НАУЧНО-ПРАКТИЧЕСКИЙ ЖУРНАЛ

ISSN 1682-0363 (print)
ISSN 1819-3684 (on-line)

БЮЛЛЕТЕНЬ СИБИРСКОЙ МЕДИЦИНЫ

BULLETIN OF SIBERIAN MEDICINE

Том 19
№ 4. 2020

ПРОФЕССОР СИБГМУ ВПЕРВЫЕ В РОССИИ ВОШЛА В СОСТАВ РЕДКОЛЛЕГИИ ЗАРУБЕЖНОГО ЖУРНАЛА «PLOS NEGLECTED TROPICAL DISEASES»

Заведующий кафедрой факультетской педиатрии с курсом детских болезней лечебного факультета, декан лечебного факультета СибГМУ, доктор медицинских наук, профессор Ольга Федорова стала членом редакционной коллегии зарубежного высокорейтингового журнала «PLoS Neglected Tropical Diseases» (Q1).

Приглашение присоединиться к команде PLoS Community Journals было направлено Ольге Сергеевне лично от главных редакторов журнала – Пола Бриндли и Шадэна Камхави. На сегодняшний день, профессор СибГМУ является единственным российским ученым в составе постоянной редакционной коллегии журнала.

Исследовательский коллектив Ольги Федоровой, который изучает эпидемиологию описторхоза, а также его взаимосвязь с хроническими неинфекционными заболеваниями, сотрудничает с научным журналом «PLoS NTD» на протяжении нескольких лет. За это время ученые СибГМУ неоднократно публиковали в данном журнале результаты своих исследований, выполненных совместно с зарубежными партнерами.

«Вхождение ученого СибГМУ в состав редколлегии авторитетного зарубежного высокорейтингового журнала – еще один шаг на пути к успешному позиционированию университета как международного научно-исследовательского центра и к повышению узнаваемости вуза на международной академической арене», - отметила ректор СибГМУ Ольга Кобякова.

Научный междисциплинарный журнал «PLoS ONE» является авторитетным зарубежным журналом первого квартиля (Q1). Журнал включен в международную реферативную базу данных и систему цитирования «Scopus». По данным на 2019 год, показатель журнала SJR равен 2.148, h-index журнала – 121. Журнал издается некоммерческой организацией Public Library of Science. Страна издательства – США. Среди основных предметных областей публикуемых статей: медицина, сельскохозяйственные и биологические науки, биохимия, генетика и молекулярная биология.

Официальный сайт журнала «PLoS Neglected Tropical Diseases».

BULLETIN OF SIBERIAN MEDICINE

Peer-reviewed scientific-practical journal
Issued quarterly

Volume 19, No. 4, 2020

ISSN 1682-0363 (print)
ISSN 1819-3684 (online)

FOUNDER AND PUBLISHER:
Siberian State Medical University, the Ministry for Healthcare of the Russian Federation

Registered by the Ministry of the Russian Federation for Affairs of the Press, Television and Radio Broadcasting and Mass Communication Media
Certificate of registration PI No. 77-7366
dated to 26.03.2001

Bulletin of Siberian Medicine is included:
in the List of peer-reviewed scientific journals and publications issued in the Russian Federation, which should publish main scientific results of doctor's and candidate's theses

Bulletin of Siberian Medicine is indexed:
Scopus
Web of Science (WoS (ESCI))
Science Index
RSCI
Ulrich's International Periodicals Directory
Cyberleninka
DOAS

Editorial Board Office:
107, Lenin Av., Tomsk, 634050, Russian Federation
Telephone: +7-(382-2)-51-41-53.
http://bulletin.tomsk.ru
E-mail: bulletin@bulletin.tomsk.ru

Publisher: the Siberian State Medical University.
2, Moscow Trakt, Tomsk, 634050,
Russian Federation.
Editors: E.E. Stepanova, Yu.P. Gotfrid
Translate: M.E. Orlova, D. Palazza
Electronic makeup, cover design
L.D. Krivtsova

Printed in Litburo LLC,
4, Korolev Str., Tomsk, 634055, Russian Federation

Signed to print 23.12.2020
Format 60 × 84/8. Offset print.
Coated paper. Times New Roman' font.
P.l. 31,25. C.p.l. 30,5.
500 copies. Odder no 521.

The price – free.
Date of publication 26.12.2020.

БЮЛЛЕТЕНЬ СИБИРСКОЙ МЕДИЦИНЫ

Научно-практический журнал
Выходит 4 раза в год

Том 19, № 4, 2020

ISSN 1682-0363 (print)
ISSN 1819-3684 (online)

УЧРЕДИТЕЛЬ И ИЗДАТЕЛЬ:
ФГБОУ ВО «Сибирский государственный медицинский университет» Минздрава России

Журнал основан в 2001 году
Зарегистрирован в Министерстве РФ по делам печати, телерадиовещания и средств массовых коммуникаций
Свидетельство регистрации ПИ № 77-7366 от 26.03.2001 г.

Журнал входит в Перечень ведущих рецензируемых научных журналов и изданий, выпускаемых в РФ, в которых должны быть опубликованы основные научные результаты диссертаций на соискание ученой степени доктора и кандидата наук

Индексация:
Scopus
Web of Science (WoS (ESCI))
РИНЦ (Science Index)
RSCI
Ulrich's International Periodicals Directory
Cyberleninka
DOAS

Редакция:
634050, г. Томск, пр. Ленина, 107.
Тел.: (382-2)-51-41-53.
http://bulletin.tomsk.ru
E-mail: bulletin@bulletin.tomsk.ru

Оригинал-макет:
Издательство СибГМУ.
634050, г. Томск, Московский тракт, 2.
Редакторы: Е.Е. Степанова, Ю.П. Готфрид
Перевод: М.Е. Орлова, Дж. Палацца
Электронная верстка, дизайн обложки Л.Д. Кривцова

Отпечатано в ООО «Литбюро»,
634055, г. Томск, ул. Королёва, 4.

Подписано в печать 23.12.2020 г.
Формат 60 × 84/8. Печать офсетная.
Бумага мелованная. Гарнитура «Times New Roman».
Печ. л. 31,25. Усл. печ. л. 30,5.
Тираж 500 экз. Заказ 703.

Цена – свободная.
Дата выхода в свет 26.12.2020.

Подписной индекс 10650 в Объединенном каталоге «Пресса России» и интернет-каталоге агентства «Книга-Сервис».

СОДЕРЖАНИЕ

CONTENTS

УДК 616.379-008.64-021.6:611.36/.37.018.1:612.349.8]-092.9
https://doi.org/10.20538/1682-0363-2020-4-6-13

Insulin-positive cells in liver and exocrine part of pancreas in animals with experimental diabetes mellitus

Baykenova M.B.[1, 2], Chereshnev V.A.[1], Sokolova K.V.[1, 2], Gette I.F.[1], Emelianov V. V.[2], Danilova I.G.[1]

[1] *Institute of Immunology and Physiology, Ural Branch of the Russian Academy of Sciences (UB RAS) 106, Pervomaiskaya Str., Yekaterinburg, 620219, Russian Federation*

[2] *Ural Federal University (UrFU) named after the first President of Russia B.N. Yeltsin 19, Mira Str., Yekaterinburg, 620002, Russian Federation*

ABSTRACT

Aim. To compare the number of insulin$^+$ cells in the liver and exocrine part of the pancreas with the type of experimental diabetes, blood glycose and glycated hemoglobin (HbA_{1c}) level and with the number of Pdx1$^+$ cells.

Materials and methods. The experiment was carried out on 25 male Wistar rats (weighting (303.0 ± 25.3) g) that were divided into 3 groups: the first group consisted of intact animals, the second had animals with experimental diabetes type 1, and the third with animals with experimental diabetes type 2. Biochemical, immunohistochemical, ELISA methods and statistical analysis were used.

Results. Insulin$^+$ and Pdx1$^+$ cells of rats with experimental diabetes were found in the liver and exocrine part of pancreas. The highest number of insulin$^+$ cells in the liver was detected in type 2 diabetes (T2D). A strong positive correlation between the number of insulin$^+$ cells in the liver and level of glycosylated hemoglobin in theblood was revealed in both type 1 and type 2 diabetes.

Conclusion. Insulin$^+$ cells are detected in the liver and acinar part of pancreas of both intact rats and rats with experimental diabetes. Group with T2D is characterized by the highest number of insulin$^+$ cells in the liver compared with type 1 diabetes (T1D). The localization of insulin$^+$ cells in the liver changes depending on the type of diabetes. In T2D insulin$^+$ cells are located in all parts of liver acini, meanwhile in animals with T1D such cells are mainly detected in the periportal area. The expression of Pdx1$^+$ in acinar cells of pancreas and liver cells is likely a mechanism for their reprogramming into insulin$^+$ cells in experimental diabetes mellitus.

Key words: diabetes mellitus, pancreas, liver, insulin$^+$ cells, Pdx1$^+$ cells.

Conflict of interest. The authors declare the absence of obvious or potential conflict of interest related to the publication of this article.

Source of financing. This work was financially supported by the Russian Science Foundation, grant No. 16-1500039-P and the budget project No. AAAA-A18-118020590108-7 of the Institute of Immunology and Physiology, UB RAS.

Conformity with the principles of ethics. The study was approved by the local Ethics Committee at the Institute of Immunology and Physiology, UB RAS (Protocol No-d-TM-2016-20).

For citation: Baykenova M.B., Chereshnev V.A., Sokolova K.V., Gette I.F., Emelianov V.V., Danilova I.G. Insulin-positive cells in liver and exocrine part of pancreas in animals with experimental diabetes mellitus. *Bulletin of Siberian Medicine.* 2020; 19 (4): 6–13. https://doi.org/10.20538/1682-0363-2020-4-6-13.

✉ *Baykenova Madina B.,* e-mail: m.b.baikenova@urfu.ru.

Инсулин-позитивные клетки печени и экзокринной части поджелудочной железы у животных с экспериментальным сахарным диабетом

Байкенова М.Б.[1,2], Черешнев В.А.[1], Соколова К.В.[1,2], Гетте И.Ф.[1], Емельянов В.В.[2], Данилова И.Г.[1]

[1]Институт иммунологии и физиологии Уральского отделения Российской академии наук (ИИФ УрО РАН) Россия, 620049, г. Екатеринбург, ул. Первомайская, 106

[2] Уральский федеральный университет (УФУ) имени первого Президента России Б.Н. Ельцина Россия, 620002, г. Екатеринбург, ул. Мира, 19

РЕЗЮМЕ

Цель исследования: сопоставить количество инсулин-положительных (инсулин$^+$) клеток печени и экзокринной части поджелудочной железы с концентрацией глюкозы и гликированного гемоглобина (HbA_{1c}) в крови, а также с количеством Pdx1-положительных (Pdx1$^+$) клеток в этих органах при различных типах сахарного диабета в эксперименте.

Материалы и методы. Эксперимент проводился на 25 самцах крыс (линия Wistar, масса (303,0 ± 25,3) г), которые были разделены на три группы: 1-я – интактные животные, 2-я – животные с экспериментальным сахарным диабетом 1-го типа, 3-я – животные с экспериментальным сахарным диабетом 2-го типа. В работе осуществляли биохимический, иммуноферментный, иммуногистохимический и статистический анализы.

Результаты. В печени и экзокринной части поджелудочной железы крыс с экспериментальным сахарным диабетом 1-го и 2-го типов обнаружены инсулин$^+$ и Pdx1$^+$-клетки. Наибольшее количество инсулин$^+$-клеток в печени отмечается при сахарном диабете 2-го типа. Установлена корреляция между количеством инсулин$^+$-клеток в печени и концентрацией HbA_{1c} в крови при сахарном диабете 1-го и 2-го типов.

Заключение. Инсулин$^+$-клетки определяются в печени и экзокринной части поджелудочной железы интактных животных и крыс, у которых воспроизведена модель сахарного диабета 1-го и 2-го типов. Животные с экспериментальным сахарным диабетом 2-го типа характеризуются большим количеством инсулин$^+$-клеток печени по сравнению с крысами с экспериментальным сахарным диабетом 1-го типа. В зависимости от типа сахарного диабета в печени меняется локализация инсулин$^+$-клеток. При экспериментальном сахарном диабете 2-го типа инсулин$^+$-клетки печени расположены во всех частях печеночной дольки, тогда как у животных с экспериментальным сахарным диабетом 1-го типа эти клетки обнаруживаются преимущественно перипортально. Вероятно, экспрессия Pdx1$^+$ в ацинарных клетках поджелудочной железы и клетках печени представляет собой механизм их перепрограммирования в инсулин$^+$-клетки при экспериментальном сахарном диабете.

Ключевые слова: сахарный диабет, поджелудочная железа, печень, инсулин$^+$-клетки, Pdx1$^+$-клетки.

Конфликт интересов. Авторы декларируют отсутствие явных и потенциальных конфликтов интересов, связанных с публикацией настоящей статьи.

Источник финансирования. Работа выполнена при поддержке гранта РНФ (№ 16-1500039-П) и бюджетной темы ИИФ УрО РАН (№ АААА-А18-118020590108-7).

Соответствие принципам этики. Исследование одобрено этическим комитетом Института иммунологии и физиологии УрО РАН (протокол No-d-ТМ-2016-20).

Для цитирования: Байкенова М.Б., Черешнев В.А., Соколова К.В., Гетте И.Ф., Емельянов В.В., Данилова И.Г. Инсулин-позитивные клетки печени и экзокринной части поджелудочной железы у животных с экспериментальным сахарным диабетом. *Бюллетень сибирской медицины.* 2020; 19 (4): 6–13. https://doi.org/10.20538/1682-0363-2020-4-6-13.

INTRODUCTION

The relevance of the study of diabetes mellitus (DM) is due to its prevalence, high level of disability in patients and their high mortality rate. Currently, more than 422 million people worldwide have diabetes [1]. The exponential increase in the number of patients with diabetes requires new therapeutic strategies to reduce the socio-economic burden of this disease [2]. Diabetes is a chronic disease characterized by hyperglycemia, which is the result of absolute or relative insulin deficiency. Both classic forms of diabetes are characterized by the inability of pancreatic beta (β) cells to satisfy the body's need for insulin secretion due to either an almost complete loss in type 1 diabetes (T1D) or a deficit of β-cells as a result of insulin resistance in type 2 diabetes (T2D). The deficit in β-cell mass, which is up to 90% in long-standing T1D and approximately 65% in long-standing T2D is considered to be a consequence of β-cell destruction [3].

Insulin synthesis is specific for pancreatic islets' β-cells and is tightly controlled at the transcription level. The transcription factor Pdx1 determines the transcription rate and stability of insulin m-RNA. Pdx1 is both a factor of β-cell differentiation during embryogenesis and a regulator of the insulin-producing function of islet cells in mature islets of Langerhans [4]. In the differentiation process of pancreatic cells, the expression of the Pdx1 gene is enhanced in β-cells, while in exocrine and duct cells, the expression of this gene, on the contrary, is gradually reduced. It is believed that the activity of the Pdx1 gene is preserved in a differentiated state only in β-cells [5]. However, currently insulin$^+$ cells have been detected in exocrine part of the pancreas, in the brain, bone marrow, spleen, liver and adipose tissue of animals [6, 7].

Since the liver and pancreas are of endodermal origin in ontogenesis, there is an assumption that both tissues include the same precursor cells that can differentiate both into hepatocytes and pancreatic β-cells. Moreover, hepatocytes and pancreatic β-cells express a large group of specific transcription factors and also use the same type of glucose transporter into the cell (GLUT2) including it in the metabolism through phosphorylation with glucokinase [8].

Based on the preceding, the aim of our research was to compare the number of insulin$^+$ cells in the liver and exocrine part of pancreas with the blood glucose and glycated hemoglobin (HbA_{1c}) levels and with the number of Pdx1$^+$ cells in these organs in different types of diabetes mellitus in the experiment.

MATERIALS AND METHODS

Experiment was carried out on 25 male Wistar rats weighting 303.0 ± 25.3 g that were divided into 3 groups: the first of intact animals (n = 10), the second of experimental diabetes type 1 (T1D) (n = 8), the third of experimental diabetes type 2 (T2D) (n = 7). T1D was modeled by intraperitoneal (i.p.) injection of alloxan, diluted in 0.85% sodium chloride solution in a total dose 170 mg/kg of animal's body mass, according to the modified author's method [9]. T2D was induced by i.p. injection of streptozotocin diluted in citrate buffer in a dose 65 mg/kg with preventive (15 minutes before) i.p. injection of nicotinamide dissolved in water in a dose 110 mg/kg [10]. The animals were sacrificed by ether overdose on the 30th day from the beginning of the experiment after taking blood from the tail vein. After median laparotomy pancreases and livers were removed and fixed in 10% neutral formalin for 24 hours. After being washed for 8 hours, tissue was subjected to standard histological protocol using Automatic Tissue Processor Leica TP 1020 (Leica Microsystems, Germany) and Tissue Embedding Station Leica EG1160 (Leica Microsystems, Germany). Tissue slides 3–4 μm thick were made using Leica SM2000 K Sliding microtome (Leica Microsystems, Germany).

To confirm experimental diabetes, plasma glucose, glycated hemoglobin (HbA_{1c}) and insulin concentrations were determined in the blood. To detect glucose and glycated hemoglobin (HbA_{1c}) concentration, standard kits for biochemical analysis were used (VectorBest, Russia; GLIKOGEMTEST, Russia). To measure blood insulin, Rat/Mouse Insulin ELISA kit (Millipore, USA) and Automatic immunofermental analyzer LAZURITE (Dynex Technologies, USA) were used.

Immunohistochemical examination of the pancreas and liver was performed using mouse anti-proinsulin and insulin (clone INS04+INS05, Invitrogen, USA) and anti-Pdx1 antibodies (Abcam, USA) according to standard protocols. Tissue sections were incubated with primary antibodies in 1: 200 dilution for 16 hours at 4 °C. Detection of insulin was performed, using the avidin–biotin–peroxidase complex. To detect Pdx, Goat anti-Mouse IgG (H + L) conjugated with fluorescent dye Texas

Red (ThermoFisher, USA) was used. Negative and positive tissue controls were used to check the protocol and exclude non-specific binding. As positive control for immunohistochemical determination of insulin and Pdx1, pancreatic tissue sections of intact rats were taken [11, 12]. Negative control was carried out on the similar tissue sections and using the same protocols, excluding primary antibodies [12, 13].

Analysis of tissue slides and calculation of insulin$^+$ cells were performed using light microscope Leica DM 2500 (Leica, Germany) and Video TesT-Morphology 5.0 software (Video TesT Ltd., Russia), calculation of Pdx1$^+$ cells was carried out with the help of a confocal laser scanning microscope LSM 710 (CarlZeiss, Germany) and ZEN 2.0 (CarlZeiss, Germany) software.

The number of insulin$^+$ cells and Pdx1$^+$ cells in exocrine part of pancreas per 1 mm^2 of a pancreatic slide was calculated. In the liver, the number of insulin$^+$ cells and Pdx1$^+$ cells in hepatic plates in all zones of hepatic lobule was determined. In sinusoidal capillaries, the following parameters were calculated: the total number of sinusoidal cells throughout the entire hepatic lobule and the total number of insulin$^+$ sinusoidal cells, located in all parts of hepatic lobule per 1 mm^2 of a hepatic tissue slide. Functional activity of insulin$^+$ cells was evaluated based on the optical density (OD) of their cytoplasm.

Statistical analysis was performed using Statistica 6.0 (DELL, USA) and Microsoft Excel 2003 (Microsoft, USA). To test the hypothesis of homogeneity of two independent samples, the nonparametric Mann – Whitney *U*-test and Kruskal – Wallis test were used. The results were considered significant at $p < 0.05$. The data were presented as the mean and the standard error of the mean ($M \pm m$). To reveal the relationship between the number of insulin$^+$ cells, Pdx1$^+$ cells and the concentration of glucose and glycated hemoglobin (HbA_{1c}) in blood, the Pearson pairwise linear correlation coefficient (r) was calculated.

RESULTS

Blood glucose and glycated hemoglobin (HbA_{1c}) levels in experimental T1D and T2D rats are significantly higher in comparison with intact rats, while blood insulin concentration decreases only in T1D. In T2D rats the level of blood insulin is significantly higher than in the T1D group, which is typical of T2D (Table 1).

Table 1

Concentration of glucose, HbA1c and insulin in the blood of rats in all experimental groups, $M \pm m$

Parameter	Group 1 (intact animals)	Group 2 (animals with T1D)	Group 3 (animals with T2D)
Glucose, mmol/L	5.00 ± 0.30	10.88 ± 0.46*	10.90 ± 0.50*
HbA_{1c}, %	4.40 ± 0.30	6.73 ± 0.78*	6.58 ± 0.97*
Insulin, mkg/L	1.28 ± 0.19	0.50 ± 0.09*	1.00 ± 0.13 #

*difference as compared with intact animals ($p < 0.05$); #difference as compared with T1D group ($p < 0.05$) (here and in Tables 2–4).

Immunohistochemical analysis showed the presence of insulin+ and Pdx1+ cells in the exocrine part of pancreas and in all zones of the hepatic lobule of experimental animals (Figure).

The number of insulin$^+$ and Pdx1$^+$ cells in the exocrine pancreas in T1DM and T2DM does not differ from their number in intact animals. The number of insulin$^+$ cells in the liver of animals with T1DM and T2DM is higher than in intact animals. In T1D insulin$^+$ cells in the liver are primary localized in the periphery of the hepatic lobule, while in T2D such cells are in all zones of the hepatic lobule. The total amount of insulin$^+$ and Pdx1$^+$ cells was counted throughout the hepatic lobule. Additionally, the data on the number of insulin$^+$ cells in the peripheral zone of the hepatic lobule are shown separately. The number of Pdx1$^+$ cells in the liver of rats with experimental diabetes is bigger than in intact rats. This parameter in T1D rats is higher than the similar parameter in intact animals (Table 2).

Optical density (OD) of cytoplasm in insulin$^+$ cells of the liver and pancreas in T1D is less than in the intact group (Table 3). In animals with experimental T1D, contrary to rats with experimental T2D, insulin production in insulin$^+$ sinusoidal cells increases, since the optical density of cytoplasm in these cells is higher in comparison with the similar parameter in intact animals and animals with experimental T2D (Table 3).

The number of insulin$^+$ sinusoidal cells increases in different types of diabetes in comparison with the similar parameter in intact animals. This parameter reaches the highest value in rats with experimental T2D, while these cells are localized in all zones of the hepatic lobule (Table 4).

To determine the relationship between the number of hepatic insulin$^+$ cells and Pdx1$^+$ cells and the level of glucose in rat blood, a pairwise linear correlation coefficient was used (Table 5).

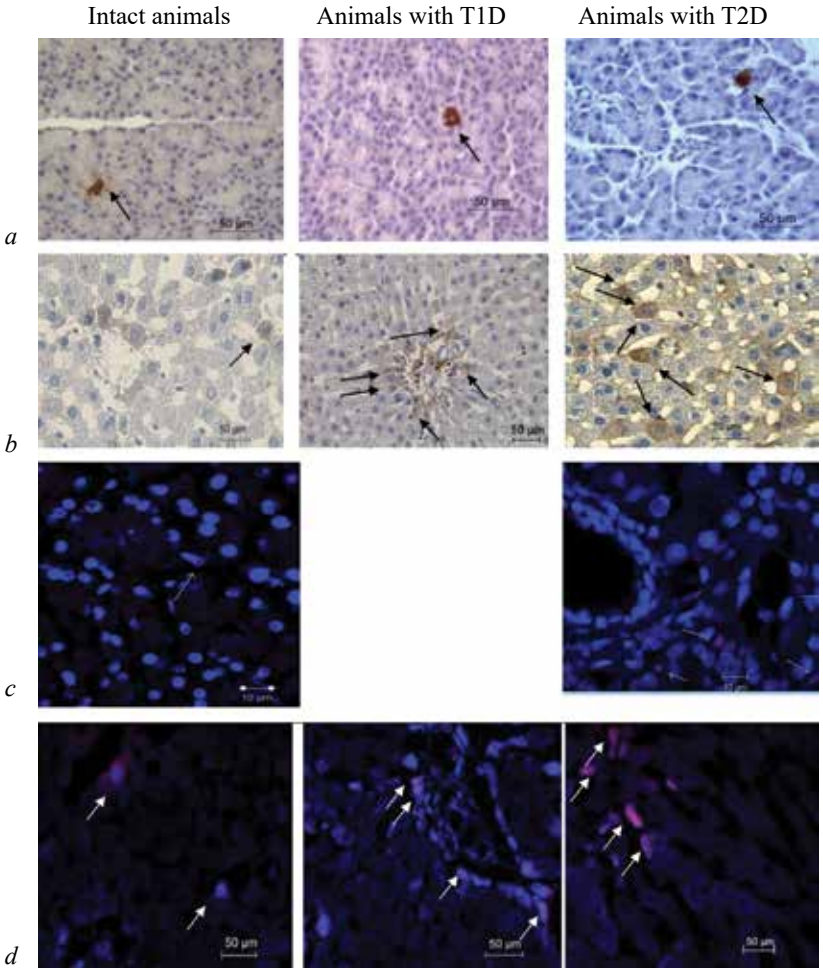

Figure. Pancreas (*a, c*) and liver (*b, d*) of intact animals, animals with experimental T1D and animals with experimental T2D; immunohistochemical staining for insulin (*a, b*) and immunofluorescent staining for Pdx1$^+$ (*c, d*). Insulin$^+$ and Pdx1$^+$ cells are shown by arrows, ×400

Table 2

Number of insulin$^+$ and Pdx1$^+$ cells in the liver and exocrine part of pancreas (*N*/mm^2 of the organ tissue), *M* ± *m*			
Parameter	Group 1 (intact animals)	Group 2 (animals with T1D)	Group 3 (animals with T2D)
Number of insulin$^+$ cells in exocrine pancreas, N/mm^2 of pancreas	3.50 ± 0.54	3.67 ± 0.73	3.15 ± 0.34
Number of Pdx1$^+$ cells in exocrine pancreas, N/mm^2 of pancreas	27.34 ± 4.92	–	21.54 ± 3.22
Number of insulin$^+$ cells in liver, N/mm^2 of liver	14.26 ± 0.84	24.86 ± 2.36*	151.50 ± 7.34*#
Number of insulin$^+$ cells in hepatic plates in the peripheral zone, N/mm^2	0	13.58 ± 3.08*	41.10 ± 4.93* #
Number of Pdx1$^+$ cells in liver, N/mm^2 of liver	32.11 ± 2.14	42.72 ± 1.59*	34.09 ± 2.46

Table 3

Optical density (OD) of cytoplasm in insulin$^+$ cells of the liver and exocrine part of the pancreas (in conventional units), *M* ± *m*			
Parameter	Group 1 (intact animals)	Group 2 (animals with T1D)	Group 3 (animals with T2D)
OD of cytoplasm in insulin$^+$ cells in the exocrine pancreas	0.44 ± 0.02	0.37 ± 0.02*	0.42 ± 0.02
OD of cytoplasm in insulin$^+$ cells in hepatic plates	0.20 ± 0.01	0.17 ± 0.012*	0.19 ± 0.01
OD of cytoplasm in insulin$^+$ sinusoidal cells	0.29 ± 0.24	0.35 ± 0.01*	0.30 ± 0.01#

Table 4

Number of sinusoidal and insulin$^+$ sinusoidal cells in the liver of experimental animals, $M \pm m$

Parameter	Group 1 (intact animals	Group 2 (animals with T1D)	Group 3 (animals with T2D)
Total number of sinusoidal cells, N/mm² of liver	387.11 ± 14.19	645.22 ± 33.95*	713.15 ± 33.47*#
Total number of insulin$^+$ sinusoidal cells, N/mm²	13.82 ± 0.63	19.19 ± 0.89*	37.80 ± 3.39*#
Number of insulin$^+$ sinusoidal cells in the peripheral zone of the hepatic lobule, N/mm² of liver parenchyma, N/mm²/ (%)	0.63 ± 0.03 (4.6 ± 0.02%)	5.64 ± 0.32* (29.7 ± 2.80%)*	17.91 ± 2.71*# (48.1 ± 7.70%)*#

Table 5

Coefficients of pairwise linear correlation between the number of insulin$^+$ cells and Pdx1$^+$ cells and concentration of glucose and HbA_{1c} in the rat blood. Coefficients of pairwise linear correlation between the number of insulin$^+$ cells and Pdx1+ cells in the rat liver

Type of cell	Glucose	HbA_{1c}	Pdx1$^+$ cells
Insulin$^+$ cells in liver in T1D	0.13	0.84	–0.49
Insulin$^+$ cells in liver in T2D	0.58	0.98	–0.25
Pdx1$^+$ cells in liver T1D	0.84	0.47	–
Pdx1$^+$ cells in liver in T1D	0.26	0.41	–

The obtained data indicate a strong positive correlation between the number of insulin+ liver cells and the level of glycated hemoglobin in blood, which is evidence of strong hyperglycemia during a month, both in T1D and T2D. At the same time, positive correlation between the number of hepatic insulin$^+$ cells and concentration of glucose, measured in rat blood on the 30th day of the experimental diabetes is weak in T1D and of moderate strength in T2D. It was established that there is a weak inverse correlation between the number of insulin$^+$ cells and Pdx1$^+$ cells in liver (Table 5). Thus, the number of insulin$^+$ cells in T1D is less than in T2D, however, the number of Pdx1$^+$ cells increases as compared with T2D. Interrelation between the HbA1c concentration and the number of Pdx1$^+$ cells in T1D and T2D is weak. The coefficient of pairwise linear correlation between concentration of glucose and Pdx1$^+$ cells in T1D is relatively high, while T2D is characterized by a lower interrelation between these parameters.

DISCUSSION

Insufficient quantity and dysfunction of insulin-producing β-cells in pancreatic islets are the main causes of hyperglycemia and the associated complications arising in T1DM and T2DM [14]. The search for methods, aimed at increasing the number and functional activity of preserved β-cells in diabetes, is a promising strategy for treatment of both diabetes types. Insulin$^+$ cells, found in various organs, are attracting more and more researchers' attention because they can partially compensate for the damage of β-cells of pancreatic islets in diabetes mellitus [15]. The quantity and localization of insulin$^+$ cells in the liver and exocrine pancreas, depending on the type of the experimental diabetes mellitus, were studied in this work.

Insulin$^+$ cells are found in the parenchyma of the liver and pancreas (outside the pancreatic islets) in small quantity in intact animals. In the rat pancreas, the number of these cells remains constant in T1D and T2D. The optical density of the cytoplasm of these cells also does not differ under the conditions of T1D and T2D models.

Depending on the type of diabetes, there are differences not only in the number of insulin$^+$ cells (in T2D their number is almost 5 times greater than in the liver of animals with T1D), but also in the localization of these cells. In T2D, insulin$^+$ cells are located in all parts of the hepatic lobule, while in animals of the T1D group these cells are found mainly in the peripheral zone. The structure, size and location of insulin$^+$ cells in the liver correspond to hepatocytes.

Liver sinusoidal cells (LSC) are located along the hepatic sinusoids and make up about 33% of liver parenchyma cells. Endothelial cells, stellate macrophages (Kupffer cells), perisinusoidal lipocytes (Ito cells), pit cells, and dendritic cells are referred to as LSC. LSC are capable of phagocytosis and pinocytosis and are involved in a wide range of immunological reactions [17].

When analyzing the number of LSC, it was determined that their number increases in both types of DM, but to a greater extent in DM2. According to the results of the study, in T2D the number of insulin$^+$ sinusoidal cells is higher than in T1D. Counting the number of insulin$^+$ sinusoidal cells in the peripheral zone of the hepatic lobule is necessary to compare this parameter with the number of insulin$^+$ cells in hepatic plates (presumably hepatocytes), located in the similar zone. Since there is evidence [6] that

insulin$^+$ hepatocytes are localized mainly in the first (peripheral) zone of the hepatic lobule, the number of insulin$^+$ sinusoidal cells, located in the intermediate (second) zone, is not indicated. As compared with pancreatic β-cells, insulin$^+$ hepatocytes are generally characterized by a lower optical density of cytoplasm, which indicates a relatively low concentration of insulin in these cells and reflects their low functional activity. An increase in the number of this type of cells can be both the result of insulin synthesis in the cells themselves and their ability for endocytosis of extracellular insulin [18].

Pancreatic and duodenal Pdx1 is a key factor in development, proliferation, and functioning of β-cells in pancreatic islets [19]. The protein is able to bind to the insulin gene promoter, GLUT2, glucokinase and other, regulating gene expression of these proteins [20]. It is believed that Pdx1 can reprogram any cells by stimulating insulin synthesis in them [21]. We observed differences in change in the number of Pdx1$^+$ liver cells in experimental models of diabetes mellitus: in T1DM their number significantly increases, in T2DM their number does not change. The pairwise linear correlation coefficient indicates a strong relationship between the number of Pdx1$^+$ liver cells and the HbA1c concentration in blood, which reflects the severity of hyperglycemia during the experiment. Likely, in the model of T1DM, insulin-producing cells in liver do not compensate for the lack of insulin, therefore, additional production of Pdx1 is required. On the contrary, in animals with T2D, the normalization of blood insulin concentration does not require further reprogramming of hepatocytes into insulin-producing cells. It also cannot be ruled out that the reason of the revealed differences between animals with T1DM and T2DM may be explained by the involvement of other transcription factors, Nkx 6.1 in the differentiation of insulin-producing cells in particular [5]. The obtained data allow us to put forward a hypothesis about the existence of an inverse relationship between the insulin concentration in blood and the production of Pdx1 in hepatocytes as a mechanism for compensating for hypoinsulinemia in diabetes.

Thus, the lack of insulin in experimental DM1 and DM2 can be compensated for by increasing the number of insulin-producing cells in liver and exocrine pancreas. Reprogramming of differentiated cells such as hepatocytes into insulin$^+$ cells can be considered a mechanism for obtaining more insulin-producing cells. New approaches in the treatment of diabetes, aimed at increasing the expression of Pdx1 and the number of insulin$^+$ cells in various organs, appear to be extremely promising.

CONCLUSION

It has been shown for the first time that in experimental T1DM and T2DM there is an increase in the number of insulin$^+$ and Pdx1$^+$ cells in the rat liver. In animals with experimental T1DM, insulin$^+$ liver cells are found mainly in the peripheral zone of the hepatic lobule. In experimental T2DM, insulin$^+$ cells are located in all parts of the hepatic lobule, and the number of Pdx1$^+$ cells does not differ from that in intact animals. A strong positive correlation between the number of insulin$^+$ cells in the liver and the HbA_{1c} concentration in blood was found in both T1DM and T2DM. The correlation between the number of insulin$^+$ cells in liver and the glucose concentration in rat blood on the 30th day of the experiment is weak in T1DM and moderate in T2DM.

REFERENCES

1. Harris-Hayes M., Schootman M., Schootman J.C., Hastings M.K. The role of physical therapists in fighting the type 2 diabetes epidemic. *J. Orthop. Sports. Phys.Ther.* 2020; 50(1): 5–16.
2. Salinno C., Cota P., Bastidas-Ponce A., Tarquis-Medina M., Lickert H, Bakhti M. β-Cell maturation and identity in health and disease. *International Journal of Molecular Sciences*. 2019; 20 (21): 5417–5422.
3. Moin A.S.M., Butler A.E. Alterations in betacell identity in type 1 and type 2 diabetes. *Current Diabetes Reports*. 2019; 19 (9): 83. DOI: 10.1007/s11892-019-1194-6.
4. Hui H., Perfetti R. Pancreas duodenum homeobox-1 regulates pancreas development during embryogenesis and islet cell function in adulthood. *European Journal of Endocrinology.* 2002; 146 (2): 129–141. DOI: 10.1530/eje.0.1460129.
5. Oster A., Jensen J., Serup P., Galante P., Madsen O.D., Larsson L.I. Rat endocrine pancreatic development in relation to two homeobox gene products (Pdx-1 and Nkx 6.1). *Histochem. Cytochem.* 1998; 46 (6): 707–715.
6. Kojima H., Fujimiya M., Matsumura K., Nakahara T., Hara M., Chan L. Extrapancreatic insulin producing cells in multiple organs in diabetes. *PNAS.* 2004; 101(8): 2458–2463. DOI: 10.1073/pnas.0308690100.
7. Beamish C.A., Strutt B.J., Arany E.J., Hill D.J. Insulin-positive, Glut2-low cells present within mouse pancreas exhibit lineage plasticity and are enriched within extra-islet endocrine cell clusters. *Islets.* 2016; 8 (3): 65–82. DOI: 10.1080/19382014.2016.1162367.
8. Dong-Sik H., Juyoung S., Ji-Won K., Heon-Seok P., Jae-Hyoung C., Kun-Ho Y. Generation of functional insulin-producing cells from neonatal porcine liver-derived cells by PDX1/VP16, BETA2/NeuroD and MafA. *PLoS One*. 2013; 8 (11): 76–79.

9. Danilova I.G., Gette I.F. Method for modeling alloxan diabetes. RF Patent No. 2534411; 2014 (in Russ.).
10. Spasov A.A., Voronkova M.P., Singur G.L., Chepljaeva N.I., Chepurnova M.V. Experimental model of type 2 diabetes. *Biomedicine.* 2011; (3): 12–18 (in Russ.).
11. Hewitt S.M., Baskin D.G., Frevert C.W., Stahl W.L., Rosa-Molinar E. Controls for immunohistochemistry: the Histochemical Society's standards of practice for validation of immunohistochemical assays. *J. Histochem. Cytochem.* 2014; 62 (10): 693–697. DOI: 10.1369/0022155414545224.
12. Seeberger K.L., Anderson S.J., Ellis C.E., Yeung T.Y., Korbutt G.S. Identification and differentiation of PDX1 β-cell progenitors within the human pancreatic epithelium. *World J. Diabetes*. 2014; 5 (1): 59–68. DOI: 10.4239/wjd.v5.i1.59.
13. Immunohistochemical methods: manual; trans. from English, ed. by G.A. Frank, P.G. Mal'kov. Moscow, 2011: 224.
14. Geerts A. History, heterogeneity, developmental biology, and functions of quiescent hepatic stellate cells. Semin. Liver Dis. 2001; 21: 311–35.
15. Kojima H., Fujimiya M., Terashima T., Kimura H., Chan L. Extrapancreatic proinsulin/insulin-expressing cells in diabetes mellitus: Is history repeating itself? *Endocr. J*. 2006; 53 (6):715–722.
16. Okada T., Kimura A., Kanki K., Nakatani S., Nagahara Y., Hiraga M. et al. Liver Resident macrophages (Kupffer cells) share several functional antigens in common with endothelial cells. *Scandinavian Journal of lmmunology Experimental Immunology*. 2016; 83: 139–150.
17. Banin V.V., Belousova T.A., Bykov V.L. et al. Terminologia histologica International terms on cytology and human histology with the official list of Russian equivalents: reference guide; ed. by V.V. Banin, V.L. Bykov. Moscow: GEOTAR-Media, 2009: 272 (in Russ.). ISBN 978-5-9704-1443-9.
18. Vekemans K., Braet F. Structural and functional aspects of the liver and liver sinusoidal cells in relation to colon carcinoma metastasis. *World J. Gastroenterol*. 2005; 1 (33): 5095–5102. DOI: 10.3748/wjg.v11.i33.5095.
19. Chakrabarti S.K., James J.C., Mirmira R.G. Quantitative assessment of gene targeting in vitro and in vivo by the pancreatic transcription factor, PDX1. Importance of chromatin structure in directing promoter binding. *J. Biol. Chem.* 2002; 277: 13286–13293.
20. Andrali S., Smapley M, Vanderford N., Ozcan S. Glucose regulation of insulin gene expression in pancreatic β-cells. *Biochemical Journal* 2008; 415 (1): 1–10.
21. Koblas T., Leontovyc I., Loukotova S., Kosinova L., Saudek F. Reprogramming of pancreatic exocrine cells AR42J into insulin-producing cells using mRNAs for PDX1, Ngn3, and MafA transcription Factors. *Official Journal of the American Society of Gene & Cell Therapy.* 2016; 5: 1–12.

Authors contribution

Baykenova M.B. – work with experimental animals, implementation of the laboratory part of the study, statistical processing of the results. Chereshnev V.A. – critical revision of the manuscript for important intellectual content. Sokolova K.V. – work with experimental animals, implementation of the laboratory part of the study, statistical processing of the results.Gette I.F. – conception and design of the study, setting up of the experiment, modeling of DM. Emelianov V.V. – analysis and interpretation of the obtained data, drafting of the text of the article. Danilova I.G. – analysis and interpretation of the obtained data, drafting of the text of the article.

Authors information

Baykenova Madina B., Junior Researcher, Institute of Immunology and Physiology UB RAS; Post-Graduate Student, UrFU named after the first President of Russia B.N. Yeltsin, Yekaterinburg, Russian Federation. ORCID 0000-0001-5697-0370.

Chereshnev Valeriy A., Dr. Sci. (Med.), Professor, Academician of RAS, Principal Researcher, Institute of Immunology and Physiology UB RAS, Yekaterinburg, Russian Federation. ORCID 0000-0002-5777-8097.

Sokolova Ksenia V., Junior Researcher, Institute of Immunology and Physiology UB RAS; Post-graduate Student, UrFU named after the first President of Russia B.N. Yeltsin, Yekaterinburg, Russian Federation. ORCID 0000-0002-7024-4110.

Gette Irina F., Cand. Sci. (Biology), Senior Researcher, Institute of Immunology and Physiology UB RAS, Yekaterinburg, Russian Federation. ORCID 0000-0003-3012-850X.

Emelianov Victor V., Cand. Sci. (Med.), Associate Professor, Department of Immunochemistry, Department of Medical Biochemistry and Biophysics, UrFU named after the First President of Russia B.N. Yeltsin, Ekaterinburg, Russian Federation. Research ID 57191753352.

Danilova Irina G., Dr. Sci. (Biology), Associate Professor, Head of the Laboratory of Morphology and Biochemistry, Institute of Immunology and Physiology UB RAS, Yekaterinburg, Russian Federation. ORCID 0000-0001-6841-1197.

(✉) **Baykenova Madina B.,** e-mail: m.b.baikenova@urfu.ru.

Received: 18.02.2020
Accepted: 29.09.2020

УДК 616-008.9-021.6:613.24/.25.038]-092.9:599.323.4
https://doi.org/10.20538/1682-0363-2020-4-14-20

High-fat, high-carbohydrate diet–induced experimental model of metabolic syndrome in rats

Birulina J.G.[1], Ivanov V.V.[1], Buyko E.E.[1, 2], Bykov V.V.[1, 3], Smagliy L.V.[1], Nosarev A.V.[1], Petrova I.V.[1], Gusakova S.V.[1], Popov O.S.[1], Vasilev V.N.[1]

[1] *Siberian State Medical University*
2, Moscov Trakt, Tomsk, 634050, Russian Federation

[2] *National Research Tomsk Polytechnic University*
30, Lenina Av., Tomsk, 634050, Russian Federation

[3] *Innovative Pharmacology Research*
79/4, Elizarovikh Str., Tomsk, 634021, Russian Federation

ABSTRACT

Aim. The study is focused on development of high-fat, high-carbohydrate diet-induced experimental model of metabolic syndrome (MS) in rats.

Materials and methods. The 6-week old Wistar rats *(n* = 20) were used for study. *Rats were* separated into control and *experimental* groups. The rats from the control group were fed standard rat chow. The rats from the experimental group had a high-fat, high-carbohydrate diet rich in lard (17%) and fructose (17%) and drank 20% fructose solution. At the end of the study, body weight and blood pressure (BP) were assessed. After 12 weeks of a diet load, an oral glucose tolerance test (GTT) and insulin tolerance test (ITT) were carried out. Lipid and protein biochemical parameters in plasma were analyzed. Adipose tissue and liver were measured at the end of the study. The levels of triacylglycerol (TAG) and cholesterol (Ch) in the liver were determined by enzymatic methods.

Results. High-fat, high-carbohydrate diet *feeding* in rats for 12 weeks led to BP elevation and increase in the *adipose tissue*/body weight ratio. Hyperglycemia, impaired glucose tolerance and insulin resistance were found in rats with MS by means of GTT and ITT. Elevation of plasma TAG level was observed in the experimental group, although plasma total Ch and HDL-Ch did not differ from those of controls. *Liver*/body weight ratio and the level of TAG and Ch in the liver were elevated in rats with MS.

Conclusion. Experimental rat model of diet-induced MS reproduces many aspects of MS in humans. This model may be useful for studying the pathophysiology of MS and methods for its prevention and treatment.

Key words: metabolic syndrome, high-fat, high-carbohydrate diet, obesity, dyslipidemia, hyperglycemia, insulin resistance.

Conflict of interest. The authors declare the absence of obvious or potential conflict of interest related to the publication of this article.

Source of financing. The study was funded by RFBR and Tomsk region according to the research project No. 19-415-703015 (No. 18-44-700009, 18-44703008) and by the Council for Grants of the President of the Russian Federation (CS-143.2020.4).

Conformity with the principles of ethics. The study was carried out in compliance with the principles of humanity set out in the directives of the European Community (86/609 / EEC) and the Declaration of Helsinki. The study was approved by the Ethics Committee at Siberian State Medical University (Protocol No. 7793 of 27.05.2019).

For citation: Birulina J.G., Ivanov V.V., Buyko E.E., Bykov V.V., Smagliy L.V., Nosarev A.V., Petrova I.V., Gusakova S.V., Popov O.S., Vasilev V.N. High-fat, high-carbohydrate diet-induced experimental model of metabolic syndrome in rats. *Bulletin of Siberian Medicine.* 2020; 19 (4): 14–20. https://doi.org/10.20538/1682-0363-2020-4-14-20.

✉ *Birulina Julia G.,* e-mail: birulina20@yandex.ru.

Экспериментальная модель метаболического синдрома у крыс на основе высокожировой и высокоуглеводной диеты

Бирулина Ю.Г.[1], Иванов В.В.[1], Буйко Е.Е.[1,2], Быков В.В.[1,3], Смаглий Л.В.[1], Носарев А.В.[1], Петрова И.В.[1], Гусакова С.В.[1], Попов О.С.[1], Васильев В.Н.[1]

[1] *Сибирский государственный медицинский университет (СибГМУ)*
Россия, 634050, г. Томск, Московский тракт, 2

[2] *Национальный исследовательский Томский политехнический университет (НИ ТПУ)*
Россия, 634050, г. Томск, пр. Ленина, 30

[3] *ООО «Инновационные фармакологические разработки» (ООО «Ифар»)*
Россия, 634021, г. Томск, ул. Елизаровых, 79/4

РЕЗЮМЕ

Цель. Разработать экспериментальную модель метаболического синдрома (МС) у крыс на основе высокожировой и высокоуглеводной диеты.

Материалы и методы. Исследование выполнено на 20 самцах крыс линии Вистар, которые были распределены на контрольную и опытную группы. Крысы контрольной группы находились на стандартной диете. Крысы опытной группы в течение 12 нед получали высокожировую и высокоуглеводную диету, содержащую животный жир (17%), фруктозу (17%) и 20%-й раствор фруктозы вместо питьевой воды. В конце исследования у животных измеряли массу тела, артериальное давление (АД), проводили глюкозотолерантный (ГТТ) и инсулинотолерантный (ИТТ) тесты. В плазме крови определяли отдельные показатели липидного обмена, в печени – содержание триацилглицеролов (ТАГ) и холестерина (ХС).

Результаты. Содержание животных на высокожировой и высокоуглеводной диете в течение 12 нед приводило к повышению АД, увеличению удельной массы висцеральной жировой ткани. Выполнение ГТТ и ИТТ позволило выявить у крыс с МС гипергликемию, нарушение толерантности к глюкозе и инсулинорезистентность. Было обнаружено увеличение концентрации ТАГ в плазме крови крыс опытной группы, при этом уровень общего ХС не отличался от контроля. У крыс с МС наблюдалось увеличение удельной массы печени, а также содержания в ней ТАГ и ХС.

Заключение. Полученная экспериментальная модель диет-индуцированного метаболического синдрома воспроизводит большинство типичных признаков МС у человека и может быть полезна в изучении патофизиологических основ развития МС и методов его профилактики и лечения.

Ключевые слова: метаболический синдром, высокожировая и высокоуглеводная диета, ожирение, дислипидемия, гипергликемия, инсулинорезистентность.

Конфликт интересов. Авторы декларируют отсутствие явных и потенциальных конфликтов интересов, связанных с публикацией настоящей статьи.

Источник финансирования. Исследование выполнено при финансовой поддержке РФФИ и Томской области в рамках научного проекта № 19-415-703015 (№ 18-44-700009, 18-44703008) и Совета по грантам Президента Российской Федерации (МК-143.2020.4).

Соответствие принципам этики. Исследование выполнено с соблюдением принципов гуманности, изложенных в директивах Европейского сообщества (86/609/EEC) и Хельсинкской декларации. Исследование одобрено локальным этическим комитетом СибГМУ (протокол № 7793 от 27.05.2019).

Для цитирования: Бирулина Ю.Г., Иванов В.В., Буйко Е.Е., Быков В.В., Смаглий Л.В., Носарев А.В., Петрова И.В., Гусакова С.В., Попов О.С., Васильев В.Н. Экспериментальная модель метаболического синдрома у крыс на основе высокожировой и высокоуглеводной диеты. *Бюллетень сибирской медицины.* 2020; 19 (4): 14–20. https://doi.org/10.20538/1682-0363-2020-4-14-20.

INTRODUCTION

The prevalence of metabolic syndrome (MS) in modern society has been increasing rapidly over the last few years, which has caused an increase in morbidity and mortality. According to the International Diabetes Federation (IDF), 25–68% of people worldwide suffer from MS [1, 2]. Significant factors in the development of MS are abdominal obesity and insulin resistance [3, 4]. IDF defines MS as a condition of visceral obesity and at least two of the following parameters: high levels of triacylglycerols (TAG), low levels of high-density lipoproteins (HDL), high blood pressure (BP) and hyperglycemia [1]. Thus, MS is a complex of metabolic, hormonal and hemodynamic disorders that increases the risk of type 2 diabetes, non-alcoholic fatty liver disease and cardiovascular diseases [3, 5, 6].

To study the pathophysiological mechanisms of the MS development and methods for its prevention and therapy, it is necessary to develop accessible experimental models [7, 8, 9]. One of these approaches is focused on the use of animals with a genetic defect causing the development of various MS-typical pathological changes. Additionally, there is another approach to induce these disorders using special diets [7]. In recent years, the combination of a high-fat diet with a high content of carbohydrates (also referred to as the "Western diet", "the cafeteria diet") has become widespread [10, 11, 12]. It was shown that animal fats (lard or beef fat) are more effective for MS modeling compared with vegetable fats [11]. Glucose [12], fructose [13, 14] or sucrose [15] can be used as carbohydrates added to the diet. Such a diet is similar to the nutrition of a modern person and is considered as the most adequate for MS modeling and reproducing of the pathogenetic factors and the phenomenology of metabolic disorders in MS.

In this regard, the aim purpose of the study was to develop an experimental model of MS in rats based on a high-fat, high-carbohydrate diet.

MATERIALS AND METHODS

The MS model was performed using male Wistar rats (20 animals with weight of 200–250 g, 6 weeks-old). The studies were carried out in compliance with the principles of the European Community Directives (86/609/EEC) and the Declaration of Helsinki. Animals were fed ad libitum and housed in a 12-h light/dark cycle. Rats were separated into control (n = 8) and experimental (n = 12) groups. The rats from the control group were fed with standard chow for laboratory rats ("Delta Feeds", Biopro, Russia, total calories 3000 kcal/kg). The rats from the experimental group were fed with a high-fat, high-carbohydrate diet rich in lard (17%), fructose (17%) and drinking water was replaced with a 20% fructose solution (total calories 4,400 kcal/kg, 54% energy from fat).

Before and at the end of the study body weight and BP ("Systola", Neurobotics, Russia) were assessed. In the last week of the experiment, glucose tolerance (GTT) and insulin tolerance (ITT) tests were carried out [11, 16]. Fasted animals (12 h of food deprivation) were injected intragastrically with a glucose solution at a dose of 2 g/kg (D-glucose, Sigma-Aldrich, USA) or subcutaneously injected with short-acting insulin at a dose of 0.75 IU/kg ("NovoRapid Penfil", Denmark). The glucose concentration in the blood obtained from the rat's tail vein was determined after 0, 15, 30, 60, 90, and 120 min by spectrophotometric enzymatic method using a commercial kit ("Glucose-Novo V-8054", Vector-Best, Russia). The glucose utilization rates (K_{ITT}, % glucose/min) were calculated as $K_{ITT} = (0.693/t_{1/2}) \times 100$, $t_{1/2}$ – the time of the reduction of plasma glucose concentration by half after insulin administration [17]. Blood plasma was obtained by centrifugation (4 °C, 8,000 g, 6 min) and stored at −20 °C for subsequent analysis. The TAG, total cholesterol (Ch), and HDL-Ch plasma concentrations were measured with a biochemical analyzer (RX Imola, Randox, Japan).

At the end of the experiment the rats were euthanized by CO_2 asphyxiation. Visceral adipose tissue and liver were obtained and weighed using analytical balance, the ratios of their weight regarding to the body weight were calculated. The concentrations of TAG and Ch in the liver (mg/g of tissue) were determined after the extraction of the lipid fraction from the liver samples (50 mg) with chloroform-methanol (2:1) by the method of J. Folch [18]. The TAG and Ch levels in extracted lipids were determined by enzymatic methods using commercial kits (Chronolab, Spain). Before the analysis, a 20% chloroform solution of Thesit detergent (Sigma-Aldrich, USA) was added to the chloroform phase. Chloroform was removed by a stream of nitrogen; emulsified lipids were dissolved in distilled water. Reagents from the kits for the TAG and Ch determination were added directly to the aqueous emulsion. The Atherogenic Index of Plasma (AIP) was calculated [19].

Data were presented as mean and standard deviation ($M \pm SD$). The correspondence of the obtained

quantitative indicators to the normality was determined using the Shapiro-Wilk W-test. For statistical significance measuring between two groups the Student t-test was performed using the IBM SPSS Statistics 21 software. The alpha level of significance for all experiments was set at $p < 0.05$.

RESULTS

Experimental models of MS reproduce most of the specific signs of the human metabolic syndrome such as excess weight, visceral obesity, insulin resistance, impaired glucose tolerance, dyslipidemia, and arterial hypertension [8, 9].

High-fat, high-carbohydrate diet *feeding* of rats for 12 weeks led to systolic blood pressure (SBP) and diastolic blood pressure (DBP) elevation and increase in the *adipose tissue*/body weight ratio *and liver*/body weight ratio (Table 1).

One of the typical features of MS is central obesity. However, feeding the animals with a special diet does not always lead to a significant increase in the body weight [11, 12, 20]. In our experiment the final body weight did not differ between control and experimental groups. A possible explanation of this finding is the fact that animals of the experimental groups consumed less of the food enriched in fat and fructose, probably due to the higher caloric intake with this diet.

Table 1

Effect of high-fat and high-carbohydrate diet on the physiological parameters of rats from the control and experimental group (Metabolic syndrome model), *M ± SD*

Parameter	Group	
	Control ($n = 8$)	Metabolic syndrome ($n = 12$)
Body weight, g	425.8 ± 25.6	463.1 ± 22.4 ($p = 0.101$)
SBP, mm Hg	124.1 ± 9.2	136.2 ± 8.3 ($p = 0.007$)
DBP, mm Hg	87.4 ± 10.2	100.3 ± 13.6 ($p = 0.036$)
Adipose tissue/body weight ratio, g	2.4 ± 0.3	4.9 ± 1.3 ($p = 0.001$)
Liver/body weight ratio, g	2.7 ± 0.4	3.5 ± 0.3 ($p = 0.002$)
Food intake, g/day/group	130.2 ± 8.4	101.7 ± 9.8 ($p = 0.005$)
Fluid intake, ml/day/group	249.5 ± 11.9	347.5 ± 12.6 ($p = 0.011$)

Note. Here and in the Table 2: p – the level of statistical significance of differences in comparison with control.

At the same time, the *adipose tissue*/body weight ratio of the experimental rats, including mesenteric, epididymal and retroperitoneal fat, increased for more than 2 times, which is also an important symptom of MS. Obtained experimental data indicates the presence of obesity in rats of the experimental group (Table 1). This information is consistent with data from other diet-induced models of MS [12, 14, 21].

Feeding of experimental rats with high-fat, high-carbohydrate diet for 12 weeks led to hyperglycemia. It can be evidenced by an increased fasting plasma glucose level (Table 2). According to GTT, at 30 min after glucose administration, the blood glucose level in rats of the experimental group exceeded the level in the control group by 25.2% ($p = 0.005$). After 60 min, the blood glucose level in rats of the control and experimental groups began to gradually decrease, remaining high in the group of rats with MS model: the difference was 32.4% ($p = 0.003$). After 2 hours, the glucose level in the control group almost returned to the initial level, while in the experimental group it remained increased by 10% ($p = 0.093$) (Fig. 1, *a*). The area under the curve of glucose concentration – time ($AUC_{0\text{-}120}$) in the experimental group was 809.9 ± 81.9 mmol/l × 120 min and exceeded the control group value (585.5 ± 53.1 mmol/l × 120 min, $p = 0.001$) (Fig. 1, *b*).

It is known that ITT can detect a change in the target cells response to insulin, which may be caused by a decrease in the sensitivity or number of insulin receptors [5, 22]. A gradual decrease of the glucose concentration in the blood of animals of the control and experimental groups was observed after subcutaneous injection of insulin. However, its level remained higher in the experimental group at the point of 30 min after the injection of insulin (the difference after 30 min was 30.1% ($p = 0.002$), after 60 min – 32.5% ($p = 0.001$), after 2 hours – 25.7% ($p = 0.011$) (Fig. 2, a)). The area under the curve "glucose concentration – time" ($AUC_{0\text{-}120}$) in the experimental group was 440.9 ± 57.4 mmol/l × 120 min and exceeded the same parameter in the control group (307.1 ± 31.1 mmol/l × 120 min, $p = 0.004$).

The progression of insulin resistance in the group of animals with MS model was confirmed by the study of K_{ITT}. It was found that K_{ITT} in rats fed a high-fat and high-carbohydrate diet was 1.3 ± 0.7% glucose/min, which is 36.5% lower than that parameter in the control group (2.1 ± 0.7 % glucose/min, $p = 0.001$) (Fig. 2, b). Thus, hyperglycemia, along with glucose tolerance and insulin resistance, indicates the development of MS in animals.

Dyslipidemia as the characteristic of MS demonstrates both quantitative and qualitative changes in the

blood lipoproteins composition. The most important signs of dyslipidemia are: an increased level of TAG in very low-density lipoproteins (VLDL-Ch), which are the main transporters of endogenous fat synthesized in the liver. At the same time, the level of Ch in low-density lipoproteins (LDL-Ch) increases, and also decreases in high-density lipoproteins (HDL-Ch) [4].

In this study, rats of the experimental group had shown an increase in plasma TAG concentration by 2.1 times compared with the control group. This phenomenon may occur due to the excessive consumption of fructose with the diet that leads to the activation of lipogenesis in the liver [13, 23]. The total Ch level in animals fed with high-fat, high-carbohydrate diet did not significantly increase. At the same time, the level of atherogenic LDL-Ch increased in rats of the experimental group, while the level of HDL-Ch did not change (Table 2).

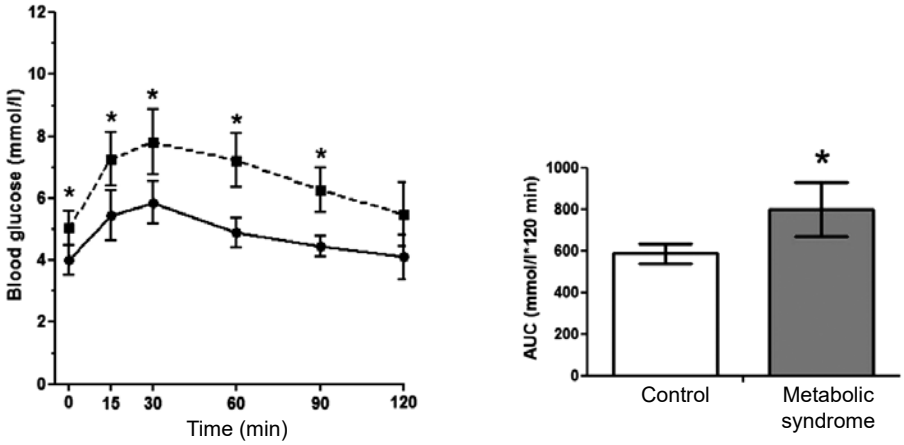

a *b*

Fig. 1. Dynamics of the blood glucose concentration in rats (*a*) and the area under the curve "glucose concentration-time" (*b*) in the oral glucose tolerance test**.** Here and in Fig. 2: the control group (solid line) and experimental group (dashed line). **p* < 0.05 in comparison with the control group

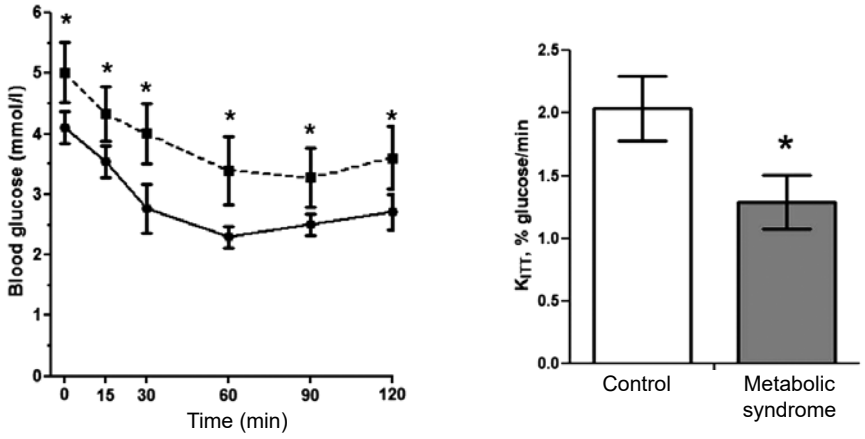

a *b*

Fig. 2. Dynamics of insulin-stimulated decrease in blood glucose concentration in rats (*a*) and glucose disposal rate (*b*) in the insulin tolerance test

Table 2

Effect of high-fat and high-carbohydrate diet on the biochemical parameters of plasma in rats from the control and experimental groups (Metabolic syndrome), *M* ± *SD*

Group	Parameter				
	Fasting glucose, mmol/l	TAG, mmol/l	Total Ch, mmol/l	HDL-Ch, mmol/l	LDL-Ch, mmol/l
Control (*n* = 8)	4.0 ± 0.5	1.8 ± 0.8	2.4 ± 0.5	0.9 ± 0.3	1.3 ± 0.3
Metabolic syndrome (*n* = 12)	5.3 ± 0.6 (*p* = 0.021)	3.7 ± 0.9 (*p* = 0.001)	2.8 ± 0.7 (*p* = 0.062)	0.8 ± 0.1 (*p* = 0.201)	1.9 ± 0.5 (*p* = 0.044)

The literary data on changes in the Ch levels and HDL-Ch, LDL-Ch levels in the blood of animals with diet-induced MS differ significantly. Some researchers have noted an increase in the total Ch content in plasma, for example, in experiments with diets rich in fructose or fats and fructose [10, 24]. Others noticed an absence of any changes in the level of Ch [12]. Data on the content of HDL-Ch in plasma also vary, with a predominance of facts on its reduction [15]. AIP of rats fed with a high-fat and high-carbohydrates diet had increased threefold (0.2 ± 0.1 in the control group versus 0.6 ± 0.2 in the experimental group, $p = 0.001$). This indicator is widely used in clinical medicine in case to assess cardiovascular risk in patients. This parameter is considered as a potential biomarker for early cardiovascular diseases diagnosis [25].

It is known that feeding of animals with high-fat [14] or high-fat and high-carbohydrate [21, 26] diets leads to the significant metabolic changes in the liver, as it can be noticed during a non-alcoholic steatohepatosis. In our experiment, there was an increase in the *liver*/body weight ratio in animals with the MS model, as well as an increase in the liver TAG level by 1.8 times (4.3 ± 1.5 mg/g in the control group versus 7.8 ± 3.4 mg/g in the experimental group, $p = 0.005$). Ch liver level had increased by 2.4 times ($1.1 \pm \pm 0.4$ mg/g in the control group versus 2.6 ± 0.6 mg/g in the experimental group, $p = 0.020$). Thus, the results of the study demonstrate that a high-fat and high-carbohydrate diet can contribute to the development of fatty liver disease.

CONCLUSION

It has been established that the use of the proposed high-fat and high-carbohydrate diet in rats reproduces most of the typical MS features: obesity, increased blood pressure, hyperglycemia, decreased glucose tolerance, insulin resistance, and dyslipidemia with triglyceridemia. This diet is similar to the high-calorie diet of a modern man. This model of diet-induced MS may be useful in studying the causes of the metabolic and hemodynamic disorders development and progression in the state of MS, as well as in exploring the potential approaches to its prevention and treatment.

REFERENCES

1. Alberti K.G., Zimmet P., Shaw J. Metabolic syndrome-a new world-wide definition. A consensus statement from the International Diabetes Federation. *Diabet. Med.* 2006; 23 (5): 469–480. DOI: 10.1111/j.1464-5491.2006.01858.x.
2. Saklayen M.G. The global epidemic of the metabolic syndrome. *Curr. Hypertens. Rep.* 2018; 20 (2): 12. DOI: 10.1007/s11906-018-0812-z.
3. Aydin S., Aksoy A., Aydin S., Kalayci M, Yilmaz M., Kuloglu T., Citil C., Catak Z. Today's and yesterday's of pathophysiology: Biochemistry of metabolic syndrome and animal models. *Nutrition*. 2014; 30 (1): 1–9. DOI: 10.1016/j.nut.2013.05.013.
4. Potenza M.V., Mechanick J.I. The metabolic syndrome: definition, global impact, and pathophysiology. *Nutr. Clin. Pract.* 2009; 24 (5): 560–577. DOI: 10.1177/0884533609342436.
5. Fowler M.J. Microvascular and macrovascular complications of diabetes. *Clinical Diabetes*. 2008: 77–82. DOI: 10.2337/diaclin.26.2.77.
6. Rojtberg G.E. Metabolic syndrome. Moscow: MED-M54 press-inform, 2007: 224 (in Russ.).
7. Kravchuk E.N., Galagudza M.M. Experimental models of metabolic syndrome. *Arterial Hypertension*. 2014; 20 (5): 377–383 (in Russ.). DOI: 10.18705/1607-419X-2014-20-5-377-383.
8. Bayrasheva V.K., Pchelin I.Y., Egorova A.E., Vasilkova V.N., Kornyushin O.V. Experimental models of alimentary obesity in rats. *Juvenis Scientia*. 2019; 9–10: 8–13 (in Russ.). DOI: 10.32415/jscientia.2019.09-10.02.
9. Kwitek A.E. Rat models of metabolic syndrome. *Methods Mol. Biol.* 2019; 2018: 269–285. DOI: 10.1007/978-1-4939-9581-3_13.
10. Panchal S.K., Brown L. Rodent models for metabolic syndrome research. *J. Biomed. Biotechnol*. 2011; 2011: 351982. DOI: 10.1155/2011/351982.
11. Gancheva S., Zhelyazkova-Savova M., Galunska B., Chervenkov T. Experimental models of metabolic syndrome in rats. *Scripta Scientifica Medica.* 2015; 47 (2): 23–30. DOI: 10.14748/ssm.v47i2.1145.
12. Moreno-Fernández S., Garcés-Rimón M., Vera G., Astier J., Landrier J.F., Miguel M. High fat/high glucose diet induces metabolic syndrome in an experimental rat model. *Nutrients*. 2018; 10 (10): 1502. DOI: 10.3390/nu10101502.
13. Lim J.S., Mietus-Snyder M., Valente A., Schwarz J.M., Lustig R.H. The role of fructose in the pathogenesis of NAFLD and the metabolic syndrome. *Nat. Rev. Gastroenterol. Hepatol.* 2010; 7: 251–264. DOI: 10.1038/nrgastro.2010.41.
14. Panchal S.K., Poudyal H., Iyer A., Nazer R., Alam A., Diwan V., Kauter K., Sernia C., Campbell F., Ward L., Gobe G., Fenning A., Brown L. High-carbohydrate high-fat diet-induced metabolic syndrome and cardiovascular remodeling in rats. *J. Cardiovasc. Pharmacol.* 2011; 57 (5): 611–624. DOI: 10.1097/FJC.0b013e31821b1379.
15. Sadowska J., Bruszkowska M. Comparing the effects of sucrose and high-fructose corn syrup on lipid metabolism and the risk of cardiovascular disease in male rats. *Acta Sci. Pol. Technol. Aliment.* 2017; 16 (2): 231–240. DOI: 10.17306/J.AFS.0482.
16. Dupas J., Feray A. Goanvec C., Guernec A., Samson N., Bougaran P., Guerrero F., Mansourati J. Metabolic syndrome and hypertension resulting from fructose enriched diet in Wistar rats. *Biomed. Res. Int.* 2017; 2017: 2494067. DOI: 10.1155/2017/2494067.

17. Patarrao R.S., Lautt W.W., Macedo M.P. Assessment of methods and indexes of insulin sensitivity. *Rev. Port. Endocrinol. Diabetes Metab.* 2014; 9 (1): 65–73. DOI: 10.1016/j.rpedm.2013.10.004.
18. Folch J., Lees M., Sloane-Stanley G.H. A simple method for the isolation and purification of total lipides from animal tissues. *J. Biol. Chem.* 1957; 226 (1): 497–509.
19. Dobiásová M., Frohlich J. The plasma parameter log (TG/HDL-C) as an atherogenic index: correlation with lipoprotein particle size and esterification rate in apoB-lipoprotein-depleted plasma (FER (HDL)). *Clin. Biochem.* 2001; 34 (7): 583–588. DOI: 10.1016/s0009-9120(01)00263-6.
20. Nagai Y., Yonemitsu S., Erion D.M., Iwasaki T., Stark R., Weismann D., Dong J., Zhang D., Jurczak M.J., Löffler M.G., Cresswell J., Yu X.X., Murray S., Bhanot S., Monia B.P., Bogan J.S., Samuel V., Shulman G.I. The role of peroxisome proliferator-activated receptor gamma coactivator-1 beta in the pathogenesis of fructose-induced insulin resistance. *Cell Metab.* 2009; 9 (3): 252–264. DOI: 10.1016/j.cmet.2009.01.011.
21. Dos Santos Lacerda D., Garbin de Almeida M., Teixeira C., De Jesus A., Da Silva Pereira J.E., Martins Bock P., Pegas Henriques J.A., Gomez R., Dani C., Funchal C. Biochemical and physiological parameters in rats fed with high-fat diet: the protective effect of chronic treatment with purple grape juice (Bordo Variety). *Beverages*. 2018; 4 (4): 100. DOI: 10.3390/beverages4040100.
22. Tkachuk V.A., Vorotnikov A.V. Molecular mechanisms of insulin resistance development. *Diabetes Mellitus.* 2014; 2: 29–40 (in Russ.). DOI: 10.14341/DM2014229-40.
23. Schaefer E.J., Gleason J.A., Dansinger M.L. Dietary fructose and glucose differentially affect lipid and glucose homeostasis. *J. Nutr*. 2009; 139 (6): 1257–1262. DOI: 10.3945/jn.108.098186.
24. Alam M.A., Kauter K., Brown L. Naringin improves diet-induced cardiovascular dysfunction and obesity in high carbohydrate, high fat diet-fed rats. *Nutrients*. 2013; 5 (3): 637–650. DOI: 10.3390/nu5030637.
25. Fernández-Macías J.C., Ochoa-Martínez A.C., Varela-Silva J.A., Pérez-Maldonado I.N. Atherogenic index of plasma: novel predictive biomarker for cardiovascular illnesses. *Arch. Med. Res.* 2019; 50 (5): 285–294. DOI: 10.1016/j.arcmed.2019.08.009.
26. Basaranoglu M., Basaranoglu G., Sabuncu T., Sentürk H. Fructose as a key player in the development of fatty liver disease. *World J. Gastroenterol*. 2013; 19 (8): 1166–1172. DOI: 10.3748/wjg.v19.i8.1166.

Authors contribution

Birulina J.G., Ivanov V.V. – conception and design, drafting of the manuscript. Smagliy L.V., Vasilev V.N., Popov O.S. – interpretation and analysis of the data. Nosarev A.V., Petrova I.V., Gusakova S.V. – substantiation of the manuscript, approval of the manuscript for publication. Buyko E.E., Bykov V.V. – experimental part of the study.

Authors information

Birulina Julia G., Cand. Sci. (Biology), Assistant Professor, Department of Biophysics and Functional Diagnostics, Siberian State Medical University, Tomsk, Russian Federation. ORCID 0000-0003-1237-9786.

Ivanov Vladimir V., Cand. Sci. (Biology), Head of the Center for Preclinical Research of Central Research Laboratory, Siberian State Medical University, Tomsk, Russian Federation. ORCID 0000-0001-9348-4945.

Buyko Evgeniy E., Laboratory Assistant, Center for Preclinical Research of Central Research Laboratory, Siberian State Medical University, Research School of Chemistry & Applied Biomedical Sciences, National Research Tomsk Polytechnic University, Tomsk, Russian Federation. ORCID 0000-0002-6714-1938.

Bykov Vladimir V., Post-Graduate Student, Department of Biochemistry and Molecular Biology with a Course of Clinical Laboratory Diagnostics, Head of the Department of Pharmacological Research, Innovative Pharmacology Research, Tomsk, Russian Federation. ORCID 0000-0002-5145-2184.

Smagliy Lyudmila V., Cand. Sci. (Med.), Assistant Professor, Department of Biophysics and Functional Diagnostics, Siberian State Medical University, Tomsk, Russian Federation. ORCID 0000-0002-5263-027X.

Nosarev Alexey V., Dr. Sci. (Med.), Professor, Department of Biophysics and Functional Diagnostics, Siberian State Medical University, Tomsk, Russian Federation. ORCID 0000-0002-0119-9707.

Petrova Irina V., Dr. Sci. (Biology), Professor, Department of Biophysics and Functional Diagnostics, Siberian State Medical University, Tomsk, Russian Federation. ORCID 0000-0001-9034-4226.

Gusakova Svetlana V., Dr. Sci. (Med.), Head of the Department of Biophysics and Functional Diagnostics, Siberian State Medical University, Tomsk, Russian Federation. ORCID 0000-0001-5047-8668.

Popov Oleg S., Dr. Sci. (Med.), Professor, Department of General Surgery, SSMU, Tomsk, Russian Federation.

Vasilev Vladimir N., Dr. Sci. (Biology), Professor, Department of Physical Education and Health, SSMU, Tomsk, Russian Federation.

(✉) **Birulina Yulia G.,** e-mail: birulina20@yandex.ru.

Received 03.03.2020
Accepted 29.09.2020

УДК 616.61-089.819.843-097.1
https://doi.org/10.20538/1682-0363-2020-4-14-20

Donor – recipient selection using epitope mismatches in kidney transplantation

Vatazin A.V., Zulkarnaev A.B., Stepanov V.A.

Moscow Regional Research and Clinical Institute
Build. 6, 61/2, Schepkina Str., 129110, Moscow, Russian Federation

ABSTRACT

Aim. To evaluate the potential option of selecting donor – recipient pairs by using the number of epitope mismatches.

Materials and methods. An observational cohort study was carried out, which included 824 adult recipients of ABO compatible deceased donor kidneys. The end point was a transplant loss. If a recipient with a functioning graft died, the observation was censored. The number of epitope mismatches (EpMM) was calculated using open source information on the population frequency of haplotypes and the repertoire of epitopes with confirmed immunogenicity. All possible combinations of the donor and recipient genotypes were compiled, and the probability of each combination was calculated. After that, the number of donor epitopes absent in the recipient was calculated for each combination with a non-zero probability, whereupon the weighted mean EpMM was calculated, where the weight coefficient was the normalized probability of occurrence of each combination.

Results. All of the donor – recipient pairs had HLA-mismatches (HLA MM): 1.9% of recipients had 1 HLA MM, 6.7% had 2 HLA MM, 29.9% had 3 HLA MM, 38.5% had 4 HLA MM, 18.1% had 5 HLA MM, and 4.9% had 6 HLA MM. The HLA MM impacted graft survival was determined: log-rank test $p < 0.0001$, Breslow test $p < 0.0001$. The median values and the interquartile ranges of EpMM were 6 [4; 7], 12 [7.74; 17.25], 18 [14; 22], 24 [20; 30], 30.5 [25; 37] and 36 [26.5; 44.5] for the cases of 1, 2, 3, 4, 5 and 6 HLA MMs, respectively. An increase in HLA MM resulted in a higher risk of developing donor-specific anti-HLA antibodies (DSA). Hazard ratio (HR) = 1.21 [95% confidence interval (CI): 0.7; 1.9], 1.71 [95% CI: 1.22; 2.36], 2.04 [95% CI: 1.42; 2.73], 2.25 [95% CI: 1.63; 2.96], 2.59 [95% CI: 2.03; 3.29] for 2, 3, 4, 5, and 6 HLA MM, respectively, versus HLA MM = 1. An increase in EpMM also resulted in a higher risk of developing DSA. HR = 1.66 [95% CI: 1.09; 2.47], 2.1 [95% CI: 1.46; 2.91], 2.41 [95% CI: 1.86; 3.03], 2.61 [95% CI: 2.12; 3.12], 2.77 [95% CI: 2.26; 3.33] for 10–19, 20–29, 30–39, 40–49 and >50 EpMM, respectively, versus EpMM < 10. An increase in HLA MM was associated with an increased risk of transplant loss. HR = 1.24 [95% CI 0.7; 2.15], 1.48 [95% CI 0.86; 2.33], 1.88 [95% CI 1.32; 2.52], 2.41 [95% CI 2; 2.93], 2, 98 [95% CI 2.59; 3.46] at 2, 3, 4, 5, and 6 HLA MM, respectively, versus HLA MM = 1. An increase in EpMM also was associated with an increased risk of transplant loss. HR = 1.71 [95% CI 1.1; 2.49], 2.11 [95% CI 1.59; 2.68], 2.4 [95% CI 1.96; 2.86], 2.59 [95% CI 2.17; 3.04], 2.71 [95% CI 2.31; 3.15] at 10–19, 20–29, 30–39, 40–49 and >50 EpMM, respectively, versus EpMM < 10. In order to demonstrate the effectiveness of EpMM accounting, we analyzed graft survival among the patients with 4 HLA MM. With the number of EpMM in the range from 10 to 24 and from 25 to 43 the difference in survival rates was statistically significant, but only at the late stages of the post-transplant period: log-rank test $p = 0.0067$, Breslow test $p = 0.0982$. The median survival for EpMM 10–24 was 10.33 [95% CI 9.05; 11.61] years, for EpMM 22–43 – 8.67 [95% CI 7.68; 9.66] years, HR 1.537 [95% CI 1.114; 2.12]. At the same time, it was not the median of survival that increased, but the proportion of patients with a functioning graft: at 10–24 EpMM after 15 years, 18.28% [95% CI 8.2; 31.67] grafts functioned, while at 25–43 EpMM only 4.75% [95% CI 0.94; 13.64] functioned.

Conclusion. In the routine practice of a transplantation center with a short waiting list of its own, it might be possible to improve the kidney transplant survival as a result of considering epitope mismatches, thus reducing the risk of developing donor-specific anti-HLA antibodies and ensuring a higher graft survival rate. This method can be used for additional ranking of transplantation candidates depending on the number of epitope mismatches within the fixed number of HLA-mismatches and thus select the optimal one. Besides, it is theoretically possible to use this method as an alternative to the traditional donor/recipient histocompatibility evaluation. Additional research is required.

✉ *Zulkarnaev Alexey B.,* e-mail: 7059899@gmail.com.

Key words: kidney transplantation, HLA, epitope, eplet, tissue compatibility, recipient selection, donor-specific antibodies, anti-HLA antibodies.

Conflict of interest. The authors declare the absence of obvious or potential conflict of interest related to the publication of this article.

Source of financing. The study was supported by the grant of the President of the Russian Federation for the state support of young Russian scientists (No. MD-2253.2018.7) were used for this study. This source of funding was not involved in determining the structure of the study, data collection, analysis and interpretation, as well as the decision to publish the results.

Conformity with the principles of ethics. The study was approved by the local Ethics Committee at Moscow Regional Research and Clinical Institute (Protocol No. 9 of 12.10.2017).

For citation: Vatazin A.V., Zulkarnaev A.B., Stepanov V.A. Donor – recipient selection using epitope mismatches in kidney transplantation. *Bulletin of Siberian Medicine.* 2020; 19 (4): 21–29. https://doi.org/10.20538/1682-0363-2020-4-21-29.

Селекция пары «донор – реципиент» с учетом эпитопных несоответствий при трансплантации почки

Ватазин А.В., Зулькарнаев А.Б., Степанов В.А.

Московский областной научно-исследовательский клинический институт им. М.Ф. Владимирского (МОНИКИ им. М.Ф. Владимирского)
Россия, 129110, Москва, ул. Щепкина, 61/2, к. 6

РЕЗЮМЕ

Цель. Оценить потенциал селекции пары «донор – реципиент» с учетом количества эпитопных несовпадений.

Материалы и методы. Проведено обсервационное ретроспективное когортное исследование, в которое включено 824 совершеннолетних реципиента трупной почки, совместимых по группе крови. Конечной точкой считали утрату трансплантата. В случае смерти реципиента с функционирующим трансплантатом наблюдение подвергали цензурированию. Подсчет количества эпитопных несовпадений (EpMM) проводили с использованием информации из общедоступных ресурсов о популяционной частоте гаплотипов и репертуаре эпитопов с подтвержденной иммуногенностью. Составлялись все возможные сочетания генотипов донора и реципиента, подчитывали вероятность каждого сочетания. Затем для каждого сочетания с ненулевой вероятностью определяли количество эпитопов донора, отсутствующих у реципиента. После этого вычисляли взвешенное среднее EpMM, где весовым коэффициентом была нормированная вероятность появления каждого сочетания.

Результаты. Все пары «донор – реципиент» имели HLA несовместимости (HLA MM): 1,9% – 1 HLA MM, 6,7% – 2 HLA MM, 29,9% – 3 HLA MM, 38,5% – 4 HLA MM, 18,1% – 5 HLA MM, 4,9% – 6 HLA MM. Различия в HLA MM влияли на выживаемость трансплантатов: log-rank test $p < 0{,}0001$, Breslow test $p < 0{,}0001$. Медиана (*Me*) и интерквартильный размах [Q_1; Q_3] EpMM составили 6 [4; 7], 12 [7,74; 17,25], 18 [14; 22], 24 [20; 30], 30,5 [25; 37] и 36 [26,5; 44,5] для 1, 2, 3, 4, 5 и 6 HLA MM соответственно. Увеличение HLA MM было связано с ростом риска появления донор-специфических анти-HLA антител (ДСА). Отношение рисков (HR) = 1,21 [95%-й доверительный интервал (95%-й ДИ) 0,7; 1,9], 1,71 [95%-й ДИ 1,22; 2,36], 2,04 [95%-й ДИ 1,42; 2,73], 2,25 [95%-й ДИ 1,63; 2,96], 2,59 [95%-й ДИ 2,03; 3,29] при 2, 3, 4, 5 и 6 HLA MM соответственно по отношению к HLA MM = 1. Увеличение EpMM также было связано с ростом риска появления ДСА. HR = 1,66 [95%-й ДИ 1,09; 2,47], 2,1 [95%-й ДИ 1,46; 2,91], 2,41 [95%-й ДИ 1,86; 3,03], 2,61 [95%-й ДИ 2,12; 3,12], 2,77 [95%-й ДИ 2,26; 3,33] при 10–19, 20–29, 30–39, 40–49 и >50 EpMM соответственно по отношению к EpMM < 10. Увеличение HLA MM было связано с ростом риска утраты трансплантата. HR = 1,24 [95%-й ДИ 0,7; 2,15], 1,48 [95%-й ДИ 0,86; 2,33], 1,88 [95%-й ДИ 1,32; 2,52], 2,41 [95%-й ДИ 2; 2,93], 2,98 [95%-й ДИ 2,59; 3,46] при 2, 3, 4, 5 и 6 HLA MM соответственно по отношению к HLA MM = 1. Для демонстрации эффективности учета EpMM мы проанализировали выживаемость трансплантатов у пациентов с HLA MM = 4. Выживаемость при 10–24 и 25–43 EpMM различалась статистически значимо, но только на поздних этапах посттрансплантационного периода: log-rank test $p = 0{,}0067$, Breslow test $p = 0{,}0982$. Медиана выживаемости для EpMM 10–24 составила 10,33 [95%-й ДИ 9,05; 11,61] лет, для EpMM 22–43 – 8,67 [95%-й ДИ 7,68; 9,66] лет, HR = 1,537 [95%-й

ДИ 1,114; 2,12]. При этом главным образом увеличивалась не медиана выживаемости, а доля больных с функционирующим трансплантатом: при 10–24 EpMM через 15 лет 18,28% [95%-й ДИ 8,2; 31,67] трансплантатов функционировало, тогда как при 25–43 EpMM – только 4,75% [95%-й ДИ 0,94; 13,64].

Заключение. В рутинной практике трансплантационного центра с небольшим, обособленным листом ожидания учет эпитопных несоответствий может улучшить результаты трансплантации почки: снизить риск появления донор-специфичных анти-HLA антител и повысить выживаемость трансплантатов. Применение этого метода позволяет дополнительно ранжировать кандидатов на трансплантацию в зависимости от количества эпитопных несовпадений в рамках фиксированного количества HLA несовпадений и выбрать оптимального. Вместе с тем существует теоретическая возможность использования этого метода в качестве альтернативы традиционной оценке тканевой совместимости донора и реципиента. Необходимы дополнительные исследования.

Ключевые слова: трансплантация почки, HLA, эпитоп, эплет, тканевая совместимость, выбор реципиента, донор-специфичные антитела, анти-HLA антитела.

Конфликт интересов. Авторы декларируют отсутствие явных и потенциальных конфликтов интересов, связанных с публикацией настоящей статьи.

Источник финансирования. Работы были выполнены с использованием средств гранта Президента Российской Федерации для государственной поддержки молодых российских ученых (№ МД-2253.2018.7). Данный источник финансирования не участвовал в определении структуры исследования, сборе, анализе и интерпретации данных, а также принятии решения опубликовать полученные результаты.

Соответствие принципам этики. Исследование одобрено локальным этическим комитетом МОНИКИ им. М.Ф. Владимирского (протокол № 9 от 12.10.2017).

Для цитирования: Ватазин А.В., Зулькарнаев А.Б., Степанов В.А. Селекция пары «донор – реципиент» с учетом эпитопных несоответствий при трансплантации почки. *Бюллетень сибирской медицины.* 2020; 19 (4): 21–29. https://doi.org/10.20538/1682-0363-2020-4-21-29.

INTRODUCTION

Over the history of clinical transplantology, the histocompatibility between the donor and the recipient has always been one of the key factors on which kidney allograft survival depended. As is known that the smaller the number of HLA-mismatches (HLA-MM), the better the survival rate of the graft. This has been proven both in the case of deceased donor kidney transplantation [1] and in the case of living donor kidney transplantation [2].

Despite the fact that the effect of this factor gradually decreases over the years, it still remains important in the current era of immunosuppression therapy.

Each HLA-antigen comprises a unique repertoire of epitopes. At that, some of them are totally unique and peculiar only to the specific allelic variant of a molecule (private epitopes), and some can be common for several HLA-molecules (public epitopes) [3].

Existence of public epitopes determines the possibility of selecting the donor/recipient pair based on this information.

The aim of the study was to evaluate the potential option of selecting donor/recipient pairs using the number of epitope mismatches.

MATERIALS AND METHODS

Study design and patients. An observational retrospective cohort study was conducted which included 824 adult recipients. All of the patients underwent transplantation of a deceased donor kidney compatible by ABO blood group. The end point was a transplant loss. If a recipient with a functioning graft died, the observation was censored.

In all cases, HLA-typing was performed (HLA A, B and DR loci). Before 2003, the serological HLA-typing was used (the split antigen level), while later, low resolution HLA-genotyping by means of SSO or SSP methods (allelic group level) was utilized. The crossmatch test (complement dependent lymphocytotoxic test) was negative in all cases. The anti-HLA antibody screenings were performed using multiplex technology on Luminex platform with LIFECODES Lifescreen Deluxe (Immucor) reagents, while identification of antibodies were done with the sets of LIFECODES LSA.

Patient data are presented in Table 1.

Table 1

Patient data	
Parameter	Value
Recipient sex M/F, %	58/42
Age of recipients, years, *Me* [Q_1; Q_3]	43 (27; 50)
Time on dialysis before transplantation, months, *Me* [Q_1; Q_3]	34 (14; 42)
Repeated transplantation, %	9
Preexisting antibodies (PRA* ≥ 10%)	12.8
Age of donors, years, *Me* [Q_1; Q_3]	38.1 (31.2; 51.8)
Brain death donor/asystolic donor, %	46/54
Preservation time, h, *Me* [Q_1; Q_3]	8.4 (6; 14)
Follow up observation period, years, *Me* [Q_1; Q_3]	8.1 (4.8; 10.4)

* panel-reactive antibody

RESULTS

The recipients demonstrated different levels of compatibility with the donor kidney (Fig. 1).

At that, HLA-incompatibility remains an important parameter that determines long term graft survival (Fig. 2).

Generally, differences in HLA-A locus compatibility significantly affected graft survival: log-rank test $p = 0.0005$, Breslow test $p = 0.0049$. The median survival for the 0, 1 and 2 HLA-A MM were 9.5 [95% CI 8.77; 10.23], 8.42 [95% CI 8; 8.87] and 8.33 [95% CI: 7.71; 8.96] years, respectively. Pair-wise comparisons: 0–1 HLA-A MM – log-rank $p = 0.0092$, Breslow $p = 0.0107$, HR 1.32 [95% CI 1.079; 1.615]; 1–2 HLA-A MM – log-rank $p = 0.2157$, Breslow $p = 0.3156$, HR 1.114 [95% CI 0.936; 1.326]; 0–2 HLA-A MM log-rank $p = 0.0003$, Breslow $p = 0.0012$, HR 1.485 [95% CI 1.204; 1.831].

Differences in HLA-B locus compatibility significantly affected graft survival: log-rank test $p = 0.0034$, Breslow test $p = 0.0008$. The median survival for the 0, 1 and 2 HLA-B MM were 9.99 [95% CI 8.38; 11.6], 8.67 [95% CI 8.1; 9.26] and 8.25 [95% CI 7.81; 8.69] years, respectively. Pair-wise comparisons: 0–1 HLA-B MM – log-rank $p = 0.0656$, Breslow $p = 0.0632$, HR 1.353 [95% CI 0.997; 1.836]; 1–2 HLA-B MM – log-rank $p = 0.0424$, Breslow $p = 0.1363$, HR 1.19 [95% CI 1.009; 1.404]; 0–2 HLA-B MM log-rank $p = 0.0031$, Breslow $p = 0.0076$, HR 1.582 [95% CI 1.213; 2.062].

Differences in HLA-DRB1 locus compatibility significantly affected graft survival: log-rank test $p < 0.0001$, Breslow test $p < 0.0001$. The median survival for the 0, 1 and 2 HLA-DR1 MM were 10.08 [95% CI 9.15; 11.02], 9 [95% CI 8.47; 9.53] and 8.25 [95% CI 7.58; 8.92] years, respectively. Pair-wise comparison: 0–1 HLA-DR1 MM – log-rank $p = 0.0021$, Breslow $p = 0.0152$, HR 1.472 [95% CI 1.166; 1.858]; 1–2 HLA-DR1 MM – log-rank $p = 0.0038$, Breslow $p = 0.0146$, HR 1.283 [95% CI 1.084; 1.52]; 0–2 HLA-DR1 MM log-rank $p < 0.0001$, Breslow $p < 0.0001$, HR 1.888 [95% CI 1.532; 2.237].

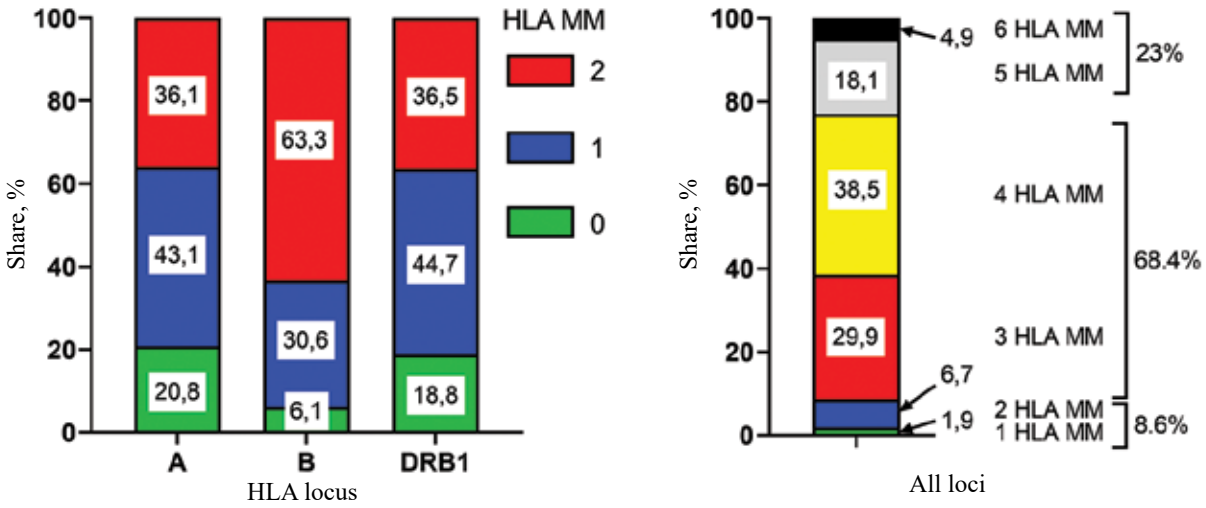

Fig. 1. HLA incompatibility distribution: HLA MM – the number of donor antigens absent in the recipient

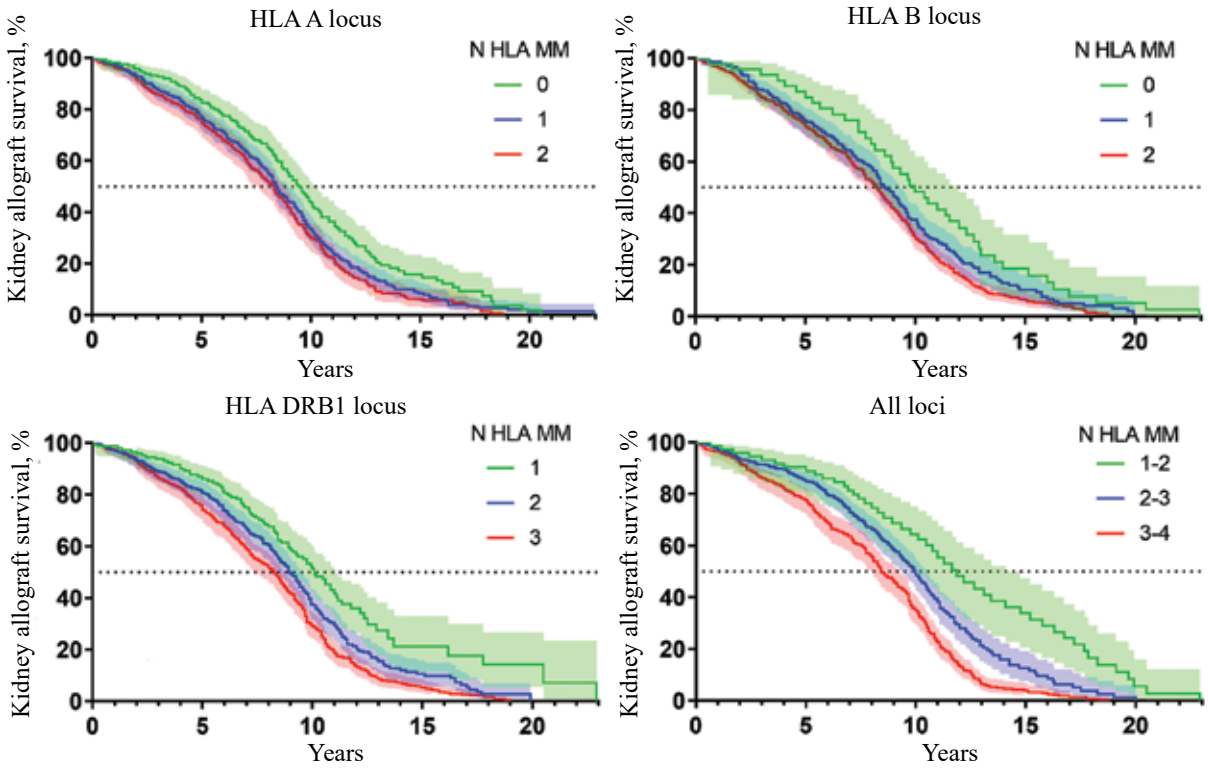

Fig. 2. Death-censored graft survival. The graphs depict the results of assessment of differences according to the log-rank criterion for three curves

Altogether, the differences in compatibility across all loci significantly affected graft survival: log-rank test $p < 0.0001$, Breslow test $p < 0.0001$. The median survival for 1-2 HLA MM, 3-4 HLA-MM and 5-6 HLA-MM were 11.85 [95% CI 9.93; 13.78], 10 [95% CI 9.4; 10.6] and 8.42 [95% CI 7.82; 9.02] years, respectively. Pair-wise comparisons: 1-2 HLA MM and 3-4 HLA MM – log-rank $p = 0.001$, Breslow $p = 0.041$, HR 1.617 [95% CI 1.233; 2.121]; 3-4 HLA MM and 5-6 HLA MM – log-rank $p < 0.0001$, Breslow $p < 0.0001$, HR 1.531 [95% CI 1.286; 1.824]; 1-2 HLA MM and 5-6 HLA MM log-rank $p < 0.0001$, Breslow $p < 0.0001$, HR 2.365 [95% CI 1.863; 3.002].

We calculated the average number of epitope mismatches for each HLA-MM quantity (Fig. 3).

An increase in numbers of HLA-mismatches and epitope mismatches significantly heightens the risk of anti-donor anti-HLA antibodies development and of graft loss (Fig. 4).

In order to demonstrate that it is possible to apply the method of donor/recipient pair selection based on epitope mismatches in practice, we analyzed graft survival in case of 4 HLA-mismatches (the most common variant at our center) (Fig. 5). The patients were divided into two groups: the ones with EpMM less or equaling the median (the average number) and the ones with higher values.

The difference in graft survival rates for the 10-24 EpMM and 25-43 EpMM was statistically significant, but only at late stages of the post-transplant period: log-rank test $p = 0.0067$, Breslow test $p = 0.0982$. The median survival for the 10-24 EpMM was 10.33 [95% CI 9.05; 11.61] years, for the 25-43 EpMM – 8.67 [95% CI 7.68; 9.66] years, HR 1.537 [95% CI 1.114; 2.12].

DISCUSSION

At present (data date: August 2019), the modern HLA nomenclature includes 28 serologically identifiable antigens of HLA A locus, 62 antigens of HLA B locus, 24 antigens of HLA DRB1 locus [7]. Considering the enormous amount of potential combinations, it becomes evident that in order to select the optimal recipient, the waiting list must be comprised of thousands of transplant candidates. Unified waiting lists of this kind exist in Europe (Eurotransplant) and in the USA (United Network for Organ Sharing).

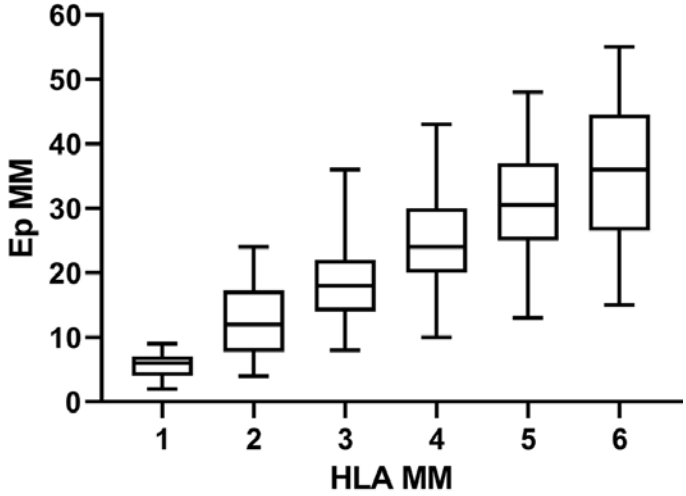

Fig. 3. Concordance between HLA MM and the estimated number of EpMM: тhe graph shows the median, interquartile range, minimum and maximum values, HLA MM – the number of donor antigens absent in the recipient, EpMM – the number of donor epitopes absent in the recipient.

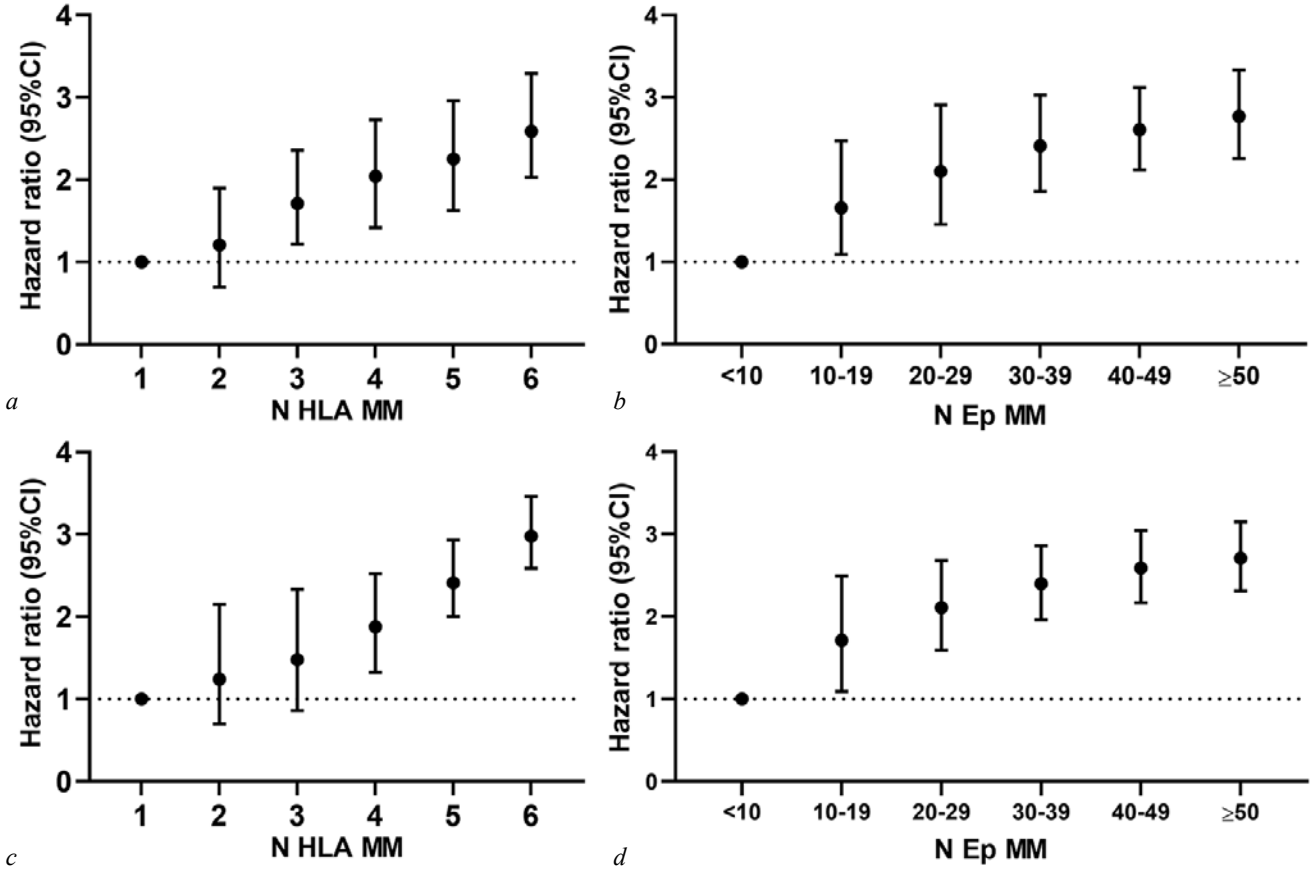

Fig. 4. The relationship between the risk of *de novo* donor-specific antibody development and HLA MM (*a*), EpMM (*b*), тhe relationship between the risk of graft loss and HLA MM (*c*), EpMM (*d*)

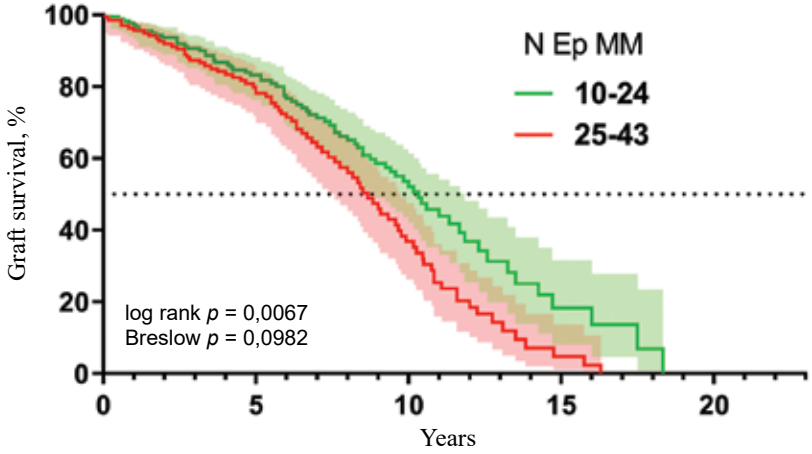

Figure 5. Death-censored graft survival in patients with 4 HLA mismatches: EpMM – the number of donor epitopes absent in the recipient, тhe median of EpMM in patients with HLA MM = 4 was 24

In Russia, each transplantation center keeps a waiting list of its own, which substantially hinders selection of the optimal recipient in terms of histocompatibility. Most of the recipients (68.4% according to the data of our center) receive a graft carrying 3 to 4 mismatched antigens, as waiting for a better match would mean substantially longer waiting times. As we have shown before [8], extended waiting for transplantation while on dialysis worsens the comorbid background, which, in turn, reduces transplantation probability and leads to a higher risk of death.

At the same time, the question of relative significance of such factors as the comorbid background and histocompatibility at various stages of waiting remains unresolved. At that, the importance of histocompatibility remains high. As we have demonstrated, the lower the number of HLA-mismatches, the better the graft survival rate, and this dependence is statistically significant.

However, it is remarkable that even with the total number of mismatches in terms of three loci considered, the median survival increases, though moderately (11.85 [95%CI 9.93; 13.78] years in case of 1–2 mismatches and 8.42 [95%CI 7.82; 9.02] years in case of 5–6 mismatches). Clinical interpretations of this fact can differ. On the one hand, it may be regarded as a confirmation of immunosuppression effectiveness, thus, histocompatibility becomes less significant. On the other hand, it indicates its insufficient effectiveness at the late stages of the post-transplantation period. Good histocompatibility generally leads to a substantial increase in the number of patients with a functioning graft in the late period rather than to the extension of the mean time of the graft functioning (median survival). Thus, in 15 years 33.8% [95% CI 20.6; 47.41] of patients with 1 or 2 HLA MM had their graft still functioning. In cases of 3 or 4 mismatches the graft remained functioning with 12.8% [95% CI 7.76; 19.2] of patients, and in cases of 5 or 6 mismatches with 3.6% [95% CI 1.84; 6.21] of patients only.

Most recipients get grafts with 4 HLA-mismatches (with consideration to HLA-A, HLA-B and HLA-DRB1 loci only). At that, each of them is deemed a totally equal candidate for the transplant in terms of histocompatibility. We believe it would be a promising possibility to be able to additionally rank candidates within the fixed HLA value taking into account EpMM. The expediency of application of such an approach to selecting the donor/recipient pair remains one of the main questions.

A major cause of graft loss at later periods is antibody-mediated rejection, which accounts for approximately 50% of cases [9]. At that, it is already known that an increase in HLA-mismatches leads to a higher risk of occurrence of *de novo* DSA [10]. We have convincing evidence to support this fact (Fig. 4*a*). An increase in HLA MM and an increase in EpMM both significantly heightened the risk of *de novo* DSA occurrence. At that, the rate of risk increase was somewhat different: the risk increase in line with the increase of HLA MMs is linear (r^2 = 0.9873). At the same time, the relation between the risk and EpMM is described quite well by the logarithmic approximation (r^2 = 0.9991). In

other words, an increase in the number of HLA MMs proportionally increases the "antigen load" and the risk of antibodies occurrence, while to EpMM this risk seems to relate in a more complex manner. We did not notice a significant increase in risk with two HLA MM compared with one HLA MM. In view of that, pursuance of accounting epitope mismatches within the fixed amount of HLA MMs (in addition to the traditional approach to selecting the donor/recipient pair) seems to be promising when it comes to the reduction of the "antigen load". When the number of EpMM increases from > 10 to the range of 10 to 19, the risk of DSAs gets substantially higher. It is an important aspect in the context of this research, for, as is shown in Figure 3, the EpMM quantity of 10 to 19 can correspond both to 2 and to 6 HLA MMs. This, in its turn, defines whether it is potentially possible to select donor/recipient pairs using epitope mismatches not in addition, but as an alternative to the traditional approach. In order to evaluate the validity of this hypothesis, additional research is required.

Four and more HLA MMs entailed a substantial risk of losing the graft function. Considering this fact, one is to admit that most of our recipients initially have an unfavorable "immunological profile" due to poor histocompatibility of donors and recipients. Considering the current state of affairs in transplantology assistance, one can presume that this will be applicable to the vast majority of transplantology centers in Russia.

The form of relation between the risk of graft loss and HLA-MMs can be well described using the exponential approximation (r^2 = 0.9978). At that, if the number of EpMM exceeds 10, it substantially increases the risk of the graft loss; this relation is also well described by means of logarithmic approximation (r^2 = 0.9976). At the same time, the benefits of its use in selection of donor/recipient pairs become evident only after a long-term follow-up: we have noticed substantial differences over a long-term period only. Even though it leads only to a moderate increase in the median survival (from 8.67 to 10.33 years Fig. 5), it makes it possible to increase substantially the share of recipients who have the graft still functioning in the long-term period: with 10 to 24 EpMM 18.28% [95 CI 8.2%; 31.67] of grafts were still functioning 15 years later, while only 4.75% with 25 to 43 EpMM [95 CI 0.94; 13.64].

Research limitations. Firstly, the study was retrospective. Secondly, the study was based on a large amount of clinical material collected over a long period of time (around 30 years). In our analysis we did not consider factors such as immunosuppressive therapy. At the same time, it is evident that the immunosuppression approaches have substantially evolved over this period of time [1, 2]. Thirdly, knowledge of antigenicity and immunogenicity consistently grows; we used the base [10] that was up-to-date in August 2019. It is entirely possible that the results might differ if we repeat our calculations using a more recent and updated base.

CONCLUSION

Summarizing all of the above, we come to a conclusion that in a routine practice of a transplantation center with a short individual waiting list, consideration of epitope mismatches will make it possible to improve kidney transplantation results, reducing the risk of developing donor specific anti-HLA antibodies and increasing graft survival. Using this method, it will be possible to perform additional ranking of transplant candidates, depending on the number of epitope mismatches within the fixed number of HLA-mismatches, and thus select the optimal one. Besides, theoretically it might be possible to use this method as an alternative to the traditional evaluation of histocompatibility between the donor and the recipient. Additional research is required.

REFERENCES

1. Shi X., Lv J., Han W., Zhong X., Xie X., Su B., Ding J. What is the impact of human leukocyte antigen mismatching on graft survival and mortality in renal transplantation? A meta-analysis of 23 cohort studies involving 486,608 recipients. *BMC Nephrol*. 2018; 19 (1): 116. DOI: 10.1186/s12882-018-0908-3.
2. Williams R.C., Opelz G., Weil E.J., McGarvey C.J., Chakkera H.A. The risk of transplant failure with HLA mismatch in first adult kidney Allografts 2: living donors, summary, guide. *Transplant Direct*. 2017; 3 (5): e152. DOI: 10.1097/TXD.0000000000000664.
3. Rodey G.E., Fuller T.C. Public epitopes and the antigenic structure of the HLA molecules. *Crit. Rev. Immunol*. 1987; 7 (3): 229–267.
4. The National Marrow Donor Program Database. URL: https://bioinformatics.bethematchclinical.org/
5. The Allele Frequency Net Database. URL: http://www.allelefrequencies.net
6. HLA Epitope Registry Database. URL: https://www.epregistry.com.br/
7. HLA nomenclature website. URL: http://hla.alleles.org/nomenclature/index.html

8. Vatazin A.V., Zulkarnaev A.B., Stepanov V.A. Survival analysis of patients on the waiting list for kidney transplantation in terms of competing risks. *Russian Journal of Transplantology and Artificial Organs*. 2019; 21 (1): 35–45 (in Russ.). DOI: 10.15825/1995-1191-2019-1-35-45.
9. Gaston R.S., Cecka J.M., Kasiske B.L. Evidence for antibody-mediated injury as a major determinant of late kidney allograft failure. *Transplantation*. 2010; 90 (1): 68–74. DOI: 10.1097/TP.0b013e3181e065de.
10. Campos A., Malheiro J., Tafulo S., Santos S., Dias L., Martins S., Almeida M., Pedroso S., Henriques A.C., Cabrita A. Increase of allosensitization after a kidney graft failure: Predictors and effect on retransplantation outcomes. *Nefrologia*. 2017; 37 (4): 397–405. DOI: 10.1016/j.nefro.2016.11.020.

Authors information

Vatazin Andrey V., Dr. Sci. (Med.), Professor, Principal Researcher, Surgical Department of Kidney Transplantation, Moscow Regional Research and Clinical Institute, Moscow, Russian Federation. ORCID 0000-0001-8497-0693.

Zulkarnaev Alexey B., Dr. Sci. (Med.), Leading Researcher, Associate Professor, Surgical Department of Kidney Transplantation, Moscow Regional Research and Clinical Institute, Moscow, Russian Federation. ORCID 0000-0001-5405-7887.

Stepanov Vadim A., Cand. Sci. (Med.), Senior Researcher, Surgical Department of Kidney Transplantation, Moscow Regional Research and Clinical Institute, Moscow, Russian Federation ORCID 0000-0002-0881-0599.

(✉) **Zulkarnaev Alexey B.,** e-mail: 7059899@gmail.com.

Received 04.09.2019
Accepted 25.12.2019

УДК 577.21:618.19-006.6]-036
https://doi.org/10.20538/1682-0363-2020-4-30-37

Studying GATA3, FOXA1, and ELF5 transcription factors in the evaluation of prognosis in luminal breast cancer patients

Vtorushin S.V.[1, 2], Vasilchenko D.V.[1, 2], Zavyalova M.V.[1, 2], Krakhmal' N.V.[1, 2], Patalyak S.V.[2]

[1] *Siberian State Medical University*
2, Moscow Trakt, Tomsk, 634050, Russian Federation

[2] *Cancer Research Institute, Tomsk National Research Medical Center of the Russian Academy of Sciences*
5, Kooperativny Str., Tomsk, 634050, Russian Federation

ABSTRACT

Background. The identification of predictive molecular markers of luminal breast cancer will help to assess the risk of developing distant metastases and determine a personalized approach to predicting the outcome of the disease during hormone therapy.

The aim of the study was to investigate the relationship between the transcription factors GATA3, FOXA1, and ELF5 in the tumor and the occurrence of distant metastases in patients with luminal subtype of breast cancer during adjuvant hormone therapy.

Materials and methods. The study included 101 patients with breast cancer (aged from 30 years to 81 years, average age (54.8 ± 10.3) years), with stages $T_{1–4}N_{1–3}M_0$ of the disease. The follow-up period was at least 5 years. The inclusion criteria for the study were luminal molecular genetic subtype of the tumor and lack of preoperative treatment. The exclusion criterion was stage IV disease. The study of transcription factors was carried out by the immunohistochemical method using polyclonal antibodies to GATA3, FOXA1, and ELF5, manufactured by Flarebio (Austria).

Results. Low expression of FOXA1 and ELF5 in the tumor was associated with the development of distant metastases (p = 0.000015 and p = 0.000002, respectively). In addition, it was found that high incidence of hematogenous metastases was associated with heterogeneous expression of FOXA1 ($\chi 2$ = 6.42; p = 0.01) and ELF5 ($\chi 2$ = 14.46; p = 0.0001) in the tumor. No similar differences were found in the study of GATA3 expression.

Conclusion. The level of expression of transcription factors FOXA1 and ELF5 and their distribution in the primary tumor can be considered as potential molecular markers in assessing the risk of hematogenous metastasis in patients with luminal breast cancer.

Key words: luminal breast cancer, transcription factors GATA3, FOXA1, ELF5, prognosis, distant metastases.

Conflict of interest. The authors declare the absence of obvious or potential conflicts of interest related to the publication of this article.

Source of financing. This work was supported by the Presidential Grant NSh-2701.2020.7 "Development of new approaches to predicting the course of breast and lung carcinomas taking into account the morphological and molecular genetic heterogeneity of the tumor".

Conformity with the principles of ethics. All patients signed informed consent to participate in the study. The work was carried out in accordance with the principles of voluntariness and confidentiality in accordance with the "Fundamentals of the legislation of the Russian Federation on the protection of public health" (Decree of the President of the Russian Federation of December 24, 1993 No. 2288) on the basis of the permission of the local committee on biomedical ethics of the Research Institute of Oncology of the Tomsk Scientific Research Center (Protocol No. 4994 of 27.10.2016).

For citation: Vtorushin S.V., Vasilchenko D.V., Zavyalova M.V., Krakhmal' N.V., Patalyak S.V. Studying GATA3, FOXA1, and ELF5 transcription factors in the evaluation of prognosis in luminal breast cancer patients. *Bulletin of Siberian Medicine.* 2020; 19 (4): 30–37. https://doi.org/10.20538/1682-0363-2020-4-30-37.

✉ *Vtorushin Sergey V.,* e-mail: wtorushin@rambler.ru.

Исследование факторов транскрипции GATA3, FOXA1, ELF5 в оценке прогноза у больных люминальным раком молочной железы

Вторушин С.В.[1, 2], Васильченко Д.В.[1, 2], Завьялова М.В.[1, 2], Крахмаль Н.В.[1], Паталяк С.В.[2]

[1] Сибирский государственный медицинский университет (СибГМУ)
Россия, 634050, г. Томск, Московский тракт, 2

[2] Научно-исследовательский институт (НИИ) онкологии,
Томский национальный исследовательский медицинский центр (НИМЦ) Российской академии наук
Россия, 634050, г. Томск, пер. Кооперативный, 5

РЕЗЮМЕ

Актуальность. Выявление предсказательных молекулярных маркеров люминального рака молочной железы (РМЖ) позволит оценить риск развития отдаленных метастазов и определить персонализированный подход к прогнозированию течения заболевания при проведении гормонотерапии.

Цель. Изучить взаимосвязь транскрипционных факторов GATA3, FOXA1, ELF5 в опухоли с возникновением отдаленных метастазов у больных люминальным подтипом РМЖ при проведении адъювантной гормонотерапии.

Материалы и методы. В исследование включена 101 больная РМЖ (возраст от 30 лет до 81 года, средний возраст (54,8 ± 10,3) года), стадии $T_{1–4}N_{1–3}M_0$. Срок наблюдения составил не менее 5 лет. Критериями включения в исследование явились: люминальный молекулярно-генетический подтип опухоли, отсутствие предоперационного лечения. Критерий исключения – IV стадия заболевания. Исследование транскрипционных факторов проводилось иммуногистохимическим методом с использованием поликлональных антител фирмы Flarebio (Австрия) к GATA3, FOXA1 и ELF5.

Результаты. Выявлено значимое снижение процента экспрессии FOXA1 и ELF5 в опухоли при развитии отдаленных метастазов (p = 0,000015 и p = 0,000002 соответственно). Кроме того, показано, что большая частота развития гематогенных метастазов сопряжена с гетерогенной экспрессией в опухоли FOXA1 (χ^2 = 6,42; p = 0,01) и ELF5 (χ^2 = 14,46; p = 0,0001). Подобных отличий в отношении экспрессии GATA3 не обнаружено.

Заключение. Уровень и характер экспрессии транскрипционных факторов FOXA1 и ELF5 в первичной опухоли могут рассматриваться в качестве потенциальных молекулярных маркеров в оценке риска гематогенного метастазирования у больных люминальным подтипом карциномы молочной железы.

Ключевые слова: люминальный рак молочной железы, факторы транскрипции GATA3, FOXA1, ELF5, прогноз, отдаленные метастазы.

Конфликт интересов. Авторы декларируют отсутствие явных и потенциальных конфликтов интересов, связанных с публикацией настоящей статьи.

Источник финансирования. Работа выполнена при финансовой поддержке гранта Президента НШ-2701.2020.7 «Разработка новых подходов к прогнозированию течения карцином молочной железы и легких с учетом морфологической и молекулярно-генетической гетерогенности опухоли».

Соответствие принципам этики. Все пациенты подписали информированное согласие на участие в исследовании. Работа проведена согласно принципам добровольности и конфиденциальности в соответствии с «Основами законодательства РФ об охране здоровья граждан» (Указ Президента РФ от 24.12.1993 № 2288) на основании разрешения локального комитета по биомедицинской этике НИИ онкологии Томского НИМЦ (протокол № 4994 от 27.10.2016).

Для цитирования: Вторушин С.В., Васильченко Д.В., Завьялова М.В., Крахмаль Н.В., Паталяк С.В. Исследование факторов транскрипции GATA3, FOXA1, ELF5 в оценке прогноза у больных люминальным раком молочной железы. *Бюллетень сибирской медицины.* 2020; 19 (4): 30–37. https://doi.org/10.20538/1682-0363-2020-4-30-37.

INTRODUCTION

In recent decades, the overall incidence of breast cancer (BC) in women has remained consistently high, with a slight increase in overall five-year survival rate. In Russia, breast cancer is the leading oncological pathology in the female population and accounts for 20.9%, occupying the largest share in the age group 30–59 years [1, 2].

Recently, transcription factors (TFs) have attracted the greatest interest as significant predictors of the course of primary breast cancer.

GATA binding protein 3 (GATA3) is a transcription factor of the zinc finger family, which normally regulates the proliferation and differentiation of breast luminal cells [3]. Mutation of this transcription factor plays an important role in breast cancer carcinogenesis, ranking third after TP53 and PIK3CA mutations [4]. A group of researchers (METABRIC Group) analyzed 2,433 and 2,000 breast carcinoma tissue samples for significant mutations and found that mutant GATA3 tumors in a subgroup of patients with ER + breast cancer had a low grade of malignancy and, therefore, a favorable prognosis and better overall 10-year survival rat [5]. Positive expression of GATA3 in breast carcinoma in the immunohistochemical study is also associated with a better prognosis and survival, and loss of expression is characterized by opposite effects [6].

The data on the relationship of this transcription factor with the development of metastases available in the literature are also contradictory and ambiguous. In one of the studies, a discrepancy between the expression level of the described transcription factor in the primary tumor and in the lymph nodes affected by metastases was found. The authors of the work showed that in some cases positive expression of GATA3 was observed in the affected lymph nodes with negative expression of the marker in the primary breast tumor and vice versa [7]. In a number of other studies, the authors evaluated the expression characteristics of GATA3 in hematogenous metastases of breast carcinoma of various localization and found that during the development of metastatic foci in the lungs, the expression of the TF under study was significantly lower in comparison with the parameters of its expression in metastases of other organs and tissues. The data obtained may indicate the possible involvement of GATA3 in the mechanisms that prevent metastasis [8, 9].

Forkhead box A1 (FOXA1), or hepatic nuclear factor 3α (HNF3α), like GATA3, is a transcription factor that not only plays a key role in the embryonic development of various organs and tissues, but also participates in breast tumorigenesis [10]. The data available in the literature suggest a possible significant potential of GATA3 in assessing the prognosis and response to hormone therapy [11, 12]. According to a number of authors, breast cancer patients in whom primary tumors were characterized by positive FOXA1 expression in ER +/PR+ status had longer overall and disease-free survival [13, 14]. The prognosis of the disease in patients was primarily determined by the fact that FOXA1 was involved in the epithelial-mesenchymal transition (EMT), interacting with the key transcription factors Twist1 and Slug, which led to a decrease in overall survival [15].

E74-like factor 5 (ELF5), a transcription factor of the E26 family (ETS), is involved in the development of breast tissue, while its primary role consists in formation of alveoli and transformation of progenitor cells into mature acinar cells [16]. This TF plays an essential role in EMT; in particular, the inhibitory effect of ELF5 on EMT in breast cancer was shown [17]. It was demonstrated in MCF-7 mouse models that the expression of this marker in the tumor can be associated with resistance to hormone therapy [18].

Thus, the data available in the literature remain controversial, which suggests the need to study the transcription factors ELF5, FOXA1, and GATA3 in patients with breast cancer in order to clarify the mechanisms of tumor progression and consider the studied markers in relation to possible assessment of prognosis for creating a personalized approach to treatment of the disease.

The aim of the study was to investigate the relationship between the expression of the transcription factors GATA3, FOXA1, and ELF5 in the tumor and the occurrence of distant metastases in patients with luminal subtype of breast cancer during adjuvant hormone therapy.

MATERIALS AND METHODS

The study included 101 patients with breast cancer (aged from 30 to 81 years, mean age 54.8 ± 10.3 years), stage $T_{1-4}N_{1-3}M_0$. All patients were treated at the Cancer Research Institute, Tomsk National Research Medical Center. The diagnosis of breast

cancer was established on the basis of core biopsy of the tumor in accordance with the WHO classification (2012). The molecular biological subtype of the neoplasm was assessed by immunohistochemistry (IHC). Antibodies to ER (clone 1D5, Dako), PR (clone PgR636, Dako), Ki-67 (clone MIB-1, Dako), and Her2 / neu (polyclonal, c-erB-2, Dako) were used. The patients did not receive preoperative treatment. In terms of surgical treatment, all women underwent surgery in form of radical mastectomy or sectoral resection (breast-conserving treatment). In 33% of patients at the time of diagnosis, menstrual function was preserved, and 68% of patients were menopausal. After the surgical stage, all patients received hormone therapy with tamoxifen or aromatase inhibitors. The observation period was at least 5 years. The primary documents were analyzed, such as medical histories and outpatient records, the presence of local recurrence of the disease and the presence and localization of distant tumor metastases were assessed. The inclusion criteria for the study were luminal molecular tumor subtype and absence of preoperative treatment. The exclusion criterion was stage IV of the disease.

When examining the surgical material, the size of the tumor node, breast tissue outside the formation, the state of the resection margins, as well as all removed axillary lymph nodes were assessed for the presence of metastatic lesions. The tumor grade was determined according to the Nottingham Histologic Grade (Elston modification of the Bloom–Richardson grading system). In the tumor stroma, the severity of infiltration by immune cells was assessed in points (1 point – no infiltration or weakly pronounced, 2 points – moderately pronounced, 3 points – strongly pronounced).

IHC of transcription factors was carried out according to the standard technique. We used polyclonal rabbit antibodies to GATA3 (dilution 1 : 200), FOXA1 (dilution 1 : 200), and ELF5 (dilution 1 : 150) produced by Flarebio (Austria). The interpretation of the staining results included the following features: the presence of marker expression (positive or negative expression) and the intensity of expression of the marker under study (on a scale from 1 to 3 points). The percentage of tumor cells with positive immunostaining was counted (the count was performed per 1,000 cells in 10 fields of view at ×40). In addition, the type of the distribution of the expression of the studied transcription factors in the tumor was assessed. In case of uniform staining in the tumor cells, regardless of the intensity of the marker expression, the expression was considered homogeneous. The presence of foci with positive and negative expression in the tumor section, as well as foci with varying degrees of staining intensity, the distribution pattern was considered heterogeneous.

Statistical analysis of the data was carried out using the Statistica v.10 package using analysis of variance, χ^2 test, and nonparametric Mann–Whitney *U*-test. Thee data were presented as the median and interquartile range Me ($Q_1 \div Q_3$). Results with significant differences at $p < 0.05$ were discussed.

RESULTS AND DISCUSSION

At the first stage, we analyzed the frequency of expression of the studied transcription factors in the tumor and possible combinations of these markers in patients with luminal BC. The frequency of occurrence of positive staining was as follows: in 96 (95.1%) patients, positive nuclear staining of the GATA3 marker was noted, in 5 cases (4.9%), the expression of the marker was negative. Positive expression of FOXA1 was detected in 91 (90.1%) patients, negative – in 10 (9.9%) patients; at the same time, positive expression of the ELF5 factor was noted in 89 (88.1%) cases, in 12 (11.9%) cases, this factor was not detected in the tumor.

Analysis of the combination of the expression of all three studied transcription factors showed fairly high variability of their co-expression. The phenotype GATA3 + FOXA1 + ELF5 + was dominant in the study group of patients and amounted to 78.2% (79 / 101). In 8 cases, the tumor showed positive staining only with antibodies to GATA3 and FOXA1 (GATA3 + FOXA + ELF5). In 4 cases, the tumor cells had the GATA3-FOXA1 + ELF5 + phenotype. In 3 cases, the neoplasm had the GATA3 + FOXA1-ELF5- phenotype, and in 5 patients the neoplasm had GATA3 + FOXA1-ELF5 +. It should be emphasized that 1 case in the study group was characterized by the presence of only positive expression of ELF5 (GATA3-FOXA1-) and 1 case had negative expression of all three studied markers in the primary tumor (GATA3-FOXA1-ELF5-).

Our analysis showed that the frequency of positive expression and the variant of the co-expression of all three studied transcription factors did not have any significant differences in the follow-

ing clinical and morphological signs: the age of the patients, menstrual status, the luminal subtype (A, B1, B2), the stage of cancer. It was also shown that the percentage of positively stained tumor cells for GATA3, FOXA1, and ELF5 did not statistically differ depending on the above mentioned clinical and morphological parameters.

We have previously shown that there is a relationship between the expression of markers ELF5 and FOXA1 and such an important parameter as the size of the primary tumor. In addition, it was found that the character of GATA3 and ELF5 expression was associated with the rate of lymph node metastases [19].

At the follow-up stages, local tumor recurrence was diagnosed in 9 out of 101 (8.9%) patients. In 8 (88.9%) cases, local tumor recurrence developed in the area of the postoperative scar, and in 1 (11.1%) case in the remaining breast tissue after organ-preserving treatment. In 7 (77.8%) cases, tumor recurrence was represented by a single node, while in 2 (22.2%) cases, multiple tumor lesions were noted. Assessment of the expression of transcription factors in the tumor did not reveal significant dependence of the expression on the rate of recurrence in the studied group of patients.

Distant metastases were diagnosed in 15 out of 101 (14.8%) patients. The site of metastatic foci and the time of their occurrence after surgery were assessed. Isolated bone metastases were found in 9 out of 15 cases (60%). In 6 cases (40%), multiple metastatic lesions of the bones and visceral organs were observed. It was of interest to study the clinical, morphological, and molecular characteristics of the tumor in patients with luminal BC depending on the development of hematogenous spread. The incidence of distant metastases was associated with the size of the primary tumor (p = 0.002) and regional lymph node metastases (χ^2 = 10,9, p = 0.00095). There was a clear tendency towards a higher rate of hematogenous dissemination with an increase in the grade of tumor (χ^2 = 4.9, p = 0.08). However, the development of distant metastases was not associated with the Ki67 proliferative activity index of tumor cells (p = 0.8) and the luminal subtype of the neoplasm (p = 0.6). At the same time, significant differences were revealed in the expression of estrogen and progesterone receptors. Thus, in the group of patients with distant metastases, the expression (%) of both types of receptors was significantly lower (Table 1).

Table 1

Indicators of expression of sex hormone receptors in the tumor depending on the presence of distant metastases in patients with luminal breast cancer

Hormone receptors	Expression in the tumor, %, *Me* $Q_1 \div Q_3$	
	Absence of hematogenous metastases	Presence of hematogenous metastases
ER	94.7 (70÷100)	69.3 (51.5÷93) p_{1-2} = 0.02
PR	83 (59.5÷98)	49 (32÷74.4) p_{1-2} = 0.038

Analysis of the relationship between the expression of the studied transcription factors in the tumor in groups of patients and the presence or absence of hematogenous metastases revealed significant differences in the percentage of FOXA1 and ELF5 expression. It was found that with the development of distant metastases, the percentage of FOXA1 and ELF5 expression in the cells of the primary tumor is significantly lower than in patients with no signs of disease progression. No such differences in the expression of the GATA3 marker were recorded (Table 2).

Table 2

Indicators of expression of transcription factors in the tumor depending on the presence of distant metastases in patients with luminal breast cancer

Transcription factors	Expression in the tumor, % (*Me* $Q_1 \div Q_3$)	
	Absence of hematogenous metastases	Presence of hematogenous metastases
GATA3	100 (98 ÷ 100)	100 (100 ÷ 100)
FOXA1	100 (90.3 ÷ 100)	70 (42 ÷ 76) p_{1-2} = 0.000015
ELF5	100 (100 ÷ 100)	76 (65 ÷ 100) p_{1-2} = 0.000002

The study showed a relationship between the nature of the distribution of the studied marker expression and the frequency of hematogenous metastases.

Most often, hematogenous metastases were observed with heterogeneous expression of factors FOXA1 (Fig. 1) (χ^2 = 6.42, p = 0.01) and ELF5 (χ^2 = 14.46, p = 0.0001) in the tumor (Table 3).

When studying the distribution pattern of GATA3 expression in the tumor (Fig. 2) and the rate of distant metastases, no significant differences were revealed. Infiltration of a tumor by immune cells is an important component of the microenvironment that affects the processes of proliferation, angiogenesis,

Table 3

Rate of distant metastasis depending on the distribution of FOXA1 and ELF5 expression in patients with luminal breast cancer

Distribution of the marker expression in the primary tumor	Distant metastases, abs. number (%)	
	Absence of hematogenous metastases	Presence of hematogenous metastases
	FOXA1	
Homogeneous (n = 45)	44 (97%)	1(3%)
Heterogeneous (n = 46)	36 (78.2%)	10 (21.8%)
	ELF5	
Homogeneous (n = 56)	54 (96.4%)	2 (3.6%)
Heterogeneous (n = 33)	21 (63.6%)	12 (36.4%)

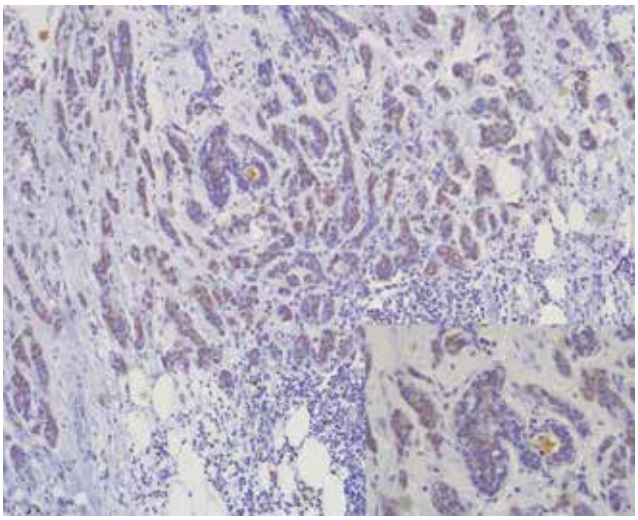

Fig. 1. Moderately pronounced heterogeneous nuclear expression of FOXA1 in tumor cells of invasive breast carcinoma, ×100. The lower right corner shows the presence of tumor cells with positive and negative expression, ×400. ICH

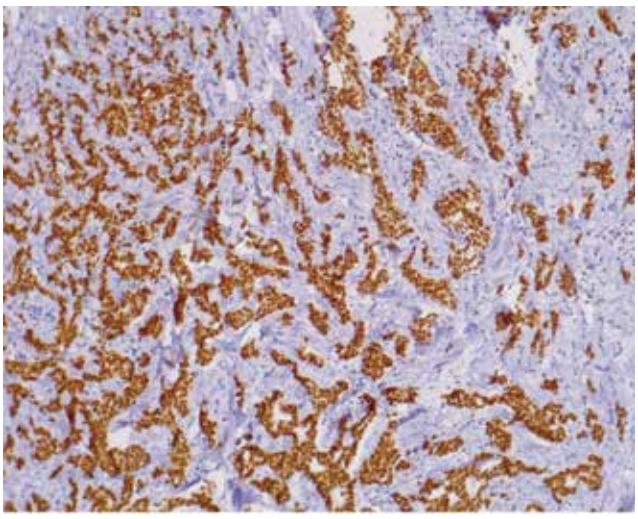

Fig. 2. Positive homogeneous nuclear expression of GATA3 in tumor cells of invasive breast carcinoma, ×100. ICH

and invasion and can determine the characteristics of tumor progression, since it is involved in the mechanisms of the metastatic cascade. The expression of the studied transcription factors in the tumor was analyzed depending on the degree of inflammatory infiltration in the neoplasm stroma. The study showed that the expression of GATA3, FOXA1, and ELF5 did not differ in tumors with different degree of infiltration with immune cells. The expression of the latter had no significant association with the incidence of distant metastases (p = 0.57).

The study of GATA3, FOXA1, and ELF5 in the primary tumor in patients with the luminal subtype of breast cancer showed a clear relationship between their expression and the development of hematogenous metastasis. The identified relationship between the low expression of ELF5 and FOXA1 and the rate of hematogenous metastasis can be explained in different ways. On the one hand, the revealed patterns can be caused by the pathogenetic influence of these factors on proliferation of tumor cells and angiogenesis, being a manifestation of EMT activation as a key mechanism in the development of hematogenous progression. It is known that the transcription factors ELF5 and FOXA1 have a suppressive effect on EMT. Therefore, a decrease in the level of their expression in the tumor may promote the activation of important factors Twist1 and Slug. However, these aspects require further study. On the other hand, hematogenous progression in the group of patients with low expression of FOXA1 and ELF5 with their heterogeneous distribution in the tumor along with low expression of ER and PR can determine the development of resistance to hormonal therapy and, therefore, become the pathogenetic basis of treatment inefficiency and disease progression.

CONCLUSION

The results of this study demonstrate the clinical significance of the transcription factors FOXA1 and ELF5 in assessing the risk of distant metastasis in patients with luminal BC subtype and can be used to predict the course of the disease when choosing the management tactics for this category of patients. Analysis of these transcription factors in the tumor can be performed at the preoperative stage during a standard immunomorphological study and considered as additional tumor parameters when planning the patient's treatment strategy.

REFERENCES

1. Rebecca L., Kimberly D., Ahmedin J. Cancer statistics. 2020. *Ca: Cancer J. Clin*. 2020; 70 (1): 7–30. DOI: 10.3322/caac.21590.
2. Kaprin A.D., Starinsky V.V., Petrova G.V. Statistics on malignant tumors in Russia in 2018 (incidence and mortality). Moscow: National Medical Research Radiological Centre of the Ministry of Health of the Russian Federation, 2019 (in Russ.).
3. Shaoxian T., Baohua Y., Xiaoli X., Yufan C., Xiaoyu T., Hongfen L., Rui B., Xiangjie S., Ruohong S., Wentao Y. Characterisation of GATA3 expression in invasive breast cancer: differences in histological subtypes and immunohistochemically defined molecular subtypes. *J. Clin. Pathol*. 2017; 70 (11): 926–934. DOI: 10.1136/jclinpath-2016-204137.
4. Koboldt D., Fulton R., McLellan M. et al. Comprehensive molecular portraits of human breast tumors. *Nature*. 2012; 490 (7418): 61–70. DOI: 10.1038/nature11412.
5. Pereira B., Chin S.F., Rueda O.M., Vollan H.K., Provenzano E., Bardwell H.A., Pugh M., Jones L., Russell R., Sammut S.J., Tsui D.W., Liu B., Dawson S.J., Abraham J., Northen H., Peden J.F., Mukherjee A., Turashvili G., Green A.R., McKinney S., Oloumi A., Shah S., Rosenfeld N., Murphy L., Bentley D.R., Ellis I.O., Purushotham A., Pinder S.E., Borresen-Dale A.L., Earl H.M., Pharoah P.D., Ross M.T., Aparicio S., Caldas C. The somatic mutation profiles of 2,433 breast cancers refines their genomic and transcriptomic landscapes. *Nature Comm*. 2016; 7: 11479. DOI: 10.1038/ncomms11479.
6. Liu J., Prager-van der Smissen W.J., Look M.P., Sieuwerts A.M., Smid M., Meijer-van Gelder M.E., Foekens J.A., Hollestelle A., Martens J.W. GATA3 mRNA expression, but not mutation, associates with longer progression-free survival in ER-positive breast cancer patients treated with first-line tamoxifen for recurrent disease. *Cancer Letters*. 2016; 376 (1): 104–109. DOI: 10.1016/j.canlet.2016.03.038.
7. Calvo J., Sanchez-Cid L., Munoz M., Lozano J.J., Thomson T.M., Fernandez P.L. Infrequent oss of luminal differentiation in ductal breast cancer metastasis. *PLoS One*. 2013; 8 (10): e78097. DOI: 10.1371/journal.pone.0078097.
8. McCleskey B.C., Penedo T.L., Zhang K., Hameed O., Siegal G.P., Wei S. GATA3 expression in advanced breast cancer: prognostic value and organ-specific relapse. *Am. J. Clin. Pathol.* 2015; 144 (5): 756–763. DOI: 10.1309/AJCP-5MMR1FJVVTPK.
9. Soni A., Ren Z., Hameed O., Chanda D., Morgan C.J., Siegal G.P., Wei S. Breast cancer subtypes predispose the site of distant metastases. *Am. J. Clin. Pathol.* 2015; 143 (4): 471–478. DOI: 10.1309/AJCPYO5FSV3UPEXS.
10. Rakha E.A., Pareja F.G. New advances in molecular breast cancer pathology. *Semin. Cancer Biol.* 2020; S1044-579X (20): 30080–30088. DOI: 10.1016/j.semcancer.2020.03.014.
11. Fu X., Pereira R., De Angelis C., Veeraraghavan J., Nanda S., Qin L., Cataldo M.L., Sethunath V., Mehravaran S., Gutierrez C., Chamness G.C., Feng Q., O'Malley B.W., Selenica P., Weigelt B., Reis-Filho J.S., Cohen O., Wagle N., Nardone A., Jeselsohn R., Brown M., Rimawi M.F., Osborne C.K., Schiff R. FOXA1 upregulation promotes enhancer and transcriptional reprogramming in endocrine-resistant breast cancer. *Proc. Natl. Acad. Sci. U S A*. 2019. 116 (52): 26823–26834. DOI: 10.1073/pnas.1911584116.
12. Forma E., Jozwiak P., Ciesielski P., Zaczek A., Starska K., Brys M., Krzeslak A. Impact of OGT deregulation on EZH2 target genes *FOXA1* and *FOXC1* expression in breast cancer cells *PLoS One.* 2018; 13 (6): e0198351. DOI: 10.1371/journal.pone.0198351.
13. He K., Zeng H., Xu X., Li A., Cai Q., Long X. Clinicopathological significance of forkhead box protein A1 in breast cancer: a meta-analysis. *Exper. Ther. Med*. 2016; 11 (6): 2525–2530. DOI: 10.3892/etm.2016.3229
14. Shou J., Lai Y., Xu J., Huang J. Prognostic value of FOXA1 in breast cancer: a systematic review and meta-analysis. *The Breast*. 2016; 27: 35–43. DOI: 10.1016/j.breast.2016.02.009.
15. Xu Y., Qin L., Sun T., Wu H., He T., Ya Z., Mo Q., Liao L., Xu J. Twist1 promotes breast cancer invasion and metastasis by silencing Foxa1 expression. *Oncogene*. 2017; 36 (8): 1157–1166. DOI: 10.1038/onc.2016.286.
16. Oakes S.R., Naylor M.J., Asselin-Labat M.L., Blazek K.D., Gardiner-Garden M., Hilton H.N., Kazlauskas M., Pritchard M.A., Chodosh L.A., Pfeffer P.L., Lindeman G.J., Visvader J.E., Ormandy C.J. The ets transcription factor Elf5 specifies mammary alveolar cell fate. *Genes Dev*. 2008; 22 (5): 581–586. DOI: 10.1101/gad.1614608.
17. Chakrabarti R., Hwang J., Andres Blanco M., Wei Y., Lukacisin M., Romano R.A., Smalley K., Liu S., Yang Q., Ibrahim T., Mercatali L., Amadori D., Haffty B.G., Sinha S., Kang Y. Elf5 inhibits the epithelial-mesenchymal transition in mammary gland development and breast cancer metastasis by transcriptionally repressing Snail2. *Nature Cell Biology*. 2012; 14 (11): 1212–1222. DOI: 10.1038/ncb2607.
18. Kalyuga M., Gallego-Ortega D., Lee H.J., Roden D.L., Cowley M.J., Caldon C.E., Stone A., Allerdice S.L., Valdes-Mora F., Launchbury R., Statham A.L., Armstrong N., Alles M.C., Young A., Egger A., Au W., Piggin C.L., Evans C.J., Ledger A., Brummer T., Oakes S.R., Kaplan W., Gee J.M., Nicholson R.I., Sutherland R.L., Swarbrick A., Naylor M.J., Clark S.J., Carroll J.S., Ormandy C.J. ELF5 Suppresses estrogen sensitivity and underpins the acquisition of antiestrogen resistance in luminal breast cancer. *PLoS Biol*. 2012; 10 (12): e1001461. DOI: 10.1371/journal.pbio.1001461.
19. Vtorushin S.V., Vasilchenko D.V., Krakhmal' N.V., Patalyak S.V. Association of GATA3, FOXA1, and ELF5 with clinical and morphological parameters of luminal breast cancer subtype. *Journal of Siberian Medical Sciences*. 2019; (4): 62–74 (in Russ.). DOI: 10.31549/2542-1174-2019-4-62-74.

Authors contribution

Vtorushin S.V. – conception and design, analysis and interpretation of data. Vasilchenko D.V. – analysis and interpretation of data, review of publications on the topic of the manuscript. Zavyalova M.V. – analysis and interpretation of data. Krakhmal' N.V. – carrying out of immunohistochemical studies, analysis of data. Patalyak S.V. – selection of cases for research, work with medical records, analysis of data.

Authors information

Vtorushin Sergey V., Dr. Sci. (Med.), Associate Professor, Professor, Pathology Department, Siberian State Medical University, Tomsk, Russian Federation; Head of the Pathology Department, Cancer Research Institute, Tomsk National Research Medical Center, Tomsk, Russian Federation. ORCID 0000-0002-1195-4008.

Vasilchenko Dmitrii V., Assistant, Pathology Department, Siberian State Medical University, Tomsk, Russian Federation. ORCID 0000-0002-9780-0770.

Zavyalova Marina V., Dr. Sci. (Med.), Professor, Head of the Pathological Anatomy Department, Siberian State Medical University, Tomsk, Russian Federation; Leading Researcher, Pathology Department, Cancer Research Institute, Tomsk National Research Medical Center, Tomsk, Russian Federation. ORCID 0000-0001-9429-9813.

Krakhmal' Nadezhda V., Cand. Sci. (Med.), Associate Professor, Pathology Department, Siberian State Medical University, Tomsk, Russian Federation. ORCID 0000-0002-1909-1681.

Patalyak Stanislav V., Cand. Sci. (Med.), Head of the Oncology department of day hospital, Cancer Research Institute, Tomsk National Research Medical Center, Tomsk, Russian Federation. ORCID 0000-0002-9468-1980.

(✉) **Vtorushin Sergey V.,** e-mail: wtorushin@rambler.ru.

Received 29.05.2020
Accepted 29.09.2020

УДК 612.821.44:57.042.2
https://doi.org/10.20538/1682-0363-2020-4-38-45

Features of brain activity in alcohol dependence in the task of inhibitory control

Galkin S. A.[1], Peshkovskaya A. G.[1], Roshchina O.V.[1], Kisel N.I.[1], Ivanova S. A.[1, 2], Bokhan N. A.[1, 2]

[1] *Mental Health Research Institute, Tomsk National Research Medical Center (NRMC) of the Russian Academy of Sciences*
4, Aleutskaya Str., Tomsk, 634014, Russian Federation

[2] *Siberian State Medical University (SSMU)*
2, Moscow Trakt, Tomsk, 634050, Russian Federation

ABSTRACT

Aim. To study neurophysiological correlates of inhibitory control to determine the features of inhibition processes in alcohol dependence.

Materials and methods. 77 patients with alcohol dependence were examined (42 men and 35 women) (F10. 2 according to ICD-10). Patients were examined using a test to assess inhibitory control – Go / No – Go. According to the task performance, patients were divided into two groups: group 1 – without inhibitory control impairments, group 2 – with impaired inhibitory control. During execution of test, electroencephalogram recordings were made according to the "10–20" system. The values of spectral power and coherence of θ-, α- and β-rhythms were analyzed. Statistical processing was carried out using nonparametric Mann – Whitney U-test and Wilcoxon W-test.

Results. In patients with impaired inhibitory control, there was a decrease in the spectral power of the α-rhythm in the frontal cortex ($p = 0.003$), whereas in patients without inhibitory control disorders – in the Central cortex ($p = 0.036$). Patients with impaired inhibitory control responded by increasing β-power to cognitive stimulus in the occipital ($p = 0.014$), left temporal ($p = 0.009$) and right temporal ($p = 0.008$) cortex, while patients without inhibitory control disorders showed an increase in β-power only in the occipital ($p = 0.007$) and left temporal ($p = 0.002$) cortex. According to coherence data, patients with impaired inhibitory control have greater involvement of brain structures during the "Go/No–go" test in all frequency ranges.

Conclusion. Patients with and without impaired inhibitory control have regional differences in changes in brain bioelectric activity during the "Go/No–go" test.

Key words: alcohol dependence, inhibitory control, electroencephalography, diagnostics.

Conflict of interest. The authors declare the absence of obvious or potential conflicts of interest related to the publication of this article.

Source of financing. The study was supported by the Tomsk Region Administration and Russian Foundation for Basic Research grant 19-413-703007.

Conformity with the principles of ethics. All the participants of the study had signed the informed consent. The study was approved by the local Ethics Committee at Mental Health Research Institute, Tomsk National Research Medical Center of the Russian Academy of Sciences (Protocol No. 114 of 22.10.2018).

For citation: Galkin S. A., Peshkovskaya A. G., Roshchina O.V., Kisel N.I. , Ivanova S. A., Bokhan N. A. Features of brain activity in alcohol dependence in the task of inhibitory control. *Bulletin of Siberian Medicine.* 2020; 19 (4): 38–45. https://doi.org/10.20538/1682-0363-2020-4-6-14.

✉ *Galkin S.A.,* e-mail: s01091994@yandex.ru.

Особенности мозговой активности при алкогольной зависимости в задаче на ингибиторный контроль

Галкин С.А.[1], Пешковская А.Г.[1], Рощина О.В.[1], Кисель Н.И.[1], Иванова С.А.[1, 2], Бохан Н.А.[1, 2]

[1] Научно-исследовательский институт (НИИ) психического здоровья, Томский национальный исследовательский медицинский центр (НИМЦ) Российской академии наук
Россия, 634014, Томск, ул. Алеутская, 4

[2] Сибирский государственный медицинский университет (СибГМУ)
Россия, 634050, Томск, Московский тракт, 2

РЕЗЮМЕ

Цель: изучить нейрофизиологические корреляты ингибиторного контроля для определения особенностей процессов торможения при алкогольной зависимости.

Материалы и методы. Обследованы 77 пациентов (42 мужчины и 35 женщин) с алкогольной зависимостью (F10.2 по МКБ-10). Пациенты обследованы с помощью теста для оценки ингибиторного контроля – Go / No – go. По результатам этого теста пациенты были разделены на две группы: группа 1 – без нарушения ингибиторного контроля, группа 2 – с нарушением ингибиторного контроля. Во время выполнения теста проводилась запись электроэнцефалограммы по системе 10-20. Анализировались значения спектральной мощности и когерентности θ- α- и β-ритмов. Статистическая обработка проводилась с применением непараметрического *U*-критерия Манна – Уитни и *W*-критерия Вилкоксона.

Результаты. У пациентов с нарушенным ингибиторным контролем происходило снижение спектральной мощности α-ритма во фронтальной коре головного мозга ($p = 0,003$), тогда как у пациентов без нарушений ингибиторного контроля – в центральной коре ($p = 0,036$). Пациенты с нарушенным ингибиторным контролем реагировали повышением β-мощности на когнитивный стимул в затылочной ($p = 0,014$), левой височной ($p = 0,009$) и правой височной ($p = 0,008$) коре, при этом у пациентов без нарушений ингибиторного контроля наблюдалось повышение β-мощности только в затылочной ($p = 0,007$) и левой височной ($p = 0,002$) коре. По данным когерентности у пациентов с нарушением ингибиторного контроля наблюдается большая вовлеченность мозговых структур во время выполнения теста Go / No – go во всех частотных диапазонах.

Заключение. Пациенты с нарушением и без нарушения ингибиторного контроля имеют региональные различия в изменениях биоэлектрической активности головного мозга в процессе выполнения теста Go / No – go.

Ключевые слова: алкогольная зависимость, ингибиторный контроль, электроэнцефалография, диагностика.

Конфликт интересов. Авторы декларируют отсутствие явных и потенциальных конфликтов интересов, связанных с публикацией настоящей статьи.

Источник финансирования. Исследование выполнено при поддержке Администрации Томской области и гранта РФФИ 19-413-703007.

Соответствие принципам этики. Все участники исследования подписали информированное согласие. Исследование одобрено локальным этическим комитетом НИИ психического здоровья Томского НИМЦ (протокол № 114 от 22.10.2018).

Для цитирования: Галкин С.А., Пешковская А.Г., Рощина О.В., Кисель Н.И., Иванова С.А., Бохан Н.А. Особенности мозговой активности при алкогольной зависимости в задаче на ингибиторный контроль. *Бюллетень сибирской медицины.* 2020; 19 (4): 38–45. https://doi.org/10.20538/1682-0363-2020-4-38-45.

INTRODUCTION

Understanding the psychological and neural processes that lead to alcohol-related disorders is an urgent task in both health care and neuroscience [1, 2].Current research has linked the inability to abstain from alcohol consumption, as well as maintain long-term remission, with impaired cognitive functions that regulate behavior, in particular, weakened executive control [1, 3]. Inhibitory processes are important components in controlling behavior [3]. Adaptive inhibitory functioning reflects the ability to stop a potential behavioral response to an external stimulus [4].

The Go/No-Go method is widely used for evaluating the processes of inhibition in higher-order executive functioning [5]. A number of studies have shown a decrease in response inhibition in patients with alcohol use dependence (AUD) to the No-go signal [1, 6, 7]. It is believed that alcohol consumption affects both the suppression of the response to the stimulus and its processing, which leads to the actualization of an erroneous response (response error) to the No–go signal [6, 7]. However, some researchers found no differences in the Go/No-Go task between patients with AUD and moderate drinkers in healthy people [6, 8]. A number of authors are inclined to believe that there is not always a deficit of inhibitory control in alcohol dependence [3]. Thus, the question of violation of inhibitory control in people with alcohol dependence is still open.

Recording and analyzing the bioelectric activity of the brain is one of the most accessible tools for studying the neurophysiological foundations of mental disorders [9, 10]. Spectral and coherent analysis of the main rhythms of the electroencephalogram (EEG) are the most widely used in research. It is believed that changes in the spectral characteristics (amplitude, power) of the EEG are associated with the neurotransmitter systems restructuring in the CNS [11]. Coherence of electrical signals is a quantitative indicator of the synchronicity of involvement of various cortical departments in any process [9].

The use of the method of assessing the bioelectric activity of the brain in psychiatry and drug therapy can expand the available data on the neurophysiological profile of patients with alcohol use dependence. However, despite the high availability and informative nature of EEG, studies of neurophysiological correlates of inhibitory control disorders in AUD are insufficient. Thus, the aim of our work was to study the neurophysiological correlates of inhibitory control to determine the features of inhibition processes in alcohol dependence.

MATERIALS AND METHODS

Materials. The study was conducted on the basis of the Department of the clinic of the Mental Health Research Institute (Department of addictive conditions) Tomsk national research medical center of the Russian Academy of Sciences, according to the Protocol approved by the local ethics Committee at the Mental Health Research Institute (Protocol No. 114 of October 22, 2018).

We examined 77 patients (42 men, 35 women, age 45 [38; 51] years) with a diagnosis of: mental disorders and behavioral disorders associated with substance use, alcohol dependence syndrome (F10. 2 according to ICD-10), after detoxification. Based on the literature data on various profiles of electrophysiological indicators in right-handed and left-handed people, right-handers were selected for the study group using a questionnaire of lateral characteristics. Diagnostic evaluation and clinical qualification of the disorder were performed using ICD-10 diagnostic criteria, patient anamnestic data, and a set of standardized psychometric tools. The inclusion criteria were verified diagnosis of an addictive disorder (alcohol dependence) according to ICD-10, voluntary consent to participate in the study, normal or adjusted to normal vision, and age 18–55 years. The exclusion criteria were the presence of chronic somatic diseases in the acute stage, epilepsy, severe organic brain damage, traumatic brain injuries of any severity, mental retardation, and refusal to participate in the study.

Methods. The Hamilton Anxiety Scale (HAM-A) and the Clinical Global Impression Scale (CGI-S) were used as psychometric tools. Data on the age of AUD disease, education, the number of hospitalizations and the amount of alcohol consumption were taken from the patient's medical history.

The inhibitor control was evaluated using a computerized Go/ No – go test (Fig. 1). Patients had to press the button when a green signal appeared on the computer screen (the Go signal) and not press the button when a red signal appeared (the No-go signal). The signals were presented in random order. The time of presentation of the signal was 500 ms, and the interval between signals was 800 ms.

Recording and evaluation of bioelectric activity of the brain was performed on a 16-channel Neuropoligraph EEG using the international system "10–20" (Fig. 2). The cutoff frequencies of upper and lower frequency filters were 30 and 1.5 Hz. The study procedure included recording the background EEG at rest with open eyes (1 min), after which the patients

performed a "Go/No – Go" test with simultaneous EEG registration. Artefact fragments were deleted from the EEG recordings. The signals were processed using fast Fourier transform, and the values of absolute spectral power (mV^2) and coherence for θ- (4–7 Hz), α- (8–13 Hz) and β- (14–30 Hz) rhythms were analyzed.

Statistical analysis. Statistical data processing was performed using the Statistica 10.0 program. Statistical data is presented in the form of *Me* [Q_1; Q_3]. Verification of agreement with the normal distribution law was performed using the Shapiro – Wilk test. The obtained data did not follow the normal distribution law. The nonparametric Mann – Whitney test was used to evaluate differences between two independent samples (group 1 vs. group 2) and the Wilcoxon test to evaluate differences between two related samples (rest EEG vs. EEG test). The differences were considered statistically significant at a significance level of $p < 0.05$.

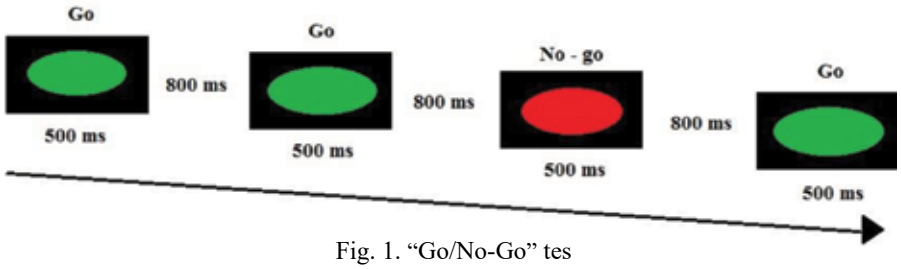

Fig. 1. "Go/No-Go" tes

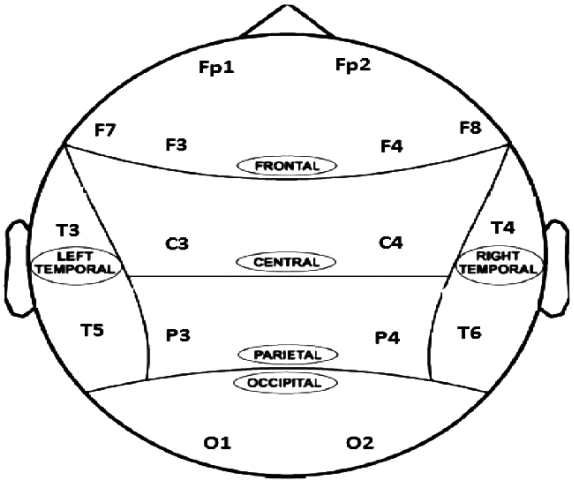

Fig. 2. Scheme of EEG

RESULTS

According to the obtained data of the Go/No-Go test, patients were divided into two groups: patients who did not make mistakes on the No-go signal (group 1) and patients with errors on the No-go signal (group 2) (Table 1).

Table 1

Answers to the "Go/No – Go" test

Characteristic	Group 1, $n = 30$	Group 2, $n = 30$	p
Number of errors per Go signal	10 [7; 13]	8 [3; 13]	0.092
Number of errors per No-go signal	–	4 [3; 7]	–
Reaction time (ms)	461 [455; 498]	489 [466; 500]	0.015

Median [Q_1; Q_3]; p – the level of statistical significance when comparing groups using the Mann – Whitney criterion.

Patients from group 2 have fewer errors on the Go signal compared to patients from group 1, but no statistically significant differences were found ($p > 0.05$). However, patients in group 2 had statistically significantly higher response times ($p < 0.05$).

Demographic and clinical characteristics of the studied groups of patients are presented in Table 2. There were no statistically significant differences in gender, age, level of education, duration of the disease, CGI-S scales (the average assessment of general health after detoxification corresponds to the indicator "moderate disorder") and HAM-A (symptoms of anxiety in both groups) ($p > 0.05$). Compared with patients from group 1 (without violation of inhibitory control), patients from group 2 showed a statistically significantly higher number of hospitalizations over the entire medical history ($p = 0.024$) and alcohol consumption (days per week) over the past 6 months ($p = 0.032$).

Table 2

Demographic and clinical characteristics of patients

Characteristic	Group 1	Group 2	p
Composition	18 men; 12 women	24 men; 23 women.	0.43; 0.35
Age (years)	44 [39; 50]	44 [36; 51]	0.915
Education (years)	13 [11; 14]	13 [11; 15]	0.501
Duration of the disease (years)	10 [4; 13]	9 [5; 12]	0.119
Number of hospitalizations	1 [1; 2]	3 [2; 4]	0.024
Amount of alcohol consumption in the last 6 months. (day per week)	2 [1; 4]	4 [2; 4]	0.032
CGI-S	4 [4; 5]	4 [4; 5]	0.522
HAM-A	19 [10; 25]	19 [12; 23]	0.702

Median [Q_1; Q_3]; p – the level of statistical significance when comparing groups using the Mann – Whitney criterion.

According to the background values of spectral power and coherence of α-, β- and θ-EEG rhythms, patients with errors for the No-go inhibitor signal did not differ significantly from patients without errors ($p > 0.05$). We were able to divide patients qualitatively only by changes in the EEG during the "Go/No – Go" test. Thus, an intragroup analysis of brain bioelectric activity rearrangements in group 2 patients revealed a statistically significant decrease in the spectral power of the α-rhythm in the frontal cortex ($p = 0.003$) and a decrease in α-coherence in Fp1–Fp2 ($p = 0.021$), T3–T4 ($p = 0.003$), Fp1–T3 ($p = 0.003$), T3–O1 ($p = 0.002$) and C3–O1 ($p = 0.034$) during the Go/No-Go test. Whereas in group 1 patients, there was a statistically significant decrease in the spectral power of the α-rhythm in the Central cortex ($p = 0.036$) and a decrease in α-coherence in Fp1–Fp2 ($p = 0.014$), C3–C4 ($p = 0.018$), T3–T4 ($p = 0.004$) and T3–O1 ($p = 0.012$) during the "Go/No – Go" test (Fig. 3).

Group 2 patients responded to a cognitive stimulus in the occipital ($p = 0.014$), left temporal ($p = 0.009$), and right temporal ($p = 0.008$) cortex with increased β-power. And with decreased β-coherence in Fp1–Fp2 ($p = 0.001$), F3–F4 ($p = 0.001$), F7–F8 ($p = 0.006$), C3–C4 ($p = 0.001$), P3–P4 ($p = 0.001$), T3–T4 ($p = 0.001$), T5–T6 ($p = 0.004$), FP1–T3 ($p = 0.045$), FP2–T4 ($p = 0.037$), T3–O1 ($p = 0.004$), T4–O2 ($p = 0.001$), and C3–O1 (v0.005). Patients from group 1 showed an increase in β-power only in the occipital ($p = 0.007$) and left temporal ($p = 0.002$) cortex, as well as a decrease in β-coherence in Fp1–Fp2 ($p = 0.001$), F3–F4 ($p = 0.002$), F7–F8 ($p = 0.009$), C3–C4 ($p = 0.003$), P3–P4 ($p = 0.04$), T3–T4 ($p = 0.002$), T3–O1 ($p = 0.02$), T4–O2 ($p = 0.02$) and C3–O1 ($p = 0.03$) (Fig. 4).

Changes in the slow-wave rhythm (θ-rhythm) in the studied groups of patients with AUD during the "Go/No – Go" test are shown in Fig. 5. Patients in group 2 had a statistically significant decrease in θ-rhythm coherence in Fp1–Fp2 ($p = 0.018$), F7–F8 ($p = 0.009$), T3–T4 ($p = 0.043$), Fp1–T3 ($p = 0.001$), Fp1–C3 ($p = 0.021$), T3–O1 ($p = 0.001$), T4–O2 ($p = 0.001$), C3–O1 ($p = 0.009$), and C4–O2 ($p = 0.004$) during the test. At the same time patients from group 1 showed a decrease in θ-rhythm coherence only in F7–F8 ($p = 0.026$), O1–O2 ($p = 0.007$) and T3-T4 ($p = 0.04$).

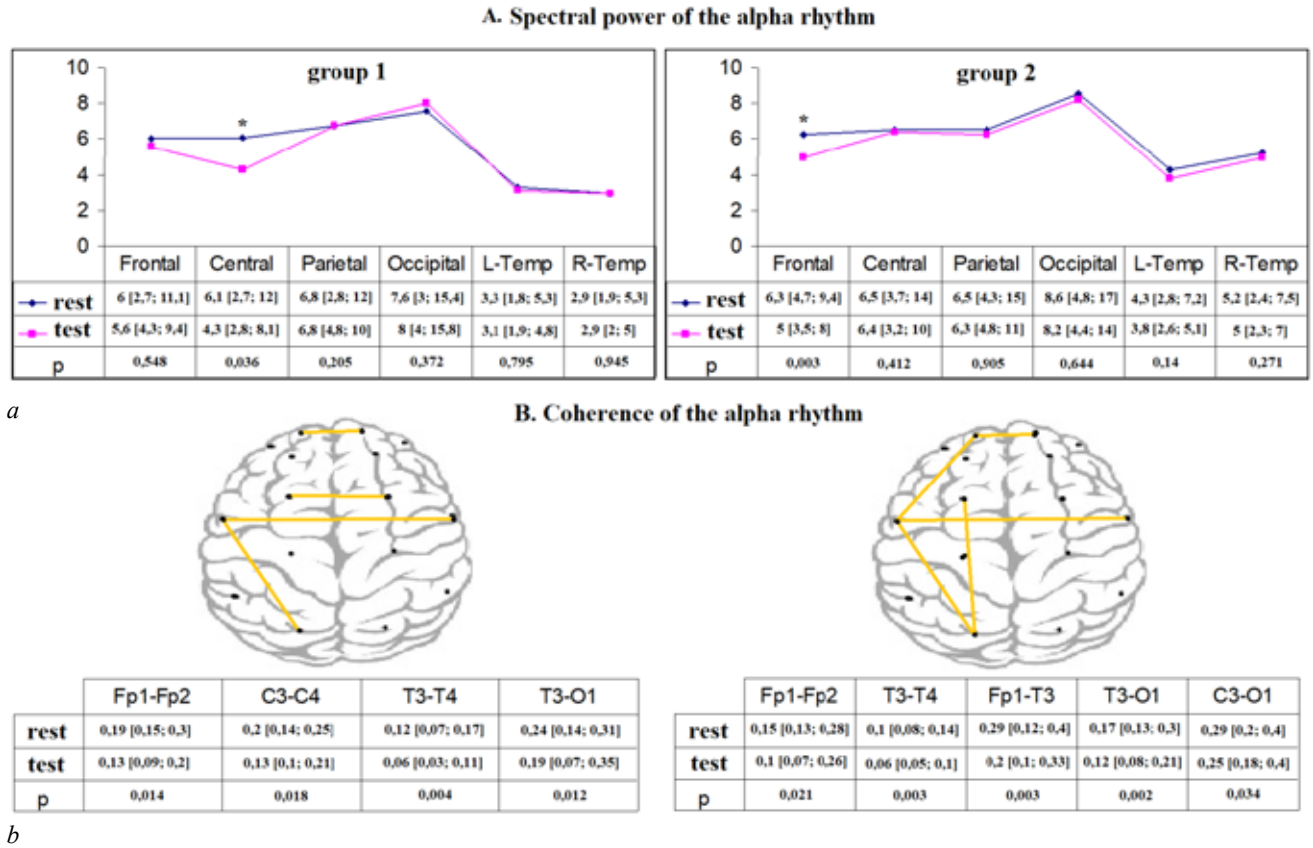

Fig. 3. Dynamics of EEG alpha rhythm during the "Go/No – Go" test,
Median [Q_1; Q_3]: * level of statistical significance when comparing groups using Wilcoxon criterion at $p < 0.05$

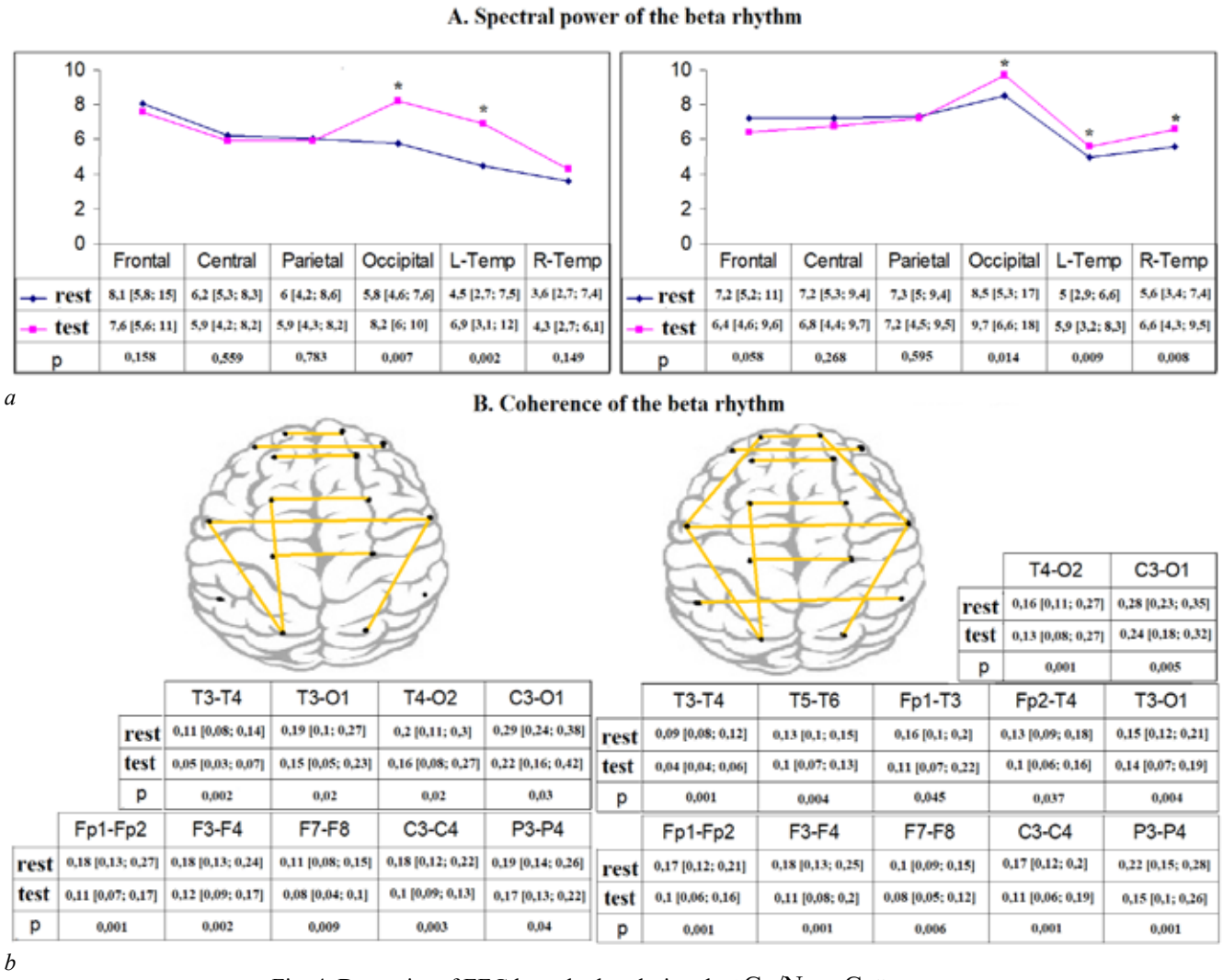

Fig. 4. Dynamics of EEG beta rhythm during the "Go/No – Go" test,
Median [Q_1; Q_3]; * level of statistical significance when comparing groups using Wilcoxon criterion at $p < 0.05$

DISCUSSION

In this study, behavioral characteristics of inhibitory control and its neural correlates were studied using the "Go/No – Go" method to determine the features of inhibition processes in AUD. The data obtained are consistent with the results of some studies using the cognitive "Go/No – Go" task in patients with AUD [4, 6, 12]. It was found that patients with impaired inhibitory control (group 2) had a more severe course of AUD than patients from group 1: more hospitalizations and alcohol consumption per week. Moreover, there is evidence that impaired inhibitory control complicates the symptoms of AUD and increases resistance to therapy [12].

The results of the electrophysiological study revealed a number of important differences. First, in patients with impaired inhibitory control during the "Go/No – Go" test, there was a decrease in the spectral power of the α-rhythm in the frontal cortex, while in patients without impaired inhibitory control this occurred in the central cortex. As a rule, the weakening of inhibitory control is reflected in the form of a decrease in the prefrontal cortex activity [1, 13, 14]. Consequently, the observed decrease in α-activity during the Go/No-Go task in the frontal cortex may objectively reflect a lack of brain resources in suppressing the response to a stimulus. A decrease in the spectral power of the α-rhythm in the central cortex in patients without inhibitory control violations may reflect the processes of triggering behavior (suppression of the response to a stimulus) [13]. Secondly, we found an unusual increase in β-activity in the occipital-temporal cortex during the "Go/No – Go" task, and in patients with impaired inhibitory control, changes

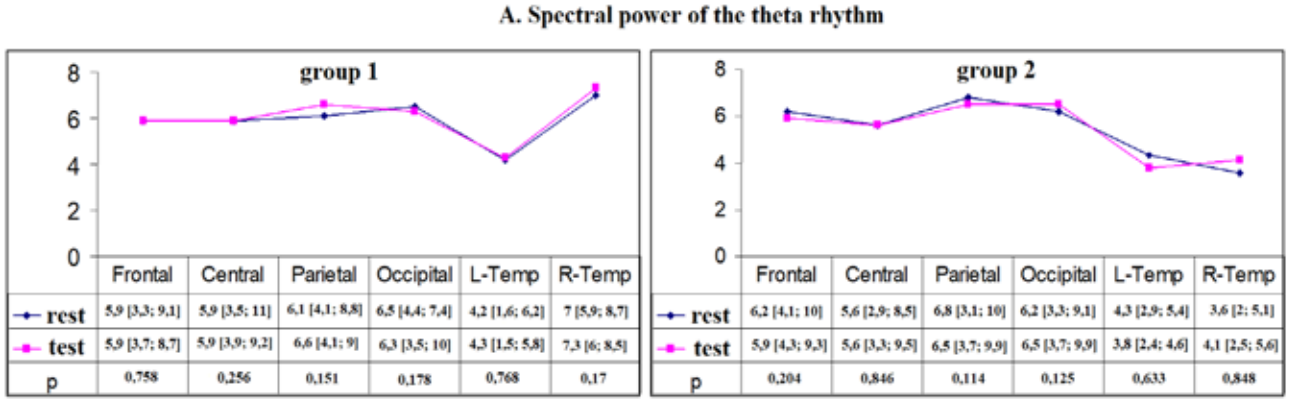

	Frontal	Central	Parietal	Occipital	L-Temp	R-Temp
rest	5,9 [3,3; 9,1]	5,9 [3,5; 11]	6,1 [4,1; 8,8]	6,5 [4,4; 7,4]	4,2 [1,6; 6,2]	7 [5,9; 8,7]
test	5,9 [3,7; 8,7]	5,9 [3,9; 9,2]	6,6 [4,1; 9]	6,3 [3,5; 10]	4,3 [1,5; 5,8]	7,3 [6; 8,5]
p	0,758	0,256	0,151	0,178	0,768	0,17

	Frontal	Central	Parietal	Occipital	L-Temp	R-Temp
rest	6,2 [4,1; 10]	5,6 [2,9; 8,5]	6,8 [3,1; 10]	6,2 [3,3; 9,1]	4,3 [2,9; 5,4]	3,6 [2; 5,1]
test	5,9 [4,3; 9,3]	5,6 [3,3; 9,5]	6,5 [3,7; 9,9]	6,5 [3,7; 9,9]	3,8 [2,4; 4,6]	4,1 [2,5; 5,6]
p	0,204	0,846	0,114	0,125	0,633	0,848

a

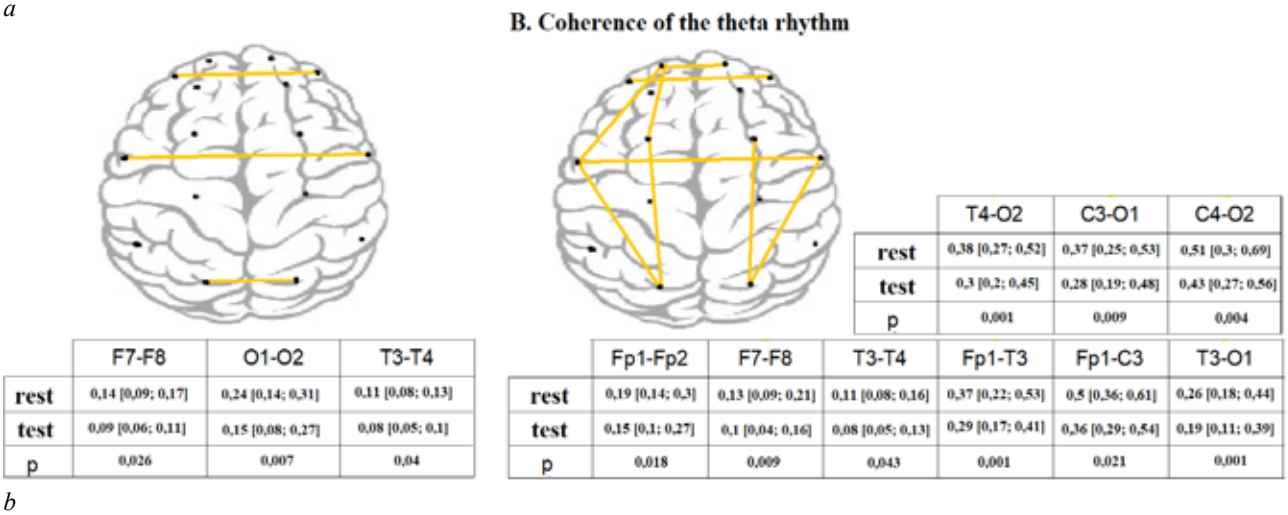

	T4-O2	C3-O1	C4-O2
rest	0,38 [0,27; 0,52]	0,37 [0,25; 0,53]	0,51 [0,3; 0,69]
test	0,3 [0,2; 0,45]	0,28 [0,19; 0,48]	0,43 [0,27; 0,56]
p	0,001	0,009	0,004

	F7-F8	O1-O2	T3-T4
rest	0,14 [0,09; 0,17]	0,24 [0,14; 0,31]	0,11 [0,08; 0,13]
test	0,09 [0,06; 0,11]	0,15 [0,08; 0,27]	0,08 [0,05; 0,1]
p	0,026	0,007	0,04

	Fp1-Fp2	F7-F8	T3-T4	Fp1-T3	Fp1-C3	T3-O1
rest	0,19 [0,14; 0,3]	0,13 [0,09; 0,21]	0,11 [0,08; 0,16]	0,37 [0,22; 0,53]	0,5 [0,36; 0,61]	0,26 [0,18; 0,44]
test	0,15 [0,1; 0,27]	0,1 [0,04; 0,16]	0,08 [0,05; 0,13]	0,29 [0,17; 0,41]	0,36 [0,29; 0,54]	0,19 [0,11; 0,39]
p	0,018	0,009	0,043	0,001	0,021	0,001

b

Fig. 5. Dynamics of EEG theta rhythm during the "Go/No – Go" test,
Median [Q_1; Q_3]; * level of statistical significance when comparing groups using Wilcoxon criterion at $p < 0.05$

were observed in both hemispheres. These changes may be due to the fact that when inhibitory control is violated, there is an increased need to activate additional parts of the brain to perform cognitive function. Third, in terms of coherence parameters, we observed significant brain structures involvement in patients with impaired inhibitory control during the Go/No-Go test, and in all frequency ranges. This also confirms the conclusion that the functional activity of the cortex is deficient in patients with AUD with impaired inhibitory control.

CONCLUSION

In general, the results of this study allow us to supplement and improve the understanding of neural functioning in cognitive processes, especially inhibitory control in patients with AUD. Our study showed the ability of the EEG method to detect differences in the electrical activity of the brain during the Go/No-Go task among patients with AUD with or without impaired inhibitory control. A better understanding of the various correlates of alcohol-related behavior and neural effects on regulatory processes can help in the diagnosis of AUD, as well as in the creation of predictive criteria for pathological attraction to alcohol.

REFERENCES

1. Ahmadi A., Pearlson G., Meda S., Dager A., Potenza M., Rosen R., Austad C., Raskin S., Fallahi C., Tennen H., Wood R., Stevens M. Influence of alcohol use on neuronal response to Go/No-Go task in college drinkers. *Neuropsychopharmacology*. 2013; 38 (11): 2197–2208. DOI: 10.1038/npp.2013.119.
2. Petit G., Cimochowska A., Kornreich C., Hanak C., Verbanck P., Campanella S. Neurophysiological correlates of response inhibition predict relapse in detoxifield alcoholic patients: some preliminary evidence from event-related potentials. *Neuropsychiat., Dis. Treat.* 2014; 10: 1025–1037. DOI: 10.2147/NDT.S61475.
3. Lopez-Caneda E., Roriguez S., Cadaveira F., Corral M., Doallo S. Impact of alcohol use on inhibitory control (and vice versa) during adolescence and young adulthood: a review. *Alcohol and Alcoholism*. 2014; 49 (2): 173–181. DOI: 10.1093/alcalc/agt168.
4. Field M., Wiers R., Christiansen P., Fillmore M., Verster J.

Acute alcohol effects on inhibitory control and implicit cognition: implications for loss of control over drinking. *Alcohol Clin. Exp. Res.* 2010; 34 (8): 1346–1352. DOI: 10.1111/j.1530-0277.2010.01218.x.
5. Marakshina J. A. the lateral asymmetry in the task of suppressing the response: electrophysiological investigation of cognitive control. *The Oretical and Experimental Psychology*. 2016; (3): 17–26 (in Russ.).
6. Ames S., Wong S., Bechara A., Cappelli C., Dust M., Grenard J., Stacy A. Neural correlates of a Go/NoGo task with alcohol stimuli in light and heavy young drinkers. *Behav. Brain. Res*. 2014; 274: 382–389. DOI: 10.1016/j.bbr.2014.08.039.
7. Simmonds D., Pekar J., Mostofsky S. Meta-analysis of Go/No–go tasks demonstrating that fMRI activation associated with response inhibition is task-dependent. *Neuropsychologia*. 2008; 46 (1): 224–232. DOI: 10.1016/j.neuropsychologia.2007.07.015.
8. Zhao X., Qian W., Fu L., Maes J. Deficits in go/no-go task performance in male undergraduate high-risk alcohol users are driven by speeded responding to go stimuli. *The American Journal of Drug and Alcohol Abuse*. 2017;43 (6): 656–663. DOI: 10.1080/00952990.2017.1282502.
9. Melnikova T.S., Lapin I.A., Sarkisyan V.V. Review of the use of coherent EEG analysis in psychiatry. *Social and clinical psychiatry*. 2009; (1): 90–94 (in Russ.).
10. Yanina A.S. Features of alpha-activity of the brain on the background of meditative psychological training. *Bulletin of Siberian medicine*. 2016; (3): 95–101 (in Russ.). DOI: 10.20538/1682-0363-2016-3-95-101.
11. Cherniy V.I., Andronova I.A., Gorodnik G.A., Cherniy T.V., Nazarenko K.V., Andronova M.A. Study of EEG predictors of neurotransmitter and neuroglial activity in patients with acute cerebral insufficiency of different Genesis. *Emergency Medicine.* 2016; (4): 45–56 (in Russ.).
12. Trusova A.V., Klimanova S.G. Cognitive control in alcohol dependence: a review of current research. *Clinical and medical Psychology: Research, Training*, *Practice.* 2015. (3): 9 (in Russ.).
13. Jackson J., Karnani M., Zemelman B., Burdakov D., Lee A. Inhibitory control of prefrontal cortex by the claustrum. *Neuron.* 2018; 99 (5): 1029–1039. DOI: 10.1016/j.neuron.2018.07.031.
14. Sallard E., Mouthon M., De Pretto M., Spierer L. Modulation of inhibitory control by prefrontal anodal tDCS: A crossover doubleblind sham-controlled fMRI study. *PLoS ONE*. 2018; 13 (3): e0194936. DOI: 10.1371/journal.pone.0194936.

Authors contribution

Galkin S.A. – development of the research concept, neurophysiological examination of the sample, data analysis, drafting of the article. Peshkovskaya A.G. – design of the study. Roshchina O.V. – clinical and psychopathological examination of the sample. Kisel N.I. – clinical and psychopathological examination of the sample. Ivanova S.A. – final approval of the manuscript for publication. Bokhan N.A. – final approval of the manuscript for publication.

Authors information

Galkin Stanislav A., Post-Graduate Student, Mental Health Research Institute, Tomsk NRMC, Tomsk, Russian Federation. ORCID 0000-0002-7709-3917.

Peshkovskaya Anastasia G., Researcher, Mental Health Research Institute, Tomsk NRMC, Tomsk, Russian Federation. ORCID 0000-0002-3951-395X.

Roshchina Olga V., Researcher, Mental Health Research Institute, Tomsk NRMC, Tomsk, Russian Federation. ORCID 0000-0002-2246-7045.

Kisel Nataliya I., Cand. Sci. (Med.), Mental Health Research Institute, Tomsk NRMC, Tomsk, Russian Federation. ORCID 0000-0002-5607-7491.

Ivanova Svetlana A., Dr. Sci. (Med.), Professor, Head of the Laboratory of Molecular Genetics and Biochemistry, Deputy Director for Science, Mental Health Research Institute, Tomsk NRMC, Tomsk, Russian Federation. ORCID 0000- 0001-7078-323X.

Bokhan Nikolay A., Dr. Sci. (Med.), Professor, Academician of the Russian Academy of Sciences, Director of the Mental Health Research Institute, head of the Department of Psychiatry, Psychotherapy, Narcology with the course of Medical Psychology, SSMU, Tomsk, Russian Federation. ORCID 0000-0002-1052-855X.

(✉) **Galkin S.A.,** e-mail: s01091994@yandex.ru.

Received 18.11.2019
Accepted 30.04.2020

УДК 616.894-053.8-021.6-092:612.822.56
https://doi.org/10.20538/1682-0363-2020-4-46-52

Aberrant angiogenesis in brain tissue in experimental Alzheimer's disease

Gorina Ya.V., Komleva Yu.K., Osipova E.D., Morgun A.V., Malinovskaya N.A., Lopatina O.L., Salmina A.B.

Krasnoyarsk State Medical University named after Prof. V.F. Voino-Yasenetsky
1, Partizana Zheleznyaka Str., Krasnoyarsk, 660022, Russian Federation

ABSTRACT

The aim was to study the molecular mechanisms of the violation of the structural and functional integrity of the blood-brain barrier in chronic neurodegeneration of the Alzheimer's type associated with the development of cerebral angiopathy.

Materials and methods. The transgenic model of Alzheimer's disease is the B6SLJ-Tg line mice (APPSwFlLon, PSEN1*M146L*L286V) 6799Vas group which includes 9 months aged males. The control group included C57BL/6xSJL mice, males aged 9 months.

Results. The total length of the vessels in the area of the dentate gyrus is 2.5 times greater in transgenic animal models of Alzheimer's disease than in animals of the control group ($p < 0.01$). The average diameter of blood vessels in all areas of the hippocampus is smaller compared with the control ($p < 0.05$). Transgenic modeling of neurodegeneration in the CA2 zone of the hippocampus increases the relative area of tissue with increased permeability of blood-brain barrier (BBB) (17.80 [9.15; 36.75]) compared to control (1.38 [0.04; 7.60]) at $p < 0.05$. A similar difference ($p < 0.05$) is also observed in the hippocampal area CA1. A tendency ($p > 0.05$) to decrease the number of CD31+ endothelial cells in the dentate gyrus of the hippocampus (21.52 [17.56; 24.50]) in animals of the experimental group compared with the control group (23.08[21.18; 29.84]) was detected. A similar situation is observed in the CA2 and CA3 areas of the hippocampus.

Conclusion. Neurodegenerative changes in the hippocampus of animals with a transgenic AD model are associated with impaired microcirculation in the brain tissue as a result of a reduction in the diameter and branching of blood vessels, and damage and increased permeability of BBB.

Key words: angiogenesis, blood-brain barrier, CD31, Alzheimer's disease.

Conflict of interest. The authors declare the absence of obvious or potential conflicts of interest related to the publication of this article.

Source of funding. This work was supported by the grant awarded by the President of the Russian Federation for state support of leading scientific schools of the Russian Federation (6240.2018.7).

Compliance with ethical standards. The experiments were carried out after consideration of the application and protocol for the use of laboratory animals at a meeting of the bioethical commission at the local Ethics Commission at Krasnoyarsk State Medical University of the Russian Ministry of Health (Protocol No. 3 of October 08.10.2018).

For citation: Gorina Ya.V., Komleva Yu.K., Osipova E.D., Morgun A.V., Malinovskaya N.A., Lopatina O.L., Salmina A.B. Aberrant angiogenesis in brain tissue in experimental Alzheimer's disease. *Bulletin of Siberian Medicine.* 2020; 19 (4): 46–52. https://doi.org/10.20538/1682-0363-2020-4-46-52.

✉ *Gorina Yana V.,* e-mail: yana_20@bk.ru.

Аберрантный ангиогенез в ткани головного мозга при экспериментальной болезни Альцгеймера

Горина Я.В., Осипова Е.Д., Моргун А.В., Малиновская Н.А., Комлева Ю.К., Лопатина О.Л., Салмина А.Б.

Красноярский государственный медицинский университет (КрасГМУ) имени профессора В.Ф. Войно-Ясенецкого
Россия, 660022, г. Красноярск, ул. Партизана Железняка, 1

РЕЗЮМЕ

Цель – изучение молекулярных механизмов нарушения структурно-функциональной целостности гематоэнцефалического барьера (ГЭБ) при хронической нейродегенерации альцгеймеровского типа, ассоциированной с развитием церебральной ангипопатии.

Материалы и методы. Опытная группа – генетическая модель болезни Альцгеймера (БА) – мыши линии B6SLJ -Tg(APPSwFlLon,PSEN1*M146L*L286V)6799Vas, самцы в возрасте 9 мес. Контрольная группа – мыши линии C57BL/6 x SJL, самцы в возрасте 9 мес.

Результаты. У животных с генетической моделью БА в зубчатой извилине гиппокампа общая длина сосудов в 2,5 раза больше, чем у контрольной группы ($p < 0,01$), при этом средний диаметр сосудов во всех областях гиппокампа меньше по сравнению с контролем ($p < 0,05$). Выявлено, что при генетическом моделировании нейродегенерации в CA2 зоне гиппокампа наблюдается увеличение относительной площади ткани с повышенной проницаемостью ГЭБ (17,80 [9,15;36,75]) по сравнению с контролем (1,38 [0,04;7,60]) при $p < 0,05$. Подобное различие ($p < 0,05$) наблюдается и в зоне CA1 гиппокампа. У животных опытной группы выявлена тенденция ($p > 0,05$) к снижению количества CD31+ эндотелиальных клеток в зубчатой извилине гиппокампа (21,52 [17,56; 24,50]) по сравнению с контролем (23,08 [21,18; 29,84]). Аналогичная ситуация наблюдается в зонах CA2 и CA3 гиппокампа.

Заключение. Нейродегенеративные изменения в гиппокампе животных с генетической моделью БА ассоциированы с нарушением микроциркуляции в ткани головного мозга в результате сокращения диаметра и разветвленности сосудов, повреждения и повышения проницаемости ГЭБ.

Ключевые слова: ангиогенез, гематоэнцефалический барьер, CD31, болезнь Альцгеймера.

Конфликт интересов. Авторы декларируют отсутствие явных и потенциальных конфликтов интересов, связанных с публикацией настоящей статьи.

Источник финансирования. Работа выполнена при поддержке гранта Президента РФ для государственной поддержки ведущих научных школ РФ (RSh-6240.2018.7).

Соответствие принципам этики. Исследование одобрено локальным этическим комитетом КрасГМУ (протокол № 3 от 08.10.2018).

Для цитирования: Горина Я.В., Осипова Е.Д., Моргун А.В., Малиновская Н.А., Комлева Ю.К., Лопатина О.Л., Салмина А.Б. Аберрантный ангиогенез в ткани головного мозга при экспериментальной болезни Альцгеймера. *Бюллетень сибирской медицины*. 2020; 19 (4): 46–52. https://doi.org/10.20538/1682-0363-2020-4-46-52.

INTRODUCTION

Alzheimer's disease (AD) is a common neurodegenerative disease among older people, characterized by the accumulation of beta-amyloid plaques, neurofibrillary tangles, and death of neuronal cells [1]. Experimental data established using magnetic resonance imaging indicate that AD without concomitant pathological disorders is much less common than dementia, accompanied by pronounced vascular changes [2]. This confirms the significant contribution of vascular disorders to the development of cognitive dysfunction and, as a consequence, neurodegeneration.

It is believed that beta-amyloid (Aβ) contributes to the damage to microvessels, the development of cerebral amyloid angiopathy (CAA), rupture of the vascular wall, and impaired cerebral perfusion [3]. Thus,

as a result of a study of the brain of patients with AD with multiple cerebral microbleeds, low levels of Aβ in the cerebrospinal fluid were revealed. This is probably the result of an increased cerebral intravascular deposition of Aβ, which leads to a violation of the integrity of the vascular wall, causing microbleeding [4]. In addition, studies on two models of transgenic lines of mice with stroke (APPswe / PS1dE9 and tg2576) showed that cerebrovascular disorders affect the clearance of Aβ and, therefore, contribute to its deposition in the brain area with pronounced damaged blood vessels [5]. Also, brain damage caused by impaired cerebral circulation increases the expression of amyloid beta precursor protein (APP) and, therefore, Aβ cleavage. Thus, against the background of Aβ deposition, which causes cerebrovascular dysfunction, subsequent ischemia can enhance the expression of APP and Aβ cleavage, forming positive feedback and leading to a violation of the structural and functional integrity of the neurovascular unit (an integrated unit that consists of microvascular endothelial cells functionally associated with neurons, astrocytes, pericytes, and extracellular matrix components) [6].

It is important to note that with age, the permeability of the blood-brain barrier increases in patients with vascular dementia, namely, in sections of brain tissue (hippocampus and cortex), and an accumulation of neurotoxic blood proteins (thrombin, albumin, and immunoglobulins) is observed [7]. In addition, a violation of the BBB integrity in the hippocampus, especially the CA1 area and the dentate gyrus, correlates with the development of cognitive dysfunction and the destruction of pericytes [8].

Thus, a violation of the BBB integrity may contribute to the progression of AD associated with the development of CAA. However, the molecular mechanisms underlying the pathogenesis are not completely clear. The purpose of this study is to study the mechanisms of violation of the structural and functional integrity of the BBB in chronic Alzheimer's type neurodegeneration associated with the development of CAA.

MATERIALS AND METHODS

The experimental group consisted of transgenic mice models of AD (a model of the formed neurodegenerative changes) mice of the B6SLJ-Tg line (APPSwFlLon,PSEN1*M146L*L286V)6799Vas, males aged 9 months (n = 5). The control group consisted of C57BL/6xSJL mice, males aged 9 months (n = 5). These mouse lines were obtained from The Jackson Laboratory.

In vivo study of BBB permeability was performed by evaluating the permeability of the Evans blue dye in sections of the brain 4–5 hours after its intraperitoneal injection (2% solution in 0.9% NaCl solution, in a volume of 4 ml/kg of animal weight) according to the protocol described [9]. Transcardial perfusion of the brain with 10% formalin was performed to the animals. The Evans blue dye fluorescence area percent of the total area of the vessels in the field of view in the coronal sections of the brain (thickness 50 μm) was calculated using confocal microscopy. Evaluation of the CD31 expression (Abcam, ab28364, rabbit polyclonal, 1: 1000) on free-floating sections was carried out using the standard method of simultaneous combined staining of the drug (free-floating sections staining protocol from Abcam, USA) [10]. The percentage of cells expressing CD31 was calculated (of the total cell number in the vascular region in the field of view, calculated from the nuclei of DAPI-positive cells localized in the vascular region) in three fields of view. Confocal microscopy was performed using an Olympus FV10i-W microscope (Japan). When analyzing photographs, Olympus FLUOVIEW Viewer 4.0 (Japan) was used.

The study of the features of the formation of the vascular network (angiogenesis) was conducted by the microscopic method using a ZOE microscope with photofixation and subsequent processing of the obtained photographs in ImageJ v1.43 (USA). The total length of the vasculature, the number of visible vessels, the number of branch points of the vessels, and the average diameter of the vessels in 1 mm^3 of the hippocampal tissue in the areas CA1, CA2, CA3, dentate gyrus (DG) were calculated.

Statistical analysis of the results was carried out using the Statplus Professional program, assembly 5.9.8.5/Core v.5.9.3.33 using nonparametric statistical methods in GraphPad6.0 program. To compare the performance in independent samples, the Mann – Whitney test was used. Differences were considered significant at $p \leq 0.05$. The results are presented in the form Me [Q_1; Q_3], where Me is the median, Q_1 is the lower quartile, Q_3 is the upper quartile, and p is the significance level.

RESULTS

It was revealed that the total length of the vessels in the dentate gyrus region in transgenic animals is 2.5 times greater than in animals of the control group (p = 0.006) (Fig. 1,*a*). Moreover, the total number of vessels in the CA1 area and the dentate gyrus exceed-

ed the values of the control animals 2.5 and 3 times, respectively ($p = 0.008$) (Fig. 1*b*). However, the number of branch points of blood vessels was significantly higher (1.5–2 times) in the CA1, CA2, CA3 regions in the control animals compared with the animals of the experimental group (Fig. 1,*c*). The mean vessel diameter was statistically significantly smaller in animals with a transgenic model of AD than in animals of the control group in all studied areas of the hippocampus (Fig. 1*d*). Thus, the formation of CAA is accompanied by remodeling of the vascular network of the hippocampus.

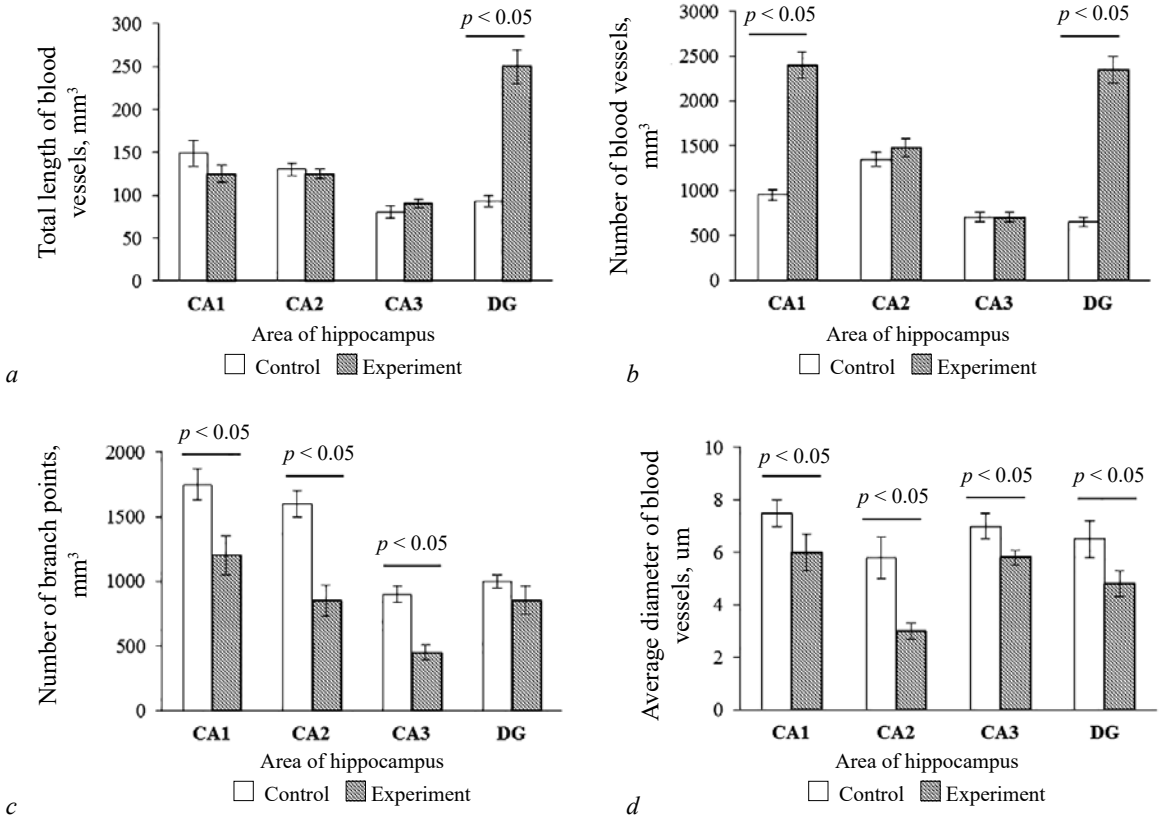

Fig. 1. Features of the vascular network (angiogenesis) in certain areas of the hippocampus in the experimental groups: *a* – total length of blood vessels, mm^3, *b* – number of blood vessels, mm^3, *c* – number of branch points, mm^3, *d* – average diameter of blood vessels; experimental group – animals with a transgenic model of Alzheimer's disease, control group – wild-type animals

We evaluated BBB permeability using Evans blue as a marker for BBB damage. We found that the relative area of brain tissue containing Evans blue dye in the CA2 zone of the hippocampus of transgenic animals is statistically significantly ($p = 0.025$) greater (17.80 [9.15; 36.75]) compared to the control group (1.38 [0.04; 7.60]) (Fig. 2,*a*). A similar statistically significant difference ($p = 0.033$) is also observed in the CA1 zone of the hippocampus (Fig. 2,*a*). The tendency ($p = 0.149$) to increase the relative area containing the dye in the dentate gyrus of the hippocampus is observed in animals of the experimental group (7.37 [1.25; 27.83]) compared with the control group (1.11 [0.05]; 6.35]) (Fig. 2,*a*). A similar situation ($p = 0.157$) was also detected in the CA3 zone of the hippocampus (Fig. 2,*a*).

The results above formed our interest in assessing the expression pattern of one of the endothelial cell markers, namely, CD31, in various hippocampal subregions in animals with a transgenic model of AD. We revealed a tendency ($p = 0.223$) to decrease the number of CD31+ endothelial cells in the dentate gyrus of the hippocampus in animals of the experimental group (21.52 [17.56; 24.50]) compared with the control group (23.08 [21.18; 29.84]) (Fig. 2,*b*). A similar situation is observed in the CA2 and CA3 zones of the hippocampus (Fig. 2,*b*). However, a statistically significant ($p = 0.028$) increase in the number of CD31+ cells in the CA1 hippocampal subregion is observed in animals with a transgenic model of AD (30.41 [20.50; 31.82]) compared with the control group (22.56 [15, 70; 25.34]) (Fig. 2,*b*).

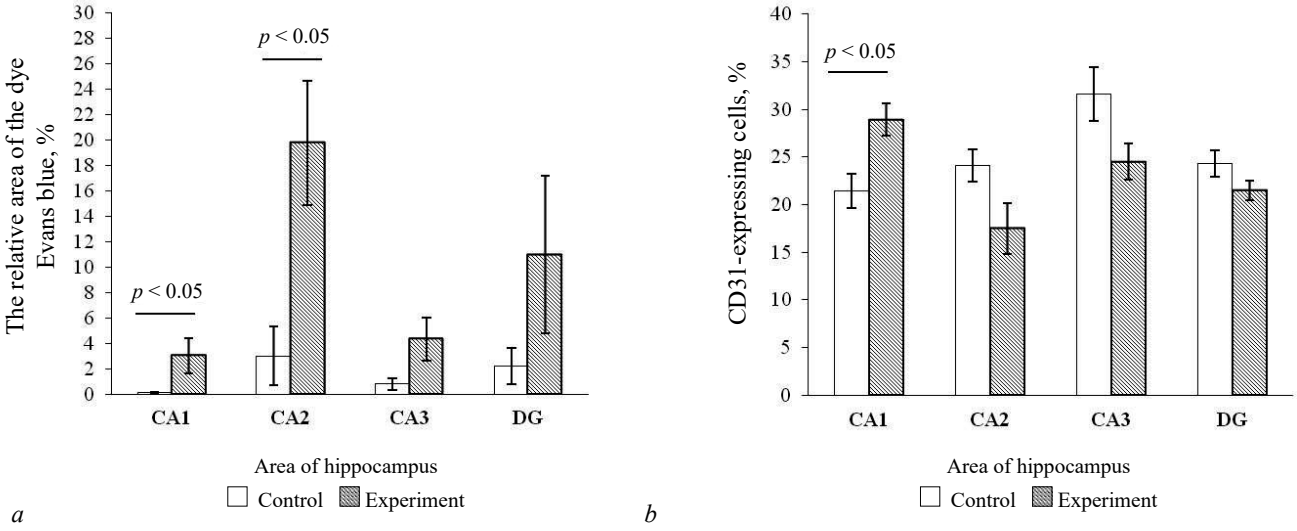

Fig. 2. Permeability of BBB *in vivo* and an expression of CD31: *a* – the amount dye of Evans blue in certain areas of the hippocampus (%) in the experimental groups; *b* – the number of cells expressing CD31 in certain areas of the hippocampus (%) in the experimental groups; experimental group – animals with a transgenic model of Alzheimer's disease, control group – wild-type animals

DISCUSSION

CAA has been shown to play a key role in the pathogenesis of dementia. CAA is most common with the development of a sporadic form of AD, which indicates the presence of a pronounced relationship between AD and cerebral angiopathy. In addition, various microvascular disorders, in particular, decreased capillary density, vascular atrophy, and endothelial dysfunction are observed in the brain with AD progression [11]. It is known that the action of angiogenic growth factors and cytokines in brain tissue leads to the activation of endothelial cells. This promotes the formation of a microvascular network, which increases local microcirculation, inducing the flow of oxygen and nutrients into the affected tissue. The endothelium also has a direct local effect, producing at least 20 paracrine factors that affect neighboring cells. Although many of these factors are anti-apoptotic, toxic substances, including neurotoxins and Aβ precursors, are also released in microvessels of affected tissues [12].

Our study showed significant changes in the microvascular bed of the hippocampus in animals with formed manifestations of chronic neurodegeneration. At the same time, the CA1 subregion of the hippocampus is the most affected area (an increase in the total number of vessels, a decrease in the number of branches of the vasculature, and a decrease in the average diameter of microvessels). Since we found that high levels of CD31 cells remained in precisely this hippocampal subregion, it is logical to assume that the CA1 zone and the dentate gyrus of the hippocampus dominate in the process of the microvascular network remodeling during Alzheimer's type neurodegeneration. Thus, the processes of the microvascular bed remodeling are multidirectional in the hippocampal subregions in animals with experimental AD: neoangiogenesis is typical for the CA1 zone of the hippocampus and the dentate gyrus, and local microcirculation disorders due to the reduction in the diameter and branching of the vessels is typical for the CA2 and CA3 subregions.

These results are consistent with the data on the intensification of the brain neoangiogenesis in experimental animals during Alzheimer's neurodegeneration [13]. This may be accompanied by the development of pathological BBB permeability due to the impaired expression of tight junction proteins of cerebral endothelial cells. At the microvascular level, endothelial cell and BBB dysfunction may be associated with decreased cerebral blood flow and hypoxia. In addition, Aβ concentration in microvessels can contribute to further damage to endothelial cells, which may be one of the links in the AD pathogenesis [14]. An impaired, due to endothelial dysfunction, Aβ drainage can lead to the accumulation of amyloid plaques in the brain parenchyma. Experimental data show [15] that the action of Aβ on proteins of tight and adhesive junctions can change the BBB permeability. Damage to the BBB leads to the death of neuronal cells, glia acti-

vation, and immune infiltration into the parenchyma. This has negative consequences for the affected areas of the brain: hormonal dysregulation in hypothalamic lesions [16], cognitive impairment in hippocampal lesions [17], which contribute to the progression of AD.

Thus, our results indicate that an increase in BBB permeability is most characteristic of the CA2 subregion of the hippocampus, to a lesser extent, the CA1 sub-region, and, most likely, the dentate gyrus of the hippocampus. A significant increase in BBB permeability may be associated with intensive neoangiogenesis, microvessel remodeling (decreased branching of vessels and a reduction in mean vessel diameter, and an increased expression of CD31 in the CA1 hippocampal subregion) against the background of the development of CAA.

CONCLUSION

It was found that neurodegenerative changes in the hippocampus of transgenic mice related to the Aβ accumulation are associated with the local disturbance of microcirculation. This is a consequence of a reduction in the diameter and branching of blood vessels, an increase in BBB permeability, and suppression of neoangiogenesis (except the CA1 subregion) as the disease progresses. These observations emphasize the importance of future research for a clear understanding of the molecular mechanisms of cerebral microcirculatory disorders and a violation of the structural and functional integrity of the BBB in chronic Alzheimer's disease neurodegeneration.

REFERENCES

1. Kumfor F., Piguet O. Emotion recognition in the dementias: brain correlates and patient implications. *Neurodegener Dis. Manag.* 2013; 3 (3): 277–288. DOI: 10.2217/nmt.13.16.
2. Chui H.C., Ramirez-Gomez L. Clinical and imaging features of mixed Alzheimer and vascular pathologies. *Alzheimers Res. Ther.* 2015; 7 (1): 21. DOI: 10.1186/s13195-015-0104-7.
3. Kalaria R.N. Small vessel disease and Alzheimer's dementia: pathological considerations. *Cerebrovasc Dis.* 2002; 13(2): 48–52. DOI: 10.1159/000049150.
4. Goos J.D.C., Kester M.I., Barkhof F., Klein M., Blankenstein M.A., Scheltens P. van der Flier W.M. Patients with Alzheimer disease with multiple microbleeds. *Stroke.* 2009; 40 (11): 3455–3460. DOI: 10.1161/STROKEAHA.109.558197.
5. Garcia-Alloza M., Gregory J., Kuchibhotla K.V., Fine S., Wei Y., Ayata C., Frosch M.P., Greenberg S.M., Bacskai B.J. Cerebrovascular lesions induce transient β-amyloid deposition. *Brain.* 2011; 134 (12): 3694–3704. DOI: 10.1093/brain/awr300.
6. Uryu K., Laurer H., McIntosh T., Praticò D., Martinez D., Leight S., Lee V.M., Trojanowski J.Q. Repetitive mild brain trauma accelerates Aβ deposition, lipid peroxidation, and cognitive impairment in a transgenic mouse model of alzheimer amyloidosis. *J. Neurosci.* 2002; 22 (2): 446–454. DOI: 10.1523/JNEUROSCI.22-02-00446.2002.
7. Sengillo J.D., Winkler E.A., Walker C.T., Sullivan J.S., Johnson M., Zlokovic B.V. Deficiency in mural vascular cells coincides with blood-brain barrier disruption in Alzheimer's disease. *Brain Pathol.* 2013; 23 (3): 303–310. DOI: 10.1111/bpa.12004.
8. Montagne A., Barnes S.R., Sweeney M.D., Halliday M.R., Sagare A.P., Zhao Z., Toga A.W., Jacobs R.E., Liu C.Y., Amezcua L., Harrington M.G., Chui H.C., Law M., Zlokovic B.V. Blood-brain barrier breakdown in the aging human hippocampus. *Neuron.* 2015; 85 (2): 296–302. DOI: 10.1016/j.neuron.2014.12.032.
9. Manaenko A., Chen H., Kammer J., Zhang J. H., Tang J. Comparison evans blue injection routes: intravenous versus intraperitoneal, for measurement of blood-brain barrier in a mice hemorrhage model. *J. Neurosci. Methods.* 2011; 195 (2): 206–210. DOI: 10.1016/j.jneumeth.2010.12.013.
10. Encinas J.M., Enikolopov G. Identifying and quantitating neural stem and progenitor cells in the adult brain. *Methods Cell Biol.* 2008; 85: 243–272. DOI: 10.1016/S0091-679X(08)85011-X.
11. Kalaria R.N. Neuropathological diagnosis of vascular cognitive impairment and vascular dementia with implications for Alzheimer's disease. *Acta Neuropathol.* 2016; 131 (5): 659–685. DOI: 10.1007/s00401-016-1571-z.
12. Grammas P., Moore P., Weigel P.H. Microvessels from Alzheimer'sdisease brains kill neurons in vitro. *Am. J. Pathol.* 1999; 154 (2): 337–342. DOI: 10.1016/S0002-9440(10)65280-7.
13. Biron K.E., Dickstein D.L., Gopaul R., Jefferies W.A. Amyloid triggers extensive cerebral angiogenesis causing blood brain barrier permeability and hypervascularity in Alzheimer's disease. *PLoS One.* 2011; 6 (8): e23789. DOI: 10.1371/journal.pone.0023789.
14. Burgmans S., van de Haar H. J., Verhey F. R. J., Backes W. H. Amyloid-β interacts with blood-brain barrier function in dementia: a systematic review. *J. Alzheimers Dis.* 2013; 35 (4): 859–873. DOI: 10.3233/JAD-122155.
15. Marco S., Skaper S.D. Amyloid beta-peptide1-42 alters tight junction protein distribution and expression in brain microvessel endothelial cells. *Neurosci. Lett.* 2006; 401 (3): 219–224. DOI: 10.1016/j.neulet.2006.03.047.
16. Jais A., Brüning J.C. Hypothalamic inflammation in obesity and metabolic disease. *J. Clin. Invest.* 2017; 127 (1): 24–32. DOI: 10.1172/JCI88878.
17. Davidson T.L., Monnot A., Neal A.U., Martin A.A., Horton J.J., Zheng W. The effects of a high-energy diet on hippocampal-dependent discrimination performance and blood-brain barrier integrity differ for diet-induced obese and diet-resistant rats. *Physiol. Behav.* 2012; 107 (1): 26–33. DOI: 10.1016/j.physbeh.2012.05.015..

Authors contribution

Gorina Ya.V. – analysis and interpretation of immunohistochemical data. Osipova E.D. – assessment of the features of the formation of the vascular network (angiogenesis). Morgun A.V. – analysis and interpretation of angiogenesis research data. Malinovskaya N.A. – assessment of BBB permeability. Komleva Yu.K. – conception and design. Lopatina O.L. – design drawings. Salmina A.B. – critical revision for important intellectual content and final approval of the manuscript for publication.

Authors information

Gorina Yana V., Cand. Sci. (Pharmacy), Associate Professor, Department of Biological Chemistry, Krasnoyarsk State Medical University, Krasnoyarsk, Russian Federation. ORCID 0000-0002-3341-1557.

Osipova Elena D., Senior Teacher, Department of Biological Chemistry, Krasnoyarsk State Medical University, Krasnoyarsk, Russian Federation. ORCID 0000-0002-9718-1260.

Morgun Andrei V., Dr. Sci. (Med.), Assistant, Pediatrics Department of the Institute of Post-graduate Education, Krasnoyarsk State Medical University, Krasnoyarsk, Russian Federation. ORCID 0000-0002-9644-5500.

Malinovskaya Nataliya A., Dr. Sci. (Med.), Professor, Department of Biological Chemistry of Krasnoyarsk State Medical University, Krasnoyarsk, Russian Federation. ORCID 0000-0002-0033-3804.

Komleva Yuliya K., Cand. Sci. (Med.), Associate Professor, Department of Biological Chemistry, Krasnoyarsk State Medical University, Krasnoyarsk, Russian Federation. ORCID 0000-0001-5742-8356.

Lopatina Olga L., Dr. Sci. (Biology), Professor, Department of Biological Chemistry, Krasnoyarsk State Medical University, Krasnoyarsk, Russian Federation. ORCID 0000-0002-7884-2721.

Salmina Alla B., Dr. Sci. (Med.), Professor, Head of the Department of Biological Chemistry, Head of the Research Institute of Molecular Medicine and Pathological Biochemistry, Krasnoyarsk State Medical University, Krasnoyarsk, Russian Federation. ORCID 0000-0002-9170-0867.

(✉) **Gorina Yana V.,** e-mail: yana_20@bk.ru.

Received 25.08.2019
Accepted 25.12.2019

УДК 616.33-006.6:612.015
https://doi.org/10.20538/1682-0363-2020-4-53-60

Redox forms of glutathione in malignant lesions of the stomach with varying aggressiveness degrees

Goroshinskaya I.A., Surikova E.I., Frantsiyants E.M., Neskubina I.V., Nemashkalova L.A., Medvedeva D.E., Maslov A.A.

National Medical Research Centre for Oncology
63, 14 Liniya Str., Rostov-on-Don, 344037, Russian Federation

ABSRACT

Aim. To study the levels of reduced and oxidized glutathione (GSH and GSSG, respectively), as well as the thiol status in gastric cancer (GC) tumors of various histological types and grades.

Materials and methods. The indicators were determined by ELISA methods in tumor, peritumoral and visually intact tissues obtained during surgery from 52 patients with GC: 18 patients had a G1-2 adenocarcinoma (AC), 8 with G3 AC, 6 with signet ring cell cancer (SRCC), 14 with combined gastric lesions (CGL) – AC with signet ring cell fragments, 6 with patients with a component of undifferentiated cancer, G4.

Results. In the groups of patients with low-differentiated and undifferentiated tumors, the GSH content in the tumor tissue and the peritumoral zone was higher than in the group of patients with well- and moderately-differentiated tumors. Tumor GSH levels in G3 AC and SRCC exceeded the values in visually intact tissues. Moreover, in the visually intact tissue of patients with SRCC, GSH level was reduced relative to G1-2 AC and CGL. GSH in all tissues of patients with CGL was higher than in patients with G1-2 AC. The lowest level of GSSG in the tumor tissue was registered in SRCC: 27.5% lower than in G1-2 AC and 30.3% lower than in G3 AC. Patients with undifferentiated tumors (G4 AC) had the highest GSH content in all studied tissues: by 29.9% in tumor; by 40.7% in peritumoral zone; and in visually intact tissue not only GSH, but also GSSG was increased by 22.5–25.5% in comparison with AC G1-2. G4 AC was also characterized by a sharp increase in the thiol status in tumor tissues by 80.2 and 89.9% higher than in visually intact and peritumoral tissues, and it was statistically higher than in AC G1-2, AC G3, SRCC and CGL. The ratio of GSH and GSSG was the most informative.

Conclusion. Poor AC differentiation (in the row G1-2, G3, G4) and a change of histological tumor type (AC, SPL and SRCC), i.e. an increase in tumor aggressiveness, were accompanied by the enhancement of reductive processes in tumor tissue, as evidenced by the statistically significant increase in the GSH/GSSG coefficient and a sharp increase in the thiol status in G4 AC.

Key words: stomach cancer, various tumor histotypes, tumor tissue, peritumoral and visually intact zones, reduced glutathione, oxidized glutathione, thiol status.

Conflict of interest. The authors declare the absence of obvious or potential conflict of interest related to the publication of this article.

Source of financing. The study was performed as part of the state assignment of National Medical Research Centre for Oncology for 2018–2020 No. AAAA18-118072790016-2 “Development of prognostic algorithms based on the detection of new laboratory factors for the prognosis of malignant tumors”.

Conformity with the principles of ethics. All patients signed an informed consent. The study was approved by the Ethics Committee at Rostov Research Institute of Oncology (Protocol No. №11/1 of 03.11.2016).

For citation: Goroshinskaya I.A., Surikova E.I., Frantsiyants E.M., Neskubina I.V., Nemashkalova L.A., Medvedeva D.E., Maslov A.A. Redox forms of glutathione in malignant lesions of the stomach with varying aggressiveness degrees. *Bulletin of Siberian Medicine.* 2020; 19 (4): 53–60. https://doi.org/10.20538/1682-0363-2020-4-53-60.

✉ *Goroshinskaya Irina A.,* e-mail: iagor17@mail.ru.

Редокс формы глутатиона при злокачественном поражении желудка разной степени агрессивности

Горошинская И.А., Сурикова Е.И., Францянц Е.М., Нескубина И.В., Немашкалова Л.А., Медведева Д.Е., Маслов А.А.

Национальный медицинский исследовательский центр (НМИЦ) онкологии
Россия, 344037, г. Ростов-на-Дону, ул. 14-я линия, 63

РЕЗЮМЕ

Цель: изучить уровень восстановленного и окисленного глутатиона (GSH и GSSG соответственно), а также тиоловый статус в опухолях рака желудка (РЖ) различных гистологических типов и разной степени дифференцировки.

Материалы и методы. Показатели определены методами иммуноферментного анализа в образцах опухоли, перитуморальной зоны и визуально интактной ткани. Образцы получены во время операции у 52 больных РЖ, в том числе у 18 – с аденокарциномой (АК) G1-2, 8 – с АК G3, 6 – с перстневидноклеточным раком (ПКР), 14 – с сочетанным поражением желудка (СПЖ) и 6 – с компонентом недифференцированного рака G4.

Результаты. В группах больных с низкодифференцированными и недифференцированными опухолями содержание GSH в ткани опухоли и перифокальной зоны было выше, чем в группе больных с высоко- и умеренно дифференцированными опухолями. При АК G3 и ПКР уровень GSH в опухолевой ткани значимо превышал уровень в визуально интактной ткани. При этом в визуально интактной ткани больных ПКР содержание GSH было ниже, чем при АК G1-2 и СПЖ. При СПЖ уровень GSH во всех тканях был выше, чем при АК G1-2.

Наиболее низкий уровень GSSG в ткани опухоли отмечен при ПКР: на 27,5% ниже, чем при АК G1-2, и на 30,3% относительно АК G3. При АК G4 наблюдалось самое высокое содержание GSH во всех исследованных тканях: в опухоли – на 29,9%, в перифокальной зоне – на 40,7%, а в визуально интактной ткани не только GSH, но и GSSG на 22,5–25,5% по сравнению со значениями у больных АК G1-2. Для G4 также характерен высокий уровень тиолового статуса в ткани опухоли – на 80,2 и 89,9% выше, чем в визуально интактной ткани и перитуморальной зоне, и он был значимо выше (на 68–96%), чем при АК G1-2, АК G3, ПКР и СПЖ. Наиболее информативным оказалось соотношение восстановленной и окисленной форм глутатиона.

Заключение. При снижении дифференцировки АК (в ряду G1-2, G3, G4) и изменении гистологического типа опухоли (АК, СПЖ и ПКР), т.е. при увеличении агрессивности неоплазмы, происходит усиление восстановительных процессов в опухолевой ткани, о чем свидетельствует статистически значимо более высокий коэффициент GSH/GSSG и уровень тиолового статуса в случае АК G4.

Ключевые слова: рак желудка, различные гистотипы опухоли, ткани опухоли, перетуморальная и визуально интактная зона, восстановленный глутатион, окисленный глутатион, тиоловый статус.

Конфликт интересов. Авторы декларируют отсутствие явных и потенциальных конфликтов интересов, связанных с публикацией настоящей статьи.

Источник финансирования. Исследование выполнялось в рамках госзадания НМИЦ онкологии на 2018–2020 гг. № АААА-А18-118072790016-2 «Разработка прогностических алгоритмов на основе выявления новых лабораторных факторов прогноза течения злокачественных опухолей».

Соответствие принципам этики. Все пациенты подписали информированное согласие. Исследование одобрено советом по этике Ростовского научно-исследовательского онкологического института (протокол № 11/1 от 03.11.2016).

Для цитирования: Горошинская И.А., Сурикова Е.И., Францянц Е.М., Нескубина И.В., Немашкалова Л.А., Медведева Д.Е., Маслов А.А. Редокс формы глутатиона при злокачественном поражении желудка разной степени агрессивности. *Бюллетень сибирской медицины.* 2020; 19 (4): 53–60. https://doi.org/10.20538/1682-0363-2020-4-53-60.

INTODUCTION

Gastric cancer (GC), which is a malignant tumor originating from the epithelium of the gastric mucosa, remains one of the most common diseases in the world. According to world statistics, GC is the fifth leading cause of cancer death and affects about 1 million people every year [1–3].

The main histological type of GC is adenocarcinoma, divided by the degree of differentiation into well-differentiated G1, moderately-differentiated G2 and low-differentiated adenocarcinoma G3. According to US statistics, the incidence of adenocarcinoma approaches 90% of all stomach tumors [4].

Another histological type of GC is signet ring cell cancer (SRCC), the frequency of which is increasing, according to some authors [5]. Gastric SRCC is usually associated with poor survival and low treatment efficacy in comparison with gastric adenocarcinoma. However, a meta-analysis showed no differences in survival between patients with SRCC and non-SRCC in the general population. The authors found that the early stages of SRCC were associated with a better prognosis, while advanced SRCC was associated with a worse prognosis [6].

Undifferentiated carcinoma is a relatively rare disease of the stomach, the incidence in Europe is about 1400 cases per year with mortality reaching 1250 cases per year [7]. This is the most aggressive form of stomach disease with absolutely atypical cells that are unable to differentiate. Its characteristic features are rapid predominantly infiltrative growth and metastasis in the early stages. In 75% of patients, undifferentiated gastric cancer metastasizes at the beginning of treatment.

The ability to produce a large number of reactive oxygen species (ROS) is one of the characteristic features of cancer cells that distinguish them from normal cells. This leads to an increased dependence of tumor cells on the antioxidant defense system [8]. Understanding the biology of redox processes that underlie the development of oncological pathology, and the mechanisms of their functioning, is of great importance for the development of new therapeutic approaches targeting resistant tumors based on changes in the redox status of a neoplasm and its surrounding tissues [9, 10]. This determines the relevance of studying the redox characteristics of a particular tumor and its environment, especially in tumors of the stomach.

Glutathione plays a central role in protecting cells from oxidative damage, which makes it one of the main active components of cancer pathophysiology [11]. Reduced glutathione and glutathione-dependent enzymes are of great importance for the normal functioning of the intestinal epithelium of the stomach, which refers to tissues that are characterized by continuous cell renewal, and the constancy of the epithelial structure is ensured only by coordinating the proliferation, differentiation, and apoptosis phases. If the balance of redox processes is disturbed, the initiation of malignant transformation and the progression of neoplasia are possible [12, 13].

In the human body, glutathione is present in several redox forms, among which the most important are reduced glutathione (GSH) and oxidized glutathione (GSSG). Reduced glutathione accounts for up to 98% of the total pool of glutathione under normal conditions [14]. The concentration and role of GSH are differentiated and depend on the type of cells. GSH is a soluble antioxidant that is present in high cellular concentrations (1–10 mM) in the cytoplasm, mitochondria, and nucleus. Mitochondria contain 10% of the cellular glutathione [15]. Red blood cells are rich in glutathione and contain 99% of the GSH content versus 1% present in plasma [16]. Plasma contains only about 20 μM glutathione with the dominant form of GSSG [17].

Earlier, we showed the features of redox systems in tumor tissue and surrounding tissues of gastric adenocarcinoma [18], as well as changes in the antioxidant status of the blood in patients with gastric cancer [19].

The aim of this study was to compare the levels of reduced and oxidized glutathione, as well as the thiol status in various histological types of stomach tumors. The indicators were studied in tumor tissue, peritumoral zone and conditionally healthy tissue in patients with gastric adenocarcinoma of different differentiation degrees, signet ring cell cancer and combined gastric lesions.

MATERIALS AND METHODS

This study included tissues obtained during the operation of 52 patients with gastric cancer (28 men and 24 women), divided into 5 groups according to the tumor histotype: adenocarcinoma G1–2 – 18 patients (T2–4N0–2M0); G3 adenocarcinoma – 8 patients (T2–4N0–3M0); adenocarcinoma with the presence of undifferentiated cells (G3 + G4) – 6 patients (T2–4N1–3M0–1); combined gastric lesion (adenocarcinoma G2 or G3 with the presence of signet ring cell fragments) – 14 patients (T3–4 N0–3M0–1); signet ring cell cancer – 6 patients (T1–4N1–3M0–1). The groups were comparable by gender and age (50–84 years).

Histological control was performed in all cases. All patients gave voluntary informed consent for the use of biological material. The content of reduced and oxidized glutathione (redox forms of glutathione), as well as the thiol status were studied by ELISA methods in the tissues of the tumor, peritumoral zone, and conditionally healthy tissues (visually intact) obtained on the resection line.

Statistical processing of the results was carried out using the Statistika 6.0 software package according to the Student's *t*-test for two independent samples, as well as using the non-parametric Mann – Whitney criterion. The samples were preliminarily checked for compliance with the normal distribution according to the Shapiro–Wilk *W*-test for small samples. Correction for comparison multiplicity was performed using the FDR control (False Discovery Rate control: Benjamini, Hochberg, 1995) [20]. The differences were considered statistically significant at $p < 0.05$, and the level of the statistical trend towards significance was observed at $0.1 > p > 0.05$. In the tables, the data were presented in the form $M \pm m$, where M is the sample mean; m is the error of the mean.

RESULTS

The predominance of patients with well- and moderately-differentiated adenocarcinoma in the study is consistent with the data presented in other studies [21].

As can be seen in Table 1, the content of GSH in the tumor tissue was higher than in the conditionally healthy tissue of the stomach in all groups of patients with gastric cancer; however, significant differences were detected only in SRCC. The GSSG content in SRCC and in patients with T4 status and at IV stage of the process, on the contrary, was significantly lower in the tumor tissue compared with conditionally healthy tissue.

Table 1

The content of reduced (μg/g tissue) and oxidized (ng/g tissue) glutathione in the tumor tissue and adjacent areas in patients with gastric cancer with different histology and stages of the malignant process, $M \pm m$

Histology	Tumor	Peritumoral zone	Conditionally healthy tissue
Adenocarcinoma G1-2, $n = 18$			
GSH	871.04 ± 40.07	790.79 ± 39.64	837.51 ± 21.27
GSSG	499.14 ± 22.54	513.73 ± 23.17	473.97 ± 14.71
Adenocarcinoma (AC) G3, $n = 8$			
GSH	968.46 ± 39.8	942.99 ± 47.87	808.05 ± 66.76
GSSG	519.02 ± 28.61	554.12 ± 27.39	456.04 ± 45.91
Combined tumor (AC + SRCC), $n = 14$			
GSH	983.02 ± 29.9	943.79 ± 32.87	958.51 ± 56.21
GSSG	460.48 ± 25.04	$p < 0.025$ 464.5 ± 13.71	502.49 ± 19.58
SRCC, $n = 6$			
GSH	810.95 ± 40.6 $p_1 = 0.095$ $p_2 < 0.02$	718.21 ± 16.45 $p_1 = 0.01$ $p_2 < 0.002$	693.01 ± 17.86 $p < 0.002$ $p_2 < 0.03$ $p_{tum} < 0.05$
GSSG	361.69 ± 26.46 $p = 0.02$ $p_1 = 0.01$	440.18 ± 37.28	504.72 ± 15.51 $p_{tum} < 0.002$
SRCC and combined tumor, $n = 20$			
GSH	925.66 ± 30.57	876.11 ± 33.18	878.86 ± 48.14
GSSG	430.84 ± 21.53 $p_1 = 0.075$	457.2 ± 14.36	503.16 ± 14.24 $p_{tum} < 0.02$ $p_{per} < 0.03$
Undifferentiated tumor (G3+G4), $n = 6$			
GSH	1,131.16 ± 111.22 $p < 0.075$ $p_3 < 0.07$	1,112.53 ± 113.2 $p < 0.02$ $p_2 = 0.095$	1,026.22 ± 29.04 $p < 0.0006$ $p_3 < 0.00001$
GSSG	527.52 ± 34.13. $p_3 = 0.01$	$p_3 = 0.018$ 512.63 ± 59.58	594.65 ± 11.3 $p < 0.001$

Table 1 (continued)

Histology	Tumor	Peritumoral zone	Conditionally healthy tissue
T4 or IV st., $n = 10$			
GSH	905.48 ± 56.31	800.98 ± 46.2 $p_2 < 0.035$ $p_4 = 0.010$	812.67 ± 32.93 $p_3 < 0.03$ $p_4 = 0.0006$
GSSG	436.2 ± 26.66	459.8 ± 27.5	515.77 ± 15.51 $p_{tum} < 0.04$

Note. Statistical significance of differences with FDR multiplicity correction: p – relative to AC G1-2, p_1 – relative to AC G3, p_2 – relative to combined lesion, p_3 – relative to SRCC, p_4 – relative to AC G4, p_{tum} – relative to tumor tissue, p_{per} – relative to peritumoral tissue.

In the groups of patients with low-differentiated and undifferentiated tumors, the GSH content in the tumor tissue and the peritumoral zone was higher than in the group of patients with well- and moderately-differentiated tumors. In SRCC, the level of GSSG in the tumor tissue was lower by 27.5% relative to AC G1-2 and by 30.3% relative to AC G3 (p = 0.01-002). Moreover, in conditionally healthy tissue of patients with SRCC, the GSH content was reduced by 17.3% relative to AC G1-2 ($p < 0.002$). Patients with undifferentiated cancer (AC G4) were characterized by an increase in the GSH content in all the tissues examined: by 29.9% in the tumor, by 40.7% in the peritumoral zone, while healthy tissues showed an increase in both GSH (by 22.5%) and GSSG (by 25.5%) compared with values in patients with AC G1-2.

The most informative was the ratio of the reduced and oxidized forms of glutathione ($GSH/GSSG \times 10^{-3}$), presented in Table 2.

Table 2

The ratio of the reduced and oxidized forms of glutathione in the tumor tissue and adjacent areas in patients with gastric cancer with different histology and stages of the malignant process

Histology	Tumor	Peritumoral zone	Conditionally healthy tissue
Adenocarcinoma G1-2, $n = 18$	1.656 ± 0.081	1.611 ± 0.102	1.815 ± 0.087
Adenocarcinoma (AC) G3, $n = 8$	1.89 ± 0.094	1.701 ± 0.004	1.83 ± 0.115
Combined tumor (AC + SRCC), $n = 14$	2.228 ± 0.153 $p < 0.005$	2.058 ± 0.098 $p < 0.015$ $p_1 < 0.05$	1.947 ± 0.136
SRCC, $n = 6$	2.29 ± 0.161 $p < 0.005$	1.689 ± 0.137 $p_{tum} = 0.018$	1.383 ± 0.073 $p < 0.05$ $p_1 = 0.05$ $p_2 = 0.075$ $p_{tum} < 0.001$
SRCC and combined tumor, $n = 20$	2.249 ± 0.113 $p < 0.005$	1.947 ± 0.087 $p < 0.05$ $p_{tum} = 0.039$	1.778 ± 0.113 $p_{tum} < 0.015$
Undifferentiated tumor (G3 + G4), $n = 6$	2.246 ± 0.357 $p < 0.05$	2.205 ± 0.09 $p < 0.02$ $p_1 < 0.001$ $p_3 < 0.05$	1.728 ± 0.052 $p_3 < 0.01$ $p_{per} < 0.005$
T4 or IV st., $n = 10$	2.146 ± 0.093 $p < 0.005$	1.755 ± 0.066 $p_4 = 0.001$ $p_{tum} = 0.003$	1.596 ± 0.09 $p_{tum} < 0.005$

Note. Statistical significance of differences with FDR multiplicity correction: p – relative to AC G1-2, p_1 – relative to AC G3, p_2 – relative to combined lesion, p_3 – relative to SRCC, p_4 – relative to AC G4, p_{tum} – relative to tumor tissue, p_{per} – relative to peritumoral tissue.

In patients with undifferentiated cells (G3 + G4), this coefficient was higher than in patients with G1–2 by 35.6% ($p < 0.05$) in the tumor tissue and by 36.9% in the peritumoral zone ($p < 0.02$). In patients with tumor germination in the serous membrane and spreading to neighboring structures (T4), as well as at stage IV of the process, this indicator was higher than in patients with G1–2 by 30% ($p < 0.005$). The highest ratio of the

reduced and oxidized forms of glutathione was found in the tumors of patients with SRCC, which was higher than in patients with G1–2 by 38.3% ($p < 0.005$). The value in the tumors of patients with combined gastric lesions exceeded the value at G1–2 by 34.5%.

The data on the thiol status are presented in Table 3. As can be seen in the table, 4 out of 16 patients with well- and moderately-differentiated adenocarcinoma had high values of this indicator in tumor tissue, and in the whole group it was higher than in patients with low-differentiated adenocarcinoma by 70.4% ($p < 0.005$). The level of the indicator in patients with SRCC and patients with combined lesions of the stomach occupied an intermediate position.

Table 3

The thiol status μg/g tissue in the tumor tissue and adjacent areas in patients with gastric cancer with different histology and stages of the malignant process, $M \pm m$

Histology	Tumor	Peritumoral zone	Conditionally healthy tissue
Adenocarcinoma G1-2, $n = 16$ $n = 4$ $n = 12$	156.62 ± 9.93 218.74 ± 5.84 125.91 ± 7.41	132.94 ± 10.04	124.16 ± 11.97
Adenocarcinoma (AC) G3, $n = 8$	91.91 ± 10.75 $p < 0.005$	115.1 ± 9.8	110.88 ± 15.94
Combined tumor (AC+SRCC), $n = 14$	128.76 ± 14.78	104.43 ± 5.54	115.76 ± 14.39
SRCC, $n = 6$	129.0 ± 19.58	122.26 ± 15.49	130.69 ± 10.52
SRCC and combined tumor, $n = 20$	128.83 ± 11.61	109.78 ± 6.09	120.24 ± 10.51
Undifferentiated tumor (G3+G4), $n = 6$	217.26 ± 15.71 $p < 0.02$ $p_1 < 0.0001$ $p_2 = 0.09$ $p_3 < 0.02$	114.39 ± 16.91 $p_{tum} < 0.005$	120.58 ± 20.43 $p_{tum} = 0.004$
T4 or IV st., $n = 10$	114.17 ± 20.76 $p = 0.09$	119.23 ± 5.81	115.85 ± 10.13

Note. Statistical significance of differences with FDR multiplicity correction: p – relative to AC G1-2, p_1 – relative to AC G3, p_2 – relative to combined lesion, p_3 – relative to SRCC, p_{tum} – relative to tumor tissue.

The high level of the thiol status in the tumor tissue of adenocarcinoma with the presence of undifferentiated cells (G4) was of interest: 80.2% and 89.9% higher than in the visually intact tissue and peritumoral zone ($p < 0.005$). It was 38.7% higher ($p < 0.02$) than in the tumor tissue of AC G1-2, 136.4% higher ($p < 0.0001$) than in AC G3, and 68.6% higher ($p < 0.02$) than in SRCC and combined lesions.

DISCUSSION

A study of the levels of glutathione redox forms showed that the GSH content in the tumor tissue was higher than in the conditionally healthy stomach tissue in all groups of patients with gastric adenocarcinoma, but the degree of difference depended on the histological type and differentiation of the tumor. The redox status of glutathione, i.e. the ratio of reduced and oxidized glutathione, was most disturbed in the tumor tissue in SRCC. It should be noted that the reduced / oxidized glutathione ratio within the cell is considered to be one of the most important parameters that characterizes the level of oxidative stress [22].

A high level of GSH in patients with low-differentiated adenocarcinoma, and especially in patients with undifferentiated cells in the tumor, as well as a significantly higher ratio of reduced and oxidized forms of glutathione in patients with SRCC, combined gastric lesions and undifferentiated gastric carcinoma indicate the role of reduced glutathione in maintaining the ability of the tumor to grow and progress.

Apart from being a powerful antioxidant, reduced glutathione has a number of functions that are not related to ROS protection. It is involved in the detoxification of electrophilic compounds (xenobiotics), as well as in the metabolism of the prostaglandins and leukotrienes, in the transport of amino acids and in the absorption of trace elements from the intestine, mainly iron and selenium. However, the dominant role of GSH is undoubtedly as an antioxidant. It is not only a trap of free radicals, but it also deals with the restoration of damaged cells. Due to the presence of a thiol group (-SH) in a molecule, GSH has the ability to protect other thiol groups in proteins from oxidative damage [14]. In this regard, the almost twice as high

thiol status detected only in tumor tissue in undifferentiated tumors of the stomach is of interest for further research and analysis. The most important functions of SH groups in biological systems include the formation of complexes with metal ions, participation in the oxidation reactions and the formation of thiol radicals and disulfides [17]. As an antioxidant, GSH lowers ROS levels during enzymatic and non-enzymatic reactions. It regenerates other oxidized low molecular weight antioxidants, for example, vitamin C and vitamin E. Moreover, it is involved in the restoration of protein molecules, nucleic acids and lipids damaged in peroxidation processes, and in maintaining the sulfhydryl groups of proteins in a reduced state, which is necessary for DNA repair and expression [23–25]. The oxidized form, glutathione disulfide (GSSG), can be reduced to GSH. Consequently, the GSH / GSSG ratio is considered an important indicator of the redox balance in cells, and a higher ratio means less oxidative stress [26].

The latest *in vitro* studies are of undoubted interest, showing that both reduced and oxidized glutathione inhibit the formation of superoxide (O_2^-) by inhibiting the quinoid oxidation of adrenaline [27]. This enhances the importance of further studies of the glutathione redox forms in pathological conditions and may lead to a change in the prevailing ideas about the exclusive role of reduced glutathione as an antioxidant and require some adjustment of the alleged participation mechanisms of the glutathione system in carcinogenesis and antitumor effects.

CONCLUSION

An analysis of our data and the above information on the characteristics of the antioxidant role of glutathione contributes to the understanding of its involvement in malignant progression in various histotypes of gastric tumors. Poor differentiation of adenocarcinoma (in the row G1–2, G3, G4) and a change in the histological type of the tumor (adenocarcinoma, combined lesion of the stomach, SRCC), i.e. an increase in the aggressiveness of the tumor, was accompanied by an increase in the reductive processes of the tumor tissue, as evidenced by the statistically significant increase in the GSH/GSSG coefficient and a sharp increase in the thiol status in undifferentiated tumors (G4). An increase in GSH with poor differentiation of adenocarcinoma, as well as a higher ratio of the reduced and oxidized forms of glutathione in patients with SRCC, combined lesions and undifferentiated adenocarcinoma of the stomach, indicate the probable participation of reduced glutathione in maintaining the tumor's ability to grow and progress.

REFERENCES

1. Jemal A., Bray F., Center M.M., Ferlay J., Ward E., Forman D. Global cancer statistics. *Cancer Journal for Clinicians.* 2011; 61 (2): 69–90. DOI: 10.3322/caac.20107.
2. Torre L.A., Bray F., Siegel R.L., Ferlay J., Lortet-Tieulent J., Jemal A. Global cancer statistics, 2012. *CA Cancer J. Clin.* 2015; 65 (2): 87–108. DOI: 10.3322/caac.21262.
3. Sitarz R., Skierucha M., Mielko J., Offerhaus G.J.A., Maciejewski R., Polkowski W.P. Gastric cancer: epidemiology, prevention, classification, and treatment. *Cancer Manag. Res.* 2018; 10: 239–248. DOI: 10.2147/CMAR.S149619.
4. American Cancer Society. Cancer Facts & Figures 2016. Atlanta: American Cancer Society; 2016.
5. Henson D.E., Dittus C., Younes M. et al. Differential trends in the intestinal and diffuse types of gastric carcinoma in the United States, 1973–2000: increase in the signet ring cell type. *Arch. Pathol. Lab. Med.* 2004; 128 (7): 765–770. DOI: 10.1043/1543-2165(2004)128<765:DTITIA>2.0.CO;2.
6. Nie R.C., Yuan S.Q., Li Y.F., Chen Y.M., Chen X.J., Zhu B.Y., Xu L.P., Zhou Z.W., Chen S., Chen Y.B. Clinicopathological characteristics and prognostic value of signet ring cells in gastric carcinoma: A Meta-Analysis. *Journal of Cancer.* 2017; 8 (17): 3396–3404. DOI: 10.7150/jca.21017.
7. Gatta G., Capocaccia R., Trama A., Martínez-García C.; RARECARE Working Group. The burden of rare cancers in Europe. *Adv. Exp. Med. Biol*. 2010; 686: 285–303. DOI: 10.1007/978-90-481-9485-8_17.
8. Prasad S., Gupta S.C., Tyagi A.K. Reactive oxygen species (ROS) and cancer: Role of antioxidative nutraceuticals. *Cancer Letters.* 2017; 387: 95–105. DOI: 10.1016/j.canlet.2016.03.042.
9. Policastro L.L., Ibañez I.L., Notcovich C., Duran H.A., Podhajcer O.L. The tumor microenvironment: characterization, redox considerations, and novel approaches for reactive oxygen species-targeted gene therapy. *Antiox. & Redox Sign.* 2013; 19: 854–895. DOI: 10.1089/ars.2011.4367
10. Castaldo S.A., Freitas J.R., Conchinha N.V., Madureira P.A. The tumorigenic roles of the cellular redox regulatory systems. *Oxid. Med. Cell. Longev.* 2015; Article ID 8413032. DOI: 10.1155/2016/8413032.
11. Andrisic L., Dudzika D., Barbasa C., Milkovicb L., Grunec T., Zarkovic N. Short overview on metabolomics approach to study pathophysiology of oxidative stress in cancer. *Redox Biology*. 2018; 14: 47–58. DOI: 10.1016/j.redox.2017.08.009.
12. Oktyabrsky O.N., Smirnova G.V. Redox regulation of cellular functions. *Biochemistry.* 2007; 72(2): 158–175 (in Russ.).
13. Dawane J.S., Pandit V.A. Understanding redox homeostasis and its role in cancer. *J. Clin. Diagnos. Res.* 2012; 6(10): 1796–1802. DOI: 10.7860/JCDR/2012/4947.2654.
14. Mironczuk-Chodakowska I., Witkowska A.M., Zujko M.E. Endogenous non-enzymatic antioxidants in the human body. *Advances in Medical Sciences.* 2018; 63(1): 68–78. DOI: 10.1016/j.advms.2017.05.005.

15. Marí M., Morales A., Colell A., García-Ruiz C., Fernández-Checa J.C. Mitochondrial glutathione, a key survival antioxidant. *Antioxid. Redox. Signal.* 2009; 11 (11): 2685–2700. DOI: 10.1089/ARS.2009.2695.
16. Samuelsson M., Vainikka L.,Öllinger K. Glutathione in the blood and cerebrospinal fluid: a study in healthy male volunteers. *Neuropeptides.* 2011; 45 (4): 287–292. DOI: 10.1016/j.npep.2011.05.004.
17. Lushchak V.I. Glutathione homeostasis and functions: potential targets for medical interventions. *J. Amino Acids.* 2012; 2012: 736837. DOI: 10.1155/2012/736837.
18. Surikova E.I., Goroshinskaja I.A., Nerodo G.A., Frantsiyants E.M., Malejko M.L., Shalashnaja E.V., Kachesova P.S., Nemashkalova L.A., Leonova A.V. Activity of redox-regulatory systems in the tumor and surrounding tissues in various histological types of tumors. *Biomedical Chemistry*. 2016; 62 (2): 187–192. DOI: 10.18097/PBMC20166202187.
19. Francijanc E.M., Orlovskaja L.A., Shalashnaya E.V., Musienko N.V., Anapaljan V.H. Changes in the antioxidant status of the blood of patients with inoperable gastric cancer after chemotherapy. *Problems in Oncology.*1999; 45(6): 607–611 (in Russ.).
20. Korn E.L., Troendle J.F., McShane L.M., Simon R. Controlling the number of false discoveries: application to high-dimensional genomic data. *Journal of Statistical Planning and Inference*. 2004; 124 (2): 379–398. DOI: 10.1016/S0378-3758(03)00211-8.
21. Wang D., Wang B., Wang R., Zhang Z., Lin Y., Huang G., Lin S., Jiang Y., Wang W., Wang L., Huang Q. High expression of EGFR predicts poor survival in patients with resected T3 stage gastric adenocarcinoma and promotes cancer cell survival. *Oncology Letters.* 2017; 13 (5): 3003–3013. DOI: 10.3892/ol.2017.5827.
22. Proskurnina E.V. Methods for assessing free radical blood homeostasis. Dissertation. Moscow, 2018: 221 (in Russ.).
23. Aquilano K., Baldelli S., Ciriolo M.R. Glutathione: new roles in redox signaling for an old antioxidant. *Front. Pharmacol.* 2014; 5: 196. DOI: 10.3389/fphar.00196.
24. Alli J.A., Kehinde A.O., Kosoko A.M., Ademowo O.G. Oxidative stress and reduced vitamins C and E levels are associated with multi-drug resistant tuberculosis. *J. Tuberc. Res*. 2014; 2: 52–58. DOI: 10.4236/jtr.2014.21006.
25. Chatterjee A. Reduced glutathione: a radioprotector or a modulator of DNA-repair activity? *Nutrients*. 2013; 5 (2): 525–542. DOI: 10.3390/nu5020525.
26. Sentellas S., Morales-Ibanez O., Zanuy M., Albertí J.J. GSSG/GSH ratios in cryopreserved rat and human hepatocytes as a biomarker for drug induced oxidative stress. *Toxicol. Vitr.* 2014; 28 (5): 1006–1015. DOI: 10.1016/j.tiv.2014.04.017.
27. Sirota T.V. Effect of the sulfur-containing compounds on the quinoid process of adrenaline autoxidation; potential neuroprotectors. *Biomedical Chemistry.* 2019; 65 (4): 316–323 (in Russ.). DOI: 10.18097/PBMC20196504316.

Authors contribution

Goroshinskaya I.A. – analysis and interpretation of the results and literature data, statistical processing of the results, writing and design of the article. Surikova E.I. – analysis of clinical indicators of patients to divide them into groups, participation in the selection of literature. Frantsiyants E.M. – final approval of the manuscript for publication. Neskubina I.V. – determination of parameters. Nemashkalova L.A. – preparation of tissues for research. Medvedeva D.E. – collection of material for research and provision of information on patients. Maslov A.A. – diagnosis, determination of a treatment plan for patients included in the study, operations.

Authors information

Goroshinskaya Irina A., Dr. Sci. (Biology), Professor, Senior Researcher, National Medical Research Centre for Oncology, Rostov-on-Don, Russian Federation. ORCID 0000-0001-6265-8500.

Surikova Ekaterina I., Cand. Sci. (Biology), Senior Researcher, National Medical Research Centre for Oncology, Rostov-on-Don, Russian Federation. ORCID 0000-0002-4318-7587.

Frantsiyants Elena M., D. Sci. (Biology), Professor, Deputy General Director for Science, National Medical Research Centre for Oncology, Rostov-on-Don, Russian Federation. ORCID 0000-0003-3618-6890.

Neskubina Irina V., Cand. Sci. (Biology), Senior Researcher, National Medical Research Centre for Oncology, Rostov-on-Don, Russia Russian Federation. ORCID 0000-0002-7395-3086.

Nemashkalova Lyidmila A., Researcher, National Medical Research Centre for Oncology, Rostov-on-Don, Russian Federation. ORCID 0000-0003-2713-8598.

Medvedeva Dar'ja E., Oncologist, Post-Graduate Student, National Medical Research Centre for Oncology, Rostov-on-Don, Russian Federation.

Maslov Andrey A., Dr. Sci. (Med.), Professor, Head of the Department of Abdominal Oncology No. 3, National Medical Research Centre for Oncology, Rostov-on-Don, Russian Federation. ORCID 0000-0003-4902-5789.

(✉) **Goroshinskaya Irina A.,** e-mail: iagor17@mail.ru.

Received: 03.09.2019
Accepted: 30.04.2020

УДК 612.216.2:616.23/.24-002.2:616.24-006.6
https://doi.org/10.20538/1682-0363-2020-4-61-66

Changes in the ventilation function of the lungs during the formation of chronic obstructive pulmonary disease and its combination with lung cancer

Dobner S.Yu.[1], Dubakov A.V.[2], Porovskiy Ya.V.[2], Tuzikov S.A.[1, 2], Miller S.V.[1], Rodionov E.O.[1, 2]

[1] *Cancer Research Institute, Tomsk National Research Medical Center (NRMC) of Russian Academy of Sciences*
5, Kooperativny Str., Tomsk, 634009, Russian Federation

[2] *Siberian State Medical University*
2, Moscow Trakt, Tomsk, 634050, Russian Federation

ABSTRACT

Aim. To study the ventilation function of the lungs in patients with varying degrees of severity of chronic obstructive pulmonary disease (COPD) and in patients with COPD combined with lung cancer (LC), as well as to establish the features of its disorders using spirography and body plethysmography.

Materials and methods. A clinical and functional study of 57 individuals was carried out with 10 healthy patients (control group), 30 patients with COPD and 17 patients in whom LC was combined with COPD using the Masterlab Pro diagnostic complex (Erich Jaeger, Germany).

Results. In patients with early COPD, a decrease in MEF_{75} (a ventilation parameter characterizing small airway patency) is the most informative. With the progression of bronchial obstruction, both restrictive and obstructive disorders, characterized by a decrease in FEV_1, VC, a change in the structure of the total lung capacity in the form of an increase in the RV/TLC ratio such as an increase in the RV/TLC ratio and an increase in bronchial resistance were recorded. In patients with LC and mild COPD, pulmonary volumes, capacities, flow-volume loop and bronchial resistance parameters did not differ from patients with COPD with a similar bronchial obstruction. In patients with LC and more severe COPD, in contrast to patients suffering from a similar severity of COPD, a decrease in the patency of large, medium and small diameter bronchi (PEF, MEF_{25}, MEF_{50}, MEF_{75}) was detected, which indicated development of generalized bronchial obstruction.

Conclusion. Modern diagnostics of pulmonary ventilation disorders in patients with LC and COPD should be aimed at identifying the disease, and drug therapy should target maximum leveling of reversible components of bronchial obstruction in order to increase the functional reserve of the respiratory system and reduce the risk of postoperative complications caused by COPD.

Key words: chronic obstructive pulmonary disease, lung cancer, pulmonary ventilation function, spirography, bodyplethysmography.

Conflict of interest. The authors declare the absence of obvious or potential conflicts of interest related to the publication of this article.

Source of financing. The authors received no specific funding for this work.

Conformity to the principles of ethics. All patients signed an informed consent to participate in the study. The study was approved by the local Ethics Committee at Cancer Research Institute, Tomsk NRMC (Protocol No. 10 of 26.09.2016).

For citation: Dobner S.Yu., Dubakov A.V., Porovskiy Ya.V., Tuzikov S.A., Miller S.V., Rodionov E.O. Changes in the ventilation function of the lungs during the formation of chronic obstructive pulmonary disease and its

✉ *Dobner Svetlana Yu.,* e-mail: dobnersv@gmail.com.

combination with lung cancer. *Bulletin of Siberian Medicine.* 2020; 19 (4): 61–66. https://doi.org/10.20538/1682-0363-2020-4-61-66.

Изменение вентиляционной функции легких в процессе формирования хронической обструктивной болезни легких и при ее сочетании с раком легкого

Добнер С.Ю.[1], Дубаков А.В.[2], Поровский Я.В.[2], Тузиков С.А.[1, 2], Миллер С.В.[1], Родионов Е.О.[1, 2]

[1] Научно-исследовательский институт (НИИ) онкологии, Томский национальный исследовательский медицинский центр (НИМЦ) Российской академии наук
Россия, 634009, г. Томск, пер. Кооперативный, 5

[2] Сибирский государственный медицинский университет (СибГМУ)
Россия, 634050, г. Томск, Московский тракт, 2

РЕЗЮМЕ

Цель. Изучение вентиляционной функции легких у пациентов с различной степенью тяжести хронической обструктивной болезни легких (ХОБЛ) и при ее сочетании с раком легкого (РЛ), а также установление особенностей респираторных нарушений с помощью спирографии и бодиплетизмографии.

Материалы и методы. Проведено клинико-функциональное исследование 57 лиц (10 здоровых (группа контроля), 30 больных с ХОБЛ и 17 больных, у которых РЛ сочетался с ХОБЛ) при помощи диагностического комплекса Masterlab Pro (Erich Jaeger, Германия).

Результаты. При начальной стадии ХОБЛ наиболее информативно снижение максимального объема скорости на уровне 75% от форсированной жизненной емкости легких ($МОС_{75}$) – вентиляционного показателя, характеризующего проходимость мелких дыхательных путей. При прогрессировании бронхиальной обструкции отмечались как обструктивные, так и рестриктивные нарушения, характеризующиеся снижением объема форсированного выдоха за первую секунду, жизненной емкости легких, изменением структуры общей емкости легких в виде увеличения отношения остаточного объема легких к общей емкости легких и повышения бронхиального сопротивления. У пациентов, страдающих РЛ в сочетании с нетяжелой ХОБЛ, показатели вентиляции легких и бронхиальное сопротивление не отличались от пациентов с ХОБЛ, имеющих аналогичную степень бронхиальной обструкции. При РЛ в сочетании с более тяжелой ХОБЛ, в отличие от пациентов, страдающих аналогичной тяжестью ХОБЛ, установлено снижение проходимости бронхов крупного, среднего и мелкого диаметра (пиковая объемная скорость, $МОС_{25}$, $МОС_{50}$, $МОС_{75}$), свидетельствующее о развитии генерализованной бронхиальной обструкции.

Заключение. Современная диагностика нарушений вентиляции легких у больных РЛ в сочетании с ХОБЛ должна быть направлена на выявление, а медикаментозная терапия – на максимальное нивелирование обратимых компонентов бронхиальной обструкции с целью повышения функционального резерва системы дыхания и снижения риска послеоперационных осложнений, вызванных ХОБЛ.

Ключевые слова: хроническая обструктивная болезнь легких, рак легкого, вентиляционная функция легких, спирография, бодиплетизмография.

Конфликт интересов. Авторы декларируют отсутствие явных и потенциальных конфликтов интересов, связанных с публикацией настоящей статьи.

Источник финансирования. Авторы заявляют об отсутствии финансирования.

Соответствие принципам этики. Все пациенты подписали информированное согласие на проведение исследования. Исследование одобрено локальным этическим комитетом НИИ онкологии, Томский НИМЦ (протокол № 10 от 26.09.2016).

Для цитирования: Добнер С.Ю., Дубаков А.В., Поровский Я.В., Тузиков С.А., Миллер С.В., Родионов Е.О. Изменение вентиляционной функции легких в процессе формирования хронической обструктивной болезни легких и при ее сочетании с раком легкого. *Бюллетень сибирской медицины.* 2020; 19 (4)/61–66. https://doi.org: 10.20538/1682-0363-2020-4-61-66.

INTRODUCTION

Chronic obstructive pulmonary disease (COPD) and lung cancer (LC) usually coexist and represent a row of clinical problems [1–3]. At the same time, COPD more often leads to a decrease in the external respiration function and is a factor determining the frequency of complications and the risk of death in some patients with LC [4, 5].

The diagnosis of COPD is largely functional. Characteristics of the pulmonary ventilation function (PVF), namely, the forced expiratory volume during the first second of the test (FEV_1), vital capacity (VC), and the Tiffno index are the "gold standard" for diagnosing COPD [1]. However, often at the onset of the disease, obstructive disorders developing in the distal parts of the bronchial tree are more effectively diagnosed using parameters of maximal expiratory flow (MEF) of the forced expiratory flow and body plethysmography [6, 8]. Body plethysmography additionally allows to determine bronchial resistance (Raw), to diagnose manifestations of lung hyperinflation, which are used in pulmonology as reliable signs of bronchial obstruction and changes in the lung tissue elastance [7, 8]. Identification of abnormality of these parameters helps early diagnosis of COPD and more effective treatment of this common lung pathology [8].

Annually, 63–65 thousand people fall ill with LC in Russia, and 1.04 million people in the world, which makes up 12.8% of all recorded neoplasm cases [9]. A characteristic feature of everyday clinical practice is an increase in the number of patients operated on in older age groups and a high percentage of postoperative complications [2, 4]. Soon, a further increase in demographic aging of the population and an increase in the number of patients with comorbid pathology are expected [10, 11].

In this regard, the increased interest in assessing COPD as a factor that can lead to complications in the perioperative period in patients with LC is understandable [4, 5]. The use of existing effective methods for diagnosing PVF disorders in this group of patients is an important task for modern scientific research.

The purpose of the study was to study PVF in patients with varying COPD severity and in patients with LC and COPD, as well as to identify the characteristics of PVF disorders using spirography and body plethysmography.

MATERIALS AND METHODS

To meet the aim of the research, clinical and functional study of 57 patients was carried out with 10 healthy patients (control group), 30 patients with COPD and 17 patients with LC and COPD. The sample of subjects included in the study was formed from patients being treated at the therapeutic clinic of Siberian State Medical University and the Department of Thoracic Oncology of Cancer Research Institute, Tomsk NRMC.

According to the PVF study, 8 patients with COPD had clinical signs of bronchitis and small bronchi obstruction, but FEV_1 was normal (group 0). The remaining 22 patients were diagnosed with COPD according to the COPD diagnostic criteria [1]: in group 1 (10 subjects) – $FEV_1 \geq 80\%$ of the proper values; in group 2 (12 subjects) $FEV_1 < 80\%$ of the proper values – 7 patients had $50\% \leq FEV_1 < 80\%$, and 5 patients – $30\% \leq FEV_1 < 50\%$ of the proper values. In 6 patients with LC + COPD, FEV_1 was $\geq 80\%$ of the proper values (group 3), in the remaining 11 patients (group 4), FEV_1 was $< 80\%$ of the proper values, in 9 of them – $50\% \leq FEV_1 < 80\%$, and in 2 – $30\% \leq FEV_1 < 50\%$ of the proper values.

PVF was evaluated on a Masterlab Pro diagnostic complex (Erich Jaeger, Germany). The test was conducted in the morning on an empty stomach in conditions of relative rest in the orthostatic position of a patient. None of the patients in study groups received any bronchoactive agents for COPD. Spirography and pneumotachography methods analyzed respiratory minute volume (RMV), vital capacity (VC), forced expiratory volume during the first second of the test (FEV_1), Tiffno index (FEV_1/VC), flow-volume loop parameters (FVL) – peak expiratory flow (PEF), maximum expiratory flow occurring at the point that is 25% of FVC from the beginning of the exhalation (MEF_{25}), maximum expiratory flow occurring at the point that is 50% of FVC from the beginning of the exhalation (MEF_{50}), maximum expiratory flow occurring at the point that is 75% of FVC from the beginning of the exhalation (MEF_{75}). Body plethysmography determined the structure of total lung capacity (TLC): residual lung volume (RV), residual lung volume to total lung capacity ratio (RV/TLC), as well as bronchial resistance (Raw).

The average age of patients with COPD (group 2) was 59.7 ± 3.0 years, they were older than the subjects in the control group, patients of group 0 and group 1 (52.6 ± 2.7; 48.2 ± 3.0; 49.0 ± 2.2, respectively). The average age of patients with LC and COPD (group 3) was 56.7 ± 2.0, while of patients in group 4 is was 60.8 ± 2.0. Patients of group 3 were older than patients

of group 1. There were no statistical differences in age between patients of groups 2 and 4.

COPD confirmation was carried out by collecting complaints, medical history, physical examination and the questionnaire for the COPD diagnosis (CAT and mMRC scales) [1, 12]. Groups of patients with LC and COPD (groups 3 and 4) included patients with IIA – n IIIB stages of LC. Group 3 included 6 patients, 3 patients of them had stage II, another 3 patients had stage IIIA. Group 4 included 3 patients with IIA–B stage of non-small cell lung cancer, 7 patients with IIIA stage and 1 patient with IIIB stage. Central LC was diagnosed in 12 (70.6%) patients and peripheral LC in 5 patients (29.4%).

The study inclusion criteria were the following: smoking; absence of other lung and severe somatic pathology, which could affect the parameters of external respiratory function at the moment of inclusion in the study; absence of regular baseline and symptomatic COPD therapy, and consent to participate in the study.

Statistical analysis of the obtained data was carried out on a personal computer using the statistical software package Statistica 10. The normal distribution was checked by the Shapiro – Wilk method. Due to the lack of normal distribution, when comparing group averages for quantitative characters, the Mann – Whitney test was used. Quantitative data are presented as the median *Me*, the 25th and 75th percentiles *(LQ; UQ)*. The differences were considered statistically significant at $p \leq 0.05$.

RESULTS AND DISCUSSION

When analyzing the PVF parameters presented in the Table, it was found that in patients with COPD (group 0), bronchial patency at the level of MEF_{75} was on average lower than in healthy subjects in the absence of differences in FEV_1, as well as other flow and volume ventilation characteristics. In group 1, there was a decrease in the average values of FEV_1, Tiffno index, VC, and FVL (MEF_{25}, MEF_{50}, MEF_{75}) compared with the average values of the control group and a decrease in FEV_1, MEF_{25}, MEF_{50}, MEF_{75} with an increase in RV, RV/TLC in comparison with group 0. In addition, with an increase in obstruction, the patients of group 2 demonstrated an additional decrease in VC, an increase in RV, RV/TLC compared with the healthy subjects of group 0, as well as a pronounced tendency (85.2%) to increase RV/TLC compared with group 1.

The restructuring in the TLC structure, detected in patients with COPD in the form of an increase in RV/TLC with a progressive decrease in FEV_1, indicated the development of pulmonary hyperinflation (PHI), the formation of "air trapping", an increase in lung volumes at the end of spontaneous expiration by the valve obstruction mechanism at the level of small airways [7, 13, 14] Studies show that PHI leads to unfavorable functional effects: respiratory muscle weakness, limited respiratory volume increase during exercise stress, positive end-expiratory pressure, and alveolar hypoventilation [8, 14].

Raw in patients with COPD in group 0 and group 1 was in the reference range and did not differ from the control group (Table). In contrast, Raw in group 2 averaged 153.6%, and was significantly higher than in the control group and in patients of group 0 and group 1.

When analyzing the PVF parameters of patients with LC and COPD presented in the table below, it was found that in patients with degree 1 of obstruction (group 3), the average bronchial patency was reduced in comparison with control subjects and patients of group 0, in the absence of differences in parameters with COPD patients of group 1, who had a similar degree of reduction in FEV_1. When comparing the PVF of patients with LC and COPD of group 4 and patients with COPD with a similar reduction in FEV_1 (group 2), the studied pulmonary volumes and capacities did not differ, however, in patients of group 4, PEF, MEF_{25}, MEF_{50}, MEF_{75} were decreased, which testified to widespread, generalized obstruction. Moreover, between the analyzed groups there were no differences in the magnitude of bronchial resistance (Raw).

It can be assumed that in this case, local stenosis or complete obturation of the bronchial lumen (dystelectasis, atelectasis) by a neoplasm, limited in length, leads to impaired ventilation of the lung tissue. At the same time, the Euler – Liliestrand mechanism restricts blood flow through the hypoventilated area, thereby preventing venous blood bypass, and the unaffected areas of the lungs can compensate for the loss of ventilation.

Despite the positive results achieved in the technique of surgical treatment for LC combined with COPD, the final effects of the treatment remain not entirely satisfactory, primarily due to the significant number of postoperative complications caused by COPD [15].

Studies have shown that tobacco smoking, and in a lesser extent exposure to other pathogenic particles or gases, is a major risk factor for developing COPD. These factors cause an inflammatory process in the

lungs, progression of which leads to typical pathophysiological disorders: mucus hypersecretion and ciliary dysfunction, airflow limitation and hyperinflation, pulmonary hypertension and systemic effects, forming reversible and irreversible components of bronchial obstruction [6]. It can be expected that modern functional diagnostics and effective drug therapy of the reversible component of bronchial obstruction will open prospects for improving the perioperative results in patients with LC and COPD.

Table

Results of comparison (p) of PVF parameters in the control group, in patients with COPD and in patients with LC combined with COPD, *Me (LQ; UQ)*

Parameter	Healthy (c) (n = 10)	COPD			COPD + LC		p				
		0 (n = 8)	1 (n = 10)	2 (n = 12)	3 (n = 6)	4 (n = 11)	0-c	1-c 1-0	2-c 2-0 2-1	3-c 3-0 3-1	4-2 4-3
VC	117.6 (107.7; 129.6)	106.4 (98.5; 112.5)	104.2 (97.0; 108.7)	93.3 (87.6; 100.3)	106.9 (106.2; 108.7)	91.8 (85.7; 93.1)	0.062	0.023 0.824	<0.001 0.037 0.013	0.074 0.846 0.415	0.406 0.001
FEV_1	109.1 (102.0; 117.0)	107.8 (104.3; 117.7)	94.5 (85.7; 104.0)	44.4 (38.0; 65.3)	91.5 (86.9; 98.2)	73.9 (65.9; 80.9)	1.0	0.013 0.037	<0.001 <0.001 <0.001	0.004 0.008 0.745	0.056 <0.001
PEF	127.3 (113.7; 145.2)	127.4 (106.2; 145.7)	105.1 (94.1; 116.8)	44.6 (40.6; 74.3)	106.7 (97.5; 115.0)	78.4 (55.5; 101.8)	0.859	0.028 0.051	<0.001 <0.001 <0.001	0.057 0.175 0.828	0.023 0.087
MEF_{25}	122.1 (100.0; 141.6)	123.3 (101.2; 142.2)	77.6 (65.2; 86.7)	15.4 (11.7; 34.3)	60.4 (50.9; 75.8)	37.6 (31.3; 72.5)	0.657	0.003 0.001	<0.001 <0.001 <0.001	0.003 0.002 0.158	0.031 0.070
MEF_{50}	83.9 (76.0; 102.6)	95.7 (80.1; 110.6)	47.2 (39.2; 57.3)	11.5 (7.5; 17.1)	54.1 (46.7; 66.2)	36.6 (24.1; 46.9)	0.656	<0.001 0.001	<0.001 <0.001 <0.001	0.003 0.012 0.278	0.018 0.035
MEF_{75}	85.0 (60.8; 110.6)	50.0 (35.6; 62.4)	25.9 (21.9; 37.1)	9.2 (5.6; 19.8)	37.9 (30.7; 44.6)	26.4 (14.0; 33.4)	0.033	0.007 <0.001	<0.001 <0.001 <0.001	0.004 0.272 0.083	0.006 0.009
RV	99.7 (93.1; 110.0)	79.2 (63.7; 102.3)	105.2 (92.8; 129.9)	141.3 (132.1; 150.5)	127.0 (92.5; 136.4)	120.8 (110.2; 142.2)	0.083	0.496 0.045	0.003 0.001 0.044	0.175 0.045 0.405	0.218 0.763
RV/TLC	90.5 (87.3; 94.6)	74.6 (70.6; 95.5)	104.6 (83.7; 120.0)	121.6 (115.1; 130.6)	102.1 (81.1; 105.4)	116.4 (107.1; 124.1)	0.109	0.121 0.016	0.001 <0.001 0.056	0.481 0.272 0.329	0.295 0.003
Raw	73.7 (42.7; 94.0)	67.1 (51.5; 80.2)	65.3 (52.3; 126.0)	139.5 (101.9; 197.8)	98.3 (86.4; 119.2)	132.4 (94.5; 174.4)	0.859	0.405 0.789	0.002 0.004 0.011	0.074 0.081 0.447	0.622 0.269

Note: c – control group.

CONCLUSION

1. In patients with early COPD, a decrease in MEF_{75} (ventilation parameter characterizing small airway patency) is the most informative. With the progression of bronchial obstruction, obstructive and restrictive disorders develop, which are characterized by a decrease in FEV_1, VC, a change in the structure of the total lung capacity in the form of an increase in the RV/TLC ratio, indicating the development of pulmonary hyperinflation. It was found that a high degree of obstructive disorders leads to increased bronchial resistance.

2. In patients with LC and mild COPD, pulmonary volumes, capacities, flow-volume loop and bronchial resistance parameters did not differ from patients with COPD with a similar degree of bronchial obstruction.

3. In patients with LC and COPD with a greater degree of obstructive disorders, in contrast to COPD with the same degree of reduction in FEV_1, the development of generalized bronchial obstruction at the level of bronchi of large, medium and small diameter (PEF, MEF_{25}, MEF_{50}, MEF_{75}) was determined in the absence of differences in static and dynamic pulmonary volumes, and bronchial resistance.

REFERENCES

1. Chuchalin A.G., Avdeev S.N., Aysanov Z.R., Belevskiy A.S., Leshchenko I.V., Meshcheryakova N.N., Ovcharenko S.I., Shmelev E.I. Federal clinical guidelines for the diagnosis and treatment of chronic obstructive pulmonary disease. *Pulmonology.* 2014; 3: 15–36 (in Russ.).
2. Dai J., Yang P., Cox A., Jiang G. Lung cancer and chronic obstructive pulmonary disease: From a clinical perspective. *Oncotarget.* 2017; 8 (11): 18513–18524. DOI: 10.18632/oncotarget.14505.
3. Miller D.S., Pashkovskaya D.V., Porovskiy Ya.V., Rodionov E.O., Miller S.V., Tuzikov S.A. Early clinical symptoms of lung cancer in clinical practice. *Science of the Young (Eruditio Juvenium)*. 2019: 7 (2): 240–246. DOI: 10.23888 / HMJ201972240-246.
4. Vinnik Yu.A., Gavrilov A.Yu. Features of the development and prevention of complications in patients planned pulmonectomy lung cancer, depending on the functional state of the respiratory system. *Ukrainian Journal of Surgery*. 2012; 3 (18): 12–16 (in Russ.).
5. Kim E.S., Kim Y.T., Kang C.H., Park I.K., Bae W., Choi S.M., Lee J., Park Y.S., Lee C.H., Lee S.M., Yim J.J., Kim Y.W., Han S.K. Prevalence of and risk factors for postoperative pulmonary complications after lung cancer surgery in patients with early-stage COPD. *Int. J. Chron. Obstruct. Pulmon. Dis.* 2016; 11: 1317–1326. DOI: 10.2147/COPD.S105206.
6. Shustov S.B., Kurenkova I.G., Kharitonov M.A., Asyamov K.V. Violations of the function of external respiration in various forms of pulmonary pathology. *Pulmonology.* 2017; 27 (3): 410–418 (in Russ.). DOI: 10.18093/0869-0189-2017-27-3-410-418.
7. Savushkina O.I., Chernyak A.V. Clinical application of the method of body pletismography. *Practical Pulmonology.* 2013; 2: 38–41 (in Russ.).
8. Avdeev S.N. Pulmonary hyperinflation in patients with COPD. *Consilium medicum*. 2006; 8 (3): 75–80 (in Russ.).
9. Davydov M.I., Petrovskiy A.V. Oncology. Clinical recommendations. Moscow: Association of Oncologists of Russia, 2018: 976 (in Russ.).
10. Chaulin A.M., Duplyakov D.V. Cardiovascular diseases and chronic obstructive pulmonary disease etiopatogenetic relationship and clinical significance (literature review). *The Sibirian Medical Journal.* 2020; 35 (2): 26–34 (in Russ.). DOI: 10.29001/2073-8552-2020-35-2-26-34.
11. Porovskiy Ya.V., Tetenev F.F. Comorbidity in medical practice. *Siberian Medical Review.* 2015; 4 (92): 5–11 (in Russ.).
12. Global strategy for the diagnosis, management, and prevention of chronic obstructive pulmonary disease (updated 2019). URL: https://goldcopd.org/wp-content/uploads/2019/11/GOLD-2020-REPORT-ver1.1wms.pdf
13. Tetenev K.F., Tetenev F.F., Ageyeva T.S., Bodrova T.N., Karzilov A.I., Mesko P.Y. Mechanisms of counteracting flap-valve bronchial obstruction in case of obstructive pulmonary emphysema. *Bulletin of Siberian Medicine*. 2015; 14 (4): 75–81. DOI: 10.20538/1682-0363-2015-4-75-81.
14. Avdeev S.N. Noninvasive ventilation in hospitalized patients with chronic obstructive pulmonary disease. *Bulletin of Siberian Medicine*. 2017; 16 (2): 6–19. DOI: 0.20538/1682-0363-2017-2-6-19.
15. Kotiv B.N., Dzidzava I.I., Popov V.A., Kuznetsov I.M. Surgical treatment of lung cancer in patients with low functional reserves of the respiratory and circulatory system. *Bulletin of the Russian Military Medical Academy.* 2016; 2 (54): 241–246 (in Russ.).

Authors contribution

Dobner S.Yu. – conception and design, analysis and interpretation of data, substantiation of the manuscript. Dubakov A.V. – conception and design, analysis and interpretation of data, substantiation of the manuscript. Porovskiy Ya.V. – conception and design, analysis and interpretation of data, substantiation of the manuscript, critical revision for important intellectual content. Tuzikov S.A. – conception and design, analysis and interpretation of data, substantiation of the manuscript, critical revision for important intellectual content, final approval of the manuscript for publication. Miller S.V. – analysis and interpretation of data. Rodionov E.O. – analysis and interpretation of data.

Authors information

Dobner Svetlana Yu., Physician, Cardiologist, Functional Diagnostics Doctor, Cancer Research Institute, Tomsk NRMC, Tomsk, Russian Federation. ORCID 0000-0002-0338-3786.

Dubakov Aleksey V., Cand. Sci. (Med.), Doctor, Department of Biophysics and Functional Diagnostics, Siberian State Medical University, Tomsk, Russian Federation.

Porovskiy Yaroslav V., Dr. Sci. (Med.), Professor, Department of Introduction into Internal Diseases with a Course of Therapy, Pediatric Department, Siberian State Medical University, Tomsk, Russian Federation. ORCID 0000-0003-3378-0608.

Tuzikov Sergey A., Dr. Sci. (Med.), Head of the Department of Thoracic Oncology, Cancer Research Institute, Tomsk NRMC; Professor, Oncology Department, Siberian State Medical University, Tomsk, Russian Federation. ORCID 0000-0002-0884-1838.

Miller Sergey V., Dr. Sci. (Med.), Leading Researcher, Department of Thoracic Oncology, Cancer Research Institute, Tomsk NRMC, Tomsk, Russian Federation. ORCID 0000-0002-5365-9840.

Rodionov Evgeniy O., Cand. Sci. (Med.), Senior Researcher, Department of Thoracic Oncology, Cancer Research Institute, Tomsk NRMC; Assistant of Oncology Department, Siberian State Medical University, Tomsk, Russian Federation. ORCID 0000-0003-4980-8986.

(✉) **Dobner Svetlana Yu.,** e-mail: dobnersv@gmail.com.

Received: 23.12.2019
Accepted: 30.04.2020

УДК 618.11-006.6-085.28-034.23.015.8:616.15:575.174.015.3
https://doi.org/10.20538/1682-0363-2020-4-67-72

Parameters of the glutathione system and thioredoxin in blood plasma and ascites and *GSTP1* Ile105Val gene polymorphism as factors of resistance to platinum-containing chemotherapy in ovarian cancer patients

Dolgova D.R.[1], Gening T.P.[1], Abakumova T.V.[1], Gening S.O.[1, 2], Antoneeva I.I.[1, 2], Fedotova A.Yu.[1]

[1] *Ulyanovsk State University*
42, Lva Tolstogo Str., Ulyanovsk, 432017, Russian Federation

[2] *Regional Clinical Oncologic Center*
90, 12 Sentyabrya Str., Ulyanovsk, 432017, Russian Federation

ABSTRACT

Background. Chemotherapy is one of the main types of treatment in ovarian cancer. Standard first-line treatment includes platinum drugs. Every fifth patient develops chemoresistance after platinum-containing first line therapy. Glutathione detoxification systems play an important role in platinum drugs utilization.

Aim. To assess the redox status of blood plasma and ascitic fluid in ovarian cancer patients before and after neoadjuvant platinum-containing chemotherapy (NACT).

Materials and methods. We determined the activity of the glutathione system and thioredoxin levels in blood plasma before and after NACT and in the ascitic fluid before NACT, and the presence of *GSTP1* gene polymorphism (Ile105Val (rs1695), Ala114Val (rs1138272) in 30 III–IV FIGO stage ovarian cancer patients. Patients were divided into 3 groups: NR – no relapse in 2 years after last chemotherapy course; R1 – relapse in less than 6 months; R2 – relapse in more than 6 months.

Results. We established an increase of the glutathione-transferase activity and a decrease of the GSH level in plasma after chemotherapy in R1 patients, and an opposite dynamic of glutathione-transferase and GSH in the R2 group. Thioredoxin level in plasma of all patients was lower than in the control group; differences in levels between groups were not statistically significant. *GSTP1* 105Val allele was more frequently present in patients than in the control group, and more frequently in R2 than in R1.

Conclusion. The increase in plasma glutathione-transferase and glutathione-reductase levels can be a prognostic marker of early relapse. Thioredoxine dynamics do not correlate with the chemotherapy response. The presence of the *GSTP1* 105Val allele is a risk factor for ovarian cancer development, but a protective factor against early relapse.

Key words: ovarian cancer, ascites, chemoresistance, glutathione system, *GSTP1* gene polymorphism.

Conflict of interest. The authors declare the absence of obvious or potential conflict of interest related to the publication of this article.

Source of financing. This work was supported by the grant awarded by the President of the Russian Federation (MK-3196.2018.7).

Conformity with the principles of ethics. The study was approved by the local Ethics Committee of the Institute of Medicine, Ecology and Physical Education of the UlSU (Protocol No. 9 of 15.09.2015). All patients signed an informed consent.

For citation: Dolgova D.R., Gening T.P., Abakumova T.V., Gening S.O., Antoneeva I.I., Fedotova A.Yu. Parameters of the glutathione system and thioredoxin in blood plasma and ascites and *GSTP1* Ile105Val gene polymorphism as factors of resistance to platinum-containing chemotherapy in ovarian cancer patients. *Bulletin of Siberian Medicine.* 2020; 19 (4): 67–72. https://doi.org/10.20538/1682-0363-2020-4-67-72.

✉ *Dolgova Dinara R.,* e-mail: dolgova.dinara@yandex.ru.

Параметры глутатионовой системы и тиоредоксина в плазме крови и асците и полиморфизм гена *GSTP1* Ile105Val как факторы резистентности к платиносодержащей химиотерапии у больных раком яичников

Долгова Д.Р.[1], Генинг Т.П.[1], Абакумова Т.В.[1], Генинг С.О.[1, 2], Антонеева И.И.[1, 2], Федотова А.Ю.[1]

[1] *Ульяновский государственный университет (УлГУ)*
Россия, 432017, г. Ульяновск, ул. Л. Толстого, 42

[2] *Областной клинический онкологический диспансер (ОКОД)*
Россия, 432017, г. Ульяновск, ул. 12 Сентября, 90

РЕЗЮМЕ

Введение. Химиотерапия является одним из основных видов лечения распространенного рака яичников (РЯ). У каждой пятой пациентки развивается химиорезистентность после платиносодержащей терапии первой линии. Система детоксикации глутатиона играет важную роль в утилизации платиновых препаратов из опухолевых клеток.

Цель. Оценить окислительно-восстановительный статус плазмы крови и асцитической жидкости у больных РЯ до и после неоадъювантной платиносодержащей химиотерапии (НАХТ).

Материалы и методы. Мы определили активность глутатионовой системы и уровень тиоредоксина в плазме крови до и после НАХТ и в асцитической жидкости до НАХТ у 30 пациентов на III–IV стадиях (по FIGO) рака яичников. Пациенты были разделены на три группы: БР – без рецидивов в течение 2 лет после завершения химиотерапии; Р1 – рецидив заболевания в течение 6 мес после завершения химиотерапии первой линии; Р2 – рецидив после 6 мес от момента завершения химиотерапии первой линии.

Результаты. Установлено увеличение активности GT и снижение уровня GSH в плазме после химиотерапии у пациентов с Р1, а также противоположная динамика GT и GSH в группе Р2. Уровень тиоредоксина в плазме у всех пациентов был ниже, чем в контрольной группе; различия в уровнях между группами не были статистически значимыми. Аллельный вариант 105Val гена *GSTP1* выявлялся с более высокой частотой у пациентов с РЯ, чем в контроле, и чаще в группе Р2, чем у Р1.

Заключение. Повышение активности GST и GR в плазме больных РЯ может быть прогностическим маркером раннего рецидива. Динамика тиоредоксина не коррелирует с ответом на химиотерапию. Присутствие аллеля 105Val в гене *GSTP1* является фактором риска развития рака яичников, но защитным фактором против раннего рецидива.

Ключевые слова: рак яичников, асцитическая жидкость, химиорезистентность, глутатионовая система, полиморфизм гена *GSTP1*.

Конфликт интересов. Авторы декларируют отсутствие явных и потенциальных конфликтов интересов, связанных с публикацией настоящей статьи.

Источник финансирования. Работа выполнена при поддержке гранта Президента Российской Федерации (№ МК-3196.2018.7).

Соответствие принципам этики. Исследование одобрено локальным этическим комитетом Института медицины, экологии и физической культуры УлГУ (протокол № 9 от 15.09.2015). Все пациенты подписали информированное согласие на участие в исследовании.

Для цитирования: Долгова Д.Р., Генинг Т.П., Абакумова Т.В., Генинг С.О., Антонеева И.И., Федотова А.Ю. Параметры глутатионовой системы и тиоредоксина в плазме крови и асците и полиморфизм гена *GSTP1* Ile105Val как факторы резистентности к платиносодержащей химиотерапии у больных раком яичников. *Бюллетень сибирской медицины.* 2020; 19 (4): 67–72. https://doi.org/10.20538/1682-0363-2020-4-67-72.

INTRODUCTION

The increased glutathione system activity underlies the resistance to platinum-containing chemotherapy (CT) in ovarian cancer (OC), among other causes. Binding to SH-groups of glutathione inactivates cisplatin, with mainly glutathione-S-transferases (GST) providing the neutralization [1]. Platinum-resistant cells demonstrate a higher activity of GST in the cytosol compared with the original platinum-sensitive SKOV3 and SGC7901 cells, and the GSTP inhibition increases the cytotoxicity of platinum drugs by 4 times [2]. GST plays a role in drug resistance by providing the direct detoxifying effect and the MAP kinase pathway inhibition. GST modulates the tumor response to platinum-containing CT in OC [43]. GST activity in ovarian cancer ascites negatively correlates with the sensitivity to platinum drugs and positively correlates with the risk of recurrence. The expression of the glutathione-dependent enzymes genes reflects the adaptive antioxidant potential and can take part in drug resistance development [4].

The limited data are available on the thiol cell detoxification systems, represented by thioredoxin (Trx) and glutaredoxin, the regulators of the redox potential, cell proliferation, and DNA repair. Some authors propose that thioredoxin contributes to the formation of doxorubicin and cisplatin resistance, protecting cells from the oxidative stress and inhibiting the apoptosis through protein kinases ASK1 and JNK1 [5].

The aim of the study was to assess the parameters of the glutathione system and thioredoxin in blood plasma and ascites and polymorphism of the *GSTP1* Ile105Val gene as factors of chemoresistance in patients with advanced ovarian cancer.

MATERIALS AND METHODS

The study included 30 patients (median age 62 years; lower quartile – 45, upper quartile – 65) with verified OC presenting with ascites (performance status according to ECOG – 0–2, life expectancy at least 6 months). The patients were treated with 2–4 cycles of the neoadjuvant chemotherapy (NACT) according to the AP regimen (cisplatin 75 mg/m² and doxorubicin 40 mg/m² intravenously in the 1st day every 3 weeks) and, subsequently, cytoreductive surgery and adjuvant chemotherapy. Ascitic fluid (AF) for analysis was taken before starting chemotherapy. The cell-free fraction was collected after centrifugation at 1,500 rpm for 10 min. With dynamic observation, all patients were divided into groups: NR – no relapse; R1 – early relapse, relapse-free period up to 6 months; R2 – late relapse, relapse-free period from 6 to 12 months. In the plasma of patients before treatment and after NACT and AF before treatment, the activity of the glutathione system components was determined: glutathione-S-transferase (GST), glutathione reductase (GR), glutathione peroxidase (GPO), and the level of reduced glutathione (GSH) [6, 7]; thioredoxin (Trx) level was evaluated by ELISA (Cloud Clone Corp., USA). Genomic DNA for the analysis of *GSTP1* gene polymorphisms Ile105Val (rs1695), Ala114Val (rs1138272) was isolated with a "DNA express blood" kit (NPF Litech, Moscow). Genotyping of the samples was performed by allele-specific real-time PCR with Taq-Man probes (Syntol, Moscow). The control group consisted of 20 apparently healthy women (median age 52, lower quartile 45; upper quartile 58). Quantitative data are presented as median and lower and upper quartiles. Due to the abnormal distribution in the groups, the nonparametric Kruskal – Wallis test was used to describe the statistical differences (the differences were considered significant at $p \leq 0.05$). The frequencies of the *GSTP1* Ile105Val gene polymorphism, as well as the correspondence of the distribution of the observed genotype frequencies to the theoretically expected ones from the Hardy – Weinberg equilibrium, were checked using the $\chi 2$ test. To assess the relative risk of developing an event, the OR (odds ratio) value and confidence intervals were calculated using an on-line calculator in case-control studies (http://gen-exp.ru/calculator_or.php). Statistical data processing was carried out using the Statistica 13.0 software package.

RESULTS

The activity of GST statistically significantly differs between the groups of OC patients, depending on the time to the recurrence. Plasma GST activity in patients of the R1 group is several times higher than the values GST in the control, R2 and NR groups both before and after NACT (Fig. 1,*a*). The same dynamics exists in the AF: the early relapse is associated with high enzyme activity before treatment (Fig. 1,*b*). The high detoxification potential of GST may reduce the effectiveness of platinum-containing NACT by conjugating the drug, along with a decrease in free GSH. After NACT, the enzyme activity in all studied groups slightly decreases, while remaining elevated in the R1 group. The decrease in the plasma GST activity after NACT is associated with a longer relapse-free period.

The main function of GR is to maintain glutathione in the reduced form, which conjugates with exogenous toxins. The change in GR activity in the plasma of OC patients is similar to the dynamics of GST in plasma (Fig. 1,*a*), which suggests a decrease in the enzymatic recovery of GSSG after NACT.

In the R1 group, the lowest GSH values are found in blood plasma in comparison with all other groups studied (Table 1). In the NR group, low plasma GSH values

are observed before treatment, and a sharp increase (by 3.5 times) happens after NACT, which possibly reflects an increase in the antioxidant status and may act positively, preventing the formation of resistance to doxorubicin and cisplatin.

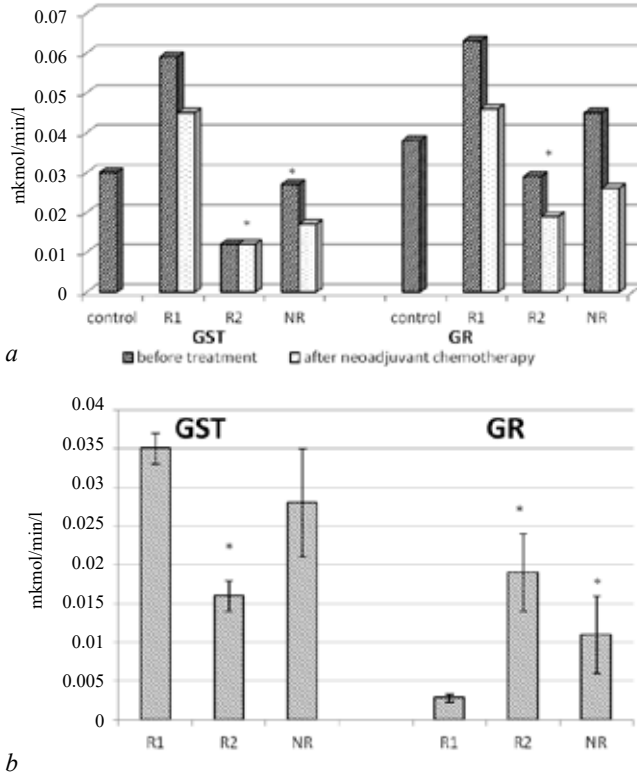

Fig.1. Level of GST and GR in plasma (*a*) and ascitic fluid (*b*), depending on the duration of the relapse-free period: * marked data are significantly different from the group R1

The activity of GPO, utilizing hydrogen peroxide, is lower than the control in blood plasma in all groups and does not differ significantly (Table 1).

Ascites sampling may reveal additional factors to clarify the molecular biological "portrait" of the ovarian tumor [8]. We found that the R1 group had the lowest GSH values in AF, while the maximum level was in the R2 group (Table 1). Thus, an increase in GST and a decrease in GSH in plasma after NACT may be markers of early relapse. In contrast, low GST activity and high GSH levels in plasma and ascites occurred in the group of NR patients.

Trx may play a role in the mechanisms of antitumor drug resistance; this effect is tissue-specific and depends on the microenvironment [9]. We found that the Trx level in blood plasma, decreased in all groups compared to the control, did not differ significantly before and after platinum-containing chemotherapy (Fig. 2).

Tumor sensitivity to cisplatin is determined by the activity of detoxification enzymes, which include GST, and the activity depends on gene polymorphism [10]. When comparing two groups, patients with OC and controls, we found that the presence of a functionally weakened *GSTP1* allele (genotype Ile/Val or Val/Val) in the genotype is a risk factor for OC (OR = 1.82; 95% CI 1.1–2.8; $p = 0.035$). The *GSTP1114Val* allele is associated with a decrease in the functional activity of the enzyme and is also more common in OC patients than in the controls (19% versus 5.5%; OR = 3.20; 95% CI 1.5–6.8; $p = 0.023$). In the R1 group, compared with the R2 patients, the Ile/Ile *GSTP1* genotype is more common (OR = 4.30; 95% CI 1.25–14.81; $p = 0.034$).

Table 1

GSH and GPO levels in plasma and AF in patients with advanced OC before and after NACT, *Me* (Q_1–Q_3)

Parameters	GSH, mmol/l			GPO, μmol/min/l		
	R1, $n = 12$	R2, $n = 8$	NR, $n = 10$	R1, $n = 12$	R2, $n = 8$	NR, $n = 10$
Plasma of primary patients	19.72 (15.64–22.44)	72.8 (54.0–95.5) $p = 0.00005$	25.16 (23.8–30.2) $p = 0.003$	9.075 (3.675–11.835)	7.905 (4.372–12.278) $p = 0.653$	11.048 (10.83–11.67) $p = 0.101$
Plasma of patients after completing NACT	28.9 (14.96–44.4)	47.5 (27.3–74.45) $p = 0.219$	105.5 (53.16–121.00) $p = 0.0006$	10.477 (10.41–11.07)	10.695 (6.405–17.10) p=0.477	8.28 (8.1–9.24) $p = 0.619$
Ascitic fluid of OC patients before treatment	19.72 (17–27.2)	101 ***(93–112.5)*** $p = 0.003$	32 20.4–98.5 $p = 0.160$	19.2 (12.3–30.3)	7.073 (4.22–9.82) $p = 0.037$	19.83 (15.75–25.62) $p = 0.802$
Control	80.72 (76.5–82.3)			52.01 (50.5–54.0)		

DISCUSSION

Ovarian carcinogenesis provokes a prooxidant state, both in the tumor and in the adjacent normal tissues, and the subsequent chemotherapy aggravates this condition. In the late stages of OC, depletion of antioxidant resources occurs. The glutathione system in the blood plasma can move to a higher level of functioning and provide protection of macromolecules from reactive oxygen species. We describe such observation in the group of patients with a long relapse-free period. Conversely,

the decrease in the antioxidant proteins favors the survival of a tumor and the metastasis development. We observed significantly lower values of GSH and Trx levels in plasma in the group of OC patients with relapses in comparison to the NR group. The glutathione system plays a dual role in the process of carcinogenesis [11].

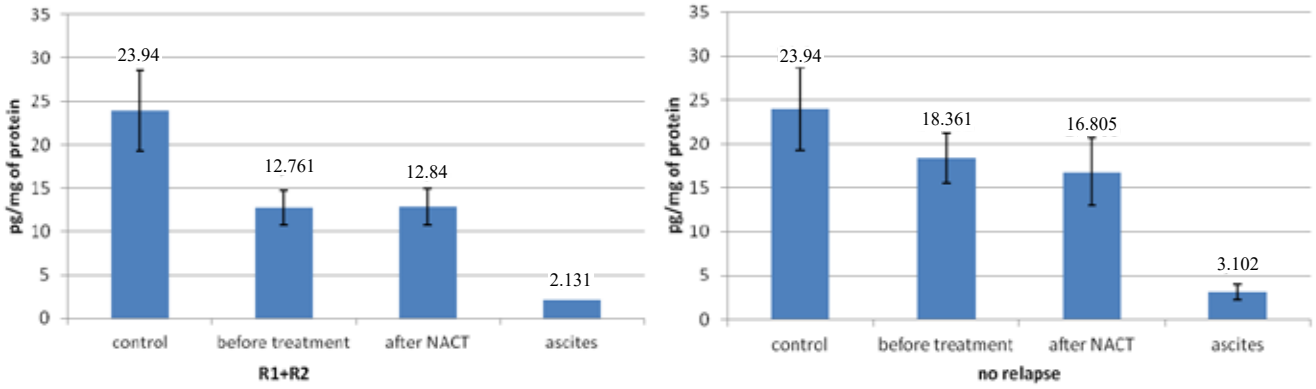

a *b*

Fig. 2. Level of thioredoxin in plasma and ascitic fluid of patients with OC before and after NACT with early and late relapse (R1 + R2) (*a*) and without relapse for 2 years (NR) (*b*)

On the one hand, its low activity disrupts the inactivation of carcinogens. The decrease in the concentrations of GSH and GSH-dependent enzymes in plasma and ascites are observed with tumor progression. Earlier in the experiment, we established a tendency towards a decrease in lipid peroxidation and oxidative modification of proteins in ascites with the progression of OC [12]. On the other hand, GSH and Trx in tumor reduce the cytotoxic effect of cisplatin; low levels of Trx in the cytoplasm of OC cells are associated with an increase in progression-free survival [13]. The observed dynamics of Trx levels in plasma and ascites needs further studying of the Trx role in the formation of OC cells clones with a high antioxidant status.

GSTP activity differs depending on the substrate; with the GSTP1105Val allele, the overall survival in OC patients is reduced after the platinum-containing chemotherapy [14]. Thus, it can be assumed that overexpression of the GSTP gene determines the resistance of OC cells to platinum-containing CT.

CONCLUSION

The platinum-containing NACT has a significant effect on the functional state of the glutathione system in the plasma of OC patients. The patients of the early relapse group have decreased GSH and Trx levels, and increased activity of GST and GR in plasma after NACT. In patients with no relapse in 2 years, an increase in the antioxidant status of plasma is observed: the levels of GSH and thioredoxin are increased, and the activity of GST is decreased. In general, the system of glutathione and glutathione-dependent blood plasma enzymes dynamically changes its profile during ovarian carcinogenesis and may be used for assessing individual sensitivity to platinum-containing chemotherapy, as a prognostic marker for early relapse. The presence of the Ile105Val allele in the GSTP1 gene is a risk factor for the development of ovarian cancer, but a protective factor against early relapse.

REFERENCES

1. Siddik Z.H. Cisplatin: mode of cytotoxic action and molecular basis of resistance. *Oncogene.* 2003; 22 (47): 7265–7279. DOI: 10.1038/sj.onc.1206933.
2. Zou M., Hu X., Xu B., Tong T., Jing Y., Xi L., Zhou W., Lu J., Wang X., Yang X., Liao F. Glutathione S-transferase isozyme alpha 1 is predominantly involved in the cisplatin resistance of common types of solid cancer. *Oncol. Rep.* 2019; 41 (2): 989–998. DOI: 10.3892/or.2018.6861.
3. Boss E.A., Peters W.H., Roelofs H.M., Boonstra H., Steegers E.A., Massuger L.F. Glutathione-S-transferases P1-1 and A1-1 in ovarian cystfluids. *Eur. J. Gynaecol. Oncol.* 2001; 22 (6): 427–432.
4. Kalinina E.V., Chernov N.N., Saprin A.N., Kotova Y.N., Remizov V.I., Shcherbak N.P. Expression of genes for redox-dependent glutathione S-transferase isoforms GSTP1-1 and GSTA4-4 in tumor cell during the development of doxorubicin resistance. *Bulletin of Experimental Biology and Medicine.* 2007; 143 (3): 298–301 (in Russ.).
5. Kalinina E., Chernov N., Novichkova M., Nurmuradov N. Thioredoxins, glutaredoxins and peroxiredoxins in redox-dependent formation of cancer cell resistance. *Free Radical Biology and Medicine.* 2017; 108 (S1): 34–35.
6. Habig W.H., Pabst M.J., Jakoby W.B. Glutathione S-transferases. The first enzymatic step in mercapturic acid formation. *J. Biol. Chem.* 1974; 249 (22): 7130–7139.
7. Maltsev G.Yu., Tyshko N.V. Methods for determining the

content of glutathione and the activity of glutathione reductase in erythrocytes. *Hygiene and Sanitation.* 2002; 2: 67–69 (in Russ.).
8. Villert A.B., Kolomiets L.A., Yunusova N.V., Ivanova A.A. Ascites as a subject of studies in ovarian cancer. *Siberian Journal of Oncology.* 2019; 18 (1): 116–123. DOI: 10.21294/1814-4861-2019-18-1-116-123 (in Russ.).
9. Pontikakis S., Papadaki C., Tzardi M., Trypaki M., Sfakianaki M., Koinis F., Lagoudaki E., Giannikaki L., Kalykaki A., Kontopodis E., Saridaki Z., Malamos N., Georgoulias V., Souglakos J. Predictive value of *ATP7b, BRCA1, BRCA2, PARP1, UIMC1 (RAP80), HOXA9, DAXX, TXN (TRX1), THBS1 (TSP1)* and *PRR13 (TXR1)* genes in patients with epithelial ovarian cancer who received platinum-taxane first-line therapy. *Pharmacogenomics J.* 2017; 17 (6): 506–514. DOI: 10.1038/tpj.2016.63.
10. Woolston C.M., Deen S., Al-Attar A., Shehata M., Chan S.Y., Martin S.G. Redox protein expression predicts progression-free and overall survival in ovarian cancer patients treated with platinum-based chemotherapy. *Free Radic. Biol. Med.* 2010; 49 (8): 1263–1272. DOI: 10.1016/j.freeradbiomed.2010.07.008.
11. Nunes S.C., Serpa J. Glutathione in ovarian cancer: a double-edged sword. *Int. J. Mol. Sci.* 2018; 19 (7): 1882. DOI: 10.3390/ijms19071882.
12. Abakumova T.V., Dolgova D.R., Gening S.O., Gening T.P., Antoneeva I.I. Prognostic role of ascetic fluid redox system parameters in patients with ovarian cancer. *Ulyanovsk Medico-biological Journal.* 2018; (3): 80–86. DOI: 10.23648/UMBJ.2018.31.17218 (in Russ.).
13. Greenwood H.E., McCormick P.N., Gendron T., Glaser M., Pereira R., Maddocks O.D.K., Sander K., Zhang T., Koglin N., Lythgoe M.F., Årstad E., Hochhauser D., Witney T.H. Measurement of tumor antioxidant capacity and prediction of chemotherapy resistance in preclinical models of ovarian cancer by positron emission tomography. *Clin. Cancer Res.* 2019; 25(8): 2471–2482. DOI: 10.1158/1078-0432.CCR-18-3423.
14. Moiseyev A.A., Khrunin A.V., Pavlyushina E.M., Pirogova N.A., Gorbunova V.A., Limborskaya S.A. Polymorphism of glutathione-S-transferase genes and outcomes of ovarian cancer chemotherapy. *Journal of N.N. Blokhin Russian Cancer Research Center.* 2008; 19 (1): 59–63 (in Russ.).

Authors contribution

Dolgova D.R. – conception and design of the study, interpretation of the data. Antoneeva I.I. – selection of a clinical base for analysis. Fedotova A.Yu. – analysis and interpretation of the data. Gening S.O. – substantiation of the manuscript and revision of the content. Abakumova T.V. – analysis and interpretation of the data. Gening T.P. – final review of the manuscript for publication.

Authors information

Dolgova Dinara R., Cand. Sci. (Biology), Associate Professor, Department of Physiology and Pathophysiology, Institute of Medicine, Ecology and Physical Education, UlSU, Ulyanovsk, Russian Federation. ORCID 0000-0001-5475-7031.

Gening Tatyana P., Dr. Sci. (Biology), Professor, Head of the Department of Physiology and Pathophysiology, UlSU, Ulyanovsk, Russian Federation; ORCID 0000-0002-5117-1382.

Abakumova Tatyana V., Cand. Sci. (Biology), Associate Professor, Department of Physiology and Pathophysiology, Institute of Medicine, Ecology and Physical Education, UlSU, Ulyanovsk, Russian Federation. ORCID 0000-0001-7559-5246.

Gening Snezhanna O., Post-Graduate Student, Department of Oncology and Radiation Diagnostics, Institute of Medicine, Ecology and Physical Education, UlSU; Medical Oncologist, Department of Hemoblastoses and Solid Tumors Chemotherapy, RCOC, Ulyanovsk, Russian Federation. ORCID 0000-0001-6970-6659.

Antoneeva Inna I., Dr. Sci. (Med.), Associate Professor, Department of Oncology and Radiation Diagnostics, Institute of Medicine, Ecology and Physical Education, UlSU, Head of the Gynecological Department, RCOC, Ulyanovsk, Russian Federation. ORCID 0000-0002-1525-2070.

Fedotova Antonina Yu., Research Engineer, Medical and Biological Research Center, UlSU, Ulyanovsk, Russian Federation. ORCID0000-0003-1027-8885.

(✉) **Dolgova Dinara R.,** e-mail: dolgova.dinara@yandex.ru.

Received 08.07.2019
Accepted 30.04.2019

УДК 616.89-008.454-008.441.13-085.214:575.174.015.3
https://doi.org/10.20538/1682-0363-2020-4-73-79

Polymorphism 3435c> t of the *ABCB1* gene (rs1045642) does not affect the mirtazapine efficiency and safety profile in patients with depressive disorders comorbid with alcohol use disorder

Zastrozhin M.S.[1, 2], Grishina E.A.[2], Ryzhikova K.A.[2], Skryabin V.Yu.[1], Koporov S.G.[1], Bryun E.A.[1, 2], Sychev D.A.[2]

[1] *Moscow Research and Practical Centre on Addictions*
37/1, Lyublinskaya Str., Moscow, 109390, Russian Federation

[2] *Russian Medical Academy of Continuous Professional Education*
Build. 1, 2/1 Barrikadnaya Str., Moscow, 123995, Russian Federation

ABSTRACT

Background. Mirtazapine is used to treat patients with depressive disorders. A large proportion of patients in this group do not adequately respond to mirtazapine therapy, while many develop undesirable drug reactions of type A. According to the previous studies, P-gp is involved in the biotransformation of mirtazapine, the activity of which is highly dependent on the polymorphism of the gene encoding it.

Aim. To aim of our study was to study the effect of mirtazapine gene polymorphism on the efficacy and safety of mirtazapine therapy in patients with depressive disorders, comorbid with alcohol dependence.

Materials and methods. The study included 119 male patients with depressive disorders, comorbid with alcohol dependence (age 38.7 ± 16.0 years). As a therapy, mirtazapine was used at a dose of 37.8 ± 13.8 mg / day. Evaluation of the effectiveness profile was carried out using psychometric scales. The safety profile was evaluated using the UKU Side-Effect Rating Scale. Genotyping was carried out by polymerase chain reaction in real time.

Results. In the course of the study, results statistically significant in terms of evaluating efficacy and safety were not obtained (HAMD scores at the end of the course of therapy: (CC) 2.5 [2.0; 4.0], (CT) 2.0 [1.0; 3.0] and (TT) 2.0 [1.0; 3.0], $p > 0.999$; according to the UKU scale: (CC) 3.0 [2.8; 3.0], (CT) 3.0 [3.0; 3.0] and (TT) 3.0 [3.0; 3.0], $p > 0.999$).

Conclusion. The study of 119 patients with depressive disorders comorbid with alcohol dependence showed that 3435C> T polymorphism of the *ABCB1* gene (rs1045642) does not affect the clinical efficacy and safety of mirtazapine.

Key words: mirtazapine, *ABCB1*, pharmacogenetics, biotransformation, personalized medicine, depressive disorder, alcohol use disorder.

Conflict of interest. The authors declare no obvious or potential conflict of interest related to the publication of this article.

Source of financing. This work was supported by the grant of the Russian Science Foundation (Project No. 18-75-10073).

Conformity with the principles of ethics. The study was approved by the local Ethics Committee at the Russian Medical Academy of Continuous Professional Education of the Ministry of Health of the Russian Federation (Protocol No. 6 of 16.05.2017). All patients signed an informed consent.

For citation: Zastrozhin M.S., Grishina E.A., Ryzhikova K.A., Skryabin V.Yu., Koporov S.G., Bryun E.A., Sychev D.A. Polymorphism 3435c> t of the *ABCB1* gene (rs1045642) does not affect the mirtazapine efficiency

✉ *Zastrozhin Mikhail S.,* e-mail: mszastrozhin@gmail.com.

and safety profile in patients with depressive disorders comorbid with alcohol use disorder. *Bulletin of Siberian Medicine.* 2020; 19 (4): 73–79. https://doi.org/10.20538/1682-0363-2020-4-73-79.

Полиморфизм 3435c>T гена *ABCB1* (rs1045642) не влияет на профиль эффективности и безопасности миртазипина у пациентов с депрессивными расстройствами, коморбидными с алкогольной зависимостью

Застрожин М.С., Гришина Е.А., Рыжикова К.А., Скрябин В.Ю., Копоров С.Г., Брюн Е.А., Сычёв Д.А.

[1] *Московский научно-практический центр (МНПЦ) наркологии*
Россия, 109390, г. Москва, ул. Люблинская, 37/1

[2] *Российская медицинская академия непрерывного профессионального образования (РМАНПО)*
Россия, 125993, г. Москва, ул. Баррикадная, д. 2/1, стр. 1

РЕЗЮМЕ

Введение. Миртазапин используется для лечения пациентов с депрессивными расстройствами. Немалая доля пациентов данной группы не отвечает должным образом на терапию миртазапином, при этом у многих отмечается развитие нежелательных лекарственных реакций типа А. По результатам ранее проводимых исследований показано, что в биотрансформации миртазапина принимает участие гликопротеин Р, активность которого в высокой степени зависит от полиморфизма кодирующего его гена.

Цель. Изучить влияние полиморфизма гена *ABCB1* на эффективность и безопасность терапии миртазапином у пациентов с депрессивными расстройствами, коморбидными с алкогольной зависимостью.

Материалы и методы. В исследование было включено 119 пациентов мужского пола с депрессивными расстройствами, коморбидными с алкогольной зависимостью (средний возраст (38,7 ± 16,0) лет). В качестве терапии использовали миртазапин в дозе (37,8 ± 13,8) мг/сут. Оценка профиля эффективности производилась с помощью психометрических шкал. Профиль безопасности оценивался с помощью валидизированной шкалы UKU Side-Effect Rating Scale. Генотипирование проводилось методом полимеразной цепной реакции в режиме реального времени.

Результаты. По результатам исследования не получены статистически значимые результаты в показателях оценки эффективности и безопасности (баллы по шкале HAMD в концу курса терапии: (CC) 2,5 [2,0; 4,0], (CT) 2,0 [1,0; 3,0] и (TT) 2,0 [1,0; 3,0], $p > 0,999$; по шкале UKU: (CC) 3,0 [2,8; 3,0], (CT) 3,0 [3,0; 3,0] и (TT) 3,0 [3,0; 3,0], $p > 0,999$).

Заключение. Продемонстрировано отсутствие влияния полиморфизма 3435C>T гена *ABCB1* (rs1045642) на показатель клинической эффективности и безопасности миртазапина.

Ключевые слова: миртазапин, *ABCB1*, фармакогенетика, биотрансформация, персонализированная медицина, депрессивные расстройства, алкогольная зависимость.

Конфликт интересов. Авторы декларируют отсутствие явных и потенциальных конфликтов интересов, связанных с публикацией настоящей статьи.

Источник финансирования. Исследование выполнено за счет гранта Российского научного фонда (проект № 18-75-10073).

Соответствие принципам этики. Исследование было одобрено локальным этическим комитетом Российской медицинской академии непрерывного профессионального образования Минздрава России (протокол № 6 от 16.05.2017). Все пациенты подписали информированное согласие на участие в исследовании.

Для цитирования: Застрожин М.С., Гришина Е.А., Рыжикова К.А., Скрябин В.Ю., Копоров С.Г., Брюн Е.А., Сычёв Д.А. Полиморфизм 3435C>T гена *ABCB1* (rs1045642) не влияет на профиль эффектив-

ности и безопасности миртазипина у пациентов с депрессивными расстройствами, коморбидными с алкогольной зависимостью. *Бюллетень сибирской медицины.* 2020; 19 (4): 73–79. https://doi.org/10.20538/1682-0363-2020-4-73-79.

INTRODUCTION

Depressive disorders are among the most frequently reported comorbidities in patients suffering from alcohol use disorder [1]. Antidepressants are commonly used in the depressive disorders treatment, and mirtazapine is a representative of this drug group [2]. Although tetracyclic antidepressants are included in the depressive disorders treatment guidelines, the number of resistant patients and patients with reported adverse drug reactions (ADRs) remains high [3].

Glycoprotein P (P-glycoprotein, P-gp) is involved in the pharmacokinetics of many drugs used for depressive disorders psychopharmacotherapy [4]. The gene encoding *ABCB1* is highly polymorphic, which may affect the interindividual variability in P-gp metabolic activity [5]. Changes in the protein activity may influence the rate of xenobiotic elimination including substrate drugs that, in turn, may have an impact on their effectiveness and safety profiles [6].

There are four groups of metabolizers distinguished by their metabolic rate: extensive metabolizers, poor metabolizers, intermediate metabolizers, and ultra-rapid metabolizers. Extensive metabolizers have normal metabolic rate. Poor metabolizers have mutations in the *ABCB1* gene, which may lead to a decrease in the activity of the encoded protein, as well as a slowdown in the metabolism of substrate drugs, which may lead to an increased risk of adverse drug reactions. Intermediate metabolizers have a mutation in only one of the homologous chromosomes, which reduces the P-gp activity but to a lesser degree than in poor metabolizers. Ultra-rapid metabolizers have the genetically determined increased activity of CYP3A that leads to the accelerated elimination of substrate drugs and reduces treatment effectiveness [7].

The study aimed to determine the influence of *ABCB1* gene polymorphisms on the effectiveness and safety profile of mirtazapine therapy in patients with depressive disorders, comorbid with alcohol use disorder.

MATERIALS AND METHODS

Clinical characteristics of the study subjects. 119 male patients (average age 38.71 ± 15.96 years old) were enrolled in the study. The inclusion criteria were specified as follows: the existence of two comorbid diagnoses: "Depressive episode (F32.x)", and "Mental and behavioral disorders due to use of alcohol. Dependence syndrome. Currently abstinent but in a protected environment (F.10.212)", a signed informed consent, and 16-days mirtazapine monotherapy. Exclusion criteria were specified as follows: presence of any other mental disorders, presence of severe somatic disorders (except alcoholic hepatitis and toxic encephalopathy), presence of any other psychotropic medications in treatment regimen, creatinine clearance values <50 mL/min, creatinine concentration in plasma >1.5 mg/dL (133 mmol/L), bodyweight less than 60 kg or greater than 100 kg, age of 75 years or more, and presence of any contraindications for mirtazapine use.

Therapy effectiveness and safety evaluation. To evaluate mirtazapine effectiveness several international psychometric scales were used: Penn Alcohol Craving Scale (PACS) [8] and Visual Analogue Scale (VAS) for urge to alcohol assessment [9], and the Clinical Global Impression (CGI) scale [10], Hospital Anxiety and Depression Scale (HADS) [11], and Hamilton Depression Rating Scale (HAMD) [12]. A safety profile was evaluated using the UKU Side-Effect Rating Scale (UKU) [13]. The patients were examined on days 1, 9, and 16 of mirtazapine therapy.

Genotyping. For genotyping, venous blood samples were collected into VACUETTE® (Greiner Bio-One, Austria) vacuum tubes on the 16th day of mirtazapine therapy. The DNA amplifiers "Dtlite" by DNA Technology (Russia), "CFX96 Touch Real-Time System" with CFX Manager software by Bio-Rad (USA), and the "SNP-screen" sets by Syntol (Russia) were used to perform the real-time polymerase chain reaction in order to determine the 3435C>T single-nucleotide polymorphisms (SNPs) of the *ABCB1* gene (rs1045642). The usage of two allele-specific hybridizations in every "SNP-screen" set enabled the determination of two alleles of the studied SNP separately on two fluorescence channels.

Statistical analysis. The data were analyzed with non-parametric methods using the Statsoft Statistica v. 10.0 (Dell Statistica, Tulsa, USA). The normality of sample distribution was evaluated using the Sha- piro – Wilk *W*-test and was taken into account when choosing a statistical method. The differences were considered statistically significant at $p < 0.05$ (power above 80%). Two samples of continuous independent data

were compared using the Mann – Whitney *U*-test with further correction of the obtained *p*-value using the Benjamin – Hochberg test due to the multiple comparison procedure. Several samples of continuous data were analyzed using the Kruskal – Wallis *H*-test. Correlation analysis was performed using the Spearman nonparametric test. The data is presented in the form of the median and interquartile range *Me* [*Q1*; *Q3*].

RESULTS

The *ABCB1* 3435C>T polymorphic marker (rs1045642) genotyping performed in 105 subjects have revealed the following:

• The number of patients with the CC genotype was 20 (16,8%);

• The number of patients with the CT genotype was 70 (58,8%);

• The number of patients with the TT genotype was 29 (24,4%).

The frequency distribution of genotypes corresponded to the Hardy – Weinberg equilibrium distribution (Chi2 = 4.00; *p*-value = 0.05).

The results of psychometric scales (PACS, VAS, CGI, HADS, HAMD) and side-effect rating scale (UKU) data analysis on days 1, 9, and 16 in patients who received mirtazapine are summarized in Tables 1–3, respectively.

Table 1

Psychometric scales and side-effect rating scale (UKU) data on in patients received mirtazapine, day 1 of the research, *Me* [Q_1; Q_3]

Scale	CC	CT	TT	*p*-value
PACS	11.0 [11.0; 11.0]	11.0 [11.0; 11.0]	11.0 [11.0; 11.0]	$p > 0.999$
VAS	51.0 [50.8; 52.0]	49.0 [46.0; 52.8]	49.0 [47.0; 51.0]	$p > 0.999$
CGI	5.0 [5.0; 5.0]	5.0 [5.0; 5.0]	5.0 [5.0; 5.0]	$p = 0.086$
HADS	37.0 [36.0; 38.0]	36.0 [34.2; 38.0]	37.0 [36.0; 38.0]	$p > 0.999$
HAMD	22.0 [21.0; 22.0]	22.0 [21.0; 23.0]	22.0 [21.0; 22.0]	$p = 0.636$
UKU	0.5 [0.0; 1.0]	1.0 [0.0; 1.0]	0.0 [0.0; 1.0]	$p > 0.999$

Table 2

Psychometric scales and side-effect rating scale (UKU) data on in patients received mirtazapine, day 9 of the research, *Me* [Q_1; Q_3]

Scale	CC	CT	TT	*p*-value
PACS	7.5 [7.0; 8.0]	7.0 [7.0; 8.0]	7.0 [7.0; 7.0]	$p > 0.999$
VAS	32.5 [31.0; 35.2]	32.0 [31.0; 33.8]	32.0 [30.0; 36.0]	$p > 0.999$
CGI	3.0 [3.0; 3.0]	3.0 [3.0; 4.0]	3.0 [3.0; 3.0]	$p > 0.999$
HADS	25.0 [24.0; 26.2]	24.0 [23.0; 25.0]	24.0 [22.0; 25.0]	$p > 0.999$
HAMD	15.0 [14.0; 16.0]	15.0 [13.0; 16.0]	14.0 [14.0; 15.0]	$p > 0.999$
UKU	2.0 [2.0; 2.2]	2.0 [2.0; 2.0]	2.0 [2.0; 3.0]	$p > 0.999$

Table 3

Psychometric scales and side-effect rating scale (UKU) data on in patients received mirtazapine, day 16 of the research, *Me* [Q_1; Q_3]

Scale	CC	CT	TT	*p*-value
PACS	1.0 [1.0; 1.2]	1.0 [1.0; 1.0]	1.0 [0.0; 2.0]	$p > 0.999$
VAS	5.5 [3.5; 7.2]	4.0 [3.0; 5.8]	5.0 [4.0; 6.0]	$p > 0.999$
CGI	0.0 [0.0; 1.0]	1.0 [0.0; 1.0]	1.0 [0.0; 1.0]	$p > 0.999$
HADS	4.0 [3.0; 4.0]	3.0 [1.2; 5.0]	4.0 [2.0; 5.0]	$p > 0.999$
HAMD	2.5 [2.0; 4.0]	2.0 [1.0; 3.0]	2.0 [1.0; 3.0]	$p > 0.999$
UKU	3.0 [2.8; 3.0]	3.0 [3.0; 3.0]	3.0 [3.0; 3.0]	$p > 0.999$

Figure 1 demonstrates the dynamics of changes in the HAMD scale scores among the patients with different genotypes. As shown, by the day 1 the studied groups had already had statistically significant differences: (CC) 22,0 [21,0; 22,0], (CT) 22,0 [21,0; 23,0], and (TT) 22,0 [21,0; 22,0], p = 0,035. By the 9th day of the study, statistically significant differences had ceased to be observed in carriers of different genotypes for the studied polymorphic marker: (CC) 15.0 [14.0; 16.0], (CT) 15.0 [13.0; 16.0], and (TT) 14.0 [14.0; 15.0], p = 0.627. On the last 16th day of the study, as well as on the 2nd visit, no statistical difference was obtained: (CC) 2.5 [2.0; 4.0], (CT) 2.0 [1.0; 3.0], and (TT) 2.0 [1.0; 3.0], p > 0.999. The similar dynamics of changes in scores as in the HAMD scale was obtained by other psychometric scales.

Figure 2 demonstrates the dynamics of changes in the UKU scores among the patients. As shown, by the day 1 of the research no statistically significant differences in scores for carriers of different genotypes for the studied polymorphic marker were obtained: (CC) 0.5 [0.0; 1.0], (CT) 1.0 [0.0; 1.0], and (TT) 0.0 [0.0; 1.0], p = 0.535. By day 9, statistically significant differences disappeared (were not detected): (CC) 2.0 [2.0; 2.2], (CT) 2.0 [2.0; 2.0], and (TT) 2.0 [2.0; 3.0], p = 0.502. Statistically significant differences were not obtained on the 16th day of the therapy: (CC) 3.0 [2.8; 3.0], (CT) 3.0 [3.0; 3.0], and (TT) 3.0 [3.0; 3.0], p > 0.999.

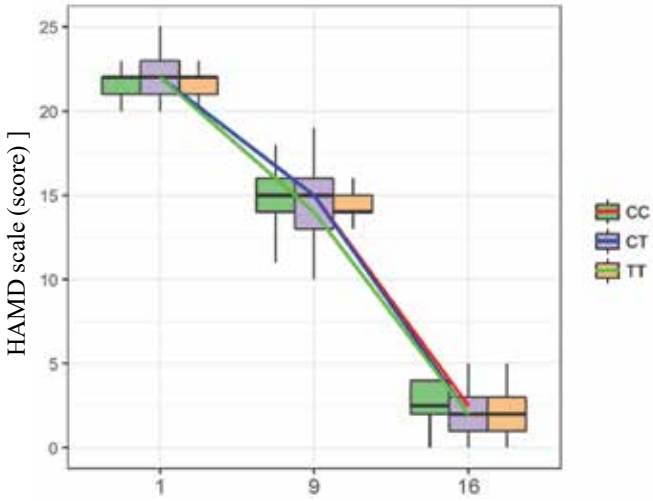

Fig. 1. Dynamics of changes in the HAMD scale scores among the patients with different genotypes in 3435C>T (rs1045642) ABCB1 polymorphic marker

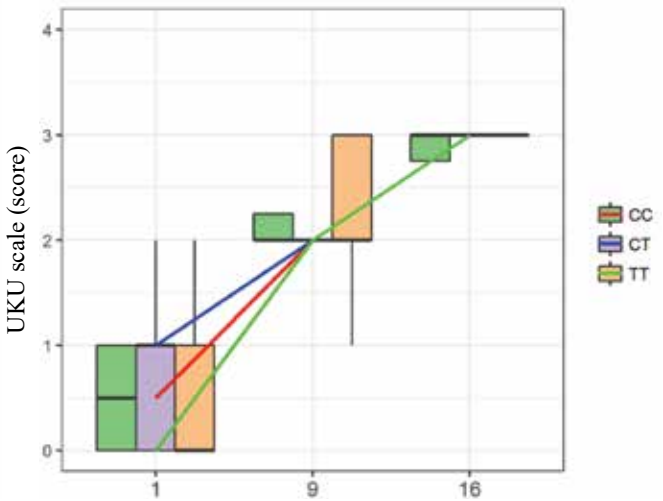

Fig. 2. Dynamics of changes in the UKU scale scores among the patients with different genotypes in 3435C>T (rs1045642) ABCB1 polymorphic marker

DISCUSSION

Statistical analysis of the data on mirtazapine clinical effectiveness and safety profile in patients with different genotypes for the 3435C>T polymorphic marker of the *ABCB1* gene (rs1045642) showed no statistically significant differences in effectiveness and safety (p > 0.999). These results may indicate the absence of the effect of this polymorphic marker on the clinical effectiveness and treatment safety of this group of patients.

Thus, according to the obtained results, which showed that the *ABCB1* gene (rs1045642) 3435C> T genetic polymorphism does not affect the effectiveness and safety rates of mirtazapine therapy in patients with depresssion disorders, comorbid with alcohol use disroder, it is possible to assume that it is not necessary to take into account the results of genotyping by the loci of this gene before prescribing mirtazapine to such patients. At the same time, prior studies manifested that *CYP2D6* gene polymorphisms should be taken into account when administering mirtazapine, as this may have an impact on the mirtazapine effectiveness and safety profile in patients with depressive disorders, comorbid with alcohol use disorder [14–16].

CONCLUSION

The current study conducted on 119 patients with depressive disorders, comorbid with alcohol use disorder, found the absence of the effect of *ABCB1* gene 3435C> T polymorphism (rs1045642) on the clinical effectiveness and safety of mirtazapine.

REFERENCES

1. Boschloo L., Vogelzangs N., Smit J.H, van den Brink W., Veltman D.J., Beekman A.T., Penninx B.W. Comorbidity and risk indicators for alcohol use disorders among persons with anxiety and/or depressive disorders: findings from the Netherlands Study of Depression and Anxiety (NESDA). *J. Affect Disord.* 2011; 131 (1–3): 233–242. DOI: 10.1016/j.jad.2010.12.014.
2. Shiv G., Akhilesh J., Manaswi G. Guidelines for the pharmacological management of depression. *Indian J. Psychiatry.* 2017; 59 (1): 34–50. DOI: 10.4103/0019-5545.196973.
3. Spear B.B., Heath-Chiozzi M., Huff J. Clinical application of pharmacogenetics. *Trends Mol. Med.* 2001; 7 (5): 201–204. DOI: 10.1016/s1471-4914(01)01986-4.
4. Peters E.J., Reus V., Hamilton S.P. The ABCB1 transporter gene and antidepressant response. *F1000 Biol. Rep.* 2009; 1: 23. DOI: 10.3410/B1-23.
5. Wolking S., Schaeffeler E., Lerche H., Schwab M., Nies A.T. Impact of genetic polymorphisms of ABCB1 (MDR1, P-Glycoprotein) on drug disposition and potential clinical implications: update of the literature. *Clin. Pharmacokinet.* 2015; 54 (7): 709–735. DOI: 10.1007/s40262-015-0267-1.
6. Ieiri I., Takane H., Otsubo K. The MDR1 (ABCB1) gene polymorphism and its clinical implications. *Clin. Pharmacokinet.* 2004; 43 (9): 553–576. DOI: 10.2165/00003088-200443090-00001.
7. Ahmed S., Zhou Z., Zhou J., Chen S.Q. Pharmacogenomics of drug metabolizing enzymes and transporters: relevance to precision medicine. *Genomics Proteomics Bioinformatics.* 2016; 14 (5): 298–313. DOI: 10.1016/j.gpb.2016.03.008.
8. Flannery B.A., Volpicelli J.R., Pettinati H.M. Psychometric properties of the Penn Alcohol Craving Scale. *Alcohol. Clin. Exp. Res.* 1999; 23 (8): 1289–1295.
9. Gould D., Kelly D., Goldstone L., Gammon J. Visual Analogue Scale (VAS). *Journal of Clinical Nursing.* 2001; 10 (5): 697–706. DOI: 10.1046/j.1365-2702.2001.00525.x.
10. Busner J., Targum S.D. The clinical global impressions scale: applying a research tool in clinical practice. *Psychiatry (Edgmont).* 2007; 4 (7): 28–37.
11. Zigmond A.S., Snaith R.P. The hospital anxiety and depression scale. *Acta Psychiatr. Scand.* 1983; 67 (6): 361–370. DOI: 10.1111/j.1600-0447.1983.tb09716.x.
12. Hamilton M. A rating scale for depression. J. Neurol. Neurosurg. *Psychiatry.* 1960; 23 (1): 56–62. DOI: 10.1136/jnnp.23.1.56.
13. Lingjaerde O., Ahlfors U.G., Bech P., Dencker S.J., Elgen K. The UKU side effect rating scale. A new comprehensive rating scale for psychotropic drugs and a cross-sectional study of side effects in neuroleptic-treated patients. *Acta Psychiatr. Scand. Suppl.* 1987; 334: 1–100. DOI: 10.1111/j.1600-0447.1987.tb10566.x.
14. Zastrozhin M.S., Skryabin V.Y., Smirnov V.V., Grishina E.A., Ryzhikova K.A., Chumakov E.M., Bryun E.A., Sychev D.A. Effects of CYP2D6 activity on the efficacy and safety of mirtazapine in patients with depressive disorders and comorbid alcohol use disorder. *Can. J. Physiol. Pharmacol.* 2019; 97 (8): 781–785. DOI: 10.1139/cjpp-2019-0177.
15. Zastrozhin M.S., Sorokin A.S., Agibalova T.V., Grishina E.A., Antonenko A.P., Rozochkin I.N., Duzhev D.V., Skryabin V.Y., Galaktionova T.E., Barna I.V., Orlova A.V., Aguzarov A.D., Savchenko L.M., Bryun E.A., Sychev D.A. Using a personalized clinical decision support system for bromdihydrochlorphenylbenzodiazepine dosing in patients with anxiety disorders based on the pharmacogenomic markers. *Hum. Psychopharmacol.* 2018; 33 (6): e2677. DOI: 10.1002/hup.2677.
16. Zastrozhin M.S., Skryabin V.Y., Miroshkin S.S., Bryun E.A., Sychev D.A. Pharmacogenetics of alcohol addiction: current perspectives. *Appl. Clin. Genet.* 2019; 12: 131–140. DOI: 10.2147/TACG.S206745.

Acknowledgments

The authors are deeply grateful to all the doctors and heads of the departments of Moscow Scientific and Practical Centre on Addictions of Moscow Department of Health for their invaluable assistance in the conduction of this study, as well as to the staff and administration of the institutions for providing the basis for laboratory research.

Authors contribution

Zastrozhin M.S. – conception and design of the study, recruitment of study participants, biomaterial sampling, carrying out of the genotyping, statistical processing of the obtained data, drafting of the article. Scryabin V.Yu. – recruitment of study participants, biomaterial sampling, carrying out of the genotyping, statistical processing of the obtained data, drafting of the article. Ryzhikova K.A. – carrying out of the genotyping, revision and editing of the article. Grishina E.A. – design of the laboratory part of the study, carrying out of the genotyping, revision and editing of the article. Koporov S.G. – conception and design of the study, assistance in resolving administrative and ethical issues, revision and editing of the article. Bryun E.A. – conception and design of the study, revision and editing of the article. Sychev D.A. – the idea of the study, conception and design of the study, revision and editing of the article. All authors made a substantial contribution to the research and preparation of the research paper, and were involved in drafting of the article or its critical revision for important intellectual content and gave final approval of the revision to be published.

Authors information

Zastrozhin Mikhail S., Cand. Sci. (Med.), Head of Laboratory of Genetics and Fundamental Studies, Moscow Research and Practical Centre on Addictions; Associate Professor, Addiction Psychiatry Department, Russian Medical Academy of Continuous Professional Education, Moscow, Russian Federation. ORCID 0000-0003-0607-4812.

Skryabin Valentin Yu., Cand. Sci. (Med.), Head of Narcology Department №16, Moscow Research and Practical Centre on Addictions, Moscow, Russian Federation. ORCID 0000-0002-4942-8556.

Grishina Elena A., Dr. Sci. (Biology), Associate Professor, Senior Researcher, Head of Biomolecular Researchers Department, Research Institute of Molecular and Personalized Medicine, Russian Medical Academy of Continuous Professional Education, Moscow, Russian Federation. ORCID 0000-0002-5621-8266.

Ryzhikova Kristina A., Junior Researcher, Biomolecular Researchers Department, Research Institute of Molecular and Personalized Medicine, Russian Medical Academy of Continuous Professional Education, Moscow, Russian Federation. ORCID 0000-0003-3505-8520.

Koporov Sergey S., Cand. Sci. (Med.), Director, Moscow Research and Practical Centre on Addictions, Moscow, Russian Federation. ORCID 0000-0003-2584-4832.

Bryun Evgeny A., Dr. Sci. (Med.), Professor, President, Moscow Research and Practical Centre on Addictions; Head of Addiction Psychiatry Department, Russian Medical Academy of Continuous Professional Education, Moscow, Russian Federation. ORCID 0000-0002-8366-9732.

Sychev Dmitry A., Dr. Sci. (Med.), Professor, Corresponding Member of the Russian Academy of Sciences, Head of Clinical Pharmacology and Therapy Department, Rector of Russian Medical Academy of Continuous Professional Education, Moscow, Russian Federation. ORCID 0000-0002-4496-3680.

(✉) **Zastrozhin Mikhail S.,** e-mail: mszastrozhin@gmail.com.

Received: 09.08.2019
Accepted: 25.12.2019

УДК 616.12-036.886:577.21
https://doi.org/10.20538/1682-0363-2020-4-80-85

ABCA1 gene promoter methylation and sudden cardiac death

Ivanova A.A.[1], Gurazheva A.A.[1], Akinshina E.I.[1], Maksimova S.V.[2], Malyutina S.K.[1], Novoselov V.P.[3], Rodina I.A.[3], Khamovich O.V.[3], Maksimov V.N.[1]

[1] *Institution of Internal and Preventive Medicine, Branch of the Institute of Cytology and Genetics, Siberian Branch of the Russian Academy of Sciences*
175/1, B. Bogatkova Str., Novosibirsk, 630089, Russian Federation

[2] *Novosibirsk State Medical University*
52, Krasny Av., Novosibirsk, 630091, Russian Federation

[3] *Novosibirsk Regional Office of Forensic Medical Examination*
134, Nemirovicha-Danchenko Str., Novosibirsk, 630087, Russian Federation

ABSTRACT

Aim. To study the association of the methylation of the promoter of the *ABCA1* gene with sudden cardiac death (SCD).

Materials and methods. The study design is based on the case-control principle. The SCD group included 150 men (mean age (46.7 ± 9.2) years) who died of sudden cardiac death according to forensic medical examination data (the main pathological diagnoses are acute circulatory failure, acute coronary insufficiency). The control group included 150 men (mean age (42.6 ± 1.2) years) who died suddenly, but not due to cardiovascular pathology. DNA was isolated by phenol-chloroform extraction from myocardial tissue. The methylation status of the *ABCA1* gene promoter was assessed by methyl-specific polymerase chain reaction. The results obtained were statistically processed in SPSS 16.0 using Pearson's test and Fisher's test with Yates' correction for continuity. $P < 0.05$ was used as a level of significance.

Results. Comparing the groups revealed statistically significant differences in the methylation status of the gene promoter ($p = 0.015$). In the SCD group, the proportion of individuals whose *ABCA1* gene promoter is methylated is statistically significantly higher compared to the control group ($p = 0.020$; OR = 5.86; 95% CI (1.28–26.89)).

Conclusion. Methylation of the promoter of the *ABCA1* gene is associated with sudden cardiac death.

Key words: sudden cardiac death, methylation, *ABCA1*, promoter.

Conflict of interest. The authors declare no obvious or potential conflict of interest related to the publication of this article.

Source of financing. The study was carried out with the financial support of the Russian Foundation for Basic Research and the Government of the Novosibirsk Region (project No. 19-415-543001).

Conformity with the principles of ethics. The study was approved by the local Ethics Committee at the Institution of Internal and Preventive Medicine (Protocol No. 77 of 04.06.2019).

For citation: Ivanova A.A., Gurazheva A.A., Akinshina E.I., Maksimova S.V., Malyutina S.K., Novoselov V.P., Rodina I.A., Khamovich O.V., Maksimov V.N. *ABCA1* gene promoter methylation and sudden cardiac death. *Bulletin of Siberian Medicine.* 2020; 19 (4): 80–85. https://doi.org/10.20538/1682-0363-2020-4-80-85.

✉ *Ivanova Anastasia A.,* e-mail: ivanova_a_a@mail.ru.

Метилирование промотора гена *ABCA1* и внезапная сердечная смерть

Иванова А.А.[1], Гуражева А.А.[1], Акиншина Е.И.[1], Максимова С.В.[2], Малютина С.К.[1], Новоселов В.П.[3], Родина И.А.[3], Хамович О.В.[3], Максимов В.Н.[1]

[1] Научно-исследовательский институт терапии и профилактической медицины (НИИТПМ) – филиал Федерального исследовательского центра «Институт цитологии и генетики» Сибирского отделения Российской академии наук (ФИЦ ИЦиГ СО РАН)
Россия, 630089, г. Новосибирск, ул. Б. Богаткова, 175/1

[2] Новосибирский государственный медицинский университет (НГМУ)
Россия, 630091, г. Новосибирск, Красный проспект, 52

[3] Новосибирское областное клиническое бюро судебно-медицинской экспертизы (НОКБСМЭ)
Россия, 630087, г. Новосибирск, ул. Немировича-Данченко, 134

РЕЗЮМЕ

Цель. Исследование ассоциации метилирования промотора гена *ABCA1* с внезапной сердечной смертью (ВСС).

Материалы и методы. Дизайн исследования построен по принципу «случай – контроль». Группа ВСС включала 150 мужчин (средний возраст (46,7 ± 9,2) года), умерших внезапной сердечной смертью согласно данным судебно-медицинской экспертизы (основные патологоанатомические диагнозы – острая недостаточность кровообращения, острая коронарная недостаточность). Контрольная группа включает 150 мужчин (средний возраст (42,6 ± 1,2) года), умерших внезапно, но не вследствие сердечно-сосудистой патологии. ДНК выделена методом фенол-хлороформной экстракции из ткани миокарда. Оценка статуса метилирования промотора гена *ABCA1* проведена методом метил-специфической полимеразной цепной реакции. Полученные результаты статистически обработаны в SPSS 16.0 с применением критерия Пирсона, критерия Фишера с поправкой Йетса на непрерывность. В качестве уровня значимости использован $p < 0,05$.

Результаты. При сравнении групп выявлены статистически значимые различия по статусу метилирования промотора гена *ABCA1* между группами ($p = 0,015$). В группе ВСС доля лиц, у которых промотор гена *ABCA1* метилирован, статистически значимо больше по сравнению с контрольной группой ($p = 0,020$; ОШ = 5,86; 95%-й доверительный интервал (1,28–26,89)).

Заключение. Метилирование промотора гена *ABCA1* ассоциировано с внезапной сердечной смертью.

Ключевые слова: внезапная сердечная смерть, метилирование, *ABCA1*, промотор.

Конфликт интересов. Авторы декларируют отсутствие явных и потенциальных конфликтов интересов, связанных с публикацией настоящей статьи.

Источник финансирования. Исследование выполнено при финансовой поддержке РФФИ и Правительства Новосибирской области (проект № 19-415-543001).

Соответствие принципам этики. Исследование одобрено локальным этическим комитетом НИИТПМ – филиалом ФИЦ ИЦИГ СО РАН (протокол № 77 от 04.06.2019).

Для цитирования: Иванова А.А., Гуражева А.А., Акиншина Е.И., Максимова С.В., Малютина С.К., Новоселов В.П., Родина И.А., Хамович О.В., Максимов В.Н. Метилирование промотора гена *ABCA1* и внезапная сердечная смерть. *Бюллетень сибирской медицины.* 2020; 19 (4): 80–85. https://doi.org/10.20538/1682-0363-2020-4-80-85.

INTRODUCTION

The term “sudden cardiac death” (SCD), according to the latest recommendations of the European Society of Cardiology, is used when a fatal outcome has developed within 1 hour from the onset of acute symptoms in the case of a known fatal cardiac pathology/found on autopsy fatal cardiac pathology/not found on autopsy of the causes of sudden death (sudden arrhythmic death). In the absence of witnesses to death, the time criterion for SCD is increased to 24 hours.

It is believed that the etiology of SCD at a young age is dominated by cardiac arrhythmias, cardiomyopathies, myocarditis and other more rare diseases, the contribution of which to the occurrence of SCD at the population level is small. At an older age, ischemic heart disease, also called coronary heart disease (CHD), heart failure, valvular defects, and secondary cardiac arrhythmias come out on top. At a young age, even after a high-quality forensic study, the cause of sudden death may remain unknown [1].

Currently, mortality due to cardiovascular diseases (CVD) occupies a leading position in the structure of mortality in the Russian population (583.1 people per 100 thousand of the population per year according to the Federal State Statistics Service of 2018) [2]. In almost half of cases, SCD develops in a provisionally healthy person who did not have any previous manifestations of cardiovascular pathology. The survival rate of patients after an episode of SCD, even while in a hospital, is still low [1].

In this regard, the identification of biomarkers that will help determine the predisposition to the development of SCD, especially in a patient without symptoms of cardiac pathology, is an important task of modern healthcare, since the existing clinical and diagnostic criteria for stratification of SCD risk play a significant role only for patients with already identified heart pathology, previous myocardial infarction and a history of sudden cardiac death. Thus, new biomarkers are essential for early primary prevention of SCD development.

SCD is a multifactorial nosology, the contribution to the development of which is made by genetic and environmental factors. To date, a huge number of polymorphisms and gene mutations associated with SCD have been identified. However, it is still unclear how genes with a critical role in the pathogenesis of SCD interact at the cellular level. It is not yet possible to use individual single nucleotide variants of genes as diagnostic markers of SCD. The data obtained during the study of DNA methylation can help to understand the mechanisms of the implementation of genetic information in the pathogenesis of SCD.

A number of studies have shown that the assessment of methylation of individual genes, as well as the results of genome-wide methylation, can be used as diagnostic markers of the risk of developing a disease (for example, atherosclerosis, CHD), the severity of symptoms, and the prognosis of the course. If epigenetic studies of this kind are carried out for many CVDs, then, according to the world literature data, DNA methylation studies of SCD have not yet been carried out.

The *ABCA1* gene (ATP binding cassette subfamily A member 1, 9q31.1) encodes a protein that is required for the removal of cholesterol from peripheral tissues. It has been shown that gene inactivation by methylation of its promoter is associated with the development of coronary artery disease, which is the most common SCD substrate among middle-aged and older people [3].

Thus, the aim of the project is to study the association of methylation of the *ABCA1* gene promoter with SCD.

MATERIALS AND METHODS

The study design is based on the case-control principle. The SCD group included 150 men (mean age (46.7 ± 9.2) years) who died of sudden cardiac death according to forensic medical examination data (the main pathological diagnoses were acute circulatory failure, acute coronary insufficiency). Criteria for exclusion from the group of sudden cardiac death were the presence of morphological changes in the heart tissue characteristic of myocardial infarction and cardiomyopathies. In addition, persons who were in a state of alcoholic and drug intoxication were excluded from the group. The control group included 150 men (mean age (42.6 ± 1.2) years) who died suddenly (1: 1 matching method), but not due to cardiovascular pathology. DNA was isolated by phenol-chloroform extraction from myocardial tissue in the group of sudden cardiac death and in the control group.

The selection of a control group from the DNA bank of people who died suddenly, and the use of DNA isolated from myocardial tissue, both in the SCD group and in the control group, were dictated by the proven tissue-specificity of DNA methylation.

The methylation status of the *ABCA1* gene promoter was assessed by methyl-specific polymerase chain reaction (PCR) on bisulfite-converted DNA. EZ DNA Methylation Kit (Zymo Research, USA) was used for bisulfite conversion of DNA samples. Methyl-specific PCR was carried out in two tubes: with primers specific for the methylated and unmethylated allele, according to the methods described in the study by H. Ghaznavi et al. [3].

The results obtained were statistically processed in SPSS 16.0 using Pearson's test, Fisher's test with Yates' correction for continuity; $p < 0.05$ was used as a level of statistical significance.

RESULTS

In the SCD group, 22% (33/150) of the *ABCA1* gene promoter is fully methylated (MM); 1.3% (2/150) is completely unmethylated (UU); 76.7% (115/150) had both methylated and unmethylated gene promoter (MU). In the control group, 27.3% (41/150) of the ABCA1 gene promoter is completely methylated; in 7.4% (11/150) it is completely unmethylated; 65.3% (98/150) had both methylated and unmethylated gene promoters. When comparing the groups, statistically significant differences in the methylation status of the *ABCA1* gene promoter were revealed between the groups ($p = 0.015$). In the SCD group, the proportion of individuals in whom the *ABCA1* gene promoter is methylated is statistically significantly greater than in the control group (MM + MU vs. UU: $p = 0.020$; OR = 5.86; 95% confidence interval (1.28–26.89)).

DISCUSSION

Epigenetic changes form the boundary between genotype and environment. It is believed that epigenetic variability may significantly contribute to the development of CVD. Over the past two decades, many studies have been conducted to find the link between DNA methylation and cardiovascular disease. DNA methylation is usually viewed in the context of CpG dinucleotide sequence (CpG sites). In mammalian somatic cells, most of the CpG sites are methylated. But CpG sites in regions of increased CpG density (CpG islands) are usually described as sites with reduced methylation. DNA methylation of the gene promoter is an important factor for the regulation of transcription [4]. It is known that hypomethylation of a gene promoter increases its expression, while hypermethylation decreases it. It is important to note that the level of methylation of individual genes is tissue-specific [5]. The accumulated knowledge suggests that epigenetic changes, such as DNA methylation abnormalities, may help to find an alternative explanation for the pathophysiology of CVD [6].

A variety of loci have been studied for methylation of individual genes for each cardiovascular phenotype. Studies of the methylation level in SCD according to the available world literature have not been carried out. However, studies have been conducted to study methylation in other CVDs that underlie SCD or have a similar pathophysiological basis. The most studied nosology in relation to methylation is coronary heart disease and its varieties.

The *ABCA1* gene (ATP binding cassette subfamily A member 1, 9q31.1) encodes a transporter of molecules across extra- and intracellular membranes. Using cholesterol as a substrate, protein functions as an efflux pump for the reverse transport of lipids in cells. Gene mutations are associated with the development of familial alpha-lipoprotein deficiency (hypoalphalipoproteinemia) and familial high-density lipoprotein deficiency [7]. Expression of the *ABCA1* gene has been identified as an independent predictor of the development of ischemic heart disease, atherosclerotic plaques, including uncalcified ones [8]. Methylation of the *ABCA1* gene promoter was identified as a significant risk factor for the development, but not the severity of the ischemic heart disease: the frequency of methylation of the promoter is higher in the group of people with ischemic heart disease compared to the control group, as well as in the older age group [3]. The methylation level of the *ABCA1* gene promoter negatively correlates with the concentration of high-density lipoprotein cholesterol in individuals with familial hypercholesterolemia. Additionally, methylation of the *ABCA1* gene is associated with a history of ischemic heart disease [7].

In a pilot study, it was shown that methylation of the *ABCA1* gene promoter can be used as a significant biomarker for early diagnosis of atherosclerosis [9]. In women in Japan, an inverse relationship between methylation of the gene promoter and the level of high-density lipoprotein cholesterol was confirmed, and a relationship was found between the methylation level of the *ABCA1* gene promoter and diet. In women with a diet enriched with vegetables and vitamins, the level of gene promoter methylation is significantly lower [10, 11]. Polymorphisms of the *ABCA1* gene are associated with the level of a number of lipid metabolism indicators: rs363717, rs2230806, rs4149313, rs9282541 – with the risk of coronary heart disease, rs2230808 – with the level of total cholesterol in the blood, rs363717, rs4149339, rs4149338 – with the increased levels of triglycerides in the blood. [9, 12, 13]. The rs2230806 polymorphism is associated with triglyceride levels in patients with severe dyslipidemia [14]. According to the meta-analysis, the level of high-density lipoprotein cholesterol is associated with the rs2246293 polymorphism [15].

According to our data, methylation of the *ABCA1* gene promoter is associated with the risk of SCD. In the SCD group, the proportion of individuals in whom the *ABCA1* gene promoter is methylated is statistically significantly higher than in the control group. According to the data of the world scientific literature, studies on the search for the relationship between

methylation of the *ABCA1* gene promoter and SCD have not been carried out. Nevertheless, foreign studies have shown that methylation of the gene promoter is associated with the risk of ischemic heart disease and impaired lipid homeostasis. Since ischemic heart disease is the most common substrate for the development of SCD in the older age group, our results are consistent. However, due to the small number of groups included in the study, additional verification of the identified association in groups with a larger size is required, with the inclusion of women in the study.

CONCLUSION

Methylation of the *ABCA1* gene promoter is statistically significantly associated with sudden cardiac death.

REFERENCES

1. Priori S.G., Blomström-Lundqvist C., Mazzanti A., Blom N., Borggrefe M., Camm J., Elliott P.M., Fitzsimons D., Hatala R., Hindricks G., Kirchhof P., Kjeldsen K., Kuck K.H., Hernandez-Madrid A., Nikolaou N., Norekvål T.M., Spaulding C., van Veldhuisen D.J. The task force for the management of patients with ventricular arrhythmias and the prevention of sudden cardiac death of the European Society of Cardiology (ESC). *G. Ital. Cardiol.* 2016; 17 (2): 108–170. DOI: 10.1714/2174.23496.
2. Federal State Statistics Service. Information and analytical materials. Natural movement of the population (in Russ.). URL: https://gks.ru/compendium/document/13269.
3. Ghaznavi H., Mahmoodi K., Soltanpour M.S. A preliminary study of the association between the *ABCA1* gene promoter DNA methylation and coronary artery disease risk. *Mol. Biol. Res. Commun*. 2018; 7 (2): 59–65. DOI: 10.22099/mbrc.2018.28910.1312.
4. Nazarenko M.S., Markov A.V., Lebedev I.N., Freidin M.B., Sleptcov A.A., Koroleva I.A., Frolov A.V., Popov V.A., Barbarash O.L., Puzyrev V.P. A comparison of genome-wide DNA methylation patterns between different vascular tissues from patients with coronary heart disease. *PLoS One.* 2015; 10 (4): e0122601. DOI: 10.1371/journal.pone.0122601.
5. Wang X., Liu A.H., Jia Z.W., Pu K., Chen K.Y., Guo H. Genome-wide DNA methylation patterns in coronary heart disease. *Herz.* 2018; 43 (7): 656–662. DOI: 10.1007/s00059-017-4616-8.
6. Banerjee S., Ponde C.K., Rajani R.M., Ashavaid T.F. Differential methylation pattern in patients with coronary artery disease: pilot study. *Mol. Biol. Rep.* 2019; 46 (1): 541–550. DOI: 10.1007/s11033-018-4507-y.
7. Guay S.P., Légaré C., Brisson D., Mathieu P., Bossé Y., Gaudet D., Bouchard L. Epigenetic and genetic variations at the *TNNT1* gene locus are associated with HDL-C levels and coronary artery disease. *Epigenomics*. 2016; 8 (3): 359–371. DOI: 10.2217/epi.15.120.
8. Infante T., Forte E., Schiano C., Punzo B., Cademartiri F., Cavaliere C., Salvatore M., Napoli C. Evidence of association of circulating epigenetic-sensitive biomarkers with suspected coronary heart disease evaluated by cardiac computed tomography. *PLoS One*. 2019; 14 (1): e0210909. DOI: 10.1371/journal.pone.0210909.
9. Ma S.C., Zhang H.P., Kong F.Q., Zhang H., Yang C., He Y.Y., Wang Y.H., Yang A.N., Tian J., Yang X.L., Zhang M.H., Xu H., Jiang Y.D., Yu Z. Integration of gene expression and DNA methylation profiles provides a molecular subtype for risk assessment in atherosclerosis. *Mol. Med. Rep.* 2016; 13 (6): 4791–4799. DOI: 10.3892/mmr.2016.5120.
10. Fujii R., Yamada H., Munetsuna E., Yamazaki M., Mizuno G., Tsuboi Y., Ohashi K., Ishikawa H., Ando Y., Hagiwara C., Maeda K., Hashimoto S., Hamajima N., Suzuki K. Dietary vegetable intake is inversely associated with ATP-binding cassette protein A1 (ABCA1) DNA methylation levels among Japanese women. *Nutrition*. 2019; 65: 1–5. DOI: 10.1016/j.nut.2019.02.010.
11. Fujii R., Yamada H., Munetsuna E., Yamazaki M., Ando Y., Mizuno G., Tsuboi Y., Ohashi K., Ishikawa H., Hagiwara C., Maeda K., Hashimoto S., Suzuki K. Associations between dietary vitamin intake, *ABCA1* gene promoter DNA methylation, and lipid profiles in a Japanese population. *Am. J. Clin. Nutr*. 2019; 110 (5): 1213–1219. DOI: 10.1093/ajcn/nqz181.
12. Lu Y., Liu Y., Li Y., Zhang H., Yu M., Kanu J.S., Qiao Y., Tang Y., Zhen Q., Cheng Y. Association of ATP-binding cassette transporter A1 gene polymorphisms with plasma lipid variability and coronary heart disease risk. *Int. J. Clin. Exp. Pathol.* 2015; 8 (10): 13441–13449.
13. Wang F., Ji Y., Chen X., Song Y., Huang S., Zhou C., Huang C., Chen Z., Zhang L., Ge J. *ABCA1* variants rs2230806 (R219K), rs4149313 (M8831I), and rs9282541 (R230C) are associated with susceptibility to coronary heart disease. *J. Clin. Lab. Anal.* 2019; 33 (6): e22896. DOI: 10.1002/jcla.22896.
14. Smirnov G.P., Malyshev P.P., Rozhkova T.A., Zubareva M.Y., Shuvalova Y.A., Rebrikov D.V., Titov V.N. The effect of ABCA1 rs2230806 common gene variant on plasma lipid levels in patients with dyslipidemia. *Klin. Lab. Diagn.* 2018; 63 (7): 410–413. DOI: 10.18821/0869-2084 -2018-63-7-410-413.
15. Ma Y., Follis J.L., Smith C.E., Tanaka T., Manichaikul A.W., Chu A.Y., Samieri C., Zhou X., Guan W., Wang L., Biggs M.L., Chen Y.D., Hernandez D.G., Borecki I., Chasman D., Rich S.S., Ferrucci L., Irvin M.R., Aslibekyan S., Zhi D., Tiwari H.K., Claas S.A., Sha J., Kabagambe E.K., Lai C.Q., Parnell L.D., Lee Y.C., Amouyel P., Lambert J.C., Psaty B.M., King I.B., Mozaffarian D., McKnight B., Bandinelli S., Tsai M.Y., Ridker P.M., Ding J., Mstat K.L., Liu Y., Sotoodehnia N., Barberger-Gateau P., Steffen L.M., Siscovick D.S., Absher D., Arnett D.K., Ordovás J.M., Lemaitre RN interaction of methylation-related genetic variants with circulating fatty acids on plasma lipids: a meta-analysis of 7 studies and methylation analysis of 3 studies in the cohorts for heart and aging research in genomic pidemiology consortium. *Am. J. Clin. Nutr*. 2016; 103 (2): 567–578. DOI: 10.3945/ajcn.115.112987.

Authors contribution

Ivanova A.A. – conception and design development, analysis and interpretation of the data. Gurazheva A.A. – carrying out of bisulfite conversion of DNA. Akinshina E.I., Maksimova S.V. – carrying out of methyl-specific PCR. Malyutina S.K. – conception and design development. Novoselov V.P., Rodina I.A., Khamovich O.V. – carrying out of the forensic medical stage of the study. Maximov V.N. – conception and design development, final approval of the article for publication.

Authors information

Ivanova Anastasia A., Cand. Sci. (Med.), Senior Researcher, Laboratory of Molecular Genetic Investigation of Internal Diseases, Institution of Internal and Preventive Medicine, Novosibirsk, Russian Federation. ORCID 0000-0002-9460-6294.

Gurazheva Anna A., Junior Researcher, Laboratory of Molecular Genetic Investigation of Internal Diseases, Institution of Internal and Preventive Medicine, Novosibirsk, Russian Federation. ORCID 0000-0003-1547-624X.

Akinshina Elena I., Junior Researcher, Laboratory of Molecular Genetic Investigation of Internal Diseases, Institution of Internal and Preventive Medicine, Novosibirsk, Russian Federation. ORCID 0000-0002-2924-9147.

Maksimova Sofya V., 3rd-Year Student, Department of Pediatrics, Novosibirsk State Medical University, Novosibirsk, Russian Federation. ORCID 0000-0002-2472-181X.

Malyutina Sofia K., Dr. Sci. (Med.), Professor, Head of the Laboratory of Etiopathogenesis and Clinical Features of Internal Diseases, Institution of Internal and Preventive Medicine, Novosibirsk, Russian Federation. ORCID 0000-0001-6539-0466.

Novoselov Vladimir P., Dr. Sci. (Med.), Professor, Head of Novosibirsk Regional Office of Forensic Medical Examination, Novosibirsk, Russian Federations. ORCID 0000-0002-6312-5543.

Rodina Irina A., Cand. Sci. (Med.), Forensic Expert Physician, Novosibirsk Regional Office of Forensic Medical Examination, Novosibirsk, Russian Federation. ORCID 0000-0003-2799-0756.

Khamovich Olesya V., Cand. Sci. (Med.), Forensic Expert Physician, Novosibirsk Regional Office of Forensic Medical Examination, Novosibirsk, Russian Federation. ORCID 0000-0002-2960-193X.

Maksimov Vladimir N., Dr. Sci. (Med.), Associate Professor, Head of the Laboratory of Molecular Genetic Investigation of Internal Diseases, Institution of Internal and Preventive Medicine, Novosibirsk, Russian Federation. ORCID 0000-0002-7165-4496.

(✉) **Ivanova Anastasia A.,** e-mail: ivanova_a_a@mail.ru.

Received 18.03.2019
Accepted 29.09.2019

УДК 616.1-089:611.14.018.74:577.152.312
https://doi.org/10.20538/1682-0363-2020-4-86-93

The role of recovered thiols in venous endothel adaptation in case of autovenous reconstruction of lower limb arteries

Kalinin R.E., Abalenikhina Yu.V., Pshennikov A.S., Vinogradov S.A.

Ryazan State Medical University
9, Vysokovoltnaya Str., Ryazan, 390026, Russian Federation

ABSTRACT

Aim. To evaluate the role of thiol status and its correlative relationship with the level of nitric oxide metabolites and vascular endothelial growth factor A (VEGF-A) in the blood plasma of patients with critical lower limb ischemia (CLI) after autovenous reconstructions of femoropopliteal segment's arteries in the setting of venous endothelium of the arterial bed.

Materials and methods. 54 patients with critical lower limb ischemia had been examined and divided into groups: synthetic prosthesis, *in situ* autovenous bypass procedure and reversed vein autovenous bypass procedure. Peripheral venous blood was taken on the 1st and 10th days, and in 1, 3 and 6 months after the operation. Nitric oxide metabolites level was examined with photocolorimetric method by reaction with Griess reagent on a microplate analyzer (Awareness Technology, USA). VEGF-A number estimation was done by ELISA test (PersonalLab, Italy) with the use of Human VEGF-A Platinum ELISA. The level of thiol (SH-) groups was estimated with the use of Ellman's reagent (SERVA, Germany) on spectrophotometer (Saint-Petersburg, Russian Federation).

Results. The concentration of VEGF-A and the level of SH-groups increase on the 10th day and after 1 month in the group of patients operated on using a synthetic prosthesis. The level of NO metabolites, the concentration of VEGF-A, and the content of SH-groups increase statistically significantly and then decrease to the initial values in the group of patients operated on by reversed vein autovenous bypass procedure. In the group of patients operated on by the *in situ* method, the level of nitric oxide metabolites increases, the concentration of VEGF-A increases on the 10th day, the level of SH-groups increases, and a positive correlation was found between the content of SH-groups and the concentration of VEGF-A.

Conclusion. NO metabolites contribute to the build-up of SH groups and VEGF-A in patients operated by the "reversed vein" method, and in patients in the *in situ* group, the concentration of VEGF-A and the level of SH groups are not affected, which may be of clinical importance when prescribing NO donors.

The revealed patterns of change in the level of recovered thiols, nitrogen oxide metabolites, VEGF-A in combination with analysis of early and late postoperative complications make it possible to conclude the advantage of autovenous reconstruction of the femoropopliteal segment due to functional adaptation of the venous endothelium compared to the group of patients, operated on by the method of "synthetic prosthesis". Method *in situ* on biochemical and angiological indicators proved to be more favorable in terms of the clinical course, than the "reversed vein" method.

Key words: nitric oxide metabolites, vascular endothelial growth factor, protein and nonprotein thiol groups, autovenous reconstruction of lower limbs arteries, reperfusion endothelial injury.

Conflict of interest. The authors declare no obvious or potential conflict of interest related to the publication of this article.

Source of financing. The research work was performed with financial support from the Russian Foundation for Basic Research in the frame of scientific project No. 18-315-00129 and scholarship of the President of the Russian Federation to young researchers and postgraduate students conducting advanced research in priority fields of the Russian economic modernization No. SP-2164.2018.4.

Conformity with the principles of ethics. All research participants gave personal informed consent approved by Ryazan State Medical University Ethics Committee (Protocol No. 1 of 16.10.2018).

✉ *Kalinin Roman E.,* e-mail: rzgmu@rzgmu.ru.

For citation: Kalinin R.E., Abalenikhina Yu.V., Pshennikov A.S., Vinogradov S.A. The role of recovered thiols in venous endothel adaptation in case of autovenous reconstruction of lower limb arteries. *Bulletin of Siberian Medicine.* 2020; 19 (4): 86–93. https://doi.org/10.20538/1682-0363-2020-4-86-93.

Роль восстановленных тиолов в адаптации венозного эндотелия при аутовенозной реконструкции артерий нижних конечностей

Калинин Р.Е., Абаленихина Ю.В., Пшенников А.С., Виноградов С.А.

Рязанский государственный медицинский университет (РязГМУ) им. акад. И.П. Павлова
Россия, 390026, г. Рязань, ул. Высоковольтная, 9

РЕЗЮМЕ

Цель. Оценить изменения тиолового статуса, выявить корреляционные связи между содержанием SH-групп и уровнем метаболитов оксида азота (NO), васкулоэндотелиальным фактором роста А (VEGF-A) плазмы крови пациентов с критической ишемией нижних конечностей (КИНК) после аутовенозных реконструкций артерий бедренно-подколенного сегмента в условиях артериального русла.

Материалы и методы. Обследованы 54 пациента с КИНК, которые разделены на три группы: шунтирование с использованием синтетического протеза, аутовенозное шунтирование по методу реверсированной вены и аутовенозное шунтирование по методу *in situ.* Забор периферической венозной крови производили на 1-е, 10-е сут, через 1, 3 и 6 мес после операции. Уровень метаболитов оксида азота оценивали фотоколориметрическим методом по реакции с реактивом Грисса на микропланшетном анализаторе (Awareness Technology, США). Определение концентрации VEGF-A осуществлялось путем иммуноферментного анализа (Personal Lab., Италия) с использованием Human VEGF-A Platinum ELISA. Содержания тиоловых (SH-) групп определяли с помощью реактива Эллмана (SERVA, Германия) на спектрофотометре СФ-2000 (г. Санкт-Петербург, Россия).

Результаты. Концентрация VEGF-A и уровень SH-групп возрастают на 10-е сут, через 1 мес в группе пациентов, оперированных с использованием синтетического протеза. Уровень метаболитов NO, концентрация VEGF-A, содержание SH-групп статистически значимо возрастают, а затем снижаются до исходных значений в группе пациентов, оперированных по методу реверсированной вены. В группе пациентов, оперированных по методу *in situ*, уровень метаболитов оксида азота повышается, концентрация VEGF-A увеличивается на 10-е сут, уровень SH-групп возрастает и выявлена положительная корреляционная связь между содержанием SH-групп и концентрацией VEGF-A.

Заключение. Метаболиты NO способствуют нарастанию SH-групп и VEGF-A у пациентов, оперированных по методу реверсированной вены, а у пациентов в группе *in situ* не влияют на концентрацию VEGF-A и уровень SH-групп, что может иметь клиническое значение при назначении доноров NO. Выявленные закономерности изменения уровня восстановленных тиолов, метаболитов оксида азота, VEGF-A в совокупности с анализом ранних и поздних послеоперационных осложнений позволяют сделать вывод о преимуществе аутовенозной реконструкции бедренно-подколенного сегмента за счет функциональной адаптации венозного эндотелия по сравнению с группой пациентов, оперированных с использованием синтетического протеза. Метод *in situ* по биохимическим и ангиологическим показателям оказался более благоприятным с точки зрения клинического течения, чем метод реверсированной вены.

Ключевые слова: метаболиты оксида азота, васкулоэндотелиальный фактор роста, белковые и небелковые тиоловые группы, аутовенозная реконструкция артерий нижних конечностей, реперфузионное повреждение эндотелия.

Конфликт интересов. Авторы декларируют отсутствие явных и потенциальных конфликтов интересов, связанных с публикацией настоящей статьи.

Источники финансирования. Исследование выполнено при финансовой поддержке РФФИ (проект № 18-315-00129) и стипендии Президента Российской Федерации молодым ученым и аспирантам, осуществляющим перспективные научные исследования и разработки по приоритетным направлениям модернизации российской экономики (№ СП-2164.2018.4).

Соответствие принципам этики. Все участники исследования подписали добровольное информированное согласие. Исследование одобрено локальным этическим комитетом РязГМУ им. акад. И.П. Павлова (протокол № 1 от 16.10.2018).

Для цитирования: Калинин Р.Е., Абаленихина Ю.В., Пшенников А.С., Виноградов С.А. Роль восстановленных тиолов в адаптации венозного эндотелия при аутовенозной реконструкции артерий нижних конечностей. *Бюллетень сибирской медицины.* 2020; 19 (4): 86–93. https://doi.org/10.20538/1682-0363-2020-4-86-93.

INTRODUCTION

The use of an autovenous conduit from the great saphenous vein (GSV) remains an acceptable method of open reconstructive vascular surgery. Currently, autovenous bypass is performed using the reverse vein method and the *in situ* method. The discussion about the advantages and disadvantages of both methods has not stopped for more than half a century: will the transformation of the autovein take the path of adaptation or maladjustment?

Published data describes a proposal on the possibility of considering the concentration of SH-groups as an indicator of the adaptive capabilities of the organism [1]. Since the 1960s, a large number of clinical studies have been performed in which a decrease in the concentration of SH-groups in the blood serum of patients with various diseases was obtained: cardiovascular disorders [2], diabetes mellitus [3], chronic renal failure [4], alcoholic cirrhosis [5] and other pathology [6]. The dynamics of changes in SH-groups against the background of autovenous reconstructions of the arteries of the lower extremities under conditions of reperfusion damage to the endothelium may turn out to be a marker for predicting the adaptive transformation of an arterialized vein.

It is known that the most important and early marker of intimal damage is endothelial dysfunction associated, first of all, with the inhibition of the production of nitric oxide (NO), the most important regulator of vascular tone [7, 8]. Nitric oxide, due to its functions, is a universal angioprotective substance on which structural changes in the vascular wall depend [9, 10]. It has been proven that NO helps to slow down the formation of neointima in the area of surgical anastomoses of an artery with a synthetic prosthesis in patients after surgery [11], therefore, it was suggested that treatment with drugs that stimulate the production of NO may have an inhibitory effect on the development of restenosis after surgery [12], acting as one of the mechanisms of long-term compensation of blood circulation. Since NO is a "short-lived" molecule, many of its protective properties are associated not only with direct action, but also with the endogenous protective systems activated by it, in particular with the activation of vasculoendothelial growth factor (VEGF) [13].

In this regard, it is relevant to study the thiol status and identify correlations between the content of SH-groups and the level of metabolites of nitric oxide, VEGF-A in blood plasma in combination with the analysis of early and late complications in patients with critical lower limb ischemia (CLI) after autovenous reconstruction of the arteries of the femoral-popliteal segment to assess the degree of adaptation of the venous endothelium in the settings of the arterial bed.

MATERIALS AND METHODS

The study included 54 patients with CLI (III–IV stage according to the Pokrovskiy – Fontaine classification), of whom there were 48 men (88.9%) and 6 women (11.1%). The average age was (64.6 ± 6.6) years. All patients gave informed consent to participate in the study and to use their bioassay. The patients were divided into three groups depending on the type of graft used for revascularization of the arteries of the femoral-popliteal segment: group A – synthetic prosthesis, group B – reversed vein and group C – *in situ* autovenous bypass grafting. Conical prostheses made of 4/8 mm polytetrafluoroethylene were used as a synthetic graft in all cases. In patients with autovenous revascularization, the ipsilateral great saphenous vein was used in all cases. Clinical groups were matched by gender, age, stage of the disease, comorbidity, initial minimum diameter of GSV, Rutherford outflow score (Table 1).

Post-operative peripheral venous blood withdrawal for evaluation of the examined biochemical indicators had been done on days 1 and 10, and on months 1, 3 and 6.

The level of nitric oxide metabolites (the total concentration of nitrates and nitrites) was determined by the photocolorimetric method by the development of color in the diazotization reaction with sulfanilamide nitrate, which is part of the Griess reagent (NevaReaktiv, Russia). Nitrites diazotize sulfanilamide, and the resulting substance reacts with azo coupling with naphthylethylenediamine to form a pink compound, the color intensity of which is proportional to the total concentration of nitrites and nitrates in the sample [14].

Table 1

Clinical characteristics of study groups

Parameter, unit of measure	Group A	Group B	Group C
Number of patients, *n*	18	18	18
Age, years	64.15 ± 6.5	64.9 ± 6.5	65.6 ± 6.9
Male, *n* (%)	16 (88.9 %)	16 (88.9 %)	16 (88.9 %)
Female, *n* (%)	2 (11.1 %)	2 (11.1 %)	2 (11.1 %)
Disease state on Pokrovskiy – Fontaine classification			
Stage III, *n* (%)	11 (61.1 %)	10 (55.6 %)	11 (61.1 %)
Stage IV, *n* (%)	7 (38.9 %)	8 (44.4 %)	7 (38.9 %)
Comorbidities			
Ischemic Heart disease, *n* (%)	12 (66.7%)	11 (61.1%)	14 (77.8%)
Hypertensive disease, *n* (%)	15 (83.3%)	16 (88.9%)	18 (100%)
Cerebrovascular diseases, *n* (%)	4 (22.2%)	3 (16.7%)	5 (27.8%)
Base Anatomic-Morphological Characteristics			
Great saphenous vein diameter on ultrasound duplex scanning, mm	-	3.5 ± 0.6	3.7 ± 0.7
Condition of outflow tract on Rutherford, points	6.1 ± 1.1	6.7 ± 1.4	6.5 ± 1.6
Type of reconstruction of infrainguinal segment arteries			
Method	Synthetic Prosthesis	Reversed vein	in situ
Above knee joint cleft	13 (72.2 %)	10 (55.6 %)	13 (72.2 %)
Below knee joint cleft	5 (27.8 %)	8 (44.4 %)	5 (27.8 %)

The color intensity was assessed in the visible spectral region with registration on a StatFax 3200 microplate analyzer (Awareness Technology, USA) at a wavelength of 540 nm and expressed in nmol/mg protein.

Determination of the active form of human vasculoendothelial growth factor A (VEGF-A) was carried out by enzyme immunoassay on Personal Lab units (Italy) using Human VEGF-A Platinum ELISA human VEGF-A (BMS277/2) (BioChimMac, Moscow, Russia). The intensity of the color measured at 450 nm is directly proportional to the concentration of VEGF-A present in the samples. The VEGF-A concentration in the samples was determined using a standard curve and expressed in pg/ml.

The level of intracellular and extracellular reducing agents was assessed by the change in the content of thiol (SH-) groups, which were determined using Ellman's reagent on an SF-2000 spectrophotometer (St. Petersburg, Russia) [15]. The reaction of sulfhydryl (thiol) groups with Ellman's reagent (5,5'-dithiobis-2-nitrobenzoic acid, SERVA, Germany) breaks the disulfide bond in the reagent and forms 2-nitro-5-thiobenzoic acid, which at alkaline pH in water turns into a quinoid form and has a bright yellow color. The resulting thionitrophilic anion is quantified on a spectrophotometer at 412 nm. To calculate the level of reduced thiols in blood plasma (in μmol/ml), the molar extinction coefficient of the Ellman reagent was taken as 14150 M^{-1} cm^{-1}.

The statistical analysis of the results of the experimental study was carried out using the Statistica 10.0 program. The normal distribution of data was checked using the Shapiro – Wilk test (W test). The results were presented as Me *[Q 1 ; Q 3]*, where Me is the median, *Q 1* is the first quartile (25%), *Q 3* is the third quartile (75%), arithmetic mean and its error $M \pm m$. To analyze the statistical significance of differences between independent samples, the Mann – Whitney rank test (U test) was used. To check the equality of the medians of several samples, the Kruskall – Wallis test was used. Spearman's coefficient *(R)* was used to assess the rank correlation. The critical level of statistical significance of the differences in the null hypothesis (p) was taken equal to 0.05.

RESULTS AND DISCUSSION

NO metabolites level does not change significantly in Group A and increases in post-operation period in groups B and C.

In groups B and C NO metabolites level significantly grows on days 1 and 10, in the period from month 1 to month 6 NO level is stable but statistically higher than before operations (Fig. 1).

Any operative intervention on arteries leads to endothelium damage which causes inflammation with adhesion and thrombocyte aggregation, proliferation and migration of smooth muscle cells into intima. Endothelium damage induces production of NO synthase-2 (NOS-2) in smooth muscle cells and endothelium [16, 17], which can explain the results reached in groups B and C. Venous conduit from great saphenous vein has functional endothelial lining and reacts on local and systemic molecular and hemodynamic

stimulants and regulates vascular tone and homeostasis which is not the case of synthetic prosthesis due to absence of endothelium in it and that is why NO metabolites level does not change in group A (Fig. 1).

Along with changes in the level of nitric oxide metabolites, vascular endothelial growth factor VEGF is one of the well-studied indicators of angiogenesis, indicating the severity of the lesion [18]. It has been proven that VEGF ensures normal growth and development of the body, wound healing. However, high levels of VEGF were found in the development of cancerous tumors and rheumatoid arthritis [19].

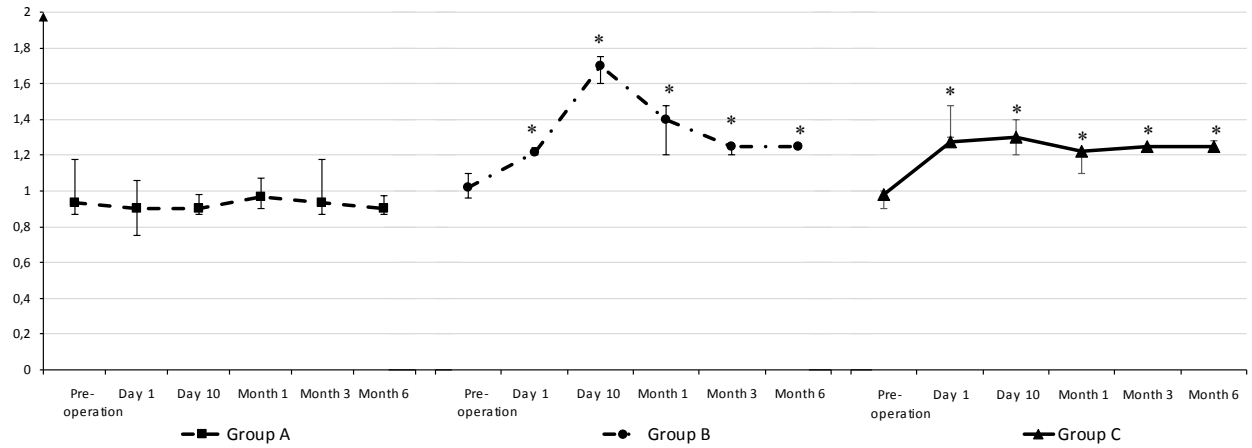

Fig. 1. NO metabolites level in blood plasma of patients with critical lower limb ischemia before and after femoropopliteal segment arteries reconstruction, *Me* [Q_1; Q_3]: * significant differences in data between pre-operation and post-operation ($p < 0.05$)

The concentration of the active form of human VEGF-A in experimental group A increases statistically significantly from the 1st day to 6 months, reaching a maximum on the 10th day. In experimental group B, the amount of VEGF-A statistically significantly increased after 1 month relative to the values before surgery. In group C, it statistically significantly increases on the 10th day after surgery and decreases in the period from 1 to 6 months relative to the values before surgery.

It is known that the survival rate of patients with a high level of VEGF is significantly lower than that of patients with a low expression of VEGF-A [18], therefore, the results obtained indicate a positive trend in autovenous bypass grafting using the *in situ* technique.

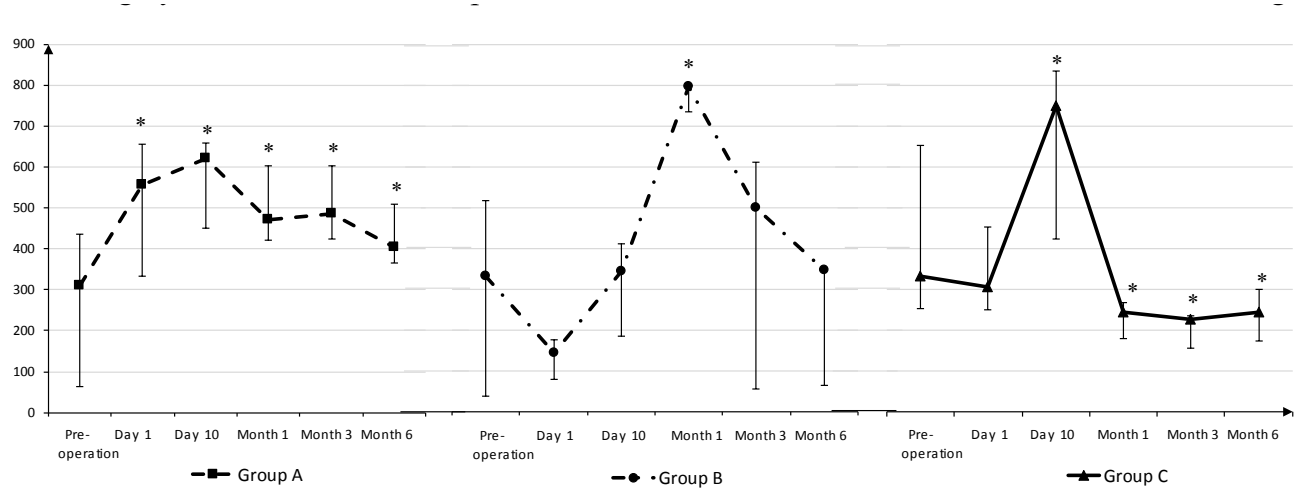

Fig. 2. Concentration of VEGF-A's active form in blood plasma of patients with critical lower limb ischemia before and after femoropopliteal segment arteries reconstruction, *Me* [Q_1; Q_3], pg/ml: * significant differences in data between pre-operation and post-operation ($p < 0.05$)

After surgery, the restoration of the body is accompanied by adaptation to new conditions. Currently, thiol-containing compounds (molecules containing-SH groups) are considered not only as a new marker of oxidative stress, but also as an indicator of homeostasis and adaptation under pathophysiological conditions [20].

The level of reduced thiols in the blood plasma of patients in groups A and B increases on the 10th day and after 1 month, and in group C it statistically significantly increases from the 10th day to the 6th month (Fig. 3).

The degree of adaptation directly depends on the concentration of thiols: the higher the degree of adaptation, the higher the level of SH-groups in the blood serum. It follows from this that the functional adaptation of the venous endothelium is higher in patients operated on by the *in situ* method, compared with the reverse vein method.

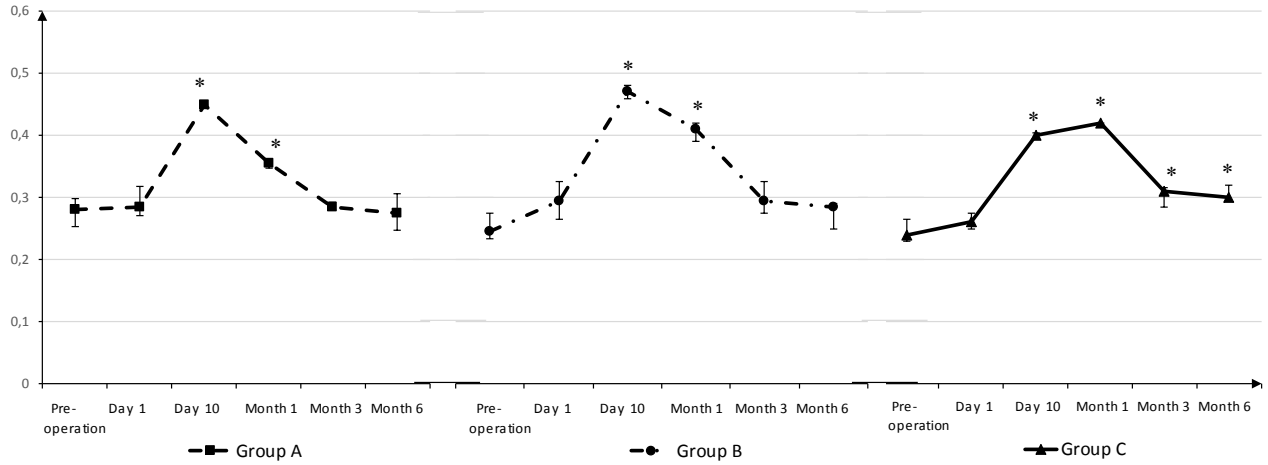

Fig. 3. Reduced thiols level in blood plasma of patients with critical lower limb ischemia before and after femoropopliteal segment arteries reconstruction, *Me* [Q_1; Q_3], μmol/ml: * significant differences in data between pre-operation and post-operation ($p < 0.05$)

Thiols are able to form reversible mixed disulfide bonds between protein and low molecular weight SH groups. The results obtained in group C indicate that oxidative stress decreases, disulfide bonds are restored to thiol groups, and thiol-disulfide homeostasis is maintained, and the body's resistance to reconstructive surgery increases. Abnormalities in thiol-disulfide homeostasis can play an essential role as a biomarker in the development of pathophysiological conditions. In patients in groups A and B, after mobilization of the body's defense reactions, which are expressed in an increase in the level of thiols, their decrease to the initial level is observed, which indicates adaptation or compensation without depletion.

The obtained biochemical results confirm the clinical observations given in Table. 2.

Table 2

Clinical characteristics of early and late complications of patients in the study groups

	Group A	Group B	Group C
Short-term results (up to 30 days)			
Thrombosis, *n* (%)	2 (10%)	2 (10%)	1 (4.5%)
First-time passableness, %	90	90	95.5
Second-time passableness, %	90	95	100
Limb salvage,%	90	95	95.5
Major amputations, *n* (%)	2 (10%)	1 (5%)	1 (4.5%)
Minor amputations, *n* (%)	1 (5%)	5 (25%)	2 (9%)
Long-term results (6 months)			
Thrombosis, *n* (%)	4 (20%)	3 (15%)	1 (4.5%)
First-time passableness, %	70	75	91
Second-time passableness, %	75	80	95.5
Limb salvage,%	80	85	95.5
Major amputations, *n* (%)	2 (10%)	2 (10%)	0
Minor amputations, *n* (%)	1 (5%)	1 (5%)	1 (4.5%)

From the perspective of early and late postoperative complications, patients in group C have a more favorable clinical picture, as indicated by a high percentage of primary and secondary patency of bypasses, a decrease in mortality, and an increase in the degree of limb preservation. The most unfavorable postoperative period according to the list of declared angiological signs is in patients in group A (see Table 2).

Interestingly, in terms of biochemical parameters in group B, positive correlations were revealed: the higher the level of nitric oxide metabolites, the higher the number of VEGF-A and SH-groups. Patients of group C showed a positive correlation between the amount of VEGF-A and free thiols, regardless of the level of nitric oxide metabolites (Table 3). Thus, in group B, NO metabolites promote the growth of SH-groups and VEGF-A, and in group C, they do not affect the concentration of VEGF-A and the level of SH-groups, which may be of clinical significance when assigning NO donors.

Table 3

Correlation ratio (R) between NO metabolites level, VEGF-A, SH-groups of patients in pre-operation and post-operation periods

	Group A	Group B	Group C
NO metabolites/VEGF-A	$R = 0.1$; $p > 0.05$	$R = 0.47$; $p < 0.01$	$R = 0.15$; $p > 0.05$
NO metabolites/SH-groups	$R = 0.15$; $p > 0.05$	$R = 0.48$; $p < 0.01$	$R = 0.065$; $p > 0.05$
VEGF-A/SH-groups	$R = 0.40$; $p < 0.01$	$R = 0.35$; $p < 0.01$	$R = 0.41$; $p < 0.01$

CONCLUSION

The obtained patterns of changes in the level of reduced thiols, nitric oxide metabolites, VEGF-A in patients with CLI indicate adaptation of the venous endothelium in the settings of the arterial bed during autovenous reconstruction of the femoropopliteal segment in comparison with the group of patients operated on using a synthetic prosthesis, which is confirmed by the analysis of early and late postoperative complications. The *in situ* method demonstrates the development of a more favorable clinical picture in terms of biochemical and angiological parameters than the reverse vein method.

REFERENCES

1. Zemtsova I., Stankevich L. The role of thiolic compounds in oxidative homeostasis maintenance in the process of athletic preparation. *Science in Olympic Sport.* 2015; 2: 37–44 (in Russ.).
2. Mangoni A.A., Zinellu A., Carru C., Attia J.R., McEvoy M. Serum thiols and cardiovascular risk scores: a combined assessment of transsulfuration pathway components and substrate/product ratios. *J. Transl. Med.* 2013; 11: 99. DOI: 10.1186/1479-5876-11-99.
3. Emmelien E.M., Pasch A., Feelisch M., Waanders F., Hendriks S.H., Mencke R., Harms G., Groenier K.H., Bilo H.J.G., Hillebrands J.-L., Goor H., Dijk P.R. Serum free thiol sin type 2 diabetes mellitus: A prospective study. *J. Clin. Transl. Endocrinol.* 2019; 16: 100182. DOI: 10.1016/j.jcte.2019.100182.
4. Otal Y., Şener A., Demircan S., Alisik M. Acute renal failure and thiol-disulfide homeostasis. *J. Nephrol. Ther.*, 2018; 8: 312. DOI: 10.4172/2161-0959.1000312.
5. Mungli P., Jeevan K., Sudeshna T. Serum total thiol status in alcohol abusers. *Asian Journal of Biochemistry.* 2008; 34 (1): 8–51. DOI: 10.3923/ajb.2008.48.51.
6. Rodosskaia N.K., Chernousova G.M. Immune system and thiols: some peculiarities of thiolexchange. *Compimmunol. Microbiol. Infect.* 2010; 33 (1): 65–71. DOI: 10.1016/j.cimid.2008.08.001.
7. Deanfield J.E., Halcox J.P., Rabelink T.J. Endothelial function and dysfunction: testing and clinical relevance. *Circulation.* 2007; 115 (10): 1285–1295. DOI: 10.1161/CIRCULATIONAHA.106.652859.
8. Morin F.C., Beierwaltes W.H., Solhaug M., Feld L.G., Waz W.R. Nitric oxide: from molecular biology to clinical nephrology. *Pediatr. Nephrol.* 1998; 12 (6): 504–511.
9. Pokrovsky V.I., Vinogradov N.A. Nitric oxide, its physiological and pathophysiological properties. *Therapeutic Archive*. 2005; 77 (1): 82–87 (in Russ.).
10. Piterková J., Luhová L., Mieslerová B., Lebeda A., Petřivalský M. Nitric oxide and reactive oxygen species regulate the accumulation of heat shock proteins in tomato leaves in response to heat shock and pathogen infection. *Plant Sci*. 2013; 207: 57–65. DOI: 10.1016/j.plantsci.2013.02.010.
11. Kalinin R.E., Suchkov I.A., Nikiforov A.A., Pshennikov A.S. Dynamics of some biochemical parameters in patients with obliterating atherosclerosis of the arteries of the lower extremities at different times after reconstructive operations. *I.P. Pavlov Russian Medical Biological Herald*. 2012; 20 (1): 42–45 (in Russ.).
12. Suchkov I.A., Pshennikov A.S., Gerasimov A.A., Agapov A.B., Kamaev A.A. Prevention of restenosis in reconstructive surgery of the great arteries. *Science of the Young – Eruditio Juvenium*. 2013; 2: 12–19 (in Russ.).
13. Dulak J. Józkowicz A., Dembinska-Kiec A., Guevara I., Zdzienicka A., Zmudzinska-Grochot D., Florek I., Wójtowicz A., Szuba A., Cooke J.P. Nitric oxide induces the synthesis of vascular endothelial growth factor by rat vascular smooth muscle cells. *Arterioscler. Thromb. Vasc. Biol.* 2000; 20 (3): 659–666. DOI: 10.1161/01.atv.20.3.659.
14. Metelskaya V.A., Gumanova N.G. Screening method for determining the level of nitric oxide metabolites in blood serum.

Russian Clinical Laboratory Diagnostics. 2005; 6: 15–18 (in Russ.).
15. Hu M.L. Measurements of protein thiol groups and glutathione in plasma. *Methods Enzymology.* 1994; 233: 381–385.
16. Vorobiev R.I. On the study of endothelial function in cardiovascular diseases. *Cardiovascular Therapy and Prevention (appendix)*. 2006; 5 (6): 76–77 (in Russ.).
17. Kuryanov P.S., Razuvaev A.S., Vavilov V.N. Intimal hyperplasia in the area of the vascular anastomosis. *Angiology and Vascular Surgery*. 2008; 14 (4): 146–151 (in Russ.).
18. Svetozarsky N.L., Artifeksova A.A., Svetozarsky S.N. Vascular endothelial growth factor: biological properties and practical significance. *Journal of Siberian Medical Sciences*. 2015; 5: 24 (in Russ.).
19. Gershtein E.S., Kushlinsky D.N., Adamyan L.V., Ognerubov N.A. Vascular endothelial growth factor is a clinically significant indicator in malignant neoplasms. *Tomsk State University Journal*. 2014; 19 (1): 10–20 (in Russ.).
20. Asoğlu M., Kiliçaslan F., Beginoğlu Ö., Fedai Ü., Akil Ö., Çelik H., Büyükaslan H. Thiol/disulphide homeostasis as a new oxidative stress marker in untreated patients with generalized anxiety disorder. *Anatolian Journal of Psychiatry*. 2018; 19 (2): 143–149. DOI: 10.5455/apd.261956.

Authors contribution

Kalinin R.E. – verification of the manuscript, critical revision of the manuscript for important intellectual content, final approval of the manuscript for publication. Abalenikhina Yu.V., Pshennikov A.S., Vinogradov S.A. – conception and design of the study, analysis and interpretation of data, drafting of the article. Abalenikhina Yu.V. – carrying out of biochemical tests. Pshennikov A.S., Vinogradov S.A. – supervision of patients in the Department of Vascular Surgery of the Regional Clinical Hospital of Ryazan, treatment and surgical correction of the magistral blood flow, sampling of biological material from patients.

Authors information

Kalinin Roman E., Dr. Sci. (Med.), Professor, Rector, Head of the Department of Cardiovascular, Endovascular, Operative Surgery and Topographic Anatomy, Ryazan State Medical University, Ryazan, Russian Federation. ORCID 0000-0002-0817-9573.

Abalenikhina Yulia V., Cand. Sci. (Biology), Associate Professor, Department of Biological Chemistry, Ryazan State Medical University, Ryazan, Russian Federation. ORCID 0000-0003-0427-0967.

Pshennikov Alexander S., Dr. Sci. (Med.), Associate Professor, Dean of the General Medicine Faculty, Professor of the Department of Cardiovascular, Endovascular, Operative Surgery and Topographic Anatomy, Ryazan State Medical University, Ryazan, Russian Federation. ORCID 0000-0002-1687-332X.

Vinogradov Sergey A., Post-Graduate Student, Department of Cardiovascular, Endovascular, Operative Surgery and Topographic Anatomy, Ryazan State Medical University, Ryazan, Russian Federation. ORCID 0000-0001-8547-4798.

(✉) **Kalinin Roman E.,** e-mail: rzgmu@rzgmu.ru.

Received 06.09.2019
Accepted 25.12.2019

УДК 616.5-006.81:577.175.82
https://doi.org/10.20538/1682-0363-2020-4-94-101

Does change in neurotransmitter brain status affect the growth of transplantable melanoma?

Kit O.I., Frantsiyants E.M., Bandovkina V.A., Kaplieva I.V., Surikova E.I., Trepitaki L.K., Cheryarina N.D., Kotieva I.M.

National Medical Research Centre for Oncology
63, 14 Liniya Str., Rostov-on-Don, 344037, Russian Federation

ABSTRACT

Aim. To study the influence of the features of aminergic brain status on the development of B16/F10 melanoma in mice with urokinase gene knockout and chronic neurogenic pain (CNP).

Materials and methods. The study included female ($n = 68$) C57BL/6 mice with the normal urokinase gene (+*uPA*) and C57BL/6-PlautmI.IBug-This Plau6FDhu/GFDhu mice with urokinase gene knockout (–*uPA*). The model of CNP was created in the animals, and in 14 days B16/F10 melanoma was transplanted. The mice were euthanized 21 days after the transplantation. Levels of adrenaline (A), noradrenaline (NA), dopamine (DA), histamine (H), serotonin (5HT), 5-hydroxyindoleacetic acid (5HIAA) were determined in the brain using standard ELISA test systems (Cusabio, China).

Results. CNP in (+*uPA*) females resulted in the reduction of almost all studied biogenic amines (BA). On the opposite, (–*uPA*) females showed an increase in NA, DA, 5HT and a decrease of H. 5HIAA increased in both CNP and gene knockout. 5HT in (+*uPA*) females with CNP decreased, while its physiological level in gene knockout mice was maintained. After 3 weeks of tumor growth in animals with CNP, (+*uPA*) mice demonstrated increased levels of studied BA (except for 5HIAA) compared to mice with CNP alone. Only H increase was observed in (–*uPA*) mice from the similar group.

Conclusion. CNP in mice inhibited A-, NA-, H- and 5HT-ergic systems of the brain; the opposite effects were registered in urokinase gene knockout, except for the H-ergic system. Combination of CNP and melanoma in (+*uPA*) female mice activated all studied BA systems, and in (–*uPA*) females – H-ergic system only. Different stressful effects, CNP, and genetic disorders (urokinase gene knockout) contributed to changes in the brain BA system functions, leading to the activation of pro- or antitumor mechanisms.

Key words: B16/F10 melanoma, melanoma course, chronic neurogenic pain, *uPA* urokinase gene knockout, mice, brain, biogenic amines.

Conflict of interest. The authors declare no obvious or potential conflict of interest related to the publication of this article.

Source of financing. The authors state that they received no funding for the study.

Conformity with the principles of ethics. The study was approved by the National Medical Research Center for Oncology, Bioethical Committee for Working with Animals (Protocol No. 4 of 10.08.2018).

For citation: Kit O.I., Frantsiyants E.M., Bandovkina V.A., Kaplieva I.V., Surikova E.I., Trepitaki L.K., Cheryarina N.D., Kotieva I.M. Does change in neurotransmitter brain status affect the growth of transplantable melanoma? *Bulletin of Siberian Medicine.* 2020; 19 (4): 94–101. https://doi.org/10.20538/1682-0363-2020-4-94-101.

✉ *Bandovkina Valeria A.,* e-mail: super.gormon@yandex.ru.

Оказывает ли влияние изменение нейротрансмиттерного статуса мозга на рост перевивной меланомы?

Кит О.И., Франциянц Е.М., Бандовкина В.А., Каплиева И.В., Сурикова Е.И., Трепитаки Л.К., Черярина Н.Д., Котиева И.М.

Национальный медицинский исследовательский центр (НМИЦ) онкологии
Россия, 344037, г. Ростов-на-Дону, ул. 14-я линия, 63

РЕЗЮМЕ

Цель. Изучить влияние особенностей аминергического статуса головного мозга у мышей при нокауте гена урокиназы и хронической нейрогенной боли (ХНБ) на развитие меланомы B16/F10.

Материалы и методы. Работа выполнена на самках мышей (n = 68) C57BL/6 – с полноценным геном урокиназы (+*uPA*) и C57BL/6-PlautmI.IBug-This Plau6FDhu/GFDhu – с нокаутом гена урокиназы (–*uPA*). Животным моделировали состояние ХНБ, через 14 сут подкожно перевивали меланому B16/F10. Забой производили через 21 сут после перевивки. В головном мозге определяли содержание адреналина (А), норадреналина (НА), дофамина (ДА), гистамина (Г), серотонина (5НТ), 5-оксииндолуксусной кислоты (5ОИУК) с помощью иммуноферментных стандартных тест-систем (Cusabio, Китай).

Результаты. У самок (+*uPA*) ХНБ приводила к снижению содержания практически всех исследованных биогенных аминов (БА). У самок (–*uPA*), напротив, отмечался рост концентрации НА, ДА, 5НТ и снижение Г. Обнаружено увеличение уровня 5ОИУК при ХНБ и нокауте. У самок (+*uPA*) с ХНБ снижался уровень 5НТ, но сохранялось его физиологическое содержание у мышей с нокаутом. Через 3 нед роста опухоли на фоне ХНБ у мышей (+*uPA*) обнаружено увеличение уровня всех изученных БА, кроме 5ОИУК, по сравнению с уровнем у мышей только с ХНБ. У мышей (–*uPA*) в аналогичной группе было увеличение только гистамина.

Заключение. ХНБ приводила к угнетению А-, НА-, Г-, 5НТ-ергических систем мозга мышей, а при нокауте гена урокиназы наблюдались противоположные эффекты, за исключением Г-ергической системы. Сочетание ХНБ и меланомы у самок мышей (+*uPA*) приводило к активации всех изученных систем БА, а у самок (–*uPA*) – только Г-ергической системы. Стрессорное воздействие – ХНБ, генетическое нарушение (нокаут гена урокиназы), способствовали изменению функционирования систем БА мозга, разнонаправленно влияя на противоопухолевые механизмы.

Ключевые слова: меланома, хроническая нейрогенная боль, нокаут гена урокиназы uPA, мыши, головной мозг, биогенные амины.

Конфликт интересов. Авторы декларируют отсутствие явных и потенциальных конфликтов интересов, связанных с публикацией настоящей статьи.

Источник финансирования. Авторы заявляют об отсутствии финансирования.

Соответствие принципам этики. Исследование одобрено биоэтическим комитетом по работе с животными Ростовского научно-исследовательского онкологического института (протокол № 4 от 10.08.2018).

Для цитирования: Кит О.И., Франциянц Е.М., Бандовкина В.А., Каплиева И.В., Сурикова Е.И., Трепитаки Л.К., Черярина Н.Д., Котиева И.М. Оказывает ли влияние изменение нейротрансмиттерного статуса мозга на рост перевивной меланомы? *Бюллетень сибирской медицины.* 2020; 19 (4): 94–101. https://doi.org/10.20538/1682-0363-2020-4-94-101.

INTRODUCTION

The brain encloses a unique microenvironment which supports physiological homeostasis and responds to pathological changes, including cancer [1]. Skin cells that perceive both external and internal changes and participate in the regulation of the homeostasis in the body are able to influence systemic regulators, and particularly the neuroamine status of the brain [2]. The close connection between skin cells and brain neurons is confirmed by studies in some neurodegenerative diseases, in particular, Parkinson disease [3], and mental disorders which are often

combined with chronic skin diseases and melanoma [4, 5]. Multifunctional biogenic amines modulate the response of the central regulatory system to various internal and external impacts and participate in the body response to stress, playing a crucial role in maintaining homeostasis [6].

A number of studies have shown that stress can retard tumor growth through the action of neuroamines on the hypothalamus and immune system [7]. Scattered experimental data show the role of biogenic amines of the brain in antitumor protection [8, 9]. With acute and chronic stress, there is a change of the level of histamine in the brain, which regulates the secretion of hormones of the hypothalamus, the anterior pituitary gland, modulates the effect of certain transmitters [10], and plays an important role in multiple diseases of the central nervous system [11]. Comorbid diseases associated with tumor growth are connected with differences in treatment, clinical management, prognosis, survival, cancer progression, and can also cause a higher risk of complications and lower quality of life.

Moreover, despite the importance of taking comorbid diseases into account, there is not enough attention to the relation between melanoma and concomitant pathology [12]. While the effect of chronic neurogenic pain (CNP) on the transmitter status of the brain is beyond dispute [13, 14], the connection between the urokinase gene knockout and the balance of brain biogenic amines is not so obvious. There are experimental data on the significant role of plasminogen activators in the processes of the brain recovery after ischemic lesion [15]. Models of animals with neural lesion that causes chronic neuropathic pain and animals with a modified genotype allow studying multiple changes that occur in the main regulatory systems, as well as their possible impact on the tumor process development.

The aim of this work was to study the influence of characteristics of the aminergic status in the mice brain at the urokinase gene knockout and chronic neurogenic pain on the development of the B16/F10 melanoma.

MATERIALS AND METHODS

The work was performed on female mice ($n = 68$). All animals were kept under natural light conditions with free access to water and food. The studies were carried out according to the requirements and conditions set out in the International Guiding Principles for Biomedical Research Involving Animals and the Order of the Ministry of Health of the Russian Federation No. 267 of 19.06.03 "On the approval of laboratory practice rules". The mice of the C57BL/6 line with a full urokinase gene (+*uPA*), $n = 34$, were obtained from Scientific Center for Biomedical Tech- nologies of Andreevka of the Federal Biomedical Agency. Animals of the C57BL/6-PlautmI.IBug-This Plau6F-Dhu/GFDhu line with urokinase gene knockout (–*uPA*) (target mutation with production of a protein being unable to bind to the urokinase-type plasminogen activator receptor), $n = 34$, were obtained from the Laboratory Animal Breeding Station of "Pushchino".

The animals were divided into 8 groups: intact (+*uPA*) females ($n = 7$); (+*uPA*) females with CNP ($n = 9$); intact (–*uPA*) females ($n = 7$), (–*uPA*) females with CNP ($n = 9$); (+*uPA*) females with melanoma ($n = 9$); (+*uPA*) females with CNP and melanoma ($n = 9$); (–*uPA*) females with melanoma ($n = 9$); (–*uPA*) females with CNP and melanoma ($n = 9$).

The modeling of CNP by ligation of the sciatic nerve from both sides, the procedure for subcutaneous transplantation of the B16/F10 melanoma into the right subscapular region, the course of the experiment and the preparation of 10% of cytosolic fractions have been described before [13]. For this work, we used the B16/F10 murine melanoma obtained from the Research Center for Oncology named after N.N. Blokhin of the Ministry of Health of the Russian Federation. The tumor proliferative pool was 71.6%. The material for transplantation of the B16/F10 melanoma was obtained from (+*uPA*) donor mice of the C57BL/6 line, second passage, on days 12-16 of tumors development. The animals with tumors were euthanized 21 days after the melanoma transplantation. The 10% cytosolic fractions were obtained from the isolated brain and prepared on 0.1 M potassium phosphate buffer pH 7.4 containing 0.1% Tween-20 and 1% BSA; all manipulations were performed on ice. The content of biogenic amines — adrenaline (A), noradrenaline (NA), dopamine (DA), histamine (H), serotonin (5HT), 5-hydroxyindoleacetic acid (5HIAA), was determined using standard ELISA test systems (Cusabio, China).

The statistical processing of the material was carried out using the Statistica 10.0 software; mean values and standard errors ($M \pm m$) were determined. The significance of differences in average values was evaluated using the Mann – Whitney U-test and Student's t-test (after checking for normal distribution using the Shapiro – Wilk test). The differences were considered significant at $p < 0.05$.

RESULTS

First, there was a study of the effect of CNP, urokinase knockout and their combination on the content of biogenic amines in the female mice brain. The results of the study of biogenic amines in the brain of (+*uPA*) females with CNP showed a decrease in the levels of adrenaline by 2.4 times, of noradrenaline by 2.3 times, of histamine by 2.1 times and serotonin by 1.9 times ($p < 0.05$) against the background of an increase in 5HIAA by 3.3 times, compared with the indicators of intact (+*uPA*) females (Table 1). The dopamine content in the brain of (+*uPA*) females did not change under the influence of CNP, but there was an increase of the DA/NA ratio by 2.3 times and a decrease of the ($p < 0.05$) A/5HT ratio by 1.3 times as well as of the 5HT/5HIAA ratio by 4.8 times.

The urokinase gene knockout in female mice had no effect on adrenaline and serotonin levels in the brain, with an increase of the noradrenaline level by 3.2 times, dopamine level by 2.9 times, and 5HIAA level by 2.0 times, but the histamine content was decreased by 2.1 times (Table 1). As a result, the 5HT/5HIAA ratio coefficient decreased by 2.5 times, the ratio of DA/NA and A/5HT did not differ from indicators of intact (+*uPA*) females.

Modeling of CNP in (–*uPA*) females resulted in a decrease in the brain level of NA and DA by 1.5 times compared to (–*uPA*) females without pain ($p < 0.05$), however, relative to (+*uPA*) females, both intact and having the CNP background, the concentration of these neurotransmitters was higher: NA by 1.7 times and 4 times, respectively, and DA by 2 times ($p < 0.05$).

In (–*uPA*) females, CNP caused a decrease in histamine by 1.8 times compared with intact (–*uPA*) and (+*uPA*) animals ($p < 0.05$), without statistically significant differences compared with (+*uPA*) females with CNP. At the same time, there was an increase in serotonin content by an average of 3 times compared with intact (–*uPA*) and (+*uPA*) animals and 5.2 times compared with (+*uPA*) females with CNP ($p < 0.05$). Modeling of CNP in (–*uPA*) mice resulted in an increase of the brain concentration of 5HIAA by 1.7 times and 1.3 times ($p < 0.05$) compared with (–*uPA*) and (+*uPA*) intact animals, respectively, while there were no significant differences compared to (+*uPA*) females with CNP. As a result, the A/5HT ratio in the brain decreased by more than 3.4 times and 2.8 times compared to intact (–*uPA*) and (+*uPA*) females and 2.1 times compared to (+*uPA*) females with CNP, and the ratio between serotonin and its 5HIAA metabolite did not differ from (+*uPA*) intact animals, but was 2.2 times higher than the one of (–*uPA*) intact animals and 4 times higher than the one of (+*uPA*) females with CNP. The DA/NA coefficient in the brain of (–*uPA*) females with CNP did not have significant differences from (–*uPA*) and (+*uPA*) of intact animals, but it turned out to be 2 times lower than that of (+*uPA*) females with CNP.

The urokinase gene knockout and CNP contributed to a change in the biogenic status of the brain in different directions. If in (+*uPA*) females, CNP caused a decrease in the A and NA level, then the urokinase gene knockout, on the contrary, resulted in an increase in the NA and DA content, but did not affect the A value. The development of CNP in (–*uPA*) females was accompanied by a decrease not only in the brain level of NA, like in (+*uPA*) females with the CNP background, but also in the level of DA; however, the levels of these catecholamines remained significantly higher than in females with a normal genome, both with and without CNP.

Only in (–*uPA*) females, the A/5HT ratio in the brain was higher than the one in (+*uPA*) females; CNP reduced the A/5HT ratio both independently and in combination with knockout. It should be noted that in females, any of the exerted effects – CNP, urokinase gene knockout, alone or in combination with CNP, resulted in an increase in the brain level of 5HIAA, a serotonin metabolite, as well as in a decrease in the histamine concentration.

Previously, we found that CNP in mice with a normal genome had a stimulating effect on the development of transplanted melanoma, which was expressed in a decrease in life expectancy and latent period, as well as in more active metastatic spreading to non-specific sites against the background of a smaller tumor volume [13]. The development of transplanted melanoma in mice with the *uPA* gene knockout was characterized by smaller tumor volumes and the absence of metastatic spreading after 3 weeks, against the background of the absence of differences in life expectancy and latent period. In female mice with the urokinase gene knockout and CNP with transplanted melanoma, a shorter life expectancy was observed, which is characteristic of animals with CNP and tumor growth, however, there was a larger latent period [16].

Taking into account the multidirectional changes in the neurotransmitter status of the brain in female mice under the influence of CNP and the urokinase gene knockout, as well as differences in the course

of malignant process, the content of biogenic amines in the brain was studied in female mice with CNP, the urokinase gene knockout and their combination after 3 weeks of growth of transplanted melanoma B16/F10.

As a control, the level of biogenic amines in (+*uPA*) female mice with self-developing melanoma (without concomitant CNP) was examined first. After 3 weeks of growth of the B16/F10 melanoma, there was an increase of the brain level of dopamine by 1.8 times ($p < 0.05$), of serotonin by 2.3 times and of 5HIAA by 1.5 times ($p < 0.05$); the content of noradrenaline, histamine and adrenaline did not have significant differences from values in intact (+*uPA*) females (Table 1). As a result, the A/5HT ratio decreased by 2.1 times, while the 5HT/5HIAA and DA/NA ratios increased by 1.5 times ($p < 0.05$).

In (+*uPA*) females with CNP, after 3 weeks of growth of melanoma in the brain, there was an increase of levels of adrenaline and dopamine by 1.4 times ($p < 0.05$), of noradrenaline by 2.2 times, of histamine by 2.0 times and of serotonin by 1.3 times ($p < 0.05$), together with a decrease in the content of 5HIAA by 2.5 times, compared with indicators in the brain of (+*uPA*) females with CNP only (Table 1). As a result, the A/5HT ratio did not differ from the values in the brain of (+*uPA*) females with CNP only, 5HT/5HIAA was 3.3 times higher, and DA/NA, on the contrary, 1.6 times ($p < 0.05$) lower. It should be noted that compared with the amine content in animals with standard transplantation of melanoma, differences were also detected: lower levels of adrenaline, serotonin and the 5HT/5HIAA ratio by 1.8 times ($p < 0.05$), 2.4 times and 2.1 times, respectively (Table 1).

Table 1

Content of biogenic amines in the brain of female C57Bl/6 mice, $M \pm m$

Parameter	Intact (+*uPA*) mice	(+*uPA*) mice + melanoma B16/F10	(+*uPA*) mice + CNP	(+*uPA*) mice + CNP + melanoma B16/F10	Intact (–*uPA*) mice	(–*uPA*) mice + melanoma B16/F10	(–*uPA*) mice + CNP	(–*uPA*) mice + CNP + melanoma B16/F10
Adrenalin, ng/g of tis.	8.5 ± 0.7	9.0 ± 0.8	3.5 ± 0.3[1]	5.0 ± 0.6[1.3.4]	8.6 ± 0.85	7.4 ± 0.69[4]	8.6 ± 0.82[3]	8.1 ± 0.78
Noradrenaline, ng/g of tis.	19.4 ± 1.8	23.2 ± 2.2	8.5 ± 1.1[1]	18.9 ± 2.0[3]	61.4 ± 5.9[1]	40.3 ± 0.38[2.4]	33.7 ± 3.1[2.3]	37.0 ± 3.2
Dopamine, ng/g of tis.	17.5 ± 1.8	31.0 ± 3.1[1]	17.9 ± 1.5	25.0 ± 2.2[1.3]	50.0 ± 4.7[1]	33.4 ± 0.31[2]	35.8 ± 3.4[2.3]	41.2 ± 3.9
Histamine, ng/g of tis.	34.9 ± 3.2	30.4 ± 2.9	16.6 ± 1.2[1]	33.5 ± 2.9[3]	16.4 ± 1.5[1]	34.0 ± 0.32[2]	18.9 ± 1.6	28.2 ± 2.7[5]
Serotonin, ng/g of tis.	0.43 ± 0.03	0.97 ± 0.05[1]	0.23 ± 0.02[1]	0.4 ± 0.03[3.4]	0.35 ± 0.03	1.9 ± 0.15[2.4]	1.2 ± 0.11[2.3]	1.2 ± 0.10[6]
5-HIAA, µg/g of tis.	0.15 ± 0.03	0.23 ± 0.03[1]	0.5 ± 0.03[1]	0.2 ± 0.01[1.3]	0.3 ± 0.03[1]	0.4 ± 0.03[2.4]	0.5 ± 0.04[2]	0.4 ± 0.03
A/5HT	19.77 ± 1.4	9.28 ± 0.73[1]	15.22 ± 1.2[1]	12.5 ± 1.2[1.4]	26.1 ± 0.24[1]	3.89 ± 0.35[2.4]	7.17 ± 0.69[2.3]	6.75 ± 0.66[6]
5HT/5HIAA	2.9 ± 0.25	4.22 ± 0.39[1]	0.6 ± 0.05[1]	2.0 ± 0.18[1.3.4]	1.1 ± 0.09[1]	4.75 ± 0.47[2]	2.4 ± 0.18[2.3]	3.0 ± 0.03[6]
DA/NA	0.9 ± 0.08	1.34 ± 0.12[1]	2.1 ± 0.20[1]	1.32 ± 0.13[1.3]	0.81 ± 0.07	0.83 ± 0.08	1.06 ± 0.09[3]	1.11 ± 0.1

Note. [1] – statistically significant compared with intact (+*uPA*) animals; [2] – statistically significant compared with intact (–*uPA*) animals; [3] – statistically significant compared with (+*uPA*) animals with CNP; [4] – statistically significant compared with (+*uPA*) animals with the B16/F10 melanoma; [5] – statistically significant compared with (–*uPA*) animals with CNP; 6 – statistically significant compared with (–*uPA*) animals with the B16/F10 melanoma.

The level of catecholamines in the brain of (–*uPA*) mice decreased 3 weeks after tumor transplantation: adrenaline by 1.2 times ($p < 0.05$), noradrenaline and dopamine by 1.5 times ($p < 0.05$), and histamine, serotonin and 5HIAA, on the contrary, increased by 2.1 times, 5.8 times and 1.3 times ($p < 0.05$), respectively, compared with (–*uPA*) females. Moreover, the A/5HT ratio turned out to be 6.7 times lower, and the 5HT/5HIAA ratio was 4.3 times higher. It should be noted that, compared with the indicators of (–*uPA*) females with melanoma without concomitant CNP, the content of NA in (–*uPA*) mice was higher by 1.7 times ($p < 0.05$), of serotonin by 2.0 times, of 5HIAA – by 1.7 times ($p < 0.05$), but there was a decrease of the ratio of A/5HT by 2.4 times and of DA/NA by 1.6 times ($p < 0.05$).

The melanoma growth in female mice with the urokinase gene knockout and CNP was characterized by a low life expectancy 1.6 times ($p < 0.05$) lower than for females with the urokinase gene knockout without CNP, but with a latent period being larger by 1.7 times ($p < 0.05$). At that, in the brain of (–*uPA*) females with

CNP after 3 weeks of growth of melanoma, only a 1.5-fold increase ($p < 0.05$) in histamine levels was detected compared with the brain indicators of (*–uPA*) females with CNP without tumor transplantation (Table 1). The main difference compared with the neurotransmitter status in (*–uPA*) females with melanoma after 3 weeks of tumor growth was the decrease in the serotonin level by 1.6 times ($p < 0.05$), resulting in an increase in the A/5HT ratio by 1.7 times ($p < 0.05$) and a decrease in the 5HT/5HIAA ratio by 1.6 times ($p < 0.05$).

DISCUSSION

The development of transplanted melanoma is accompanied by a violation of central regulatory mechanisms, while the characteristics of the tumor development may depend on the initial status and reactivity of the aminergic systems of the brain. In the course of this study, it was found that the growth of melanoma at standard transplantation to female mice, after 3 weeks of the experiment, resulted in an imbalance of the dopaminergic and noradrenergic systems, with the prevalence of the first one, as well as in the serotonergic system activation, which was expressed in an increase of levels of both serotonin and its metabolite.

First of all, it is noteworthy that CNP (in (*+uPA*) females) and the urokinase gene knockout in independent variants have different effects on the adrenergic, noradrenergic and serotonergic systems, but these are equal in relation to the histaminergic system. From the obtained results, it can be seen that CNP in (*+uPA*) females results in a decrease of almost all of the studied biogenic amines in the brain, resulting in a violation of basic mechanisms of central regulation. The urokinase gene knockout, on the contrary, activates the noradrenergic, serotonergic and dopaminergic systems in the brain of females, as well as changes the biogenic amines ratio.

The model of chronic neurogenic pain is a model of chronic prolonged stress, while animals with the urokinase knockout, although having a genetically determined disorder, do not phenotypically differ from (*+uPA*) mice of the C57BL/6 line [15]. It is known that urokinase and its receptor are found in large quantity in the developing brain [17], but their expression in the adult state is limited to certain groups of neurons, mainly in the hippocampus and some subcortical structures [18]. In our study, it was shown that the urokinase gene knockout, although it did not have phenotypic manifestations in the behavior of mice, was characterized by a significant increase in the brain levels of noradrenaline, dopamine, and serotonin, but a decrease in histamine. We suppose that the found increase in the absolute levels of dopamine, noradrenaline and serotonin, as well as a change in the balance of biogenic amines in the brain of females with the urokinase gene knockout, is one of the mechanisms that contribute to the restoration of neurogenesis and synaptic transmission of nerve endings in case of various stress impacts under conditions of genetic damage to one of the links of the urokinase system.

The growth of most types of malignant tumors depends on the balance between factors promoting proliferation, angiogenesis, migration, and survival of the cells, and those that are involved in cell differentiation, inhibit proliferation and result in apoptosis [19]. Therefore, after transplantation of malignant melanoma cells into animals with different neurotransmitter status of the brain, which was genetically determined or altered as a result of prolonged chronic exposure of neurogenic pain, the development of the malignant process may turn out to be modified due to various background states of central regulatory systems.

The decrease in biogenic amines in the brain of females under the influence of CNP resulted in a weakening of the antitumor defense of the body, which resulted in a decrease in life expectancy, latent period, and increase in activity and metastasis sites in animals. At the same time, the growth of transplanted melanoma in female mice with the urokinase gene knockout did not have significant differences in life expectancy and latent period; however, the increase in tumor volume was significantly slower than at transplanting melanoma to mice with a wild type of the urokinase gene. We suggest that the urokinase gene knockout could have an antitumor effect at the local level, as we previously showed the participation of the system of growth factors and fibrinolysis in the pathogenesis of melanoma growth in female mice [20]. Experimental studies show the interaction of serotonergic and dopaminergic systems with each other, while affecting the brain plasticity and the ability of the body as a whole to recover and adapt [21]. Noradrenaline is involved in the protection of dopaminergic neurons through enhancing the tyrosine hydroxylase expression [22]. The depletion of the noradrenergic system of the brain is often associated with hyperactivation of the hypothalamo-pituitary-adrenal axis, which characterizes various mental disorders associated with stress, such as anxiety and depression, and neurodegenerative conditions, such as Alzheimer disease and multiple sclerosis [23]. Recent studies show that this reaction has

gender differences, and females are less resistant to prolonged stress [24].

In this study, animals with CNP and the urokinase gene knockout showed a decrease in histamine levels in the brain. This fact, on the one hand, can be explained by the multifunctionality of histamine, which takes part both in nociceptive reactions and in restoration processes in the brain. The difficulty in interpreting the results of changes in neuronal amines in general and histamine in particular lies in the activation of various receptors, which results in various effects. On the other hand, an increase in aminoxidase activity may cause a decrease in histamine levels. We have detected an increase in the level of the serotonin metabolite – 5HIAA both in CNP and knockout animals. A significant difference was a decrease in serotonin in females with CNP, but the preservation of its physiological concentrations in knockout animals.

Moreover, the combined effect of CNP and (*–uPA*) results only in a decrease in the effect of the urokinase gene knockout and activation of the serotonergic system metabolism against the background of an increase in the serotonin level. There is a possibility that it was the increase in the serotonin level in the brain of females with the combination of the gene knockout with CNP that affected the increase in the latent period of tumor development, although it did not result in an increase in the life expectancy of animals.

CONCLUSION

Thus, the obtained study results indicate the undoubted effect of changes in the neurotransmitter balance of the brain under the influence of chronic neurogenic pain and genetically determined urokinase deficiency on the growth of transplanted melanoma. A better understanding of mechanisms underlying neurotransmitter function at oncogenesis, neurogenesis, and chronic comorbid diseases will make it possible to predict the possible course of the disease and to develop personalized antitumor therapy.

REFERENCES

1. Valiente M., Ahluwalia M.S., Boire A., Brastianos P.K., Goldberg S.B., Lee E.Q., Le Rhun E., Preusser M., Winkler F., Soffietti R. The evolving landscape of brain metastasis. *Trends Cancer*. 2018; 4 (3): 176–196. DOI: 10.1016/j.trecan.2018.01.003.
2. Jozic I., Stojadinovic O., Kirsner R.S.F., Tomic-Canic M. Skin under the (spot)-light: cross-talk with the central hypothalamic-pituitary-adrenal (HPA). *Axis. J. Invest. Dermatol*. 2015; 135 (6): 1469–1471. DOI: 10.1038/jid.2015.56.
3. Planken A., Kurvits L., Reimann E., Kadastik-Eerme L., Kingo K, Kõks S., Taba P. Looking beyond the brain to improve the pathogenic understanding of Parkinson's disease: implications of whole transcriptome profiling of Patients' skin. *BMC Neurol*. 2017; 17 (1): 6. DOI: 10.1186/s12883-016-0784-z.
4. Dalvin L.A., Damento G.M., Yawn B.P., Abbott B.A., Hodge D.O., Pulido J.S. Parkinson disease and melanoma: confirming and reexamining an association. *Mayo Clin. Proc*. 2017; 92 (7): 1070–1079. DOI: 10.1016/j.mayocp.2017.03.014.
5. Xie Q.W., Dai X, Tang X., Chan C.H.Y., Chan C.L.W. Risk of mental disorders in children and adolescents with atopic dermatitis: a systematic review and meta-analysis. *Front Psychol*. 2019; 10: 1773. DOI: 10.3389/fpsyg.2019.01773.
6. Shukla R.K., Dhuriya Y.K., Chandravanshi L.P., Gupta R., Srivastava P., Pant A.B., Kumar A., Pandey C.M., Siddiqui M.H., Khanna V.K. Influence of immobilization and forced swim stress on the neurotoxicity of lambda-cyhalothrin in rats: effect on brain biogenic amines and BBB permeability. *Neurotoxicology*. 2017; 60: 187–196. DOI: 10.1016/j.neuro.2016.07.002.
7. Kusuhara M., Maruyama K., Ishii H., Masuda Y., Sakurai K., Tamai E., Urakami K. A fragrant environment containing α-pinene suppresses tumor gowth in mice by modulating the hypothalamus/sympathetic nerve/leptin axis and immune system. *Integr. Cancer Ther*. 2019; 18: 1534735419845139. DOI: 10.1177/1534735419845139.
8. Ben-Shaanan T.L., Schiller M., Azulay-Debby H., Korin B., Boshnak N., Koren T., Krot M., Shakya J., Rahat M.A., Hakim F., Rolls A. Modulation of anti-tumor immunity by the brain's reward system. *Nat. Commun*. 2018; 9 (1): 2723. DOI: 10.1038/s41467-018-05283-5.
9. Menezes A.C., Carvalheiro M., Ferreira de Oliveira J.M.P., Ascenso A., Oliveira H. Cytotoxic effect of the serotonergic drug 1-(1-Naphthyl)piperazine against melanoma cells. *Toxicol. in Vitro*. 2018; 47: 72–78. DOI: 10.1016/j.tiv.2017.11.011.
10. Passani M.B., Panula P., Lin J.S. Histamine in the brain. *Front Syst. Neurosci*. 2014; 8: 64. DOI: 10.3389/fnsys.2014.00064.
11. Hu W., Chen Z. The roles of histamine and its receptor ligands in central nervous system disorders: An update. *Pharmacol. Ther*. 2017; 175: 116–132. DOI: 10.1016/j.pharmthera.2017.02.039.
12. Bebe F.N., Hu S., Brown T.L., Tulp O.L. Role, extent, and impact of comorbidity on prognosis and survival in advanced metastatic melanoma: a review. *J. Clin. Aesthet. Dermatol*. 2019; 12 (1): 16–23.
13. Kit O.I., Frantsiyants E.M., Kotieva I.M., Kaplieva I.V., Trepitaki L.K., Bandovkina V.A., Rozenko L.Ya., Cheryarina N.D., Pogorelova Yu.A. Some mechanisms of increasing malignancy of B16/F10 melanoma in female mice with chronic pain. *Russian Journal of Pain.* 2017; 2 (53): 14–20 (in Russ.).
14. Taylor B.K., Westlund K.N. The noradrenergic locus coeruleus as a chronic pain generator. *J Neurosci. Res*. 2017; 95 (6): 1336–1346. DOI: 10.1002/jnr.23956.
15. Semina E.V., Rubina K.A., Stepanova V.V., Tkachuk V.A. Participation of urokinase receptor and its endogenous ligands in brain development and formation of cognitive functions. *Russian Journal of Physiology.* 2016; 102 (8): 881–903 (in Russ.).
16. Frantsiyants E.M., Kaplieva I.V., Surikova E.I., Neskubina I.V., Bandovkina V.A., Trepitaki L.K., Lesovaya N.S., Cheryarina N.D., Pogorelova Yu.A., Nemashkalova L.A. Effect of

urokinase gene-knockout on growth of melanoma in experiment. *The Siberian Scientific Medical Journal.* 2019; 39 (4): 62–70 (in Russ.). DOI: 10.15372/SSMJ20190408.
17. Merino P., Diaz A., Manrique L.G., Cheng L., Yepes M. Urokinase-type plasminogen activator (uPA) promotes ezrin-mediated reorganization of the synaptic cytoskeleton in the ischemic brain. *J. Biol. Chem.* 2018; 293 (24): 9234–9247. DOI: 10.1074/jbc.RA118.002534.
18. Merino P., Diaz A., Jeanneret V., Wu F., Torre E., Cheng L., Yepes M. Urokinase-type plasminogen activator (uPA) binding to the uPA receptor (uPAR) promotes axonal regeneration in the central nervous system. *J. Biol. Chem*. 2017; 292 (7): 2741–2753. DOI: 10.1074 / jbc.M116.761650.
19. Cao L., Liu X., Lin E.J., Wang C., Choi E.Y., Riban V., Lin B., During M.J. Environmental and genetic activation of a brain-adipocyte BDNF/leptin axis causes cancer remission and inhibition. *Cell*. 2010; 142 (1): 52–64. DOI: 10.1016/j.cell.2010.05.029.
20. Frantsiyants E.M., Bandovkina V.A., Pogorelova Yu.A., Tkalya L.D., Cheryarina N.D. The activity of plasminogen activation system components and some factors of neoangiogenesis in the development dynamics of transplantable melanoma B16/F10. *Modern Problems of Science and Education.* 2015; 5: 617 (in Russ.).
21. Cordeiro L.M.S., Rabelo P.C.R, Moraes M.M., Teixeira-Coelho F, Coimbra C.C., Wanner S.P, Soares D.D. Physical exercise-induced fatigue: the role of serotonergic and dopaminergic systems. *Braz. J. Med. Biol. Res*. 2017; 50 (12): e6432. DOI: 10.1590/1414-431X20176432.
22. Zhu M.Y, Raza M.U., Zhan Y., Fan Y. Norepinephrine upregulates the expression of tyrosine hydroxylase and protects dopaminegic neurons against 6-hydrodopamine toxicity. *Neurochem. Int*. 2019; 31: 104549. DOI: 10.1016/j.neuint.2019.104549.
23. Urquhart M.A., Ross J.A., Reyes B.A.S., Nitikman M., Thomas S.A., Mackie K., van Bockstaele E.J. Noradrenergic depletion causes sex specific alterations in the endocannabinoid system in the Murine prefrontal cortex. *Neurobiol. Stress*. 2019; 10: 100164. DOI: 10.1016/j.ynstr.2019.100164.
24. Becker J.B., Chartoff E. Sex differences in neural mechanisms mediating reward and addiction. *Neuropsychopharmacology*. 2019; 4 (1): 166–183. DOI: 10.1038/s41386-018-0125-6.

Authors contribution

Frantsiyants E.M., Kaplieva I.V. – conception and design of the experiment. Frantsyants E.M., Kaplieva I.V., Bandovkina V.A. – analysis and interpretation of results. Bandovkina V.A., Surikova E.I. – drafting and editing of the manuscript, critical revision for important intellectual content. Trepitaki L.K. – carrying out of the experiment. Cheryarina N.D. – carrying out of ELISA analysis. Kit O.I., Frantsyants E.M., Kotieva I.M. – final approval of the manuscript for publication.

Authors information

Kit Oleg I., Dr. Sci. (Med.), Professor, Corresponding Member of the Academy of Medical Sciences, General Director of National Medical Research Centre for Oncology, Rostov-on-Don, Russian Federation. ORCID 0000-0003-3061-6108.

Frantsiyants Elena M., Dr. Sci. (Biology), Professor, Deputy General Director for Science, Head of Laboratory of Malignant Tumor Pathogenesis Study, National Medical Research Centre for Oncology, Rostov-on-Don, Russian Federation. ORCID 0000-0003-3618-6890.

Bandovkina Valerija A., Cand. Sci. (Biology), Senior Researcher, Laboratory of Malignant Tumor Pathogenesis Study, National Medical Research Centre for Oncology, Rostov-on-Don, Russian Federation. ORCID 0000-0002-2302-8271.

Kaplieva Irina V., Cand. Sci. (Med.), Senior Researcher, Laboratory of Malignant Tumor Pathogenesis Study, National Medical Research Centre for Oncology, Rostov-on-Don, Russian Federation. ORCID 0000-0002-3972-2452.

Surikova Ekaterina I., Cand. Sci. (Biology), Senior Researcher, Laboratory of Malignant Tumor Pathogenesis Study, National Medical Research Centre for Oncology, Rostov-on-Don, Russian Federation. ORCID 0000-0002-4318-7587.

Trepitaki Lidija K., Researcher, Laboratory of Malignant Tumor Pathogenesis Study, National Medical Research Centre for Oncology, Rostov-on-Don, Russian Federation. ORCID 0000-0002-9749-2747.

Cheryarina Natalia D., Laboratory Assistant, Laboratory of Malignant Tumor Pathogenesis Study, National Medical Research Centre for Oncology, Rostov-on-Don, Russian Federation. ORCID 0000-0002-3711-8155.

Kotieva Inga M., Cand. Sci. (Med.), Senior Researcher, Laboratory of Malignant Tumor Pathogenesis Study, National Medical Research Centre for Oncology, Rostov-on-Don, Russian Federation. ORCID 0000-0003-0252-4708.

(✉) **Bandovkina Valeria A.,** e-mail: super.gormon@yandex.ru.

Received 08.11.2019
Accepted 25.12.2019

УДК 6616.2-002.5:575.22](571.56)
https://doi.org/10.20538/1682-0363-2020-4-102-109

Comparative analysis of N-acetyltransferase 2 genotyping results among patients with newly diagnosed pulmonary tuberculosis residing in the Sakha Republic (Yakutia)

Krasnova N.M.[1], Efremova E.N.[2], Egorova A.A.[2], Filippova O.I.[2], Chertovskikh Y.V.[3], Rudykh Z.A.[3], Alekseeva E.A.[3], Tatarinova T.E.[3], Sokorutov D.A.[1], Val N.S.[2], Vinokurova M.K.[2], Karvchenko A.F.[2], Vengerovskii A.I.[4], Sychev D.A.[5]

[1] *M.K. Ammosov North-Eastern Federal University*
58, Belinskogo Str., Yakutsk, 677000, Russian Federation

[2] *Phthisiatry Research-Practice Center*
93, Petra Alekseeva Str., Yakutsk, 677000, Russian Federation

[3] *Republican Clinical Hospital No. 3*
34, Kirova Str., Yakutsk, 677027, Russian Federation

[4] *Siberian State Medical University*
2, Moscow Trakt, Tomsk, 634050, Russian Federation

[5] *Russian Medical Academy of Continuous Professional Education*
2/1, Barrikadnaya Str., Moscow, 125993, Russian Federation

ABSTRACT

Aim. To assess the variability of the *NAT2* gene and to comparatively analyze the prevalence of *NAT2* polymorphisms and acetylation types among Yakut and Russian patients newly diagnosed with pulmonary tuberculosis (TB), permanently residing in the Sakha Republic (Yakutia).

Materials and methods. The study included 197 patients with newly diagnosed pulmonary TB (132 Yakuts and 65 Russians) aged (43.3 ± 14.4). The following single-nucleotide polymorphisms were analyzed, using real-time polymerase chain reaction (PCR): *NAT2*5* (rs1801280, T341C), *NAT2*6* (rs1799930, G590A), *NAT2*7* (rs1799931, G857A), *NAT2*11* (rs1799929, C481T), *NAT2*12* (rs1208, A803G), and *NAT2*13* (rs1041983, C282T). Genetically determined basal metabolic rates were calculated using the NATpred online tool.

Results. 75% of residents, both of Yakut and Russian ethnicity, were identified as carriers of *NAT2* polymorphic variants known to be related to isoniazid biotransformation. *NAT2*6* and **13* allelic variants were more frequent in Yakuts (occurring in 40.9% and 64.4%, respectively); variants *NAT2*5, *6, *11, *12*, and **13* were more common in Russians (69.2; 55.4; 67.7; 69.2, and 64.6%, respectively). The *NAT2*5, *7, *11*, and **12* polymorphisms were found to be significantly ethnicity-dependent. The study established substantial prevalence of medium acetylation type (58.3%) in Yakuts and slow acetylation type in Russians (61.5%). Correlations were shown between ethnicity and different prevalence rates of rapid, medium, or slow acetylation types among patients with TB.

Conclusion. The observed *NAT2* polymorphism distribution patterns and isoniazid acetylation types among Yakut and Russian patients with newly diagnosed pulmonary TB demonstrated that pharmacologic responses can be significantly different between ethnic groups. Findings of pharmacogenetic studies in Yakut and Russian populations should be incorporated in clinical practice for personalized administration of isoniazid.

Key words: Yakut, Russian, tuberculosis, isoniazid, pharmacogenetics, polymorphism, *NAT2*, acetylation, isoniazid acetyltransferase.

✉ *Krasnova Natalia M.,* e-mail: krasnova14@mail.ru.

Conflict of interest. The authors declare no obvious or potential conflict of interest related to the publication of this article.

Source of financing. The study was financially supported by the Republican clinical hospital no. 3 of the Ministry of Health of the Sakha Republic (Yakutia).

Conformity to the principles of ethics. All patients signed an informed consent to take part in the study. The study was approved by the Ethics Committee of the Phthisiatry Research-Practice Center (Protocol No. 3 of 26.09.2018).

For citation: Krasnova N.M., Efremova E.N., Egorova A.A., Filippova O.I., Chertovskikh Y.V., Rudykh Z.A., Alekseeva E.A., Tatarinova T.E., Sokorutov D.A., Val N.S., Vinokurova M.K., Karvchenko A.F., Vengerovskii A.I., Sychev D.A. Comparative analysis of N-acetyltransferase 2 genotyping results among patients with newly diagnosed pulmonary tuberculosis residing in the Sakha Republic (Yakutia). *Bulletin of Siberian Medicine.* 2020; 19 (4): 102–109. https://doi.org/10.20538/1682-0363-2020-4-102-109.

Сравнительный анализ результатов генотипирования гена N-ацетилтрансферазы 2 у пациентов с впервые выявленным туберкулезом органов дыхания, проживающих в Республике Саха (Якутия)

Краснова Н.М.[1], Ефремова Е.Н.[2], Егорова А.А.[2], Филиппова О.И.[2], Чертовских Я.В.[3], Рудых З.А.[3], Алексеева Е.А.[3], Татаринова Т.Е.[3], Сокорутов Д.А.[1], Валь Н.С.[2], Винокурова М.К.[2], Кравченко А.Ф.[2], Венгеровский А.И.[4], Сычёв Д.А.[5]

[1] Северо-Восточный федеральный университет (СВФУ) им. М.К. Аммосова
Россия, 677000, г. Якутск, ул. Белинского, 58

[2] Научно-практический центр (НПЦ) «Фтизиатрия»
Россия, 677000, г. Якутск, ул. Петра Алексеева, 93

[3] Республиканская клиническая больница (РКБ) № 3
Россия, 677027, г. Якутск, ул. Кирова, 34

[4] Сибирский государственный медицинский университет (СибГМУ)
Россия, 634050, г. Томск, Московский тракт, 2

[5] Российская медицинская академия непрерывного профессионального образования (РМАНПО)
Россия, 125993, г. Москва, ул. Баррикадная, 2/1, стр. 1

РЕЗЮМЕ

Цель. Оценить вариабельность гена *N*-ацетилтрансферазы 2 (*NAT2*), провести сравнительный анализ распространенности его полиморфизмов гена *NAT2* и типов ацетилирования среди якутов и русских с впервые выявленным туберкулезом органов дыхания, проживающих в Республике Саха (Якутия).

Материалы и методы. В исследование включены 197 пациентов (132 якута и 65 русских) в возрасте (43,3 ± 14,4) года с впервые выявленным туберкулезом органов дыхания. Методом полимеразной цепной реакции в режиме реального времени исследованы однонуклеотидные полиморфизмы *NAT2*5* (rs1801280, T341C), *NAT2*6* (rs1799930, G590A), *NAT2*7* (rs1799931, G857A), *NAT2*11* (rs1799929, C481T), *NAT2*12* (rs1208, A803G), *NAT2*13* (rs1041983, C282T). Генетически детерминированную скорость метаболизма рассчитывали с помощью онлайн-калькулятора NATpred.

Результаты. Полиморфные варианты гена *NAT2*, ассоциированные со скоростью биотрансформации изониазида, встречаются у 75% якутов и всех русских, проживающих в Якутии. Якуты являются частыми носителями аллельных вариантов *NAT2*6* и **13* (с частотой встречаемости 40,9 и 64,4% соответственно), русские – носителями *NAT2*5, *6, *11, *12 и *13* (с частотой встречаемости 69,2; 55,4; 67,7; 69,2 и 64,6% соответственно). Распределение полиморфизмов *NAT2*5, *7, *11, *12* значимо зависит от национальности. Установлена большая распространенность промежуточного типа ацетилирования (58,3%) среди якутов, медленного типа – среди русских (61,5%). Различия распространенности быстрого, промежуточного и медленного типов ацетилирования у пациентов с туберкулезом зависят от национальности.

Заключение. Особенности распределения полиморфизмов гена *NAT2* и типов ацетилирования изониазида среди пациентов якутской и русской национальности с впервые выявленным туберкулезом органов дыхания свидетельствуют о том, что фармакологический ответ может значительно различаться среди пациентов национальных групп. Данные фармакогенетического исследования у якутов и русских необходимо учитывать в клинической практике для персонализированного применения изониазида.

Ключевые слова: якуты, русские, туберкулез, изониазид, фармакогенетика, полиморфизм, NAT2, медленный, быстрый, промежуточный, тип ацетилирования.

Конфликт интересов. Авторы декларируют отсутствие явных и потенциальных конфликтов интересов, связанных с публикацией настоящей статьи.

Источник финансирования. Исследование выполнено при финансовой поддержке ГАУ РС(Я) «Республиканская клиническая больница № 3» Министерства здравоохранения Республики Саха (Якутия).

Соответствие принципам этики. Все пациенты подписали информированное согласие на проведение исследования. Исследование одобрено локальным этическим комитетом ГБУ РС(Я) «Научно-практический центр «Фтизиатрия» (протокол № 3 от 26.09.2018).

Для цитирования: Краснова Н.М., Ефремова Е.Н., Егорова А.А., Филиппова О.И., Чертовских Я.В., Рудых З.А., Алексеева Е.А., Татаринова Т.Е., Сокорутов Д.А., Валь Н.С., Винокурова М.К., Кравченко А.Ф., Венгеровский А.И., Сычёв Д.А. Сравнительный анализ результатов генотипирования гена N-ацетилтрансферазы 2 у пациентов с впервые выявленным туберкулезом органов дыхания, проживающих в Республике Саха (Якутия). *Бюллетень сибирской медицины.* 2020; 19 (4): 102–109. https://doi.org/10.20538/1682-0363-2020-4-102-109.

INTRODUCTION

Conventionally recommended treatment for newly identified drug-sensitive pulmonary tuberculosis consists of a combination of 4 most effective anti-TB drugs, such as isoniazid, rifampicin, pyrazinamide, and ethambutol, administered in standard doses (http://cr.rosminzdrav.ru/#!/schema/943). In reality, individual differences in pharmacologic responses to these drugs, developing quite often, include poor chemotherapy outcomes in some patients, possible development of *M. tuberculosis* drug resistance followed by disease relapse, and adverse drug reactions [1]. In particular, isoniazid is a drug with a known hepatotoxic effect, which can cause liver damage with clinical manifestations ranging from asymptomatic hyperenzymemia (10–20% of patients) to severe hepatitis or acute hepatic failure (0.5–1%) [2]. Toxic liver effect is produced by highly active isoniazid metabolites, hydrazine and acetylhydrazine [3, 4].

Isoniazid is metabolized in the liver through reactions of acetylation and hydrolysis. These reactions are catalyzed by N-acetyltransferase-2 (*NAT2*) and acylamidase, respectively [5]. A *NAT2* isozyme is encoded by a highly polymorphic gene with 106 alleles established to date. *NAT2* activity is determined by single-nucleotide substitution in the backbone region of the encoding gene [6, 7]. Combinations of *NAT2* gene alleles produce a variety of isoniazid acetylation phenotypes: rapid acetylator (presence of 1 or 2 "rapid" alleles); medium acetylator (1 "slow" allele); slow acetylator (2 "slow" alleles) [5, 8].

NAT2 gene polymorphism distribution is known to vary substantially and has been shown to correlate with race, ethnic origin, and place of residence [9–11]. The aim of this study was to assess the variability of *NAT2* gene and to comparatively analyze prevalence of *NAT2* gene polymorphisms and acetylation types among Yakuts and Russians with newly identified pulmonary tuberculosis (PTB).

MATERIALS AND METHODS

Single-center, one stage, observational sampling study was conducted, including 197 patients with newly identified PTB, selected from representatives of 2 ethnic groups living in the Sakha Republic (Yakutia): 132 Yakuts (77 women, 55 men) and 65 Russians (35 women, 30 men). Patients were hospitalized to Phthisiatry Research-Practice Center in Yakutsk during the intensive chemotherapy phase. Patient's average age was 43.3 ± 14.4 years. Inclusion criteria were PTB diagnosed for the first time, age of 18 years or over, informed consent, and Yakut or Russian ethnicity. Ethnicity was established based on self-definition by patients and their parents; family trees were also analyzed to the second generation. In earlier studies, it was shown that ethnic self-definition corresponded

to microsatellite analysis in 99.9% of cases [12]. Descendants from mixed marriages and patients who did not meet any of the inclusion criteria were excluded.

Blood for genetic analysis was obtained from a superficial elbow vein. Using evacuated blood collection systems, whole blood specimens were collected in 4 mL tubes coated with finely dispersed ethylenediaminetetraacetic acid (Zhejiang Gongdong Medical Technology Co., Ltd); then desoxyribonucleic acid (DNA) was isolated using the ExtractDNA Blood reagent kit (Evrogen, Russia). Using Real-Time CFX96 Touch (Bio-Rad, USA) PCR system and GenTest-M *NAT2* (Nomotek, Russia) reagent kit, we identified the presence of the following polymorphic variants: *NAT2*5* (rs1801280, T341C), *NAT2*6* (rs1799930, G590A), *NAT2*7* (rs1799931, G857A), *NAT2*11* (rs1799929, C481T), *NAT2*12* (rs1208, A803G), and *NAT2*13* (rs1041983, C282T). Genetically determined basal metabolic rates were calculated using NATpred online calculator [13].

Statistical analysis was performed using IBM SPSS Statistics ver. 23. Pearson's chi-squared test and its modification with Yates's correction were used for analysis. Compliance of genotype distribution with Hardy – Weinberg equilibrium was checked using 95% Clopper – Pearson confidence intervals. The critical significance level p was 0.05.

RESULTS

Yakut and Russian patients newly diagnosed with TB had the following polymorphic *NAT2* gene variants known to be linked with the isoniazid biotransformation rate: *NAT2*5*, **6, *7, *11, *12,* and **13*. In Yakuts, allele and genotype distributions of *NAT2* polymorphisms were consistent with Hardy – Weinberg equation ($p > 0.05$). In Russians permanently living in Yakutia, allele and genotype distributions of *NAT2*5, *6, *7, *12*, and **13* polymorphisms complied with the Hardy – Weinberg equation, only the *NAT2*11* polymorphism did not correspond to the equilibrium (Table 1).

NAT2 polymorphic variants were found in 75% (99 / 132) of Yakut patients and in all Russian patients (65 / 65). Two most frequent allelic variants found among Yakuts were *NAT2*6* (40.9%) and *NAT2*13* (64.4%). In Russians, the following polymorphic variants were observed with almost the same frequencies: *NAT2*5, *6, *11, *12*, and **13* (69.2%, 55.4%, 67.7%, 69.2%, and 64.6%, respectively) (Table 1).

Statistically significant ethnicity-dependent differences were observed in the prevalence of single-nucleotide polymorphisms (SNPs) *NAT2*5, *7, *11, *12* (Table 1). Polymorphic variants *NAT2*6* and *NAT2*13* were equally frequent among Yakuts and Russians.

Table 1

Comparison of allele and genotype frequencies of *NAT2* gene polymorphisms in Yakuts and Russians with newly identified pulmonary tuberculosis (PTB)

Polymorphism	Yakuts (n = 132)							Russians (n = 65)						
	Genotype, n (%)			Allele, %		χ^2	P	Genotype, n (%)			Allele, %		χ^2	P
NAT2*5 (T341C)	T/T	T/C	C/C	T	C	1.17	0.558	T/T	T/C	C/C	T	C	1.28	0.527
	91 (68.9)	35 (26.5)	6 (4.6)	0.82	0.18			20 (30.8)*	36 (55.4)*	9 (13.8)*	0.58	0.42		
NAT2*6 (G590A)	G/G	G/A	A/A	G	A	0.64	0.727	G/G	G/A	A/A	G	A	0.004	0.998
	78 (59.1)	49 (37.1)	5 (3.8)	0.78	0.22			29 (44.6)	29 (44.6)	7 (10.8)	0.67	0.33		
NAT2*7 (G857A)	G/G	G/A	A/A	G	A	0.01	0.993	G/G	G/A	A/A	G	A	0.36	0.976
	94 (71.2)	35 (26.5)	3 (2.3)	0.84	0.16			56 (86.2)*	9 (13.8)*	0 (0)*	0.93	0.07		
NAT2*11 (C481T)	C/C	C/T	T/T	C	T	0.00	1.000	C/C	C/T	T/T	C	T	6.70	0.035
	90 (68.2)	38 (28.8)	4 (3.0)	0.83	0.17			21 (32.3)*	40 (61.5)*	4 (6.2)*	0.63	0.37		
NAT2*12 (A803G)	A/A	A/ G	G/G	A	G	0.17	0.916	A/A	A/ G	G/G	A	G	2.07	0.354
	91 (68.9)	38 (28.8)	3 (2.3)	0.83	0.17			20 (30.8)*	37 (56.9)*	8 (12.3)*	0.59	0.41		
NAT2*13 (C282T)	C/C	C/T	T/T	C	T	5.89	0.052	C/C	C/T	T/T	C	T	0.72	0.699
	47 (35.6)	74 (56.1)	11 (8.3)	0.64	0.36			23 (35.4)	34 (52.3)	8 (12.3)	0.62	0.38		

Note. $\chi 2$ – Pearson's chi-square test, p – statistically significant differences (< 0.05). * significant differences, compared with Yakuts, $p < 0.05$.

58.3% (77 / 132) of Yakuts with newly diagnosed TB were characterized by medium acetylators, while in 22.7% (30/132) and 18.9% (25/132) slow and rapid acetylators, respectively, were observed. Among Russians, slow type was detected in 61.5% (40 / 65), medium type – in 35.4% (23 / 65), and rapid type – in 3.1% (2 / 65).

Differences in the prevalence of 3 acetylation types significantly depended on ethnicity ($\chi^2 = 30.977$; $p = 0.000$).

Occurrence of NAT2*6, *7, and *11 genotypes among slow and medium acetylators did not differ much between Yakut and Russian patients, unlike the prevalence of NAT2*5, *12, and *13 polymorphisms, which showed statistically significant differences.

74% (57 / 77; CI [0.62–0.83]) of Yakut medium acetylators were carriers of homozygous T/T genotype of NAT2*5 (T341C). In the group of Russian patients, this carriage was observed in 39.1% of cases (9 / 23; CI [0.19–0.61]) ($p < 0.05$).

Heterozygous T/C NAT2*5 genotype was identified in 24.7% of Yakut (19 / 77; CI [0.15–0.35]) and 60.9% of Russian (14 / 23 CI [0.38–0.80]) ($p < 0.05$) medium acetylators (Table 2).

Table 2

Acetylation types in patients with PTB with different genotypes of *NAT2* gene polymorphisms

Polymorphisms	Genotype	Yakuts (n = 132)			Russians (n = 65)		
		Slow acetylator (n = 30), n (%)	Medium acetylator (n = 77), n (%)	Rapid acetylator (n = 25), n (%)	Slow acetylator (n = 40), n (%)	Medium acetylator (n = 23), n (%)	Rapid acetylator (n = 2), n (%)
NAT2*5 (T341C)	T/T	9 (30.0)	57 (74.0)	25 (100.0)	9 (22.5)	9 (39.1)	2 (100.0)
	T/C	16 (53.3)	19 (24.7)	0	22 (55.0)	14 (60.9)	0
	C/C	5 (16.7)	1 (1.3)	0	9 (22.5)	0	0
NAT2*6 (G590A)	G/G	12 (40.0)	41 (53.2)	25 (100.0)	11 (27.5)	16 (69.6)	2 (100.0)
	G/A	15 (50.0)	34 (44.2)	0	23 (57.5)	6 (26.1)	0
	A/A	3 (10.0)	2 (2.6)	0	6 (15.0)	1(4.3)	0
NAT2*7 (G857A)	G/G	16 (53.3)	53 (68.8)	25 (100.0)	32 (80.0)	22 (95.7)	2 (100.0)
	G/A	12 (40.0)	23 (29.9)	0	8 (20.0)	1 (4.3)	0
	A/A	2 (6.7)	1 (1.3)	0	0	0	0
NAT2*11 (C481T)	C/C	9 (30.0)	56 (72.7)	25 (100.0)	9 (22.5)	10 (43.5)	2 (100.0)
	C/T	18 (60.0)	20 (26.0)	0	27 (67.5)	13 (56.5)	0
	T/T	3 (10.0)	1 (1.3)	0	4 (10.0)	0	0
NAT2*12 (A803G)	A/A	9 (30.0)	57 (74.0)	25 (100.0)	10 (25.0)	8 (34.8)	2 (100.0)
	A/G	19 (63.3)	19 (24.7)	0	23 (57.5)	14 (60.9)	0
	G/G	2 (6.7)	1 (1.3)	0	7 (17.5)	1 (4.3)	0
NAT2*13 (C282T)	C/C	3 (10.0)	19 (24.7)	25 (100.0)	6 (15.0)	15 (65.2)	2 (100.0)
	C/T	18 (60.0)	56 (72.7)	0	27 (67.5)	7 (30.4)	0
	T/T	9 (30.0)	2 (2.6)	0	7 (17.5)	(4.3)	0

Among medium acetylators, 74% of Yakuts (57/77; CI [0.62–0.83]) and 34.8% of Russians (8 / 23; CI [0.16–0.57]) ($p < 0.05$) had A/A genotype of NAT2*12 (A803G). Carriers of heterozygous A/G NAT2*12 genotype were found more frequently among Russian patients (60.9%, 14 / 23; CI [0.38–0.80]), as opposed to rarer occurrence of this genotype among Yakut patients (24.7%, 19 / 77; CI [0.15–0.35]) ($p < 0.05$). C/C NAT2*13 genotype (C282T) was present in 24.7% of Yakuts (19 / 77; CI [0.15–0.35]) and 65.2% of Russians (15 / 23; CI [0.42–0.83]) ($p < 0.05$). In addition, Yakuts were more frequent carriers of T/C NAT2*13 heterozygote (72.7%, 56 / 77; CI [0.61–0.82]) than Russians (30.4%, 7 / 23; CI [0.13–0.52]) ($p < 0.05$).

DISCUSSION

Genetic diversity of the *NAT2* gene and acetylation phenotypes developed as a result of human adaption to living environment. Transition from nomadic to sedentary life profoundly changed food choices, resulting in the body being exposed to novel pathogens and xenobiotics. Further, due to the need for better survival the activity of detoxifying enzymes had been altered, producing a new heritable phenotype of biotransformation [14].

Correlation between ethnicity and the prevalence of *NAT2* gene polymorphisms has been observed across the globe. Based on data from the International Genome Sample Resource (IGSR; https://www.internationalgenome.org/), NAT2*5, *11, and *12 polymorphic variants are more prevalent among the populations of Europe and South Asia (68.4% and 56.5% (first variant); 67.6% and 53.1% (second variant); 67.2% and 58.1% (third variant)). Variants NAT2*5, *11, and *12 have been observed in 7.3%, 7.1%, and 7.7% of the population of East Asia, respectively. NAT2*7 polymorphism is frequent among native population of East Asia (31.8%), but is rare among Europeans (4.6%). NAT2*6 polymorphism has been detected in 58.7% of people living in South

Asia, showing equal rates among populations of Europe (46.9%) and East Asia (43.2%). Proportions of people carrying *NAT2*13* variant are nearly the same among Asian and European races (50.5% of Asians, 69.4% of Europeans).

Our study demonstrated higher frequencies of NAT2*6 and NAT2*13 allelic variants among Yakuts (Table 1), which complies with previously reported prevalence rates among Asians. The frequency of NAT2*5, NAT2*11, and NAT2*12 variants among Yakuts was 31.1%, 31.8%, and 31.1%, respectively, which was inconsistent with previously estimated proportions among Asian people. The allelic variant NAT2*7 had almost the same occurrence among Yakuts (28.8%) and people from East Asia (31.8%); however, its frequency was lower in the population of South Asia (13.5%).

The frequencies of NAT2*5, *6, *11, *12, and *13 polymorphic variants among Russians were 69.2%, 55.4%, 67.7%, 69.2%, and 64.6%, respectively (Table 1). The frequency of NAT2*7 polymorphism in Russians residing in Yakutia was higher than in residents of Europe (13.8% and 4.6%, respectively).

Comparative analysis of NAT2 genotype distribution showed that Russian patients were more frequent carriers of NAT2*5, *11, and *12 than Yakuts (Table 1). To date, evidence is lacking on the contribution of NAT2*5 and *11 genotypes to severity and frequency of isoniazid-induced liver damage in patients with tuberculosis. There is a known correlation between increased risk of isoniazid-induced hepatotoxicity and minor allele homozygous genotypes, compared with the same risk in carriers of major alleles of NAT*5 and *11 [15, 16].

Polymorphic variant NAT2*7 was more frequent in Yakuts (28.8%) than in Russians (13.8%) ($p < 0.05$). Genotype A/A NAT2*7 was observed in a small number of Yakut patients (2.3%) and in none of the Russian patients (Table 1). Few studies have reported inconclusive data on association between minor allele A NAT2*7 and hepatotoxicity risk. Some authors pointed out a higher risk of hepatotoxic reactions to first-line anti-TB drugs in individuals with A/A genotype, in contrast to carriers of G/G genotype [17, 18], while other researchers reported absence of such associations [2, 19].

Major alleles of NAT2*5, *6, and NAT2*7 encode synthesis of NAT2 with altered amino acid sequence and, therefore, lower activity. People with NAT2*5 allele in combination with NAT2*6, or *7 polymorphic variant are slow acetylators [8]. Geographic distribution of slow acetylators has been well studied: this phenotype occurs in 60% of the population of Europe, Middle East, North Africa, and South Asia, and in 10% of the population of East Asia and Native Americans [20].

In Yakut population, the most widespread acetylation type was medium type (58.3%), while Russians mostly were characterized by slow acetylation type (61.5%). The proportion of rapid acetylators was much larger among Yakuts, than among Russians (18.9% versus 3.1%). This is consistent with previous comparative studies among Asians and Caucasians.

In clinical practice, NAT2 polymorphism and genetically determined variability in isoniazid acetylation speed can have a considerable impact on the outcome and safety of tuberculosis pharmacotherapy. A link between liver damage rate and slow acetylation type was confirmed in several meta-analyses [21–24]. Slow acetylators showed high serum concentrations of isoniazid and its toxic metabolites [25]. Rapid acetylators had lower serum isoniazid concentrations, but higher risk of drug resistance to *M. tuberculosis* [25–28].

CONCLUSION

Our study results suggest that NAT2 gene polymorphisms linked to isoniazid acetylation have considerable prevalence rates among Yakuts and Russians. Yakuts mostly tended to be carriers of allelic variants NAT2*6 and *13, while Russians mostly carried variants NAT2*5, *6, *11, *12, and *13. Comparative analysis within the study sample showed the presence of statistically significant differences in frequencies of NAT2*5, *7, *11, and *12 genotypes, depending on ethnicity. As a result of NAT2 genotype combinations, Yakuts tended to develop mostly medium acetylation type, while Russians more often developed slow acetylation type. The observed patterns in distributions of NAT2 gene polymorphisms and acetylation types among Yakuts and Russians with newly identified TB can serve as a confirmation that pharmacologic responses can substantially differ depending on patients' ethnicity.

REFERENCES

1. Stepanova N.A., Streltsova E.N., Galimzyanov Kh.M., Kantemirova B.I. Adverse reactions to first-line anti-TB drugs. *Tuberculosis and Pulmonary Diseases*. 2016; 94 (5): 42–45 (in Russ.). DOI: 10.21292/2075-1230-2016-94-5-42-45.
2. Chan S.L., Chua A.P.G., Aminkeng F., Chee C.B.E., Jin S., Loh M., Gan S.H., Wang Y.T., Brunham L.R. Association and clinical utility of NAT2 in the prediction of isoniazid-induced

liver injury in Singaporean patients. *PLoS One.* 2017; 12 (10): e0186200. DOI: 10.1371/journal.pone.0186200.

3. Udut V.V., Dygai A.M., Vengerovsky A.I. Effects of phospholipid hepatoprotectors on apoptosis during experimental liver pathology induced by isoniazid and paracetamol. *Bulletin of Experimental Biology and Medicine*. 2012; 154 (11): 568–571. DOI: 10.1007/s10517-013-2012-9.
4. Richardson M., Kirkham J., Dwan K., Sloan D.J., Davies G., Jorgensen A.L. NAT2 variants and toxicity related to anti-tuberculosis agents: a systematic review and meta-analysis. *Int. J. Tuberc. Lung. Dis*. 2019; 23 (3): 293–316. DOI: 10.5588/ijtld.18.0324.
5. Snalina N.E., Sychev D.A. Genetic predictors of isoniazid-induced hepatotoxicity. *Molecular Medicine*. 2018; 16 (2): 31–36 (in Russ.). DOI: 10.29296/24999490-2018-02-04.
6. Jarrar Y.B., Balasmeh A.A., Jarrar W. Sequence analysis of the *N*-acetyltransferase 2 gene (N*AT2*) among Jordanian volunteers. *Libyan J. Med*. 2018; 13 (1): 1408381. DOI: 10.1080/19932820.2017.1408381.
7. Khan S., Mandal R.K., Elasbali A.M., Dar S.A., Jawed A., Wahid M., Mahto H., Lohani M., Mishra B.N., Akhter N., Rabaan A.A., Haque S. Pharmacogenetic association between gene polymorphisms and isoniazid induced hepatotoxicity: trial sequence meta-analysis as evidence. *Biosci. Rep.* 2019; 39 (1): BSR20180845. DOI: 10.1042/BSR20180845.
8. Yadav D., Kumar R., Dixit R.K., Kant S., Verma A., Srivastava K., Singh S.K., Singh S. Association of *NAT2* gene polymorphism with antitubercular drug-induced hepatotoxicity in the Eastern Uttar Pradesh population. *Cureus*. 2019; 11 (4): e4425. DOI: 10.7759/cureus.4425.
9. Dursun R., Dursun H.G., Zamani A.G., Yıldırım M.S., Çınar İ. *NAT2* gene polymorphisms in Turkish patients with psoriasis vulgaris. *Biomed. Res. Int.* 2018; 3258708. DOI: 10.1155/2018/3258708.
10. Kristensen B.E., Yakimov V., Bjorn-Mortensen K., Soborg B., Koch A., Andersson M., Birch Kristensen K., Michelsen S.W., Skotte L., Ahrendt Bjerregaard A., Blaszkewicz M., Golka K., Hengstler J.G., Feenstra B., Melbye M., Geller F. Study of correlation between the NAT2 phenotype and genotype status among Greenlandic Inuit. *EXCLI J.* 2018; 17: 1043–1053. DOI: 10.17179/excli2018-1671.
11. Sabbagh A., Darlu P., Crouau-Roy B., Poloni E.S. Arylamine N acetyltransferase 2 (NAT2) genetic diversity and traditional subsistence:a worldwide population survey. *PLoS One.* 2011; 6 (4): e18507. DOI: 10.1371/journal.pone.0018507.
12. Tang H., Quertermous T., Rodriguez B., Kardia S.L., Zhu X., Brown A., Pankow J.S., Province M.A., Hunt S.C., Boerwinkle E., Schork N.J., Risch N.J. Genetic structure, self-identified race/ethnicity, and confounding in case-control association studies. *Amer. J. Human Genet.* 2005; 76 (2): 268–275.
13. Kuznetsov I.B., McDuffie M., Moslehi R. A web-server for inferring the human N-acetyltransferase-2 (NAT2) enzymatic phenotype from *NAT2* genotype. *Bioinformatics.* 2009; 25 (9): 1185–1186.
14. Magalon H., Patin E., Austerlitz F., Quintana-Murci L., Heyer E. Population genetic diversity of the *NAT2* gene supports a role of acetylation in human adaptation to farming in Central Asia. *Eur. J. Hum. Genet.* 2008; 16 (2): 243–251. DOI: 10.1038/sj.ejhg.5201963.
15. Xiang Y., Ma L., Wu W., Liu W., Li Y., Zhu X., Wang Q., Ma J., Cao M., Wang Q., Yao X., Yang L., Wubuli A., Merle C., Milligan P., Mao Y., Gu J., Xin X. The incidence of liver injury in Uyghur patients treated for TB in Xinjiang Uyghur Autonomous Region, China, and its association with hepatic enzyme polymorphisms *NAT2, CYP2E1, GSTM1* and *GSTT1*. *PLoS One*. 2014; 9 (1): e85905. DOI: 10.1371/journal.pone.0085905.
16. Possuelo L.G., Castelan J.A., de Brito T.C., Ribeiro A.W., Cafrune P.I., Picon P.D., Santos A.R., Teixeira R.L., Gregianini T.S., Hutz M.H., Rossetti M.L., Zaha A. Association of slow N-acetyltransferase 2 profile and anti-TB drug-induced hepatotoxicity in patients from Southern Brazil. *Eur. J. Clin. Pharmacol.* 2008; 64 (7): 673–681. DOI: 10.1007/s00228-008-0484-8.
17. Cramer J.P., Lohse A.W., Burchard G.D., Fischer L., Nashan B., Zimmermann M., Marx A., Kluge S. N-acetyltransferase 2 activity in isoniazid-associated acute hepatitis requiring liver transplantation. *Transpl. Int.* 2010; 23 (2): 231–233. DOI: 10.1111/j.1432-2277.2009.00921.x.
18. An H.R., Wu X.Q., Wang Z.Y., Zhang J.X., Liang Y. *NAT2* and *CYP2E1* polymorphisms associated with antituberculosis drug-induced hepatotoxicity in Chinese patients. *Clin. Exp. Pharmacol. Physiol.* 2012; 39 (6): 535–543. DOI: 10.1111/j.1440-1681.2012.05713.x.
19. Kim S.H., Kim S.H., Bahn J.W., Kim Y.K., Chang Y.S., Shin E.S., Kim Y.S., Park J.S., Kim B.H., Jang I.J., Song J., Kim S.H., Park H.S., Min K.U., Jee Y.K. Genetic polymorphisms of drug-metabolizing enzymes and anti-TB drug-induced hepatitis. *Pharmacogenomics*. 2009; 10 (11): 1767–1779. DOI: 10.2217/pgs.09.100.
20. Kumar H.A.K., Ramesh K., Kannan T., Sudha V., Haribabu H., Lavanya J., Swaminathan S., Ramachandran G. N-acetyltransferase gene polymorphisms plasma isoniazid concentrations in patients with tuberculosis. *Indian J. Med. Res.* 2017; 145 (1): 118–123. DOI: 10.4103/ijmr.IJMR_2013_15.
21. Shi J., Xie M., Wang J., Xu Y., Liu X. Susceptibility of N-acetyltransferase 2 slow acetylators to antituberculosis drug-induced liver injury: a meta-analysis. *Pharmacogenomics.* 2015; 16 (18): 2083–2097. DOI: 10.2217/pgs.15.144.
22. Suvichapanich S., Fukunaga K., Zahroh H., Mushiroda T., Mahasirimongkol S., Toyo-Oka L., Chaikledkaew U., Jittikoon J., Yuliwulandari R., Yanai H., Wattanapokayakit S., Tokunaga K. NAT2 ultra-slow acetylator and risk of anti-tuberculosis drug-induced liver injury: a genotype-based meta-analysis. *Pharmacogenet. Genomics*. 2018; 28 (7): 167–176. DOI: 10.1097/FPC.0000000000000339.
23. Wang P.Y., Xie S.Y., Hao Q., Zhang C., Jiang B.F. *NAT2* polymorphisms and susceptibility to anti-tuberculosis drug-induced liver injury: a meta-analysis. *Int. J. Tuberc. Lung Dis.* 2012; 16 (5): 589–595. DOI: 10.5588/ijtld.11.0377.
24. Zhang M., Wang S., Wilffert B., Tong R., van Soolingen D., van den Hof S., Alffenaar J.W. The association between the *NAT2* genetic polymorphisms and risk of DILI during anti-TB treatment: a systematic review and meta-analysis. *Br.*

J. Clin. Pharmacol. 2018; 84 (12): 2747–2760. DOI: 10.1111/bcp.13722.
25. Lauterburg B., Smith C., Todd E., Mitchell J. Pharmacokinetics of the toxic hydrazine metabolites formed from isoniazid in humans. *J. Pharmacol. Exp. Ther*. 1985; 235 (3): 566–570.
26. Donald P.R., Sirgel F.A., Venter A., Parkin D.P., Seifart H.I., van de Wal B.W., Werely C., van Helden P.D., Maritz J.S. The influence of human N-acetyltransferase genotype on the early bactericidal activity of isoniazid. *Clin. Infect Dis.* 2004; 39 (10): 1425–1430.
27. Weiner M., Burman W., Vernon A., Benator D., Peloquin C.A., Khan A., Weis S., King B., Shah N., Hodge T. Low isoniazid concentrations and outcome of tuberculosis treatment with once weekly isoniazid and rifapentine. *Am. J. Respir. Crit. Care Med.* 2003; 167 (10): 1341–1347.
28. Azuma J., Ohno M., Kubota R., Yokota S., Nagai T., Tsuyuguchi K., Okuda Y., Takashima T., Kamimura S., Fujio Y., Kawase I. Pharmacogenetics-based tuberculosis therapy research group. *NAT2* genotype guided regimen reduces isoniazid-induced liver injury and early treatment failure in the 6-month four-drug standard treatment of tuberculosis: A randomized controlled trial for pharmacogenetics-based therapy. *Eur. J. Clin. Pharmacol*. 2013; 69 (5): 1091–1101. DOI: 10.1007/s00228-012-1429-9.

Authors contribution

Krasnova N.M., Efremova E.N., Egorova A.A., Filippova O.I., Vinokurova M.K., Alekseeva E.A., Chertovskykh Y.V., Rudykh Z.A., Tatarinova T.E., Sokorutov D.A., Val N.S. – carrying out of the research, statistical analysis and interpretation of data. Kravchenko A.F., Vengerovsky A.I., Sychev D.A. – conception and design, critical revision for important intellectual content, final approval of the manuscript for publication.

Authors information

Krasnova Natalia M., Cand. Sci. (Med.), Associate Professor, Department of Advanced-Level Therapy, Clinical Pharmacology and Occupational Diseases, M.K. Ammosov North-Eastern Federal University, Yakutsk, Russian Federation. ORCID 0000-0002-4811-7801.

Efremova Efrosiniya N., TB clinician, Phthisiatry Research-Practice Center, Yakutsk, Russian Federation. ORCID 0000-0001-6934-2971.

Egorova Aleksandra A., TB clinician, Phthisiatry Research-Practice Center, Yakutsk, Russian Federation. ORCID 0000-0002-3027-2731.

Filippova Olga I., TB clinician, Head of the Pulmonary TB Department, Phthisiatry Research-Practice Center, Yakutsk, Russian Federation. ORCID 0000-0003-4213-2901.

Chertovskykh Yana V., Clinical Pharmacologist, Head of the Center for Personalized Medicine, Republican Hospital no. 3, Yakutsk, Russian Federation. ORCID 0000-0003-0941-8633.

Rudykh Zoya A., Clinical Pharmacologist, Center for Personalized Medicine, Republican Hospital no. 3, Yakutsk, Russian Federation. ORCID: 0000-0001-8212-0150.

Alekseeva Elizaveta A., Biologist, Center for Personalized Medicine, Republican Hospital no. 3, Yakutsk, Russian Federation. ORCID: 0000-0001-6116-5720.

Tatarinova Tatiana E., Clinical Pharmacologist, Center for Personalized Medicine, Republican Hospital no. 3, Yakutsk, Russian Federation. ORCID 0000-0002-2616-3655.

Sokorutov Denis A., Residen, M.K. Ammosov North-Eastern Federal University, Yakutsk, Russian Federation. ORCID 0000-0002-7255-5238.

Val Natalia S., Cand. Sci. (Med.), Deputy director for medical service, Phthisiatry Research-Practice Center, Yakutsk, Russian Federation. ORCID 0000-0003-2910-1895.

Vinokurova Maria K., Dr. Sci. (Med.), Deputy director for science, Phthisiatry Research-Practice Center, Yakutsk, Russian Federation. ORCID 0000-0001-7673-3815.

Kravchenko Aleksandr F., Dr. Sci. (Med.), Director, Phthisiatry Research-Practice Center, Yakutsk, Russian Federation. ORCID: 0000-0002-9210-3407.

Vengerovsky Aleksandr I., Dr. Sci. (Med.), Professor, Honored Worker of Higher Education of the Russian Federation, Head of the Pharmacology Department, Siberian State Medical University, Tomsk, Russian Federation. ORCID 0000-0001-5094-3742.

Sychev Dmitry A., Dr. Sci. (Med.), Professor, Corresponding Member of the Russian Academy of Sciences, Head of Clinical Pharmacology and Therapy Department, Russian Medical Academy of Continuous Professional Education, Moscow, Russian Federation. ORCID 0000-0002-4496-3680.

(✉) **Krasnova Natalia M.,** e-mail: krasnova14@mail.ru.

Received 19.04.2020
Accepted 29.09.2020

УДК 616-009.7:615.216
https://doi.org/10.20538/1682-0363-2020-4-110-118

Analgesic action of hexaazaisowurtzitane derivative in somatic pain models caused by TRPA1 and TRPV1 Ion channels activation

Krylova S.G.[1], Lopatina K.A.[1], Zueva E.P.[1], Safonova E.A.[1], Povet'eva T.N.[1], Nesterova Yu.V.[1], Afanas'eva O.G.[1], Kul'pin P.V.[1], Suslov N.I.[1], Kulagina D.A.[2], Sysolyatin S.V.[2], Zhdanov V.V.[1]

[1] *Goldberg Research Institute of Pharmacology and Regenerative Medicine (GRIP&RM), Tomsk National Research Medical Center (NRMC), Russian Academy of Sciences*
3, Lenin Av., Tomsk, 634028, Russian Federation

[2] *Institute for Problems of Chemical and Energetic Technologies Siberian Branch of the Russian Academy of Sciences (IPCET SB RAS)*
1, Socialist Str., Biysk, 659322, Russian Federation

ABSTRACT

The aim of this study was to assess the analgesic action of thiowurtzine in somatogenic nociception models by activation of TRPA1 and TRPV1 ion channels.

Materials and methods. The object of the study is the compound 4-(3,4-dibromothiophenecarbonyl)-2,6,8,12-tetraacetyl-2,4,6,8,10,12-hexaazatetracyclo [5.5.0.^{03,11}.0^{5,9}]dodecane (thiowurtzine). The analgesic activity of thiowurtzine was studied under the conditions of a chemogenic activation model of TRPA1 channels (by the formalin test), and by a selective test with an agonist of TRPV1 channels (the capsaicin test). The compound was administered once *per os* in a dose range of 50–200 mg/kg (water-tween solvent) an hour before the experimental manipulations. The reference drugs were diclofenac sodium in a preventive single *per os* dose of 10 mg/kg in 1% starch gel in a volume of 0.2 ml/mouse, and ketorolac in a dose of 6 mg/kg in the same solvent, volume and route of administration.

Results. Thiowurtzine, when administered in *per os* doses of 100 and 200 mg/kg, was found to effectively block nociceptive reactions caused by activation of TRPA1 and TRPV1 ion channels. At the same time, the analgesic activity of thiowurtzine turned out to be comparable and/(or) superior to the ketorolac and diclofenac action, depending on the model situation. In addition, it was found that thiowurtzine (200 mg/kg *per os*) corresponds to diclofenac sodium (10 mg/kg *per os*) and is superior to ketorolac (6 mg/kg *per os*) in terms of anti-inflammatory severity in the formalin test.

Conclusion. The biphasicity of behavioral reactions in the prognostic formalin test do not allow for an unambiguous conclusion about the direction of the action mechanism of thiowurtzine, which confirms the polymodality hypothesis. The data obtained in the two models of somatogenic nociception do not exclude the fact that the modulation of the TRPA1 and TRPV1 activity is one of the mechanisms of the thiowurtzine analgesic action. By the key analgesic characteristics found herein, thiowurtzine proves to be a unique compound with a high therapeutic and innovation potential.

Key words: hexaazaisowurtzitane, thiowurtzine, analgesic activity, somatogenic nociception, TRP ion channels, formalin test, capsaicin, ketorolac, diclofenac, anti-inflammatory activity.

Conflict of interest. The authors declare no obvious or potential conflict of interest related to the publication of this article.

Source of financing. The study was carried out under the State Contract No. 14.N08.11.0179.

Conformity with the principles of ethics. The study was approved by the Bioethics Committee of the GRIP&RM, Tomsk NRMC (Protocol No. 96092015 of 16.09.2015).

✉ *Krylova Svetlana G.,* krylova5935@gmail.com.

For citation: Krylova S.G., Lopatina K.A., Zueva E.P., Safonova E.A., Povet'eva T.N., Nesterova Yu.V., Afanas'eva O.G., Kul'pin P.V., Suslov N.I., Kulagina D.A., Sysolyatin S.V., Zhdanov V.V. Analgesic action of hexaazaisowurtzitane derivative in somatic pain models caused by TRPA1 and TRPV1 ion channels activation. *Bulletin of Siberian Medicine.* 2020; 19 (4): 110–118. https://doi.org/10.20538/1682-0363-2020-4-110-118.

Анальгетическое действие производного гексаазаизовюрцитана на моделях соматической боли, вызванной активацией TRPA1- и TRPV1-ионных каналов

Крылова С.Г.[1], Лопатина К.А.[1], Зуева Е.П.[1], Сафонова Е.А.[1], Поветьева Т.Н.[1], Нестерова Ю.В.[1], Афанасьева О.Г.[1], Кульпин П.В.[1], Суслов Н.И.[1], Кулагина Д.А.[2], Сысолятин С.В.[2], Жданов В.В.[1]

[1] *Научно-исследовательский институт фармакологии и регенеративной медицины (НИИФиРМ) им. Е.Д. Гольдберга, Томский национальный исследовательский медицинский центр (НИМЦ) Российской академии наук*
Россия, 634028, г. Томск, пр. Ленина, 3

[2] *Институт проблем химико-энергетических технологий Сибирского отделения Российской академии наук (ИПХЭТ СО РАН)*
Россия, 659322, г. Бийск, ул. Социалистическая, 1

РЕЗЮМЕ

Цель. Оценка анальгетического действия тиовюрцина в условиях активации TRPA1- и TRPV1-ионных каналов на моделях соматогенной ноцицепции.

Материалы и методы. Объектом исследования является соединение 4-(3,4-дибромтиофенкарбонил)-2,6,8,12-тетраацетил-2,4,6,8,10,12-гексаазатетрацикло [5,5,0,$0^{3,11}$,$0^{5,9}$]додекан (тиовюрцин). Исследование анальгетической активности тиовюрцина проводили в условиях хемогенной модели активации TRPA1-каналов (формалиновый тест) и в селективном (капсаициновом тесте) с агонистом TRPV1-каналов – капсаицином. Соединение вводили однократно *per os* в диапазоне доз 50–200 мг/кг (водно-твиновый растворитель) за 1 ч до экспериментальных воздействий. В качестве референс-препаратов использовали диклофенак натрия превентивно однократно *per os* в дозе 10 мг/кг на 1%-м растворе крахмальной слизи в объеме 0,2 мл/мышь, кеторолак – в дозе 6 мг/кг в аналогичном растворителе, объеме и пути введения.

Результаты. Установлено, что тиовюрцин при превентивном однократном *per os* введении в дозах 100 и 200 мг/кг эффективно блокирует ноцицептивные реакции, обусловленные активацией TRPA1- и TRPV1-ионных каналов. При этом анальгетическая активность тиовюрцина оказалась сравнимой и (или) превосходящей действие кеторолака и диклофенака в зависимости от модельной ситуации. Кроме того, выявлено, что тиовюрцин (200 мг/кг *per os*) соответствует диклофенаку натрия (10 мг/кг *per os*) и превосходит кеторолак (6 мг/кг *per os*) по выраженности противовоспалительного действия в формалиновом тесте.

Заключение. Бифазность поведенческих реакций в прогностическом «Формалиновом тесте» не позволяет однозначно сделать вывод о направленности механизма действия тиовюрцина, что подтверждает гипотезу о полимодальности. Данные, полученные на двух моделях соматогенной ноцицепции, не исключают того, что модуляция активности рецепторов TRPA1- и TRPV1-ионных каналов является одним из механизмов его анальгетического действия. По сочетанию выявленных ключевых для анальгетика характеристик тиовюрцин является уникальным веществом с высоким терапевтическим и инновационным потенциалом.

Ключевые слова: гексаазаизовюрцитан, тиовюрцин, анальгетическая активность, соматогенная ноцицепция, TRP-ионные каналы, кеторолак, диклофенак, капсаицин, формалиновый тест, противовоспалительная активность.

Конфликт интересов. Авторы декларируют отсутствие явных и потенциальных интересов, связанных с публикацией настоящей статьи.

Источник финансирования. Работа выполнена в рамках реализации государственного контракта № 14.N08.11.0179.

Соответствие принципам этики. Исследование одобрено биоэтическим комитетом НИИФиРМ им. Е.Д. Гольдберга (протокол JACUC № 96092015 от 16.09.2015).

Для цитирования: Крылова С.Г., Лопатина К.А., Зуева Е.П., Сафонова Е.А., Поветьева Т.Н., Нестерова Ю.В., Афанасьева О.Г., Кульпин П.В., Суслов Н.И., Кулагина Д.А., Сысолятин С.В., Жданов В.В. Анальгетическое действие производного гексаазаизовюрцитана на моделях соматической боли, вызванной активацией TRPA1- и TRPV1-ионных каналов. *Бюллетень сибирской медицины.* 2020; 19 (4): 110–118. https://doi.org/10.20538/1682-0363-2020-4-110-118.

INTRODUCTION

Nowadays, one of the new trends in pharmaceutics is the synthesis of candidate molecules for use in designing non-narcotic analgesics to alleviate severe and moderate pain [1]. Three types of pain killers are principally used to treat pain of various etiologies in patients in inpatient and outpatient settings: opiate- and cannabinoid-based drugs with different analgesic activity, nonsteroidal anti-inflammatory drugs (NSAIDs), and different combinations thereof in multimodal treatment regimens [1, 2, 3]. For management of severe and moderate pain, non-narcotic analgesics could serve as opioid alternatives that act on the central and peripheral nervous systems in humans and offer a range of advantages. However, the number of possible candidate molecules of non-opioid analgesics is extremely limited. One of the up-to-date approaches to making innovative molecules is developing methods for streamlined construction and synthesis of original chemical entities.

The interdisciplinary partnership between the IPCET SB RAS and the GRIP&RM of NRMC resulted in 4-(3,4-dibromothiophenecarbonyl)-2,6,8,12-tetraacetyl-2,4,6,8,10,12-hexaazatetracyclo [5.5.0.$0^{3,11}$.$0^{5,9}$] dodecane (thiowurtzine), the world's first molecule in a new class of compounds for medical use (RU Patent No. 2565766 as of 23.09.2015). This innovative compound was created by the streamlined synthesis technique using the PASS software prediction data, and it is the ever-first in the class of hexaazaisowurtzitanes. Since the 80-ies of the last century, numerous studies focused on the synthesis of this class of compounds have primarily been of defense nature. And only in recent years, hexaazaisowurtzitane has been in use as a pharmacophore for the design of original pharmaceutical agents [4].

The previous studies revealed that this innovative compound demonstrated a pronounced analgesic activity comparable and/or superior to diclofenac sodium, ketorolac and tramadol in the "Hot plate" test and Acetic acid-induced writhing test, the model of acute visceral and deep somatic pain. Because thiowurtzine had no impact on the secretion of basic inflammation mediators (histamine, serotonin, and prostaglandin) and had no ulcerogenic activity in a dose range of 25-200 mg/kg, there was a conclusion made that it has no COX-dependent action [5]. With that, its prominent anti-inflammatory action in the arachidonic acid-induced test and its moderate action in the bradykinin- and carrageenan-induced inflammation models were validated [6]. This compound can be referred to hazard category III (lethal dose (LD_{50}) is in the range of 150–5000 mg/kg), GOST 12.1.007-76. The maximum possible single dose of thiowurtzine did not reach LD_{50} (or animal lethality). Thiowurtzine did not evoke respiratory depression nor did changes in gastrointestinal reflexes. The study into the thiowurtzine action mechanism revealed naloxone-sensitive analgesia, and no affinity to peripheral opioid receptors was proven using naloxone methiodide [5].

The above data altogether give evidence of the polymodal mechanism of the thiowurtzine action, which necessitates further research in this aspect.

The present study aimed to evaluate the analgesic action of thiowurtzine by activation of TRPA1 and TRPV1 ion channels in somatogenic nociception models such as formalin test and capsaicin test.

MATERIALS AND METHODS

The experiments were done on 50 outbred sexually mature male mouse of CD1 stock and 48 male CBA strain mice (aged 7–8 weeks) of the first category, conventional. The animals were provided by the Department of Experimental Biological Models at the GRIP&RM of Tomsk NRMC (animal health certificate available). The animal husbandry and experimental design were approved by the Bioethics Committee of the GRIP&RM (JACUC protocol No. 96092015 of 16.09.2015) and were in compliance with Directive 2010/63/EU "On the Protection of Animals Used for Scientific Purposes" of the European Parliament and

the Council of the European Union and with Order No. 199n as of 01.08.2016, of the Ministry of Health of the Russian Federation.

The experimental design, sample size, experimental regimen, and choice of statistical analysis were determined in the optimal way for this kind of research to acquire robust data for interpretation of results without expanding the number of animals. Before the experiment, each animal inside the group was assigned an individual number labeled with carbol-fuchsin marks. The animals were divided into groups randomly by body weight criterion so that the individual weight value would not deviate from the average within one group by no more than ±10%. After the experiments were completed, the mice were euthanized by the cervical dislocation method.

The innovative molecule under study represents a polynitrogen polycyclic cage compound, 4-(3,4-dibromothiophene carbonyl)-2,6,8,12-tetraacetyl-2,4,6,8,10,12-hexaazatetracyclo[5.5.0.$0^{3,11}$.$0^{5,9}$] dodecane. This is a newly synthesized compound obtained by acylation of commercially available 2,6,8,12-tetraacetyl-2,4,6,8,10,12-hexaazatetracyclo[5.5.0.$0^{3,11}$.$0^{5,9}$]dodecane with 3,4-dibromothiophene carboxylic chloroanhydride. Thiowurtzine, a colorless crystalline product with an API content of 99.0% and a single impurity content of below 0.2% (as per HPLC), Mp = 328–330°C), was characterized in full and validated by physicochemical analytical methods such as IR (ν/cm^{-1}), ^{1}H nuclear magnetic resonance (NMR) (DMSO-d6, δ, ppm) and ^{13}C NMR (DMSO-d6, δ, ppm) spectroscopies.

The therapeutic analgesic dose of thiowurtzine was estimated to be *per os* 100 mg/kg as determined in the previous studies on thiowurtzine analgesic activity [5, 6]. Here, thiowurtzine was administered in a single dose at 50–200 mg/kg (water-tween solvent) through an oral gavage one hour before experimental manipulations. The reference drugs were diclofenac sodium (Hemoharm, Russia) administered through gavage in a preventive single dose of 10 mg/kg dissolved in 1% starch mucilage in a volume of 0.2 mL/mouse, and ketorolac (Dr. Reddy's Laboratories Ltd., India) in a dose of 6 mg/kg with the same solvent, administration volume and route. The used doses of the reference drugs were equivalent to the mean therapeutic human dose. The animals of the negative control group received equivolumetric infusions of the water-tween solvent in the same regiment.

Formalin test. Formalin test, a chemogenic model of acute pain response, mimics pain reactions of different genesis (somatic traumas, burns, cuts, chemical injuries, surgical skin incisions) [7]. One of the mechanisms of the formalin nocigenic action is the activation of TRPA1 channels responding normally to cold and stimulating the development of thermal and mechanical hyperalgesia [8].

The animals were divided into 5 groups: I. Control, no treatment; II. Ketorolac, 6 mg/kg; III. Diclofenac, 10 mg/kg; IV. Thiowurtzine, 100 mg/kg; V. Thiowurtzine, 200 mg/kg. The test drug and the reference drugs were administered one hour before starting the tests. Hyperalgesia was simulated by subcutaneous injection of 20 μL/kg 2% aqueous formalin solution injected intraplantarily into the right hind paw pad after one hour. The pain response intensity in the first and second test phases were documented every second for the number and duration of behavioral patterns (flinches) of pain responses (licks, shakes) of the affected hind paw for 60 minutes. The pattern times were summated for each animal. The analgesic activity of the drugs was evaluated against the decreasing number of pain responses relative to the negative control, separately for phase I (initial 10 min after formalin injection) and phase II (from the 10th to the 60th minute following formalin injection) of the nociceptive response.

Capsaicin test. Examination of a new molecule for analgesic action in the selective test with a TRPV1 channel agonist is an essential step in exploring the specific pharmacological activity. This test helps evaluate how a compound influences the sensitivity of TRPV1 channels found basically in nociceptive neurons of the central and peripheral nervous systems [9].

The animals were divided into 5 groups: I. Control, no treatment; II. Ketorolac – 6 mg/kg; III. Thiowurtzine – 50 mg/kg; IV. Thiowurtzine – 100 mg/kg; V. Thiowurtzine – 200 mg/kg. The test drug and the reference drugs were administered one hour before starting the experiment. In an hour, a 10 μL capsaicin solution (3 μg/10 μL of 10% ethanol dissolved in 0.9% NaCl) was injected intraplantarily into the left hind paw. After injection, the paw was rubbed with ethanol to prevent capsaicin-induced skin irritation. Then, the time (latency period) to pass until response initiation (the mouse began violently shaking and licking the paw) was recorded. Afterwards, paw-lick patterns and total licking time were counted every second for 15 minutes for each mouse. The basic criteria of the drug efficacy were the total licking time and the pain reaction time.

Anti-inflammatory effect assessment. After the two tests were completed, the mice were euthanized, whereupon the both hind paws (inflamed and intact) were excised along the bone prominence below the junction of the splint bone and shin bone and above the talocalcaneal joint, and were weighed on an electronic analytical balance. The anti-inflammatory effect evaluated against the edema weight change was expressed as percentage to the control and was estimated by the appropriate formulae [10].

Statistical processing of the obtained results was performed by the variation statistics method using Statistica 6.0 software. For all the data, the mean value (X) and the standard error of the mean ($M \pm m$) were estimated, which are given in summary Tables 1, 2 together with the quantity n (number of variants in a group). Differences in the quantities under comparison were considered significant if the probability of their identity was below 5% ($p < 0.05$). Using sample coefficients of asymmetry and excess, the approximation degree of the distribution law of the test characteristic to the normal was evaluated. The non-parametric Mann – Whitney U-test was used for independent samples in the case of deviations in distributions of a characteristic from the normal. To reveal the reliability of differences in these qualitative characteristics, the Fisher transformation was used [10].

RESULTS

The modern experimental system including the nociceptive tests using electrical, thermal, mechanical, and chemical stimuli for pain modulation at different sensitivity levels can provide a range of anti-nociceptive characteristics of novel chemical entities and, in some ways, predict the nature of their analgesic action in humans [9, 11, 12].

The subcutaneous injection of formalin into the dorsal surface of the hind paw evoked a typical, biphasic, nociceptive behavioral response (Fig. 1), as evidenced by the score of pain reactions in the control mice: (30.8 ± 1.6) flinches in nociceptive phase I and (13.2 ± 2.6) in nociceptive phase II.

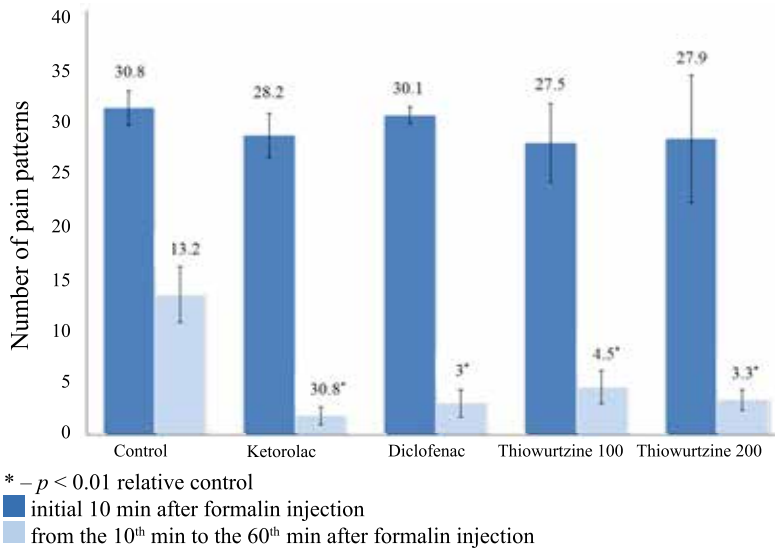

Fig. 1. Pain response in mice within 40–50 min after formalin injection

In the formalin test, which simulates a clinical model of both acute (phase I) and tonic pain (phase II), thiowurtzine exhibited an analgesic activity in the both phases [8]. In test phase I, thiowurtzine when administered as preventive single doses of 100 and 200 mg/kg via an intragastric gavage caused a statistically significant decrease in the number of initial pain reactions in the form of paw lifting, as compared to the control group; with that, no activity of the reference drugs diclofenac and ketorolac was noticed. Phase I of the formalin test characterizes acute pain in response to an injected chemical, and is mainly attributed to the direct activation of the thin unmyelinated C-fibers, most of which transmit impulses from the nociceptors;in our case, from the TRPA1 channels [7, 8, 9]. At this point of observation, thiowurtzine moderately limited the acute pain caused by the formalin-induced activation of the TRPA1 channels (Fig. 1).

In phase II of formalin-induced inflammation, thiowurtzine in doses of 100 and 200 mg/kg diminished the number of paw-lick behavioral responses typical for this test by 3.4 ($p < 0.05$) times and by 3.2 times

($p < 0.05$) as compared to the control group (Fig. 1). The analysis of the number of paw-shake patterns revealed that the test drug and the reference drugs had a similar analgesic activity. This reaction was not detected in animals which received 200 mg/kg thiowurtzine, while a 100 mg/kg dose resulted in a 5.3-fold decrease in shakes compared to the negative control, indicating a pronounced inhibition of nociceptive manifestations. The scores of pain reactions when thiowurtzine was administered in doses of 100 mg/kg (4.5 ± 1.6, $p < 0.01$) and 200 mg/kg (3.3 ± 1.0, $p < 0.01$) appeared to be similar to those of the reference drugs ketorolac (1.8 ± 0.8, $p < 0.01$) and diclofenac (3.0 ± 1.3, $p < 0.01$) in terms of formalin hyperalgesia severity.

By examining the anti-inflammatory action of thiowurtzine in phase II of nociceptive behavior, its statistically significant effect at a dose of 100 mg/kg was detected. By the reduced paw inflammatory swelling, a 200 mg/kg thiowurtzine dose (26%) was commensurable with diclofenac sodium (32%) and superior to ketorolac (14%) (Table 1).

Table 1

Indicators of anti-inflammatory action of thiowurtzine in formalin test in outbred male CD1 stock mice

Test group, dose (mg/kg), (number of animals)	Paw swelling, $M \pm m$, %	Paw swelling inhibition, %
Control, water-tween solvent ($n = 10$)	48.0 ± 2.5	–
Ketorolac, 6 ($n = 10$)	41.2 ± 4.8*	14
Diclofenac, 10 ($n = 10$)	32.8 ± 1.5*	32
Thiowurtzine, 100 ($n = 10$)	41.2 ± 2.2*	14
Thiowurtzine, 200 ($n = 10$)	35.4 ± 3.2*	26

* $p_U < 0.05$.

In test phase II, thiowurtzine diminished the tonic pain intensity due to the reduced inflammation (Table 1) in the peripheral tissues, and due to a possible change in the neuronal function of the dorsal horns of the spinal cord where the neurons of ascending pain pathways are located. The formalin test has a quite high prognostic significance when the action mechanism of novel potential analgesics are examined, as far as the opioid analgesics are known to block the both nociceptive phases, while non-steroid anti-inflammatory agents inhibit only the second phase, while local anesthetics suppress only the first phase [7, 8, 10].

The biphasic behavioral responses of the mice groups, which received thiowurtzine, do not allow for the unambiguous conclusion about the direction of the thiowurtzine action mechanism. Even though thiowurtzine exhibited a moderate anti-nociceptive effect in phase I wherein the reference drugs of the nonsteroidal anti-inflammatory group showed no activity, it effectively blocked the pain response in animals in phase II. That being said, the pain response level in phase II, judging from the shortened licking time in the thiowurtzine groups, turned out to be comparable with anti-nociceptive activities of ketorolac and diclofenac. Besides, the earlier detected naloxone-sensitive analgesia of thiowurtzine does not preclude possible involvement of opioidergic system in its antinociceptive activity in the both test phases [5]. The obtained results altogether necessitate further research in other nociceptive models.

The intraplantarily injected capsaicin solution evoked a marked nociceptive behavioral response manifested as paw licking and shaking in the control mice group. With that, all the indicators of pain reaction development and behavioral patterns were in agreement with the literature data (Table 2) and suggest that the model situation was reproduced (Table 2).

Table 2

Indicators of antinociceptive activity of thiowurtzine administered in a preventive single dose in the capsaicin test in male CBA mouse stock, $M \pm m$

Animal group, drug dose, (number of animals)	Pain reaction latency time, sec	Counts		Total licking time, sec	Pain reaction time, sec
		Licks	Shakes		
Control, purified water, ($n = 8$)	8.8 ± 1.8	9.4 ± 1.6	5.6 ± 1.3	86.6 ± 20.6	820.0 ± 31.1
Ketorolac, 6 mg/kg ($n = 10$)	25.1 ± 7.1*	5.0 ± 0.9*	1.6 ± 0.5*	38.4 ± 13.0	347.6 ± 79.6*
Thiowurtzine, 50 mg/kg ($n = 10$)	62.8 ± 21.6*	8.7 ± 2.0	2.6 ± 1.0	82.0 ± 35.1	579.4 ± 57.9*
Thiowurtzine, 100 mg/kg ($n = 9$)	18.7 ± 5.0*	6.3 ± 0.9	1.4 ± 0.4**	30.4 ± 10.2**	421.4 ± 75.0*
Thiowurtzine, 200 mg/kg ($n = 10$)	61.2 ± 20.1**	5,2 ± 1.2*	1.6 ± 0.7*	20.6 ± 5.0**	326.6 ± 86.4*

* $p_U < 0.05$; ** $p_U < 0.01$ relative to the negative control.

As one should expect, ketorolac evoked a significant decrease in pain reaction severity in male CBA mice: pain response latency period increased by 2.9 times ($p < 0.05$), paw licks declined by 1.9 times ($p < 0.05$) and paw shakes declined by 3.5 times ($p < 0.05$) compared to the control group (Table 2). It should be noted that the pain reaction time shortened by 2.4 times ($p < 0.01$). The results given above are consisted with the literature data on expressiveness of ketorolac analgesic effect.

The analysis of the results for the thiowurtzine groups allows for the conclusion of its prominent dose-dependent analgesic effect. With that, no statistically significant differences from the ketorolac group were detected. For instance, when thiowurtzine was administered in a 50 mg/kg dose, the pain response latency time was noticed to increase by a factor of 7.1 ($p < 0.05$) compared to the control group and by a factor of 1.7 compared to the ketorolac group. Based on the overall data obtained, the pain response time shortened by 1.4 times ($p < 0.05$) relative to the negative control.

The pronounced analgesic activity of thiowurtzine at 100 mg/kg manifested itself as a statistically significant increase in pain response latency, a decrease in paw shakes by 4.0 times ($p < 0.01$), a decrease in total licking time by 2.8 times ($p < 0.01$), and a decrease in pain response time by 1.9 times relative to the corresponding indicators of the control group.

In case thiowurtzine was dosed at 200 mg/kg, the difference in all test indicators was statistically significant between this group and the control group. For instance, the pain response latency increased by 7.0 times ($p < 0.05$) and paw licks and shakes decreased by 1.8 times ($p < 0.05$) and 3.5 times ($p < 0.01$), respectively, with total licking time being reduced by 4.2 times ($P < 0.01$) and pain response time being reduced by 2.5 times ($p < 0.01$) compared to the negative control. The mechanism of pain reaction development is associated with ion channels of nociceptors in tissues when exposed to chemical and mechanical injury. A capsaicin injection, a direct agonist of TRPV1 channels, can successfully provoke such an injury [9].

The findings obtained herein indicate that the test compound blocked pain progress in capsaicin-injected mice, at that the observed analgesic effect was dose-dependent, reached its maximum when thiowurtzine was dosed at 200 mg/kg, and was commensurable with the ketorolac effect.

The TRP ion channel family whose discovery was an important step in exploring the nature of pain sensation at the molecular level is currently considered as the pharmacologically most urgent biotargets of the human nervous system for analgesia [13–16]. Searching for modulators and agonists of TRP ion channels and designing high-efficacy analgesics with minimum side effects on their basis is among the priority focal areas of research labs around the world [13, 16]. The discovered properties of thiowurtzine actualize further development of unique thiowurtzine-based drugs intended for therapy of acute and moderate pain of different genesis. The pronounced anti-nociceptive activity of thiowurtzine even one hour post injection suggests a potential use of thiowurtzine-based drugs to alleviate pain syndrome in extreme cases.

CONCLUSION

Thiowurtzine when administered in a preventive single *per os* dose of 100 and 200 mg/kg was found to effectively block nociceptive reactions caused by activation of TRPA1 and TRPV1 ion channels. That being said, the thiowurtzine analgesic activity turned out to be comparable and/or superior to ketorolac and diclofenac, depending on the model situation. Besides, thiowurtzine (200 mg/kg *per os*) was found to be equivalent to diclofenac sodium (10 mg/kg *per os*) and superior in anti-inflammatory expressiveness to ketorolac (6 mg/kg *per os*) in the formalin test. The test results can assert that the pronounced anti-nociceptive action of the innovative compound in the capsaicin and formalin tests is due to the interaction with the TRPV1 and TRPA biotargets.

Moreover, all the data obtained previously may indicate that the activity modulation of TRP ion channels is one of the mechanisms of thiowurtzine's analgesic action. By the combination of the revealed key characteristics typical of an analgesic, thiowurtzine is a unique chemical entity with a high therapeutic and innovation potential.

REFERENCES

1. Sosnov A.V., Sadovnikov S.V., Semchenko F.M., Rufanov K.A., Tohmahchi V.N., Sosnova A.A., Tjurin I.A. Strong non-narcotic analgesics as a direction of pharmaceutical development. *Development and Registration of Medicines.* 2016; 14 (1): 196–206 (in Russ.).
2. Mihajlova A.S. Clinician's analgesic arsenal. *Farmateka.* 2018; (3): 50–56 (in Russ.).
3. Cawich S.O., Deonarine U., Harding H.E., Dan D., Naraynsingh V. Cannabis and postoperative analgesia: handbook of cannabis and related pathologies.

Biology, Pharmacology, Diagnosis, and Treatment. 2017; 450–458. DOI: 10.1016/B978-0-12-800756-3.00052-1.
4. Sysolyatin S.V., Kalashnikov A.I., Malykhin V.V. Reductive debenzelation of 2,4,6,8,10,12 – hexaazaisowurtzitan. *International Journal of Energetic Materials and Chemical Propulsion*. 2010; 9 (4): 365. DOI: 10.1615/IntJEnergeticMaterialsChemProp.
5. Krylova S.G., Povet'eva T.N., Zueva E.P., Suslov N.I., Amosova E.N., Razina T.G., Lopatina K.A., Rybalkina O.Yu., Nesterova Yu.V., Afanas'eva O.G., Kiseleva E.A., Sysolyatin S.V., Kulagina D.A., Zhdanov V.V. Analgesic activity of hexaazaisowurtzitane Derivatives. *Bulletin of Experimental Biology and Medicine.* 2019; 166 (4): 461–465. DOI: 10.1007/s10517-019-04372-9.
6. Lopatina K.A., Krylova S.G., Zueva E.P., Safonova E.A., Razina T.G., Rybalkina O.Ju., Povet'eva T.N., Suslov N.I., Kulagina D.A., Minakova M.Ju., Sysoljatin S.V. Study of the action mechanism of a new analgesic derivative of hexaazaisowurtzitane: effects of inflammatory mediators. *Russian Journal of Pain.* 2018; 58 (4): 68–72 (in Russ.). DOI: 10.25731/RASP.2018.04.031.
7. McNamara C.R., Mandel-Brehm J., Bautista D.M., Siemens J., Deranian K.L, Zhao M., Hayward N.J., Chong J.A., Julius D., Moran M.M., Fanger C.M. TRPA1 mediates formalin-induced pain. *Proceedings of the National Academy of Sciences of the United States of America*. 2007; 104(33):13525–13530. DOI: 10.1073/pnas.0705924104.8.
8. Tjølsen A., Berge O.G., Hunskaar S. Roslandet J. H., Hole K. The formalin test: an evaluation of the method. *Pain;* 1992: 51 (1). DOI: 10.1016/0304-3959(92)90003-T.
9. Bondarenko D.A., D'jachenko I.A., Skobcov D.I., Murashev A.N. *In vivo* models of studying of analgetic activity. *Biomedicina.* 2011; 2: 84–94 (in Russ.)
10. Mironov A.N. Preclinical drug research guide. Moscow: Grif i K. Publ., 2013:944 (in Russ.)
11. Rice A.S., Cimino-Brown D., Eisenach J.C., Kontinen V.K., Lacroix-Fralish M.L., Machin I.; Preclinical Pain Consortium, Mogil J.S., Stöhr T. Animal models and the prediction of efficacy in clinical trials of analgesic drugs: a critical appraisal and call for uniform reporting standards. *Pain*. 2008; 139: 243–247. DOI: 10.1016/j.pain.2008.08.017.
12. Barrot M. Tests and models of nociception and pain in rodents. *Neuroscience*. 2012; 211: 39–50. DOI: 10.1016/j.neuroscience.2011.12.041.
13. Lee L.Y., Hsu C.C., Lin Y.J. Lin RL, Khosravi M. Interaction between TRPA1 and TRPV1: Synergy on pulmonary sensory nerves. *Pulmonary Pharmacology & Therapeutics.* 2015; 35: 87–93. DOI: 10.1016/j.pupt.2015.08.003.
14. Gaudet R. TRP channels entering the structural era. *J. Physiol.* 2008; 586 (15): 3565–3575. DOI: 10.1113/jphysiol.2008.155812.
15. Full-spectral multiplexing of bioluminescence resonance energy transfer in three TRPV channels. *Biophysical Journal*. 2017; 112: 87–98. DOI: 10.1016/j.bpj.2016.11.3197.
16. Weyer-Menkhoff I., Lötsch J. Human pharmacological approaches to TRP-ion-channel-based analgesic drug development. *Drug Discovery* 2018; 23 (12): 2003–2012. DOI: 10.1016/j.drudis.2018.06.020.

Authors contribution

Krylova S.G. – development of the concept and design of experiments, experimentation, critical revision for important intellectual content. Lopatina K.A. – arrangement and experimentation, statistical analysis, writing. Zueva E.P. – substantiation of the manuscript and critical revision for important intellectual content. Safonova E.A. – experimentation. Povet'eva T.N. – conceptualization, experimental design, experimentation. Suslov N.I. – critical revision for important intellectual content. Nesterova Yu.V. – experimentation, statistical analysis. Afanas'eva O.G. – experimentation. Kul'pin P.V. – experimentation. Sysolyatin S.V. – synthesis of thiowurtzine. Kulagina D.A. – synthesis and provision of thiowurtzine. Zhdanov V.V. – analysis of pharmacological activity prediction results, final approval of the manuscript for publication.

Authors information

Krylova Svetlana G., Dr. Sci. (Biology), Senior Researcher of the Oncopharmacology Laboratory, GRIP&RM, Tomsk NRMC, RAS, Tomsk, Russian Federation. ORCID 0000-0003-0249-1395.

Lopatina Kseniya A., Cand. Sci. (Med.), Researcher of the Oncopharmacology Laboratory, GRIP&RM, Tomsk NRMC, RAS, Tomsk, Russian Federation. ORCID 0000-0003-4445-4859.

Zueva Elena P., Dr. Sci. (Biology), Professor, Head of the Oncopharmacology Laboratory, GRIP&RM, Tomsk NRMC, RAS, Tomsk, Russian Federation. ORCID 0000-0002-6480-6770.

Safonova Elena A., Cand. Sci. (Med.), Researcher of the Oncopharmacology Laboratory, GRIP&RM, Tomsk NRMC, RAS, Tomsk, Russian Federation. ORCID 0000-0002-0685-4192.

Poveteva Tatyana N., Dr. Sci. (Med.), Professor, Senior Researcher of Phytopharmacology and Special Nutrition Laboratory, GRIP&RM, Tomsk NRMC, RAS, Tomsk, Russian Federation. ORCID 0000-0001-8644-489X.

Nesterova Yuliya V., Cand. Sci. (Med.), Researcher of Phytopharmacology and Special Nutrition Laboratory, GRIP&RM, Tomsk NRMC, RAS, Tomsk, Russian Federation. ORCID 0000-0002-1382-926X.

Afanas'eva Olga G., Cand. Sci. (Biology), Researcher of Phytopharmacology and Special Nutrition Laboratory, GRIP&RM, Tomsk NRMC, RAS, Tomsk, Russian Federation. ORCID 0000-0002-7374-5586.

Kul'pin Pavel V., Junior Researcher Phytopharmacology and Special Nutrition Laboratory, GRIP&RM, Tomsk NRMC, RAS, Tomsk, Russian Federation. ORCID 0000-0002-7993-5639.

Suslov Nikolaj I., Dr. Sci. (Med.), Professor, Head of Phytopharmacology and Special Nutrition Laboratory, GRIP&RM, Tomsk NRMC, RAS, Tomsk, Russian Federation. ORCID 0000-0002-7993-5639.

Kulagina Daria A., Cand. Sci. (Chem.), Junior Researcher Laboratory of Medicinal Chemistry, IPCET SB RAS, Biysk, Russian Federation. ORCID 0000-0002-4673-5817.

Sysolyatin Sergey V., Dr. Sci. (Chem.), Professor, Corresponding Member of the RAS, Director, IPCET SB RAS, Biysk, Russian Federation. ORCID 0000-0002-1405-171X.

Zhdanov Vadim V., Dr. Sci. (Med.), Professor, Corresponding Member of the RAS, Director of GRIP&RM, Tomsk NRMC, RAS, Tomsk, Russian Federation. ORCID 0000-0002-9516-0204.

(✉) **Krylova Svetlana G.,** krylova5935@gmail.com.

Received 07.02.2020
Accepted 29.09.2020

УДК 60:678:611.018.4.08
https://doi.org/10.20538/1682-0363-2020-4-119-129

Biodegradable polymer composites with osteogenic potential

Lebedev S.M.[1], Chistokhin D.M.[1], Shchadenko S.V. [1], Dzuman A.N.[2], Nikolaeva O.O.[3], Mitrichenko D.V.[3], Prosolov A.B.[3], Khlusov I.A.[1-4]

[1] National Research Tomsk Polytechnic University (NR TPU)
30, Lenina Av., Tomsk, 634050, Russian Federation

[2] Siberian State Medical University (SSMU)
2, Moscow Trakt, Tomsk, 634050, Russian Federation

[3] SINTEL Research and Production Company (RPC)
45, Gerzena Str., Tomsk, 634061, Russian Federation

[4] Immanuel Kant Baltic Federal University (IKBFU)
14, A. Nevskogo Str., Kaliningrad, 236041, Russian Federation

ABSTRACT

The aim was to study the basic physico-mechanical properties of hydroxyapatite (HA) composites (up to 25–50 wt%) with polylactide (PLA-HA) and poly(e-caprolactone) (PCL-HA) prepared by melt compounding, as well as the osteogenic potential of PLA-HA *in vivo*.

Materials and methods. All biodegradable polymer composites were prepared by hot melt compounding and studied by dielectric spectroscopy in frequency domain, optical microscopy, X-ray diffraction analysis and tensile tests. An ability of PLA-5 wt% HA composites prepared by 3D-printing to induce bone tissue growth *in vivo* was detected with the help of ectopic subcutaneous test in inbred mice.

Results. Values of the real part of complex permittivity of PLA-HA and PCL-HA composites are increased by 15–30% compared to those for initial PLA and PCL, while tand loss factor tanδ does not exceed 0.02 for PLA-based composites and 0.2 for PCL-based composites. The crystallinity degree of PLA-HA composites is increased by 3 and 6 times with an increase of HA content from 25 to 50 wt% respectively compared to the indicator for PLA. The crystallinity degree of PCL-HA composites with 25 wt% HA is increased by 2 times compared to the value for PCL. It is due to the fact that HA powder particles play the role of additional nucleation centers. For all this, mechanical strength of composites diminished statistically. Even lowest HA content (5 wt%) in PLA-HA composites prepared by 3D-printing increased the incidence of ectopic osteogenesis by 40%.

Conclusion. Designed biodegradable composites have a practical use potential for bone tissue engineering.

Key words: poly(lactic acid), poly(ε-caprolactone), hydroxyapatite, melt compounding, physicochemical properties, ectopic osteogenesis, *in vivo.*

Conflict of interest. The authors declare no obvious or potential conflict of interest related to the publication of this article.

Source of financing. The study was partially supported by the Council for Grants of the President of the Russian Federation for State Support of Leading Scientific Schools of the Russian Federation (Grant No. SS-2495.2020.7).

Conformity with the principles of ethics. The study was approved by the local Ethics Committee at Immanuel Kant Baltic Federal University, Kaliningrad (Protocol No. 7 of 09.12.2015).

✉ *Lebedev Sergey M.,* e-mail: lsm70@mail.ru.

For citation: Lebedev S.M., Chistokhin D.M., Shchadenko S.V., Dzuman A.N., Nikolaeva O.O., Mitrichenko D.V., Prosolov A.B., Khlusov I.A. Biodegradable polymer composites with osteogenic potential. *Bulletin of Siberian Medicine.* 2020; 19 (4): 119–129. https://doi.org/10.20538/1682-0363-2020-4-119-129.

Биоразлагаемые полимерные композиции с остеогенным потенциалом

Лебедев С.М.[1], Чистохин Д.М.[1], Щаденко С.В.[1], Дзюман А.Н.[2], Николаева О.О.[3], Митриченко Д.В.[3], Просолов А.Б.[3], Хлусов И.А.[1, 2, 3, 4]

[1] Национальный исследовательский Томский политехнический университет (НИ ТПУ)
Россия, 634050, г. Томск, пр. Ленина, 30

[2] Сибирский государственный медицинский университет (СибГМУ)
Россия, 634050, г. Томск, Московский тракт, 2

[3] Научно-производственная компания (НПК) «Синтел»
Россия, 634061, г. Томск, ул. Герцена, 45

[4] Балтийский федеральный университет (БФУ) им. И. Канта
Россия, 236041, г. Калининград, ул. А. Невского, 14

РЕЗЮМЕ

Цель. Исследование основных физико-механических свойств композитов гидроксиапатита (ГА) (до 25–50%) с полилактидом (ПЛА-ГА) и поли(ε-капролактоном) (ПКЛ-ГА), полученных методом смешения в расплаве, а также остеогенного потенциала ПЛА-ГА *in vivo.*

Материалы и методы. Все биоразлагаемые полимерные композиции изготовлены методом горячего компаундирования в расплаве, исследованы методами диэлектрической спектроскопии в частотном ходе, оптической микроскопии, рентгеноструктурного анализа и испытаний на растяжение. Способность композитов ПЛА-5% ГА, полученных методом 3D-печати, к *in vivo* индукции роста костной ткани изучена при помощи теста подкожного эктопического костеобразования на линейных мышах.

Результаты. Значения действительной составляющей комплексной диэлектрической проницаемости композиций ПЛА-ГА и ПКЛ-ГА увеличиваются на 15–30% по сравнению с исходными ПЛА и ПКЛ, при этом тангенс угла потерь не превышает 0,02 для композиций на основе ПЛА и 0,2 – для композиций на основе ПКЛ. Степень кристалличности для композиций ПЛА-ГА, по сравнению с показателем для ПЛА, увеличивается в 3 и 6 раз при повышении содержания ГА с 25 до 50% соответственно. Для композиции ПКЛ-ГА при 25% ГА степень кристалличности увеличивается в 2 раза по отношению к значению для ПКЛ. Это обусловлено тем, что частицы порошка ГА играют роль дополнительных центров кристаллизации. При этом статистически значимо снижается прочность композитов на разрыв. Композиты ПЛА, полученные методом 3D-печати, даже с низким (5%) содержанием ГА на 40% повышают результаты эктопического остеогенеза.

Заключение. Разработанные биоразлагаемые композиции имеют потенциал практического применения в приложении к биоинженерии костной ткани.

Ключевые слова: полилактид, поли(ε-капролактон), гидроксиапатит, компаундирование в расплаве, физико-механические свойства, эктопический остеогенез, *in vivo.*

Конфликт интересов. Авторы декларируют об отсутствии явных и потенциальных конфликтов интересов, связанных с публикацией настоящей статьи.

Источник финансирования. Исследование частично выполнено при финансовой поддержке Совета по грантам Президента Российской Федерации по государственной поддержке ведущих научных школ Российской Федерации (грант № НШ-2495.2020.7).

Соответствие принципам этики. Исследование одобрено локальным этическим комитетом Инновационного парка Балтийского федерального университета им. И. Канта, г. Калининград (протокол № 7 от 09.12.2015).

Для цитирования: Лебедев С.М., Чистохин Д.М., Щаденко С.В., Дзюман А.Н., Николаева О.О., Митриченко Д.В., Просолов А.Б., Хлусов И.А. Биоразлагаемые полимерные композиции с остеогенным потенциалом. *Бюллетень сибирской медицины.* 2020; 19 (4): 119–129. https://doi.org/10.20538/1682-0363-2020-4-119-129.

INTRODUCTION

Biodegradable polymers such as poly(lactic acid) (PLA) and poly(ε-caprolactone) (PCL) are used extensively in the field of biomedical applications. In this case, biodegradable polymers are used as polymer scaffolds to assist tissue and cell growth during the bone tissue regeneration, and for drug delivery, when drugs are mixed with polymer matrix and they are gradually released as the polymer is dissolved in the body [1–8]. PLA and PCL can be degraded by microorganisms under environment conditions. In addition, PCL is susceptible to both alkaline and enzymatic hydrolysis [9–10].

Conventional single-phase polymer materials do not always meet the essential requirements of regenerative medicine therefore there is a great need to design multi-phase composites with properties similar to that of natural bone. For instance, poly(lactic acid) has a good biodegradability, however it has a very low elongation at break and brittleness limits its usage. On the other hand, poly(ε-caprolactone) has a higher elongation at break, while its degradability rate is lower than for PLA. Various organic and inorganic fillers are used to improve the properties of biodegradable composites such as mechanical properties, water uptake, degradability rate, and biocompatibility, making these materials suitable for use in the field of biomedicine. Carbon nanotubes (CNT) and carbon fibers (CF), derivatives of graphite, graphene, layered silicates, ferroelectric and piezoelectric ceramics powders, and hydroxyapatite (HA) are often used as fillers with required properties in such multi-phase biodegradable composites [7, 11–18].

For example, in [19–21], the authors showed the effectiveness of "Osteomatrix" biocomposite material, consisting of natural hydroxyapatites, aminoglycans, and collagens, for bone tissue regeneration. Defects in damaged bones were filled with "Osteomatrix" biocomposite material in the form of powder, pellets or blocks, which significantly reduced the formation time of a new bone tissue in patients.

Numerous authors have demonstrated that the addition of HA into PLA or PCL matrices can improve both biocompatibility and mechanical properties of polymer-ceramic composites because hydroxyapatite has the most similar chemical composition to human bone [1, 22–32]. Akindoyo et al. [23] reported that adding HA into PLA allows for better cell attachment and proliferation to the PLA-matrix. Adding the biostrong impact modifier (BSIM) into PLA-HA composites results in increase of impact strength, tensile and flexural properties at 5 wt% BSIM content.

Russias et al. [28] observed that PLA-based composites filled with either a fine-grained powder (average particle size – 5 μm) or larger whiskers (25–30 μm long and 5 μm in diameter) of hydroxyapatite with about 70–85 wt.% ceramic contents can be used to prepare scaffolds with mechanical properties close to those of human cortical bone.

Zhang et al. [31] showed that PLA-HA composites improve interfacial adhesion and the bending strength. Furthermore, these composites can be processed by 3D-printing [30, 31]. Shen et al. [32] reported that PLA-based biocomposites filled with HA and carbon fiber (CF) (PLA-HA-CF) were manufactured of PLA-HA-CF prepreg by hot pressing. PLA-HA-CF prepreg was prepared by mixing components in solution. They have found that biocomposites have excellent mechanical properties, for example, flexural strength, flexural modulus and shear strength reach 430 MPa, 22 GPa, 212 MPa, respectively. Water uptake of PLA-HA-CF biocomposites increased up to 5%, while the rate of mass loss was only 1.6%. After *in vitro* degradation for 3 months, the pH value of phosphate buffer solution decreases by less than 0.1, indicating that the alkaline of HA neutralizes the acid formed following the degradation of PLA by hydrolysis, which prevents the harm of acidity for the patient's body. Park et al. [33], Kim et al. [34] and Jiang et al. [35] demonstrated that the PCL-HA composites can be successfully applied to manufacture biodegradable scaffolds by 3D-printing for bone tissue engineering.

However, the majority of PLA-HA and PCL-HA composites were prepared by mixing in solution, but even for these composites, studies of the main properties are episodic in nature.

The aim of this work was to study the basic physico-mechanical properties of PLA-HA and PCL-HA

composites obtained by melt compounding, as well as *in vivo* osteogenic potential of PLA-HA composites.

MATERIALS AND METHODS

Biodegradable poly(lactic acid) (PLA, Ingeo 4043D, NatureWorks LLC, USA) and poly(ε-caprolactone) (PCL, purchased from Sigma-Aldrich, USA) were used in this work as polymer matrices. Powder of hydroxyapatite (HA) produced by mechanochemical method [36] provided by Sintel RPC LLC (Tomsk, Russia) was used as filler. All materials were used as received without an additional treatment. The filler content (*C*) in polymer composites was changed from 0 to 50 wt%. All composites were prepared by melt compounding in a measuring mixer 50 EHT (Brabender, Germany). Mixing time and processing temperature were 10 min and 190–210 °C for PLA-based composites and 80–100 °C for PCL-based composites respectively. The speed of counter-rotating blades of the mixer was changed from 30 to 90 rpm as shown in Fig. 1. Filler was gradually introduced into the polymer melt up to the required fraction, while mixing until all fillers were evenly distributed in the polymer matrix. After preparation, all composites were granulated with the granulator (Brabender, Germany).

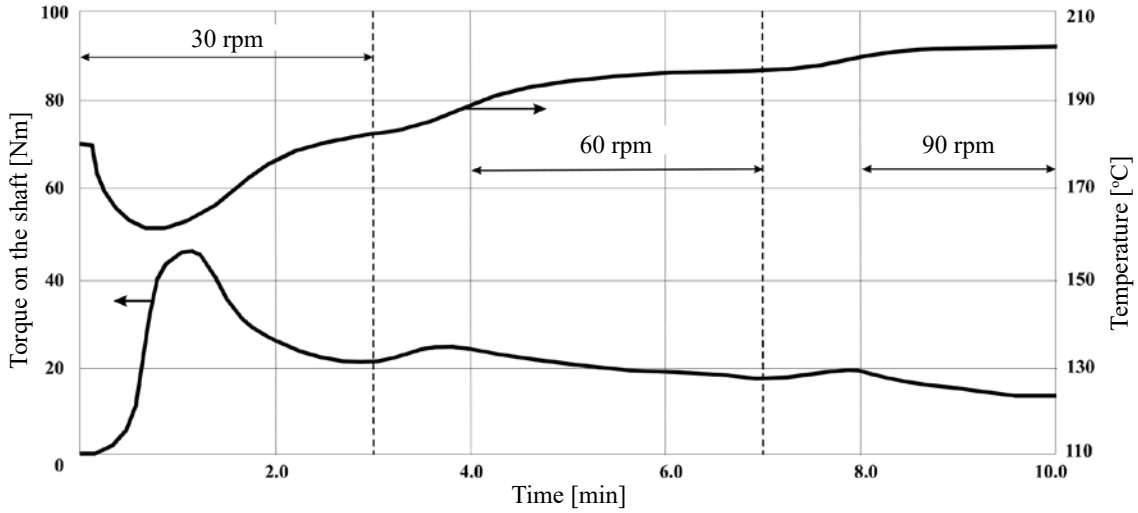

Fig. 1. Temporal diagrams of the melt temperature and torque on the agitator shaft for PLA-based composite

To prepare the samples with dimensions of 65 × 85 × (0.05–1.0) mm by hot pressing, compression molds filled with polymer composite pellets were placed into a vacuum furnace heated to 200 °C (for PLA-based composites) and to 100 °C (for PCL-based composites) for 3 hours. After that, compression molds were pressed in a hydraulic press at 20 MPa for 20 minutes. Then, the compression molds were cooled at a cooling rate of 4°C / min to ambient temperature under pressure in air.

Measurements of the ε′ real part of the $\varepsilon^*(f) = \varepsilon'(f) - \varepsilon''(f)$complex permittivity and the $\tan\delta = \varepsilon''(f)/\varepsilon'(f)$ loss factor, where ε″ is the imaginary part of the complex permittivity; $\delta = 90° - \varphi$ is the loss factor angle; and φ is the angle between voltage and current, were carried out under 3V AC voltage in the frequency range from 1 to 10^5 Hz using a "Solartron Analytical" instrument (Great Britain). From seven to ten measurements per decade in the entire investigated frequency range were carried out for all samples. Not less than three samples for each material were tested.

The morphology of developed composites, shape and dimensions of filler powder particles were studied by an optical microscopy (OM). The thickness of samples for the OM study was 50 μm.

The study of crystalline structure of polymer matrices and composites was carried out by wide angle X-ray diffraction method (XRD) by means of the "Shimadzu XRD-7000" diffractometer (CuK_α radiation λ = 1,54 Å) at an accelerating voltage on an X-ray tube of 40 kV and current of 30 mA, in the angle range of 2θ = 5–90°.

The mechanical properties of the developed polymer composites were studied using an "Instron 3345" universal tensile testing machine (USA). The elastic modulus, elongation at break, and tensile strength for all tested samples were determined from the experimentally obtained stress-strain curves.

To estimate the bioengineering potential of PLA-HA composites, three-dimensional (3D) samples prepared of 95 wt% PLA + 5 wt% HA composite were prepared in the form of disks (11 mm in diameter and 1.2 mm thick) by computer-aided design in Blender software with open source code and subsequent layer-by-layer deposition of filaments (diameter 1.75 mm) using a CreatBot Duo 3D printer (CreatBot 3D Printer, PRC) as described previously [37]. Samples prepared of pure PLA were used as control ones. To improve the bone marrow adhesion to the surface of samples, one of sample surfaces was textured with 0.3–0.5 mm wide grooves.

One of the modern methods to determine the osteogenic properties of materials and products is the ectopic (heterotopic) subcutaneous test, which makes it possible to evaluate the *in vivo* induction of differentiation of mesenchymal stem cells into osteoblasts [38].

The experiments were carried out in compliance with the principles of humane treatment of laboratory animals in accordance with the "Rules for the use of experimental animals" (Appendix to the order of the Ministry of Health of USSR No. 755 dated 12.08.1977). Animals were kept according to RD-APK 3.10.07.02-09. Drinking water was supplied to laboratory animals from the water supply system; water quality was in accordance with SanPiN 2.1.4.1074-01 (Russia). Animals were kept under artificial and natural light in accordance with the requirements of SNiP 23.05-95 (Russia).

BALB/c inbred mice were anesthetized and operated under sterile conditions. The skin was sterilized with 70% ethanol, samples with syngeneic bone marrow from femur were implanted into the lateral subcutis pockets of the venter, and the wound was sutured and treated with 70% ethanol. The procedure was described previously [39]. The bone marrow of an adult organism is the central pool and the source of mesenchymal stem cells (MSCs) [40].

Forty days later, the animals were sacrificed via CO_2 asphyxiation, and the status of the tissues around the implants was assessed. The implants were removed together with the adjacent soft tissues (tissue plates) on the "working" (textured) surface of the samples. Standard histological technique for preparing thin sections of fixed tissue lamellae and their hematoxylin and eosin staining was used [39]. Six implants were tested in both the control and experimental groups. A formation of bone and/or bone tissue with marrow in the tissue lamellae was considered as a positive result.

The ability of implants to induce bone growth was calculated as the percentage of test samples promoting the induction of bone tissue growth (IBT) with or without bone marrow in the tissue plate per the total number of implanted samples according to the formula: IBT (%) = $[N_2/N_1] \times 100\%$, where N_1 is the number of implanted samples; N_2 is the number of samples on which bone tissue growth was detected.

Statistical analyses were conducted using the STATISTICA 13.3 software package for Windows. The normality of the data distribution was defined by the Kolmogorov – Smirnov test. The mean and mean error ($M \pm m$), median and Me (Q_1–Q_3) interquartile range were calculated. To assess the statistical significance of differences, in the event that the distribution of data does not correspond to the normal distribution law, the nonparametric Mann – Whitney test was used. Statistically significant differences were considered at $p < 0.05$.

RESULTS AND DISCUSSION

The results of dielectric spectroscopy in frequency domain are presented in Fig. 2. It is obvious that frequency dependencies of $\varepsilon'(f)$ for polymer composites exhibit typical behavior: the $\varepsilon'(f)$ is monotonically decreased with frequency for both polymer matrices and composites based on them. When filling PLA with HA powder, the permittivity of PLA + 25 wt% HA composite is increased by about 12–15% compared to the initial PLA over the frequency range studied due to the higher permittivity of HA, which is about 4–9 [41]. Increase in the permittivity of PLA + 50 wt% HA composite is 23–32% compared to the initial PLA. Increase in the permittivity of PCL + 25 wt% HA composite is 1–4% compared to the initial PCL. Tan$\delta(f)$ loss factor over the studied frequency range for PLA-based composites does not exceed 0.02, while for PCL-based composites it does not exceed 0.2.

The results of OM are shown in Fig. 3. However, the filler particles form agglomerates sized around 100 μm, which are visible both for initial HA powder (Fig. 3,*a*) and for composite with filler content 25 wt% (Fig. 3,*b*). It can be seen that filler particles are quasi-uniformly distributed in the polymer matrix. Decrease in the average size of filler agglomerates for the composite with 50 wt% HA (Fig. 3,*c*) compared to that for composite PLA + 25 wt% HA is explained by de-agglomeration of filler powder particles during compounding due to an increase in the stiffness of composites.

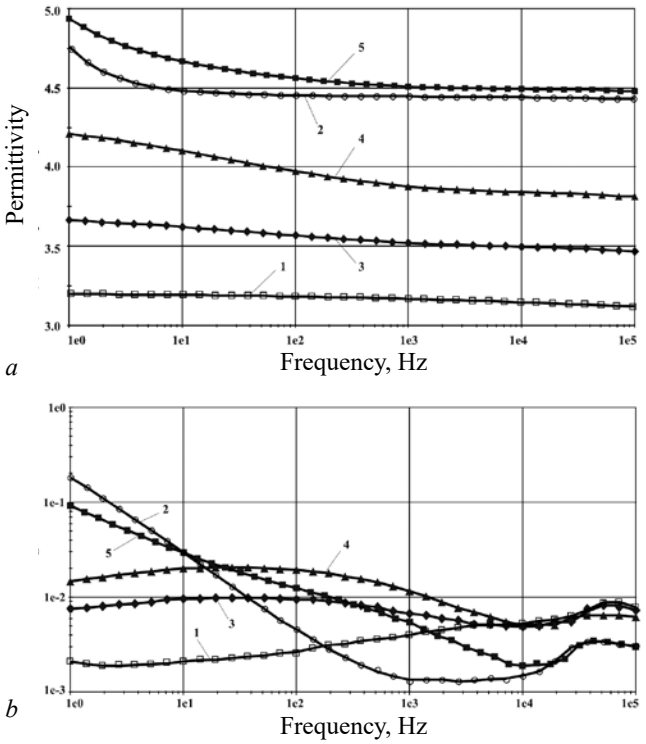

Fig. 2. Frequency dependencies of the real part of complex permittivity (relative units) (*a*) and tanδ (*b*) for: 1 – PLA; 2 – PLA+25% HA; 3 – PLA+50% HA; 4 – PCL; and 5 – PCL+25% HA

X-ray diffraction data (X-ray diffraction analysis, or XRD) for polymer matrices (PLA and PCL) and composites (PLA+HA and PCL+HA) are shown in Fig. 4. These results indicate that for PLA broad diffraction peak around 2Q » 16.2° due to reflections from (200) or (110) crystallographic planes is observed (Fig. 4,*a*). On the other hand, peaks around 26.12°, 29.16°, 32°, 40°, 46.9°, and 49.7° observed for PLA-HA composites are attributed to the characteristic diffractions peaks of HA (Fig. 4,*b* and 4,*c*) due to reflections from (002), (210), (211), (310), (222) and (213) crystallographic planes.

For initial PCL two strong reflections at 2Q » 21.4°, and 23.7°, corresponding to the (110) and (200) crystallographic planes of the PCL crystalline form are observed (Fig. 4,*d*). The characteristic peaks around 26.12°, 29.16°, 32°, 40°, 46.9°, and 49.7° for PCL-HA composites are due to the HA presence (Fig. 4,*e*), as well as for PLA-HA composites.

The degree of crystallinity for the used polymer matrices and composites based on them are listed in Table 1.

It can be seen that the crystallinity degree of PLA-HA composites is increased by 3 and 6 times for PLA + 25 wt% HA and PLA + 50 wt% HA composites, respectively, compared with the initial PLA.

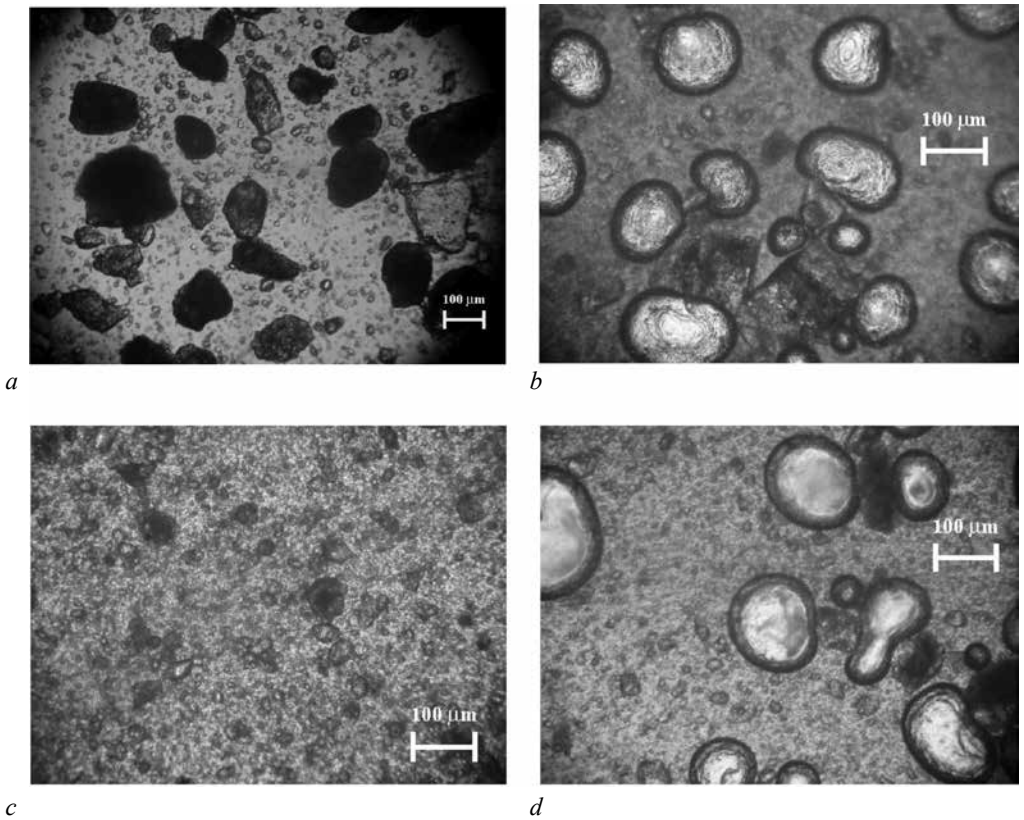

Fig. 3. OM micrographs of the HA filler powder (*a*) and PLA-HA composites: *b* – 25 wt% HA, *c* – 50 wt% HA, and *d* – PCL-HA composite with 25 wt% HA

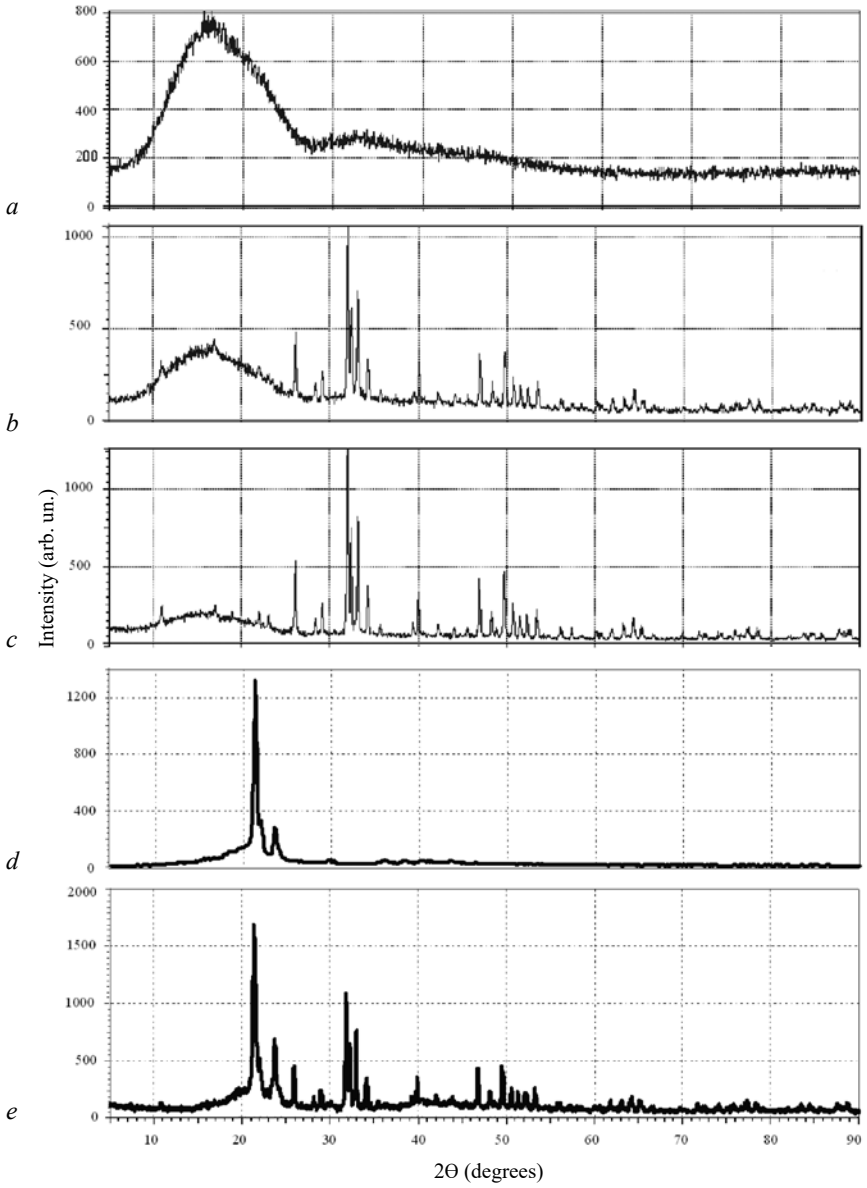

Fig. 4. XRD patterns (*a*) initial PLA; *b* – PLA-HA composite with 25 wt% HA; *c* – PLA-HA composite with 50 wt% HA; *d* – initial PCL; and *e* – PCL-HA composite with 25 wt% HA

Table 1

The degree of crystallinity of polymer matrices and composites, $M \pm m$

Material	PLA	PLA + 25 wt% HA	PLA + 50 wt% HA	PCL	PCL + 25 wt% HA
The degree of crystallinity, %	11.6 ± 0.35	37.9 ± 1.14	71.45 ± 2.14	34.7 ± 1.04	75.53 ± 2.27

The crystallinity degree of PCL + 25 wt% HA composite is increased by 2 times compared to the initial PCL. When polymer matrix is filled with HA powder, the filler particles act as an additional nucleating agent for the polymer matrix resulting in the increase of the crystallinity degree of polymer composites.

Fig. 5 demonstrates the results of tensile tests. It is seen that the addition of HA to the PLA results in a decrease in elongation and tensile strength, and only for the Young's modulus there is a tendency to increase with increasing HA content.

For PCL-based composites the changes in the studied mechanical properties are similar, with the only difference being that the values of the Young's modulus and tensile strength are significantly lower than those obtained for PLA-based composites, while the elongation for PLA-based composites is negligible compared to with PCL-based composites.

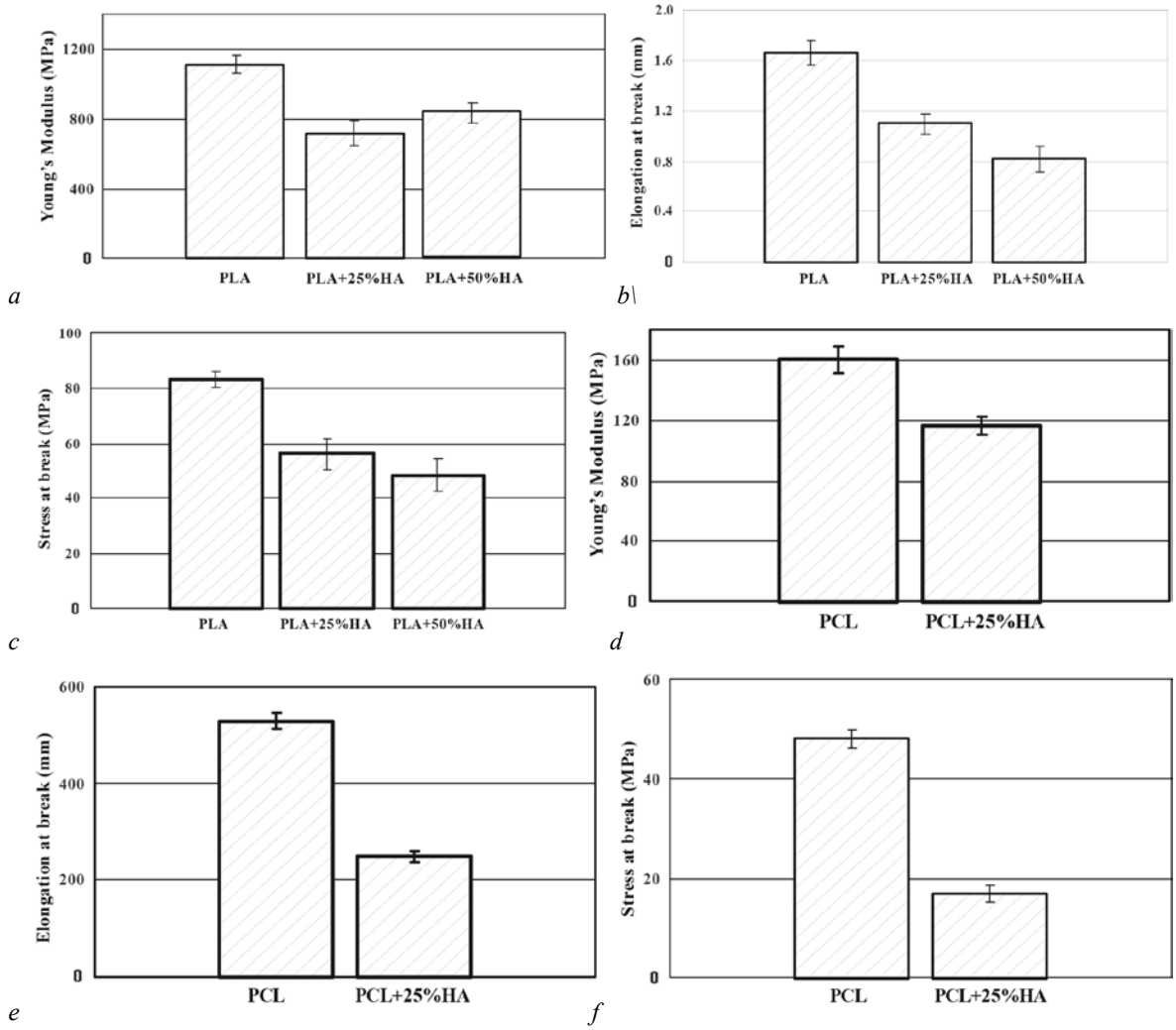

Fig. 5. The results of mechanical tests for PLA-based (*a*, *b*, *c*) and PCL-based (*d*, *e*, *f*) composites: *a*, and *d* – Young's modulus; *b* – and *e* – elongation at break; *c*, and *f* – tensile strength

Currently, biodegradable polymers and their composites are widely used in tissue bioengineering. PLA implants are one of the most popular products in clinical practice. PLA products are resorbable over time and are replaced by bone tissue, according to various authors, not earlier than 7 years after implantation [42]. It can lead to complications in the form of an inflammatory reaction to a foreign body [43]. In this regard, a development and biomedical testing of new technologies for the manufacture and modification of composites of (co)polymers and HA with controlled biodegradation are very relevant. However, at high HA content, the potential enhancement of the osteogenic properties of composites [44] is offset by a real decrease in their physicomechanical properties (Fig. 5).

During subcutaneous implantation, test materials experience a biomechanical load (shock, compression, and lateral displacement) resulting in simulated *in vivo* conditions to bone implantation. While PLA composites with a low HA content (5 wt%) were subcutaneously tested, after 40 days there were no macroscopic signs of implant destruction and inflammatory reaction (in particular, severe hyperemia of the recipient bed, and the presence of exudate). The disks were surrounded by a thin (less than 50 μm) connective tissue capsule, fixing them in the lateral subcutaneous pocket.

PLA and its composites promoted the conduction of grown tissues on the surface of the test samples. It was recorded by more than 3-fold increase in the area of tissue plates (Table 2). Histological evaluation of tissue lamellae showed induction of bone growth (IBT) as follows: 20% in the case of pure PLA samples; 60% in the case of PLA + 5 wt% HA composite scaffolds (Table 2).

Table 2

Sample effect on geometric and histological features of tissues grown from bone marrow under subcutaneous ectopic test in BALB/c mice, *Me* (Q_1–Q_3)

Test groups of samples, $n = 6$	Incidence of tissue lamella formation	IBT	Bone marrow (initial level before implantation)	Properties of tissue lamellae (after implantation)	
	%	%	Area, mm²	Area, % of bone marrow area	Histological compound
PLA	100	20	3.54 (3.49–3.72)	306 (217–504)	Bone with marrow (1 case); connective and fat tissues (4 cases)
PLA + 5 wt% HA	100	60	4.53 (3.89–4.87)	382 (327–443)	Membrane reticulated bone (2 cases); bone with marrow (1 case); connective tissue (2 cases)

Note: n – the number of test samples in each group; PLA – polylactide; PLA+5 wt% HA –hydroxyapatite (5 wt%) composite with polylactide.

Membrane reticulated bone, as well as the bone/bone marrow system formed *de novo* due to *in situ* remodeling of bone marrow applied *in vitro* were revealed on histological sections of tissue lamellae (Fig. 6).

Ectopic metaplasia of syngeneic bone marrow proceeds through the activation of a pool of donor MSCs differentiating into the precursors of chondro/osteoblasts. In turn, recipient hematopoietic stem cells repopulate the implantation site [45].

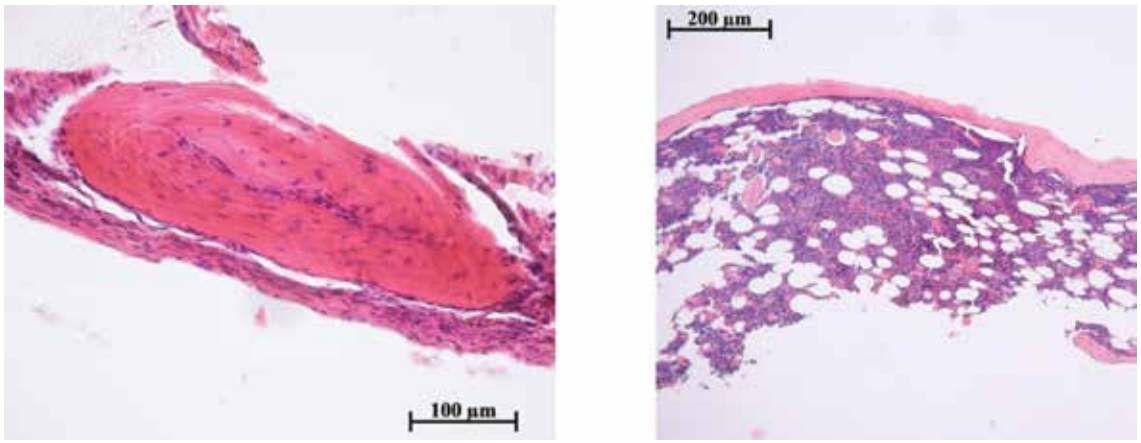

a *b*\

Fig. 6. The positive result examples of histological slices of tissue lamellae grown on PLA and PLA + 5 wt% HA samples after 40-day subcutaneous implantation: *a* – bone tissue, ×200; *b*) bone with marrow, ×100 hematoxylin-eosin staining

CONCLUSION

Biodegradable polymer PLA- and PCL-based composites filled with HA prepared by melt compounding were obtained, which allows introducing up to 25–50 wt% HA into polymer matrices. HA particles and their agglomerates with a diameter of up to 100 µm are uniformly distributed over the matrix volume, increasing the degree of surface polarization and crystallinity of composites. As a consequence of high crystallinity, the mechanical strength of the composites decreases with filling. Developed biodegradable composites can be used for practical application in various areas of regenerative medicine. In the field of bone tissue bioengineering, PLA composites obtained by 3D printing, even with a low (5 wt%) HA content, increase ectopic osteogenesis by 40%. It allows considering MSCs as a cellular target of their biological activity.

REFERENCES

1. Hutmacher D.W. Scaffolds in tissue engineering bone and cartilage. *Biomaterials*. 2000; 21 (24): 2529–2543. DOI: 10.1016/s0142-9612(00)00121-6.
2. Murariu M., Dubois P. PLA composites: from production to properties. *Adv. Drug Deliv. Rev*. 2016; 107: 17–46. DOI: 10.1016/j.addr.2016.04.003.
3. Langer R., Vacanti J.P. Tissue engineering. *Science*. 1993; 260: 920–926. DOI: 10.1126/science.8493529.
4. Gupta A.P., Kumar V. New emerging trends in synthetic biodegradable polymers – polylactide: a critique. *Europ. Polym.*

J. 2007; 43 (10): 4053–4074. DOI: 10.1016/J.EURPOLYMJ.2007.06.045.
5. Jorge P., Domingos M., Gloria A., Ciurana J. BioCell printing: Integrated automated assembly system for tissue engineering constructs. *CIRP Annals – Manufacturing Technology*. 2011; 60 (1): 271–274. DOI: 10.1016/J.CIRP.2011.03.116.
6. Elzubair A., Elias C.N., Suarez J.C.M., Lopes H.P., Vieira M.V.B. The physical characterization of a thermoplastic polymer for endodontic obturation. *J. Dent*. 2006; 34 (10): 784–789. DOI: 10.1016/j.jdent.2006.03.002.
7. Hutmacher D.W., Schantz T., Zein I., Ng K.W., Teoh S.H., Tan K.C. Mechanical properties and cell cultural response of polycaprolactone scaffolds designed and fabricated via fused deposition modeling. *J. Biomed. Mater. Res*. 2001; 55(2): 203–216. DOI: 10.1002/1097-4636(200105)55: 2<203::aid-jbm1007>3.0.co;2-7.
8. Rohner D., Hutmacher D.W., Cheng T.K., Oberholzer M., Hammer B. *In vivo* efficacy of bone-marrow-coated polycaprolactone scaffolds for the reconstruction of orbital defects in the pig. *J. Biomed. Mater. Res. B: Appl. Biomater*. 2003; 66B (2): 574–580. DOI: 10.1002/jbm.b.10037.
9. Tay F.R., Pashley D.H., Williams M.C., Raina R., Loushine R.J., Weller R.N. et al. Susceptibility of a polycaprolactone-based root canal filling material to degradation. I. Alkaline hydrolysis. *J. Endodontics*. 2005; 31 (8): 593–598. DOI: 10.1097/01.don.0000152301. 72828.61.
10. Chan-Chan L.H., Solis-Correa R., Vargas-Coronado R.F., Cervantes-Uc J.M., Cauich-Rodríguez J.V., Quintana P., Bartolo-Pérez P. Degradation studies on segmented polyurethanes prepared with HMDI, PCL and different chain extenders. *Acta Biomaterialia*. 2010; 6 (6): 2035–2044. DOI: 10.1016/j.actbio.2009.12.010.
11. Mitchell C.A., Krishnamoorti R. Dispersion of single-walled carbon nanotubes in poly(ε-caprolactone). *Macromolecules*. 2007; 40 (5): 1538–1545. DOI: 10.1021/ma0616054.
12. Raquez J.-M., Habibi Y., Murariu M., Dubois P. Polylactide (PLA)-based nanocomposites. *Prog. Polym. Sci*. 2013; 38 (10–11): 1504–1542. DOI: 10.1016/j.progpolymsci.2013.05.014.
13. Ray S.S., Bousmina M. Biodegradable polymers and their layered silicate nanocomposites: in green the 21st century materials word. *Prog. Mater. Sci*. 2005; 50: 962–1079. DOI: 10.1016/j.pmatsci.2005.05.002.
14. Murariu M., Paint Y., Murariu O., Raquez J.-M., Bonnaud L., Dubois P. Current progress in the production of PLA–ZnO nanocomposites: Beneficial effects of chain extender addition on key properties. *J. Appl. Polym. Sci*. 2015; 132: 42480. DOI: 10.1002/app.42480.
15. Murariu M., Dechief A.L., Bonnaud L., Paint Y., Gallos A., Fontaine G. et al. The production and properties of polylactide composites filled with expanded graphite. *Polym. Degrad. Stab*. 2010; 95: 889–900. DOI: 10.1016/j.polymdegradstab.2009.12.019.
16. Li S.H., Liu Q., Wijn J.R., Zhou B.L., Groot K. *In vitro* calcium phosphate formation on a natural composite material, bamboo. *Biomaterials*. 1997; 18 (5): 389–395. DOI: 10.1016/S0142-9612(96)00122-6.
17. Morvan J., Buyuktanir E., West J.L., Jákli A. Highly piezoelectric biocompatible and soft composite fibers. *Appl. Phys. Lett*. 2012; 100 (6). DOI: 10.1063/1.3683482.
18. Lebedev S.M., Amitov E.T., Mikutskiy E.A. Biodegradable electrically conductive polycaprolactone-based composites filled with carbon nanotubes. *Russian Phys. J*. 2020; 62 (10): 1753–1762. DOI: 10.1007/s11182-020-01903-0.
19. Lekishvili M.V., Balberkin A.V., Vasil'iev M.G., Kolondaev A.F., Baranetskiy A.L., Buklemishev Yu.V. The first experience of using the biocomposite material "Osteomatrix" in a bone pathology clinic, *Bulletin of Traumatology and Orthopedics named after N.N. Priorov*. 2002; 4: 80–83 (in Russ.)
20. Ivanov S.Yu., Biz'ayev N.F., Lomakin M.V., Panin A.M. Clinical results of the use of various osteoplastic materials at sinus-lifting. *Novelties in Dentistry*. 1999; 5: 51–54 (in Russ.).
21. Aglullin I.R., Safin I.R. Osteoplastics in the treatment of patients with bone defects. *Volga Region Oncology Bulletin*. 2012; 1: 42–44 (in Russ.).
22. Gonçalves E.M., Oliveira F.J., Silva R.F., Neto M.A., Fernandes M.H., Amaral M. et al. Three-dimensional printed PCL-hydroxyapatite scaffolds filled with CNTs for bone cell growth stimulation. *J. Biomed. Mater. Res. Part: B*. 2016; 104 (6): 1210–1219. DOI: 10.1002/ jbm.b.33432.
23. Akindoyo J.O., Beg M.D.H., Ghazali S., Alam A.K.M.M., Heim H.P., Feldmann M. Synergized poly(lactic acid)-hydroxyapatite composites: Biocompatibility study. *J. Appl. Polym. Sci*. 2019. DOI: 10.1002/app.47400.
24. Akindoyo J.O., Beg M.D.H., Ghazali S., Heim H.P., Feldmann M. Impact modified PLA-hydroxyapatite composites – thermo-mechanical properties. *Comp. Part A: App. Sci. Manufact.* 2018; 107: 326–333. DOI: 10.1016/j.compositesa.2018.01.017.
25. Šupová M. Problem of hydroxyapatite dispersion in polymer matrices: a review. *J. Mater. Sci. Mater. Med*. 2009; 20 (6): 1201–1213. DOI: 10.1007/s10856-009-3696-2.
26. Mao D., Li Q., Bai N., Dong H., Li D. Porous stable poly(-lactic acid)/ethyl cellulose/hydroxyapatite composite scaffolds prepared by a combined method for bone regeneration. *Carbohydrate Polymers*. 2018; 180: 104–111. DOI: 10.1016/j.carbpol.2017. 10.031.
27. Alizadeh-Osgouei M., Li Y., Wen C. A comprehensive review of biodegradable synthetic polymer-ceramic composites and their manufacture for biomedical applications. *Bioactive Mater*. 2019; 4 (1): 22–36. DOI: 10.1016/j.bioactmat.2018.11.003.
28. Russias J., Saiz E., Nalla R.K., Gryn K., Ritchie R.O., and Tomsia A.P. Fabrication and mechanical properties of PLA/HA composites: a study *in vitro* degradation. *Mater. Sci. Eng. C: Biomim. Supramol. Syst*. 2006; 26 (8): 1289–1295. DOI: 10.1016/j.msec.2005.08.004.
29. Ferri J.M., Jorda J., Montanes N., Fenollar O., and Balart R. Manufacturing and characterization of poly(lactic acid) composites with hydroxyapatite. *J. Thermoplast. Comp. Mater*. 2017; 31 (7): 865–881. DOI: 10.1177/0892705717729014.
30. Zhang H., Mao X., Du Z., Jiang W., Han X., Zhao D. et al. Three dimensional printed macroporous polylactic acid/hydroxyapatite composite scaffolds for promoting bone formation in a critical-size rat calvarial defect model. *Sci. Tech. Adv. Mater*. 2016; 17 (1). DOI: 10.1080/14686996.2016.1145532.

31. Zhang S.M., Liu J., Zhou W., Cheng L., Guo X.D. Interfacial fabrication and property of hydroxyapatite/polylactide resorbable bone fixation composites. *Curr. Appl. Phys*. 2005; 5 (5): 516–518. DOI: 10.1016/j.cap.2005.01.023.
32. Shen L., Yang H., Ying J., Qiao F., Peng M. Preparation and mechanical properties of carbon fiber reinforced hydroxyapatite/polylactide biocomposites. *J. Mater. Sci. Mater. Med*. 2009; 20 (11): 2259–2265. DOI: 10.1007/s10856-009-3785-2.
33. Park S.A., Lee S.H., Kim W.D. Fabrication of porous polycaprolactone/hydroxyapatite (PCL/HA) blend scaffolds using a 3D plotting system for bone tissue engineering. *Bioprocess Biosyst. Eng*. 2011; 34 (4): 505–513. DOI: 10.1007/s00449-010-0499-2.
34. Kim J.Y., Lee T.-J., Cho D.-W., Kim B.-S. Solid free-form fabrication-based PCL/HA scaffolds fabricated with a multi-head deposition system for bone tissue engineering. *J. Biomater. Sci*. 2010; 21 (6–7): 951–962. DOI: 10.1163/156856209X458380.
35. Jiang W., Shi J., Li W., Sun K. Morphology, wettability, and mechanical properties of polycaprolactone/hydroxyapatite composite scaffolds with interconnected pore structures fabricated by a mini-deposition system. *Polym. Eng. Sci*. 2012; 52: 2396–2402. DOI: 10.1002/pen.23193.
36. Chaikina M.V., Uvarov N.F., Ulihin A.S., Khlusov I.A. Mechanochemical synthesis of nanosized functional materials with the apatite-type structure. *Problems of Materials Science.* 2008; 54 (2): 219–232.
37. Druzhinina T.V., Talalaev S.Ya., Zakirov N.P., Shchadenko S.V., Khabibulin Sh.A., Khlusov I.A., Litvinova L.S. Cellular reactions to three-dimensional matrices of polylactic acid and hydroxyapatite generated by 3D printing. *Bull. Siberian Med.* 2016; 15 (5): 16–29. DOI: 10.20538/1682-0363-2016-5-16-29 (in Russ.).
38. Scott M.A., Levi B., Askarinam A., Nguyen A., Rackohn T., Ting K., Soo C., James A.W. Brief review of models of ectopic bone formation. *Stem Cells Dev*. 2012; 21 (5): 655–668. DOI: 10.1089/scd.2011.0517.
39. Bolbasov E.N., Popkov A.V., Popkov D.A., Gorbach E.N., Khlusov I.A., Golovkin A.S., Sinev A., Bouznik V.M., Tverdokhlebov S.I., Anissimov Y.G. Osteoinductive composite coatings for flexible intramedullary nails. *Mater. Sci. Eng. C*. 2017; 75: 207–220. DOI: 10.1016/j.msec.2017.02.073.
40. Caplan A.I. Mesenchymal stem cells. *J. Orthop. Res*. 1991; 9 (5): 641–50. DOI: 10.1002/jor.1100090504.
41. Silva C.C., Almeida A.F.L., De Oliveira R.S., Pinheiro A.G., Góes J.C., Sombra A.S.B. Dielectric permittivity and loss of hydroxyapatite screen-printed thick films. *J. Mater. Sci*. 2003; 38: 3713–3720. DOI: 10.1023/A:1025963728858.
42. Jukkala-Partio K., Laitinen O., Vasenius J., Partio E.K., Toivonen T., Tervahartiala P., Kinnunen J., Rokkanen P. Healing of subcapital femoral osteotomies fixed with self-reinforced poly-L lactide screws. An experimental long-term study in sheep. *Arch. Orthop. Trauma Surg*. 2002; 122 (6): 360–364. DOI: 10.1007/s00402-001-0379-y.
43. Bostman O.M., Pihlajamaki H.K. Late foreign-body reaction to an intraosseous bioabsorbable polylactic acid screw. A case report. *J. Bone Joint. Surg. Am*. 1998; 80 (12): 1791–1794. DOI: 10.2106/00004623-199812000-00010.
44. Zhang R., Ma P. X. Porous poly(L-lactic acid)/apatite composites created by biomimetic process. *J. Biomed. Mater. Res.* 1999; 45 (4): 285–293. DOI: 10.1002/(sici)1097-4636(19990615)45:4<285::aid-jbm2>3.0.co;2-2.
45. Fridenshtein A.Ya., Luria E.A. Cellular basics of the hematopoietic microenvironment. *Medicine*. 1980; 216 (in Russ.).

Authors contribution

Lebedev S.M., Khlusov I.A., Shchadenko S.V. – conception and design. Lebedev S.M., Chistokhin D.M., Dzuman A.N., Khlusov I.A., Shchadenko S.V. – carrying out of the practical part of the study. Nikolaeva O.O., Mitrichenko D.V., Prosolov A.B. – collection, translation and processing of data. Lebedev S.M., Khlusov I.A. – writing of the manuscript.

Authors information

Lebedev Sergey M., Dr. Sci. (Eng.), Leading Researcher, NR TPU, Tomsk, Russian Federation. ORCID 0000-0002-3367-1244.
Chistokhin Dmitry M., Engineer, NR TPU, Tomsk, Russian Federation.
Shchadenko Sergey V., Engineer, Research School of Chemistry & Applied Biomedical Sciences, NR TPU, Tomsk, Russian Federation.
Dzuman Anna N., Cand. Sci. (Med.), Associate Professor, Department of Morphology and General Pathology, SSMU, Tomsk, Russian Federation. ORCID 0000-0002-0795-0987.
Nikolaeva Olga O., Head of Production Department, SINTEL RPC, Tomsk, Russian Federation.
Mitrichenko Dmitry V., Director, SINTEL RPC, Tomsk, Russian Federation.
Prosolov Alexander B., Deputy Director for Research, SINTEL RPC, Tomsk, Russian Federation.
Khlusov Igor A., Dr. Sci. (Med.), Professor, Department of Morphology and General Pathology, SSMU; Research School of Chemical and Biomedical Technologies, NR TPU; Researcher, SINTEL RPC, Tomsk; Chief Researcher, IKBFU, Kaliningrad, Russian Federation. ORCID 0000-0003-3465-8452.

(✉) **Lebedev Sergey M.,** e-mail: lsm70@mail.ru.

Received 28.02.2020
Accepted 30.04.2020

УДК 616.127-005.8-039.35:575.174.015.3
https://doi.org/10.20538/1682-0363-2020-4-130-137

FGB, *TNFα*, *IL-1β*, *LPL*, *ITGB3*, and *TGFB1* genes polymorphism in patients with recurrent myocardial infarction

Mayanskaya S. D.[1], Garaeva L. A.[2], Teplyakov A.T.[3], Filipenko M.L. [4], Sokolova E.A.[4], Kravtsova O.A[5]., Berezikova E.N.[6]

[1] *Kazan State Medical University*
49, Butlerov Str., Kazan, 420012, Russian Federation

[2] *Kazan State Medical Academy, Branch Campus of the Russian Medical Academy of Continuous Professional Education*
11, Mushtary Str., Kazan, 420012, Russian Federation

[3] *Cardiology Research Institute, Tomsk National Research Medical Center of the Russian Academy of Sciences*
5, Kooperativny Lane, Tomsk, 634009, Russia

[4] *Institute of Chemical Biology and Fundamental Medicine, Siberian Branch of the Russian Academy of Sciences*
630090, 8, Lavrentiev Av., Novosibirsk, Russian Federation

[5] *Kazan Federal University*
18, Kremlevskaya Str., Kazan, 420008, Russian Federation

[6] *Novosibirsk State Medical University*
52, Krasnyi Av., Novosibirsk, 630091, Russian Federation

ABSTRACT

The aim. To evaluate the association of fibrinogen (*FGB*), tumor necrosis factor α (*TNF*α), interleukin 1β (*IL-1*β), lipoprotein lipase (*LPL*), platelet glycoprotein (*ITGB3*), and transforming growth factor β (*TGFB1*) genes with the incidence of recurrent myocardial infarction (MI) in patients living in the middle Volga region.

Materials and methods. The study included 104 people with recurrent MI compared to 280 people who had just one episode of MI. *TNFα* (rs1800629), *IL1B* (rs16944), *TGFB1b* (rs1800469), *FGB* (rs1800788), *ITGB3* (rs5918) and *LPL* (rs328) gene polymorphism was determined in all patients using competing TaqMan probes. Association estimation was performed with multivariate logistic regression analysis.

Results. Patients with recurrent MI much more often had *TNFα*, *IL1B*, *TGFB1b*, *FGB*, *ITGB3* and *LPL* allele and genotype polymorphism. Moreover the risk of MI increased significantly in a case of combination of *FGB* (alleles and genotypes) and *TNF*α (alleles and genotypes) gene polymorphisms (OR = 4.04, 95% CI = (1.895–8.615), $p = 0.0001$).

Conclusion. Thus, *FGB*, *LPL*, *TNF*α, *TGFB1b* and *ITGB3* gene polymorphism are associated with more severe coronary heart disease and may be a risk factor of recurrent MI development. The dominant total contribution of the *FGB* (rs1800788) and *TNF*α (rs1800629) polymorphic genes to the development of recurrent MI in the population of the middle Volga region was revealed.

Key words: recurrent myocardial infarction, gene polymorphism, *TNFα*, *IL1B*, *TGFB1b*, *FGB*, *ITGB3, LPL.*

Conflict of interest. The authors declare the absence of obvious and potential conflicts of interest related to the publication of this article.

Source of financing. The authors declare the absence of financing.

✉ *Mayanskaya Svetlana D.,* e-mail: Smayanskaya@mail.ru.

Conformity with the principles of ethics. The study was approved by the Ethics Committee at Kazan State Medical University (Protocol No. 4 of 24.05.2016).

For citation: Mayanskaya S.D., Garaeva L.A., Teplyakov A.T., Filipenko M.L., Sokolova E.A., Kravtsova O.A., Berezikova E.N. *FGB, TNFα, IL-1β, LPL, ITGB3,* and *TGFB1* genes polymorphism in patients with recurrent myocardial infarction. *Bulletin of Siberian Medicine.* 2020; 19 (4): 130–137. https://doi.org/10.20538/1682-0363-2020-4-130-137.

Особенности полиморфизма генов *FGB*, *TNFα*, *IL-1β*, *LPL*, *ITGB3* и *TGFB1* у пациентов с повторным инфарктом миокарда

Маянская С.Д.[1], Гараева Л.А.[2], Тепляков А.Т.[3], Филипенко М.Л.[4], Соколова Е.А.[4], Кравцова О.А.[5], Березикова Е.Н.[6]

[1] Казанский государственный медицинский университет (КГМУ)
Россия, 420012, г. Казань, ул. Бутлерова, 49

[2] Казанская государственная медицинская академия (КГМА) – филиал Российской медицинской академии непрерывного профессионального образования (РМАНПО)
Россия, 420012, г. Казань, ул. Муштари, 11

[3] Научно-исследовательский институт (НИИ) кардиологии, Томский национальный исследовательский медицинский центр (НИМЦ) Российской академии наук
Россия, 634012, г. Томск, ул. Киевская, 111

[4] Институт химической биологии и фундаментальной медицины Сибирского отделения Российской академии наук (ИХБФМ СО РАН)
Россия, 630090, г. Новосибирск, пр. Ак. Лаврентьева, 8

[5] Казанский (Приволжский) федеральный университет
Россия, 420008, Республика Татарстан, г. Казань, ул. Кремлевская, 18

[6] Новосибирский государственный медицинский университет (НГМУ)
Россия, 630091, г. Новосибирск, Красный пр., 52

РЕЗЮМЕ

Цель. Ассоциация полиморфизма генов фибриногена (*FGB*), фактора некроза опухоли α (*TNFα*), интерлейкина 1 β (*IL-1β*), липопротеинлипазы (*LPL*), тромбоцитарного гликопротеина (*ITGB3*) и трансформирующего фактора роста β (*TGFB1*) с риском развития повторного инфаркта миокарда (ИМ) у пациентов, проживающих на территории Среднего Поволжья.

Материалы и методы. В исследование вошли 280 человек с однократным и 104 человека с повторным ИМ. Генотипирование полиморфных локусов генов *TNFα* (rs1800629), *IL1B* (rs16944), *TGFB1b* (rs1800469), *FGB* (rs1800788), *ITGB3* (rs5918) и *LPL* (rs328) осуществляли с использованием TaqMan-зондов. Статистическую обработку данных проводили методом многофакторного логистического регрессионного анализа.

Результаты. Среди пациентов с повторным ИМ более часто встречались аллели и генотипы полиморфных маркеров генов *TNFα*, *IL1B*, *TGFB1b*, *FGB*, *ITGB3* и *LPL*. При оценке суммарного вклада полиморфизмов исследуемых генов риск повторного ИМ значительно возрастал при наличии комбинации полиморфизмов генов *FGB* (аллели и генотипы) и *TNFα* (аллели и генотипы), OR = 4,04; 95% CI 1,895–8,615; p = 0,0001.

Заключение. Таким образом, генотипы полиморфных локусов генов *FGB*, *LPL*, *TNFα*, *TGFB1b* и *ITGB3* могут быть ассоциированы с риском более тяжелого течения ишемической болезни сердца и приводить к развитию повторных инфарктов миокарда. Выявлен доминирующий суммарный вклад полиморфных локусов генов *FGB* (rs1800788) и *TNFα* (rs1800629) в развитие повторного ИМ у населения Среднего Поволжья.

Ключевые слова: повторный инфаркт миокарда, полиморфизм генов, *TNFα*, *IL1B*, *TGFB1b*, *FGB*, *ITGB3*, *LPL*.

Конфликт интересов. Авторы декларируют отсутствие явных и потенциальных конфликтов интересов, связанных с публикацией настоящей статьи.

Источник финансирования. Авторы заявляют об отсутствии финансирования.

Соответствие принципам этики. Все пациенты подписали информированное согласие на участие в исследовании. Исследование одобрено локальным этическим комитетом КГМУ (протокол № 4 от 24.05.2016).

Для цитирования: Маянская С.Д., Гараева Л.А., Тепляков А.Т., Филипенко М.Л., Соколова Е.А., Кравцова О.А., Березикова Е.Н. Особенности полиморфизма генов *FGB*, *TNFα*, *IL-1β*, *LPL*, *ITGB3* и *TGFB1* у пациентов с повторным инфарктом миокарда. *Бюллетень сибирской медицины.* 2020; 19 (4): 130–137. https://doi.org/10.20538/1682-0363-2020-4-130-137.

INTRODUCTION

Myocardial infarction is a severe cardiovascular disease with a multi-stage evolution consisting of different events. The genetic characteristics of each stage have a leading role in the determination of individual risk of atherosclerosis progression.

The key pathological processes that control coronary heart disease severity are lipid metabolism and hemostasis disorder, as well as activity of inflammatory process in atherosclerotic plaque. Several wide genome associated studies of recent years have revealed the responsibility of some gene polymorphisms for the amount and quality of production of various lipid metabolism and coagulation components and a number of cytokines, such as interleukins, transforming growth factors, adhesion molecules, etc. [1]. Remarkably, most of the studies of disease severity are mainly based on evaluating of fatal complications frequency among patients with a stable angina. However, it is assumed that a transforming growth factor is associated primarily with an increase in the size of the atherosclerotic plaque itself, and not with a thinning of its lining [2], and an increase in the activity of interleukin Ib is associated with both aggravation of stenosis and the frequency of fatal complications [3]. The study of these genes polymorphism in aspect of cardiovascular disease progression is an essential step in understanding the pathogenetic mechanisms of coronary artery occlusion, including cases of recurrent MI. Based on a number of studies, it has been suggested that mutant alleles of cytokine cascade and thrombus formation genes, encoding main pathogenetic markers of restenosis and reocclusion of coronary vessels in patients with coronary artery disease (CAD), are quite frequent [2, 4].

Thus, the aim of the research is to study features of several genes polymorphism associated with inflammation activity, lipid metabolism and hemostasis for a personalized prediction approach of recurrent MI development.

MATERIALS AND METHODS

A total of 384 participants aged 44 to 85 years (mean age 66 ± 10.7 years) who had undergone inpatient treatment in the cardiology department of City Clinical Hospital No. 7 in Kazan with acute myocardial infarction (AMI) with ST segment elevation and/or "Q" -positive MI were enrolled. All patients signed informed consent to participate in the study. AMI diagnosis was verified by biomarkers analysis results: troponins, ECG, and coronary angiography (CAG). In some patients (104 people), a previous MI was determined according to the anamnesis and previous research methods. A comparative study was conducted between a group of patients with single and repeated MI (280 and 104 patients, respectively).

All patients underwent genotyping of DNA samples isolated from peripheral blood leukocytes at the SNP of tumor necrosis factor alpha *TNFα* (rs1800629), transforming growth factor *TGFB1b* (rs1800469), interleukin 1 beta *IL1B* (rs16944), platelet glycoprotein *IT318GB* (rs16944), platelet glycoprotein chains of fibrinogen *FGB* (rs1800788) and lipoprotein lipase *LPL* (rs328) using competing TaqMan probes. Genotyping reliability was confirmed by sequencing. Oligonucleotide primers design and genes study were carried out in laboratory of pharmacogenomics of the Institute of Chemical Biology and Fundamental Medicine of the Siberian Branch of the Russian Academy of Sciences (ICBFM SB RAS).

"Genetics" and "Hardy Weinberg" statistics packages of the R-project software (www.r-project.org) were used for analysis. Compliance with the Hardy – Weinberg equilibrium was assessed using Fisher's exact test. Association of genotype with severity of

CAD was carried out using multivariate logistic regression analysis, from which OR (odds ratios), its confidence interval (95% CI) and the significance level of the results obtained (p-value) were calculated. The odds ratio was calculated adjusted for race and risk factors (gender, age, smoking, the presence of hereditary burden, arterial hypertension (AH), dyslipidemia and obesity). Analysis was carried out for four models of inheritance: dominant, additive, recessive and co-dominant. The selection of the best of several competing models was based on the Akaike Information Criterion (AIC). Data are presented as mean and mean error $M \pm m$.

RESULTS

All participants were preliminarily assessed for their clinical status and comorbidities to exclude their possible impact when analyzing association of genetic polymorphism with recurrent MI development (Table 1).

Table 1

Clinical characteristics of patients with MI (n =384)

Parameters	1 group, n = 280 (%)	2 group, n = 104 (%)	p-value
Sex: male female	1791 (64) 101 (36)	64 (61.5) 36 (38.5)	$p = 0.61$
Age (years)	64.1 ± 10.3	70.3 ± 7.2	$p = 0.31$
Blood pressure	204 (72.8)	104 (100)	$p = 0.02$
Smoking	186 (66.4)	63 (61)	$p = 0.29$
TC	5.3 ± 0.98	5.19 ± 0.99	$p = 0.38$
BMI	29.9 ± 6.2	28 ± 6.2	$p = 0.07$
Hereditary burden	190 (67.8)	63 (60.5)	$p = 0.16$
Type 2 diabetes	157 (56.0)	60 (57.6)	$p = 0.8$
CHF: with EF more 40% with EF less 40%	 194 (69.3) 86 (30.7)	 60 (57.7) 44 (42.3)	$p = 0.033$

Note. TC – total cholesterol; BMI – body mass index; CHF – chronic heart failure; EF – ejection fraction.

Thus, it was revealed that in the group with repeated MI, AH was detected significantly more often. Later, when conducting logistic regression analysis, corrections were made for this parameter, as well as for age. Taking stenosis into account, in the group with repeated MI lesions of the left coronary artery trunk and the anterior interventricular branch were observed more often. Allele frequencies were determined for all studied loci in patients in both groups. Alleles distribution of all genes in comparison groups corresponded to the Hardy – Weinberg equation.

Association of gene polymorphism with the development frequency of single and repeated MI was calculated in two variants: by presence of a polymorphic allele, as well as by genotypes among all genes, except for the *LPL* and *TNFα* genes, as their pathological genotype frequency of occurrence is too rare for a reliable assessment. Alleles and genotypes in groups association is presented in Table 2.

Table 2

Association of polymorphic allele and genotype of the studied genes with the development of recurrent MI

ONP	1 group (n = 280)	2 group (n = 104)	Additive model OR 95% CI p-value	Co-dominant model	
				Heterozygous genotype OR 95% CI p-value	Homozygous genotype OR 95% CI p-value
LPL	CC 246 CG + GG 34 + 0	CC 78 CG + GG 21 + 5	2.92 [1.39–6.11] 0.005	–	–
ITGB3	TT 213 CT + CC 64 + 3	TT 82 CT + CC 11 + 11	1.21 [0.64–2.31] p = 0,13	TC: 0.44 [0.15–1.29] p = 0.14	CC: 7.08 [1.46-34.22] p = 0.005
			AIC: 238.6	AIC: 231.86	

Table 2 (continued)

ONP	1 group (n = 280)	2 group (n = 104)	Additive model OR 95% CI p-value	Co-dominant model	
				Heterozygous genotype OR 95% CI p-value	Homozygous genotype OR 95% CI p-value
FGB	CC 145 CT + TT 110 + 25	CC 27 CT + TT 66 + 11	1.91 [1.15–3.17] p = 0.01	CT: 3.30 [1.51–7.23] p = 0.003	TT: 2.45 [0.70–8.60] p = 0.16
			AIC: 232.79	AIC: 230.94	
TGFB1	CC 139 CT + TT 118 + 23	CC 27 CT + TT 63 + 14	1.88 [1.12–3.16] p = 0.02	CT: 2.82 [1.28–6.20] p = 0.01	TT: 2.81 [0.86–9.23] p = 0.09
			AIC: 233.19	AIC: 233.23	
IL1B	CC 128 CT + TT 118 + 34	CC 41 CT + TT 47 + 16	1.36 [0.83–2.23] p = 0.23	CT: 1.31 [0.63–2.75] p = 0.47	TT: 1.89 [0.66–5.39] p = 0.23
			AIC: 239.48	TC: 0.44 [0.15–1.29] p = 0.14	
TNFa	GG 219 GA + AA 58 + 3	GG 96 GA + AA 3 + 5	0.21 [0.05–0.88] p = 0.03	-	-

Note. ONP – oligonucleotide primers; OR – odds ratio adjusted for risk factors; 95% CI – confidence interval; AIC – Akaike criterion; CC, CA, GG and others and others – genotype variants.

According to the data, five candidate genes under study were associated with recurrent MI development, taking into account corrections for comorbidities and age. As it can be seen from Table 3, polymorphism of *FGB* rs1800788, *LPL* rs328, *TNF*α rs1800629, *ITGB3* rs5918 and *TGFB1* rs1800469 had a statistically significant effect on the incidence of recurrent MI. Thus, for the *FGB* gene, a rare allele (–249T) presence (OR = 1.91, 95% CI = (1.15–3.17), p = 0.01) was associated with a higher frequency of recurrent MI development. For the *TNF* gene (–308G/A) it was possible to assess only the contribution of a rare allele, which is more common among patients without recurrent MI (OR = 0.21, 95% CI = (0.05–0.88), p = 0.03).

Besides, the rare −509T allele of *TGFB1* gene was significantly more often detected in patients with recurrent MI (OR = 1.88, 95% CI = (1.12–3.16), p = 0.002). And, finally, a strong correlation was demonstrated by genotype of the *ITGB3* gene (PlA2) homozygous for a rare allele (ORadj = 7.08, 95% CI = (1.46–34.22), p = 0.005), while the presence of one rare allele had no significant pathological effect.

Assessment of contribution of cumulative genes polymorphism effect revealed the risk of MI significant increase in combination of *FGB* rs1800788 and *TNF*α rs1800629 polymorphisms (OR = 4.04, 95% CI = (1.895–8.615), p = 0.0001), while for *LPL* rs328 and *ITGB3* rs5918 this indicator turned out to be lower than in isolation for each of the genes (OR = 3.212, 95% CI = (1.165–8.853), p = 0.030 (Table 3).

Table 3

The combined contribution of *FGB* and *TNFα* gene polymorphism in the development of recurrent MI*NFα*

Parameter	OR [95% CI] p-value
FGB rs1800788 – T allele *TNF* rs1800629 – A allele	OR = 4.04 95% CI 1.895–8.615 p = 0.0001
LPL rs328 – G allele *ITGB3* rs5918 – C allele	OR = 3.212, 95% CI = (1.165–8.853), p = 0.030

Note. OR – odds ratio adjusted for risk factors; 95% C.I. – confidence interval.

DISCUSSION

Heredity contribution to the development of coronary atherosclerosis leaves no doubt, since numerous works are devoted to the influence of genetic polymorphism on the incidence of cardiovascular complications (CVC) of coronary artery disease.

In particular, there are data of the studied SNPs of *TNF*α tumor necrosis factor alpha (−308G/A), *TGFB1b* transforming growth factor (−509 C/T), *IL1B* interleukin 1 beta (−511C/T), *FGB* fibrinogen beta chain (–249C/T) and its *ITGB3* platelet glycoprotein (PlA1 / PlA2), as well as *LPL* lipoprotein lipase (rs328) effect on various manifestations of atherosclerosis.

Thus, presence of polymorphic T allele in SNP rs1800788 in *FGB* gene is associated with incidence of MI in population, although some early studies hadn't found connection between polymorphism and level

of fibrinogen in the blood and manifestations of IHD [5]. In many studies, *TNF*α gene polymorphism is also associated with the incidence of acute cardiovascular events [6]. C-509T polymorphism of *TGFB1b* gene has been considered a protective factor against atherosclerosis for a long time due to the anti-inflammatory effect of cytokine during atherogenesis [7]. However, in recent years, many studies have shown a negative effect of polymorphism on various manifestations of atherosclerosis, possibly due to development of proliferative changes in the intima, and note the relationship of the mutant -509 T allele with the incidence of fatal CVC [2].

In most studies, *LPL* gene polymorphism has not shown a significant effect on coronary atherosclerosis incidence and severity [8], however, it is assumed to be associated with an unfavorable course along with a number of concomitant factors. In a large number of studies PlA2 polymorphism of the ITGB3 gene is associated with incidence of acute events, including in younger patients, but it is practically irrelevant for development of chronic conditions [9]. *IL1*β–511C/T polymorphism presence is associated with frequency and degree of atherosclerotic stenosis in various localizations, while data on its effect on incidence of MI are rather contradictory [10].

At the same time, most of the studies are carried out in groups of patients with CVD compared to a relatively healthy population and reflect, first of all, the risks of disease occurrence, and not its dynamics. A distinctive feature of this work is a comparative assessment of genetic polymorphism among patients with complicated atherosclerosis, namely, depending on presence of single or repeated MI with the possibility of predicting it. It was found that patients with recurrent myocardial infarction showed a significant association with polymorphism of four genes, *FGB* rs1800788, *TNF* rs1800629, *LPL* rs328, *ITGB3* rs5918, and *TGF* rs180046.

T allele in SNP rs1800788 of the *FGB* gene with high statistical significance was more common in patients with recurrent MI, which fully correlates with the data of other studies and may be explained by an increased amount of pure fibrinogen and its effect on atherothrombosis [5]. At the same time, the opposite picture was observed with the *TNFα* rs1800629 SNP. The polymorphic A allele was significantly more common in patients without signs of acute or previous MI, while normal G/G genotype was associated with an increased incidence of the disease. Whereas other studies have noted a protective role of the G allele, primarily in relation to acute events such as MI or unstable angina pectoris [11].

The *LPL* rs328 gene polymorphism contribution also manifested itself among patients with repeated MI and was highly associated with an increase in incidence of pathology. Taking into account some studies of mutant G allele effect on atherosclerosis development in patients after MI [12], a significance of this gene polymorphism specifically for patients with recurrent coronary artery occlusion can be assumed.

The polymorphism of the *ITGB3* rs5918 gene significantly increased the incidence of MI only in the case of the mutant homozygous genotype and was significant only in the group of patients who underwent repeated MI. In general, this does not contradict the data on the pathological effect of the mutant *ITGB3* rs5918 allele on the amount of fibrinogen and platelet reactivity in severe CVD [13]. The presence of the polymorphic G allele of the *TGF* rs1800469 gene was also significant only in the case of repeated MI, which may indicate the significance of excessive synthesis of the extracellular matrix in severe coronary artery disease [2].

Contribution assessment of the cumulative genes polymorphism effect allowed us to assume dominant role of polymorphic allele combinations in atherosclerosis progression risk prediction. Thus, with a combination of polymorphic alleles of the *FGB* rs1800788 and *TNF*α rs1800629 genes, the risk of recurrent myocardial infarction in patients with a single infarction increased significantly, even in comparison with the presence of a single gene polymorphism.

CONCLUSION

Thus, a correlation between *FGB* rs1800788, *LPL* rs328, *ITGB3* rs5918, *TNF*α rs1800629, and *TGF* rs1800469 genes polymorphisms and frequency of recurrent MI was revealed. Repeated MI is associated with the presence of any polymorphic genotype of the *FGB* rs1800788, *LPL* rs328, *TGFB1* rs1800469 genes and polymorphic homozygous genotype of the *ITGB3* rs5918 gene, as well as normal homozygous genotype of *TNF*α rs1800629 gene. On the contrary, the presence of polymorphic genotype of *TNF*α gene rs1800629 indicates its protective effect on the development of recurrent MI.

An increased incidence of some polymorphisms in group of patients with repeated MI compared to the group of patients with a single MI may indicate, first of all, an influence of these polymorphisms on atherosclerosis progression and enlarging of stenosis in

coronary arteries. However, this thesis requires further study.

Assessment of total contribution of *FGB* rs1800788 and *TNFα* rs1800629 genes polymorphism is appropriate to clarify both primary and recurrent myocardial infarction development risk in order to optimize diagnostic and therapeutic measures.

REFERENCES

1. Sukhija R., Fahdi I., Garza L., Fink L., Scott M., Aude W., Pacheco R., Bursac Z., Grant A., Mehta J.L. Inflammatory markers, angiographic severity of coronary artery disease, and patient outcome. *Am. J. Cardiol*. 2007; 99 (7): 879–884. DOI: 10.1016/j.amjcard.2006.11.032.
2. Koch W., Hoppmann P., Mueller J.C., Schömig A., Kastrati A. Association of transforming growth factor-β1 gene polymorphisms with myocardial infarction in patients with angiographically proven coronary heart disease. *Arterioscler. Thromb. Vasc. Biol*. 2006; 26 (5): 1114–1119. DOI: 10.1161/01.ATV.0000217747.66517.11.
3. Miranda-Malpica E., Martínez-Rios M.A., Fragoso J.M., Delgadillo-Rodríguez H., Rodríguez-Pérez J.M., González-Quesada C., Martínez-Rodríguez N., Saldaña-Mendoza A., Peña-Duque M.A., Vargas-Alarcón G. The interleukin 1B–511 polymorphism is associated with the risk of developing restenosis after coronary stenting in Mexican patients. *Hum. Immunol*. 2008; 69 (2): 116–121. DOI: 10.1016/j.humimm.2007.12.003.
4. Mcpherson T.H., Tybjaerg-Hansen A. Genetics of coronary artery disease. *Circ. Res*. 2016; 118 (4): 564–578. DOI: 10.1161/CIRCRESAHA.115.306566.
5. Titov B.V., Osmak J., Matveeva N.A., Kukava G.N., Shakhnovich R.M., Favorov A.V., Ruda M.Y., Favorova O.O. Genetic risk factors for myocardial infarction more clearly manifest for early age of first onset. *Mol. Biol. Rep*. 2017; 44 (4): 315–321. DOI: 10.1007/s11033-017-4112-5.
6. Szalai C., Füst G., Duba J., Kramer J., Romics L., Prohászka Z., Császár A. Association of polymorphisms and allelic combinations in the tumour necrosis factor-alpha-complement MHC region with coronary artery disease. *J. Med. Genet*. 2002; 39(1): 46–51. DOI: 0.1136/jmg.39.1.46.
7. Yang Y.N., Zhao B., Li X.M., Xie X., Liu F., Chen B.D. Association of a transforming growth factor-β1 polymorphism with acute coronary syndrome in a Chinese Han population. *Mol. Res*. 2014; 13 (3): 6160–6167. DOI: 10.4238/2014.April.3.2.
8. Jensen M.K., Rimm E.B., Rader D., Schmidt E.B., Sørensen T.I., Vogel U., Overvad K., Mukamal K.J. S447X variant of the lipoprotein lipase gene, lipids, and risk of coronary heart disease in 3 prospective cohort studies. *Am. Heart J*. 2009; 157 (2): 384–390. DOI: 10.1016/j.ahj.2008.10.008.
9. Verdoia M., Cassetti E., Schaffer A., Barbieri L., Giovine G.D., Nardin M., Marino P., Sinigaglia F., Luca G.D. Novara Atherosclerosis Study Group (NAS). Relationship between glycoprotein IIIa platelet receptor gene polymorphism and coronary artery disease. *Angiology*. 2015; 66 (1): 79–85. DOI: 10.1177/0003319714524296.
10. Tabrez S., Jabir N.R., Firoz C.K., Hindawi S., Shakil S., Damanhouri G.A., Zaidi S.K. Estimation of interleukin-1βpPromoter (−31 C/T and −511 T/C) polymorphisms and its level in coronary artery disease patients. *J. Cell. Biochem*. 2017; 118 (9): 2977–2982. DOI: 10.1002/jcb.25958.
11. Koch W., Kastrati A., Böttiger C., Mehilli J., von Beckerath N., Schömig A. Interleukin-10 and tumor necrosis factor gene polymorphisms and risk of coronary artery disease and myocardial infarction. *Atherosclerosis*. 2001; 159 (1): 137–144. DOI: 10.1016/s0021-9150(01)00467-1.
12. Ahmadi Z., Senemar S., Toosi S., Radmanesh S. The Association of lipoprotein lipase genes, HindIII and S447X polymorphisms with coronary artery disease in Shiraz city. *J. Cardiovasc. Thorac. Res.* 2015; 7 (2): 63–67. DOI: 10.15171/jcvtr.2015.14.
13. Grove E.L., Ørntoft T.F., Lassen J.F., Jensen H.K., Kristensen S.D. The platelet polymorphism PlA2 is a genetic risk factor for myocardial infarction. *J. Intern. Med*. 2004; 255 (6): 637–644. DOI: 10.1111/j.1365-2796.2004.01327.x.

Authors contribution

Mayanskaya S.D. – conception and plan of the research, analysis and interpretation of data. Garaeva L.A. – selection of patients for research, analysis and interpretation of data, article design. Teplyakov A.T. – advising on the concept of research and the results obtained, final approval of the manuscript for publication. Filipenko M.L. – development of the research concept, carrying out of the practical part of the study. Sokolova E.A. – carrying out of the practical part of the study, statistical processing of the results of work. Kravtsova O.A. – carrying out of the practical part of the study, editing of the article. Beresikova E.N. – clinical interpretation of the data obtained.

Authors information

Mayanskaya Svetlana D., Dr. Sci. (Med.), Professor of the Hospital Therapy Department, KSMU, Kazan, Russian Federation. ORCID 0000-0001-6701-5395.

Garaeva Liliya A., Cand. Sci. (Med.), Assistant Lecturer of the Department of Cardiology, Roentgen-endovascular and Cardiovascular Surgery, KSMU, Branch Campus of the Russian Medical Academy of Continuous Professional Education, Kazan, Russian Federation. ORCID 000-0002-9427-6037.

Teplyakov Alexandr T., Dr. Sci. (Med.), Professor, Head of Heart Failure Department, CRI, Tomsk NRMC RAS, Tomsk, Russian Federation. ORCID 0000-0003-0721-0038.

Filipenko Maxim L., Cand. Sci. (Biology), Head of the Laboratory of Pharmacogenomics, ICBFM SB RAS, Novosibirsk, , Russian Federation. ORCID 0000-0002-8950-5368.

Sokolova Ekaterina A., Cand. Sci. (Biology), Junior Researcher of the Laboratory of Pharmacogenomics, ICBFM SB RAS, Novosibirsk, , Russian Federation. ORCID 0000-0002-5715-8007.

Kravtsova Olga A., Cand. Sci. (Biology), Associate Professor of the Department of Biochemistry and Biotechnology, KFU, Kazan, Russian Federation. ORCID 0000-0002-4227-008x.

Beresikova Ekaterina N., Dr. Sci. (Med.), Associate Professor of the Department of Outpatient Therapy and General Medical Practice, NSMU, Novosibirsk, Russian Federation. ORCID 0000-0002-9630-0213.

(✉) **Mayanskaya Svetlana D.,** email: Smayanskaya@mail.ru.

Received 10.03.2020
Accepted 29.09.2020

УДК 616.127-005.8:612.115.38
https://doi.org/10.20538/1682-0363-2020-4-138-142

Receptor mechanism of infarct-limiting effect of adaptation to normobaric hypoxia

Naryzhnaya N.V., Mukhomedzyanov A.V., Tsibulnikov S.Yu., Maslov L.N.

Cardiology Research Institute, Tomsk National Research Medical Center (TNRMC), Russian Academy of Science
111a, Kievskaya Str., Tomsk, 634012, Russian Federation

ABSTRACT

The aim of the study was to investigate the involvement of bradykinin, cannabinoid and vanilloid (TRPV1 channel) receptors in the implementation of the infarct-limiting effect of chronic normobaric hypoxia (CNH).

Materials and methods. The study was performed on male Wistar rats (n = 117) weighing 250–300 g. Adaptation to CNH was modeled for 21 days at 12% pO_2, 0.3% pCO_2 and normal atmospheric pressure. A day after adaptation of rats to CNH coronary artery occlusion (45 min) and reperfusion (2 h) was performed. In the study the following compounds were used: selective cannabinoid CB1 receptor antagonist rimonabant (1 mg/kg), selective cannabinoid CB2 receptor antagonist AM630 (2.5 mg/kg), selective bradykinin B2 receptor antagonist HOE140 (50 μg/kg), and vanilloid receptor (TRPV1 channel) antagonist capsazepine (3 mg/kg). All antagonists were administered 15 min before coronary artery occlusion.

Results. Adaptation to normobaric hypoxia promoted the formation of the pronounced infarct-limiting effect. The blockade of B2 receptor eliminated the infarct-limiting effect of CNH. Blockade of cannabinoid or vanilloid receptors did not affect the infarct-limiting effect of CNH.

Conclusion. The infarct-limiting effect of CNH depends on the activation of B2 receptor, and the adaptive increase in cardiac tolerance to ischemia/reperfusion does not depend on cannabinoid or vanilloid receptors.

Key words: myocardium, ischemia, reperfusion, receptors, chronic hypoxia.

Conflict of interest. The authors declare the absence of obvious and potential conflicts of interest related to the publication of this article.

Source of financing. This work was supported by the Russian Science Foundation (Grant No. 16-15-10001). The study with HOE140 was carried out within the framework of the state assignment № AAAA-A15-115120910024-0.

Conformity with the principles of ethics. The study was approved by the local Ethics Committee at the Cardiology Research Institute, Tomsk National Research Medical Center, Russian Academy of Science (Protocol No.137 of 16.09.2015).

For citation: Naryzhnaya N.V., Mukhomedzyanov A.V., Tsibulnikov S.Yu., Maslov L.N. Receptor mechanism of infarct-limiting effect of adaptation to normobaric hypoxia. *Bulletin of Siberian Medicine.* 2020; 19 (4): 138–142. https://doi.org/10.20538/1682-0363-2020-4-138-142.

Рецепторный механизм инфаркт-лимитирующего эффекта адаптации к нормобарической гипоксии

Нарыжная Н.В., Мухомедзянов А.В., Цибульников С.Ю., Маслов Л.Н.

Научно-исследовательский институт (НИИ) кардиологии, Томский национальный исследовательский медицинский центр (НИМЦ) Российской академии наук
634012, Россия, г. Томск, ул. Киевская, 111а

✉ *Tsibulnikov Sergey Yu.,* e-mail: tsibulnikov1986@mail.ru.

РЕЗЮМЕ

Цель исследования – изучение участия брадикининовых, каннабиноидных и ваниллоидных рецепторов (TRPV1-каналов) в реализации инфаркт-лимитирующего эффекта хронической нормобарической гипоксии.

Материалы и методы. Исследование было выполнено на самцах крыс Вистар (n = 117) массой 250–300 г. Адаптацию к гипоксии (ННГ) моделировали в течение 21 сут при 12% pO_2, 0,3% pCO_2 и нормальном атмосферном давлении. Через 1 сут после адаптации у крыс воспроизводили коронарооккклюзию (45 мин) и реперфузию (2 ч). В исследовании использовали следующие препараты: селективный антагонист каннабиноидных CB1-рецепторов римонабант (1 мг/кг), селективный антагонист каннабиноидных CB2-рецепторов AM630 (2,5 мг/кг), селективный антагонист брадикининовых B2-рецепторов HOE140 (50 мкг/кг), антагонист ванилоидных рецепторов (TRPV1-каналов) капсазепин (3 мг/кг). Все антагонисты вводили за 15 мин до коронарооккклюзии.

Результаты. Адаптация к нормобарической гипоксии приводила к формированию выраженного инфаркт-лимитирующего эффекта. Блокада B2-рецепторов устраняла инфаркт-лимитирующий эффект ННГ. Блокада каннабиноидных или ваниллоидных рецепторов не влияла на инфаркт-лимитирующее действие ННГ.

Заключение. Инфаркт-лимитирующий эффект ННГ зависит от активации B2-рецепторов, а адаптационное повышение толерантности сердца к ишемии и реперфузии не зависит от каннабиноидных или ваниллоидных рецепторов.

Ключевые слова: миокард, ишемия, реперфузия, рецепторы, хроническая гипоксия.

Конфликт интересов. Авторы декларируют отсутствие явных и потенциальных конфликтов интересов, связанных с публикацией настоящей статьи.

Источник финансирования. Работа выполнена при поддержке Российского научного фонда (грант № 16-15-10001). Исследование с HOE140 выполнено в рамках госзадания № АААА-А15-115120910024-0.

Соответствие принципам этики. Исследование одобрено локальным этическим комитетом НИИ кардиологии Томского НИМЦ (протокол № 137 от 16.09.2015).

Для цитирования: Нарыжная Н.В., Мухомедзянов А.В., Цибульников С.Ю., Маслов Л.Н. Рецепторный механизм инфаркт-лимитирующего эффекта адаптации к нормобарической гипоксии. *Бюллетень сибирской медицины.* 2020; 19 (4): 138–142. https://doi.org/10.20538/1682-0363-2020-4-138-142.

INTRODUCTION

It is known that in chronic moderate hypoxia, nonspecific myocardial resistance to damage during ischemia and subsequent reperfusion is formed. However, the pathways of forming myocardial resistance during adaptation to hypoxia remain poorly understood. In particular, the receptor mechanisms of this phenomenon have not been sufficiently studied. Earlier, we found the participation of opioid receptors in the infarct-limiting [1] and cytoprotective [2] effects of adaptation to continuous hypoxia. However, other receptor mechanisms remain unexplored. At the same time, an important role of bradykinin, cannabinoid and vanilloid receptors in the regulation of the heart's tolerance to ischemia/reperfusion during ischemic and remote preconditioning is known [3–7].

The aim of this study was to investigate the participation of bradykinin, cannabinoid, and vanilloid receptors (TRPV1 channels) in the implementation of the infarct-limiting effect of continuous normobaric hypoxia (CNH).

MATERIALS AND METHODS

The study was performed on male Wistar rats (n = 117) weighing 250–300 g. Animals of the experimental groups (adapted to hypoxia) were exposed to CNH (12% pO_2, 0.3% pCO_2) at normal atmospheric pressure in the chamber for 21 days [1]. Monitoring the state of the gaseous medium was carried out using the TCOD-IR and OLC 20 sensors (Oldham) and the Bio-Nova-204G4R1 apparatus (NTO Bio-Nova) through the MX32 control unit (Oldham). 24 hours before the start of the experiment, the animals of the experimental group were removed from the hypoxic chamber. Groups of rats of normoxic control were kept under standard vivarium conditions.

Before the coronary occlusion procedure, the animals were anesthetized with α-chloralose (100 mg/kg i.p.). During subsequent manipulations, the animals were subjected to artificial ventilation with atmospheric air, which was carried out using the SAR-830 Series ventilator (Central Wisconsin Engineers Inc., Schofield, USA) through an intubated trachea. To perform coronary occlusion, the chest was opened at

the intercostal space to the left of the sternum, the heart was freed from the pericardium and a ligature was placed on the left descending coronary artery in its upper third for 45 minutes. Reperfusion was performed by releasing the ligature with visual control of the restoration of coronary circulation by hyperemia of the ischemic region [8]. The duration of reperfusion was 2 hours. To determine myocardial infarction size, the ligature, previously placed on the left coronary artery, was again tightened; the isolated heart was washed through the aorta with physiological saline, and stained with 5% potassium permanganate solution. After washing the myocardium with saline, the right ventricle was separated, both ventricles were weighed, the left ventricle was dissected into sections 1 mm thick parallel to the axis of the heart.

Sections of the left ventricle were stained with a 1% solution of 2,3,5-triphenyltetrazolium (37° C, 30 minutes) and fixed for 1 day in a 10% solution of neutral formalin [8]. Slices were scanned (Scanjet G2710), the size of the necrosis zone and the area at risk (ischemia/reperfusion zone) were determined planimetrically using the application software package. The magnitude of the infarct size was expressed as a percentage of the area at risk. The following drugs were used in the study: selective cannabinoid CB1 receptor antagonist rimonabant (1 mg/kg), selective cannabinoid CB2 receptor antagonist of AM630 (2.5 mg/kg), selective bradykinin B2 receptors antagonist HOE140 (50 μg/kg), and vanilloid receptor (TRPV1 channels) antagonist capsazepine (3 mg/kg). All antagonists were administered 15 minutes before coronary artery occlusion. The choice of doses of pharmacological agents was based on the previous data [9–12].

Statistical data processing was performed using the Statistica 6.0 software (StatSoft, Inc.). The mean value (*M*) and standard error of the mean (*SEM*) were calculated. The significance of differences between groups was determined using the nonparametric Mann – Whitney *U*-test. The critical significance level was taken as $p = 0.05$.

RESULTS

Adaptation to normobaric hypoxia led to the formation of a pronounced infarct-limiting effect, the size of the infarct formed during coronary occlusion-reperfusion, defined as the ratio of the size of necrosis to the risk zone, was 38% less than in non-adapted rats. It should be noted that the hypertrophy of the right ventricle of the myocardium is characteristic of the state of chronic hypoxia (Table 1).

Table 1

Effect of CB1 cannabinoid receptor antagonist rimonabant and CB2 cannabinoid receptor antagonist Am630 on the infarct size after 45-minute coronary occlusion and 120-minute reperfusion in rats adapted to normobaric hypoxia, *M ± SEM*

Groups	*n*	Area of necrosis, mg	Area at risk, mg	Infarct size, AN/AR(%)	Right ventricular weight, mg	Left ventricular weight, mg
Control	12	186.9 ± 14.4	351.3 ± 9.8	53.2 ± 4.8	175.1 ± 11.3	981.7 ± 13.7
Rimonabant (1 mg/kg)	12	185.6 ± 14.4	355.3 ± 9.8	48.0 ± 4.8	170.1 ± 10.3	981.7 ± 13.7
AM630 (2.5 mg/kg)	12	181.7 ± 19.4	367.1 ± 22.4	49.5 ± 7.2	173.4 ± 10.7	947.8 ± 64.6
CNH	12	124.1 ± 12.8*	369.3 ± 15.1	33.6 ± 6.8*	226 ± 12.2*	958.3 ± 12.6
CNH + rimonabant (1 mg/kg)	12	131.8 ± 13.5*	374.3 ± 17.1	35.2 ± 8.3*	225.3 ± 17.6*	989.3 ± 15.5
CNH + AM630 (2.5 mg/kg)	12	118.6 ± 13.5*	364.8 ± 17.1	32.5 ± 8.2*	233.7 ± 13.9*	969.8 ± 12.9

Note: * $p < 0.05$ compared with the control group, Mann – Whitney *U*-test. AN – area of necrosis, AR – area at risk (here and in Table 2).

It was found that the inhibition of cannabinoid CB1 receptors by the selective antagonist rimonabant did not lead to a change in the infarct size in rats adapted to CNH (Table 1). These data indicate that CB1 cannabinoid receptors are not involved in the formation of the infarct-limiting effect of CNH. The injection of the selective CB2 cannabinoid receptor antagonist AM630 also did not affect the infarct size during coronary artery occlusion and reperfusion in rats adapted to CNH (Table 1). The administration of the selective cannabinoid receptor antagonists to non-adapted rats did not lead to a change in the infarct size during the subsequent coronary occlusion (Table 1). These data suggest that CB1 and CB2 cannabinoid receptors are not involved in the infarct-limiting effect of CNH.

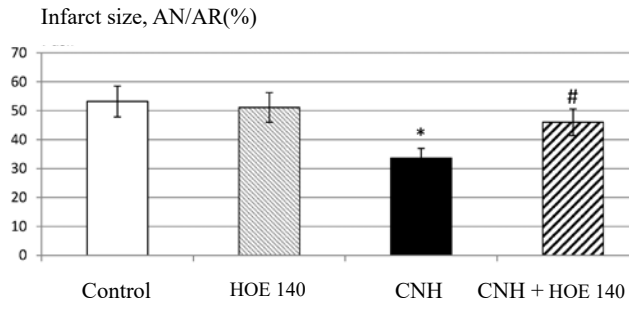

Fig. 1. Effect of the bradykinin receptor antagonist HOE 140 on the infarct size in rats after CNH

Note: * $p < 0.05$ compared with the control group, # – with the CNH group, Mann – Whitney *U*-test. AN – area of necrosis, AR – area at risk.

Blockade of bradykinin receptors by the selective antagonist HOE140 contributes to an increase in the infarct size in rats adapted to CNH (Fig. 1). Moreover, in non-adapted rats, blockade of the bradykinin receptors did not affect the infarct size. These data indicate that bradykinin receptors are involved in the formation of the infarct-limiting effect of CNH.

Inhibition of vanilloid receptors (TRPV1 channels) by the selective blocker capsazepine did not affect the infarct size in rats after a course of CNH or in non-adapted animals (Table 2). The obtained data allow us to conclude that there is no connection of TRPV1 channel activation and the formation of cardioprotection during adaptation to normobaric hypoxia.

Table 2

Effect of vanilloid receptor (TRPV1 channel) blocker capsazepine on rat infarct size after CNH, *M* ± *SEM*

Groups	*n*	Area of necrosis, mg	Area at risk, mg	Infarct size, AN/AR(%)	Right ventricular weight, mg	Left ventricular weight, mg
Control	12	186.9 ± 14.4	351.3 ± 9.8	53.2 ± 4.8	175.1 ± 11.3	981.7 ± 13.7
Capsazepine (3 mg/kg)	9	171.9 ± 18.5	353.6 ± 17.1	48.6 ± 6.2	199.4 ± 13.6	917.5 ± 19.3
CNH	12	124.1 ± 12.8*	369.3 ± 15.1	33.6 ± 6.8*	226 ± 12.2*	958.3 ± 12.6
CNH + capsazepine (3 mg/kg)	12	128.9 ± 12.2*	374.3 ± 17.1	34.7 ± 6.1*	218.1 ± 16.1*	976.6 ± 12.5

Note: * $p < 0.05$ compared with the control group, Mann – Whitney *U*-test. AN – area at necrosis, AR – area at risk.

DISCUSSION

The problem of myocardial protection in ischemic damage remains relevant, despite significant progress in this area. The reason for this is the lack of effective cardioprotective drugs that do not have strong side effects. Currently, beta-blockers, alpha-2-adrenoreceptor agonists, calcium channel blockers, nitrates, statins, and macroergic compounds are proposed to protect the myocardium from ischemic-reperfusion injury [13]. The effectiveness of a number of these drugs is insufficient for anti-ischemic protection, which, in the presence of many side effects, casts doubt on the feasibility of the use of the indicated drugs. Thus, the search for new means for myocardial protection during ischemic-reperfusion exposure remains an urgent task of modern pharmacology.

One of the ways of a directed search for such agents is a study of the mechanisms of non-specific adaptive resistance of the myocardium to ischemic damage. Thus, it is known that the myocardium of animals subjected to moderate chronic hypoxia is more resistant to ischemic effects than the myocardium of intact animals [1, 8, 14]. A study of this phenomenon has been conducted for 60 years, but many aspects of the formation of adaptive myocardial stability remain unexplored, its receptor mechanisms remain poorly understood. Previous studies in our laboratory have shown participation of opioid receptors in adaptive cardioprotection [1, 2].

This work revealed that bradykinin receptors are also involved in the mechanism of triggering the defense mechanism when adapting to chronic hypoxia. Both types of these receptors are known to be associated with Gi/o proteins that are located on the membrane of cardiomyocyte. Successive activation of receptors (opioid or bradykinin) and Gi/o proteins triggers an intracellular kinase mechanism that turns off protein kinase C, NO-synthase, tyrosine kinase, and subsequently activates ATP-sensitive potassium channels of mitochondria [14]. The result of the latter is inhibition of the opening of the pore that regulates the permeability of mitochondria (MPTP), an increase in the resistance of mitochondria to calcium ions, an improvement in the energy metabolism of mitochondria, and thus a decrease in the sensitivity of cells to the damaging effects of ischemia and reperfusion [15].

CONCLUSION

The obtained results allow us to present bradykinin receptors as one of the key mechanisms for the

formation of the infarct-limiting effect of continuous normobaric hypoxia. Taking into account the data on the important role of opioid receptors in cardioprotection in CNH [1, 2], we can talk about the implementation of the infarct-limiting effect of chronic hypoxia through Gi/o-protein-coupled opioid and bradykinin receptors. Cannabinoid receptors and TRPV1 channels do not participate in the infarct-limiting effect of adaptation to normobaric hypoxia.

REFERENCES

1. Maslov L.N., Naryzhnaia N.V., Tsibulnikov S.Y., Kolar F., Zhang Y., Wang H., Gusakova A.M., Lishmanov Y.B. Role of endogenous opioid peptides in the infarct size-limiting effect of adaptation to chronic continuous hypoxia. *Life Sci*. 2013; 93 (9–11): 373–379. DOI: 10.1016/j.lfs.2013.07.018.
2. Naryzhnaya N.V., Khaliulin I., Lishmanov Y.B., Suleiman M.S., Tsibulnikov S.Y., Kolar F., Maslov L.N. Participation of opioid receptors in the cytoprotective effect of chronic normobaric hypoxia. *Physiol. Res.* 2019; 68 (2): 245–253. DOI: 10.33549/physiolres.933938.
3. Maslov L.N., Khaliulin I., Zhang Y., Krylatov A.V., Naryzhnaya N.V., Mechoulam R., De Petrocellis L., Downey J.M. Prospects for creation of cardioprotective drugs based on cannabinoid receptor agonists. *J. Cardiovasc. Pharmacol. Ther.* 2016; 21 (3): 262–272. DOI: 10.1177/1074248415612593.
4. Gorbunov A.S., Maslov L.N., Jaggi A.S., Singh N., De Petrocellis L., Boshchenko A.A., Roohbakhsh A., Bezuglov V.V., Oeltgen P.R. Physiological and pathological role of TRPV1, TRPV2 and TRPV4 channels in heart. *Curr. Cardiol. Rev.* 2019; 15 (4): 244–251. DOI: 10.2174/1573403X15666190307112326.
5. Heusch G. Molecular basis of cardioprotection: signal transduction in ischemic pre-, post-, and remote conditioning. *Circ. Res.* 2015; 116 (4): 674–699. DOI: 10.1161/CIRCRESAHA.116.305348.
6. Randhawa P.K., Jaggi A.S.. Investigating the involvement of glycogen synthase kinase-3β and gap junction signaling in TRPV1 and remote hind preconditioning-induced cardioprotection. *Eur. J. Pharmacol*. 2017; 814: 9–17. DOI: 10.1016/j.ejphar.2017.07.045.
7. Sharma R., Randhawa P.K., Singh N., Jaggi A.S. Bradykinin in ischemic conditioning-induced tissue protection: Evidences and possible mechanisms. *Eur. J. Pharmacol*. 2015; 768: 58–70. DOI: 10.1016/j.ejphar.2015.10.029.
8. Neckář J., Szárszoi O., Herget J., Ošťádal B., Kolář F. Cardioprotective effect of chronic hypoxia is blunted by concomitant hypercapnia. *Physiol. Res*. 2003; 52 (2): 171–175.
9. Lichtman A.H., Wiley J.L., LaVecchia K.L., Neviaser S.T., Arthur D.B., Wilson D.M., Martin B.R. Effects of SR 141716A after acute or chronic cannabinoid administration in dogs. *Eur. J. Pharmacol.* 1998; 357 (2–3): 139–148. DOI: 10.1016/S0014-2999(98)00558-5.
10. Heymann H.M., Wu Y., Lu Y., Qvit N., Gross G.J., Gross E.R. Transient receptor potential vanilloid 1 inhibitors block laparotomy- and opioid-induced infarct size reduction in rats. *Br. J. Pharmacol.* 2017; 174 (24): 4826–4835. DOI: 10.1111/bph.14064.
11. Gross G.J., Hsu A., Gross E.R., Falck J.R., Nithipatikom K. Factors mediating remote preconditioning of trauma in the rat heart: central role of the cytochrome P450 epoxygenase pathway in mediating infarct size reduction. *J. Cardiovasc. Pharmacol. Ther*. 2013; 18 (1): 38–45. DOI: 10.1177/1074248412437586.
12. Toguri J.T., Moxsom R., Szczesniak A.M., Zhou J., Kelly M.E., Lehmann C. Cannabinoid 2 receptor activation reduces leukocyte adhesion and improves capillary perfusion in the iridial microvasculature during systemic inflammation. *Clin. Hemorheol. Microcirc*. 2015; 61 (2): 237–249. DOI: 10.3233/CH-151996.
13. Kozlov I.A. Prevention of complications caused by myocardial ischemia-reperfusion in noncardiac surgical procedures. *Bulletin of Siberian Medicine*. 2016; 15 (3): 102–119. DOI: 10.20538/1682-0363-2016-3-102-119 (in Russ.).
14. Naryzhnaya N.V., Maslov I.N., Khaliulin I.G., Zhang Y., Pei J.M., Tsepokina A.V., Khutornaya M.V., Kutikhin A.G., Lishmanov Y.B. Chronic continuous normobaric hypoxia augments cell tolerance to anoxia-reoxygenation: the role of protein kinases. *Russian Journal of Physiology.* 2016; 102 (12): 1462–1471 (in Russ.).
15. Prokudina E.S., Naryzhnaya N.V., Mukhomedzyanov A.V., Gorbunov A.S., Zhang Y., Yaggi A.S., Tsibulnikov S.Y., Nesterov E.A., Lishmanov Y.B., Suleiman M.S., Oeltgen P.R., Maslov L.N. Effect of chronic continuous normobaric hypoxia on functional state of cardiac mitochondria and tolerance of isolated rat heart to ischemia and reperfusion: role of μ and delta2 opioid receptors. *Physiol. Res*. 2019; 68 (6): 909–920. DOI: 10.33549/physiolres.933945.

Authors information

Naryzhnaya Natalya V., Dr. Sci. (Med.), Leading Researcher, Laboratory of Experimental Cardiology, Research Institute of Cardiology, Tomsk NRMC, Tomsk, Russian Federation. ORCID 0000-0003-2264-1928.

Mukhomedzyanov Alexander V., Junior Researcher, Laboratory of Experimental Cardiology, Research Institute of Cardiology, Tomsk NRMC, Tomsk, Russian Federation. ORCID 0000-0003-1808-556X.

Tsibulnikov Sergey Yu., Senior Researcher, Laboratory of Experimental Cardiology, Research Institute of Cardiology, Tomsk NRMC, Tomsk, Russian Federation. ORCID 0000-0003-1534-2516.

Maslov Leonid N., Dr. Sci. (Med.), Professor, Head of the Laboratory of Experimental Cardiology, Research Institute of Cardiology, Tomsk NRMC, Tomsk, Russian Federation. ORCID 0000-0002-6020-1598.

(✉) **Tsibulnikov Sergey Yu.,** e-mail: tsibulnikov1986@mail.ru.

Received 02.03.2020
Accepted 29.09.2020

УДК 612.112.3:612.112.95]:621.318.1-022.532:576.535
https://doi.org/10.20538/1682-0363-2020-4-143-150

Modification of human monocytes and macrophages by magnetic nanoparticles in vitro for cell-based delivery

Perekucha N.A.[1], Smolina P.A.[1], Demin A.M.[2], Krasnov V.P.[2], Pershina A.G.[1, 3]

[1] *Siberian State Medical University*
2, Moscow Trakt, Tomsk, 634050, Russian Federation

[2] *Postovsky Institute of Organic Synthesis, Ural Branch of Russian Academy of Sciences*
22, S. Kovalevskoy Str., Yekaterinburg, 620990, Russian Federation

[3] *National Research Tomsk Polytechnic University*
30, Lenina Av., Tomsk, 634050, Russian Federation

ABSTRACT

The aim of the study was to develop a method for the modification of human monocytes/macrophages by iron oxide magnetic nanoparticles *in vitro*.

Materials and methods. Iron oxide magnetic nanoparticles were obtained by a co-precipitation method and coated with a thin SiO_2 layer and polyethylene glycol 3000. Murine macrophage-like cell line RAW 264.7, primary human monocytes and macrophages were incubated with magnetic nanoparticles for 1–24 hours. The efficiency of cellular uptake of nanoparticles was measured using a ferrozine-based method and microcopy with Perls' Prussian blue staining. The cell viability was tested by fluorescent flow cytometry using SYTOX Green.

Results. Incubation of RAW264.7 cell, human monocytes and macrophages with magnetic nanoparticles at a concentration > 5 μg/mL on a rotator for 1 hour at 37 °C provides the loading of nanoparticles into > 99% of cells. The magnetic nanoparticles have no adverse effect on the cell viability. The RAW264.7 cells modified with nanoparticles showed no change in migration activity. The efficiency of the nanoparticle uptake by macrophages was >50 pkg (Fe)/cell.

Conclusion. According to the proposed method, macrophages loaded with magnetic nanoparticles have proved viable, they retain the ability to migrate, and therefore can be used as cell-based delivery systems for tumor diagnostic and therapy.

Key words: magnetic nanoparticles, monocytes, macrophages, cell-based delivery system.

Conflict of interest. The authors declare the absence of obvious and potential conflicts of interest related to the publication of this article.

Source of financing. State Assignment of Siberian State Medical University No. AAAA-A18-118031490008-7.

Conformity with the principles of ethics. The study was approved by the local Ethics Committee at Siberian State Medical University (Protocol No. 7698 of 25.02.2019).

For citation: Perekucha N.A., Smolina P.A., Demin A.M., Krasnov V.P., Pershina A.G. Modification of human monocytes and macrophages by magnetic nanoparticles in vitro for cell-based delivery. *Bulletin of Siberian Medicine.* 2020; 19 (4): 143–150. https://doi.org/10.20538/1682-0363-2020-4-143-150.

✉ *Pershina Alexandra G.,* e-mail: allysyz@mail.ru.

Модификация макрофагов и моноцитов человека магнитными наночастицами *in vitro* для доставки, опосредованной клетками

Перекуча Н.А.[1], Смолина П.А.[1], Дёмин А.М.[2], Краснов В.П.[2], Першина А.Г.[1, 3]

[1] *Сибирский государственный медицинский университет (СибГМУ)*
Россия, 634050, г. Томск, Московский тракт, 2

[2] *Институт органического синтеза (ИОС) им. И.Я. Постовского Уральского отделения Российской академии наук (УрО РАН)*
Россия, 620990, г. Екатеринбург, ул. С. Ковалевской, 22

[3] *Национальный исследовательский Томский политехнический университет (НИ ТПУ)*
Россия, 634050, г. Томск, пр. Ленина, 30

РЕЗЮМЕ

Цель исследования – разработать протокол модификации макрофагов и моноцитов человека магнитными наночастицами оксида железа (Fe_3O_4) *in vitro.*

Материалы и методы. Магнитные наночастицы оксида железа получены методом со-осаждения, покрыты силоксановой оболочкой и полиэтиленгликолем 3000. Макрофаги мыши линии RAW 264.7, моноциты периферической крови и макрофаги человека инкубировали с магнитными наночастицами в течение 1–24 ч. Эффективность захвата наночастиц клетками оценивали феррозиновым методом и методом микроскопии с окрашиванием на железо по Перлсу. Исследование жизнеспособности клеток выполняли методом проточной цитофлуориметрии с использованием красителя SYTOX Green.

Результаты. Инкубация макрофагов с магнитными наночастицами в концентрации >5 мкг/мл в течение 1 ч на ротаторе при 37 °С обеспечивает загрузку наночастиц в >99% клеток. Исследуемые магнитные наночастицы не оказывают негативных эффектов на жизнеспособность клеток. Клетки линии RAW 264.7, поглотившие наночастицы, сохраняют миграционную активность. Эффективность загрузки макрофагов магнитными наночастицами составляет >50 пкг (Fe)/клетку.

Заключение. Макрофаги, загруженные магнитными наночастицами согласно предложенному протоколу, являются жизнеспособными, сохраняют способность к миграции и перспективны в качестве систем доставки, опосредованной клетками, для диагностики и терапии опухоли.

Ключевые слова: магнитные наночастицы, моноциты, макрофаги, системы доставки на основе клеток.

Конфликт интересов. Авторы гарантируют отсутствие потенциальных и явных конфликтов интересов, связанных с публикацией данной статьи.

Источник финансирования. Работа выполнена в рамках государственного задания Сибирского государственного медицинского университета (No. АААА-А18-118031490008-7).

Соответствие принципам этики. Все участники исследования подписали добровольное информированное согласие. Исследование одобрено локальным этическим комитетом СибГМУ (протокол № 7698 от 25.02.2019).

Для цитирования: Перекуча Н.А., Смолина П.А., Дёмин А.М., Краснов В.П., Першина А.Г. Модификация макрофагов и моноцитов человека магнитными наночастицами *in vitro* для доставки, опосредованной клетками. *Бюллетень сибирской медицины.* 2020; 19 (4): 143–150. https://doi.org/10.20538/1682-0363-2020-4-143-150.

INTRODUCTION

Magnetic nanoparticles (MNPs) are being actively studied to develop alternative approaches to therapy [1] and diagnostics of malignant neoplasms [2, 3], including controlled drug delivery [4, 5] and monitoring the effectiveness of tumor chemotherapy [6].

However, the problem of efficient delivery of MNPs to the tumor still remains unresolved [7]. One of the promising approaches to solving this problem is using autologous leukocytes as biocontainers for the delivery of nanoparticles [8, 9]. Leukocytes are capable of active migration, as they can pass through the

endothelium of capillaries and penetrate into the intercellular space, which makes them ideal "couriers" [10], allowing them to increase the delivery efficiency by more than 100 times [11].

Among leukocytes, monocytes and macrophages are the most attractive populations for the development of a nanoparticle delivery system within cells. An important feature of monocytes and macrophages, in contrast to neutrophils, is the ability to maintain their viability for a long time after phagocytosis of particles. The pronounced phagocytic capacity of monocytes and macrophages favorably distinguishes them from lymphocytes; to efficiently load the latter with nanoparticles, special methods are needed [12].

The ability of monocytes and macrophages due to chemotaxis [13] to penetrate into hypoxic zones of tumor promises to solve the problem of impact on cancer cells in these areas, which are practically inaccessible for penetration of conventional pharmacological drugs [14].

The first step in implementing cell-based delivery systems is creating complexes of immune cells with nanoparticles. There exist several approaches [15, 16]; the main method is *in vitro* assembly, when nanoparticles either attach to the surface of the cell membrane or are internalized in cells [17, 18]. An alternative approach is using nanoparticles coated with isolated cell membranes [19].

Optimization of the parameters of cell modification with nanoparticles is important in the development of delivery systems. The modification should not lead to significant changes in the cellular immune response, the rate of differentiation, the migration ability of cells, or a decrease in viability [20].

The aim of this work was to develop a method for loading iron oxide (Fe_3O_4) MNPs into human macrophages/monocytes *in vitro*.

MATERIALS AND METHODS

Iron oxide (Fe_3O_4) MNPs with an average diameter of 10 nm were obtained by a method of co-precipitation from aqueous solutions of Fe^{2+} and Fe^{3+} salts, coated with SiO_2 and covalently modified with O-[N-(6-Maleimidohexanoyl)aminoethyl]-O′-[3-(N-succinimidyloxy)-3-oxopropyl]polyethylene glycol 3,000 (PEG). To obtain fluorescent labeled particles, Cyanine5 NHS ester (Lumiprobe, Cy5, Russia) was used. The received nanoparticles (MNP-PEG) formed stable colloidal suspensions in aqueous buffers with an average hydrodynamic diameter of 190 nm (PdI < 0.06).

RAW264.7 cells were cultured in DMEM/F12 complete medium (Thermo Fisher Scientific, USA) supplemented with 10% fetal bovine serum (FBS, Gibco, USA), L-glutamine (Glutamax, Gibco) and gentamicin at 5% CO_2, 37 °C. A scraper was used to remove adhered cells.

To isolate monocytes, peripheral blood from healthy donors was collected from the cubital vein into a vacutainer with heparin (Green Vac-Tube with Li-heparin, Green Cross) in a volume of 30 ml. Isolation of mononuclear cells from the peripheral blood of the healthy donors was carried out by centrifugation on a Ficoll 1.077 density gradient (PanEco, Russia). Isolation of monocytes from the mononuclear fraction was carried out on magnetic columns (Miltenyi Biotec) using magnetic particles with antibodies to CD14 (Miltenyi Biotec Inc., Germany). Monocytes were cultured in RPMI 1640 complete medium (PanEco) mixed with 1% L-glutamine (Glutamax, Gibco), 10% FBS, and 1% penicillin-streptomycin (PanEco). The purity of the human monocyte population was assessed using PE Mouse Anti-Human CD14 (Clone M5E2) antibodies (BD Biosciences, USA). The purity of the monocyte population was at least 97%.

To obtain macrophages, monocytes were incubated in RPMI complete medium supplemented with granulocyte-macrophage colony-stimulating factor (GM-CSF, Sigma, USA) to a concentration of 100 ng/ml for 7 days, with a medium change every 3 days. Maturation was assessed using Pacific Blue anti-human CD11b Antibody (Clone ICRF44) (Biolegend, USA) and PE anti-human CD68 Antibody (Biolegend). The purity of the macrophage population was at least 91%.

To study the uptake of nanoparticles, 10^5 cells of the RAW264.7 line in 450 μl of DMEM/F12 complete medium were introduced into 2 ml tubes or seeded in the wells of a 24-well plate. Then, 1/10 of the MNP-PEG suspension (50 μl) in phosphate-buffered saline (PBS) was added to the cells. An equivalent volume of 1 × PBS was added to control cell samples. The cells in tubes were incubated at 37 °C for 1 or 2 hours on a rotator, cells in 24-well plates were incubated for 1 hour in a CO_2 incubator.

After the incubation with MNP-PEG on a rotator, the cells were centrifuged for 7 minutes at 180 × *g*, resuspended in 1 × PBS to wash away nanoparticles, centrifuged, and the pellet was resuspended in 200 μl of 1 × PBS. After the incubation with MNP-PEG, the adherent cells were washed twice with 1 × PBS, removed with a scraper, and transferred into

2 ml tubes. The cells were centrifuged for 7 minutes at 180 *g*, the pellet was resuspended in 200 µl of 1 × PBS.

Viability was assessed on a BD Accuri C6 flow cytometer (BD Biosciences) using SYTOX Green (Thermo Fisher Scientific). For confocal microscopy, cell nuclei were stained with Hoechst 33342 in PBS (5 µg/ml). The study was carried out on a Carl Zeiss LSM 710 confocal microscope. A Prussian Blue Iron Stain Kit (Polysciences, Inc., USA) was used to detect iron in the cells. The cells were analyzed using light microscopy (Leica DMi8). The iron content in cells was determined by the ferrozine method as described in [21]. The rate of cell migration was assessed according to the proposed method [22].

Statistical analysis of the data was performed using the GraphPad Prism 7 software package. The Shapiro – Wilk test was used to control the normal distribution of the data. Data with normal distribution were presented as mean and standard deviation ($M \pm SD$). The statistical significance of differences was determined using the Student's *t*-test. For multiple comparisons, one-way ANOVA with post-hoc Dunnett's test was used. The significance level was defined as $p < 0.05$.

RESULTS

To select optimal conditions for loading cells with nanoparticles, two incubation modes were tested on RAW 264.7 cells: with cells adhered to a culture plate and in a suspension with continuous mixing on the rotator. During the incubation of RAW 264.7 and MNP-PEG in a concentration range of 0.625–5 µg/ml, it was found that MNP-PEG were more efficiently absorbed by the cells in the suspension (when incubated on the rotator) than by adherent cells. Particularly, at a concentration of MNP-PEG of 5 µg/ml after 1 hour of incubation on the plate, the proportion of Cy5-positive cells was 38.0 ± 2.5%; while during the incubation on the rotator, the percentage of the cells that were loaded with nanoparticles was 99.7 ± 0.1%. With a 2-hour increase in the incubation period on the rotator, the number of the cells that were loaded with nanoparticles grew to 99.9 ± 0.04% (Fig. 1,*a*).

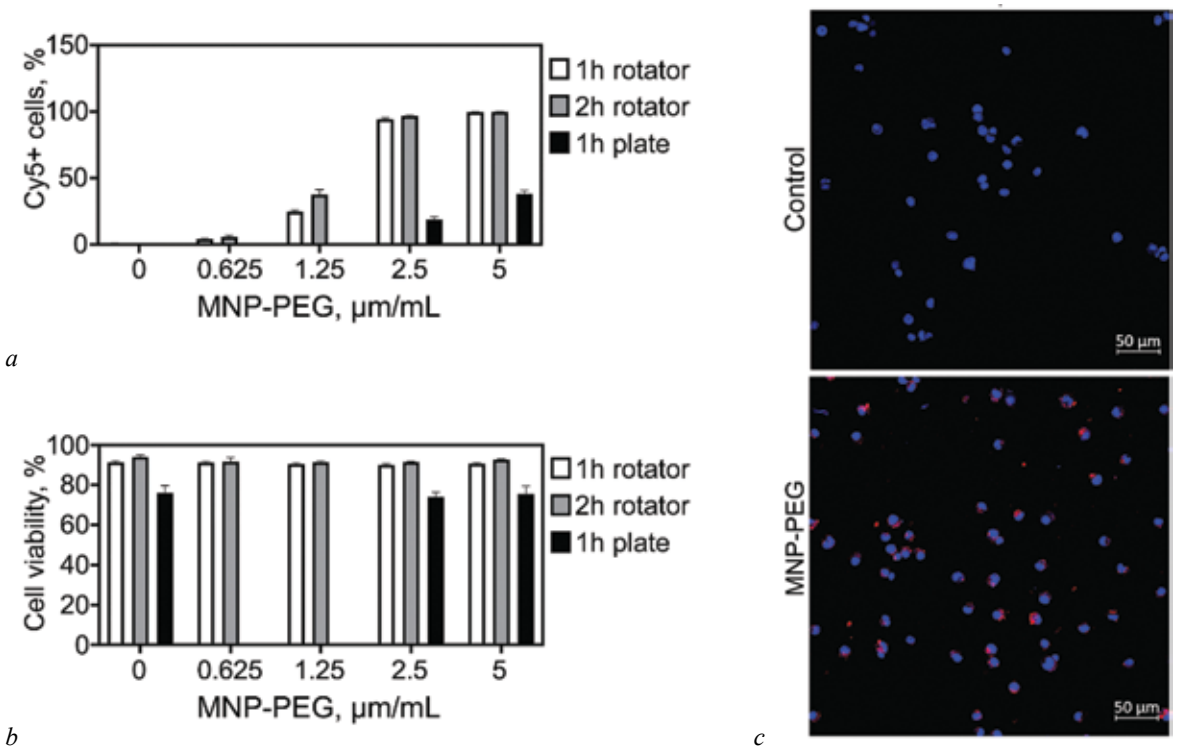

Fig. 1. Uptake of MNP-PEG by RAW264.7 cells: *a* – efficiency of MNP-PEG uptake by RAW264.7 cells under various incubation conditions; *b* – viability of RAW264.7 cells under various incubation conditions as determined by fluorescence flow cytometry with SYTOX Green; *c* – image of RAW264.7 cells incubated without nanoparticles (control) and after incubation with MNP-PEG for 1 hour on the rotator, obtained by confocal microscopy (Carl Zeiss LSM 710). Cell nuclei are colored blue (Hoechst 33342), nanoparticles are colored red (Cyanine5). Scale bar: 50 µm

After the incubation of cells with MNP-PEG on the rotator, more than 90% of RAW264.7 cells retained their viability. In particular, after 1 hour of incubation with MNP-PEG at a concentration of 5 μg/ml on the rotator, the percentage of living cells was (90.7 ± 0.3)%, which did not differ from the values obtained for controls (91.4 ± 0.8)% (Fig. 1,*b*). After the incubation of adhered cells on a plate with the addition of MNP-PEG, the proportion of dead cells was 24.5 ± 4.0% and did not differ from the value in controls (24.0 ± 3.7)%. This outcome is probably due to the negative effect of using a scraper to remove adhered cells from the plastic surface.

The efficient uptake of MNP-PEG by RAW 264.7 cells was confirmed by confocal microscopy data. In particular, Cy5-positive inclusions were observed in the cytoplasm of RAW 264.7 cells after their incubation with MNP-PEG (Figure 1*b*).

The selected incubation mode, 1 hour on the rotator at 37 °C, was further used for quantitative assessment of the efficiency of the "loading" of RAW 264.7 cells. As many as 10^6 cells were incubated with MNP-PEG at a high concentration (50 μg/ml). Then the cells were washed and resuspended in 1 × MACS buffer. After sorting on the magnetic columns, the number of cells in the washing solutions and cell suspension eluted from the column after it was removed from the magnetic separator was counted. The efficiency of magnetic sorting for RAW 264.7 cells was 77%. "Magnetically positive" cells were transferred into the wells of a 6-well plate and incubated for 2 hours in a CO_2 incubator for cell adhesion; then they were additionally washed from nanoparticles twice with 1 × PBS. Then the cells were removed from the plastic surface to determine the iron content in them. According to the ferrozine test, the efficiency of the uptake of nanoparticles by RAW264.7 macrophages was (58 ± 14) pkg/cell. According to flow cytometry data with SYTOX Green, after the modification of the cells with MNP-PEG nanoparticles, the proportion of dead cells was (9.9 + 3.6)%, which did not differ from the values obtained in controls (11.8 + 4.6)%.

When examining the "magnetically positive" RAW264.7 cells with light microscopy, a large number of Prussian blue positive granules were observed in the cytoplasm (Fig. 2).

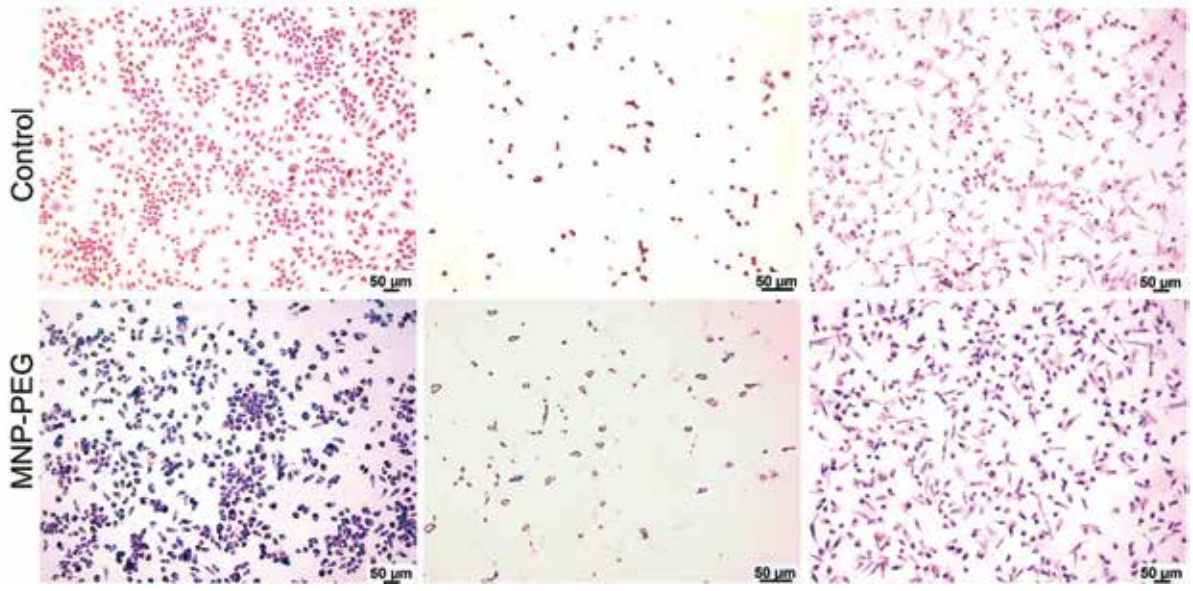

a *b* *c*

Fig. 2. Image of RAW264.7 cells (*a*), human peripheral blood monocytes (*b*) and (*c*) human monocyte-derived macrophages incubated without nanoparticles (control) and after loading with MNP-PEG and magnetic sorting. Prussian blue staining. Scale bar: 50 μm

The migration rate of RAW264.7 cells "loaded" with MNP-PEG was 12.6 μm/h (Fig. 3) and practically did not differ from the cell migration rate in controls (14.8 μm/h).

In the follow-up series of experiments, we studied the uptake of MNP-PEG by human peripheral blood monocytes and by macrophages differentiated from peripheral blood monocytes. Incubation was carried out under the conditions selected for RAW264.7 cells: non-adherent cells in a suspension were incubated with MNP-PEG at a concentration of 50 μg/ml for 1 hour on the rotator at 37 °C. MNP-PEG were absorbed by both

human monocytes and macrophages. Light microscopic images of "magnetically positive" human macrophages adhered to the plate are shown in Fig. 2,*b*.

According to the data on the iron content in cells after their incubation with MNP-PEG, it was found that the efficiency of the uptake of nanoparticles by monocytes was (46 ± 6) pkg/cell, and by macrophages, (369 ± 96) pkg/cell. The efficiency of magnetic sorting of macrophages after their "loading" with MNP-PEG was 93%. Despite the 100% modification of the cell population with nanoparticles (according to flow cytometry data), the loading density of each individual cell might vary. As a result, some cells lack enough particles to effectively retain them on the magnetic column. It is important to note that the viability of the cells loaded with MNP-PEG did not differ from the values obtained in controls.

The research into the influence of MNP-PEG on the viability of human peripheral blood mononuclear cells and monocytes after 24-hour co-incubation showed that MNP-PEG had no negative effects on cell viability (Fig. 4).

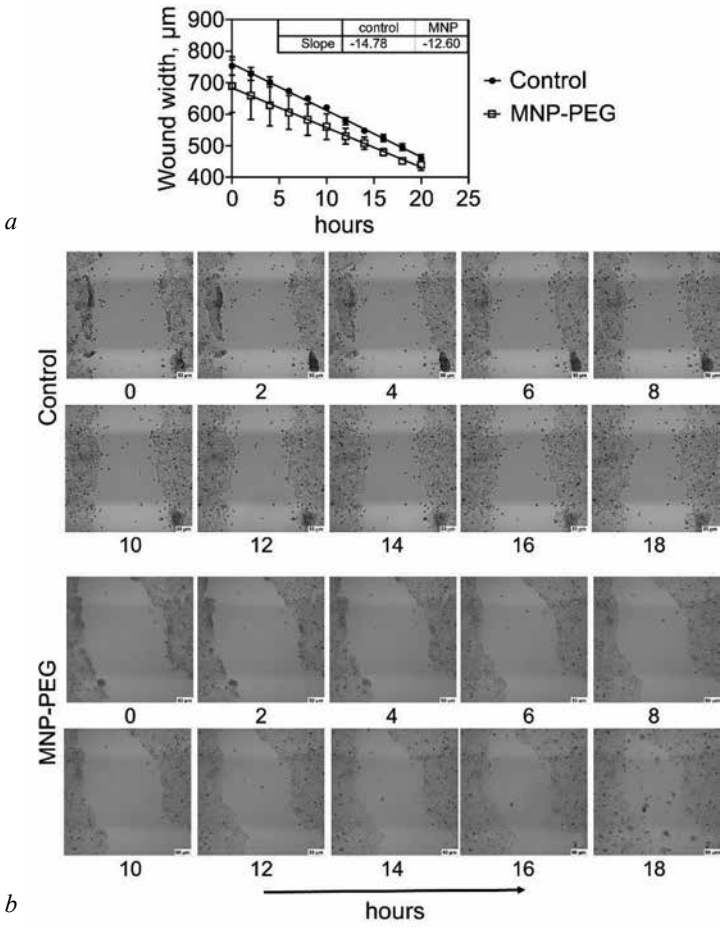

Fig. 3. Study of the migration activity of RAW264.7 cells: *a* – calculation of the migration rate of RAW264.7 cells in controls and cells loaded with MNP-PEG: *b* – images of RAW264.7 cells incubated without nanoparticles (control) and after loading with MNP-PEG and magnetic sorting, obtained within 18 hours after the formation of a "wound" on the adhesion layer

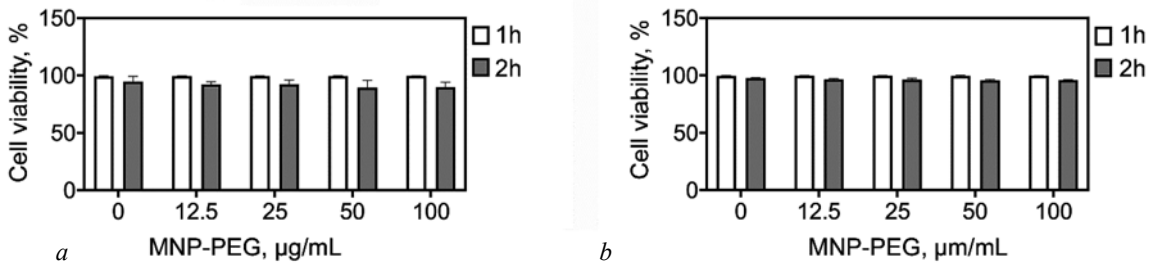

Fig. 4. Influence of MNP-PEG on the viability of human blood cells: viability of (*a*) mononuclear cells and (*b*) human peripheral blood monocytes after their incubation with MNP-PEG (12.5–100 mg/ml) for 1 and 24 hours according to fluorescence flow cytometry with SYTOX Green

DISCUSSION

Earlier experiments demonstrated successful creation of delivery systems based on monocyte-macrophage cell lines modified by nanoparticles [23], as well as on alveolar [24], peritoneal [25], and bone marrow macrophages [20]. However, research works on the uptake of nanoparticles by primary cultures of human monocyte/macrophage cells are very scarce.

The incubation period with MNPs required to achieve maximum accumulation varies considerably from 1 to 24 hours, according to the literature. It was shown that timing depends on the type of surface modification of nanoparticles [26]. According to our data, an increase in the incubation period up to 2 hours did not lead to a noticeable increase in the number of "loaded" cells; and therefore, to optimize the method, an incubation period of 1 hour was chosen.

This research work established that macrophages exhibited a more pronounced phagocytic activity towards nanoparticles, which is in line with the results of the comparative study on the uptake of nanoparticles by cells of the human monocyte-like cell line THP-1 and after their differentiation into macrophages dTHP-1 [27]: the efficiency was 6 and 50 pkg/cell for THP-1 and dTHP-1, respectively. Note that the uptake efficiency of MNP-PEG is much higher.

CONCLUSION

Iron oxide MNPs coated with SiO_2 and PEG are efficiently uptaken by RAW 264.7 mouse macrophage, human peripheral blood monocytes, and human monocyte-derived macrophages. The optimal loading conditions are incubation of non-adherent cells (in a suspension) with nanoparticles for 1 hour on the rotator at 37 °C. MNPs are absorbed by > 99% of cells in the suspension and have no cytotoxic effect on RAW 264.7 cells, human peripheral blood monocytes and macrophages. Therefore, macrophages loaded with MNPs, according to the proposed method, are viable, retain the ability to migrate, and can be used as systems for delivering magnetic nanoparticles to a tumor.

REFERENCES

1. Liu X., Zhang Y., Wang Y., Zhu W., Li G., Ma X. et al. Comprehensive understanding of magnetic hyperthermia for improving antitumor therapeutic efficacy. *Theranostics.* 2020; 10 (8): 3793–3815. DOI: 10.7150/thno.40805.
2. Yu E.Y., Bishop M., Zheng B., Ferguson R.M., Khandhar A.P., Kemp S.J. et al. Magnetic Particle Imaging: A Novel *in vivo* imaging platform for cancer detection. *Nano Lett.* 2017; 17 (3): 1648–1654. DOI: 10.1021/acs.nanolett.6b04865.
3. Lee J., Huh Y., Jun Y., Seo J., Jang J., Song H. et al. Artificially engineered magnetic nanoparticles for ultra-sensitive molecular imaging. *Nat. Med.* 2007; 13 (1): 95–99. DOI: 10.1038/nm1467.
4. Huang Y., Gao X., Chen J. Leukocyte-derived biomimetic nanoparticulate drug delivery systems for cancer therapy. *Acta Pharmaceutica Sinica B*. 2018; 8 (1): 4–13. DOI: 10.1016/j.apsb.2017.12.001.
5. Shaghasemi S.B., Virk M.M., Reimhult E. Optimization of magneto-thermally controlled release kinetics by tuning of magnetoliposome composition and structure. *Scientific Reports.* 2017; 7 (1): 1–10. DOI: 10.1038/s41598-017-06980-9.
6. Zhao H., Richardson R., Talebloo N., Mukherjee P., Wang P., Moore A. uMUC1-targeting magnetic resonance imaging of therapeutic response in an orthotropic mouse model of colon cancer. *Mol. Imaging Biol.* 2019; 21 (5): 852–860. DOI: 10.1007/s11307-019-01326-5.
7. Wilhelm S., Tavares A.J., Dai Q., Ohta S., Audet J., Dvorak H.F. et al. Analysis of nanoparticle delivery to tumours. *Nature Reviews Materials*. 2016; 1 (5): 16014. DOI: 10.1038/natrevmats.2016.14.
8. Huang Y., Gao X., Chen J. Leukocyte-derived biomimetic nanoparticulate drug delivery systems for cancer therapy. *Acta Pharmaceutica Sinica B*. 2018; 8 (1): 4–13. DOI: 10.1016/j.apsb.2017.12.001.
9. Choi M.R., Stanton-Maxey K.J., Stanley J.K., Levin C.S., Bardhan R., Akin D. et al. A cellular Trojan Horse for delivery of therapeutic nanoparticles into tumors. *Nano Letters*. 2007; 7 (12): 3759–3765. DOI: 10.1021/nl072209h.
10. Moore T.L., Hauser D., Gruber T., Rothen-Rutishauser B., Lattuada M., Petri-Fink A. et al. Cellular shuttles: monocytes/macrophages exhibit transendothelial transport of nanoparticles under physiological flow. *ACS Applied Materials & Interfaces*. 2017; 9 (22): 18501–18511. DOI: 10.1021/acsami.7b03479.
11. Han H., Eyal S., Portnoy E., Mann A., Shmuel M., Benifla M. et al. Monocytes as carriers of magnetic nanoparticles for tracking inflammation in the epileptic rat brain. *Curr. Drug Deliv*. 2019; 16 (7): 637–644. DOI: 10.2174/1567201816666190619122456.
12. Steinfeld U., Pauli C., Kaltz N., Bergemann C., Lee H.-H. T lymphocytes as potential therapeutic drug carrier for cancer treatment. *International Journal of Pharmaceutics*. 2006; 311 (1–2): 229–236. DOI: 10.1016/j.ijpharm.2005.12.040.
13. Si J., Shao S., Shen Y., Wang K. Macrophages as active nanocarriers for targeted early and adjuvant cancer chemotherapy. *Small*. 2016; 12 (37): 5108–5119. DOI: 10.1002/smll.201601282.
14. Quatromoni J.G., Eruslanov E. Tumor-associated macrophages: function, phenotype, and link to prognosis in human lung cancer. *American Journal of Translational Research*. 2012; 4 (4): 376–389.
15. Anselmo A.C., Gilbert G.B., Kumar S., Gupte V., Cohen R.E., Rubner M.F. et al. Monocyte-mediated delivery of polymeric backpacks to inflamed tissues: a generalized strategy to deliver drugs to treat inflammation. *Journal of Controlled Release*. 2015; 199: 29–36. DOI: 10.1016/j.jconrel.2014.11.027.

16. Hao J., Chen J., Wang M., Zhao J., Wang J., Wang X. et al. Neutrophils, as "Trojan horses", participate in the delivery of therapeutical PLGA nanoparticles into a tumor based on the chemotactic effect. *Drug Deliv*. 2020; 27 (1): 1–14. DOI: 10.1080/10717544.2019.1701141.
17. Irvine D.J., Hanson M.C., Rakhra K., Tokatlian T. Synthetic nanoparticles for vaccines and immunotherapy. *Chemical Reviews*. 2015; 115 (19): 11109–11146. DOI: 10.1021/acs.chemrev.5b00109.
18. Dong X., Chu D., Wang Z. Leukocyte-mediated delivery of nanotherapeutics in inflammatory and tumor sites. *Theranostics*. 2017; 7 (3): 751–763. DOI: 10.7150/thno.18069.
19. Cao H., Dan Z., He X., Zhang Z., Yu H., Yin Q. et al. Liposomes coated with isolated macrophage membrane can target lung metastasis of breast cancer. *ACS Nano*. 2016; 10(8): 7738–7748. DOI: 10.1021/acsnano.6b03148.
20. Tong Y.-I., Kang W., Shi Y., Zhou G., Lu Y. Physiological function and inflamed-brain migration of mouse monocyte-derived macrophages following cellular uptake of superparamagnetic iron oxide nanoparticles – Implication of macrophage-based drug delivery into the central nervous system. *Int. J. Pharm*. 2016; 505 (1–2): 271–282. DOI: 10.1016/j.ijpharm.2016.03.028.
21. Pershina A.G., Brikunova O.Y., Perekucha N.A., Demin A.M., Shevelev O.B., Malkeyeva D., Kiseleva E., Minin A., Kostikova L.A., Stepanov I.V., Kuznetsov D.K., Shur V.Ya., Krasnov V.P. Supporting data and methods for the characterization of iron oxide nanoparticles conjugated with pH-(low)-insertion peptide, testing their cytotoxicity and analyses of biodistribution in SCID mice bearing MDA-MB231 tumor. *Data in Brief*. 2020; 29: 105062. DOI: 10.1016/j.dib.2019.105062.
22. Justus C.R., Leffler N., Ruiz-Echevarria M., Yang L.V. *In vitro* cell migration and invasion assays. *J. Vis. Exp*. 2014; (88): 51046. DOI: 10.3791/51046.
23. Basel M.T., Balivada S., Wang H., Shrestha T. Cell-delivered magnetic nanoparticles caused hyperthermia-mediated increased survival in a murine pancreatic cancer model. *International Journal of Nanomedicine.* 2012; 7: 297–306. DOI: 10.2147/IJN.S28344.
24. Madsen S.J., Christie C., Hong S.J., Trinidad A., Peng Q., Uzal F.A. et al. Nanoparticle-loaded macrophage-mediated photothermal therapy: potential for glioma treatment. *Lasers in Medical Science*. 2015; 30 (4): 1357–1365. DOI: 10.1007/s10103-015-1742-5.
25. Choi J., Kim H.Y., Ju E.J., Jung J., Park J., Chung H.K. et al. Use of macrophages to deliver therapeutic and imaging contrast agents to tumors. *Biomaterials*. 2012; 33 (16): 4195–4203. DOI: 10.1016/j.biomaterials.2012.02.022.
26. Beduneau A., Ma Z., Grotepas C.B., Kabanov A., Rabinow B.E., Gong N. et al. Facilitated monocyte-macrophage uptake and tissue distribution of superparmagnetic iron-oxide nanoparticles. *PLoS One*. 2009; 4 (2): e4343. DOI: 10.1371/journal.pone.0004343.
27. Luciani N., Gazeaua F., Wilhelm C. Reactivity of the monocyte/macrophage system to superparamagnetic anionic nanoparticles. *J. Mater. Chem.* 2009; 19 (35): 6373–6380. DOI: 10.1039/b903306h.

Authors contribution

Perekucha N.A. – implementation of the experimental part of the study, interpretation and analysis of data, drafting of the manuscript. Smolina P.A. – implementation of the experimental part of the study. Demin A.M., Krasnov V.P. – synthesis of magnetic nanoparticles. Pershina A.G. – conception and design, interpretation and analysis of data, editing of the manuscript, critical revision of the manuscript for important intellectual content.

Authors information

Perekucha Natalya A., Junior Researcher, Center of Bioscience&Bioengineering, Central Research Laboratory, Siberian State Medical University, Tomsk, Russian Federation. ORCID 0000-0001-9310-3196.

Smolina Polina A., Student, Department of Biomedicine, Siberian State Medical University, Tomsk, Russian Federation. ORCID 0000-0001-9216-9572.

Demin Aleksandr M., Cand. Sci. (Chemistry), Senior Researcher, Laboratory of Asymmetric Synthesis, Postovsky Institute of Organic Synthesis, Yekaterinburg, Russian Federation. ORCID 0000-0002-4132-232.7

Krasnov Viktor P., Dr. Sci. (Chemistry), Professor, Head of the Laboratory of Asymmetric Synthesis, Postovsky Institute of Organic Synthesis, Yekaterinburg, Russian Federation. ORCID 0000-0003-1411-6218.

Pershina Aleksandra G., Cand. Sci. (Biology), Head of the Center of Bioscience&Bioengineering, Central Research Laboratory, Siberian State Medical University; Associate Professor, Research School of Chemical and Biomedical Engineering, National Research Tomsk Polytechnic University, Tomsk, Russian Federation. ORCID 0000-0001-7604-9722.

(✉) **Pershina Alexandra G.,** e-mail: allysyz@mail.ru.

Received 08.09.2020
Accepted 03.11.2020

УДК 616.33-021.6:62-631.42:615.24
https://doi.org/10.20538/1682-0363-2020-4-151-157

Gastroprotective effect of *Ferulopsis hystrix* (Bunge) Pimenov in ethanol-induced gastropathy

Salchak S.M.[1], Razuvaeva Ya.G.[1], Toropova A.A.[1], Arakchaa K.D.[2], Olennikov D.N.[1], Nikolaev I.G.[1]

[1] *Institute of General and Experimental Biology, Siberian Branch of the Russian Academy of Sciences 6, Sakhyanovoy Str., Ulan-Ude, 670047, Russian Federation*

[2] *Scientific Research Institute of Medical-Social Problems and Management of the Republic of Tuva 2a, Kechil-oola Str., Kyzyl, Republic of Tuva, 667003, Russian Federation*

ABSTRACT

The aim of the study was to evaluate the gastroprotective effect of dry extracts from the roots and rhizomes of *Ferulopsis hystrix* in ethanol-induced gastropathy.

Materials and methods. The studies were carried out on 68 white *Wistar* rats. Ethanol-induced gastropathy was simulated by a single intragastric administration of ethanol in the dose of 10 ml/kg. Animals of the experimental groups received medicinal forms from the roots and rhizomes of *F. hystrix*: I – decoction in a volume of 10 ml/kg; II–V – dry extracts in the dose of 200 mg/kg, obtained by extraction with purified water, 30, 40 and 70% ethanol, respectively; VI – dry extract, prepared by double extraction with 40% and single extraction with 30% ethanol for 7 days before the modeling of gastropathy. Number of structural changes was determined in the gastric mucosa. They were differentiated into small, large, and strip-like erosions. The Pauls' index was calculated for structural changes. Pathomorphological studies of the stomach were carried out.

Results. The total number of structural changes in the stomach of animals in experimental groups I, II, IV and V is 44% lower on average, in experimental group III it is 67% lower and in experimental group VI it is 3.6 times lower than in the control. The Pauls' index for large erosions in experimental groups I–V is 38–75% lower, in experimental group VI it is 83% lower than the index in the control animals. No strip-like erosions are detected in animals of experimental groups III–VI. Pauls' index for these destructions in experimental groups I and II is 7.0 and 6.5 times lower than the index in the control animals. Microscopic morphological examination registered the increase of shallow-like erosions in the stomach of animals of experimental groups. Shallow-like erosions do not reach the *muscularis mucosae*. Microcirculation disorders and leukocyte infiltration are less pronounced than in the control group.

Conclusion. *F. hystrix* has the gastroprotective effect, increasing the resistance of the gastric mucosa to the effect of ethanol. The *F. hystrix* extract prepared with 30% and 40% ethanol shows the most pronounced pharmacotherapeutic effect in ethanol-induced gastropathy.

Key words: ethanol-induced gastropathy, *Ferulopsis hystrix* (Bunge) Pimenov, gastroprotective effect.

Conflict of interest. The authors declare the absence of obvious and potential conflicts of interest related to the publication of this article.

Source of financing. The studies were carried out as part of the state assignment (No. AAAA-A17-117011810037-0).

Conformity with the principles of ethics. The study was approved by the local Ethics Committee of the Institute of General and Experimental Biology (Protocol No. 4 of 26.01.2017).

For citation: Salchak S.M., Razuvaeva Ya.G., Toropova A.A., Arakchaa K.D., Olennikov D.N., Nikolaev I.G. Gastroprotective effect of *Ferulopsis hystrix* (Bunge) Pimenov in ethanol-induced gastropathy. *Bulletin of Siberian Medicine.* 2020; 19 (4): 151–157. https://doi.org/10.20538/1682-0363-2020-4-151-157.

✉ *Salchak Saizana M.,* e-mail: saizana_salchak@mail.ru.

Гастропротективное влияние *Ferulopsis hystrix* (Bunge) Pimenov при экспериментальной этаноловой гастропатии

Салчак С.М.[1], Разуваева Я.Г.[1], Торопова А.А.[1], Аракчаа К.Д.[2], Оленников Д.Н.[1], Николаева И.Г.[1]

Институт общей и экспериментальной биологии Сибирского отделения Российской академии наук (ИОЭБ СО РАН)
Россия, 670047, г. Улан-Удэ, ул. Сахьяновой, 6

Научно-исследовательский институт медико-социальных проблем и управления Республики Тыва (НИИ МСПУ РТ)
Россия, 667003, Республика Тыва, г. Кызыл, ул. Кечил-оола, 2а

РЕЗЮМЕ

Цель. Оценка гастропротективного действия сухих экстрактов, полученных с использованием различных экстрагентов из корневищ с корнями *Ferulopsis hystrix* (Bunge) Pimenov при этаноловом повреждении желудка у белых крыс.

Материалы и методы. Эксперименты проведены на 68 самцах и самках крыс линии Вистар. Этаноловую гастропатию моделировали однократным внутрижелудочным введением этанола в дозе 10 мл/кг. Животные опытных групп (I– VI) в течение 7 сут до моделирования гастропатии получали лекарственные формы из корневищ с корнями *F. hystrix*: I – отвар в объеме 10 мл/кг; II–V – сухие экстракты в дозе 200 мг/кг, полученные путем экстракции водой очищенной, 30-, 40- и 70%-м этанолом соответственно; VI – сухой экстракт, приготовленный двукратной экстракцией 40%-м и однократной экстракцией 30%-м этанолом. В слизистой оболочке желудка определяли структурные изменения, которые дифференцировали на мелкие, крупные и полосовидные эрозии. Проводили патоморфологические исследования желудка.

Результаты. Установлено, что в I, II, IV и V опытных группах общее количество повреждений в желудке было в среднем на 44% меньше, чем в контроле, в III опытной группе – на 67% и в VI опытной группе – в 3,6 раза. Индекс Паулса для крупных эрозий в I–V опытных группах был ниже контрольного показателя на 38–75%, в VI – на 83%. Полосовидные эрозии не выявлялись у животных III–VI опытных групп; индекс Паулса для данных деструкций в I и II опытных группах был в 7,0 и 6,5 раза ниже показателя контрольных животных. В стенке желудка животных отмечались неглубокие эрозии, не достигающие мышечной пластинки слизистой оболочки; нарушения микроциркуляции и лейкоцитарная инфильтрация были менее выражены относительно контроля.

Заключение. *F. hystrix* оказывает гастропротективное влияние, повышая резистентность слизистой оболочки желудка к действию этанола. Наиболее выраженный фармакотерапевтический эффект проявляет экстракт, приготовленный двукратной экстракцией 40%-м и однократной экстракцией 30%-м этиловым спиртом.

Ключевые слова: этаноловая язва, *Ferulopsis hystrix* (Bunge) Pimenov, гастропротективное действие.

Конфликт интересов. Авторы декларируют отсутствие явных и потенциальных конфликтов интересов, связанных с публикацией настоящей статьи.

Источник финансирования. Исследования проведены в рамках выполнения госзадания (№ АААА-А17-117011810037-0).

Соответствие принципам этики. Исследование одобрено локальным этическим комитетом ИОЭБ СО РАН (протокол № 4 от 26.01.2017).

Для цитирования: Салчак С.М., Разуваева Я.Г., Торопова А.А., Аракчаа К.Д., Оленников Д.Н., Николаева И.Г. Гастропротективное влияние *Ferulopsis hystrix* (Bunge) Pimenov при экспериментальной этаноловой гастропатии. *Бюллетень сибирской медицины.* 2020; 19 (4): 151–157. https://doi.org/10.20538/1682-0363-2020-4-151-157.

INTRODUCTION

Ferulopsis hystrix (Bunge) Pimenov is a perennial plant of *Umbelliferae* family growing in Russian South Siberia and Far East [1]. The given plant was formerly classified as *Phlojodicarpus turczaninovii* Sipl. The roots and rhizomes of *F. hystrix* are used in folk and traditional medicine. For a long time, the roots of *F. hystrix* known under the name "*chuksugbai*" have been in the common use in Tuvinian folk medicine and now it holds a leading position as anti-inflammatory, wound-healing remedy, as well as in the treatment of tuberculosis and cancer [2]. In Mongolian and Buryat traditional medical systems, *F. hystrix* is a substitute of *Costus speciosus* (Tibet. *ru rta*) used in Tibetan medicine for the treatment of *rlung* of the blood, diseases of the lungs and throat, for amelioration of "compression" in the stomach and stopping of necrosis [3].

Rhizomes and roots of *F. hystrix* contain various groups of biologically active substances among which coumarins play a leading role in the pharmacological activity of the plant; their total content is 3.9–4.6% [4, 5]. Coumarins have antiviral, antibacterial and antifungal properties [6, 7]; also, they have anti-inflammatory [8] and antioxidant activity [9, 10]. The experiments on animals have shown a marked gastro-protective effect of natural and synthetic coumarins [11]. In this regard, the study of the gastro-protective effect of the *F. hystrix* roots and rhizomes is of great interest.

The aim of the study was to estimate the gastro-protective effect of the dry extracts derived from the *F. hystrix* rhizomes and roots with the use of various extraction solvents.

MATERIALS AND METHODS

The experiments were carried out on 68 white male and female Wistar rats weighing 180–200 g. The animal care was compliant with the rules of "Good Laboratory Practice" (GLP) and the Order of the Russian Health Ministry "On approval of Rules for Laboratory Practice" (No. 199N, 01.04.2016). Before the start of the experiments, the animals meeting the criteria were divided into groups taking into account the randomization principle. The experimental work followed the "European Convention for the protection of vertebrate animals used for experimental and other scientific purposes" (Strasburg, 1986).

The animals were divided into 7 groups: a control group and 6 experimental ones. The animals of group I received the decoction of *F. hystrix* in the volume 10 ml/kg prepared according to the General Monograph 1.4.1.0018.15 Infusions and decoctions. The animals of groups II–V received the dry extracts (200 mg/kg) obtained by extraction with purified water, 30, 40 and 70% ethyl alcohol respectively; the raw material-to-extraction agent ratio was 1 : 10; they were prepared at room temperature by vigorous shaking and successive vacuum drying. The animals of experimental group VI received the extract prepared by double extraction with 40% ethanol and the third extraction with 30% ethanol. The given choice of extraction solvents allowed us to obtain the extract with maximum content of extractive substances and good physical qualities [12].

According to the data of high-performance liquid chromatography, coumarins are the main components of the *F. hystrix* dry extract including peucenidin (3′-O-acetoxy-4′-O-senecioloxy-2′,3′-dihydroroselol) and skimmin (umbelliferone-7-O-glucoside; 1.26%), their content was 16.65 ± 0.33 and 1.26 ± 0.03%, respectively. The quantitative analysis of coumarins in the *F. hystrix* dry extract was performed with the HPLC method on the microcolumn liquid chromatograph Milichrom A-02 (Econova, Novosibirsk, Russia) on the column ProntoSIL-120-5-C18 AQ (2 × 75 mm, Ø 5 um; Metrohm AG, Herisau, Switzerland); mobile phase: 0.2 M $LiClO_4$ in 0.006 M $HClO_4$ (A), acetonitrile (B); gradient mode (% B): 0–26 min 5–100, 26–29 min 100; flow rate 150 µl / min; the column temperature was 35 °C; UV-detector, 330 nm. The content of coumarins was calculated with the use of calibration curves constructed using commercial reference samples of skimmin and peucenidin (> 95%; Wuhan ChemFaces Biochemical Co., Ltd., Wuhan, Hubei, PRC). The results are presented as the mean of triplicate ($M \pm SD$).

The tested medicinal forms of *F. hystrix* were introduced intragastrically to animals for 7 days and the last dose was introduced 1 hour before the injection of ulcerogenic agent. The animals of the control group received purified water according to the same scheme. The lesion of the stomach mucosa was induced by a single introduction of absolute alcohol to animals in the dose of 10 ml/kg against the background of 24-hour food deprivation [13]. One hour after the alcohol introduction, the rats were decapitated under light ether narcosis. To estimate the state of the gastric mucosa, the stomach was cut along the greater gastric curvature and the number of destructions was determined. The destructions were differentiated as small erosions (≤ 2 mm), large erosions (2–5 mm) and stripe-like

erosions (>5 mm). The Pauls' index was calculated for each kind of lesions according to the formula [13].

For patho-morphological studies, the material was fixed in 10% neutral buffered formalin, dewatered in ascending alcohol and embedded in paraffin. The sections were stained with hematoxylin and eosin.

The results obtained were processed with the use of the program Statistica for Windows 6.0. To describe statistical differences, nonparametric Mann – Whitney *U*-test was used. The results were presented as interquartile range median *Me* (Q_1; Q_3). To compare the lesion frequency in comparison groups, the Fisher test was used. The differences were significant with $p < 0.05$.

RESULTS AND DISCUSSION

Small erosions have been revealed in all control animals; large erosion in 8 animals and stripe-like erosions in 6 animals. The Pauls' index was 4.0, 2.4 and 1.1 respectively (Table 1). In the gastric mucosa of the control animals, hemorrhages and erosions in the form of narrow dehiscences resulted from desquamation of necrotic cells in surface and glandular epithelium were noted. Five in ten animals had deep lesions reaching up to muscular layer of mucous tunic that were classified as ulcers. At the bottom and edges of the ulcers, necrotic masses with signs of desquamation were revealed. In the boundary zone, massive leucocytic infiltration was noted, as well as cell elements of the glands in the state of marked dystrophy up to necrosis. In the vessels of microvasculature, nuclei of endothelial cells were bloated and plasma-impregnated and had signs of plasmarrhage and diapedetic hemorrhages found partially along the vessels or at considerable range in the form of homogeneous pink masses with a touch of erythrocytes and leucocytes. In the vessel lumina sludge phenomenon, erythro- and leucostasis were noted.

The use of the *F. hystrix* decoction and extracts prepared with the use of various solvents had gastro-protective effect increasing the resistance of gastric mucosa to ethanol impact. In the animals that received the decoction and extracts prepared with the use of water and 70% ethanol, the total number of gastric mucosa lesions was 44% less on average than in animals of the control group. Small erosions were revealed in all animals of the experimental groups; their quantity and Pauls' index were in line with the indices of animals in the control group. Large erosions were noted in 7-8 animals out of 10 in the given experimental groups. The Pauls' index for large erosions in the experimental groups I, II, and V was less than in the control group by 38, 46 and 42%, respectively. Stripe-like erosions were noted in 2 out of 8 animals in the group, which received the water extract, and in 2 out of 10 animals in the group, which received the decoction. The Pauls' index for stripe-like ulcers in the given experimental groups was 7.0 and 6.5 times lower than that in the control group. In most animals of the experimental groups I, II, and V, microscopic studies revealed hemorrhages, erosions injuring no more than two-thirds of their muscular layer of mucous tunic. Ulcers with deep necrosis of the muscular layer of mucous tunic and circumscribed by the marked leucocytic infiltration were revealed in two animals of the experimental groups I and II. The areas with signs of plasmarrhage and diapedetic hemorrhages were less marked.

In animals of the experimental groups III and IV, which received the extracts prepared with the use of 30% and 40% ethanol, the total number of destructions in the muscular layer of mucous tunic was 67 and 45% less than that in the control animals (Table 1). Small erosions were noted in 8 animals of the experimental groups III and IV; large erosions – in 6 and 8 out of 10 animals which received the extracts prepared with the use of 30% and 40% ethanol, respectively. No stripe-like erosions were noted in the animals of the given experimental groups. The Pauls' index for small and large erosions was significantly lower in the experimental group III and was 1.4 and 0.6, respectively, as compared to 2.1 and 1.6 in the experimental group IV; it was 2.9 and 4.0 times lower than these indices in the control group. Histological studies of the muscular layer of mucous tunic in the animals of the experimental groups III and IV revealed not deep erosions injuring only gastric superficial-foveolar epithelium. Single erosions penetrated into half of the muscular layer of mucous tunic. Leucocytic infiltration around erosions was marked moderately. Vessel dilatation in microvasculature along with erythro- and leucostasis and small areas of plasmarrhage and diapedetic hemorrhages were noted.

The extract of *F. hystrix* prepared with the use of 30 and 40% ethanol combination demonstrated more marked gastro-protective effect. The number of all destructions per one animal in the given experimental group was 2.5 (Table 1) that was 3.6 times less than that of the control group. No stripe-like erosions were found. Small and large erosions were noted respectively in 7 and 5 animals out of 10; the Pauls' index was 3.6 and 6.0 times lower than that in animals of the control group. Patho-histological studies of the

stomach wall in animals of the group VI revealed destructive alterations only in the gastric superficial-foveolar epithelium; its desquamation resulted in small erosions with slight leucocytic infiltration. The vessels of microvasculature were moderately dilated and plethorical with signs of erythrostasis and erythrodiapedesis; no sludge phenomenon and plasmarrhages were noted.

Table 1

The effect of *Ferulopsis hystrix* on the severity of lesions in the gastric mucosa of white rats in ethanol-induced gastropathy

Indices	Groups of animals						
	Control, $n = 10$	Experimental I, $n = 10$	Experimental II, $n = 8$	Experimental III, $n = 10$	Experimental IV, $n = 10$	Experimental V, $n = 10$	Experimental VI, $n = 10$
Total number of gastric mucosa lesions, *Me* (Q_1; Q_3)	9 (7;11)	5 (2;8) $p \le 0.05$	6 (2;8) $p \le 0.05$	3 (2;3) $p \le 0.05$	4.5 (2;8) $p \le 0.05$	5 (2;7) $p \le 0.05$	2.5 (0;4) $p \le 0.05$
Small erosions							
Number of animals with erosions, %	100	60	100	80	80	100	70
Number of destructions, *Me* (Q_1; Q_3)	4 (3;5)	3.5 (2;4)	3.5 (2;4)	2 (1;3) $p \le 0.05$	2 (2;4) $p \le 0.05$	3 (3;4)	2* (0;3)
Pauls' index	4.0	1.9	3.3	1.4	2.1	3.4	1.6
Large erosions							
Number of animals with erosions, %	80	70	75	60	80	80	50
Number of destructions, *Me* (Q_1; Q_3)	3 (2;4)	2.5 (0;4)	2 (0;3)	1 (0;1) $p \le 0.05$	2 (1;3)	2 (1;2)	0.5 (0;1) $p \le 0.05$
Pauls' index	2.4	1.5	1.3	0.6	1.6	1.4	0.4
Stripe-like erosions							
Number of animals with erosions, %	60	30	25	0 $p \le 0.01$	0 $p \le 0.01$	0 $p \le 0.01$	0 $p \le 0.01$
Number of destructions, *Me* (Q_1; Q_3)	1 (0;3)	0 (0;1)	0 (0;2) $p \le 0.05$	0	0	0	0
Pauls' index	0.84	0.12	0.125	0	0	0	0

Note: *n* – number of animals included in the analysis.

The gastro-protective effect of the medicinal forms from the roots and rhizomes of *F. hystrix* is due to the content of phenolic compounds, particularly, coumarins and flavonoids, which have antioxidant, anti-inflammatory, anticoagulant and other effects. Coumarins inhibiting the enzyme COX-2 in the lesion suppress the synthesis of inflammation mediators (histamine, serotonin), proinflammatory cytokines – IL-1β, TNF-α and other biological substances; due to this, they have an anti-inflammatory effect promoting the decrease of vascular permeability and leucocyte migration [14, 15]. The vessel-dilating effect of coumarins is due to the decrease of intracellular calcium concentration in smooth myocytes in microvasculature vessels. The decrease of thromboxane B2 synthesis in thrombocytes due to cyclooxygenase inhibition plays an important role in the mechanism of coumarin anti-coagulating effect [16]. Hence, the inhibition of thrombocyte aggregation indirectly promotes microcirculation in the stomach mucosa, which, together with the vessel dilating and anti-inflammatory effects of coumarins, explains the presence of gastro-protective activity of *F. hystrix* in ethanol-induced stomach injury in white rats. This gastro-protective effect is probably due to antioxidant properties of coumarins and flavonoids contained in *F. hystrix* and their capability to chelate mixed-valent metal ions participating in the reactions of free radical formation [17], bind formed radicals [9] and increase the resistance of cell membranes [11].

CONCLUSION

Thus, the decoction and dry extracts from rhizomes and roots of *F. hystrix* prepared with the use of various solvents have gastro-protective effect increasing the resistance of the stomach mucosa to the impact of ethanol, limiting the development of dystrophic and necrotic processes in the gastric superficial-foveolar

and glandular epithelia and preventing the development of inflammatory processes in the stomach wall of white rats. The given medicinal forms may be arranged according to their pharmacological efficiency in ascending order: water extract of *F. hystrix* < extract of *F. hystrix* prepared with the use of 70% ethanol; < extract of *F. hystrix* prepared with the use of 40% ethanol < extract of *F. hystrix* prepared with the use of 30% ethanol < extract of *F. hystrix* prepared with the use of 40 and 30% ethanol.

REFERENCES

1. Plant Resources: Wild flowering plants, their component composition and biological activity. Vol.3. Family *Fabaceae – Apiaceae*; ed.-in-chief. A.L. Budantsev. St.-Petersburg; Mocsow, 2010: 601 (in Russ.).
2. Serenot S.K. Tuva traditional medicine: medicinal plants, herbs, lichens, mushrooms with a parallel description of their use in Chinese, Mongolian and Tibetan medicine. Kyzyl: Tuva book publishing house named after Yu.Sh. Kunzegesh, 2009:118 (in Russ.).
3. Aseyeva T.A., Kuznetsova N.A., Mikhnevich L.V., Kornopoltseva T.V., Chekhirova G.V. Diseases of the digestive system: symptoms and treatment (based on Tibetan medical essays of the XII-XVII centuries). Novosibirsk: Nauka Publ., 2016: 188 (in Russ.).
4. Ganbaatar J., Shults E.E., Otgonsuren D., Radnaeva L.D. Taraskin V.V., Badamkhand D. Coumarins from *Peucedanum hystrix* growing in Mongolia. *Mongolian Journal of Chemistry.* 2014; 12: 42–49. DOI: 10.5564/mjc.v12i0.170.
5. Shul'ts E.E., Petrova T.N., Shakirov M.M., Bagryanskaya I.Yu., Taraskin V.V., Tolstikov G.A., Ganbaatar Zh., Radnaeva L.D., Otgonsuren D., Pokrovskii A.G. Plant coumarins IX. Phenolic compounds of *Ferulopsis hystrix* growing in Mongolia. Cytotoxic activity of 8,9-dihydrofurocoumarins. *Chemistry of Natural Compounds.* 2012; 48 (2): 211–217. DOI: 10.1007/s10600-012-0207-3.
6. Heide L. The aminocoumarins: biosynthesis and biology. *Natural Product. Reports.* 2009. 26 (10): 1241–1250. DOI: 10.1039/b808333a.
7. Song P.-P., Zhao J., Liu Z.-L., Duan Ya.-B., Hou Yi.-P., Zhao Ch.-Q., Wu M., Wei M., Wang N.-H., Lv Ye., Han Z.-J. Evaluation of antifungal activities and structure-activity relationships of coumarin derivatives. *Pest Management Science.* 2017; 73 (1): 94–101. DOI: 10.1002/ps.4422.
8. Kurbanova F.K., Serkerov S.V. Esterified dihydrofurocoumarins of the roots of *Seseli transcaucasica (Apiaceae*). *Plant Resources*. 2012; 48 (2): 228–233 (in Russ.).
9. Brumbarova T., Bauer P., Ivanov R. Molecular mechanisms governing *Arabidopsis iron* uptake. *Trends in Plant Science.* 2015; 20 (2): 124–133. DOI: 10.1016/j.tplants.2014.11.004.
10. Tomasz K., Rafał P., Monika S. Natural and synthetic coumarins and their pharmacological activity. *European Journal of Clinical and Experimental Medicine.* 2017; 15 (2): 169–175. DOI: 10.15584/ejcem.2017.2.12.
11. Parfenov E.A., Trapkov V.A., Shabanov P.D. Redox-regulation as a reliable platform for finding and developing new types of drugs. Search for gastroprotectors among substituted coumarins. *Reviews of Clinical Pharmacology and Drug Therapy.* 2014; 12 (4): 22–42 (in Russ.).
12. Arakchaa K.D., Nikolaev S.M., Salchak S.M., Razuvaeva Ya.G., Nikolaeva I.G., Toropova A.A., Nikolaeva G.G. The method of obtaining an agent with gastroprotective, anti-inflammatory, antioxidant activity. Patent for invention No. 2679310. Application No. 2018110207 dated 22.03.2018. IPC A61K36/23 (2006.01). Published: 07.02.2019 Bull. 4 (in Russ.).
13. Baginskaya A.I., Ferubko E.V., Kurmanova E.N., Voskobejnikova E.N., Sidelnikov N.I. Experimental models of erosive and ulcerative lesions of the stomach and duodenum. Moscow: "Russian doctor" Publ., 2017: 96 (in Russ.).
14. Ibrar A., Shehzadi S.A., Khan I. Developing hybrid molecule therapeutics for diverse enzyme inhibitory action: active role of coumarin-based structural leads in drug discovery. *Bioorganic & Medicinal Chemistry.* 2018; 26 (13): 3731–3762. DOI: 10.1016/j.bmc.2018.05.042.
15. Chauhan S., Devi U., Kumar V.R., Anwar F., Kaithwas G. Dual inhibition of arachidonic acid pathway by mulberry leaf extract. *Journal Inflammopharmacology*. 2015; 23 (1): 65–70. DOI: 10.1007/s10787-014-0223-y.
16. Cheriyan B.V, Kadhirvelu P., Nadipelly J., Shanmugasundaram J., Sayeli V., Subramanian V. Anti-nociceptive effect of 7-methoxy coumarin from *Eupatorium triplinervevahl* (Asteraceae). *Pharmacogn Magazine.* 2017; 13 (49): 81–84. DOI: 10.4103/0973-1296.197650.
17. Barot Kuldipsinh P., Jain Shailesh V., Kremer L., Singh S. Recent advances and therapeutic journey of coumarins: current status and perspectives. *Medicinal Chemistry Researsh.* 2015; 24 (7): 2771–2798. DOI: 10.1007/s00044-015-1350-8.

Authors contribution

Salchak S.M., Toropova A.A. – conception and design development, analysis and interpretation of data, critical revision for important intellectual content. Razuvaeva Ya.G., Arakchaa K.D. – substantiation of the manuscript, critical revision for important intellectual content, final approval of the manuscript for publication. Olennikov D.N., Nikolaeva I.G. – analysis and interpretation of data, critical revision for important intellectual content.

Authors information

Salchak Saizana M., Post-Graduate Student, Laboratory of Safety of Biologically Active Substances, Institute of General and Experimental Biology, Ulan-Ude, Russian Federation. ORCID 0000-0001-6244-9506.

Razuvaeva Yanina G., Dr. Sci. (Biology), Leading Researcher, Laboratory of Safety of Biologically Active Substances, Institute of General and Experimental Biology, Ulan-Ude, Russian Federation. ORCID 0000-0001-7829-1424.

Toropova Anyuta A., Cand. Sci. (Biology), Researcher, Laboratory of Safety of Biologically Active Substances, Institute of General and Experimental Biology, Ulan-Ude, Russian Federation. ORCID 0000-0003-2618-7777.

Arakchaa Kara-kys D., Cand. Sci. (Chemistry), Associate Professor, Director of the Scientific Research Institute of Medical-Social Problems and Management of the Republic of Tuva, Kyzyl, Russian Federation. ORCID 0000-0002-5128-8898.

Olennikov Daniil N., Dr. Sci. (Pharm.), Leading Researcher, Laboratory of Biomedical Research, Institute of General and Experimental Biology, Ulan-Ude, Russian Federation. ORCID 0000-0001-8194-1061.

Nikolaeva Irina G., Dr. Sci. (Pharm.), Senior Researcher, Laboratory of Safety of Biologically Active Substances, Institute of General and Experimental Biology, Ulan-Ude, Russian Federation. ORCID 0000-0002-3476-1014.

(✉) **Salchak Saizana M.,** e-mail: saizana_salchak@mail.ru.

Received 06.08.2019
Accepted 25.12.2019

УДК 611.013.85:618.36:577.27.085.2
https://doi.org/10.20538/1682-0363-2020-4-158-166

Placental growth factor exerts modulatory effects on *in vitro* activated T cells

Smetanenko E.A.[1], Leplina O.Yu.[1], Tikhonova M.A.[1], Pasman N.M.[2], Ostanin A.A.[1], Chernykh E.R.[1]

[1] *Research Institute of Fundamental and Clinical Immunology (RIFCI)*
14, Yadrintsevskaya Str., Novosibirsk, 630099, Russian Federation

[2] *Institute of Medicine and Psychology, Novosibirsk National Research State University*
2, Pirogova Str., Novosibirsk, 630090, Russian Federation

ABSTRACT

Background. Recent studies demonstrated immunosuppressive properties of vascular endothelial growth factor (VEGF-A) and identified VEGF-A as a key mediator of tumor-induced immunosuppression. Placental growth factor (PlGF) is another member of VEGF family in which dramatic elevation is associated with effective immune adaptation in successful pregnancy, whereas low concentrations are related to pregnancy complications resulting from the activation of immune system. Previously, we have shown that activated T cells express VEGF receptor type 1 (VEGFR-1), and PlGF inhibits T cell proliferation in VEGFR-1–dependent manner.

The aim of the present study was to further characterize PlGF effects on T cell responses *in vitro*.

Materials and methods. Peripheral blood mononuclear cells (PBMC) from healthy donors were stimulated with anti-CD3 monoclonal antibodies (a-CD3) in the absence or presence of PlGF and assessed for IL-10 production, programmed cell death and the expression of inhibitory receptors (PD-1, CTLA-4, Tim-3) in CD4+ and CD8+ T cell subsets.

Results. The addition of PlGF to PBMC cultures activated with a-CD3 resulted in increased percentages of IL-10-producing CD4+ and CD8+ T cells. Besides, PlGF promoted CD8+ T cells apoptosis while did not affect programmed cell death within CD4+ T cells. Notable, T cell activation with a-CD3 in the presence of PlGF was accompanied by the enhancement of PD-1-expressing cells in CD8+ T cell subset and Tim-3-expressing cells in both CD4+ and CD8+ T cells, and by the increased expression of PD-1 and Tim-3 on T cells.

Conclusion. Our *in vitro* findings indicate that PlGF can inhibit T cell responses due to the increasing interleukin-10 (IL-10) production, promoting CD8+ T cell apoptosis and enhancing the expression of PD-1 and Tim-3 inhibitory receptors. Given the elevated levels of PlGF in successful pregnancy and its decrease in gestation complications, the obtained data also suggest that PlGF-mediated suppression may be implicated into the governing immune evasion in pregnancy.

Key words: PlGF, T cells, apoptosis, IL-10, inhibitory receptors, PD-1, CTLA-4, Tim-3.

Conflict of interest. The authors declare the absence of obvious and potential conflicts of interest related to the publication of this article.

Source of financing. The study was supported by the Russian Foundation for Basic Research and the government of Novosibirsk region (Project No. 18-44-540005r-a).

Conformity with the principles of ethics. The study was approved by the local Ethics Committee of RICFI (Protocol No. 107 of 15.06.2018).

For citation: Smetanenko E.A., Leplina O.Yu., Tikhonova M.A., Pasman N.M., Ostanin A.A., Chernykh E.R. Placental growth factor exerts modulatory effects on *in vitro* activated T cells. *Bulletin of Siberian Medicine.* 2020; 19 (4): 158–166. https://doi.org/10.20538/1682-0363-2020-4-158-166.

✉ *Chernykh Elena R.,* e-mail: ct_lab@mail.ru.

Фактор роста плаценты модулирует ответ активированных *in vitro* Т-клеток

Сметаненко Е.А.[1], Леплина О.Ю.[1], Тихонова М.А.[1], Пасман Н.М.[2], Останин А.А.[1], Черных Е.Р.[1]

[1] Научно-исследовательский институт фундаментальной и клинической иммунологии (НИИФКИ) Россия, 630099, г. Новосибирск, ул. Ядринцевская, 14

[2] Новосибирский национальный исследовательский государственный университет (ННИГУ) Россия, 630090, г. Новосибирск, ул. Пирогова, 2

РЕЗЮМЕ

Актуальность. Недавние исследования выявили иммуносупрессивные свойства фактора роста эндотелия сосудов (VEGF-A) и его ключевую роль в опухоль-индуцированной иммуносупрессии. Плацентарный фактор роста (PlGF) является еще одним представителем семейства VEGF, резкое возрастание которого ассоциировано с эффективной иммунной адаптацией при успешной беременности, тогда как низкие концентрации PlGF являются предиктором гестационных осложнений на фоне активации иммунной системы. Ранее нами показано, что активированные Т-клетки экспрессируют рецепторы VEGF 1-го типа (VEGFR-1) и PlGF через связывание с VEGFR-1 ингибирует пролиферацию Т-клеток.

Цель. Дальнейшее изучение влияния PlGF на Т-клеточный ответ *in vitro*.

Материалы и методы. Мононуклеарные клетки (МНК) периферической крови здоровых доноров стимулировали моноклональными анти-CD3-антителами (a-CD3) в отсутствие и присутствии рекомбинантного PlGF и оценивали продукцию интерлейкина-10 (IL-10), уровень апоптоза и экспрессию ингибиторных рецепторов (PD-1, CTLA-4, Tim-3) в субпопуляциях CD4+ и CD8+ Т-клеток.

Результаты. Активация МНК a-CD3 в присутствии PlGF приводила к возрастанию относительного содержания CD4+ и CD8+ Т-клеток, продуцирующих IL-10. Кроме того, PlGF усиливал апоптоз активированных CD8+ Т-лимфоцитов, не влияя значимо на уровень программированной клеточной гибели CD4+ Т-клеток. Характерно, что активация Т-клеток a-CD3 в присутствии PlGF сопровождалась возрастанием PD-1 экспрессирующих клеток в субпопуляции CD8+ Т-клеток и Tim-3-экспрессирующих клеток среди CD4+ и CD8+ Т-клеток, а также повышением уровня экспрессии PD-1 и Tim-3 на Т-клетках.

Заключение. PlGF способен ингибировать Т-клеточный ответ посредством усиления продукции IL-10 и активационно-индуцированного апоптоза CD8+ Т-клеток, а также экспрессии ингибиторных рецепторов. Учитывая повышенный уровень PlGF при физиологической беременности и его снижение при гестационных осложнениях, полученные данные позволяют предполагать, что ингибиторный эффект PlGF на Т-клеточный ответ может являться еще одним механизмом, обеспечивающим защиту плода от иммунной системы матери.

Ключевые слова: PlGF, Т-клетки, апоптоз, IL-10, ингибиторные рецепторы, PD-1, CTLA-4, Tim-3.

Конфликт интересов. Авторы декларируют отсутствие явных и потенциальных конфликтов интересов, связанных с публикацией настоящей статьи.

Источник финансирования. Исследование выполнено при финансовой поддержке РФФИ и Правительства Новосибирской области (проект № 18-44-540005р-а).

Соответствие принципам этики. Исследование одобрено локальным этическим комитетом НИИФКИ (протокол № 107 от 15.06.2018).

Для цитирования: Сметаненко Е.А., Леплина О.Ю., Тихонова М.А., Пасман Н.М., Останин А.А., Черных Е.Р. Фактор роста плаценты модулирует ответ активированных *in vitro* Т-клеток. *Бюллетень сибирской медицины.* 2020; 19 (4): 158–166. https://doi.org/10.20538/1682-0363-2020-4-158-166.

INTRODUCTION

Vascular endothelial growth factor (VEGF) family proteins play a pivotal role in de-novo angiogenesis in physiological and pathological conditions. VEGF-A is the most active and the best-studied VEGF family member that mediates pro-angiogenic activity via activation of two receptors with tyrosine kinase activity, i.e. VEGFR-1 (Flt-1) and VEGFR-2 (KDR/Flk-1) [1]. Placental growth factor (PlGF) is another potent pro-angiogenic factor that is ligated exclusively with VEGFR-1 [2, 3].

Recent studies showed that VEGF-A, in addition to pro-angiogenic activity, demonstrates immunomodulating properties: (i) induces accumulation of regulatory T cells and myeloid suppressor cells, (ii) inhibits maturation of dendritic cells (DCs) and T cell functions [4], and operates as a key factor of tumour-induced immunosuppression [5]. Nevertheless, PlGF-dependent immunomodulating properties have not been extensively studied. It is known though that PlGF: (i) stimulates M2 macrophage polarisation, (ii) suppresses DC maturation, and (iii) induces regulatory B-cells [3, 6]. However, the effects of PlGF on T cell functions remain largely unexplored. According to the literature data, the effect of VEGF on T cells is mediated via VEGFR-2 [7]. At the same time, PlGF is a selective ligand for VEGFR-1, and its role in regulating functional T cell activity remains unclear.

Studies of PlGF-dependent immunomodulating properties are motivated by a putative participation of this factor in tumour escape from immune surveillance, since increased PlGF levels in most tumour types are associated with immune dysfunctions and correlate with tumour progression [8, 9]. PlGF-dependent immunomodulating activity in pregnancy evoked even stronger interest owing to significantly increased serum PlGF levels in normal pregnancy, in contrast to decreased PlGF concentrations in gestational complications [10].

During pregnancy the immune system undergoes a significant rearrangement (termed "immune adaptation") [11], which is directed on inducing tolerance to paternal alloantigens and preventing excessive inflammatory reactions. Several mechanisms underlying immune adaptation have been elucidated, including depletion of alloantigen-reactive T cells, Th1→Th2 switch and induction of regulatory T cells [11]. Recent studies have also demonstrated the role of T cell exhaustion in suppressing maternal T-cell-mediated cytotoxic activity [12, 13]. From this standpoint, immunomodulating activity of PlGF could represent yet another mechanism involved in fetal protection from the maternal immune system.

Previously, we demonstrated VEGFR-1 expression on activated T cells, whereby ligation of PlGF with VEGFR-1 resulted in inhibition of CD4+ and CD8+ T cell proliferation in mononuclear cell cultures [14]. This study aimed to elucidate the effects of PlGF on T cell responses *in vitro*, with particular reference to T-cell-derived immunosuppressive cytokine production (IL-10), T cell apoptosis and expression of inhibitory receptors (PD-1, CTLA-4, Tim-3) involved in T cell exhaustion.

MATERIALS AND METHODS

This study included 35 healthy blood donors of both genders aged 20–54 years. Peripheral blood mononuclear cells (PBMC) were isolated from heparinised venous blood using Ficoll-Verografin (p = 1.078 g/ml) gradient centrifugation. PBMC were cultivated in round-bottomed 96-well plates in RPMI-1640 cell culture medium supplemented with 10% inactivated donor AB (blood group IV) serum, 2mM HEPES-buffer, 0.3 mg/ml L-glutamine and 100 μg/ml gentamycin (all reagents were from Sigma-Aldrich, St. Louis, MO USA) at 37°C in and 5% CO_2. PBMC were stimulated in the presence of monoclonal anti-CD3 antibodies (1 μg/ml, a-CD3, ICO-90, MedBioSpektr, Moscow), 0.1–100 ng/ml PlGF (R&D Systems, Abingdon, UK). To assess proliferation, cells were incubated for 4 days, followed by pulse-labelling with 1.0 mCi/well of ^{3}H-thymidine. Cells were harvested, and radioactivity was quantitated using a Liquid Scintillation Counter SL-30 (Intertechnic, France).

In a separate set of experiments, we studied the effect of neutralising anti-VEGFR-1 antibodies (a-VEGFR-1) on suppressive PlGF properties. To this end, PBMC were stimulated with a-CD3 in the presence of PlGF (5 ng/ml) followed by cultivation in the presence or absence of neutralising a-VEGFR-1 or a-VEGFR-2 antibodies (HumanVEGFR1/Flt-1; VEGFR2/KDR/Flk-1 antibodies, 2.5 μg/ml; R&D Systems, USA), which were added to PBMC cultures concomitantly with PlGF or 24 h later.

Intracellular IL-10 expression was analysed in 48 h PBMC cultures activated by a-CD3 in the presence or absence of PlGF. Cells were labelled by anti-CD3 (Phycoerythrin, PE), CD8+ (Fluorescein isothiocyanate, FITC), CD4 (Peridinin chlorophyll, PerCP), IL-10(PE) antibodies (BD Biosciences, San Jose, CA, USA) followed by fixation/permeabilization using fixation/permeabilization Transcription Factor

Buffer Set (BD Biosciences), according to the manufacturer's instructions. Content ratio of IL-10-secreting cells in CD4+ and CD8+ T cell gates (altogether 30,000 events were collected for each sample) was analysed by flow cytometry (BD FACSCalibur).

Apoptosis of activated T cells was analysed by flow cytometry. To this end, PBMC were stimulated by a-CD3 and PlGF, as described above, and cultivated for 48 h. Cells were labelled with anti-CD4(FITC) or anti-CD8(FITC) antibodies (BD Biosciences) followed by Annexin V/7-7-amino-actinomycin D (ADD) (PE-conjugated Annexin V/7-ADDkit), according to the manufacturer's instructions. Altogether 10,000 events were assessed for each sample, and percentages of Annexin V-positive and/or 7-ADD-positive CD4+ and CD8+ T cells were analysed using CellQuest software (BD Biosciences, USA).

Cell surface expression of inhibitory receptors (PD-1, CTLA-4, Tim-3) on T cells was analysed by flow cytometry using anti-CD4(Pe), anti-CD8(FITC), anti-CTLA-4(Phycoerythrin/Cyanine dye tandem conjugate, PE-Cy5), anti-PD-1(Allophycocyanin, APC), anti-TIM-3(PerCP/Cyanine dye tandem conjugate, PerCP/Cy5.5) and relevant isotype controls (BD PharMingen, USA). Percentages and mean fluorescence intensity (MFI) of PD-1$^+$, CTLA-4$^+$, and Tim-3$^+$ cells were analysed in CD4+ and CD8+ T cell gates. Statistical analysis was performed using an analytics software portfolio Statistica 6.0 for Windows (StatSoft Inc., USA). The data are presented as Median (*Me*) with the interquartile range [Q_1–Q_3]. Related samples were compared using a nonparametric paired difference test (Wilcoxon signed-rank test) with the Bonferroni correction. Results were considered statistically significant at $p < 0.05$.

RESULTS

PlGF-mediated inhibition of a-CD3-activated T cells is VEGF-independent.

We showed previously that VEGFR-1 blockade aborted suppressive effects of PlGF on T cell proliferation in a-CD3-stimulated PBMC cultures [14], suggesting that PlGF exerted a direct inhibitory effect on T cells via ligating with its cognate receptor VEGFR-1. PlGF is also known to activate PBMC and induce VEGF production [15], which could also inhibit T cell proliferation [7]. Suppressive effects of VEGF have been described to manifest themselves from day 7 under high VEGF concentrations [7], which significantly surpassed VEGF levels present in PBMC cultures [15].

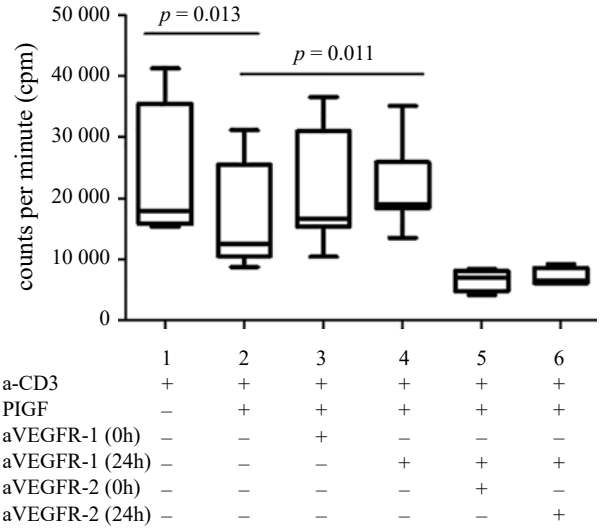

Fig. 1. Neutralising a-VEGFR-1 antibodies withdraw the inhibitory effect of PlGF on T cell proliferation: PBMC were stimulated with a-CD3-antibodies in the absence (*1*) and presence of 5 ng/ml PlGF(*2–6*); neutralising a-VEGFR-1 (*3*, *4*) or a-VEGFR-2 (*5*, *6*) antibodies were added at a dose of 2.5 μg/ml concomitantly with PlGF (*3*, *5*) or 24 h after the beginning of cultivation (*4*, *6*), counts per minute (cpm), *Me* [Q_1–Q_3], *Min–Max*, $n = 8$

In order to rule out the involvement of VEGF in the inhibitory PlGF activity, we compared blocking effects of a-VEGFR-1 and a-VEGFR-2 on PlGF-mediated suppression. Blocking antibodies were added either simultaneously with PlGF or 24 h later taking into consideration low VEGFR expression levels on unstimulated T cells followed by significant augmentation of VEGFR expression 24 h after the cultivation onset. Figure 1 shows that PlGF presence resulted in a significant (31%; 26–38%, $p = 0.013$) reduction in T cell proliferation levels in response to a-CD3 stimulation. Neutralising a-VEGFR-1 antibodies reduced PlGF suppressive activity to 9% (3–25%) if added concomitantly with PlGF and to 3% (0–16%) if added 24 h later. More pronounced inhibition of PlGF suppressive activity in the last case was likely to be due to higher VEGFR-1 expression on T cells 24 h after a-CD3 stimulation. Of note, VEGFR-2 blockade did not abrogate PlGF-mediated suppressive effects.

The effect of PlGF on IL-10 production by a-CD3-activated CD4+ and CD8+ T cells.

To study the effect of PlGF on IL-10-producing capacity of T cells, we analysed percentages of CD4+ and CD8+ T cells with intracellular IL-10 expression in cultures of a-CD3-stimulated PBMC in the presence

and absence of PlGF (Fig. 2). Activation of PBMC with a-CD3 significantly increased relative numbers of IL-10-positive cells in CD8+ T cell subpopulation ($p = 0.028$). Although we also detected an increase in IL-10-producing CD4+ T cells derived from most donors studied here, these changes were not statistically different from the baseline levels ($p = 0.06$).

The addition of PlGF to PBMC cultures increased proportion of IL-10$^+$ cells both in CD4+, and CD8+ T cell subsets, as compared to a-CD3-stimulated PBMC cultures incubated in the absence of PlGF. Of note, percentages of CD8$^+$IL-10$^+$ T cells in PBMC cultures incubated with PlGF were 2.7-fold higher, as compared to CD4$^+$IL-10$^+$ T cells ($p = 0.018$).

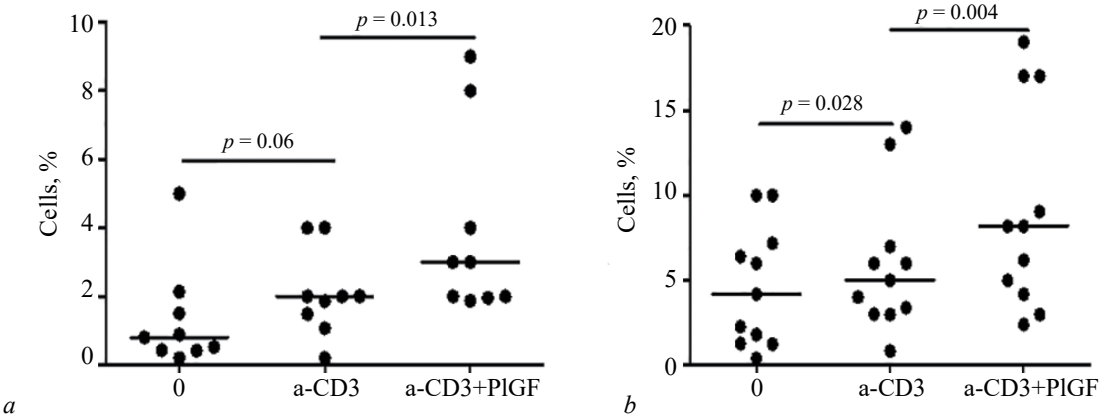

Fig. 2. PlGF increases intracellular IL-10 expression CD4+ (*a*) and CD8+ (*b*) by T lymphocytes: PBMC were cultivated in the medium (*0*) or stimulated with a-CD3 in the absence (a-CD3) and presence of 5 ng/ml PlGF (a-CD3+PlGF). After 48 h of cultivation intracellular IL-10 expression was assessed CD4+ and CD8+ T cell subpopulations using flow cytometry. The data are presented as individual values and *Me*, $n = 9–11$

PlGF enhanced apoptosis of a-CD3-activated T cells.

In order to address putative involvement of PlGF in programmed cell death regulation, we studied the effect of PlGF on the level of activation-induced apoptosis in CD4$^+$ and CD8$^+$ T cells. Apoptotic and necrotic cells were identified by a three-colour flow cytometry. Cells in early apoptosis are known to exclude a DNA-labelling vital dye 7-ADD, thus consistent with Ann$^+$/7-ADD$^-$ phenotype. Late apoptotic or necrotic cells are permeable to 7-AAD and therefore could be identified as Ann$^+$/7-ADD$^+$. Most CD4+ and CD8+ T cells in freshly isolated PBMC were viable (Ann$^-$/7-ADD$^-$ phenotype) and contained negligible proportion of apoptotic cells. Incubation of PBMC with a-CD3 for 48 h was accompanied by an increase in percentages of apoptotic cells in CD4+ and CD8+ T cell subpopulations (Fig. 3). Further supplementation of PBMC cultures with PlGF enhanced apoptosis in CD8+T cells ($p < 0.05$), but not in CD4+ T cells. Since the number of Ann$^+$/7-ADD$^-$ cells reflects only proximal (early) apoptotic events, we performed additional analysis of the total amount of Ann+ T cells (i.e. Ann$^+$/7ADD$^{-/+}$). Relative proportions of Ann+CD8+ T cells were found to be higher in a-CD3-activated PBMC incubated with PlGF than that in control a-CD3 stimulated PBMC. Meanwhile, no differences were detected in percentages of AnnV+CD4+ T cells incubated in the presence or absence of PlGF.

PlGF enhanced the expression of inhibitory receptors on activated T cells.

Overexpression of inhibitory receptors (also called inhibitory checkpoint molecules) is considered an important mechanism restraining T cell responses due to T cell exhaustion [12]. In order to assess the effects of PlGF on inhibitory receptor expression, we studied the expression of PD-1, CTLA-4, and Tim-3 on CD4+ and CD8+ T cells in 48 h PBMC cultures (Table).

PBMC stimulation with a-CD3 increased percentages of T cells expressing checkpoint molecules. Thus, relative numbers of CD4+PD-1+ and CD8+PD-1+ T cells following anti-CD3 stimulation were statistically higher, as compared to that observed in unstimulated PBMC cultures. The addition of PlGF enhanced the proportion of PD-1-positive CD8+ T cells ($p < 0.05$), with no effect on CD4+PD-1+ T cells. Ligation of T cell receptors with a-CD3 antibodies resulted in an increased proportion of CD4+ T cells co-expressing CTLA-4, while incubation with PlGF did not affect

percentages of CTLA-4-positive CD4+ or CD8+ T cells. Furthermore, a-CD3 stimulation enhanced percentages of Tim-3-positive cells in CD4+ and CD8+ T cell subpopulations, while in the presence of PlGF both CD4+Tim3+ and CD8+Tim3+ T cells showed statistically significant increase ($p < 0.05$).

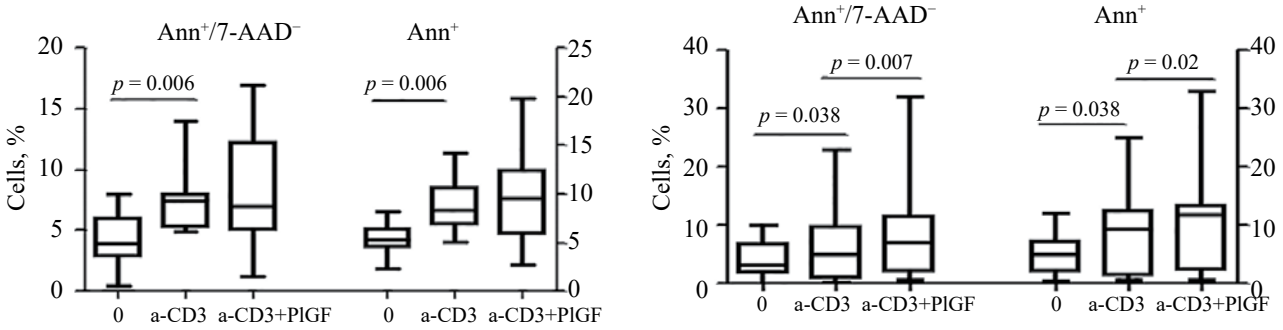

Fig. 3. PlGF enhances apoptosis of a-CD3-activated CD8+ T cells: the summarized data on the relative numbers of cells in the early apoptosis stage ($Ann^+/7ADD^-$) and the total amount of apoptotic cells (AnnV+) in CD4+ (*a*) and CD8+ (*b*) T cell gates are presented. The data from four independent experiments were analyzed using the paired Wilcoxon test, $n = 10$

Table

Effect of PlGF on the checkpoint molecules expression on a-CD3-activated CD4+ and CD8 + T cells, *Me* [Q_1–Q_3], $n = 8$

PBMC	$CD4^+$ T cells (%)			$CD8^+$ T cells, %		
	PD-1	CTLA-4	Tim-3	PD-1	CTLA-4	Tim-3
0	3.7 [2.2–4.3]	4.6 [2.1–7.1]	2.9 [2.0–3.6]	2.3 [1.6–2.8]	0.4 [0.1–0.8]	0.7 [0.1–1.6]
a-CD3	6.0* [3.0–8.5]	7.0* [2.4–10.2]	3.7* [2.7–5.3]	3.2* [2.4–4.2]	0.3 [0.1–0.7]	2.4* [1.6–3.2]
a-CD3+PlGF	5.5* [4.5–8.1]	7.3* [4.2–10.0]	5.0*# [3.3–6.6]	3.8 *# [2.9–4.5]	0.5 [0.3–0.7]	5.1*# [3.3–6.1]

Note. The percentage of PD-1, CTLA-4 and Tim-3-positive cells in the gates of CD4+ and CD8+ T lymphocytes was evaluated in 48-hour cultures of unstimulated PBMC (0) and PBMC activated by anti-CD3-antibodies in the absence of (a-CD3) and in the presence of 5 ng/ml PlGF (a-CD3+PlGF).

* $p < 0.05$ – significance of differences compared with unstimulated PBMC; # $p < 0.05$ – significance of differences compared with a-CD3-activated PBMC.

Importantly, PlGF not only increased percentages of PD-1- and Tim-3-positive T cells, but also enhanced the expression of these receptors on T cells. Thus, treatment of PBMC in the presence of PlGF facilitated the enhancement of mean fluorescence intensity (MFI) of PD-1 staining on CD4+ T cells from (37.1 ± 3.5) to (47.8 ± 5.8), while on CD8+ T cells MFI of PD-1 staining increased from (38 ± 3.3) to (47.0 ± 4.1) ($p < 0.05$). MFI of Tim-3 staining increased on CD4+ T cells in the presence of PlGF from (41.0 ± 4.2) to (49.0 ± 4.9), as well as on CD8+ T cells from (44.0 ± 4.5) to (49.0 ± 5.3) ($p < 0.05$). Taken together, activation of PBMC in the presence of PlGF resulted in moderate, but statistically significant augmentation of expression levels of PD-1 and Tim-3 *on both* CD4+ and CD8+ T cells.

DISCUSSION

The data obtained in this study showed that inhibitory effects of PlGF on T cell proliferation in a-CD3-stimulated PBMC cultures were mediated via VEGFR-1, and that these effects were not associated with a probable increase in VEGF production by activated PBMC [15], as judged from the fact that VEGFR-2 blockade did not withdraw suppressive effects of PlGF. In addition, it was demonstrated that PlGF: enhanced IL-10 production by activated CD4+ and CD8+ T cells, aggravated apoptosis of CD8+ T cells, and increased expression of inhibitory receptors PD-1 and Tim-3 on T cells, implying an important role of PlGF/VEGFR-1 signal transduction pathway in modulation of T cell functions.

VEGFR-1 has been reported to possess low tyrosine kinase activity, which for a long time supported a paradigm that considered VEGFR-1 exclusively a ligand-trapping receptor [2]. However, it was subsequently shown that this receptor was expressed on haemopoietic precursors, monocytes/macrophages and DCs, and that VEGFR-1-dependent signalling pathway was involved in mobilisation of bone marrow precursors, activation and migration of monocytes, and regulation of DC maturation and cell proliferation [3, 16, 17]. Moreover, recent studies demonstrated that VEGFR-1-mediated signalling in hypoxic condi-

tions activated STAT3 transcription factor [8], which plays an important role in regulating T cell functions by inhibiting proliferation and IL-2-producing capacity of T cells [18]. These observations are in agreement with our data that PlGF exerts inhibitory effect on T cell proliferation by binding to VEGFR-1.

This study identified an interesting property of PlGF – this factor stimulated IL-10 production by activated T cells. Y.L. Lin et al. demonstrated previously that PlGF modulated cytokine-secreting function of T cells indirectly via a DC-dependent mechanism. Thus, PlGF-modified DCs enhanced IL-13 and IL-5 production by allogeneic T cells without affecting IL-10 production in mixed leukocyte culture [6]. These results stress important differences between direct and DC-mediated effects of PlGF.

J.Y. Shin et al. described the augmentation of IL-10 production due to VEGF mediated ligation of VEGFR-1 on activated spleen T cells and CD4+ T cell line [19], which supports the ability of VEGFR-1 to exert direct effects on T cells. However, the authors did not detect suppression of T cell proliferation under conditions of VEGFR-1 activation. This fact is likely explained by PlGF and VEGF exerting different effects when binding to VEGFR-1 due to the activation of different downstream transcription factors [17].

IL-10 is known to be a key immunosuppressive cytokine involved in restricting immune responses and inducing tolerance in pregnancy [20]. Suppressive effects of IL-10 are mediated principally via generation of tolerogenic DCs, induction of regulatory T cells and activation of anti-inflammatory JAK1/STAT3 signalling pathway in T cells [21]. Inhibitory effects of IL-10 are most clearly demonstrated with regard to CD4+ T cells, in which endogenous IL-10 production constitutes an important regulatory mechanism restraining CD4+ T cell functions [22]. The effect of IL-10 on CD8+ T cell functions is far less unambiguous. Indeed, in tumour growth IL-10 could activate and stimulate expansion of cytotoxic CD8+ T cells [23], whereas in chronic infection a direct inhibitory effect of IL-10 on CD8+ T cells has been described [24]. Our data suggests that PlGF is capable of enhancing IL-10 production not only by CD4+, but also CD8+ T cells. However, whether IL-10 production underlies the suppressive effects of PlGF on T cell proliferation, with particular reference to CD8+ T cells, remains an open question and awaits further investigations.

Importantly, this study also revealed that PlGF could enhance both apoptosis of CD8+ T cells and expression of inhibitory receptors (PD-1 and Tim-3) on T cells. The ability of PlGF to modulate apoptosis levels was recently demonstrated using an experimental lung emphysema model [25]. The authors showed that PlGF increased apoptosis of lung epithelium via activation of c-Jun N-terminal kinase (JNK) and protein kinase C. Our study demonstrated that PlGF enhanced apoptosis of activated CD8+ T cells for the first time.

Interestingly, PlGF also increased the relative numbers of PD-1+ cells, and specifically in CD8+ (but not CD4+) T cell subpopulation, suggesting that PlGF-mediated augmented apoptosis of CD8+ T cells could be associated with enhanced PD-1 expression. An important role of PD-1 inhibitory receptors in suppressing cytotoxic T cell functions has been convincingly demonstrated previously in cancer [26], and recently in pregnancy [27]. PD-1-dependent signalling has been shown to inhibit T cells via various mechanisms, including apoptosis induction [28]. Furthermore, increased expression of checkpoint molecules could reflect T cell exhaustion state [12].

In addition to PD-1 up-regulation, treatment with PlGF enhanced relative numbers of Tim-3-positive cells, and notably both in CD8+ and CD4+ T cell subpopulations. Tim-3 is another checkpoint molecule involved in the formation of T cell exhaustion status, thus playing an important role in suppressing maternal immune responses against fetal alloantigens during successful pregnancy [29]. T. Voronet et al. demonstrated for the first time that *VEGF*-A strengthened expression of various inhibitory checkpoint molecules (PD-1, CTLA-4, Tim-3) on CD8+ T cells in tumour-bearing mice by engaging a VEGFR-2 signalling pathway [30]. These authors also detected simultaneous expression of several inhibitory receptors on CD8+ T cells in the presence of high VEGF concentrations.

Our data showed that angiogenic factors have stimulating effects on checkpoint molecule expression on human T cells, and, in particular, we demonstrated that PlGF enhanced the expression of PD-1 and Tim-3 on T cells. Along with this, if the stimulatory effect of PlGF on PD-1 expression was observed only in CD8+ T cell subpopulation, the influence of PlGF on Tim-3 expression was detected in both CD4+ and CD8+ T cell subpopulations. A co-expression analysis of different inhibitory receptors was beyond the scope of this investigation, which is a study limitation. However, the increase of both CD8+PD-1+ and CD8+-Tim-3 T cells associated with reduced CD8+ T cell proliferation in cultures with PlGF, implies that the up-regulation of checkpoint molecules on the surface

of T cells could mediate inhibitory effects of PlGF on T cells.

The data obtained in this study infer that PlGF could be considered a novel immunomodulator in pregnancy. Indeed, serum PlGF concentrations are known to increase during normal pregnancy, while declining PlGF levels observed in placental hypoxia serve as a predictor factor of pre-eclampsia and intrauterine growth retardation [10]. In spite of the high prognostic value of PlGF levels, its pathophysiological significance has not been fully elucidated. Taking into consideration an important role of immune adaptation in successful pregnancy paralleled by pronounced immune impairments observed in women with pre-eclampsia [31, 32], we hypothesise that PlGF is involved in immune modulation in normal pregnancy, while reduced PlGF levels facilitate immune system activation leading to the development of pregnancy complications.

CONCLUSION

Taken together, this study showed that PlGF enhanced IL-10 production by activated CD4+ and CD8+ T cells, apoptosis of CD8+ T cells, and expression of inhibitory receptors PD-1 and Tim-3 on T cells, evidencing an important role of PlGF/VEGFR-1 signalling pathway in modulating T cell functions. Taking into account enhanced PlGF levels in normal pregnancy paralleled by their reduction during pregnancy complications, we envisage that inhibitory effects of PlGF on T cell responses could constitute yet another mechanism governing immune evasion in pregnancy.

REFERENCES

1. Stuttfeld E., Ballmer-Hofer K. Structure and function of VEGF receptors. *IUBMB Life.* 2009; 61 (9): 915–922. DOI: 10.1002/iub.234.
2. De Falco S. The discovery of placenta growth factor and its biological activity. *Exp. Mol. Med.* 2012; 44 (1): 1–9. DOI: 10.3858/emm.2012.44.1.025.
3. Dewerchin M., Carmeliet P. PlGF: a multitasking cytokine with disease-restricted activity. *Cold Spring Harb. Perspect Med*. 2012; 2 (8): a011056. DOI: 10.1101/cshperspect.a011056.
4. Voron T., Marcheteau E., Pernot S., Colussi O., Tartour E., Taieb J., Terme M. Control of the immune response by pro-angiogenic factors. *Front Oncol.* 2014; 4: 70. DOI: 10.3389/fonc.2014.00070.
5. Lapeyre-Prost A., Terme M., Pernot S., Pointet A.L., Voron T., Tartour E., Taieb J. Immunomodulatory activity of VEGF in cancer. *Int. Rev. Cell Mol. Biol.* 2017; 330: 295–342. DOI: 10.1016/bs.ircmb.2016.09.007.
6. Lin Y.L., Liang Y.C., Chiang B.L. Placental growth factor down-regulates type 1 T helper immune response by modulating the function of dendritic cells. *J. Leukoc. Biol.* 2007; 82 (6): 1473–1480. DOI: 10.1189/jlb.0307164.
7. Ziogas A., Gavalas N., Tsiatas M., Tsitsilonis O., Politi E., Terpos E., Rodolakis A., Vlahos G., Thomakos N., Haidopoulos D., Antsaklis A., Dimopoulos M., Bamias A. VEGF directly suppresses activation of T cells from ovarian cancer patients and healthy individuals via VEGF receptor Type 2. *Int. J. Cancer*. 2012; 130 (4): 857–864. DOI: 10.1002/ijc.26094.
8. Albonici L., Giganti M., Modesti A., Manzari V., Bei R. Multifaceted role of the placental growth factor (PlGF) in the antitumor immune response and cancer progression. *Int. J. Mol. Sci*. 2019; 20 (12): e2970. DOI: 10.3390/ijms20122970.
9. Meng F.-J., Xiao S.-X., Zhang Y., Wang W., Wang B., Fan X.-Y. Prognostic significance of placenta growth factor expression in patients with multiple cancers: a meta-analysis. *Int. J. Clin. Exp. Med*. 2015; 8 (8): 12726–12735.
10. Lecarpentier É., Vieillefosse S., Haddad B., Fournier T., Leguy M., Guibourdenche J., Tsatsaris V. Placental growth factor (PlGF) and sFlt-1 during pregnancy: physiology, assay and interest in preeclampsia. *Ann. Biol. Clin. (Paris)*. 2016; 74 (3): 259–267. DOI: 10.1684/abc.2016.1158.
11. Morelli S., Mandal M., Goldsmith L.T., Kashani B.N., Ponzio N.M. The maternal immune system during pregnancy and its influence on fetal development. *Research and Reports in Biology.* 2015; 6: 171–189. DOI: 10.2147/RRB.S80652.
12. Slutsky R., Romero R., Xu Y., Galaz J., Miller D., Done B., Tarca A.L., Gregor S., Hassan S.S., Leng Y., Gomez-Lopez N. Exhausted and senescent T cells at the maternal-fetal interface in preterm and term labor. *J. Immunol. Res.* 2019: 3128010. DOI: 10.1155/2019/3128010.
13. Xu Y., Wang S., Lin Y., Li D., Du M. Tim-3 and PD-1 regulate CD8+ T cell function to maintain early pregnancy in mice. *J. Reprod. Dev.* 2017; 63 (3): 289–294. DOI: 10.1262/jrd.2016-177.
14. Chernykh E.R., Leplina O.Yu., Tikhonova M.A., Batorov E.V., Ostanin A.A. Vascular Endothelial Growth Factor Receptor-1 Signaling as a Novel Mechanism of T Cell Suppression in Tumor Neoangiogenesis. *Medical Immunology (Russia)*. 2019; 21 (4): 653–660 (in Russ.). DOI: 10.15789/1563-0625-2019-4-653-660.
15. Bottomley M., Webb N., Watson C., Holt L., Bukhari M., Denton J., Freemont A., Brenchley P. Placenta growth factor (PlGF) induces vascular endothelial growth factor (VEGF) secretion from mononuclear cells and is co-expressed with VEGF in synovial fluid. *Clin. Exp. Immunol.* 2000; 119 (1): 182–188. DOI: 10.1046/j.1365-2249.2000.01097.x.
16. Dikov M., Ohm J., Ray N., Tchekneva E.E., Burlison J., Moghanaki D., Nadaf S., Carbone D.P. Differential roles of vascular endothelial growth factor receptors 1 and 2 in dendritic cell differentiation. *J. Immunol.* 2005; 174 (1): 215–222. DOI: 10.4049/jimmunol.174.1.215.
17. Koch S., Tugues S., Li X., Gualandi L., Claesson-Welsh L. Signal transduction by vascular endothelial growth factor receptors. *Biochem. J.* 2011; 437 (2): 169–183. DOI: 10.1042/BJ20110301.
18. Oh H., Yu C.R., Golestaneh N., Amadi-Obi A., Lee Y.S., Eseonu A., Mahdi R.M., Egwuagu C.E. STAT3 protein promotes T-cell survival and inhibits interleukin-2 production through up-regulation of Class O Forkhead transcription factors. *J. Biol. Chem.* 2011; 286 (35): 30888–30897. DOI: 10.1074/jbc.M111.253500.

19. Shin J.Y., Yoon I.H., Kim J.S., Kim B., Park C.G. Vascular endothelial growth factor-induced chemotaxis and IL-10 from T cells. *Cell Immunol.* 2009; 256 (1–2): 72–78. DOI: 10.1016/j.cellimm.2009.01.006.
20. Mobini M., Mortazavi M., Nadi S., Zare-Bidaki M., Pourtalebi S., Arababadi M.K. Significant roles played by interleukin-10 in outcome of pregnancy. *Iran J. Basic Med. Sci.* 2016; 19 (2): 119–124.
21. Sabat R., Grütz G., Warszawska K., Kirsch S., Witte E., Wolk K., Geginat J. Biology of interleukin-10. *Cytokine Growth Factor Rev.* 2010; 21 (5): 331–344. DOI: 10.1016/j.cytogfr.2010.09.002.
22. Jankovic D., Kugler D., Sher A. IL-10 production by CD4+ effector T cells: a mechanism for self-regulation. *Mucosal. Immunol.* 2010; 3 (3): 239–246. DOI: 10.1038/mi.2010.8.
23. Emmerich J., Mumm J.B., Chan I.H., LaFace D., Truong H., McClanahan T., Gorman D.M., Oft M. IL-10 directly activates and expands tumor-resident CD8(+) T cells without de novo infiltration from secondary lymphoid organs. *Cancer Research.* 2012; 72 (14): 3570–3581. DOI: 10.1158/0008-5472.CAN-12-0721.
24. Smith L.K., Boukhaled G.M., Condotta S.A., Mazouz S., Guthmiller J.J., Vijay R., Butler N.S., Bruneau J., Shoukry N.H., Krawczyk C.M, Richer M.J. Interleukin-10 directly inhibits CD8+ T cell function by enhancing N-glycan branching to decrease antigen sensitivity. *Immunity.* 2018; 48 (2): 299-312: e5. DOI: 10.1016/j.immuni.2018.01.006.
25. Hou H., Cheng S., Chung K., Wei S., Tsao P., Lu H., Wang H., Yu C. PlGF mediates neutrophil elastase-induced airway epithelial cell apoptosis and emphysema. *Respir. Res.* 2014; 15 (1): 106. DOI: 10.1186/s12931-014-0106-1.
26. Chiu Y.M., Tsai C.L., Kao J.T., Hsieh C.T., Shieh D.C., Lee Y.J., Tsay G.J., Cheng K.S., Wu Y.Y. PD-1 and PD-L1 up-regulation promotes T-cell apoptosis in gastric adenocarcinoma. *Anticancer Res.* 2018; 38 (4): 2069–2078. DOI: 10.21873/anticanres.12446.
27. Meggyes M., Miko E., Szigeti B., Farkas N., Szereday L. The importance of the PD-1/PD-L1 pathway at the maternal-fetal interface. *BMC Pregnancy Childbirth*. 2019; 19 (1): 74. DOI: 10.1186/s12884-019-2218-6.
28. Shi F., Shi M., Zeng Z., Qi R., Liu Z., Zhang J., Yang Y., Tien P., Wang F.S. PD-1 and PD-L1 up-regulation promotes CD8(+) T-cell apoptosis and postoperative recurrence in hepatocellular carcinoma patients. *Int. J. Cancer.* 2011; 128 (4): 887–896. DOI: 10.1002/ijc.25397.
29. Banerjee H., Kane L.P. Immune regulation by Tim-3. *F1000Res.* 2018; 7: 316. DOI: 10.12688/f1000research.13446.1.
30. Voron T., Colussi O., Marcheteau E., Pernot S., Nizard M., Pointet A., Latreche S., Bergaya S., Benhamouda N., Tanchot C., Stockmann C., Combe P., Berger A., Zinzindohoue F., Yagita H., Tartour E., Taieb J., Terme M. VEGF-A modulates expression of inhibitory checkpoints on CD8+ T cells in tumors. *J. Exp. Med.* 2015; 212 (2): 139–148. DOI: 10.1084/jem.20140559.
31. Laresgoiti-Servitje E. A leading role for the immune system in the pathophysiology of preeclampsia. *J. Leukoc. Biol.* 2013; 94 (2): 247–257. DOI: 10.1189/jlb.1112603.
32. Geldenhuys J., Rossouw T., Lombaard H., Ehlers M., Kock M. Disruption in the regulation of immune responses in the placental subtype of preeclampsia. *Front Immunol.* 2018; 9: 1659. DOI: 10.3389/fimmu.2018.01659.

Acknowledgements

The authors are grateful to A. Delvig for providing language help in drafting the text of the article.

Authors contribution

Smetanenko E.A. – working with cell cultures. Leplina O.Yu. – working with cell cultures, analysis and interpretation of data. Tikhonova M.A. – preparation of samples for flow cytometry, flow cytometry testing of the samples. Pasman N.M. – analysis and interpretation of data. Ostanin A.A. – conception and design, drafting of the article. Chernykh E.R. – conception and design, analysis and interpretation of data, drafting of the article, final approval of the manuscript for publication.

Authors information

Smetanenko Ekaterina A., Post-Graduate Student, Laboratory of Cellular Immunotherapy, RIFCI, Novosibirsk, Russian Federation.

Leplina Olga Yu., Dr. Sci. (Med.), Leading Researcher, Laboratory of Cellular Immunotherapy, RIFCI, Novosibirsk, Russian Federation. ORCID 0000-0003-3169-8643.

Tikhonova Marina A., Cand. Sci. (Biology), Senior Researcher, Laboratory of Cellular Immunotherapy, RIFCI, Novosibirsk, Russian Federation. ORCID 0000-0002-2366-1667.

Pasman Natalia M., Dr. Sci. (Med.), Professor, Head of the Department of Obstetrics and Gynecology, Institute for the Medicine and Psychology, NSU, Novosibirsk, Russian Federation.

Ostanin Alexander A., Dr. Sci. (Med.), Professor, Head Researcher, Laboratory of Cellular Immunotherapy, RIFCI, Novosibirsk, Russian Federation. ORCID 0000-0001-6895-938X.

Chernykh Elena R., Dr. Sci. (Med.), Professor, Corresponding Member of the RAS, Head of the Laboratory of Cellular Immunotherapy, RIFCI, Novosibirsk, Russian Federation. ORCID 0000-0003-2346-6279.

(✉) **Chernykh Elena R.,** e-mail: ct_lab@mail.ru.

Received: 11.12.2019
Accepted: 30.04.2020

УДК 616.527.4-039-097
https://doi.org/10.20538/1682-0363-2020-4-167-173

Features of polymorbid pathology in patients with autoimmune bullous dermatosis

Ufimtseva M.A., Izmozherova N.V., Gurkovskaya E.P., Bochkarev Yu.M.

Ural State Medical University
3, Repin Str., Yekaterinburg, 620028, Russian Federation

ABSTRACT

Background. Autoimmune bullous dermatosis (ABD) is a group of inherited and acquired skin diseases, the main morphological elements of which are the bullas, developed as a result of autoantibody production directed against protein structures of the epidermis and dermo-epidermal junction, leading to epidermal detachment and blistering on the skin and mucous membranes.

The aim of the research was to analyze the detection rate and structure of polymorbid pathology in patients with autoimmune bullous dermatoses and to determine the Charlson index and 10-year survival in patients before and after prescription of glucocorticosteroid therapy.

Materials and methods. The research included retrospective and prospective stages. At the first stage, the analysis of primary medical records was carried out, and histories of 70 patients over 18 years old, before the onset of autoimmune bullous dermatosis were analyzed. Clinical and epidemiological data were taken into account, the main and concomitant diagnoses were determined in accordance with ICD X. The Charlson index was calculated for all patients, the 10-year survival rate of patients with autoimmune bullous dermatoses was determined.

Results. Polymorbid pathology was recorded in 81.4% of patients, before the onset of autoimmune bullous dermatosis. 48.6% of patients had two or more concomitant diseases. Among patients with diseases of internal organs, those with cardiovascular pathology (52.8%) occupied the first place, patients with gastroenteric pathology (41.4%) occupied the second place, patients with endocrinopathy held the third place (20.0%). The Charlson index median in patients of this group was 2.5 (1–3), the risk of fatal outcome over a 10-year period was 16.5%. Subsequently, after the onset of autoimmune bullous dermatosis, 65.7% of patients required the prescription of glucocorticosteroid therapy. Decompensation of concomitant pathology was diagnosed in 39.1% of patients, therefore they needed consultation of related specialists. The median polymorbidity index increased to 3.5 (2–5), the risk of a death increased to 34.5% ($p < 0.05$).

Conclusion. Polymorbid pathology worsens the course of autoimmune bullous dermatoses, increases the risk of disability and mortality, especially in patients receiving systemic glucocorticosteroid therapy, and therefore these patients should be under regular medical check-up not only of a dermatovenereologist, but also of related specialists.

Key words: autoimmune bullous dermatosis, polymorbidity, Charlson index, glucocorticosteroids.

Conflict of interest. The authors declare the absence of obvious and potential conflicts of interest related to the publication of this article.

Source of financing. The authors state that they received no funding for the study.

Conformity with the principles of ethics. The study was approved by the local Ethics Committee at Ural State Medical University (Protocol No. 10 of 12.16.2016).

For citation: Ufimtseva M.A., Izmozherova N.V., Gurkovskaya E.P., Bochkarev Yu.M. Features of polymorbid pathology in patients with autoimmune bullous dermatosis. *Bulletin of Siberian Medicine.* 2020; 19 (4): 167–173. https://doi.org/10.20538/1682-0363-2020-4-167-173.

✉ *Gurkovskaya Evgeniya P.,* e-mail: gurkovskaya-e@mail.ru.

Особенности полиморбидной патологии у больных аутоиммунными буллезными дерматозами

Уфимцева М.А., Изможерова Н.В., Гурковская Е.П., Бочкарев Ю.М.

Уральский государственный медицинский университет (УГМУ)
Россия, 620028, г. Екатеринбург, ул. Репина, 3

РЕЗЮМЕ

Цель. Изучить частоту выявления и структуру полиморбидной патологии у больных аутоиммунными буллезными дерматозами. Определить индекс полиморбидности Чарлсон и 10-летнюю выживаемость у больных до и после назначения глюкокортикостероидной терапии.

Материалы и методы. Исследование включало ретроспективный и проспективный этапы. На первом этапе проведен анализ первичной медицинской документации, 47 амбулаторных карт и 23 историй болезни больных старше 18 лет до дебюта аутоиммунного буллезного дерматоза. Учитывали клинико-эпидемиологические данные, основной и сопутствующий диагнозы устанавливали в соответствии с Международной классификацией болезней 10-го пересмотра. Всем пациентам рассчитан индекс Чарлсон, определена 10-летняя выживаемость больных аутоиммунными буллезными дерматозами.

Результаты. Полиморбидная патология до дебюта аутоиммунного буллезного дерматоза зафиксирована у 81,4% больных. У 48,6% пациентов выявлено два и более сопутствующих заболевания. Наиболее часто диагностируются заболевания сердечно-сосудистой системы (первое ранговое место – 52,8%), затем патология желудочно-кишечного тракта (второе ранговое место – 41,4%), на третьем месте – эндокринопатии (20,0%). Медиана индекса Чарлсон у больных данной группы составила 2,5 (1–3), риск летального исхода за 10-летний период 16,5%. Впоследствии 65,7% пациентам, после дебюта аутоиммунного буллезного дерматоза, потребовалось назначение системных глюкокортикостероидов. Декомпенсация сопутствующей патологии диагностирована у 39,1% пациентов. Медиана индекса полиморбидности возросла до 3,5 (2–5), риск развития летального исхода увеличился до 34,5% ($p < 0,05$).

Заключение. Полиморбидная патология ухудшает течение и прогноз аутоиммунных буллезных дерматозов, увеличивает риск инвалидизации и смертности, в особенности у пациентов, получающих системную глюкокортикостероидную терапию, в связи с чем больные должны находиться на диспансерном учете не только у врача-дерматовенеролога, но и смежных специалистов.

Ключевые слова: аутоиммунные буллезные дерматозы, полиморбидность, индекс Чарлсон, глюкокортикостероиды.

Конфликт интересов. Авторы декларируют отсутствие явных и потенциальных конфликтов интересов, связанных с публикацией настоящей статьи.

Источник финансирования. Авторы заявляют об отсутствии источника финансирования.

Соответствие принципам этики. Исследование одобрено локальным этическим комитетом УГМУ (протокол № 10 от 16.12.2016).

Для цитирования: Уфимцева М.А., Изможерова Н.В., Гурковская Е.П., Бочкарев Ю.М. Особенности полиморбидной патологии у больных аутоиммунными буллезными дерматозами. *Бюллетень сибирской медицины.* 2020; 19 (4): 167–173. https://doi.org/10.20538/1682-0363-2020-4-167-173.

INTRODUCTION

Autoimmune bullous dermatosis (ABD) is a group of hereditary and acquired skin diseases that is formed as a result of the production of autoantibodies to various structures of the dermoepidermal compound, leading to epidermal detachment and blistering [1, 2]. The most severe ABD leading to permanent disability, as well as mortality, include acantholytic pemphigus, Lever's bullous pemphigoid, Dühring's herpetiform dermatitis, and acquired and congenital epidermolysis bullosa [3, 4].

Currently, mortality in ABD remains at a high level and varies from 15.0% to 30.0% despite pathogenetic treatment with systemic glucocorticosteroids

(GCS) and immunosuppressants [5, 6]. The prognosis of the disease also depends on polymorbidity. Researchers point out that ABD is often associated with diabetes, hypothyroidism, and inflammatory bowel disease, and an increased risk of stroke is observed in patients of this group [7, 8]. The presence of polymorbid pathology leads to a deterioration in the condition of ABD patients, an uncontrolled course of concomitant diseases and their resistance to basic therapy, a decrease in life quality, adherence of patients to drug therapy, and increased rates of patient disability and mortality [9].

Most studies of domestic and foreign scientists come down to identifying the most common diseases in ABD patients and do not include an assessment of the diagnosed polymorbidity severity, which is relevant, as it will enable to predict the course of both ABD and concomitant pathology, as well as to determine the death risk.

The aim of the research is to study the detection frequency and structure of polymorbid pathology in patients with autoimmune bullous dermatoses, to determine the Charlson polymorbidity index and 10-year survival in patients before and after glucocorticosteroid therapy.

MATERIALS AND METHODS

The study included retrospective and prospective stages. At the first stage, the analysis of primary medical documentation was carried out: 47 ambulatory medical records and 23 patient charts of subjects older than 18 years before the onset of autoimmune bullous dermatosis. Clinical and epidemiological data were taken into account. The main and concomitant diagnoses were established in accordance with the International Classification of Diseases, 10th Revision (ICD-10). Polymorbidity was registered by the number of nosologies in one patient. To assess somatic pathology, the Charlson index was determined. The overall score is the total of each patient's comorbid conditions (weighted according to severity and age) and points for each decade of life if a patient exceeded the age of 40.

The diseases assessed by calculating the Charlson index include cardiovascular diseases, dementia, chronic lung diseases, connective tissue diseases, peptic ulcer disease, liver damage, diabetes mellitus, kidney disease, liver disease, malignant neoplasms, and acquired immunodeficiency syndrome. Depending on the severity of concomitant diseases, the number of accrued points may be equal to 1, 2, 3 and 6.

With the help of the Charlson index, 10-year survival of patients with autoimmune bullous dermatoses was predicted. At the second stage, a clinical and instrumental examination of this group of patients was carried out, after the debut of autoimmune bullous dermatosis and the prescription of basic therapy. Statistical processing of the obtained data was carried out using the Excel 2000 and Statistica 13 packages. The median, upper and lower quartiles were calculated *Me* (Q_1–Q_3), nonparametric statistical methods (χ^2) with continuity correction were used. The level of statistical significance of the differences was considered at $p < 0.05$.

RESULTS

According to the retrospective analysis of primary medical documentation of 70 patients with autoimmune bullous dermatoses (ABD), 81.4% (57/70) of them had polymorbid pathology diagnosed before the debut of bullous dermatosis. The median age in the group of men with ABD was 49 years (interquartile range (IQR): 41.5–63.0 years), and in the group of women it was 56 years (IQR: 45.0–67.5). In 48.6% (34/70) patients, two or more concomitant diseases were detected.

Moreover, in the structure of the internal organs pathology, diseases of the cardiovascular system were diagnosed in 52.8% (37/70) patients, pathology of the gastrointestinal tract was registered in 41.4% (29/70) patients, endocrinopathies were observed in 20.0 % (14/70) patients, diseases of the musculoskeletal system were found in 15.7% (11/70) of ADB patients (Table). Patients also had diseases such as bronchial asthma, renal cell cancer, colon adenocarcinoma, senile cataract.

It is noteworthy that among 37 patients with cardiovascular pathology, all ABD patients showed arterial hypertension. Moreover, every second patient had stage 2 or stage 3 of high blood pressure. In 56.7% (21/37) of patients with arterial hypertension, target organs were affected (left ventricular hypertrophy, atherosclerotic plaques of the magistral vessels, creatinine clearance <60 ml/min), and in 35.1% (13/37) associated clinical conditions (ACC) were identified. Among patients with ACCs, 29.7% (11/37) patients with pathology of the cardiovascular system demonstrated coronary heart disease, 8.1% (3/37) patients had a history of myocardial infarction, 24.3% (9/37) patients were diagnosed with chronic heart failure, and 5.4% (2/37) patients had chronic renal failure. Atherogenic dyslipidemia

was reported in 13.5% (5/37) patients with ABD. It should be noted that two of the three patients with previously established arterial hypertension subsequently required the prescription of high daily doses of systemic glucocorticosteroids due to the onset of ABD.

Table

The comorbidity structure in patients with autoimmune bullous dermatosis, *n* = 70

№	Chapter of the ICD-10	Total	
		n	%
1	Chapter IX. Diseases of the circulatory system	37	52.8
2	Chapter XI. Diseases of the digestive system	29	41.4
3	Chapter IV. Endocrine, nutritional and metabolic diseases	14	20.0
4	Chapter XIII. Diseases of the musculoskeletal system and connective tissue	11	15.7
5	Chapter XIV. Diseases of the genitourinary system	7	10.0
6	Chapter VII. Diseases of the eye and adnexa	7	10.0
7	Chapter X. Diseases of the respiratory system	5	7.1
8	Chapter II. Neoplasms	4	5.8
9	Chapter V. Mental and behavioural disorders	2	2.8
10	Chapter VI. Diseases of the nervous system	1	1.4
	Total number of patients with pathology of internal organs	57	81.4

Note. The total number of observations exceeds 100.0% due to the presence of several pathological conditions in one person.

In the structure of the gastrointestinal tract (GIT) diseases, in 65.5% (19/29) of ABD patients with gastrointestinal pathology, endoscopic signs of gastritis were diagnosed, every third patient suffered from chronic cholecystitis and / or chronic pancreatitis. 10.3% (3/29) patients had a history of gastric ulcer. It should be noted that only two ABD patients with gastrointestinal complaints had a history of esophagogastroduodenoscopy. In one case, esophagitis was diagnosed, in another, erosion was found throughout the organ, which was regarded as a manifestation of erosive esophagitis. However, these manifestations regressed after the use of systemic glucocorticosteroids prescribed due to the debut of ABD. One patient had an esophageal stricture of unknown etiology.

In 72.7% (8/11) ABD patients with pathology of the musculoskeletal system, first detected or previously established osteoporosis and osteopenia were observed. It should be noted that therapy in these patients, before inclusion in the study, consisted of taking NSAIDs and calcium preparations.

Among endocrinopathies, 57.1% (8/14) ABD patients were diagnosed with type 2 diabetes mellitus, this pathology was detected before taking systemic glucocorticosteroids. And 28.5% (4/14) patients were diagnosed with autoimmune thyroiditis.

Pathology of the visual organs was detected in seven patients with ABD, patients with senile cataract occupy the first rank place, and every second patient required surgical treatment. Two patients were diagnosed with conjunctivitis and blepharitis.

Diseases of other organs and systems, such as bronchial asthma, chronic pyelonephritis, sensory polyneuropathy, iron deficiency anemia, were found in isolated cases. It should be noted that 4 out of 70 ABD patients were diagnosed with a malignant neoplasm, which could be a trigger factor in the development of paraneoplastic pemphigus and Lever's bullous pemphigoid.

The Charlson polymorbidity index was calculated for all patients with ABD. The median Charlson index in patients with ABD was 2.5 (1–3), the risk of death over a 10-year period is 16.5%. No gender differences were observed when comparing the Charlson index. A high proportion of patients with arterial hypertension, chronic heart failure, type 2 diabetes mellitus, gastric and duodenal ulcer was found. None of the ABD patients reported diseases included in the calculation of the Charlson index: peripheral vascular damage, transient cerebrovascular accident, collagenosis, liver cirrhosis without portal hypertension, acute cerebrovascular accident with hemiplegia or paraplegia, acute and chronic lymphoid or myeloid leukemia, lymphomas, cirrhosis of the liver with portal hypertension, acquired immunodeficiency syndrome.

Six concomitant diseases were registered in one man with Lever's bullous pemphigoid before the onset of ABD, including renal cell carcinoma of the right

kidney, coronary heart disease: post-infarction cardiosclerosis (2007), voltage angina pectoris (II functional class), hypertension (III stage, risk 4), chronic heart failure (II functional class), type 2 diabetes mellitus, cataract, and benign prostatic hyperplasia. The Charlson index was 8 and the risk of death was more than 79.0% (Figure).

Figure. Patient A., 63 year, Lever's bullous pemphigoid

It should be noted that after the onset of ABD, 65.7% (46/70) of patients required the prescription of pathogenetic therapy, namely systemic glucocorticosteroid therapy. Patients with acantholytic pemphigus, bullous pemphigoid Lever, acquired bullous epidermolysis were treated with medium and high daily doses of glucocorticosteroids. During treatment, 39.1% (18/46) of patients receiving systemic glucocorticosteroid therapy were diagnosed with decompensation of concomitant pathology.

In 29,7% (11/37) patients with diseases of the cardiovascular system, there was a lack of correction of arterial hypertension of varying degrees. Of these, nine patients reported an increase in blood pressure, requiring correction of antihypertensive therapy by a cardiologist.

Decompensation of type 2 diabetes mellitus was diagnosed in every second patient with previously established endocrinopathy (7/14), so all patients needed an endocrinologist's consultation with a view to adjusting the dose of sugar-lowering drugs.

After the prescription of systemic glucocorticosteroid therapy for patients with ABD, the Charlson index was re-calculated. The Charlson index median in 65.7% (46/70) of patients with ABD treated with glucocorticosteroid therapy was 3.5 (2–5), which reliably indicates an increased risk of death to 34.5% ($p < 0.05$) in a comparative analysis. It should be noted that in this group of patients, the polymorbidity index increased by one, and the risk of death increased by 18.0%, compared with indicators before the debut of ABD and the prescription of glucocorticosteroid therapy.

DISCUSSION

Despite the low prevalence of ABD, according to domestic and foreign researchers, mortality reaches 30.0%, which is due to both the disease severity and the development of complications during treatment [10, 11]. In this regard, patients with ABD should be kept at the dispensary of a dermatovenerologist throughout their lives [12].

In the last decade, doctors and scientists all over the world report the effect of polymorbid pathology on the clinical course of the disease, quality of life, treatment effectiveness of the underlying disease and its prognosis, noting that the more concomitant diseases the patient has, the worse the patient's quality of life and the higher the risk of death are [13, 14]. Foreign authors point out that the most common concomitant diseases in patients with ABD were cardiovascular, infectious and autoimmune diseases, metabolic disorders, while mortality in these patients was significantly higher than in patients of the same age without ABD [15]. According to the results of the study, polymorbid pathology was detected in 81.4% of patients, while more than two concomitant diseases were found in 48.6% of patients.

M. Pishgahi and N. Namazi (2018) evaluated the risk of developing atrial fibrillation in ABD patients. The authors note that mortality among bullous dermatoses patients with diseases of the cardiovascular system, such as coronary heart disease and arrhythmia, is higher than in the population. Scientists report a high risk of developing atrial arrhythmias in patients with

acantholytic pemphigus, while the risk is increased in patients taking high doses of glucocorticosteroids [16, 17].

We obtained similar data, however, the study revealed high comorbidity in patients with ABD with arterial hypertension and type 2 diabetes mellitus, which is due to the drug therapy of the underlying disease – prolonged use of oral glucocorticosteroids. At the same time, it should be noted that diabetes, after the prescription of high-dose glucocorticosteroid therapy, develops a more severe course and needs early prevention.

Most foreign studies come down to assessing the incidence of concomitant diseases in patients with ABD without assessing the polymorbidity index and taking into account the severity of the comorbid disease diagnosed by them [18, 19]. The study was the first to conduct a comprehensive examination of patients with ABD with the determination of the Charlson index, which is the "gold standard" in various types of studies to assess polymorbidity. With its help, you can predict the risk of death, as well as personify a follow-up plan for patients receiving long-term high-dose glucocorticosteroid therapy.

CONCLUSION

Polymorbid pathology was detected in 81.4% of patients before the debut of ABD. The most common pathologies were hypertension, pathology of the gastrointestinal tract, type 2 diabetes mellitus and osteoporosis. After the debut of ABD and the prescription of systemic glucocorticosteroid therapy, decompensation of somatic pathology was observed in 39.1% of patients. The presence of polymorbid pathology is a negative predictive factor that increases the risk of death, as evidenced by the high Charlson index. Thus, ABD patients receiving systemic glucocorticosteroid therapy need to be registered at the dispensary, not only by a dermatovenereologist, but also by related specialists.

REFERENCES

1. Samtsov A.V., Belousova I.E. Bullous dermatosis. St. Petersburg: Publishing and Printing Company "KOSTA" Publ, 2012: 144 (in Russ.).
2. Skripkin Y.K., Butov Y.S., Ivanova O.L. Dermatovenereology. National guideline. Moscow: GEOTAR-Media Publ, 2011: 1024 (in Russ.).
3. Mahneva N.V. A modern view on the diagnosis and treatment of autoimmune bullous dermatoses. *International Journal of Applied and Fundamental Research.* 2011; 9: 15–17 (in Russ.).
4. Kubanov A.A., Znamenskaya L.F., Abramova T.V. Differential diagnosis of bullous dermatosis. *Vestnik Dermatologii i Venerologii.* 2016; 6: 43–56 (in Russ.).
5. Ghiasi M., Daneshpazhooh M., Ismonov M., Chams-Davatchi C. Evaluation of autoimmune bullous diseases in elderly patients in Iran: A 10-Year Retrospective Study. *Skinmed*. 2017; 15 (3): 175–180.
6. Patsatsi A., Lamprou F., Kokolios M., Stylianidou D., Trigoni A., Kalampalikis D., Sotiriadis D. Spectrum of autoimmune bullous diseases in Northern Greece. A 4-year Retrospective Study and Review of the Literature. *Acta Dermatovenerol. Croat*. 2017; 25 (3): 195–201.
7. Lai Y.C., Yew Y.W., Lambert W.C. Bullous pemphigoid and its association with neurological diseases: a systematic review and meta-analysis. *J. Eur. Acad. Dermatol. Venereol.* 2016; 30 (12): 2007–2015. DOI: 10.1111/jdv.13660.
8. Liu Y.D., Wang Y.H., Ye Y.C., Zhao W.L., Li L. Prognostic factors for mortality in patients with bullous pemphigoid: a meta-analysis. *Arch. Dermatol. Res*. 2017; 309 (5): 335–347. DOI: 10.1007/s00403-017-1736-1.
9. Jeon H.W., Yun S.J., Lee S.C., Won Y.H., Lee J.B. Mortality and comorbidity profiles of patients with bullous pemphigoid in Korea. *Ann. Dermatol*. 2018; 30 (1): 13–19. DOI: 10.5021/ad.2018.30.1.13.
10. Khamaganova I.V., Malyarenko E.N., Denisova E.V., Vorontsova I.V., Plieva K.T. Error in the diagnosis of vulgar pemphigus: a clinical case. *Russian Journal of Skin and Venereal Diseases*. 2017; 20 (1): 30–33 (in Russ.).
11. Bulgakova A.I., Khismatullina Z.R., Hamzina G.R. Prevalence, etiological aspects and clinical manifestations of pemphigus. *International Dental Review*. 2017; 1: 24–29 (in Russ.).
12. Lykova S.G., Reshetnikova T.B., Spitsyna A.V. Acantholytic pemphigus: pathogenetic mechanisms and features of corticosteroid therapy. *Sib. Journal of Dermatology and Venerology.* 2001; 1: 9–13 (in Russ.).
13. Kridin K., Zelber-Sagi S., Bergman R. Risk factors for lethal outcome in patients with pemphigus: a retrospective cohort study. *Eur. J. Dermatol*. 2018; 28 (1): 26–37. DOI: 10.1684/ejd.2018.3252.
14. Försti A.K., Jokelainen J., Timonen M., Tasanen K. Risk of death in bullous pemphigoid: A Retrospective Database Study in Finland. *Acta Derm. Venereol*. 2016; 96 (6): 758–761. DOI: 10.2340/00015555-2347.
15. Ren Z., Hsu D.Y., Brieva J., Silverberg N.B., Langan S.M., Silverberg J.I. Hospitalization, inpatient burden and comorbidities associated with bullous pemphigoid in the U.S.A. *Br. J. Dermatol.* 2017; 176 (1): 87–99. DOI: 10.1111/bjd.14821.
16. Pishgahi M., Dadkhahfar S., Robati R.M., Kheradmand Z., Shahidi-Dadras M., Zargari O., Elpern D.J. Electrocardiographic changes after high-dose corticosteroid pulse therapy in pemphiguspatients. *J. Dermatolog. Treat*. 2018; 29 (8); 802–805. DOI: 10.1080/09546634.2018.1466980.
17. Namazi N., Ariaeenejad S., Azad M.E., Pishgahi M. Risk of atrial fibrillation in pemphigus vulgaris. *Indian Dermatol. Online J.* 2018; 9 (4): 275–277. DOI: 10.4103/idoj.IDOJ_205_17.

18. Chiu Y.W., Chen Y.D., Hua T.C., Wu C.H., Liu H.N., Chang Y.T. Comorbid autoimmune diseases in patients with pemphigus: a nationwide case-control study in Taiwan. *Eur. J. Dermatol.* 2017; 27 (4): 375–381. DOI: 10.1684/ejd.2017.3060.

19. Charlson M., Wells M.T., Ullman R., King F., Shmukler C. The Charlson comorbidity index can be used prospectively to identify patients who will incur high future costs. *PLoS One.* 2014; 9 (12): e112479. DOI: 10.1371/journal.pone.0112479.

Authors contribution

Ufimtseva M.A., Bochkarev Yu.M. – dermatology consultation, editing of the article. Izmozherova N.V. – polymorbid pathology consultation, editing of the article. Gurkovskaya E.P. – conduction of the clinical study, preparation of the article.

Authors information

Ufimtseva Marina A., Dr. Sci. (Med.), Associate Professor, Head of the Department of Dermatovenerology and Life Safety, Ural State Medical University, Yekaterinburg, Russian Federation. ORCID 0000-0002-4335-9334.

Izmozherova Nadezhda V., Dr. Sci. (Med.), Associate Professor, Head of the Department of Pharmacology and Clinical Pharmacology, Ural State Medical University, Yekaterinburg, Russian Federation. ORCID 0000-0001-7826-9657.

Gurkovskaya Evgenia P., Assistant, Department of Dermatovenerology and Life Safety, Ural State Medical University, Yekaterinburg, Russian Federation. ORCID 0000-0001-7535-5429.

Bochkarev Yurii M., Cand. Sci. (Med.), Associate Professor, Department of Dermatovenerology and Life Safety, Ural State Medical University, Yekaterinburg, Russian Federation. ORCID 0000-0001-6298-7216.

(✉) **Gurkovskaya Evgenia P.,** e-mail: gurkovskaya-e@mail.ru.

Received 19.07.2019
Accepted 30.04.2020

УДК 616.896-053.2-076.5:577.15
https://doi.org/10.20538/1682-0363-2020-4-174-178

Features of the cytokine profile in children with autism spectrum disorder

Khudiakova M.I.[1], Cherevko N.A.[1], Novikov P.S.[1], Berezovskaya K.V.[2]

[1] *Siberian State Medical University*
2, Moscow Trakt, Tomsk, 634055, Russian Federation

[2] *Center of Family Medicine*
22, Trifonova Str., Tomsk, 634055, Russian Federation

ABSTRACT

The aim of the study was to reveal the particularities of the concentration of cytokines IL4, IL6, IL10, IL17, IFNγ in blood serum in children with autism spectrum disorder (ASD).

Materials and methods. The blood samples obtained from children of two study groups: children with autism spectrum disorder (n = 93) and clinically healthy children (n = 30), served as the material for the study. Cytokine concentrations were determined in blood serum using the Bender Medsystems (Austria) kits for IL17A and Vector-Best (Russia) kits for IL4, IL6, IL10, IFNγ. Serum cytokine concentrations were determined by enzyme immunoassay using kits for IL17A (Bender Medsystems, Austria), IL4, IL6, IL10, IFNγ (Vector-Best, Russia). Assessment of cognitive and psychophysiological indicators in children was performed using the Autism Treatment Evaluation Checklist (ATEC).

Results. The concentrations of IL17A (U = 54; p = 0.015) and IFNγ (U = 4.64; p = 0.006) were increased and the concentrations of IL6 (U = 327; p = 0.001) and IL4 (U = 177; p = 0.001) were decreased in children with ASD.

The concentration of IL6 correlates with the concentration of IL4 (r = 0.68; $p < 0.05$). The concentration of IL17A correlates with the concentration of IFNγ (r = 0.41; $p < 0.05$), IL6 (r = 0.87; $p < 0.05$) and ATEC score (r = 0.24; $p < 0.05$) in the group of children with ASD.

Conclusion. The cytokine imbalance in children with ADS, which was observed in the study, confirms the hypothesis of their participation in the development of the disease and clearly shows the Th17 immunoregulation pathway in the pathogenesis of the autism spectrum disorder.

Key words: autism spectrum disorder, cytokines, neuroimmune inflammation, interleukin 17A.

Conflict of interest. The authors declare the absence of obvious and potential conflicts of interest related to the publication of this article.

Source of financing. The study was sponsored by the Center of Family Medicine (Tomsk, Russia), “Sozidaniye” charity fund (Moscow, Russia), and Association of Parents of Autistic Children “AURA” (Tomsk, Russia).

Conformity with the principles of ethics. All parents of the children signed an informed consent for complex research and processing of personal data. The study was approved by the local Ethics Committee at the Center of Family Medicine (Protocol No. 7 of 18.03.2019).

For citation: Khudiakova M.I., Cherevko N.A., Novikov P.S. , Berezovskaya K.V. Features of the cytokine profile in children with autism spectrum disorder. *Bulletin of Siberian Medicine.* 2020; 19 (4): 174–178. https://doi.org/10.20538/1682-0363-2020-4-174-178.

✉ *Khudiakova M.I.,* e-mail: khudiakovami@mail.ru.

Особенности цитокинового профиля у детей с расстройством аутистического спектра

Худякова М.И.[1], Черевко Н.А.[1], Новиков П.С.[1], Березовская К.В.[2]

[1] Сибирский государственный медицинский университет (СибГМУ)
Россия, 634055, г. Томск, Московский тракт, 2

[2] ООО «Центр семейной медицины»
Россия, 634050, г. Томск, ул. Трифонова, 22

РЕЗЮМЕ

Цель работы: выявить уровень концентрации цитокинов IL-4, I-L6, IL-10, IL-17, IFNγ в сыворотке крови у детей с расстройством аутистического спектра (РАС).

Материалы и методы. Материалом исследования служили образцы крови, полученные от детей двух групп исследования: детей с расстройством аутистического спектра (n = 93) и клинически здоровых детей (n = 30). Средний возраст в обеих группах составил (7 ± 2) лет.

В сыворотке крови методом иммуноферментного анализа определяли концентрацию цитокинов IL-17A (с применением набора Bender Medsystems, Австрия) и IL-4, IL-6, IL-10, IFNγ (Вектор-Бест, Россия). Оценку когнитивных и психофизиологических показателей проводили с помощью анкеты Autism Treatment Evaluation Checklist (ATEC).

Результаты. У детей с РАС повышены значения концентрации IL-17A (U = 54; p = 0,015) и IFNγ (U = 4,64; p = 0,006) и снижены – IL-6 (U = 327; p = 0,001) и IL-4 (U = 177; p = 0,001) по сравнению с этими показателями у детей в контрольной группе. Установлены корреляции между концентрацией IL-6 и IL-4 (r = 0,68; p < 0,05); между IL-17A и IFNγ (r = 0,41; p < 0,05), IL-6 (r = 0,87; p < 0,05), количеством баллов ATEC (r = 0,24; p < 0,05) у детей с РАС.

Заключение. Установленный нами дисбаланс цитокинов у детей с РАС подтверждает гипотезу его участия в развитии РАС и свидетельствует об Th17-направлении иммунорегуляции в патогенезе расстройств аутистического спектра.

Ключевые слова: расстройство аутистического спектра, цитокины, нейроиммунное воспаление, интерлейкин 17А.

Конфликт интересов. Авторы декларируют отсутствие явных и потенциальных конфликтов интересов, связанных с публикацией настоящей статьи.

Источник финансирования. Работа выполнена за счет средств ООО «Центр семейной медицины» (г. Томск), благотворительного фонда «Созидание» (г. Москва), с участием ТРОО «АРДА «АУРА» (г. Томск).

Соответствие принципам этики. Все родители детей подписали информированное согласие. Исследование одобрено этическим комитетом ООО «Центра семейной медицины» (протокол № 7 от 18.03.2019).

Для цитирования: Худякова М.И., Черевко Н.А., Новиков П.С., Березовская К.В. Особенности цитокинового профиля у детей с расстройством аутистического спектра. *Бюллетень сибирской медицины.* 2020; 19 (4): 174–178. https://doi.org/10.20538/1682-0363-2020-4-174-178.

INTRODUCTION

Autism spectrum disorder (ASD) is a current problem of the 21st century. More new cases of the disease are being revealed every passing year. According to the statistics, the prevalence of ASD is 1:68 among children under 8 years of age [1].

The analysis of scientific data related to ASD over the last 5 years demonstrates the significant growth in global interest in the disease. However, the exact mechanism of ASD pathogenesis remains unknown. One of the modern theories of ASD development is the neuroimmune inflammation hypothesis, which is

associated with food intolerance and cognitive dysfunctions involving innate and acquired immunity and microbiota [2, 3]. In our previous studies, we identified the peculiarities of food hypersensitivity in children with ASD [4].

In this regard, the study of the role of interleukin 17 (IL17) which is thought to be responsible for immune homeostasis control in intestine mucosa, interleukin 6 (IL6), interferon gamma (IFNγ), and anti-inflammatory cytokines such as interleukin 4 (IL4) and interleukin 10 (IL10) in ASD pathogenesis in children is of current interest.

The study aims to reveal the peculiarities of the concentration of cytokines IL4, IL6, IL10, IL17, IFNγ in blood serum in children with an autism spectrum disorder.

MATERIALS AND METHODS

The study was held in the outpatient department of the Center of Family Medicine (Tomsk, Russia). A total of 123 children selected for the study were split into two groups. The main group was represented by 93 children with a varying severity level of ASD diagnosed 4–5 years ago. 30 somatically healthy children were selected for the control group. The average age of the children in both groups was (7 ± 2) years. Differentiated food hypersensitivity reactions were detected in both groups of children [4].

All parents of the children signed an informed consent for complex research and processing of personal data.

The blood samples taken from antecubital subcutaneous veins in fasting subjects served as the material of the study. Concentrations of IL4, IL6, IL10, IL17, IFNγ were assessed. Cytokines concentrations were determined in blood serum using the Bender Medsystems (Austria) kits for IL17A and Vector-Best (Russia) kits for IL4, IL6, IL10, IFNγ.

To assess the cognitive and psychophysiological changes in children with ADS and to determine the disease severity during the period of blood samples analysis the parents of the children were asked to fill the special questionnaire, the Autism Treatment Evaluation Checklist (ATEC) in accordance with their observations. The scores of the questionnaire of children from the control group were less than 10, confirming the absence of the disease in those children.

The statistical analysis was performed using the IBM SPSS Statistics 23.0 (USA) software. The obtained data were processed using Kolmogorov – Smirnov test, Mann – Whitney U-test, Wilcoxon signed-rank test, and Spearman's rank correlation coefficient. Two-sided p-values of < 0.05 were considered statistically significant.

RESULTS AND DISCUSSION

The results of the study listed in the Table 1 show that the IL17A concentration in children with ASD is significantly higher than in the control group ($U = 54$; $p = 0.015$).

Table 1

Cytokines concentration in children with ADS and children from the control group

Cytokines, pg/ml	Children with ADS		Control group	
	Med	IQR	Med	IQR
IL4	1.75*	1.00–14.93	16.30	15.58–17.13
IL6	3.20*	1.00–15.33	15.75	18.30–20.43
IL10	17.45	15.38–20.89	17.50	16.28–19.48
IL17A	9.58*	3.76–26.75	6.85	2.95–15.05
IFNγ	14.90*	13.12–16.10	13.35	11.85–14.20

* $p < 0.05$ in children with ADS compared with healthy children; Note. *Med* – median; *IQR* – interquartile range.

IL17A is the pro-inflammatory cytokine produced by several human immune cells such as Th17, neutrophils, peripheral blood mononuclear cells, type 3 innate lymphoid cells (ILC 3). The majority of these cells are situated in barrier tissues where they take part in homeostasis control in the intestine. The cytokines IL17A, IL17F and IL22 produced by ILC 3 cells enhance the barrier function of the intestine by stimulating mucin and antimicrobial peptide production [6]. The disturbance in Th17 cells regulation and IL17A production is associated with the progression of numerous inflammatory and autoimmune diseases including intestinal inflammatory diseases [7].

In literature sources, there are data concerning the IL17A effector role in children's behavioral anomalies caused by maternal immune activation, which shows the relation of neuroinflammatory state and behavioral manifestations [8, 9].

It is important to note that the highest IL17A blood concentrations among the children selected for our study were detected in severe disease manifestations cases determined according to the results of the ATEC test ($r = 0.24$; $p < 0.05$). It may indicate that the increase of IL17A concentration in serum is closely associated with the ADS severity degree.

The IL17 concentration increase in blood serum of children with ADS may be interrelated with the higher levels of IFNγ ($r = 0.41$; $p < 0.05$). According to the present data, the increase in IFNγ production is

associated with the Th17 cell plasticity. The repeated stimulation with various microbial antigens in differentiated cells leads to transcriptional changes in the Th17 line. Examples of such plasticity are Th17/Th1-cells or ILC3 cells which are able to produce both IL17A and IFNγ [10, 11]. In return, IL17A is a stimulator of pro-inflammatory cytokines (such as IFNγ and IL12) produced by macrophages [12]. It may explain the increase of IFNγ concentration in the blood serum of children with ADS comparing with the results in the control group ($U = 4.64$; $p = 0.006$). According to the literature sources, the direct action of IFNγ in high concentrations may interfere with the normal development of the neural system affecting dendrites morphology and synapses formation which can lead to ADS development [13].

According to the results of our study, the IL17A concentration in children with ADS changes in a unidirectional way with the levels of IL6 ($r = 0.87$; $p < 0.05$), concentration of which in children with ADS was decreased ($U = 327$; $p = 0.001$). It is well-known that IL6 is the key factor in Th17 cell differentiation [14]. It is the multi-purpose cytokine which may cause the cell responses to mediating inflammation, neurogenesis, gliogenesis, cell growth, and survival as well as myelinization and demyelination in CNS [15]. Moreover, it has regenerative and anti-inflammatory activity and participates in metabolic and neural processes regulation [16]. Consequently, IL6 takes part in immune system activation, hypothetically causing the development of the ADS-like phenotype in descendants [17].

Whereas, in the group of children with ADS the levels of IL6 correlate with IL4 concentration ($r = 0.68$; $p < 0.05$), which was significantly lower in children with ADS comparing with the control group ($U = 177$; $p = 0.001$). It is proved that IL4 participates in cognitive processes as a neuroprotector [18]. It becomes active during CNS inflammation, causes alternative activation of glia cells, and protects them from apoptosis. Probably, the IL4 concentration decrease is associated with ADS development.

According to the obtained data, there is no significant difference in IL10 concentration in both groups.

CONCLUSION

The cytokine imbalance in children with ADS, which was observed in our study, confirms the hypothesis of their participation in the development of the disease and clearly shows the Th17 immunoregulation pathway in the pathogenesis of the autism spectrum disorder. However, further studies of the cytokine features in ADS patients are required. It will allow understanding of the mechanism underlying the progression of neurodegenerative diseases, such as ADS, caused by inflammation.

REFERENCES

1. Christensen D.L., Baio J., Braun K.V.N., Bilder D., Charles J., Constantino J.N. Prevalence and characteristics of autism spectrum disorder among children aged 8 years-autism and developmental disabilities monitoring network. *MMWR Surveillance Summaries*. 2016; 65 (3): 1–23. DOI: 10.15585/mmwr.ss6503a1.
2. Hu C.C., Xu X., Xiong G.L., Xu Q., Zhou B.R., Li C.Y., Qin Q., Liu C.X., Li H.P., Sun Y.J., Yu X. Alterations in plasma cytokine levels in Chinese children with autism spectrum disorder. *Autism Research*. 2018; 11 (7): 989–999. DOI: 10.1002/aur.1940.
3. Fattorusso A., Di Genova L., Dell'Isola G.B., Mencaroni E., Esposito S. Autism spectrum disorders and the gut microbiota. *Nutrients*. 2019; 11 (3): 521. DOI: 10.3390/nu11030521.
4. Hudjakova M.I., Cherevko N.A., Skirnevskaja A.V., Rosenstein A.Z., Rozenshtejn M.Ju, Kondakov S.Je., Berezovskaia. K.V. Features of food hypersensitivity in children with autism spectrum disorder. *Acta Biomedica Scientifica*. 2019; 4(5): 61–68. (in Russ.) DOI: 10.29413/ABS.2019-4.5.10
5. Eftekharian M.M., Ghafouri-Fard S., Noroozi R., Omrani M.D., Arsang-Jang S., Ganji M., Gharzi V., Noroozi H., Komaki A., Mazdeh M., Taheri M. Cytokine profile in autistic patients. *Cytokine*. 2018; 108: 120–126. DOI: 10.1016/j.cyto.2018.03.034.
6. Ohnmacht C., Marques R., Presley L., Sawa S., Lochner M., Eberl G. Intestinal microbiota, evolution of the immune system and the bad reputation of pro-inflammatory immunity. *Cellular Microbiology*. 2011; 13 (5): 653–659. DOI: 10.1111/j.1462-5822.2011.01577.x.
7. Wilke C.M., Bishop K., Fox D., Zou W. Deciphering the role of Th17 cells in human disease. *Trends in Immunology*. 2011; 32: 603–611. DOI: 10.1016/j.it.2011.08.003.
8. Wong H., Hoeffer C. Maternal IL-17A in autism. *Experimental Neurology*. 2018; 299 (PtF): 228–240. DOI: 10.1016/j.expneurol.2017.04.010.
9. Choi G.B., Yim Y.S., Wong H., Kim S., Kim H., Kim S.V., Hoeffer C.A., Littman D.R., Huh J.R. The maternal interleukin-17a pathway in mice promotes autism-like phenotypes in offspring. *Science*. 2016; 351 (6276): 933–939. DOI: 10.1126/science.aad0314.
10. Sandquist I., Kolls J. Update on regulation and effector functions of Th17 cells. *F1000 Research*. 2018; 7: 205. DOI: 10.12688 / f1000research.13020.1.
11. Duhen R., Glatigny S., Arbelaez, C.A., Blair T.C., Oukka M., Bettelli E. Cutting edge: The pathogenicity of IFN-γ–producing Th17 cells is independent of T-bet. *The Journal of Immunology*. 2013; 190 (9): 4478–4482. DOI: 10.4049/jimmunol.1203172.
12. AL-Ayadhi L.Y., Mostafa G.A.. Elevated serum levels of interleukin-17A in children with autism. *Journal of Neuroinflammation*. 2012; 9 (1): 158. DOI: 10.1186 / 1742-2094-9-158.

13. Leipzig N.D., Xu C., Zahir T., Shoichet M.S. Functional immobilization of interferon-gamma induces neuronal differentiation of neural stem cells. *Journal of Biomedical Materials Research Part A.* 2010; 93 (2): 625–633. DOI: 10.1002/jbm.a.32573.
14. Kuchroo V.K., Awasthi A. Emerging new roles of Th17 cells. *European Journal of Immunology*. 2012; 42 (9): 2211–2214. DOI: 10.1002/eji.201242872.
15. Erta M., Quintana A., Hidalgo J. Interleukin-6, a major cytokine in the central nervous system. *International Journal of Biological Sciences*. 2012; 8 (9): 1254–1266. DOI: 10.7150/ijbs.4679.
16. Scheller J., Chalaris A., Schmidt-Arras D., Rose-John S. The pro- and anti-inflammatory properties of the cytokine interleukin-6. *Biochimica et Biophysica Acta*. 2011; 1813(5): 878–888. DOI: 10.1016/j.bbamcr.2011.01.034.
17. Atladottir H.O., Thorsen P., Ostergaard L., Schendel D.E., Lemcke S., Abdallah M., Parner E.T. Maternal infection requiring hospitalization during pregnancy and autism spectrum disorders. *Journal of Autism and Developmental Disorders*. 2010; 40 (12): 1423–1430. DOI: 10.1007/s10803-010-1006-y.
18. Gadani S.P., Cronk J.C., Norris G.T., Kipnis J. IL-4 in the brain: a cytokine to remember. *The Journal of Immunology*. 2012; 189 (9): 4213–4219. DOI: 10.4049/jimmunol.1202246.

Authors information

Khudiakova Maria I., External PhD Student, Siberian State Medical University, Tomsk, Russian Federation. ORCID 0000-0002-6320-5017.

Cherevko Natalia A., Dr. Sci. (Med.), Professor of the Department of Allergology and Immunology, Siberian State Medical University, Tomsk, Russian Federation. ORCID 0000-0003-1023-4137.

Novikov Pavel S., External PhD Student, Siberian State Medical University, Tomsk, Russian Federation.

Berezovskaya Ksenia V., General Practitioner, Pediatrician, Center of Family Medicine, Tomsk, Russian Federation.

(✉) **Khudiakova M.I.,** e-mail: khudiakovami@mail.ru.

Received 07.02.2020
Accepted 29.09.2020

УДК 616.24-002.5-078.75- 092.4
https://doi.org/10.20538/1682-0363-2020-4-179-188

Expression of pro-inflammatory and co-stimulatory molecules on the surface of macrophages in vitro in patients with pulmonary tuberculosis

Churina E.G.[1, 2], Sitnikova A.V.[1], Urazova O.I.[1, 2], Novitskiy V.V.[1, 2], Patysheva M.R.[2, 4], Golubchikov P.N.[5], Stepanova E.P.[5]

[1] Siberian State Medical University
2, Moscow Trakt, Tomsk, 634050, Russian Federation

[2]National Research Tomsk State University
36, Lenina Av., Tomsk, 634050, Russian Federation

[3]Tomsk State University of Control Systems and Radioelectronics
40, Lenina Av., Tomsk, 634050, Russian Federation

[4] Cancer Research Institute, Tomsk National Research Medical Center, the Russian Academy of Sciences
5, Kooperativny Str., Tomsk, 634009, Russian Federation

[5] Tomsk Phthisiopulmonological Medical Center
17/1, R. Luksemburg Str., Tomsk, 634009, Russian Federation

ABSTRACT

The aim of this study was to identify features of the expression of pro-inflammatory and co-stimulatory molecules on the surface of macrophages *in vitro* in patients with pulmonary tuberculosis, based on the clinical form of the disease and sensitivity of the pathogen to anti-TB drugs.

Materials and methods. 40 patients (36 men and 4 women) with pulmonary tuberculosis (TB) were examined: 18 patients (16 men and 2 women, average age (44.56 ± 8.10) years) with disseminated tuberculosis (DTB) and 22 patients (20 men and 2 women, average age (46.54 ± 5.24) years) with infiltrative tuberculosis (ITB). Of those, 30 patients had *Mycobacterium tuberculosis* (MBT) sensitive to the basic anti-TB drugs (ATBD), and 10 patients had MBT resistant to first-line anti-TB drugs. Venous blood was the study material. To isolate monocytes from the whole blood in order to transform them into macrophages, ficoll density gradient centrifugation with gradient density of 1.077 g/cm^3 was used followed by immunomagnetic separation of CD14$^+$ cells. Monocytes were cultured in a complete culture medium X-VIVO 10 with gentamicin and phenol red with the addition of the macrophage colony-stimulating factor (M-CSF) (5 ng/ml) at a concentration of 1×10^6 cells/ml with the following stimulators: interleukin (IL) 4 (10 ng/ml) and interferon (IFN) γ (100 ng/ml). Immunophenotyping of macrophages was performed using monoclonal antibodies to CD80, CD86, and HLA-DR on a Beckman Coulter CytoFLEX LX flow cytometer (Beckman Coulter, USA). The analysis of the obtained data was carried out using the CytExpert 2.0 software application. The results were analyzed using statistical methods.

Results. The number of intact and cytokine-stimulated (IL-4 and IFNγ) CD80-positive macrophages in patients with ITB and drug-resistant TB (DR TB) exceeded their number not only in healthy donors, but also in patients with DTB and drug-sensitive TB (DS TB), respectively. In addition, an increase in CD86 expression on the surface of macrophages was registered in patients with ITB and DR TB after adding IFNγ (M1-activation inducer) to the suspension culture. In contrast, in patients with DTB and DS TB, the number of macrophages with expression of B7 family co-stimulating molecules decreased or remained within the normal values in the absence of a reaction to cytokines during cytokine induction. Deficiency of HLA-DR-positive macrophages was found in all TB patients. The minimal number of macrophages expressing HLA-DR was found in patients with DTB and DS TB after cell incubation with IL-4 (M2-activation inducer).

Conclusion. Evaluation of the expression of B7 (CD80/86) and HLA-DR membrane molecules on macrophages in TB patients allows to conclude that anti-TB immune response is impaired at stages of antigen presentation (in all

✉ *Churina Elena G.,* e-mail: Lena1236@yandex.ru.

examined patients with TB) and co-stimulation (in DTB and DS TB). An increase in the expression of macrophage surface molecules CD80 (with M1- and M2-stimulation) and CD86 (with M1-stimulation) in patients with ITB and DR TB indicates an increase in cell reactivity in these forms of TB. In addition, deficit of expression of HLA-DR (a key marker of pro-inflammatory cell activation) on the surface of macrophages in TB can be considered as a general (independent of the clinical form of the disease and drug sensitivity of the pathogen) pathogenetic factor of immune imbalance in pulmonary tuberculosis.

Key words: macrophages, pulmonary tuberculosis, innate immunity, immune response, co-stimulating molecules, IL-4, IFNγ, CD80, CD86, HLA-DR.

Conflict of interest. The authors declare the absence of obvious and potential conflicts of interest related to the publication of this article.

Source of financing. The reported study was funded by Council for Grants of the President of the Russian Federation for leading scientific schools (No. SS-2690.2018.7) and the RFBR, project No. 19-315-90018.

Conformity with the principles of ethics. All patients participating in the study signed an informed consent. The study was approved by the local Ethics Committee at Siberian State Medical University (Protocol No. 5648 of 27.11.2017).

For citation: Churina E.G., Sitnikova A.V., Urazova O.I., Novitskiy V.V., Patysheva M.R., Golubchikov P.N., Stepanova E.P. Expression of pro-inflammatory and co-stimulatory molecules on the surface of macrophages *in vitro* in patients with pulmonary tuberculosis. *Bulletin of Siberian Medicine.* 2020; 19 (4): 179–188. https://doi.org/10.20538/1682-0363-2020-4-179-188.

Экспрессия провоспалительных и костимулирующих молекул на макрофагах *in vitro* у больных туберкулезом легких

Чурина Е.Г.[1, 2], Ситникова А.В.[1], Уразова О.И.[1, 3], Патышева М.Р.[2, 4], Новицкий В.В.[1, 3], Голубчиков П.Н.[5], Степанова Е.П.[5]

[1] *Сибирский государственный медицинский университет (СибГМУ)*
Россия, 634050, г. Томск, Московский тракт, 2

[2] *Национальный исследовательский Томский государственный университет (НИ ТГУ)*
Россия, 634050, г. Томск, пр. Ленина, 36

[3] *Томский государственный университет систем управления и радиоэлектроники(ТУСУР)*
Россия, 634050, г. Томск, пр. Ленина, 40

[4] *Научно-исследовательский институт (НИИ) онкологии, Томский национальный исследовательский медицинский центр (НИМЦ) Российской академии наук*
Россия, 634009, г. Томск, пер. Кооперативный, 5

[5] *Томский фтизиопульмонологический медицинский центр*
634009, г. Томск, ул. Р. Люксембург, 17

РЕЗЮМЕ

Цель работы – установить особенности экспрессии провоспалительных и костимулирующих молекул на макрофагах *in vitro* у больных туберкулезом легких в зависимости от клинической формы заболевания и чувствительности возбудителя к противотуберкулезным лекарственным средствам.

Материалы и методы. Обследованы 40 пациентов (36 мужчин и 4 женщины): 18 пациентов с диссеминированным туберкулезом легких (ДТБ) (16 мужчин и 2 женщины, средний возраст (44,56 ± 8,10) лет) и 22 пациента с инфильтративным туберкулезом легких (ИТБ) (20 мужчин и 2 женщины, средний возраст (46,54 ± 5,24) лет) с туберкулезом легких (ТБ). Из них было 30 пациентов, выделяющих *Mycobacterium tuberculosis* (МВТ), чувствительные к основным противотуберкулезным средствам (ПТС), и 10 пациентов, выделяющих МВТ, устойчивые к лекарственным средствам основного ряда противотуберкулезной терапии. Группу сравнения составили 15 здоровых доноров с сопоставимыми характеристиками по полу и возрасту.

Материалом исследования являлась венозная кровь. Для выделения моноцитов из цельной крови с целью их трансформации в макрофаги использовали метод центрифугирования в градиенте фиколла плотностью 1,077 г/см^3 с последующей иммуномагнитной сепарацией CD14$^+$ клеток. Моноциты культивировали в полной питательной среде X-VIVO 10 с добавлением колониестимулирующего фактора макрофагов (M-CSF) (5 нг/мл) в концентрации 1×10^6 клеток/мл со стимуляторами: интерлейкином (IL) 4 (10 нг/мл) и интерфероном (IFN) γ (100 нг/мл). Иммунофенотипирование макрофагов проводили с использованием моноклональных антител к CD80, CD86, HLA-DR на проточном цитометре Beckman Coulter CytoFLEX LX (Beckman Coulter, США). Анализ полученных данных осуществляли при помощи программного приложения CytExpert 2.0 (Beckman Coulter, США). Полученные результаты анализировали статистическими методами.

Результаты. Количество интактных и стимулированных цитокинами (IL-4 и IFNγ) CD80-позитивных макрофагов у больных ИТБ и с лекарственно-устойчивым ТБ (ЛУ ТБ) превышало их число не только у здоровых доноров, но и у больных ДТБ и с лекарственно-чувствительным ТБ (ЛЧ ТБ) соответственно. Кроме того, у больных ИТБ и ЛУ ТБ регистрировалось повышение экспрессии CD86 на макрофагах после добавления в суспензионную культуру IFNγ (индуктор M1-активации). У больных ДТБ и ЛЧ ТБ количество макрофагов с экспрессией костимулирующих молекул семейства B7 при индукции цитокинами, напротив, снижалось или сохранялось в пределах нормы в отсутствие реакции на цитокины. Дефицит HLA-DR-позитивных макрофагов обнаруживался у всех больных ТБ. Минимальное число макрофагов, экспрессирующих HLA-DR, установлено у больных ДТБ и ЛЧ ТБ после инкубации клеток с IL-4 (индуктор M2-активации).

Заключение. Оценка экспрессии мембранных молекул B7 (CD80/86) и HLA-DR на макрофагах у больных ТБ позволяет сделать вывод о нарушениях противотуберкулезного иммунного ответа на стадии презентации антигена (у всех обследованных больных ТБ) и костимуляции (при ДТБ и ЛЧ ТБ). Увеличение экспрессии макрофагами поверхностных молекул CD80 (при M1- и M2-стимуляции) и CD86 (при M1-стимуляции) у больных ИТБ и ЛУ ТБ свидетельствует о повышении реактивности клеток при данных формах течения ТБ. Наряду с этим дефицит экспрессии на макрофагах HLA-DR (ключевого маркера провоспалительной активации клеток) при ТБ можно рассматривать как общий (не зависящий от клинической формы болезни и лекарственной чувствительности возбудителя) патогенетический фактор иммунного дисбаланса при туберкулезе легких.

Ключевые слова: макрофаги, туберкулез легких, врожденный иммунитет, иммунный ответ, костимулирующие молекулы, IL-4, IFNγ, CD80, CD86, HLA-DR.

Конфликт интересов. Авторы декларируют отсутствие явных и потенциальных конфликтов интересов, связанных с публикацией настоящей статьи.

Источник финансирования. Исследование выполнено при финансовой поддержке Совета по грантам Президента Российской Федерации для ведущих научных школ (НШ-2690.2018.7) и РФФИ в рамках научного проекта № 19-315-90018.

Соответствие принципам этики. Пациенты подписали информированное согласие. Исследование одобрено локальным этическим комитетом СибГМУ (протокол № 5648 от 27.11.2017).

Для цитирования: Чурина Е.Г., Ситникова А.В., Уразова О.И., Патышева М.Р., Новицкий В.В., Голубчиков П.Н., Степанова Е.П. Экспрессия провоспалительных и костимулирующих молекул на макрофагах *in vitro* у больных туберкулезом легких. *Бюллетень сибирской медицины.* 2020; 19 (4): 179–188. https://doi.org/10.20538/1682-0363-2020-4-179-188.

INTRODUCTION

It is known that immunity is a complex of factors of life-sustaining activity of an organism aimed at maintaining body homeostasis. Acquired resistance to tuberculosis is a result of complex immune responses with involvement of macrophages, dendritic cells, lymphocytes, and granulocytes. At the same time, macrophages and human lymphatic system serve as a "phylogenetic cradle" for the causative agent of tuberculosis infection and promote the formation of symbiotic relationships between *Mycobacterium tuberculosis* (MBT) and a host organism [1]. Macrophages play a crucial role in the successful realization of innate immunity mechanisms in during pathogen invasion into mucous membranes of the respiratory tract (including MBT).

Macrophages are the most ancient immunocompetent cells. They represent a heterogeneous population of resident professional antigen presenting cells. The macrophage is the main effector cell in protecting the host from pathogens and regulating the innate and adaptive immune responses. Macrophages are involved in remodeling and restoration of damaged tissues [2, 3]. Versatility and plasticity of macrophages make it

possible for a rapid conversion of their functional phenotype in the focus of inflammation. This heterogeneity is determined by the ability of macrophages to implement different programs of activation in response to various stimuli, such as cytokine signals and signals associated with cell damage or penetration of the pathogen- and damage-associated molecular pattern molecules (DAMPs/PAMPs) into the body. In classic activation, macrophages maintain the course of an acute inflammatory Th1-dependent immune response while simultaneously performing the effector function (M1-activation). In alternative activation, macrophages acquire an anti-inflammatory phenotype resulting in their functional realignment and they start performing a tolerogenic function promoting fibrogenesis and enhanced cell proliferation (M2-activation) [4, 5].

The classic macrophage activation leading to polarization of their maturation towards M1-cells is induced by interferon (IFN) γ produced by type 1 T-helpers (Th1) and natural killers (NK) cells as well as tumor necrosis factor (TNF) α and bacterial lipopolysaccharides (LPS) [6]. Interleukins (IL) 4 and 10 are the main differentiation factors for alternatively activated M2-macrophages [7, 8]. Toll-like receptors (TLR) on the surface and inside macrophages recognize patterns of pathogenicity and, thus, trigger the activation of innate immunity. Molecules of the major histocompatibility complex (MHC) (HDL-DR) and co-stimulating molecules of the B7 group form a functionally important group of surface macrophage molecules. The expression of MHC-II molecules is enhanced by cell activation; CD80 and CD86 act as co-stimulating molecules. The former appears on the macrophage surface only after activation, the latter is expressed constitutively, but in antigen induction the intensity of expression increases [9–11].

Inflammation is the major effector mechanism of innate immunity which is implemented in the lungs in response to *M. tuberculosis* invasion into alveolar macrophages. This occurs if macrophages do not perform a phagocytic function for some reason. The effectiveness of inflammatory and regenerative potential of macrophages is determined, first of all, by their functional phenotype and the intensity of pro-inflammatory molecule expression on the cells.

Thus, the aim of this study was to identify the features of the expression of pro-inflammatory and co-stimulatory molecules on the surface of macrophages *in vitro* in patients with pulmonary tuberculosis, depending on the clinical form of the disease and sensitivity of the pathogen to anti-TB drugs.

MATERIALS AND METHODS

We examined 40 patients (36 men and 4 women): 18 patients with disseminated tuberculosis (DTB) (16 men and 2 women, average age (44.56 ± 8.10) years) and 22 patients with infiltrative tuberculosis (ITB) (20 men and 2 women, average age (46.54 ± 5.24) years). The diagnosis was established on the basis of medical history data, clinical findings, results of an X-ray examination of the lungs, and bacteriological and microscopic examination of the sputum.

Drug sensitivity of the pathogen to the basic ATBD was examined in all patients with TB. According to this criterion, 30 patients secreted MBT sensitive to the basic ATBD and 10 patients secreted MBT resistant to the first line ATBD (isoniazid, rifampicin, streptomycin, ethambutol). The exclusion criteria were under the age of 20 years and over 55 years, the presence of allergies, and severe concomitant diseases of infectious and non-infectious origin. 15 healthy donors with comparable characteristics by age and gender composed the comparison group.

The material for the study was venous blood collected from healthy donors and TB patients. Blood sampling was carried out once, in the middle of the disease course, before the start of anti-TB chemotherapy. To isolate monocytes from the whole blood with the aim of their following transformation into macrophages, the method of magnetic separation of $CD14^+$ monocytes (MACS MultiStand, Germany) was used according to the manufacturer's instructions (Miltenyi Biotec GmbH, Germany).

20 ml of the whole venous blood was collected into vacuum blood collection systems with an anticoagulant (K_3-EDTA). The blood was diluted with phosphate-buffer saline (PBS) at a 1:1 ratio and layered over 15 ml of ficoll with a density of 1.077 g/cm^3.
The samples were centrifuged for 30 min at 0.016 g. The resulting mononuclear fraction was collected and washed from PBS twice. After that, 5 ml of PBS was added, and the mixture was stirred; then the number of mononuclear cells was counted using an automatic cell counter Scepter 2,0 (Merck Millipore, Germany). The cell suspension was centrifuged, the supernatant was removed, and the appropriate volume of MACS Separation Buffer (containing bovine serum albumin (BSA), EDTA, and 0.09% azide) and $CD14^+$ magnetic particles (Micro Beads, Germany) were added based on the number of cells, followed by incubation for 40 min. The resulting suspension underwent positive magnetic separation according to the manufacturer's protocol (Miltenyi Biotec, Germany).

IN VITRO MACROPHAGE CULTIVATION

Monocytes were cultivated in X-VIVO 10 complete growth-supporting medium with gentamycin and phenol red (Lonza, Switzerland) at a concentration of 1×10^6 cell/ml with the addition of M-CSF (5 ng/ml; RnD Systems, USA). Recombinant cytokines IL-4 (10 ng/ml; PeproTech, USA) (for M2-cell activation) and IFNγ (100 ng/ml PeproTech, USA) (for M1-cell activation) were used for additional cell induction. The samples had been cultivated in the CO_2-incubator for 6 days at 37 ° C and 7.5% of CO_2 without additional stimulation and with the addition of M1- and M2-activation cytokines.

IMMUNOPHENOTYPING OF MACROPHAGES

Macrophage phenotyping was performed on the sixth day of cultivation. To collect cells, a plate with the cell culture was placed on ice and held for 10 minutes, then the cells were collected using a cell scraper (Cell-scraper, USA). Monoclonal antibodies to CD80, CD86, and HLA-DR (eBioscience, USA) were added for immunophenotyping of macrophages. Measurement of cell suspensions was implemented using Beckman Coulter CytoFLEX flow cytometer (Beckman Coulter, USA). The analysis of obtained data was performed using CytExpert 2.0 software application (Beckman Coulter, USA).

SPSS Statistics 17.0 and Microsoft Excel were used for statistical analysis of the obtained data. The data were presented as the median (Me) and 25th and 75th percentiles (1st and 3rd quartiles: Q_1 and Q_3 respectively). To perform a comparative analysis, the non-parametric Mann – Whitney test with the Benjamini – Hochberg correction was applied. The results of statistical analysis were considered significant at $p < 0.05$.

RESULTS

When studying the expression of co-stimulating B7 molecules (CD80 / CD86) and HLA-DR activation marker on the surface of macrophages, it was found that the number of macrophages expressing CD80 molecules in patients with ITB was higher than in patients of the control group and patients with DTB. In DTB patients, it was lower than in healthy donors (Table 1, Fig. 1). The addition of IFNγ to cell cultures in patients with ITB was accompanied by an increase in the expression of CD80. The addition of IL-4 to the cell culture, on the contrary, was accompanied by a decrease in the CD80 expression, compared with its value in the absence of stimulation (Table 1). In DTB, the level of cytokine-induced expression of CD80 did not significantly differ from normal values, but in the absence of stimulation it was significantly lower than in healthy patients (Table 1).

Table 1

Expression of pro-inflammatory markers on the surface of macrophages depending on the clinical form of the disease in patients with TB, %, *Me* (Q_1–Q_3)

Markers of macrophages	Groups of comparison	During cultivation without stimulation	During cultivation with IL-4 (M2-stimulation)	During cultivation with IFNγ (M1-stimulation)
CD80	Healthy donors	23.11 (15.14–27.11)	15.25 (7.53–25.14)	20.32 (10.91–31.44)
	Patients with DTB	12.23 (8.42–25.13) $p_1 = 0.012$	11.65 (8.01–26.13)	18.70 (9.34–28.27)
	Patients with ITB	48.60 (24.17–51.14) $p_1 = 0.014$ $p_2 = 0.022$	41.61 (20.15–53.23) $p_1 = 0.015$ $p_2 = 0.031$	58.50 (28.73–70.35) $p_1 = 0.021$ $p_2 = 0.012$ $p_4 = 0.014$
CD86	Healthy donors	11.12 (8.52–28.01)	43.51 (32.53–54.55) $p_3 = 0.012$	23.22 (10.01–31.14) $p_3 = 0.016$ $p_4 = 0.025$
	Patients with DTB	14.14 (9.37–21.52)	13.48 (4.73–19.04) $p_1 = 0.012$	15.52 (7.14–25.37) $p_1 = 0.013$
	Patients with ITB	16.54 (9.22–27.63)	19.12 (8.56–23.14) $p_1 = 0.021$	27.02 (15.23–39.14) $p_2 = 0.012$ $p_3 = 0.015$ $p_4 = 0.034$
HLA-DR	Healthy donors	95.61 (76.66–98.73)	97.33 (85.41– 98.43)	96.66 (76.32–99.32)
	Patients with DTB	71.12 (51.33–83.72) $p_1 = 0.021$	57.71 (33.62–77.71) $p_1 = 0.022$ $p_3 = 0.025$	74.16 (42.74–84.23) $p_1 = 0.017$ $p_4 = 0.014$

Table 1 (continued)

Markers of macrophages	Groups of comparison	During cultivation without stimulation	During cultivation with IL-4 (M2-stimulation)	During cultivation with IFNγ (M1-stimulation)
HLA-DR	Patients with ITB	75.44 (51.51–87.53) $p_1 = 0.012$	67.51 (45.63–78.42) $p_1 = 0.013$	62.51 (44.72–83.43) $p_1 = 0.024$

Note: p_1 – the level of statistical significance of differences compared to the value of the indicator in healthy donors; p_2 – compared to the value in patients with DTB; p_3 – compared to the value during in vitro cell culture without stimulation; p_4 – compared to the value during *in vitro* cell culture with IL-4 (M2-stimulation).

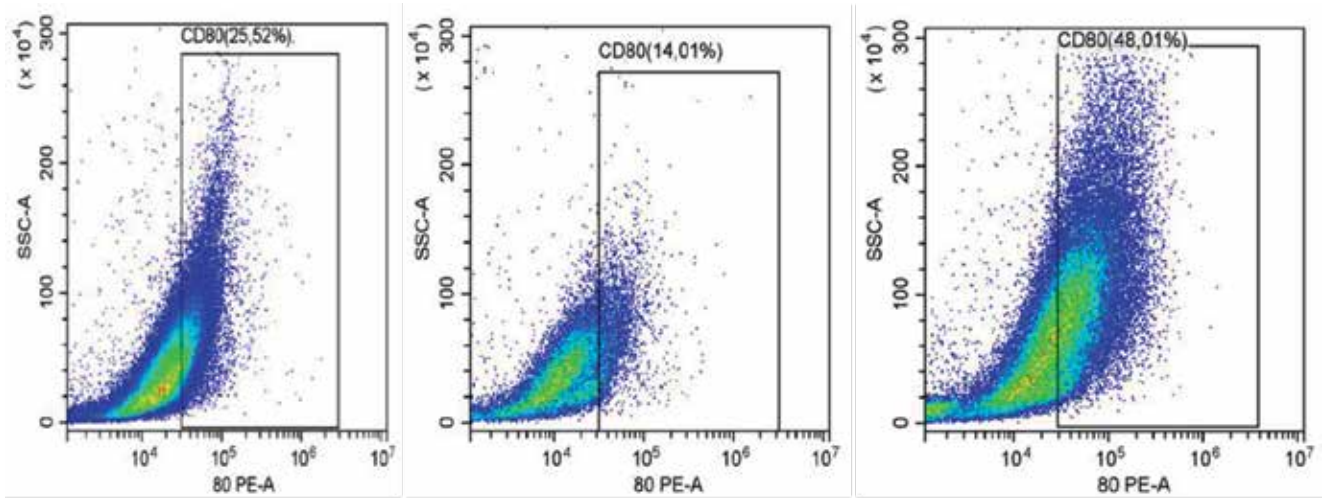

a *b* *c*

Fig. 1. The expression of CD80 on macrophages in patients with pulmonary tuberculosis depending on the clinical form of the disease, %: *a* – in healthy donors; *b* – in patients with DTB; *c* – in patients with ITB

The analysis of CD80 expression in TB patients depending on sensitivity of MBT to ATBD revealed the maximum number of CD80-positive macrophages in patients with DR TB compared to their number in healthy donors and patients with DS TB (Table 2). Herewith, in patients with DR TB, the expression of CD80 on the surface of macrophages stimulated by IL-4 and IFNγ cytokines was significantly higher than that on unstimulated cells (Table 2). In patients with DS TB after IFNγ induction of cells (M1-activation), the number of CD80-positive macrophages corresponded to that in healthy patients but was 1.9 times higher than with IL-4 stimulation (M2-activation) and without the addition of cytokines (Table 2).

In patients with TB, there were no differences in the expression of CD86 molecules by macrophages in the absence of stimulation by recombinant cytokines, regardless of the clinical form of the disease. When adding cytokines to the cell culture, the expression of CD86 on the surface of macrophages in healthy donors increased by 3.9 times in response to IL-4 induction (M2-activation) and 2.1 times in response to IFNγ induction (M1-activation), as opposed to values without stimulation. In patients with ITB, the number of CD86-expressing macrophages upon IFNγ induction was higher than in DTB patients and compared with their number in the absence of stimulation and with IL-4 induction of cells (it decreased, on the contrary) (Table 1). In addition, under IFNγ effects, an increase in CD86 expression by macrophages was observed in DR TB in comparison with patients with DS TB and in healthy donors, as well as in comparison with expression of the marker by unstimulated macrophages and during induction of cells by IL-4 (Table 2).

The analysis of the expression of HLA-DR-activating marker on the surface of macrophages revealed its decrease in patients with TB compared with the group of healthy donors, regardless of the clinical form of the disease and sensitivity of the pathogen to ATBD (Table 1, 2, Fig. 3). The maximum decrease in the number of macrophages expressing HLA-DR was observed in patients with DTB and DR TB after incubation of cells with IL-4, as opposed to their number in cell culture without stimulation and during IFNγ induction (Table 1, 2).

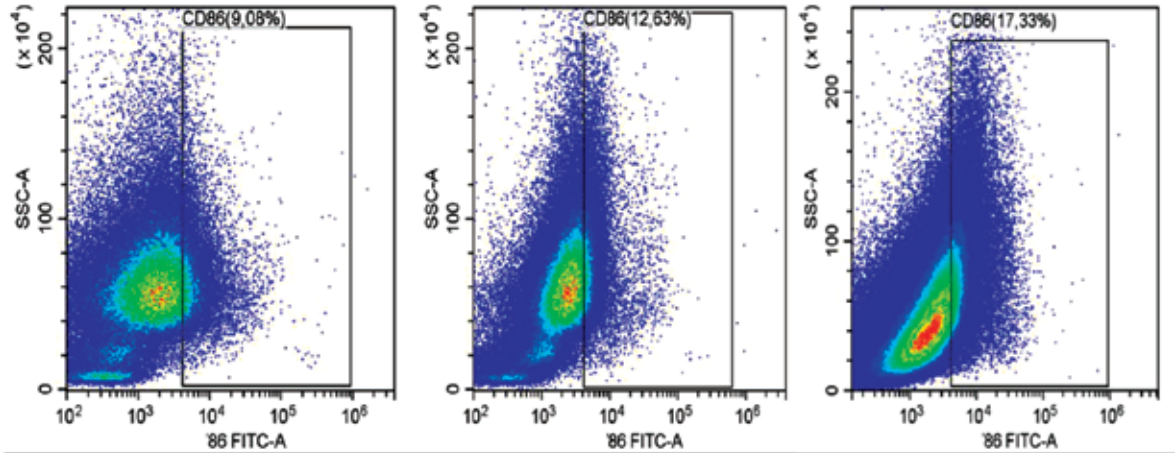

a *b* *c*

Fig. 2. The expression of CD86 on the surface of macrophages in patients with pulmonary tuberculosis depending on the clinical form of the disease, %: *a* – in healthy donors; *b* – in patients with DTB; *c* – in patients with ITB

Table 2

The expression of pro-inflammatory markers on the surface of macrophages depending on drug sensitivity of the pathogen to anti-TB drugs, %, *Me* (Q_1–Q_3)

Markers of macrophages	Groups of comparison	During cultivation without stimulation	During cultivation with IL-4 (M2-stimulation)	During cultivation with IFNγ (M1-stimulation)
CD80	Healthy donors	23.11 (15.14 –27.11)	15.25 (7.53 –25.14)	20.32 (10.91–31.44)
	Patients with DS TB	11.01 (9.21–26.63) $p_1 = 0.041$	12.22 (10.02–28.41)	23.55 (11.5–34.24) $p_3 = 0.025$ $p_4 = 0.017$
	Patients with DR TB	51.22 (23.11–68.33) $p_1 = 0.015$ $p_2 = 0.022$	62.33 (37.21–71.42) $p_1 = 0.037$ $p_2 = 0.025$ $p_3 = 0.027$	61.22 (32.45–70.66) $p_1 = 0.026$ $p_2 = 0.022$ $p_3 = 0.011$
CD86	Healthy donors	11.12 (8.52–28.01)	43.51 (32.53–54.55) $p_3 = 0.010$	23.22 (10.01–31.14) $p_3 = 0.015$ $p_4 = 0.024$
	Patients with DS TB	14.02 (8.51–21.44)	13.54 (10.25–25.11) $p_1 = 0.031$	17.23 (10.32–28.55)
	Patients with DR TB	18.22 (9.25–30.45) $p_1 = 0.030$	25.23 (14.01–36.12) $p_1 = 0.042$ $p_2 = 0.010$	34.45 (18.23–41.56) $p_1 = 0.024$ $p_2 = 0.014$ $p_3 = 0.012$ $p_4 = 0.021$
HLA-DR	Healthy donors	95.61 (76.66–98.73)	97.33 (85.41–98.43)	96.66 (76.32–99.32)
	Patients with DS TB	69.23 (56.25–86.12) $p_1 = 0.012$	55.12 (43.22–75.23) $p_1 = 0.022$ $p_3 = 0.011$	66.23 (42.5–84.23) $p_1 = 0.031$ $p_3 = 0.015$
	Patients with DR TB	80.23 (59.12–94.54) $p_1 = 0.044$ $p_2 = 0.012$	76.12 (49.52–90.13) $p_1 = 0.034$ $p_2 = 0.012$	72.12 (57.32–86.42) $p_1 = 0.035$ $p_2 = 0.014$

Note: p_1 – the level of statistical significance of differences compared to the value of the indicator in healthy donors; p_2 – in patients with DS TB; p_3 – in in vitro cell culture without stimulation; p_4 – in in vitro cell culture with IL-4 (M2-stimulation).

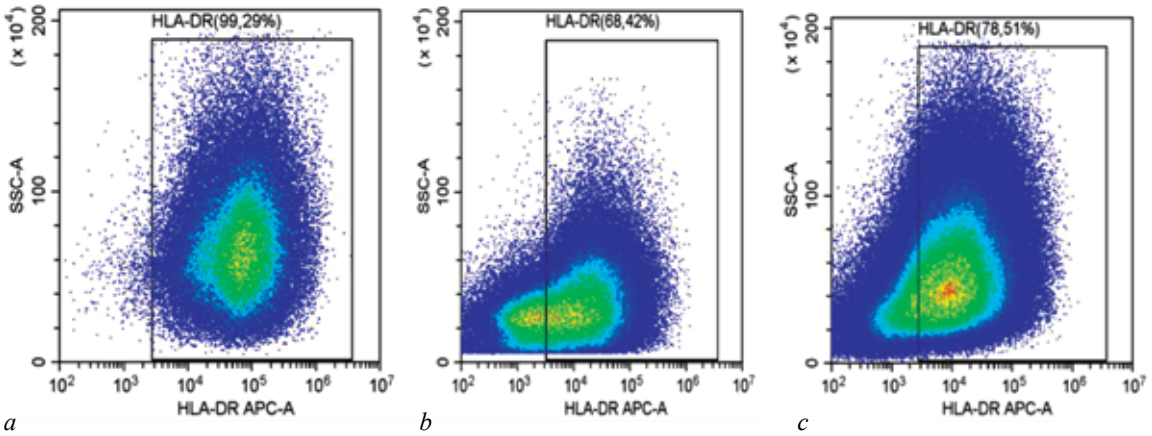

Fig. 3. The expression of HLA-DR on the surface of macrophages in patients with pulmonary tuberculosis depending on the clinical form of the disease, %: *a* – in healthy donors; *b* – in patients with DTB; *c* – in patients with ITB.

DISCUSSION

Analysis of the expression of pro-inflammatory markers, namely B7 co-stimulatory molecules (CD80, CD86) and HLA-DR marker of activation on the surface of macrophages, showed that the number of macrophages expressing HLA-DR, which is necessary for implementation of their antigen-presenting function, was reduced in patients with DTB and ITB, especially during M2-activation of cells. Interestingly, macrophage expression of CD80 and CD86 molecules in patients with TB was multidirectional. For instance, we observed a significant increase in the number of CD80-positive cells in patients with ITB, especially during stimulation with IFNγ (at M1-activation), while in patients with DTB, the number of $CD80^+$ macrophages decreased (Table 1, Fig. 1). It should be noted that in DR TB, the expression of the CD80 molecule sharply increased both during M1- and M2-activation of macrophages (Table 2).

The expression of the CD86 molecule on the surface of unstimulated macrophages did not generally differ from that in the control group. However, it increased during M1-activation of cells in patients with infiltrative and drug resistant TB (Table 1, 2). It may be assumed that intensive expression of CD86 co-stimulating molecule during *in vitro* differentiation of cells into M1-macrophages in ITB and DR TB was caused by the preservation of their pro-inflammatory potential. At the same time, natural expression of CD86 on the surface of macrophages regardless of the antigen load and mediator stimulation should be taken into account.

It is known that co-stimulating CD80 and CD86 molecules are the members of the B7 family [12]. CD80 and CD86 markers were found not only on the surface of dendritic cells, activated B-lymphocytes, and macrophages [13], but also on the surface of non-professional antigen-presenting cells [14]. The CD80 molecule, often in the tandem with CD86, plays an important role in the regulation of both adaptive and innate immune responses. These molecules are ligands for the CD28 receptor on the surface of naive T-lymphocytes, and their interaction is an important co-stimulating signal in immunological synapse between a macrophage and a T-cell, which leads to the activation, proliferation, and differentiation of T-lymphocytes in a necessary direction [15]. CD80 is a key marker of the activation of macrophages and it is not expressed on the surface of cells in the absence of the antigen load [16]. In inflammation, interaction of the macrophage with the receptor on the surface of the T-lymphocyte via MHC-II leads to the activation of CD80 [13].

HLA-DR is constitutively expressed on the surfaces of monocytes, macrophages, and dendritic cells. Monocytes of a healthy human also express HLA-DR molecules on their surface at high density. Previously, while investigating in vitro dendritic cells transformed from blood monocytes in patients with TB, we had showed enhanced generation of tolerogenic dendritic cells (HLA-DR-negative) associated with an imbalance of their cytokine secretory activity [17].

HLA-DR expression on the surface of monocytes and macrophages is crucial for the presentation of microbial peptides by T-cells, which contributes to the initiation of the adaptive immune response [18]. The negative role of decreased expression of HLA-DR on the surface of macrophages has been shown. Mono-

cytes and macrophages with reduced or no expression of HLA-DR are not able to perform their antigen-presenting function. The change in the expression of HLA-DR on the surface of monocytes/macrophages is considered to be an informative marker of the dynamics of the immune response in critical conditions [19]. A decrease in the number of HLA-DR-positive monocytes has been described in severe injuries, in the postoperative period, in acute pancreatitis, and burn injury [20, 21]. In the development of hospital-acquired infection, a decrease in the expression of HLA-DR on the surface of monocytes determines the development of sepsis [22].

Thus, a significant decrease in the number of HLA-DR-positive cells (especially in patients with DTB) established by us indicates impairment of the mechanism of classic activation of macrophages and their antigen-presenting and effector functions.

CONCLUSION

According to the obtained findings, changes in *in vitro* expression of CD80/CD86 co-stimulating molecules on the surface of macrophages in patients with TB are multidirectional. In case of DTB and DS TB, the number of intact (unstimulated) CD80-positive macrophages is lower than the normal value; and in ITB and DR TB, the number of such macrophages is higher than the normal value, both in the absence of stimulation and with M2- and especially M1-activation of macrophages. The latter in association with an increase in the expression of CD80 during IFNγ-mediated M1-induction of macrophages in ITB and DR TB patients indicates an increase in pro-inflammatory reactivity of cells in these forms of TB. The absence of increase or, on the contrary, a decrease in expression of CD80 and CD86 on the surface of macrophages in response to cytokine stimulation in patients with DTB and DS TB along with a deficiency of the expression of HLA-DR may be considered as a pathogenetic factor of the immune imbalance, a manifestation of secondary immune deficiency in pulmonary tuberculosis, and an indicator of an unfavorable prognosis of the disease.

REFERENCES

1. Novitskiy V.V., Urazova O.I., Strelis A.K., Voronkova O.V., Filinyuk O.V., Shilko T.A. Pathology of the immunity: a cause or consequence of TB infection? *Bulletin of Siberian Meedicine*. 2006; 5 (2):70–74 (in Russ.).
2. Murray P., Wynn T. Protective and pathogenic functions of macrophage subsets. *Nat. Rev. Immunol.* 2011; 11 (11): 723–737. DOI: 10.1038/nri3073.
3. Churina E.G., Sitnikova A.V. *Urazova O.I.,* Chumakova S.P., *Vins M.V.,* Beresneva A.E.., Novitskiy V.V. Macrophages in bacterial diseases of the lungs: phenotype and functions (review). *Bulletin of Siberian Mdicine.* 2019; 18(1): 142–154 (in Russ.). DOI: 10.20538/1682-0363-2019-1-142-154.
4. Swirski F.K., Nahrendorf M. Leukocyte behavior in atherosclerosis, myocardial infarction, and heart failure. *Science*. 2013; 339 (6116): 161–166. DOI: 10.1126/science.1230719.
5. Possamai L.A., Thursz M.R., Wendon J.A., Antoniades C.G. Modulation of monocyte/macrophage function: a therapeutic strategy in the treatment of acute liver failure. *J. Hepatol*. 2014; 61 (2): 439–445. DOI: 10.1016/j.jhep.2014.03.031.
6. Cassetta L., Cassol E., Poli G. Macrophage polarization in health and disease. *Sci. World J*. 2011; 11: 2391– 2402. DOI: 10.1100/2011/213962.
7. Hussell T., Bell T. Alveolar macrophages: plasticity in a tissue-specific context. *Immunol*. 2014; 14 (2): 81–93. DOI: 10.1038/nri3600.
8. Hoeffel G., Ginhoux F. Ontogeny of tissue-resident macrophages. *Immunology*. 2015; 6: 486. DOI: 10.3389/fimmu.2015.00486.
9. Schenk M., Fabri M., Krutzik S.R., Lee D.J., Vu D.M., Sieling P.A., Montoya D., Liu P.T., Modlin R.L. Interleukin-1β triggers the differentiation of macrophages with enhanced capacity to present mycobacterial antigen to T cells. *Immunology*. 2014; 141 (2): 174–180. DOI: 10.1111/imm.12167.
10. Gordon S., Martinez F.O. Alternative activation of macrophages: mechanism and functions. *Immunity*. 2010; 32 (5): 593–604. DOI: 10.1016/j.immuni.2010.05.007.
11. Martinez F.O., Sica A., Mantovani A., Locati M. Macrophage activation and polarization. *Front. Biosci.* 2008; 1 (13): 453–461. DOI: 10.2741/2692.
12. Peyravian N., Gharib E., Moradi A., Mobahat M., Tarban P., Azimzadeh P., Nazemalhosseini-Mojarad E., Asadzadeh Aghdaei H. Evaluating the expression level of co-stimulatory molecules CD 80 and CD 86 in different types of colon polyps. *Curr. Res. Transl. Med.* 2018; 66 (1): 19–25. DOI: 10.1016/j.retram.2017.11.003.
13. Owen J., Punt J., Stranford S., Jones P., Kuby J. Kuby Immunology. New York: W.H. Freeman & Co., 2013: 574.
14. Scarpa M., Brun P., Scarpa M., Morgan S., Porzionato A., Kotsafti A., Bortolami M., Buda A., D'Incà R., Macchi V., Sturniolo G.C., Rugge M., Bardini R., Castagliuolo J., Angriman I., Castoro C. CD80-CD28 signaling controls the progression of inflammatory colorectal carcinogenesis. *Oncotarget*. 2015; 6(24): 20058–20069. DOI: 10.18632 / oncotarget.2780.
15. Ganesan A., Moon T.C., Barakat K.H. Revealing the atomistic details behind the binding of B7–1 to CD28 and CTLA-4: A comprehensive protein-protein modelling study. *Biochimica et Biophysica Acta (BBA)*. 2018; 1862 (12): 2764–2778. DOI: 10.1016/j.bbagen.2018.08.010.
16. Wang L.X., Mei Z.Y., Zhou J.H., Yao Y.S., Li Y.H., Xu Y.H., Li J.X., Gao X.N., Zhou M.H., Jiang M.M., Gao L., Ding Y., Lu X.C. Low dose decitabine treatment induces CD80 expression in cancer cells and stimulates tumor specific cytotoxic T lymphocyte responses. *PLoS One.* 2013; 8 (5): e62924. DOI: 10.1371/journal.pone.0062924.

17. Urazova O.I., Churina E.G., Hasanova R.R., Novitskiy V.V., Poletika V.S. Association between polymorphisms of cytokine genes and secretion of IL-12p70, IL-18, and IL-27 by dendritic cells in patients with pulmonary tuberculosis. *Tuberculosis*. 2019; 115: 56–62.
18. Zhuang Y., Peng H., Chen Y., Zhou S., Chen Y. Dynamic monitoring of monocyte HLA-DR expression for the diagnosis, prognosis, and prediction of sepsis. *Front. Biosci. (Landmark Ed).* 2017; 22: 1344–1354. DOI: 10.2741/4547.
19. Venet F., Lukaszewicz A.C., Payen D., Hotchkiss R., Monneret G. Monitoring the immune response in sepsis: a rational approach to administration of immunoadjuvant therapies. *Curr. Opin. Immunol.* 2013; 25 (4):477–483. DOI: 10.1016 / j. coi.2013.05.006.
20. Monneret G.,Venet F.,Pachot A., Lepape A. Monitoring immune dysfunctions in the septic patient: a new skin for the old ceremony. *Mol. Med*. 2008; 14 (1-2): 64–78. DOI: 10.2119/2007-00102.
21. Monneret G., Lepape A.,Voirin N., Bohe J.,Venet F., Debard A.L. Persisting low monocyte human leukocyte antigen-DR expression predicts mortality in septic shock. *Intensive Care Med.* 2006; 32 (8): 1175–1183. DOI: 10.1007/s00134-006-0204-8.
22. Grimaldi D., Louis S., Pène F., Sirgo G., Rousseau C., Claessens Y. E., Vimeux L., Cariou A., Mira J. P., Hosmalin A., Chiche J. D. Profound and persistent decrease of circulating dendritic cells is associated with ICU-acquired infection in patients with septic shock intensive care. *Med*. 2011; 37 (9): 1438–1446. DOI: 10.1007/s00134-011-2306-1.

Authors contribution

Churina E.G. – design of the study, analysis of literature, statistical processing and interpretation of research results, drafting of the manuscript. Sitnikova A.V. – sample preparation of biomaterial, implementation of immunomagnetic separation and flow cytometry, methods, drafting of the manuscript. Urazova O.I. – material and technical support of laboratory research, interpretation of results, drafting, design and translation of the manuscript. Patysheva M.R. – implementation of immunomagnetic separation and flow cytometry, consulting assistance in designing the study. Novitskiy V.V. – consultations on hematological aspects of the study, editing of the manuscript. Stepanova E.P. – interaction with patients, collection of the biomaterial. Golubchikov P.N. – interaction with patients, consultations on phthisiological and pulmonological aspects of the study.

Authors information

Churina Elena G., Dr. Sci. (Med.), Professor, Department of Pathophysiology, Siberian State Medical University; Professor, Department of Organic Chemistry, Leading Researcher at the Laboratory of Translational Cellular and Molecular Biomedicine, National Research Tomsk State University, Tomsk, Russian Federation. ORCID 0000-0002-8509-9921.

Sitnikova Anjelika V., Post-Graduate Student, Department of Pathophysiology, Siberian State Medical University, Tomsk, Russian Federation.

Urazova Olga I., Dr. Sci. (Med.), Professor, Corresponding Member of RAS, Head of the Pathophysiology Division, Siberian State Medical University; Professor, Department of Complex Information Security of Computer Systems, Tomsk State University of Control Systems and Radioelectronics, Tomsk, Russian Federation. ORCID 0000-0002-9457-8879.

Novitskiy Vyacheslav V., Dr. Sci. (Med.), Professor, Academician of RAS, Honored Scientist of Russia, Professor of the Pathophysiology Division, Siberian State Medical University; Professor of the Department of Complex Information Security of Computer Systems, Tomsk State University of Control Systems and Radioelectronics, Tomsk, Russian Federation. ORCID 0000-0002-9577-8370.

Patysheva Marina R., Junior Researcher, Laboratory of Tumor Progression Biology of the Cancer Research Institute, Tomsk NRMC; Junior research scientist, Laboratory of Translational Cellular and Molecular Biomedicine, NR TSU, Tomsk, Russian Federation. ORCID 0000-0001-5758-7330.

Golubchikov Petr N., Deputy Chief Physician for Medicine, Tomsk Phthisiopulmonological Medical Center, Tomsk, Russian Federation.

Stepanova Ekaterina P., TB Specialist, Pulmonologist, Head of the Department for patients with respiratory tuberculosis, Tomsk Phthisiopulmonological Medical Tomsk, Russian Federation.

(✉) **Churina Elena G.,** e-mail: Lena1236@yandex.ru.

Received 18.06.2020
Accepted 29.09.2020

УДК 613.86:004.738]-053.6(571.5)
https://doi.org/10.20538/1682-0363-2020-4-189-197

Internet addiction in adolescents in Central Siberia: analysis of prevalence and structure of consumed content

Evert L.S.[1, 2], Tereshchenko S.Yu.[1], Zaitseva O.I.[1, 2], Semenova N.B.[1], Shubina M.V.[1]

[1] Krasnoyarsk Scientific Center of the Siberian Branch of the Russian Academy of Sciences (KSC SB RAS), Research Institute of Medical Problems of the North – a separate unit of KSC SB RAS
3G, Partizana Zheleznyaka Str., Krasnoyarsk, 660022, Russian Federation

[2] Khakass State University named after N.F. Katanov
68, Khakasskaya Str., Abakan, 655000, Republic of Khakassia, Russian Federation

ABSRACT

The aim of this study was to investigate the prevalence of Internet addiction (IA) and the structure of consumed content among adolescents in Central Siberia.

Materials and methods. From January to May 2019, 3,012 adolescents (45.8% of boys and 54.2% of girls) aged 12–18 years were examined (average age 14.5 ± 1.3 years). Younger adolescents (12–14 years old) accounted for 52.5%, and seniors (15–18 years old) accounted for 47.5%. Peculiarities of online behavior were evaluated according to Chen's Internet Addiction Scale (CIAS) adapted by V.L. Malygin and K.A. Feklisov; a total CIAS score of ≥ 65 indicated Internet addiction. Gambling addiction was rated according to the Game Addiction Scale for Adolescents, and addiction to social networks was rated according to the Social Media Disorder Scale. The structure of the consumed content was estimated in the overall sample and in two age groups. The data obtained were processed by non-parametric statistical methods using the Statistica 12.0 software. Quantitative characteristics are presented as the median and the interquartile range *Me* (Q_{25} – Q_{75}), binary signs are represented as a share (%) and the confidence interval. The significance of the differences (p) for quantitative indicators was evaluated by Mann – Whitney *U*-test and for binary characters by Pearson's $\chi 2$ criterion. The differences between the groups were considered statistically significant at $p \leq 0.05$.

Results. The overall prevalence of IA was 6.9%, adaptive use of the Internet was observed in 49.4% of adolescents, non-adaptive use was registered in 43.6% of cases. The frequency of Internet addiction increases with age: from 6.0% in 12–14 year-old adolescents to 8.0% in 15–18 year-old adolescents ($p = 0.0324$). Content consumed by adolescents included gambling addiction (11%), addiction to social networks (8.0%), mixed IA (2.6%), and undifferentiated Internet addiction (2.8%). Younger adolescents are more often dependent on online games (12.2%), social networks (9.3%), and mixed IA (3.3%), while in older adolescents, undifferentiated IA is more often observed (39.5%).

Conclusion. High level of IA prevalence in adolescents in Central Siberia confirms the relevance of this problem and indicates the need to develop preventive measures aimed at maintaining child and adolescent health.

Keywords: adolescents, Internet, Internet addiction, consumed content.

Conflict of interest. The authors declare the absence of obvious or potential conflicts of interest related to the publication of this article.

Source of financing. The study was supported by the Russian Foundation for Basic Research (No. 18-29-22032/18).

Conformity with the principles of ethics. The study was approved by the local Ethics Committee at the Research Institute of Medical Problems of the North (RI MPN) – a separate unit of the KSC SB RAS (Protocol No. 1 of 16.01.2019).

For citation: Evert L.S., Tereshchenko S.Yu., Zaitseva O.I., Semenova N.B., Shubina M.V. Internet addiction in adolescents in Central Siberia: analysis of prevalence and structure of consumed content. *Bulletin of Siberian Medicine.* 2020; 19 (4): 189–197. https://doi.org/10.20538/1682-0363-2020-4-189-197.

✉ *Evert Lidiya S.,* e-mail: lidiya_evert@mail.ru.

Интернет-зависимость у подростков Центральной Сибири: анализ распространенности и структура потребляемого контента

Эверт Л.С.[1,2], Терещенко С.Ю.[1], Зайцева О.И.[1,2], Семенова Н.Б.[1], Шубина М.В.[1]

[1] *Красноярский научный центр Сибирского отделения Российской академии наук (ФИЦ КНЦ СО РАН), Научно-исследовательский институт медицинских проблем Севера (НИИ МПС) – обособленное подразделение ФИЦ КНЦ СО РАН*
Россия, 660022, г. Красноярск, ул. Партизана Железняка, 3Г

[2] *Хакасский государственный университет (ХГУ) им. Н.Ф. Катанова*
Россия, 655000, Республика Хакасия, г. Абакан, ул. Хакасская, 68

РЕЗЮМЕ

Цель данного исследования – изучение распространенности интернет-зависимости (ИЗ) и структуры потребляемого контента у подростков Центральной Сибири.

Материалы и методы. С января по май 2019 г. обследованы 3 012 подростков (45,8% мальчиков и 54,2% девочек) в возрасте 12–18 лет (средний возраст 14,5 ± 1,3). Младшие подростки (12–14 лет) составили 52,5%, старшие (15–18 лет) – 47,5%. Особенности онлайн-поведения оценивались по шкале интернет-зависимости Чена (CIAS) в адаптации В.Л. Малыгина, К.А. Феклисова; величина общего CIAS-балла, равная 65 и выше, свидетельствовала о наличии интернет-зависимости.

Игровая зависимость оценивалась по шкале Game Addiction Scale for Adolescents, зависимость от социальных сетей – по шкале The Social Media Disorder Scale. Структура потребляемого контента оценена в общей выборке и двух возрастных группах. Полученные данные обработаны методами непараметрической статистики в программе Statistica 12. Количественные признаки представлены в виде медианы и интерквартильного размаха Me (Q_{25}–Q_{75}), бинарные признаки – как доля (%) и доверительный интервал. Значимость различий p для количественных показателей оценивалась по U-критерию Манна – Уитни, для бинарных признаков – по критерию $\chi 2$ Пирсона. Различия между группами считались статистически значимыми при $p \leq 0,05$.

Результаты. Общая распространенность ИЗ составила 6,9%, адаптивное пользование интернетом отмечалось у 49,4% подростков, неадаптивное – у 43,6%. Частота встречаемости интернет-зависимости увеличивается с возрастом: с 6,0% у подростков 12–14 лет до 8,0% – у подростков 15–18 лет ($p = 0,0324$). Потребляемый подростками контент включал игровую зависимость (11%), зависимость от социальных сетей (8,0%), смешанную (2,6%) и недифференцированную интернет-зависимость (2,8%). У младших подростков чаще формируется зависимость от онлайн-игр (12,2%), социальных сетей (9,3%) и смешанная (3,3%), у старших подростков – недифференцированная ИЗ (39,5%).

Заключение. Высокий уровень распространенности ИЗ у подростков Центральной Сибири подтверждает актуальность данной проблемы и свидетельствует о необходимости разработки профилактических мероприятий, направленных на сохранение здоровья детского подросткового населения.

Ключевые слова: подростки, интернет, интернет-зависимость, потребляемый контент.

Конфликт интересов. Авторы декларируют отсутствие явных и потенциальных конфликтов интересов, связанных с публикацией настоящей статьи.

Источник финансирования. Исследование выполнено при финансовой поддержке Российского фонда фундаментальных исследований (№ 18-29-22032/18).

Соответствие принципам этики. Письменное информированное согласие на участие в исследовании было подписано родителями подростков младше 15 лет или самими школьниками в возрасте старше 15 лет. Исследование одобрено локальным этическим комитетом НИИ МПС ФИЦ КНЦ СО РАН (протокол № 1 от 16.01.2019).

Для цитирования: Эверт Л.С., Терещенко С.Ю., Зайцева О.И., Семенова Н.Б., Шубина М.В. Интернет-зависимость у подростков Центральной Сибири: анализ распространенности и структура потребляемого контента. *Бюллетень сибирской медицины.* 2020; 19 (4): 189–197. https://doi.org/10.20538/1682-0363-2020-4-189-197.

INTRODUCTION

Currently, the problem of Internet addiction (IA) around the world is becoming an alarming issue due to its high prevalence and an upward trend, which requires immediate solutions, especially for adolescents and youth [1–3]. The Internet is the newest means of communication that has both positive and negative impact on the human psyche [4], and at the same time it imposes special demands on the physical and mental health of a modern person [5].

According to cross-national epidemiological studies, the prevalence of IA in adolescents in European countries varies and ranges from 4.4% in Italy (83.4% of adaptive Internet use (AIU), 12.2% of maladaptive Internet use (MIU)), 5.1% in Germany (79.7% of AIU, 15.2% of MIU), 7.2% in Spain (75.5% of AIU, 17.3% of MIU), 8.7% in Romania (68.9% of AIU, 22.4% of MIU), and up to 11.5% in Estonia (63.4% of AIU, 25.1% of MIU) [6]. In countries of the Asia-Pacific region, the numbers are as follows: 6.2% in Japan, 9.6% in China, 9.7% in South Korea, 14.1% in Malaysia, 16.4% in Hong Kong, and 21.1% in the Philippines [7]. The prevalence of Internet addiction among adolescents in various regions of Russia varies from 4.2% in Moscow [8] and 12.0% in Khabarovsk [9] to 38% in several other Russian regions [10]. In recent years, Russia has seen a trend towards an increase in Internet-addicted users [11]. Significant differences in the results obtained in different countries suggest that the prevalence of IA depends on many factors, including social and ethnocultural ones, geographic location, country and place of residence (city / village), ethnicity, lack of a unified methodology, and differences in the used diagnostic tools and applied assessment criteria [12].

It should be noted that most of the conducted studies contain the results of investigating the prevalence and structure of online behavior and often include analysis of psychopathological conditions and emotional disorders, but, unfortunately, do not always describe the structure of consumed content, which makes it difficult to evaluate and compare the presented data. At the same time, studying the peculiarities of teenagers surfing the Internet is undoubtedly an important aspect in preventing Internet addiction. A review of a large number of studies on the prevalence of computer games among youth and adolescents around the world showed that 0.2–12.3% of those surveyed meet the criteria for gaming addiction [13].

In recent years, there has been a marked increase in the addiction of adolescents to social media (from 1.6% to 34%, according to various authors) [14]. However, the risks of frequent and prolonged use of social media for the development of IA remain insufficiently explored. Different authors use different screening methods and clipping modes, which makes it difficult to compare the results of all studies.

Internet addiction is a complex multidimensional phenomenon, not limited solely to addictive or dependent behavior of the subject or to their social, psychological, and psychophysiological characteristics [15]. It is determined by the specifics of modern relationships between young people, with the Internet being a part of their subculture, as well as by individual properties that regulate the integrative development of their personality [16], the level of social tension, low living standards, and other objective reasons [17–19]. Still, in all cases, the Internet functions as the background for their development. Teenagers are the most susceptible to gaming and Internet addiction [20, 21].

Only a small number of studies have been devoted to investigating the frequency of IA and the structure of consumed content in adolescents in the Russian Federation in general and in Siberian region, in particular, using clear diagnostic criteria and valid methods, which makes it difficult to conduct a comparative analysis of the results. In the context of the presented data, studying the prevalence and structure of Internet addiction and the characteristics of online content consumed by adolescents of different age groups and in different regions is a priority area of scientific research, the ultimate goal of which is substantiation and development of effective methods for correcting and preventing Internet-addictive behavior in children and adolescent.

The aim of this study was to investigate the prevalence of Internet addiction (IA) and the structure of consumed content among adolescents in Central Siberia. Two hypotheses were put forward: 1) the prevalence and severity of IA will be associated with the age of adolescents, 2) the structure of consumed content will be different in different age groups.

MATERIALS AND METHODS

From January to May 2019, random samples of adolescents aged 12–18 years (males and females) were examined. The overall number of examined adolescents was 3,012 people (mean age (14.5 ± 1.3) years), they were students of 10 general educational institutions in 5 districts of Krasnoyarsk. Younger adolescents (12–14 years old) accounted for 52.5%, while older adolescents (15–18 years old) made up

47.5%. The study was approved by the Ethics Committee at the Research Institute of Medical Problems of the North and supported by the RFBR grant No. 18-29-22032/18. The necessary information was collected through questionnaires after obtaining a written informed consent to participate in the study from adolescents over 15 years of age and from parents for adolescents under 15 years. The inclusion criteria were age of 12–18 years, permanent residence in the city of Krasnoyarsk, status of a student of a comprehensive school, and written informed consent from parents to participate in the study. Criteria for exclusion were the following: age under 12 and over 18 years, residence outside the city of Krasnoyarsk, lack of the status of a comprehensive school student, and refusal to participate in the study. All studied indicators were analyzed in general for the whole group of the examined adolescents and for two separate age groups: 12–14 years (1,580 people) and 15–18 years (1,432 people).

We applied the terminological apparatus used in conducting international medical and social studies of online behavior disorders in adolescents [6]. Three types of online behavior were considered: 1) adaptive Internet use (AIU), in which there is a minimal risk of Internet addiction behavior; 2) maladaptive Internet use (MIU), in which there is a tendency to the emergence of Internet-addictive behavior; 3) pathological Internet use (PIU), in which there is a pronounced and stable pattern of Internet addictive behavior, or Internet addiction (IA).

To verify the type of online behavior of adolescents, Chen's Internationally Accepted Internet Addiction Scale was used (CIAS) [22], adapted by V.L. Malygin and K.A. Feklisov [23]. The criterion for the presence of Internet addiction was the overall CIAS score ≥ 65. The score of 27–42 indicated the absence of Internet addiction (or AIU), the score of 43–64 was used to indicate maladaptive Internet use (MIU).

Analysis of the content structure of online behavior in adolescents was carried out using the Russian version of the Game Addiction Scale for Adolescents, a questionnaire for assessing gambling addiction [24], and the Social Media Disorder Scale, a questionnaire on social media addiction [25]. In the structure of the consumed content, the following types of addiction were distinguished: gaming addiction, social media addiction, mixed Internet addiction (the presence of both gaming and social media addiction), and undifferentiated Internet addiction (adolescents with IA that was confirmed by the overall CIAS score ≥ 65, who did not have gaming or social media addiction, but who showed predominance of other types of online activities).

Statistical data processing was carried out by non-parametric statistical methods using the Statistica 12.0 software. The results of quantitative trait analysis are presented in the form of the median (*Me*) and the interquartile range ($Q_{25} – Q_{75}$). Binary features are presented as % share and the confidence interval estimated by the Wilson score interval. The achieved level of significance of differences (p) for quantitative indicators was determined by the Mann – Whitney U-test and for binary signs by the Pearson's $\chi 2$ criterion. The differences between the groups were considered statistically significant at $p \leq 0.05$.

RESULTS

Of all the adolescents included in the survey, 2,936 people completed the CIAS. The analysis of the questionnaire scale values revealed that adaptive Internet use (AIU) is typical for 49.4% (1,451/2,936) of respondents, CI = 47.6–51.2%; maladaptive Internet use (MIU) was observed in 43.6% (1,281/2,936) of adolescents, CI = 41.9–45.4%; and pathological Internet use (PIU) was detected in 6.9% (204/2,936) of the examined, CI = 6.1–7.9%; these adolescents were identified as Internet addicts.

Analysis of online behavior in terms of age differences demonstrated a decrease in adaptive Internet use and an increase in the pathological Internet use (Internet addiction) with age. Therefore, adaptive use of the Internet was typical of 51.2% (786/1,536) of adolescents aged 12–14 years, CI = 48.7–53.7%, and of 47.5% of the examined teenagers (665/1,400) aged 15–18 years , CI = 44.9–50.1% (p = 0.0469). The incidence of maladaptive Internet use was comparable among adolescents in both compared groups: 42.8% (658/1,536), CI = 40.4–45.3%, in adolescents of the younger age group and 44.5% (623/1,400), CI = 41.9–47.1%, in the examined older age group (p = 0.3646). There were more Internet-addicted adolescents in the older age group compared to the younger one: 8.0% (112/1,400), CI = 6.7–9.5% versus 6.0% (92/1,536), CI = 4.9–7.3% (p = 0.0324). We should note the absence of significant differences in the share (%) of occurrence of key Internet addiction symptoms and problems related to Internet addiction in the age groups of 12–14 and 15–18 years in the compared groups of teenagers with AIU, MIU, and PIU (indicating the presence of Internet addiction). At the same time, the analysis of the quantitative values of the scales of key Internet addiction symptoms (KIAS)

revealed the presence of statistically significant differences between the above mentioned age groups (Table 1).

Table 1

Quantitative values of the scales of the key Internet addiction symptoms in the age groups of 12–14 and 15–18 years (boys + girls), *Me* (Q_{25}–Q_{75})

Indicators	Groups examined		*p* (using the Mann – Whitney *U*-test)
	12–14 years old (*n* = 1,579)	15–18 years old (*n* = 1,442)	
Total score on the Key Symptoms of Internet Addiction (IA-Sym) scale	2.0 19.0–30.0	25.0 20.0–30.0	0.0507
Total score on the Internet Addiction Problem Scale (IA-RP)	17.0 14.0–21.0	17.0 15.0–22.0	0.0382
Total CIAS score	42.0 35.0–51.0	43.0 35.0–52.0	0.0364

The analysis of the content consumed by adolescents revealed that 11.0% of respondents (331/3,012) had addiction to online games, CI = 9.9–12.2%; social media addiction was found in 8.0% (241/3,012) of cases, CI = 7.1–9.0%; mixed IA was identified in 2.6% (79/3,012) of individuals, CI = 2.1–3.3%, and undifferentiated IA – in 2.8% (85/3,012) of adolescents, CI = 2.3–3.5%.

When analyzing the structure of consumed content in adolescents of two age groups, it was found that gambling addiction, social media addiction, and mixed type of addiction (combined online communication with gaming) were significantly more often registered in adolescents of a younger age group (Figure). Adolescents of the younger age group were characterized by higher values of gambling addiction indicators: 10.0 (7.0–14.0), in comparison with the older group: 10.0 (7.0–13.0), $p < 0.0001$.

With age, adolescents have a decrease in interest in online gaming: from 12.2% (193/1,580), CI = 10.7–13.9% in the younger age group to 9.6% (138/1,432), CI = 8.2–11.3% in the older group ($p = 0.0239$). Communication using social media attracts attention of a larger number of younger adolescents – 9.3% (147/1,580), CI = 8.0–10.8%, compared with their older peers – 6.6% (94/1,431), CI = 5.4–8.0% ($p = 0.0057$). Adolescents aged 12–14 years were also characterized by a higher incidence of mixed Internet addiction (in which there was a combination of enthusiasm for Internet games and communication via social media) – 3.3% (52/1,580), CI = 2.5–4.3%, as opposed to the value of 1.9% (27/1,431), CI = 1.3–2.7% in the group of older adolescents ($p = 0.0161$). The prevalence of undifferentiated Internet addiction was comparable in both age groups: 34.3% (36/105), CI = 25.9–43.8% in the 12–14 year-old group and 39.5% (49/124), CI = 31.4–48.3%, in the group of 15–18 year-olds ($p = 0.4143$) (Figure).

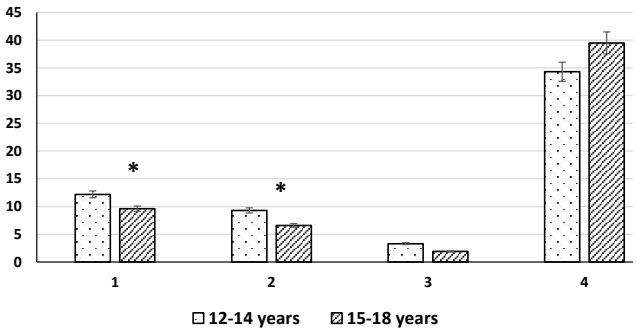

Figure. Distribution of adolescents of two age groups of 12–14 and 15–18 years (m + d) according to the prevalence of gaming addiction (1), addiction to social networks (2), mixed Internet addiction (3), and undifferentiated (4) Internet addiction in adolescents of two age groups, %

* statistically significant differences between the groups.

DISCUSSION

For the first time in Central Siberia, we conducted a large-scale screening of online behavior of adolescents (3,012 people) and analyzed the age-related characteristics of Internet addiction and consumed online content. Internet addiction was detected in 6.9% of adolescents, adaptive use of the Internet was typical of 49.4% of individuals, and maladaptive Internet use was reported for 43.6% of the examined teenagers. The study confirmed our hypothesis about the growth of pathological Internet use among Krasnoyarsk adolescents with age. For example, it was found that adolescents of the older age group tend to be more addicted to the Internet (8.0%) compared to their younger peers (6.0 %, $p = 0.0324$). This trend was also confirmed by the direction of changes in the quantitative indicators of the analyzed scales: the older group of adolescents was characterized by higher indexes on the scale of the key Internet addiction symptoms, and adolescents of the younger age group were characterized by higher quantitative values on the total gaming addiction score.

Our second assumption was that the structure of consumed online content depends on age. The results of our comparative analysis confirmed that the

features of consumed online content of adolescents of a younger age group differ from those of the older age group and include higher frequency of occurrence of gambling addiction, social media addiction, and mixed Internet addiction, while the prevalence of undifferentiated Internet addiction is more or less similar for both age groups.

According to a number of studies conducted in various countries, the prevalence of IA among adolescents varies from 1 to 18%, depending on the compared age, ethnosocial groups, applied questionnaires, and diagnostic criteria [26]. So, in Europe, IA was detected in 1–11% of adolescents (on average, in 4.4% of examined individuals); in the USA, the proportion of Internet-addicted adolescents in the total sample varied from 0.3 to 8.1% [6, 27, 28]. According to our data, the incidence rate of IA (6.9% in the total sample) was comparable with the prevalence of IA in adolescents in Spain (7.2%) [6] and Japan (6.2%) [7], and in some cases it differed from screening results in other countries. So, the frequency of IA that was established for Krasnoyarsk schoolchildren was higher than that for Moscow and the Moscow region adolescents (4.2%) [8], as well as for adolescents in Italy (4.4%) and Germany (5.1%) [6]. At the same time, the % of IA occurrence in the examined adolescents was lower than that in the teenage populations of Romania (8.7%), Estonia (11.5%) [6], and some other regions in Russia, for example, Khabarovsk (12.0%) [9]. Recent studies have shown that in Asian countries (China, Hong Kong, South Korea, etc.), the prevalence of IA among teenagers and young adults is significantly higher than in Europe and the USA and ranges from 9 to 37.9% [29, 30].

In the context of the presented data, our results were generally lower than those provided by researchers from Asian countries. The level of IA verified by us among Krasnoyarsk adolescents was lower than in China (9.6%), South Korea (9.7%), Malaysia (14.1%), Hong Kong (16.4%), and the Philippines (21.1%) [7]. In our work, we also compared the structure of the content consumed by schoolchildren of Krasnoyarsk with similar characteristics of online behavior of adolescents in other countries. It is known that the main components in the structure of the content consumed by Internet addicts are gaming addiction and social media addiction. A study of the prevalence of online gaming among young people in many countries of the world showed that the frequency of occurrence of *gaming addiction* in the studied populations of adolescents and students ranges from 0.2 to 12.3% [13, 16]. The number of schoolchildren with gaming addiction in Krasnoyarsk (11% from the total sample) turned out to be comparable with the data for adolescents in Croatia (12.3%), but exceeded the indexes for GB (0.8%), Hong Kong (0.9%), Denmark (1.3%), Germany (2.2%), the United Kingdom (2.2%), Italy (2.6%), Serbia (3.1%), Norway (3.4%), Lithuania (4.2%), Sweden (4.2%), Cyprus (4.4%), Spain (4.6%), Finland (4.8%), Romania (4.9%), and Albania (5.3%) [13].

The frequency of *social media addiction* that was identified for Internet-addicted adolescents in Krasnoyarsk (8% from the total sample) turned out to be higher than the level of this parameter in Nigeria (1.6%), comparable to the parameter value in Peru (8.6%), but lower than this indicator in China (12%) and Hong Kong (34%) [14] as well as in the Netherlands (11%) [31].

Thus, all three psychometric tools used (CIAS, Social Media Disorder scale (SMDS), and Game Addiction Scale for Adolescents (GASA)) show that the prevalence of pathological use of the Internet among urban adolescents in Central Siberia is lower than in most Asian countries, but it exceeds the average European level. The ambiguity of population data obtained in different countries suggests that the prevalence rates of IA depend on many factors, including social and ethnocultural features, research methodology, diagnostic tools, and assessment criteria.

To date, several etiopathogenetic models of formation of Internet-addictive behavior in adolescents have been proposed [32]. Some researchers suggest the presence of predominantly neurobiological risk factors, which are associated with the insufficient maturity of certain parts of the adolescent's brain, which is manifested by insufficient effectiveness of volitional control, high impulsivity, and excessively activated reward circuitry [33, 34]. However, the biopsychosocial model is the most recognized by researchers today; it involves a combination of psychosocial problems (especially problems in relationships with parents and peers) and neurobiological risk factors [32, 35, 36].

The biopsychosocial model of IA formation in adolescents can explain the differences in IA prevalence through both ethnically determined spectrum of secretion and reception of neurotransmitters and sociocultural characteristics of the populations. Analysis of the available literature shows that insufficient attention is paid to the ethnic factor in the analysis of IA prevalence. For example, in the fundamental systematic review by S.E. Luczak et al. [37] that was devoted to

ethnic differences in 11 forms of addictive behavior in the classification by S. Sussman, M. Lisha, and M. Griffiths, only one study could be found (cited earlier in the review by D.J. Kuss et al. [38]) that had been taking the ethnic factor of IA into account.

The study by T.M. Yates et al. [39] examined 1,470 college students with similar sociocultural living conditions according to a single protocol and showed higher incidence of Internet addiction among representatives of Asian nationalities (8.6%), compared to non-Asians (3.8%). The same review cited a number of sources showing high frequency of computer games addiction in non-European Americans (indigenous people, Negroids), compared to representatives of the Caucasian race [37].

In a large, multicenter (11 countries) European study of Internet addiction in adolescents, the most pronounced comorbidity with suicidal behavior, depression, and anxiety was revealed, but the contribution of each comorbidity factor varied from country to country. The authors concluded that there is a need for further research in this direction with the obligatory allowance for sociocultural and, possibly, ethnic (genetic) differences [40, 41]. From our point of view, analysis that would be considering the role of ethno-geographic differences in the prevalence of ethno-genotypic characteristics of populations seems to be a promising direction in the neurogenetics of addiction in adolescents, especially in such a multinational country as the Russian Federation.

We are currently implementing a research project supported by the Russian Foundation for Basic Research "Internet addiction in adolescents in Central Siberia: prevalence, content structure, ethno-geographical differences, mental and somatic comorbidity, neurotransmitter associations and genetic predictors", the data of which was partially used in this article. The project investigates the prevalence of Internet addiction, its degrees of severity, addiction patterns, and content variants for adolescents in large, ethnically different cities in Central Siberia (Krasnoyarsk, Abakan, Kyzyl). In addition, it is planned to study the associative role of candidate neurotransmitters and conduct a population analysis of polymorphisms in the candidate genes of oxytocinergic, dopaminergic, serotonergic, noradrenalinergic, melatoninergic, and nicotine neurotransmitter systems of IA formation. The research design developed for this project involves further psycho-neurobiological comparison, which, in accordance with our hypothesis, will allow to identify specific predictor genes and neurotransmitters that correspond to certain patterns of adolescent online behavior, taking into account the ethno-social characteristics of populations. The results of the study will help to open up new perspectives in assessing the fundamental neurobiological causes of IA formation and personalizing treatment strategy for Internet-addicted adolescents.

CONCLUSION

Modern epidemiology of Internet addiction based on valid diagnostic approaches, with mandatory consideration of regional, age, gender, and ethno-social factors as well as the range of consumed content is currently a priority area. From this perspective, the novelty of this study consists in the fact that for the first time the largest sample (including testing of 3,012 respondents aged 12–18 years) was gathered to investigate the prevalence of Internet addiction in Russian adolescents using the CIAS scale adapted by V.L. Malygin and K.A. Feklisov. It is a validated psychometric tool that allows for cross-national and cross-cultural comparisons, which was developed specifically for adolescents. For the first time, data were obtained on the prevalence of IA among urban adolescents in Central Siberia. Pathological Internet-addicted behavior was recorded in 6.9% of teenagers from the unbiased school sample in Krasnoyarsk.

The results of the study demonstrate fairly high prevalence of Internet addiction and borderline types of online behavior in adolescents, which confirms the urgency of the problem of Internet addiction in adolescents. The obtained data indicate the need for further study of the characteristics of online behavior of adolescents and the structure of the content they consume. Further research should be devoted to investigation of Internet addiction with account of gender, ethnicity, characteristics of regional and environmental living conditions, and risk factors for IA formation for optimizing treatment and preventive measures in the adolescent population of Internet users.

REFERENCES

1. Schneider L.A., King D.L., Delfabbro P.H. Family factors in adolescent problematic Internet gaming: a systematic review. *Journal of Behavioral Addictions*. 2017; 6 (3): 321–333. DOI: 10.1556/2006.6.2017.035.
2. Moawad G.E., Ebrahem G.G.S. The relationship between use of technology and parent-adolescents social relationship. *Journal of Education and Practice*. 2016; 7 (14): 168–178.
3. Ballarotto G., Volpi B., Marzilli E., Tambelli R. Adolescent internet abuse: A study on the role of attachment to parents and peers in a large community sample. *BioMed Research*

International. 2018; Article ID 5769250: 10. DOI: 10.1155/2018/5769250.
4. Azab H.M., Effat S.M.A., Aly H.Y., Mahmoud O.A.A.. Correlation of internet addiction with anxiety, depression and personalitytraits – Upper Egyptstudy. *Sohag Medical Journal*. 2019; 23 (1):142–153. DOI: 10.21608 / smj.2019.41384.
5. Sukhotina N.K. Children's mental health and its determinants. *Journal of Neurology and Psychiatry.* 2013; 5 (2): 16–22 (in Russ.).
6. Kaess M., Durkee T., Brunner R, Carli V, Parzer P, Wasserman C. Pathological Internet use among European adolescents: psychopathology and selfdestructive behaviours. *Eur. Child Adolesc. Psych*. 2014; 23 (11): 1093–1020. DOI: 10.1007/s00787-014-0562-7.
7. Mak K.K., Lai C.M., Ko C.H., Chou C., Kim D.I., Watanabe H. et al. Psychometric properties of the Revised Chen Internet Addiction Scale (CIAS-R) in Chinese adolescents. *J. Abnorm. Child. Psychol.* 2014;42(7): 1237–1245.
8. Malygin V.L., Khomeriki N.S., Antonenko A.A. Individual psychological features of teenagers as risk factors for Internet addiction formation. *Medical Psychology in Russia: Electronic Scientific Journal.* 2015; 7 (30): 7 (in Russ.). URL: http://mprj.ru (ac- cessed on 09.08.2019).
9. Ragulina M.V. Emotional ill-being of Internet-addicted teenagers. *Scientific Trends: Pedagogy and Psychology.* 2017 (in Russ.). DOI: 10.18411/spc-04-12-2017-24.
10. Titova V.V., Katkov A.L., Chugunov A.N. Internet addiction: causes and mechanisms of formation. Diagnosis and approaches to prevention and treatment. *Pediatrician.* 2014; 5 (4): 132–139 (in Russ.).
11. Varlamova S.N., Goncharova E.R., Sokolova I.V. Internet addiction of teenagers in metropolitan cities: criteria and typology. *Monitoring of Public Opinion*. 2015; 2 (125):165– (in Russ.). DOI: 18210.14515/monitoring.
12. Pontes H.M., Kuss D., Griffiths M. Clinical psychology of Internet addiction: a review of its conceptualization, prevalence, neuronal processes, and implications for treatment. *Neuroscience and Neuroeconomics*. 2015; 4 (11): 23.
13. Calado F., Alexandre J., Griffiths M.D. Prevalence of adolescent problem gambling: A systematic review of recent research. *J. Gambl. Stud*. 2017; 33: 397–424. DOI: 10.1007/s10899-016-9627-5.
14. Online social network site addiction: A comprehensive review. 2015; 2 (2): 175–184.
15. Weinnstein A. Internet addiction: diagnosis, comorbidity, and treatment. *Medical Psychology in Russia: electronic scientific journal.* 2015; 4 (33): 3. URL: http://mprj.ru (accessed on 12.08.2019) (in Russ.).
16. Khomeriki N.S. Individual psychological features of teenagers who are prone to Internet addiction. *Mental Health*. 2013; 5 (84): 49–51 (in Russ.).
17. Individual differences in implicit learning abilities and impulsive behavior in the context of Internet addiction and Internet Gaming Disorder under the consideration of gender. *Addictive Behaviors Reports*. 2017; 5: 19–28. DOI: 10.1016/j.abrep.2017.02.002.
18. Internet gaming disorder: Trends in prevalence 1998–2016. *Addictive Behaviors*. 2017; 75: 17–24. DOI: 10.1016/j.addbeh.2017.06.010.
19. Mindfulness facets and problematic Internet use: A six-month longitudinal study. *Addictive Behaviors*. 2017; 72: 57–63. DOI: 10.1016/j.addbeh.2017.03.018.
20. Karacic S., Oreskovic S. Internet addiction through the phase of adolescence: A questionnaire study. *JMIR Mental Health*. 2017; 4 (2). Article e11. DOI: 10.2196/mental.5537.
21. Reiner I.A., Tibubos N., Hardt J., Müller K., Wölfling K., Beutel M.E. Peer attachment, specific patterns of internet use and problematic internet use in male and female adolescents. *European Child and Adolescent Psychiatry*. 2017; 26 (10): 1257–1268. DOI: 10.1007/s00787-017-0984-0.
22. Chen S.-H., Weng L.-J., Su Y.-J., Wu H.-M., Yang P.-F. Development of chinese internet addiction scale and its psychometric study. *Chinese Journal of Psychology*. 2003; 45: 251–266. DOI: 10.1037/t44491-000.
23. Malygin V.L., Feliksov K.A. Internet addiction. Diagnostic criteria and methods: textbook. M.: MSMSU; 2011: 32 (in Russ.).
24. Lemmens J.S., Valkenburg P.M., Peter J. Development and validation of a game addiction scale for adolescents. *Media Psychol*. 2009; 12 (1): 77–95. DOI: 10.1080/15213260802669458.
25. Van den Eijnden R.J.J.M., Lemmens J.S., Valkenburg P.M. The social media disorder scale. *Computers in Hum. Behav*. 2016; 61: 478–487. DOI: 10.1016/j.chb.2016.03.038.
26. Cerniglia L., Zoratto F., Cimino S., Laviola G., Ammaniti M., Adriani W. Internet addiction in adolescence: neurobiological, psychosocial and clinical issues. *Neuroscience & Biobehavioral Reviews*. 2017; 76: 174–184. DOI:10.1016/j.neubiorev.2016.12.024.
27. Floros G., Fisoun V., Siomos K. Internet addiction in the island of hippokrates: impact of gender and age in teenage use and abuse of the internet. *European Psychiatry*. 2010; 25: 414. DOI: 10.1016/S0924-9338(10)70410-7.
28. Kuss D.J., van Rooij A., Shorter G.W., Griffiths M.D., van de Mheen D. Internet addiction in adolescents: Prevalence and risk factors. *Computers in Human Behavior*. 2013; 29 (5): 1987–1996. DOI: 10.1016/j.chb.2013.04.002.
29. Wang H., Zhou X., Lu C., Wu J., Deng X., Hong L. Problematic internet use in high school students in Guangdong Province, China. *PLoS One*. 2011; 6 (5). Article ID e19660. DOI: 10.1371/journal.pone.0019660.
30. Takahashi M., Adachi M., Nishimura T., Hirota T., Yasuda S., Kuribayashi M., Nakamura K. Prevalence of pathological and maladaptive Internet use and the association with depression and health-related quality of life in Japanese elementary and junior high school-aged children. *Soc. Psych. Psychiatr. Epidemiol*. 2018; 53 (12): 1349–1359. DOI: 10.1007/s00127-018-1605-z.
31. Jelenchick L.A., Hawk S.T., Moreno M.A. Problematic internet use and social networking site use among Dutch adolescents. *J. Adolesc. Med. Health.* 2016; 28 (1): 119–121. DOI: 10.1515/ijamh-2014-0068.
32. Cimino S., Cerniglia L. A longitudinal study for the empirical validation of an etiopathogenetic model of internet addiction in adolescence based on early emotion regulation. *BioMed Research International*. 2018; 2018: 4038541. DOI: 10.1155/2018/4038541.

33. Hong S.B., Zalesky A., Cocchi L., Fornito A., Choi E.J., Kim H.H., Suh J.E., Kim C.D., Kim J.W., Yi S.H. Decreased functional brain connectivity in adolescents with internet addiction. *PLoS One*. 2013; 8 (2): e57831. DOI: 10.1371/journal.pone.0057831.
34. Kuss D.J., Lopez-Fernandez O. Internet addiction and problematic Internet use: A systematic review of clinical research. *World J. Psychiatry*. 2016; 6 (1): 143–176. DOI: 10.5498/wjp.v6.i1.143.
35. Griffiths M. A 'components' model of addiction within a biopsychosocial framework. *Journal of Substance Use*. 2005; 10 (4): 191–197. DOI: 10.1080/14659890500114359.
36. Kim H.S., Hodgins D.C. Component model of addiction treatment: A pragmatic transdiagnostic treatment model of behavioral and substance addictions. *Front. Psychiatry*. 2018; 9: 406. DOI: 10.3389/fpsyt.2018.00406.
37. Luczak S.E., Khoddam R., Yu S., Wall T.L., Schwartz A., Sussman S. Review: Prevalence and co-occurrence of addictions in US ethnic/racial groups: Implications for genetic research. *Am. J. Addict*. 2017; 26 (5): 424–436. DOI: 10.1111/ajad.12464.
38. Kuss D.J., Griffiths M.D., Karila L., Billieux J. Internet addiction: a systematic review of epidemiological research for the last decade. *Curr. Pharm. Des*. 2014; 20 (25): 4026–4052. DOI: 10.2174/13816128113199990617.
39. Yates T.M., Gregor M.A., Haviland M.G. Child maltreatment, alexithymia, and problematic internet use in young adulthood. *Cyberpsychol. Behav. Soc. Netw*. 2012; 15 (4): 219–225. DOI: 10.1089/cyber.2011.0427.
40. Durkee T., Carli V., Floderus B., Wasserman C., Sarchiapone M., Apter A., Balazs J.A., Bobes J., Brunner R., Corcoran P., Cosman D., Haring C., Hoven C.W., Kaess M., Kahn J.P., Nemes B., Postuvan V., Saiz P.A., Varnik P., Wasserman D. Pathological internet use and risk-behaviors among European adolescents. *Int. J. Environ. Res. Public. Health*. 2016; 13 (3). DOI: 10.3390/ijerph13030294.
41. Kaess M., Parzer P., Brunner R., Koenig J., Durkee T., Carli V., Wasserman C., Hoven C.W., Sarchiapone M., Bobes J., Cosman D., Varnik A., Resch F., Wasserman D. Pathological internet use is on the rise among European adolescents. *J. Adolesc. Health*. 2016; 59 (2): 236–239. DOI: 10.1016/j.jadohealth.2016.04.009.

Authors contribution

Evert L.S. – analysis and interpretation of data, drafting of the manuscript. Tereshchenko S.Yu. – conception and design of the study. Zaitseva O.I. – justification of the manuscript. Semenova N.B. – final approval of the manuscript for publication. Shubina M.V. – critical revision of the manuscript for important intellectual content.

Authors information

Evert Lidia S., Dr. Sci. (Med.), Chief Researcher, Clinical Department of Somatic and Mental Health of Children, RI MPN, KSC SB RAS, Krasnoyarsk; Professor, Department of General Professional Disciplines, KSU named after N.F. Katanov, Abakan, Russian Federation. ORCID 0000-0003-0665-7428.

Tereshchenko Sergey Yu., Dr. Sci. (Med.), Professor, Head of the Clinical Department of Somatic and Mental Health of Children, RI MPN, KSC SB RAS, Krasnoyarsk, Russian Federation. ORCID 0000-0002-1605-7859.

Zaitseva Olga I., Dr. Sci. (Med.), Chief Researcher, Laboratory of Clinical Pathophysiology, RI MPN, KSC SB RAS, Krasnoyarsk, Russian Federation. ORCID 0000-0001-7199-2308;

Semenova Nadezhda B., Dr. Sci. (Med.), Chief Researcher of the Clinical Department of Somatic and Mental Health of Children, RI MPN, KSC SB RAS, Krasnoyarsk, Russian Federation. ORCID 0000-0002-2790-7740.

Shubina Margarita V., Junior Researcher, Clinical Department of Somatic and Mental Health of Children, RI MPN, KSC SB RAS, Krasnoyarsk, Russian Federation. ORCID 0000-0002-6724-1058.

(✉) **Evert Lidiya S.,** e-mail: lidiya_evert@mail.ru.

Received 06.10.2019

Accepted 25.12.2019

УДК 616-001.17-06:616.12
https://doi.org/10.20538/1682-0363-2020-4-198-206

Cardiac disorders in burn injury

Vatutin N.T.[1, 2], Ignatenko G.A.[1], Taradin G.G.[1, 2], Eshchenko E.V.[3], Goncharuk M.S.[1, 2], Kulikova S.O.[1]

[1] M. Gorky Donetsk National Medical University
16, Ilyicha Av., Donetsk, 283003, Donetsk People's Republic (Ukraine)

[2] V.K. Gusak Institute of Urgent and Recovery Surgery
47, Leninsky Av., Donetsk, 283045, Donetsk People's Republic (Ukraine)

[3] Myrnograd Center for Primary Health Care
20, Sobornaya Str., Myrnograd, 85323, Ukraine

ABSTRACT

The presented review highlights the peculiarities of cardiovascular system damages in burn injury. The epidemiological data on the incidence of thermal injuries are reported. The pathogenic mechanisms of heart disorders during various periods of burn injury, as well as pathological changes in the myocardium are examined in detail. The main clinical manifestations of heart damage on the background of burn disease have been identified (heart failure, myocarditis, infectious endocarditis, cardiac arrhythmias and conduction disturbances, myocardial infarction). Special attention is paid to laboratory and instrumental methods for investigation of the heart with a discussion of the benefits and disadvantages of each method. The manuscript discusses the main therapeutic approaches for the management of burn patients with cardiac pathology, as well as the possibilities of using and the effectiveness of modern treatment methods aimed at improving survival, diminishing the severity of cardiovascular disorders and improving the prognosis of such patients.

Key words: thermic burns; burn injury, heart in burn trauma, heart failure; pathogenesis, pathomorphology, clinical picture; diagnosis, management.

Conflict of interest. The authors declare the absence of obvious or potential conflicts of interest related to the publication of this article.

Source of financing. The authors received no specific funding for this work.

For citation: Vatutin N.T., Ignatenko G.A., Taradin G.G., Eshchenko E.V., Goncharuk M.S., Kulikova S.O. Cardiac disorders in burn injury. *Bulletin of Siberian Medicine.* 2020; 19 (4): 198–206. https://doi.org/10.20538/1682-0363-2020-4-198-206.

Поражение сердца при ожоговой болезни (обзор литературы)

Ватутин Н.Т.[1, 2], Игнатенко Г.А.[1], Тарадин Г.Г.[1, 2], Ещенко Е.В.[3], Гончарук М.С.[1, 2], Куликова С.О.[1]

[1] Донецкий национальный медицинский университет (ДонНМУ) имени М. Горького
Донецкая Народная Республика (Украина), 283003, г. Донецк, пр. Ильича, 16

[2] Институт неотложной и восстановительной хирургии (ИНВХ) имени В.К. Гусака
Донецкая Народная Республика (Украина), 283045, г. Донецк, пр. Ленинский, 47

✉ *Taradin Gennadii G.,* e-mail: taradin@inbox.ru.

[3] *Мирноградский центр первичной медико-санитарной помощи*
Украина, 85323, г. Мирноград, ул. Соборная, 20

РЕЗЮМЕ

Обзор посвящен особенностям поражений сердечно-сосудистой системы при ожоговой болезни. Приведены эпидемиологические данные о распространенности термических поражений. Подробно рассмотрены патогенетические механизмы повреждения сердца в различные периоды ожоговой травмы, а также патоморфологические изменения миокарда. Выделены основные клинические проявления поражений сердца на фоне ожоговой болезни (сердечная недостаточность, миокардит, инфекционный эндокардит, нарушения ритма и проводимости сердца, инфаркт миокарда). Особое внимание уделено лабораторным и инструментальным методам исследования состояния сердца с обсуждением преимуществ и недостатков каждого метода. Рассмотрены основные терапевтические подходы ведения ожоговых больных с кардиальной патологией, а также возможности и эффективность использования современных методов лечения, направленных на улучшение выживаемости, выраженности сердечно-сосудистых нарушений и улучшение прогноза таких пациентов.

Ключевые слова: термические ожоги, ожоговая болезнь, сердце при ожоговой травме, сердечная недостаточность, патогенез, патоморфология, клиническая картина, диагностика, лечение.

Конфликт интересов. Авторы декларируют отсутствие явных и потенциальных конфликтов интересов, связанных с публикацией настоящей статьи.

Источник финансирования. Авторы заявляют об отсутствии финансирования.

Для цитирования: Ватутин Н.Т., Игнатенко Г.А., Тарадин Г.Г., Ещенко Е.В., Гончарук М.С., Куликова С.О. Поражение сердца при ожоговой болезни (обзор литературы). *Бюллетень сибирской медицины.* 2020; 19 (4): 198–206. https://doi.org/10.20538/1682-0363-2020-4-198-206.

INTRODUCTION

Thermal damage is a serious medical, social and economic problem. It is related to the high frequency of burn injuries in everyday life, at work and during military conflicts, the complexity and duration of treatment of the patients, frequent disability and high mortality. According to the data, 11 million people worldwide sought medical care for burns in 2004. The risk of burns tends to increase with lower socioeconomic status, and up to 90% of burns occur in low- or middle-income countries. According to WHO, about 180 thousand cases of deaths caused by burns are registered annually worldwide [1]. In Ukraine, the overall incidence of thermal injuries is also quite high and accounts for 152 cases per 100 thousand inhabitants. In the Russian Federation, 251,480 burns were recorded in 2018, which is 171.2 cases per 100 thousand people [3].

With widespread and deep burns, a clinically pronounced generalized reaction of the body develops. It begins in the first hours after the injury and lasts not only the entire period of the wound existence, but also some time after the complete restoration of the skin covering. This complex set of interconnected pathophysiological changes and clinical manifestations that occurs in response to a burn injury is called a “burn disease” [4].

Thermal trauma is accompanied by a number of deviations and disorders in the activities of the body as a whole and, in particular, cardiac disorders. The diverse spectrum of morphological changes in the myocardium is observed in extensive burns. There are decrease in myocardial contraction, various rhythm and conduction disturbances, and development of heart failure (HF). Thus, according to some data, signs of myocarditis are revealed in 20–40% of cases, and signs of arrhythmia and heart block are seen in about 35% of cases of burn disease.

Heart damage in burn injury with underlying cardiovascular diseases can approach significant severity and not only be the cause of severe HF, but also the death of injured patients [5]. The initial presence of cardiopulmonary pathology in the burned patient increases the risk of developing myocardial infarction (MI) or death by more than 6 times. Nevertheless, despite the high occurrence of burns and common heart damage, special characteristics of cardiac pathology are poorly highlighted in the literature, and data on pathophysiological events, current diagnostic and treatment methods are revealed scantily.

PATHOPHYSIOLOGY

The burn disease has a complex multicomponent pathogenesis, the individual links of which become prevailing in different time periods after a burn injury. On the first day after injury, hypovolemia, hemodynamic shifts and disturbances of microcirculation develop. Then, severe intoxication occurs (the first 1–2 weeks) and later, infectious complications emerge. In this regard, four periods are distinguished during the burn disease: burn shock (first 3–5 days), acute burn toxemia (5–10 days), septicotoxemia (from 11 days to complete wound healing), and recovery.

In the first hours of the burn injury, even in the absence of massive shifts in the body's water spaces, the severity of the patient's condition is associated with pain syndrome and psycho-emotional stress, which serve as a trigger for the neuroendocrine response. The primary reaction occurs at the level of the spinal neural-reflex arcs with irritation of the sympathetic nervous system and the release of catecholamines into circulation, which leads to vasospasm, increased total peripheral vascular resistance, centralization of circulation, ultimately resulting in the occurrence of peripheral tissue hypoxia and acidosis.

These events are exacerbated by impairment of respiratory function (a decrease in the respiratory volume and vital capacity of lungs), which, in turn, leads to a decrease in blood oxygen saturation and tissue oxygenation, the accumulation of underoxidized metabolic products, and the development of respiratory and metabolic acidosis. Simultaneously, there is a short increase in the stroke and minute volume of the heart, an increase in blood pressure (BP), which subsequently drops as hypovolemia deteriorates.

An increase in blood coagulability, microthrombosis and alterations in microcirculation occur, which deteriorates tissue hypoxia and acidosis. In this setting, a paralytic expansion of capillaries emerges, and microcirculatory and electrolyte disturbances increase. Subsequently, pathological depolarization of the cell membranes of cardiomyocytes with alteration of their permeability develops.

Several hours post burn, a profound shock state develops due to the loss of preload as burn edema advances [6].

Immediately post burn, cardiac function is inhibited due to the pro-inflammatory effect of interleukin-1B and tumor necrosis factor-alpha (TNFα), which can be blocked by CD14 knockout or slowed down due to kappa B nuclear factor blockers [7]. In the 48 hours post burn, tachycardia develops with increasing cardiac output (CO) and myocardial inflammation occurs due to β-adrenergic influence [8]. The decrease in the right ventricular ejection fraction [9], observed after endotoxemia, can be mitigated by thromboxane blockade. Initially, after the increase in total vascular resistance in catabolic phase of systemic inflammation and sepsis, vasoplegia develops deteriorating cardiogenic and redistributive shock leading in turn to multi-organ failure.

It was established [10] that, in case of burn injury, acidosis causes the increase in the cytosolic calcium content in cardiomyocytes, the secretion of pro-inflammatory cytokines by these cells, and activation of the apoptosis and autophagy processes. Myocardial damage in a burn injury leads to an alteration of its contractility and the development of HF. Inflammatory cytokines (TNFα, interleukin-6) contribute to the development of diastolic dysfunction of the left ventricle (LV).

At the moment of thermal exposure to the skin, a huge number of cells are destroyed and damaged with the release of a bulk of various biologically active substances: inflammatory mediators (kinins, serotonin, histamine, acute phase proteins, complement factors, etc.). All of them have a vasoactive effect and significantly increase the permeability of the vascular wall. In burn patients, metabolic imbalance along with disorders of the endocrine, respiratory systems and psychoemotional status affect the cardiovascular system [11].

Another mechanism of myocardial damage in burn disease is the hyperproduction of reactive oxygen species and lipid radicals. An excess of free radicals causes cardiomyocyte membrane permeability disturbances, change in ionic homeostasis, damage to their genetic apparatus and activation of programmed mechanisms of cell death [12].

An imbalance in the acid-base state and the electrolyte content (in particular, hyper- or hypokalemia), specific to a burn disease, can lead to various disturbances in the cardiac conduction and heart rate, including life-threatening arrhythmias.

In conditions of tissue destruction caused by burns, proteins of the injured patient acquire the properties of autoantigens. In this case, antibodies produced by the patient's body interact with both pathologically altered and normal tissue components, cardiomyocytes, in particular. One of the mechanisms responsible for the development of autosensitization is the formation of tissue and microbial antigen associations, in which the microbial part acts as an adjuvant. All these pro-

cesses can lead to the development of burn myocarditis.

In the period of burn toxemia and septicotoxemia due to the initiation of the secondary bacterial infections, various cardiac infective complications are also possible. In this setting, myocarditis, pericarditis and infectious endocarditis (IE) may develop.

PATHOMORPHOLOGY

Morphological examinations also indicate heart damage in case of the burn disease. Those who died in the first days of the burn injury the section show signs of circulatory disorders, edema of the interstitial and perivascular tissue, foci of protein and fatty degeneration. During autopsy during the period of septicotoxemia in the burn disease, heart sizes were enlarged in the transverse direction, its walls became flabby, the cavities were extended and were filled with massive variegate blood clots. Histological examination of such myocardium revealed widespread dystrophic changes, especially pronounced in the LV wall, small damage areas and small-focal myocyte necrosis.

Pathological cardiac changes during septicotoxemia of the burn disease are characterized by widespread dystrophic lesions and edema of the interstitial and perivascular myocardial tissue. In persons of young and middle age, injuries of this nature occurred most often in the setting of sepsis. In older people with a previous heart disease, extensive dystrophic myocardial lesions were detected without generalization of the infection.

CLINICAL PICTURE

Heart failure (HF) plays a significant role in the clinical picture of heart damage in burn disease. In small lesions (up to 10% of the total body surface area (TBSA)), only moderate tachycardia and slight increase in BP can be observed in the injured. In more extensive and deeper burns (over 10–15% of TBSA) in the first period of the burn disease, dyspnea, palpitations and chest pain often occur. Acrocyanosis, tachycardia and diminishing of the first sound at the cardiac apex are clinically detected. BP rises slightly during the erectile phase of burn shock and decreases in the torpid phase. In some cases indicating an unfavorable prognosis, refractory arterial hypotension develops in the early stages after thermal injury. In patients with initial arterial hypertension, BP during shock usually drops to normal values and often remains at the same level throughout the subsequent period of the disease [4].

In toxemia phase injured may remain shortness of breath, palpitations and chest pain. Due to tachycardia, systolic murmur at the apex, the decrease in BP and expansion of the heart borders are often determined.

In the period of septicotoxemia, pericarditis and endocarditis often develop which may be one of the reasons for the development and progression of HF. In these cases, the fluid infusion in large volumes used in the treatment of burn injured can deteriorate their condition due to the significant increase in pre- and afterload.

Electrolyte imbalance (hyper- or hypokalemia), myocardial ischemia and MI, myocarditis or underlying cardiac pathology can cause various rhythm and conduction disturbances in burn injured patients. These changes can occur within 6–8 hours after the injury, therefore, the sooner the measures will be taken to prevent and compensate them, the greater is the likelihood of a favorable course of the burn disease and the lower incidence of its serious complications [4].

A relatively rare, but very severe complication of the burn disease is acute coronary syndrome, including the development of MI. Vasospastic forms of acute coronary insufficiency in burn disease are described, in the origin of which the release of endogenous nickel possessing a powerful vasoconstrictor effect is considered [13]. M. Caliskan et al. [14] have demonstrated that vasoconstriction of the coronary arteries and arterioles are caused by stress factors and increased activity of the sympathetic tone attributable to the burn injury. Moreover, the authors found that vasoconstriction causes a worsening of systolic and diastolic LV function, a decrease in the reserve of coronary blood velocity reflecting microvascular dysfunction in the absence of obstruction or narrowing of the coronary arteries lumen [14].

There are also descriptions of cases of the development of stress-induced cardiomyopathy (Takotsubo) with severe hemodynamic abnormalities in setting of the burn injury. Results of studies confirm the basic concept of post-traumatic heart damage as stress-induced cardiomyopathy and have demonstrated the potential importance of stress in accelerating fatal outcome in patients with injuries and thermal burns.

DIAGNOSIS

Laboratory tests. It is known that during the first 3–4 days in burn injured, there is most often an increase in potassium in blood, which can be the cause of the development of various cardiac rhythm and conduction disturbances including life-threatening ones.

Estimation of troponin levels is currently used as a standard biomarker for diagnostics MI and acute coronary syndrome [15, 16]. In case of the burn disease, an increase in blood levels of myocardial damage markers, such as cardiac troponins and creatine phosphokinase MB-fractions is observed. Moreover, the degree of their elevation reflects the severity of myocardial damage.

In this context, it should be noted that an increase in troponin levels occurs under the influence of a wide range of non-cardiac and cardiac factors, such as physical endurance training, sepsis and other serious diseases, including stroke, pulmonary embolism [17], pericarditis, myocarditis, Takotsubo syndrome [18], acute coronary syndrome, acute HF, tachyarrhythmias, etc. It is suggested that TNFα increases the permeability of the cell membrane under stress or inflammation and is considered a possible mechanism responsible for increasing troponin levels [15].

Due to the above mentioned non-cardiac causes, many authors have shown that troponin levels can be increased in burns of significant areas. The increase in troponin levels usually occurs in patients with burns affecting ≥15% of TBSA and during the first 72 hours after injury. In one study, no patients with burns <20% of TBSA showed the increase in troponin, despite matched age, weight, and gender characteristics with those whose burn area exceeded 20% of TBSA. Data from the prospective study that found correlation between elevated troponin T levels and regional abnormalities of LV wall movement in patients with the burn area > 20% of TBSA were presented. None of the patients with identified regional impairment of LV wall movement showed the normal level of cardiac troponin. It is noteworthy that in experimental studies and in burn injured, the decrease in the troponin level was revealed after surgical escharotomy (surgical excision of an eschar) [15].

The concentration of brain natriuretic peptide and its precursor (NT-proBNP) in blood plasma reflects the degree of hemodynamic load on the heart. There are suggestions that these indicators can be used to assess the prognosis of burned patients in extremely serious conditions. Thus, the level of NT-proBNP closely correlates with the size of the burn area, the degree of fluid retention, the severity of organ failure, and mortality rates. In addition, the determination of the level of brain natriuretic peptide in the blood serum is considered to be a simple and informative method for detecting HF in patients with severe burns during resuscitation procedures in the setting of shock.

Electrocardiography (ECG). On the ECG records, a decrease in voltage, sinus tachycardia, various rhythm disturbances (atrial fibrillation and atrial flutter, premature cardiac beats, supraventricular and ventricular tachycardia, ventricular fibrillation), conduction disturbances and pathological changes in the initial and final parts of the ventricular complex can be determined. There is often an increase in the QT dispersion with close correlation of this indicator with severity of the heart damage. Concerning the heart rate variability determined by 24-hour Holter ECG monitoring, it was found that abnormal heart rate variability during the immediate postburn period is strongly predictive of death [19, 20]. In burn injury, the inhibition of the wave structure of the heart rhythm and the total spectrum power indicators are observed [21]. S.Y. Joo et al. [20] revealed a sympathetic predominance during daytime and a decreased parasympathetic activity during nighttime in burn injured patients.

Transthoracic and transesophageal echocardiography (TEE) has important diagnostic value in severe patients, since it allows evaluate the myocardial structure and function, clarify causes of HF. According to the results of a systematic review regarding the importance of using TEE in 128 burn patients, the main pathological findings were deterioration of systolic and diastolic LV function, detection of vegetation on the heart valves, pulmonary hypertension, pericardial effusion and right ventricular HF. The advantages of TEE over transthoracic echocardiography are the possibility of a more accurate assessment of valve function, myocardial contractility and, perhaps most important, monitoring the adequacy of acute hemodynamic recovery and preload in the acute phase of resuscitation. TEE is especially informative in assessing the structure of heart valves to confirm or exclude IE and its complications, due to the proximity of the location of the high-frequency ultrasonic transducer to the heart. Given the susceptibility of burn injured to local and general infectious complications, IE can develop in any patient, regardless of the burn area. Nevertheless, thorough discussion of the indications for TEE is necessary considering the relative invasiveness of the method, the frequent thermal damage to the oral cavity and pharynx, the infrequent but existing probability of rupture of the esophagus and the risk of bacteremia.

Coronary angiography is used in patients with a clinical picture of acute coronary syndrome or acute myocardial infarction, which, as already noted, can develop against a background of the burn injury.

MANAGEMENT

In addition to the appropriate treatment of burn wounds during a shock period, the burn disease treatment includes the management of pain and patient exaltation, hypovolemia amelioration, replacement of the circulating blood volume, hemodynamic stabilization, metabolic disorders correction and infection control [22].

Procedural pain complicates the patient management and leads to the use of aggressive methods to combat it such as administration of potent opioids, ketamine, and regional or general anesthesia. Unfortunately, high doses of opioids are associated with several serious adverse effects such as depressed consciousness and the risk of developing delirium, hypotension, respiratory depression and not infrequently obstipation. Therefore, there is an obvious need to reduce the number of doses of opioid administrating throughout treatment, and at the same time to provide a tolerable level of pain [23].

It was shown that intravenous infusion of lidocaine starting with a bolus dose (1 mg/kg) and then in the form of a continuous infusion (180 mg/hour) is not accompanied by adverse effects and had a 25% opioid sparing effect [23].

Given massive volumes of solution transfusions during this period, it is recommended to provide inotropic myocardial support with dopamine at a dose of 5–10 mg/kg/min. At this dosage dopamine improves myocardial contractility and increases CO. When signs of congestive HF appear, the volume of infusion therapy should be reduced and diuretics should be administered.

Detoxification, the infection control and the correction of homeostasis are the main targets in the treatment of burn toxemia [22]. It is necessary to conduct timely and adequate correction of the acid-base state and electrolyte imbalance emerging in patients with severe burn injury. With the development of life-threatening disorders of cardiac rhythm and conduction (ventricular fibrillation, ventricular tachycardia, asystole, electromechanical dissociation, some forms of supraventricular tachycardia), active antiarrhythmic therapy is indicated and emergency resuscitation measures are fulfilled.

Non-emergency antiarrhythmic therapy is prescribed in cases where arrhythmia or heart block do not influence significantly a patient's condition. Therefore, in sinus tachycardia, β-blockers (propranolol, bisoprolol) or calcium antagonists (verapamil, diltiazem) are usually used.

For the treatment of hemodynamically relevant sinus bradycardia, atropine (0.5–2.0 mg), isoprenaline (2–20 μg/min by intravenous administration) or pacing are applied.

Extrasystoles usually do not require active antiarrhythmic therapy, since the prognosis for this form of arrhythmia depends entirely on the basic underlying process and the degree of structural damage of the heart. Class II and III of antiarrhythmic drugs, omacor are used to terminate extrasystoles of high grades (coupled, salvos, early) that cause hemodynamic disturbances in people with severe cardiac pathology (MI, myocarditis, severe LV dysfunction).

With the aim to terminate atrial fibrillation (AF) or flutter, electric cardioversion (ECV) or antiarrhythmic drugs (propafenone, procainamide, amiodarone or sotalol) are administered. If it is impossible to terminate AF, digoxin, verapamil or β-blockers are used to control the ventricular rate. Due to the high risk of thromboembolic complications, the treatment by anticoagulants is considered.

Paroxysms of atrioventricular tachycardia are stopped by vagal tests, intravenous infusion of adenosine triphosphate (10–30 mg), adenosine (6–12 mg) or verapamil. Transesophageal pacing and ECV are also effective. Radiofrequency catheter ablation is considered as a radical way to treat this arrhythmia.

The most effective treatment for acute coronary syndrome and MI is an urgent percutaneous coronary intervention with the maximally rapid restoration of coronary blood flow.

In recent years, the effectiveness of various approaches to the prevention of myocardial damage and dysfunction arising from burns has been actively studied. The possibility of using angiotensin-converting enzyme inhibitors, drugs that modulate ion channels, anti-inflammatory agents, antioxidants, metabolic drugs and cardioprotectors, has been considered for this purpose.

The issue of prescribing propranolol to adult patients who suffered thermal injury is being actively debated in order to reduce the hypermetabolic response [24–27]. Propranolol is being successfully used to block the effects of endogenous catecholamines which are involved as the first mediators of the hypermetabolic response. In the first stages of the burn injury, the level of catecholamines in the blood is increased by 10 times. The hyperdynamic type of circulation, an increase in the level of basal metabolism and the catabolism of skeletal muscle proteins taken together produce distinctly negative effect on the patient's

organism. The effects of propranolol in the burn patient include a decrease in thermogenesis, terminating or slowing down tachycardia, a decrease in CO and energy consumption at rest. The dosage used is individual for each patient, however, a reduction in heart rate by 20% causes a decrease in heart load and fatty infiltration (secondarily to a decrease in peripheral lipolysis). It has been shown that propranolol enhances the intracellular circulation of amino acids, which leads to a decrease in atrophy of muscle tissue, thereby increasing muscle mass. Carvedilol may have additional advantages due to its ability to block α-adrenergic receptors and remove free radicals [6].

The use of ozone therapy is scientifically grounded for the treatment of thermal lesions. Medical ozone has bactericidal and analgesic effects. It improves microcirculation, normalizes immunity and the oxidative-antioxidant state of blood and cells. There is the evidence that, during ozone therapy of patients with severe thermal injuries, the functional activity of the myocardium and CO increase. Moreover, an antiarrhythmic effect is observed, myocardial ischemia decreases (with an improvement in the processes of myocardial repolarization on the ECG), hemodynamic parameters improve.

A number of studies have shown that early surgical intervention (necrotomy, necrectomy, dermabrasion with xenoplasty, autodermoplasty), optimization of the wound process using a culture of fetal human embryonic fibroblasts, stem cells [28, 29], adequate transfusion and antibacterial therapy can reduce complications of the burn disease and decrease mortality.

The beneficial effect of listening to music on the course of a burn disease is shown. Thus, according to a meta-analysis [30], which covered 17 randomized controlled trials and 804 patients with burn injury, listening to music helped alleviate pain, decrease in anxiety and reduce heart rate.

PROGNOSIS

Although the most obvious consequences of thermal injury are associated with damage of the skin, systemic reactions that occur during burn disease affect many organs and tissues, including the heart, often causing an unfavorable outcome at the onset of the disease and having a negative effect in the long term. Therefore, according to data provided by J.M. Duke et al. [31] who compared individuals without a history of burns, patients with burn injuries over the age of 45 years were 1.46 times more often (95% confidence interval (CI): 1.36–1.56) and almost 3 times longer (95% CI: 2.60–3.25) were hospitalized due to pathology of the cardiovascular system. Patients with a history of burns were more often hospitalized for coronary heart disease (1.21, 95% CI: 1.07–1.36), HF (2.29, 95% CI: 1.85–2.82), cerebrovascular pathology (1.57, 95% CI: 1.33–1.84), and had higher mortality rates from cardiovascular diseases (1.11, 95% CI: 1.02–1.20). Similar data were obtained among pediatric patients under the age of 15 years who suffered from thermal trauma [32]. According to L. Knowlin et al. [5] derangements in cardiac function can last for two years in pediatric patients post burn.

CONCLUSION

In summary, it should be emphasized that timely diagnosis of heart damage in burn disease, treatment and prevention of its occurrence, including correction of electrolyte disorders, adequate antibiotic therapy, and the use of cardiovascular drugs can improve the quality of treatment and reduce the mortality of such patients.

REFERENCES

1. Burns. Newsletter. World Health Organization. URL: https://www.who.int/ru/news-room/fact-sheets/detail/burns (access: 06.03.2018) (in Russ.).
2. Greenhalgh D.G. Management of burns. *N. Engl. J. Med*. 2019; 380 (24): 2349–2359. DOI: 10.1056/NEJMra1807442.
3. Socially significant diseases of the Russian population in 2018. Statistical digest of 2018 of the Ministry of Healthcare of the Russian Federation. Moscow. URL: https://www.rosminzdrav.ru/ministry/61/22/stranitsa-9 (access: 31.07.2019) (in Russ.).
4. Shabanov V.E., Demenko V.V., Savin Yu.N., Alekseev A.A., Krutikov M.G., Bobrovnikov A.E. Clinical recommendations for the provision of medical care to victims of thermal injury in emergency situations. Moscow: 2015: 2–37 (in Russ.).
5. Knowlin L., Reid T., Williams F., Cairns B., Charles A. Burn mortality in patients with preexisting cardiovascular disease. *Burns.* 2017; 43 (5): 949–955. DOI: 10.1016/j.burns.2017.01.026.
6. Culnan D.M.,Capek K.D., Sheridan R.L. Etiology and prevention of multisystem organ failure. *Total Burn Care*. 2018; 30: 307–317. DOI:10.1016/b978-0-323-47661-4.00030-7.
7. Nielson C.B., Duethman N.C., Howard J.M., Moncure M., Wood J.G. Burns: pathophysiology of systemic complications and current management. *J Burn Care Res*. 2017; 38 (1): e469–e481. DOI:10.1097/BCR.0000000000000355.
8. Guillory A.N., Clayton R.P., Herndon D.N., Finnerty C.C. Cardiovascular dysfunction following burn injury: what we have learned from rat and mouse models. *Int J Mol Sci*. 2016; 17 (1): 53. DOI:10.3390/ijms17010053.
9. Coz Y.A., Aguinaga M.M., Buch K.P., Disselkamp M.A. Hospital and intensive care unit management of decompensated pulmonary hypertension and right ventricular failure. *Heart Fail Rev.*2016;21(3):323-346. DOI: 10.1007/s10741-015-9514-7.

10. Hur J., Yang H.T., Chun W., Kim J.H., Shin S.H., Kang H.J., Kim H.S. Inflammatory cytokines and their prognostic ability in cases of major burn injury. *Ann. Lab. Med*. 2015; 35 (1): 105–110. DOI: 10.3343/alm.2015.35.1.105.
11. Leung B., Younger J.F., Stockton K., Muller M., Paratz J. Cardiovascular risk profile in burn survivors. *Burns*. 2017; 43 (7): 1411–1417. DOI: 10.1016/j.burns.2017.07.010.
12. Szczesny B., Brunyánszki A., Ahmad A., Oláh G., Porter C., Toliver-Kinsky T., Sidossis L., Herndon D.N., Szabo C. Time-dependent and organ-specific changes in mitochondrial function, mitochondrial DNA integrity, oxidative stress and mononuclear cell infiltration in a mouse model of burn injury. *PLoS One*. 2015; 10 (12): e0143730. DOI: 10.1371/journal.pone.0143730.
13. Culnan D.M., Sood R. Coronary vasospasm after burn injury: first described case series of a lethal lesion. *J. Burn Care Res*. 2018; 39 (6): 1053–1057. DOI: 10.1093/jbcr/irx032.
14. Caliskan M., Turk E., Karagulle E., Ciftci O., Oguz H., Kostek O., Moray G., Haberal M. Coronary flow velocity reserve in burn injury: a prospective clinical cohort study. *J. Burn Care Res*. 2016; 37 (5): 400–408. DOI: 10.1097/BCR.0000000000000302.
15. William A., Schneider H.G., Smith C., Cleland H. The incidence and significance of raised troponin levels in acute burns. *J. Burn Care Res*. 2018; 39 (5): 729–735. DOI: 10.1093/jbcr/irx020.
16. Thygesen K., Alpert J.S., Jaffe A.S., Chaitman B.R., Bax J.J., Morrow D.A., White H.D.; ESC Scientific document group. Fourth universal definition of myocardial infarction (2018). *Eur. Heart J.* 2019; 24 (3): 237–269. DOI: 10.1093/eurheartj/ehy462.
17. Vatutin N.T. Pulmonary Thromboembolism. Donetsk: 2019; 193 (in Russ.).
18. VatutinN.T., TaradinG.G., SmirnovaA.S., El'-KhatibM.A., GritsenkoIu.P., BortD.V., KartamyshevaE.V., GasendichE.S. Takotsubosyndrome: the current state of the problem. Review of recommendations ESC-HFA 2016. *Practical Angiology.* 2016: 3 (74): 56–70. (in Russ.).
19. Loguidice M.J., Schutt R.C., Horton J.W., Minei J.P., Keeley E.C. Heart rate variability as a predictor of death in burn patients. *J. Burn Care Res*. 2016; 37 (3): e227–233. DOI: 10.1097/BCR.0000000000000260.
20. Joo S.Y., Hong A.R., Lee B.C., Choi J.H., Seo C.H. Autonomic nerve activity indexed using 24-h heart rate variability in patients with burns. *Burns*. 2018; 44 (4): 834–840. DOI: 10.1016/j.burns.2017.12.012.
21. Pugachev M.I., Livarskii A.P., Salukhov V.V., Ivchenko E.V., Kharitonov M.A., Shustov S.B. Heart rate variability as an indicator of the condition of patients with severe burn injury. *Military Medical Journal*. 2017: 8: 24–33 (in Russ.).
22. Lundy J.B., Chung K.K., Pamplin J.C., Ainsworth C.R., Jeng J.C., Friedman B.C. Update on severe burn management for the intensivist. *J. Intensive Care Med*. 2016; 31 (8): 499–510. DOI: 10.1177/0885066615592346.
23. Abdelrahman I., Steinvall I., Elmasry M., Sjoberg F. Lidocaine infusion has a 25% opioid-sparing effect on background pain after burns: a prospective, randomised, double-blind, controlled trial. *Burns*. 2020; 46 (2): 465–471. DOI: 10.1016/j.burns.2019.08.010.
24. Nuñez-Villaveiran T., Sanchez M., Millan P., Garcia-de-Lorenzo A. Systematic review of the effect of propanolol on hypermetabolism in burn injuries. *Med. Intensiva*. 2015; 39 (2): 101–113. DOI: 10.1016/j.medin.2014.08.002.
25. Brown D.A., Gibbons J., Honari S., Klein M.B., Pham T.N., Gibran N.S. Propranolol dosing practices in adult burn patients: implications for safety and efficacy. *J. Burn Care Res*. 2016; 37 (3): 218–226. DOI: 10.1097/BCR.0000000000000240.
26. Guillory A.N., Herndon D.N., Silva M.B., Andersen C.R., Edgu-Fry E., Suman O.E., Finnerty C.C. Propranolol kinetics in plasma from severely burned adults. *Burns*. 2017; 43 (6): 1168–1174. DOI: 10.1016/j.burns.2016.10.019.
27. Manzano-Nunez R., Garcia-Perdomo H.A., Ferrada P., Ordoñez Delgado C.A., Gomez D.A., Foianini J.E. Safety and effectiveness of propranolol in severely burned patients: systematic review and meta-analysis. *World J. Emerg Surg*. 2017; 12: 11. DOI: 10.1186/s13017-017-0124-7.
28. Ahmadi A.R., Chicco M., Huang J., Qi L., Burdick J., Williams G.M., Cameron A.M., Sun Z. Stem cells in burn wound healing: A systematic review of the literature. *Burns*. 2019; 45 (5): 1014–1023. DOI: 10.1016/j.burns.2018.10.017.
29. Francis E., Kearney L., Clover J. The effects of stem cells on burn wounds: a review. *Int. J. Burns Trauma*. 2019; 9 (1): 1–12.
30. Li J., Zhou L., Wang Y. The effects of music intervention on burn patients during treatment procedures: a systematic review and meta-analysis of randomized controlled trials. *BMC Complement Altern. Med.* 2017; 17 (1): 158. DOI: 10.1186/s12906-017-1669-4.
31. Duke J.M., Randall S.M., Fear M.W., Boyd J.H., Rea S., Wood F.M. Understanding the long-term impacts of burn on the cardiovascular system. *Burns*. 2016; 42 (2): 366–374. DOI: 10.1016/j.burns.2015.08.020.
32. Duke J.M., Randall S.M., Fear M.W., Boyd J.H., Rea S., Wood F.M. Long-term effects of pediatric burns on the circulatory system. *Pediatrics*. 2015; 136 (5): e1323–1330. DOI: 10.1542/peds.2015-1945.

Authors contribution

Vatutin N.T. – creation of a common idea, final editing and approval of the manuscript for publication. Ignatenko G.A. – cooperation of authors, creation of a structural review concept, final editing of the manuscript. Taradin G.G. – literature search, drafting of the sections "Clinical picture" and "Diagnosis", editing of the manuscript. Yeshenko E.V. – literature search, drafting of the sections "Pathophysiology" и "Pathomorphology". Goncharuk M.S. – literature search, drafting of the sections "Management", "Prognosis" Kulikova S.O. – primary search of literature sources and their analysis, systematization of data, sorting of literature by category, design of the manuscript.

Authors information

Vatutin Nikolai T., Dr. Sci. (Med.), Professor, Head of the Department of Hospital Therapy, M. Gorky Donetsk National Medical University; Head of the Department of Cardiac Surgery and Emergency Cardiology, V.K. Gusak Institute of Urgent and Recovery Surgery, Donetsk, Donetsk People's Republic/Ukraine. ORCID 0000-0003-4307-1522.

Ignatenko Grigorii A., Dr. Sci. (Med.), Professor, Corresponding Member of NAMSU, Head of the Department of Propaedeutic and Internal Medicine, M. Gorky Donetsk National Medical University, Donetsk, Donetsk People's Republic/Ukraine. ORCID 0000-0003-3611-1186.

Taradin Gennadii G., Cand. Sci. (Med.), Head of the Department, M. Gorky Donetsk National Medical University; Senior Researcher, Department of Cardiac Surgery and Emergency Cardiology, V.K. Gusak Institute of Urgent and Recovery Surgery, Donetsk, Donetsk People's Republic/Ukraine. ORCID 0000-0003-3984-8482.

Eshchenko Evgeniia V., General Practitioner, Municipal Noncommercial Enterprise Myrnograd Center for Primary Health Care, Myrnograd, Ukraine. ORCID 0000-0001-9180-7827.

Goncharuk Maksim S., Assistant, the Department of Hospital Therapy, M. Gorky Donetsk National Medical University, Donetsk, Donetsk People's Republic/Ukraine. ORCID 0000-0001-6345-0138

Kulikova Svetlana O., Student, Gorky Donetsk National Medical University, Donetsk, Donetsk People's Republic/Ukraine. ORCID 0000-0001-9252-2452.

(✉) **Taradin Gennadii G.,** e-mail: taradin@inbox.ru.

Поступила в редакцию 11.11.2019
Подписана в печать 30.04.2020

УДК 004.946:37.09:616.1-052-021.131
https://doi.org/10.20538/1682-0363-2020-4-207-214

Virtual patients as the basis for problem-based learning of cardiologists

Karas S.I.[1, 2], Arzhanik M.B.[1, 2], Kara-Sal E.E.[1], Grakova E.V.[1], Vasiltseva O.Y.[1], Ussov W.Y.[1], Vaizov V.Kh.[1], Zavadovsky K.V.[1], Gulyaev V.M.[1], Baev A.E.[1], Kolganov S.O.[3], Kochetkov S.B.[3], Datsuk V.V.[3], Korneeva T.B.[4], Nozdrin G.K.[5]

[1] *Cardiology Research Institute, Tomsk National Research Medical Center, Russian Academy of Sciences (CRI, TNRMC RAS)*
111a, Kievskaya Str., Tomsk, 634012, Russian Federation

[2] *Siberian State Medical University (SSMU)*
2, Moscow Trakt, Tomsk, 634050, Russian Federation

[3] *National Research Tomsk Polytechnic University (NR TPU)*
30, Lenina Av., Tomsk, 634050, Russian Federation

[4] *Elecard-Med Ltd.*
3/539, Razvitia Av., Tomsk, 634055, Russian Federation

[5] *Contek-Soft Ltd.*
3, Razvitia Av., Tomsk, 634055, Russian Federation

ABSTRACT

Implementation of virtual patients allows avoiding risks for patient safety, using the standardized clinical situations repeatedly, and providing remote access to information. In order to create virtual patients, the project team comprised of specialists competent in the diverse subject areas. Every virtual patient is a structural model for a diagnostic and treatment process of a real patient augmented with textual and multimedia information. A sample comprising of 50 archival clinical charts of patients with typical cardiovascular diseases and rare pathology variants was formed. Textual information from medical records is supplemented with the multimedia results of instrumental and laboratory studies. Created data and knowledge base of virtual patients was designated for a demonstration of complete cardiovascular cases to the trainees in linear trajectory with an option of Web-access. The virtual patient repository will become a factual basis for problem-based distance learning of medical students and physicians.

Key words: virtual patients, case-based technologies, case study, distance learning, standardization, multimedia, Web-service, gamification, repository, database, knowledge base.

Conflict of interest. The authors declare no obvious or potential conflicts of interest related to the publication of this article.

Source of financing. This study was supported by the Russian Foundation for Basic Research (grant No. 19-013-00231).

For citation: Karas S.I., Arzhanik M.B., Kara-Sal E.E., Grakova E.V., Vasiltseva O.Y., Ussov W.Y., Vaizov V.Kh., Zavadovsky K.V., Gulyaev V.M., Baev A.E., Kolganov S.O., Kochetkov S.B., Datsuk V.V., Korneeva T.B., Nozdrin G.K. Virtual patients as the basis for problem-based learning of cardiologists. *Bulletin of Siberian Medicine.* 2020; 19 (4): 207–214. https://doi.org/10.20538/1682-0363-2020-4-207–214.

✉ *Karas Sergey I.,* e-mail: ksi@cardio-tomsk.ru.

Виртуальные пациенты как база проблемно ориентированной подготовки врачей-кардиологов

Карась С.И.[1, 2], Аржаник М.Б.[1, 2], Кара-Сал Э.Э.[3], Гракова Е.В.[1], Васильцева О.Я.[1], Усов В.Ю.[1], Ваизов В.Х.[1], Завадовский К.В.[1], Гуляев В.М.[1], Баев А.Е.[1], Колганов С.О.[4], Кочетков С.Б.[4], Дацюк В.В.[4], Корнеева Т.Б.[5], Ноздрин Г.К.[4]

[1] Научно-исследовательский институт (НИИ) кардиологии, Томский национальный исследовательский медицинский центр (НИМЦ) Российской академии наук
Россия, 634012, г. Томск, ул. Киевская, 111а

[2] Сибирский государственный медицинский университет (СибГМУ)
Россия, 634050, г. Томск, Московский тракт, 2

[3] Национальный исследовательский Томский политехнический университет (НИ ТПУ)
Россия, 634050, г. Томск, пр. Ленина, 30

[4] Общество с ограниченной ответственностью (ООО) «Элекард-Мед»
Россия, 634055, пр. Развития, 3/539

[5] Общество с ограниченной ответственностью (ООО) «Контек-Софт»
Россия, 634055, пр. Развития, 3

РЕЗЮМЕ

Виртуальные пациенты позволяют избежать рисков в отношении реального больного, неоднократно использовать стандартизованные клинические ситуации, обеспечить удаленный доступ к информации. Для создания виртуальных пациентов в команду проекта включены специалисты с компетенциями в разных предметных областях. Каждый виртуальный пациент является структурированной моделью лечебно-диагностического процесса реального больного, наполненной текстовой и мультимедийной информацией. Сформирована выборка из 50 архивных историй болезни пациентов с типичными сердечно-сосудистыми заболеваниями и редкими вариантами патологии. Текстовая информация из историй болезни дополнена мультимедийными результатами инструментальных и лабораторных исследований. Созданная база данных и знаний о виртуальных пациентах предназначена для демонстрации обучающимся завершенных случаев кардиоваскулярных заболеваний в линейной траектории с возможностью Web-доступа. Репозиторий виртуальных пациентов станет фактологической основой проблемно ориентированного дистанционного обучения студентов и врачей.

Ключевые слова: виртуальные пациенты, case-технологии, анализ прецедента, дистанционное обучение, стандартизация, мультимедиа, Web-сервис, геймификация, репозиторий, база данных, база знаний.

Конфликт интересов. Авторы декларируют отсутствие явных и потенциальных конфликтов интересов, связанных с публикацией настоящей статьи.

Источники финансирования. Исследование выполнено при поддержке Российского фонда фундаментальных исследований (грант № 19-013-00231).

Для цитирования: Карась С.И., Аржаник М.Б., Кара-Сал Э.Э., Гракова Е.В., Васильцева О.Я., Усов В.Ю., Ваизов В.Х., Завадовский К.В., Гуляев В.М., Баев А.Е., Колганов С.О., Кочетков С.Б., Дацюк В.В., Корнеева Т.Б., Ноздрин Г.К. Виртуальные пациенты как база проблемно ориентированной подготовки врачей-кардиологов. *Бюллетень сибирской медицины.* 2020; 19 (4): 207–214. https://doi.org/10.20538/1682-0363-2020-4-207–214.

INTRODUCTION

Problem-based learning is viewed as one of the principal approaches in medical education focusing on the development of skills for making clinical and diagnostic decisions [1]. These professional competencies are formed in the very process of solving diverse problems regarding patient health. A trainee should be directly involved in a treatment of the patient to develop the clinical decision making skills, which may not coincide with the desires of real-life patients and have

limitations in terms of medical insurance. The risks of problem-based learning in medical school can be minimized by using the descriptions of complete clinical cases and simulation methods to avoid direct contact with patients.

In this regard, virtual patients are widely implemented in the medical education abroad. The term "virtual patient" has various interpretations including standardized clinical cases performed by actors or volunteers, computerized robots, and multimedia computer models of clinical situations. Virtual patients may serve as a basis for learning based on the case studies and effectively implemented in the clinical disciplines [2–4]. Conceptual cases may be developed based on the clinical charts so the virtual patients are created for further online use [5].

This paper reviews the development of a simulation format that has been used abroad since late 20th century to develop decision making skills of trainees [6–8]. The computerized multimedia simulations for diagnosis and treatment allow avoiding the risks of incorrect or inappropriate actions towards a real patient. The systematic reviews and meta-analyses demonstrate the pedagogic effectiveness of virtual patients as well as the interest of trainees to this educational technology where the interactivity of trainees increases and they get motivation for team work with a certain gamification of clinical training [9–12].

Hereinafter, the term "virtual patient" will be viewed as a computer multimedia interactive simulation of scenarios for the diagnosis and treatment of patients [13]. A virtual patient can have a real depersonalized prototype or be a result of developer imagination, i.e. fully virtual. The use of real scenarios of treatment and diagnostic process is one of the approaches to creating of virtual patients. An incorporation of depersonalized data from the clinical charts and multimedia results of diagnostic studies into this model results in a complete case virtualization and allows ensuring a remote access to this information.

The aim of this paper is to describe the method for creation of virtual patients as a model of treatment and diagnostic process of patients with cardiovascular diseases.

MATERIALS AND METHODS

Project team for creation of virtual patients comprised of the physicians, specialists in radiology and functional diagnostics, software programmers, and analysts. The virtual patient was a compilation of textual and multimedia diagnostic and clinical information. The creation of every virtual patient involved descriptions of a real clinical case. Analytical work allowed to determine the common structure for information representation and to develop the user interface and scenarios for presenting information about virtual patient to the trainees.

The information basis of project consisted of 50 depersonalized archival medical records of cardiovascular patients and multimedia results of studies stored in the corresponding databases. Apart from the texts of complete cases, the test results and medical conclusions regarding electrocardiograms (ECG), Holter monitoring, echocardiography, ultrasound examinations of carotid, femoral, and renal arteries, pleural cavity, and pericardium, multi-slice computed tomography, magnetic resonance imaging, angiography, X-ray examination, laboratory diagnostics, and treatment tactics were used.

Completeness and consistency of depersonalized information in each clinical case was evaluated by the experienced clinical teachers. After expert evaluation, information was transferred to the analysts in the form of approved textual prototypes and files. They were systematically named to be posted in the tables carried out in the PostgreSQL database management system. Multimedia information model of virtual patients was developed using Web technologies: Java Script (framework Vue.js) and Twitter bootstrap. Database was hosted on a server with an option of remote access to the information. Successful implementation of the project was pre-defined by the fact that the specialists of the team were competent in diverse subject areas.

RESULTS

In order to create virtual patients, the team of developers had to answer several essential questions regarding the content:

- Where can the required information be obtained from?
- Which structure would ensure the creation of integral image of a virtual patient?
- What are the trajectories of virtual patient presentation to users?

Two diagnostic categories were considered while establishing the sample of archival cases. The first category comprised typical, most frequently occurring cases of cardiovascular diseases. Several cases with distinct comorbidities and treatments were selected within each clinical entity. One part of clinical charts represented standard cases, which were essential for training

of medical residents and inexperienced physicians. The other part provided an opportunity to demonstrate creative approach to physicians and was of interest to the specialists advancing their qualification.

The second subgroup of clinical records represented the rare occurring variants of cardiovascular pathology potentially leading to serious consequences for a patient. The most interesting cases with rare clinical manifestation were included, which could hardly be demonstrated to the trainees in real life. All medical records in the sample were depersonalized.

The next stage was the analysis of a large pool of textual information present in medical records. Descriptions of anamnesis vitae, past medical history, and pharmacological anamnesis were edited and introduced into the tables of virtual patient database. However, every clinical chart contains a fraction of information which does not play an essential role to clinical decision making. If the results of diagnostic studies do not provide any new information pivotal for establishing diagnosis, they may be omitted from the virtual patient structure.

On the contrary, if a patient has not been investigated for some reason, though study results could be potentially informative, the results may be extracted from record of another patient with similar clinical manifestation, anatomy, and demographic characteristics. Therefore, the necessary multimedia images and recordings (echocardiography, ultrasound, ECG, coronary angiography, MRI, angiography, etc.) were accumulated as a result of a team work of analysts and medical personnel.

It was decided to withdraw from using the patient animations, essentially gamifying the training. Information model of a treatment and diagnostic process, i.e. a superposition of interrelated data on its dynamics in the textual and multimedia formats, is primarily necessary to form and improve the skills of clinical and diagnostic decision making. This superposition is the information image of virtual patient.

A real process of patient treatment in the hospital settings involves periodic contacts with the medical personnel and paraclinical services, periodic laboratory and instrumental studies, periodic treatment correction, and modification of plans for the future. This predetermines discretion of the created multimedia computer model of treatment and diagnostic process.

Not all the records in a medical chart are equally important for an attending physician and, therefore, for the development of medical competencies of trainees. In this context, the analysts made the decision on discreet representation of information in the form of discrete units. They were designated for the trainees as a "visit" and represented information in chronological consequence according to the stages of treatment and diagnostic process of the case. The prototypes of two virtual patients were created as an example of this approach to information presentation. After that, the structure of patient description was redefined, broadened, and approved by the clinical teachers.

The number of visits may differ in virtual patients because not all contacts of the patient with medical personnel generate information useful for the treatment and diagnostic process. The medical records containing new diagnostic and clinically significant data were selected and the list of acceptable formats of textual, graphic, and video information was established for virtual patient. This stage of work resulted in a template where information from the archival medical records and multimedia databases was prepared for all virtual patients. The information units generally corresponded to the traditional sections of a clinical case and served as the basis for the development of relational database tables.

The analytical work with clinical teachers resulted in establishing the prototypes of screen forms, which underwent expertise and, after modification, were implemented as the screen templates for various clinical and diagnostic situations of virtual patients. The screen forms are supplemented with the tab pages containing all information components of the visit; the day of a hospitalization is designated on the tab page to allow an accurate evaluation of the events course by the trainees (Fig. 1). The tab page of the first visit is slightly different because it represents information at the moment of admission (patient anamnesis vitae and case history, results of previous diagnostic studies and physical examination at admission, differential diagnosis, administered symptomatic treatment, and plan of the following diagnostic procedures).

The structure and pattern of information units on the tab pages of follow-up visits do not change, but the volume of information may differ. Anamnesis vitae and case history are available on the pages of all virtual patient visits. However, data regarding the complaints, administered studies, differential diagnosis, prescribed drugs, etc. are specified for the given visit. The number of tab pages (similar to the number of visits) is non-constant; the trainee may shift between tab pages along a free trajectory.

Chronologically, the last tab page of a case corresponds to the situation of patient discharge and ultimately contains the document with epicrisis of a patient stay in hospital (Fig. 2). The images and video recordings of diagnostic examinations are placed on the tab pages for the visits following their administration.

The results of instrumental and laboratory methods are incorporated into the virtual patient structure as the scanned ECG recordings, fragments of video recordings for echocardiography, angiography, and vascular ultrasound, tomography images, and X-ray pictures with the textual medical specialist opinion (Fig. 3 and 4). Based on the current guidelines of the European Society of Cardiology and the Russian Cardiology Society, compendiums of drugs are created with specification of doses and dosage frequency for treatment of a patient.

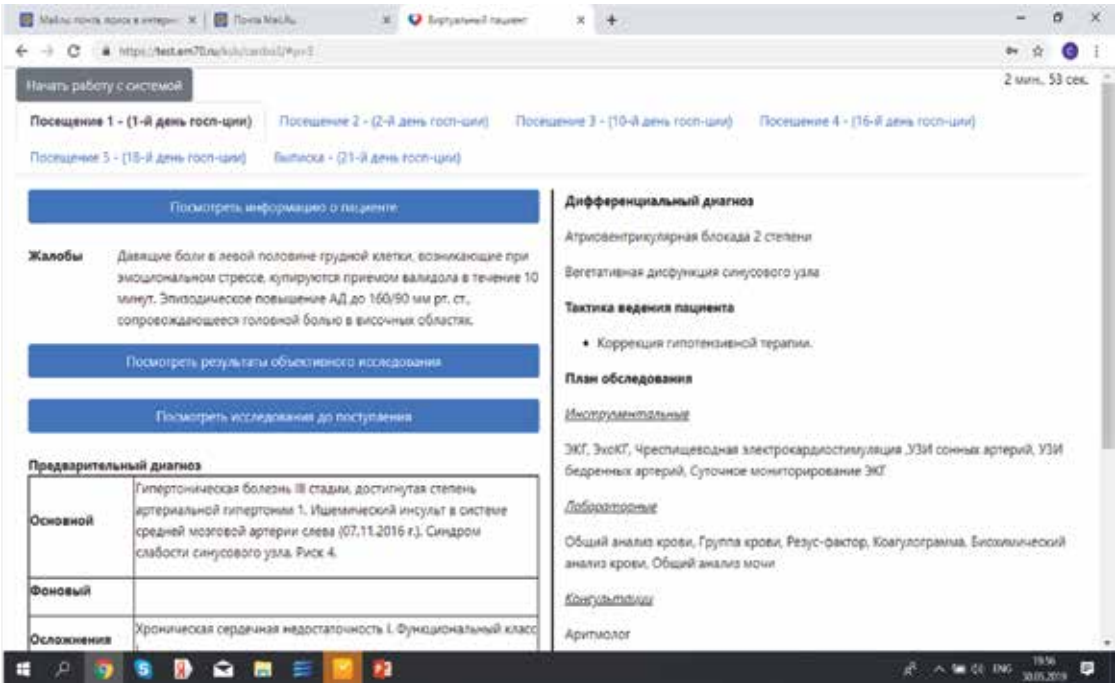

Fig. 1. Organization of the virtual patient interface

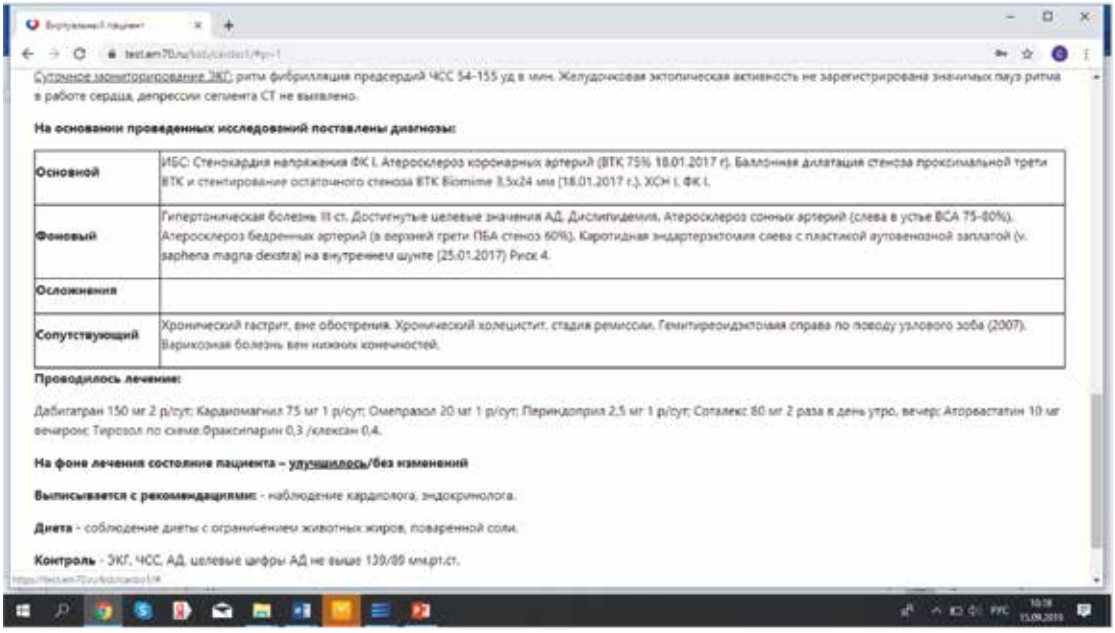

Fig. 2. Epicrisis at the final tab page of virtual patient

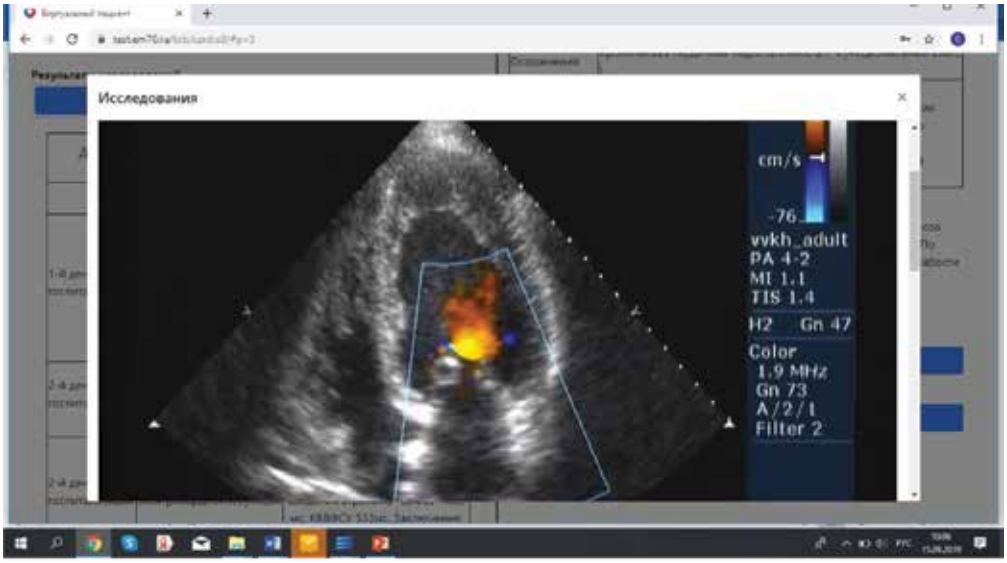

Fig. 3. Presentation of echocardiography results for virtual patient

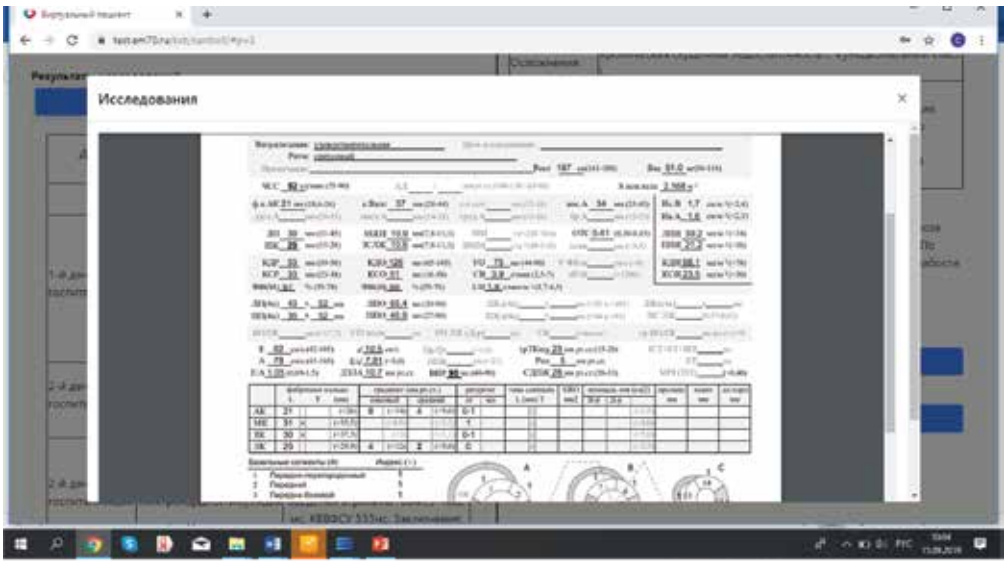

Fig. 4. Presentation of concluding remarks on the results of examination

DISCUSSION

The implementation of virtual patients is a definite innovation for Russian higher medical education. This educational technology has several advantages compared with education requiring contact with real patients or computerized mannequins. It also has some limitations. Considering this debate, one may discuss the optimality of virtual patients for the formation of clinical and diagnostic competencies. In medical education, the patient safety, pedagogic effectiveness, and costs may be considered the most essential characteristics.

First of all, the formation of competencies for decision making and their evaluation using the computer simulations are absolutely safe for the real patients. There is no need to receive patient permission for a trainee to participate in the treatment and diagnostic process; there is no need to wait for a rare in-hospital case; and there is no need to apprehend the sanctions of an insurance company if "something goes wrong".

An opportunity to repeat the same clinical situation indefinite number of times is a very essential aspect of physician training as it is impossible to achieve with real-life patients. The standardization of terms and criteria for evaluation of task performance is the advantageous characteristic of virtual patient education technology, which is hardy achievable in a framework of teaching the clinical disciplines. The presence of real comprehensive results of instrumental studies in

the standardized formats (.dcm, .avi, .jpg, etc.) allows importing them into the computer models of treatment and diagnostic process, i.e. virtual patients.

Pedagogic effectiveness of virtual patients is shown in a significant number of publications. There are not only the developed recommendations for their creation [14], but the certain proposals for the development of virtual patient-based clinical thinking skills [15]. The virtual cases, compared with the traditional medical records on paper, stimulate interaction between the trainees who are actively involved in the process. The branching trajectory makes virtual patient more realistic and useful for trainees, but it complicates the task and increases the frequency of mistakes [16]. All participants of pedagogic process notice the prospects of virtual patients for the medical education, whereas the capabilities of distance learning and decision-making skill testing make this technology unique.

The cost aspect of this educational technology is quite essential. The cost of development for each virtual patient case is one of the limiting factors for their widespread implementation in higher education and constitutes at least $10,000–20,000 abroad [17]. Average prime cost of creating one virtual patient with a linear trajectory of demonstration in this project was less than $1,000 with one-year implementation period.

The limitations of computer simulations in the clinical training include the absence of contact with patients and, as a consequence, the unawareness of patient psychological features and insufficient awareness of other personal characteristics. Even without animation, this educational technology gamifying the learning process, which results in attenuation of essential motivating factors and responsibility level of the trainees for their decision-making.

Upon comparing expected advantages and disadvantages, one may consider the virtual patients an optimal educational technology in clinical disciplines in the distance and face-to-face electronic formats.

The next step of ongoing project will be the development of with branching structure. It would simulate different variants of treatment and diagnostic process with integrated rating system for the evaluation of trainee decisions. The informational basis for the clinical and diagnostic tasks will be the materials from virtual patients. In a framework of branching clinical and diagnostic tasks, there will be an opportunity for changing the trajectory of presenting information to the trainees. The interactivity of educational technology will significantly expand and will consist in making the step-by-step solutions affecting the choice of further trajectory for completing the task.

Linear and branching multimedia models of the treatment and diagnostic process will be included in the repository of virtual patients with access for users in the form of Web-service. This resource will become the factual basis for problem-based technology of distance learning and advanced medical training of physicians.

CONCLUSION

The employed multimedia model of treatment and diagnostic process is designated for demonstration of complete cases of cardiovascular cases to the trainees along a liner trajectory. The interactivity of product is minimal and implies free choice of an information unit visit or (and) multimedia recording depending on the level of knowledge and interest of trainees. The software product complies with the technical design specification developed earlier. It passed the preliminary testing of content quality, clinical and diagnostic information sufficiency, and friendliness of information presentation on screen forms and browsing trajectory of educational content. Web-access to the materials of virtual patient is technologically implemented, which may be used for an in-person electronic learning format and distance advanced professional training of physicians.

As a result of the project competing, 50 virtual patients have been created to date for the higher medical education and postgraduate medical training. This database is hosted on the server at http://virtual.cardio-tomsk.ru as a component of factual basis for the problem-based learning technology and continuous medical education of physicians.

REFERENCES

1. Barrows H.S.,Tamblyn R.M. Problem-based learning: An approach to medical education. Springer Publishing Company, 1980: 224.
2. Lee R., Kwan C.Y. The use of problem-based learning in medical education. *J. Med. Education*. 1997; 1: 149–158.
3. Savery J. R. Overview of problem-based learning: definitions and distinctions. *Interdisciplinary Journal of Problem-Based Learning*. 2006; 1 (1). DOI: 10.7771/1541-5015.1002.
4. Berman N., Fall L.H., Smith S., Levine D.A., Maloney C.G., Potts M., Siegel B., Foster-Johnson L. Integration strategies for using virtual patients in clinical clerkships. *Acad. Med*. 2009; 84 (7): 942–949. DOI: 10.1097/ACM.0b01 3e3181a8c668.
5. Poulton T., Conradi E., Kavia S., Round J., Hilton S.R. The replacement of 'paper' cases by interactive online virtual patients in problem – based learning. *Medical Teacher*. 2009; 31(8): 752–758. DOI: 10.1080/01421590903141082.

6. Harless W., Drennon G., Marxer J., Root J., Miller G. CASE: a computer-aided simulation of the clinical encounter. *J. Med. Educ.*1971; 46.(5): 443–448.
7. Ellaway R.H., Davies D. Design for learning: deconstructing virtual patient activities. *Med. Teacher.* 2011; 33 (4): 303–310. DOI: 10.3109/0142159X.2011.550969.
8. Posel N., McGee J.B., Fleiszer D.M. Twelve tips to support the development of clinical reasoning skills using virtual patient cases. *Medical Teacher.* 2015; 37 (9): 813–818. DOI: 10.3109/0142159X.2014.993951.
9. Cook D., Erwin P., Triola M. Computerized Virtual Patients in Health Professions Education: A Systematic Review and Meta-Analysis. *Academic Medicine.* 2010; 85 (10): 1589–1602. DOI: 10.1097/ACM.0b013e3181edfe13.
10. Hege I., Kononowicz A., Tolks D., Edelbring S., Kublmeyer K. A qualitative analysis of virtual patient descriptions in healthcare education based on a systematic literature review. *BMC Med Educ.* 2016; 16:146. DOI: 10.1186/s12909-016-0655-8.
11. Consorti F., Mancuso R., Nocioni M. et al. Efficacy of virtual patients in medical education: A meta-analysis of randomized studies. *Computers & Education.* 2012; 59 (3): 1001–1008. DOI: 10.1016/j.compedu.2012.04.017.
12. Toro-Troconis M., Mellström U., Partridge M.R., Meeran K., Barrett M., Higham J. Designing game-based learning activities for virtual patients in Second Life. *J. Cyber Therapy & Rehabilitation*. 2008; 1 (3): 227–239.
13. Karas S. Virtual patients as a format for simulation learning in the continuing medical education. *Bulletin Siberian Medicine.* 2020; 19 (1): 140–149 (in Russ.) DOI: 10.20538/1682-0363-2020-1-140-149.
14. Huwendiek S., Reichert F., Bosse H.-M., DeLeng B.A., Van Der Vlueten C., Haag M., Hoffman G.F., Tönshoff B. Design principles for virtual patients: A focus group study among students. *Med. Educ.* 2009; 43 (6): 580–588. DOI: 10.1111/j.1365-2923.2009.03369.x.
15. Poulton T., Balasubramaniam C. Virtual patients: A year of change. *Med. Teacher.* 2011; 33 (11): 933–937. DOI: 10.3109/0142159X.2011.613501.
16. Huwendiek S., de Leng B.A. Virtual patient design and curricular integration evaluation toolkit. *Med. Educ*. 2010; 44 (5): 519. DOI: 10.1111/j.1365-2923.2010.03665.x.
17. Cendan J., Lok B. The use of virtual patients in medical school curricula. *Adv. Physiol. Educ.* 2012; 36 (1): 48–53. DOI: 10.1152/advan.00054.2011.

Acknowledgments

The authors thank the Russian Foundation for Basic Research for financial support of the project (grant No. 19-013-00231), leaders and employees of Elecard-Med and Contec-Soft for effective implementation of the analytical and software aspects of the project, and Dr. Yana J. Anfinogenova for translating the manuscript in the English language.

Authors information

Karas Sergey I., Dr. Sci. (Med.), Head of Department, CRI, TNRMC RAS; Professor, Department of Medical and Biological Cybernetics, SSMU, Tomsk, Russian Federation.

Arzhanik Marina B., Cand. Sci. (Ped.), Associate Professor, Department of Medical and Biological Cybernetics, SSMU, Tomsk, Russia.

Kara-Sal Eres E., Master's Student, NR TPU, Tomsk, , Russian Federation.
Grakova Elene V., Dr. Sci. (Med.), Principal Scientist, CRI, TNRMC RAS, Tomsk, Russian Federation.
Vasiltsceva Oksana Ya., Dr. Sci. (Med.), Senior Scientist, CRI, TNRMC RAS, Tomsk, , Russian Federation.
Ussov Vladimir Yu., Dr. Sci. (Med.), Head of Department, CRI, TNRMC RAS, Tomsk, , Russian Federation.
Vaizov Valery Kh., Cand. Sci. (Med.), Physician, CRI, TNRMC RAS, Tomsk, Russian Federation.
Zavadovsky Konstantin V., Dr. Sci. (Med.), Head of Department, CRI, TNRMC RAS, Tomsk, Russian Federation.
Gulyaev Vsevolod M., Cand. Sci. (Med.), Physician, CRI, TNRMC RAS, Tomsk, Russian Federation.
Baev Andrey E., Cand. Sci. (Med.), Head of Department, CRI, TNRMC RAS, Tomsk, Russian Federation.
Kolganov Sergey O., Director, Elecard-Med Ltd. Tomsk, Russian Federation.
Kochetkov Sergey B., Head of Department, Elecard-Med Ltd. Tomsk, Russian Federation.
Datscuk Valery V., Programmer, Elecard-Med Ltd. Tomsk, Russian Federation.
Korneeva Tatyana B., Head of Department, Contek-Soft Ltd. Tomsk, Russian Federation.
Nozdrin Georgy K., Programmer, Elecard-Med Ltd. Tomsk, Russian Federation.

(✉) **Karas Sergey I.,** e-mail: ksi@cardio-tomsk.ru.

Received 30.03.2020
Accepted 29.09.2020

УДК 611.018.2:576.31
https://doi.org/10.20538/1682-0363-2020-4-215-225

Extracellular matrix as a cellular information microenvironment

Naumova L.A., Starodumova V.A.

Surgut State University
1, Lenina Str., Surgut, Khanty-Mansiysk Autonomous Area – Yugra, 628412, Russian Federation

ABSTRACT

The article discusses modern ideas about the role of extracellular matrix (ECM) and cellular elements of connective tissue (CT) in tissue homeostasis in normal and pathological conditions. The works of recent years reflect a shift of interests concerning the study of many pathological processes, particularly carcinogenesis, to the state of the ECM and CT cells, which are considered as active components of the tissue that determine the processes of cellular proliferation, differentiation, migration, and apoptosis. The most important properties of the ECM attracting the attention of researchers include mechanotransduction, leading to the activation of cytoskeletal mechanisms and various cell signaling pathways; modeling of the effects of various cytokines, growth factors, and hormones; maintenance of the stem cell niches; influence on the emergence and course of the tumor process, in particular, formation of a cancerized field and premetastatic niches; and the epithelial-mesenchymal transition (EMT). Currently, CT cells are also an important object of study, in particular, fibroblasts, which are the main producers of ECM components. The attention of researchers is directed primarily to cancer-associated fibroblasts, the phenotype of which forms in the tissue long before the tumor appears. New knowledge about the role of ECM and CT cells in tissue homeostasis determines new approaches to treatment of many diseases, such as systemic sclerosis, tumors, etc.

Key words: extracellular matrix, epithelial-stromal relations and carcinogenesis, fibroblast, field cancerization, premetastatic niches.

Conflict of interest. The authors declare no obvious or potential conflicts of interest related to the publication of this article.

Source of financing. The authors received no specific funding for this work.

For citation: Naumova L.A., Starodumova V.A. Extracellular matrix as a cellular information microenvironment. *Bulletin of Siberian Medicine.* 2020; 19 (4): 215–225. https://doi.org/10.20538/1682-0363-2020-4-215–225.

Экстрацеллюлярный матрикс как информационная клеточная микросреда

Наумова Л.А., Стародумова В.А.

Сургутский государственный университет (СурГУ)
Россия, 628412, Ханты-Мансийский автономный округ – Югра, г. Сургут, ул. Ленина, 1

РЕЗЮМЕ

Рассматриваются современные представления о роли экстрацеллюлярного матрикса (ЭЦМ) и клеточных элементов соединительной ткани (СТ) в тканевом гомеостазе в норме и патологии. Работы последних лет отражают смещение интересов при исследовании многих патологических процессов, в частности опухолевого роста, в область состояния ЭЦМ и клеток СТ, которые рассматриваются как активные компоненты ткани, определяющие процессы пролиферации, дифференцировки клеток, миграции и апоптоза. К важнейшим свойствам ЭЦМ, привлекающим внимание исследователей, относится механотрансдукция, ведущая к активации цитоскелетных механизмов и различных сигнальных клеточных путей; моделирование эффектов

✉ *Naumova Lyudmila A.,* e-mail: naumovala@yandex.ru.

цитокинов, факторов роста и гормонов; поддержание ниш стволовых клеток; влияние на возникновение и течение опухолевого процесса, в частности формирование опухолевого поля и преметастатических ниш, а также эпителио-мезенхимальный переход. Важным объектом исследования в настоящее время являются и клетки СТ, в частности фибробласты – основные продуценты компонентов ЭЦМ. Внимание исследователей привлекают, прежде всего, опухоль-ассоциированные фибробласты, фенотип которых формируется в ткани задолго до появления опухоли. Расширение представлений о роли ЭЦМ и клеточных элементов СТ в тканевом гомеостазе определяет новые подходы к лечению многих заболеваний – органных склерозов, опухолей и других.

Ключевые слова: экстрацеллюлярный матрикс, эпителио-стромальные отношения и канцерогенез, фибробласт, опухолевое поле, преметастатические ниши.

Конфликт интересов. Авторы декларируют отсутствие явных и потенциальных конфликтов интересов, связанных с публикацией настоящей статьи.

Источник финансирования. Авторы заявляют об отсутствии финансирования.

Для цитирования: Наумова Л.А., Стародумова В.А. Экстрацеллюлярный матрикс как информационная клеточная микросреда. *Бюллетень сибирской медицины.* 2020; 19 (4): 215–225. https://doi.org/10.20538/1682-0363-2020-4-215–225.

INTRODUCTION

In recent years, ideas about extracellular matrix (ECM), which was previously considered mainly as a physical scaffold for cells and tissues, have changed significantly. Numerous studies confirm that the ECM is a physiologically active component of living cells and tissues that is responsible for the most important processes in them. The ECM (fibrous structures and the ground substance) along with various cellular elements (fibroblasts, macrophages, lymphocytes, mast cells, endothelium of microvessels) belongs to the components of connective tissue (CT) that functions under normal and pathological conditions on the basis of the feedback and cooperative interaction of its cells with one another, ECM, blood cells, and organ parenchyma (or epithelium of the mucous membranes) [1–3].

Due to communication between cellular elements and their microenvironment, which evolves during the development of tissues, a unique molecular composition of the ECM is formed, which has a powerful effect on the biochemical and biophysical processes in cells through adhesive contacts between cells and ECM proteins and determines the epithelial-stromal interactions [4].

The most important properties of the ECM that are attracting the attention of researchers at present include the mechanotransduction, which leads to the activation of cytoskeletal mechanisms and various cell signaling pathways; modeling of the effects of various signaling molecules, which makes it possible to consider the CT system as the most important information environment of the body [2]; maintenance of stem cell niches; influence on the emergence and course of the tumor process, in particular, formation of a cancerized field and premetastatic niches; and the epithelial-mesenchymal transition (EMT). New knowledge about the role of the ECM and cell elements of CT in maintaining tissue homeostasis is essential for understanding the treatment strategy in many diseases, including the tumor process.

EXTRACELLULAR MATRIX AS A PHYSIOLOGICALLY ACTIVE COMPONENT OF THE LIVING TISSUE

ECM is a complex which has a three-dimensional composition represented by fibrous structures, or different types of collagens (28 types are currently known), and various proteins of the ground substance (glycoproteins and proteoglycans), which forms a cellular microenvironment determining intercellular and cell-matrix adhesive contacts and is responsible for cell polarity, phenotype, proliferation, migration, and intercellular communication processes [4–6].

ECM components are created and arranged by resident cells in accordance with the characteristics of the tissue. Thus, type I and V collagen predominate in the interstitial stroma and type IV collagen predominates in the basement membranes. The main producers of ECM components are fibroblasts, the most important CT cells [4, 7].

Being a network of proteins to which various signaling molecules can bind, the ECM controls the most

important processes in living cells and tissues through modeling the effects of growth factors (GF), cytokines (CK), and hormones. At the same time, the ECM is a highly dynamic structure; it is constantly remodeled by matrix metalloproteinases (MMPs) with participation of their tissue inhibitors and various GFs [4, 7, 8].

Most post-translational modifications in the ECM are not encoded by DNA but are the result of physiological and pathological processes in the tissues. Factors of post-translational changes in the ECM include changes of MMP activity (during inflammation, fibrosis), nitrosylation and glycosylation of the ECM proteins, as well as cross-linking and isomerization, which significantly change the viscosity, elasticity, and rigidity of the ECM. Post-translational remodeling of the ECM can be both a consequence of the pathological process, and a link in its pathogenesis, for example, in development of fibrosis and cancer. Therefore, the products of degradation of type II collagen, which are formed during rheumatic diseases and enter the systemic circulation, acquire the properties of signaling molecules [4], and endostatin that is produced from degradation of type XVIII collagen becomes the most powerful anti-angiogenic factor [7].

The main functional modifiers of the ECM include proteoglycans, or proteins containing glycosaminoglycans (GAGs), which are covalently linked to them. GAGs are long, negatively charged repeating disaccharide units that are represented by heparin sulfate, chondroitin/dermatan sulfate, hyaluronan, or keratan sulfate. Transmembrane proteoglycans (integrins, syndecans, discoidins), pericellular proteoglycans (perlecan, decorin, etc.), and extracellular proteoglycans (hyalectans and five classes of proteoglycans containing leucine, or small leucine-rich proteoglycans (SLRPs)) are distinguished [4].

Proteoglycans play a major role in transmission of signals from the ECM to the cell and are, in fact, cell receptors for the adhesive molecules of the ECM. They are responsible for the interaction of the cell with the microenvironment, or for intercellular and cell-matrix interactions, participate in tissue hydration and formation of collagen, modulate the effects of GF and CK, and influence cell proliferation, cell adhesion, reparative processes, and tumor growth [4, 7, 8].

Laminin and fibronectin are among the most important glycoproteins of the ECM. Laminin is a three-dimensional glycoprotein consisting of α, β, and γ-chains. It can form up to 60 unique laminins, but only 16 combinations are currently known. Due to integrin binding, laminins are able to create a dynamic connection between the cell and the ECM. Fibronectin as a multi-domain protein provides mechanosensitive interaction between the cell and the ECM and formation of the fibrillar network [4].

Thus, protein molecules of the ECM are considered as paracrine signaling molecules, which, along with GFs, CK, and hormones, have a profound effect on tissue homeostasis.

MECHANICAL PROPERTIES OF THE EXTRACELLULAR MATRIX

A cell cannot exist or undergo proliferation and differentiation without its mechanical environment. The cells assess the stiffness of their microenvironment using lamellopodia and universal transmembrane proteins of the ECM: integrins and syndecans. Integrins, which are the main mechanosensors of the cell, bind to fibronectin, laminin, and collagens of the ECM through various combinations of their heterodimers. On the other hand, they bind to the intracellular actin cytoskeleton through vinculin, talin, and other proteins, mechanically integrating extracellular and intracellular compartments. Recognition of the mechanical properties of the microenvironment by a cell and its reaction to the biophysical properties of the ECM are called mechanotransduction [4, 9].

Conformational changes in the integrin cytoplasmic domains lead to activation of several cell signaling pathways associated with the activity of kinases and phosphatases, in particular, mitogen-activated proteinkinases (MAPs) and guanosine triphosphate phosphatases (Rho GTPase). The association of syndecans with fibronectin leads to synergy of the effects of integrin and syndecan with respect to the activation of signaling cascades through focal adhesion kinase (FAK) and subsequent stabilization of the focal adhesion complex. Tissue cells have diverse receptors for various components of the ECM [4, 6, 10]. Thus, CD34 is a receptor for hyaluronan, 67kDa-laminin is the receptor for laminin, and discoidin domain receptor (DDRs) is the receptor for collagen [4, 5, 11].

The mechanosensitivity of adhesion complexes formed by integrins and syndecans is currently an area of active research, yet much remains to be learned about the pathways providing ECM-mediated cellular responses [4, 7, 9].

To transmit external information, biochemical and biophysical repeaters work together. It is assumed that simultaneous interaction of thousands of intregrin receptors with binding sites in networks of anisotropic ECM allows cells to have a topological description

of the chemical and mechanical properties of the microenvironment, with subsequent conversion of this information into intracellular signals generating appropriate cellular responses, such as position, cell polarity, differentiation, growth, protein synthesis, and regulation of energy processes [9]. One striking example of a mechanosensitive genetic regulator is a pair of transcriptional coactivators: the yes-associated protein (YAP) and the transcriptional coactivator with the PDZ-binding motif (TAZ). The role that YAP/TAZ (which are proto-oncogenic transcriptional regulators) play in cellular processes reflects the importance of mechanotransduction both in normal conditions (regenerative processes) and in pathology, in particular, in the development of fibrosis and cancer [4, 7, 12].

It was found that during cultivation, the differentiation of mesenchymal stem cells (MSCs) into osteocytes, myocytes, or neurons depends on the elasticity of collagen matrices, i.e., mechanotransduction. When blocking myosin II, a key molecule of mechanotransduction signaling pathways, MSCs become insensitive to ECM elasticity and its effect on differentiation processes. The composition of the ECM, or the adhesion gradient (haptotaxis), is a coordinated process between adhesion and anti-adhesion which significantly affects the rate of cell migration. Thus, pronounced migration of fibroblasts is observed during cultivation on fibronectin, and it is absent during cultivation on a mixture of fibronectin/laminin or laminin [4].

In fact, the ECM exhibits a dynamic plan of cell development, which is best reflected by the phenomena of branching, budding and formation of tubular structures during embryogenesis [4].

Therefore, spatial orientation of cells and tissue homeostasis as a whole are determined by mechanotransduction or biophysical signals from the ECM, which are transformed into biochemical signals regulating gene transcription in the cell. Dysregulation of ECM remodeling, in particular, during the formation of fibrosis, significantly changes the fate of cells and leads to development of various diseases, such as disorders of the cardiovascular and musculoskeletal systems and tumor growth [4, 8, 9, 11].

EXTRACELLULAR MATRIX IN THE MAINTENANCE OF STEM CELL NICHES

The most important property of ECM is maintenance of stem cell niches [4, 13]. A niche is formed by an ensemble of stromal cells and components of the ECM produced by them. A niche is characterized primarily by spatial organization and provides intercellular and cell-matrix interactions necessary for implementation of appropriate differentiation of embryonic stem cells, which give rise to various cell lines, or somatic stem cells, which are necessary for tissue repair [14].

Maintaining stem cell niches is crucial for normal functioning of the epithelial tissues which belong to the border tissues of the body and are characterized not only by high intensity of physiological regeneration, but also by high frequency of damage and intensive reparative regeneration [3, 13, 14]. At the same time, in tissues which cells were previously considered post-mitotic, a low level of cell renewal is maintained throughout life due to stem cells niches [14].

A niche is represented by stem cells, their progeny and specific niche ECM. The niche provides integration of various signals received by stem cells (autocrine, paracrine, systemic, and cell-matrix signals) through adhesion and mechanotransduction receptors, which allows to coordinate the responses of stem cells to changing tissue needs. Stromal cells, in particular fibroblasts, play an essential role in maintaining niches of resident stem cells through activation of Wnt, Notch, and BMP signaling pathways [13].

The methodology for preservation of stem cell niches proves that adhesion to the basement membrane alone is insufficient for their maintenance; the proliferative capability of cells is related to their spatial location and the influence of mechanical force, in particular rotational force which ensures the mitotic spindle orientation during the final phase of the cell cycle [15]. The function of many stem cells decreases during life, which may underlie aging of the body [14], as well as formation of various types of pathology. Thus, it was found that the development of habitual miscarriages is largely associated with aging of endometrial stem cell niches [16].

Progress in understanding the principles of stem cell niche existence (identification of niche factors and signaling pathways) can be of great importance for regenerative medicine and tissue engineering [13, 14]. Although some intercellular and cell-matrix interactions in the niches of resident stem cells are well-studied (such as stem cell niches of the skin, intestines, hair follicles, mammary gland, and nerve trunks), many components of stem cell niches are still understudied. [14]. So, the question of cell dedifferentiation or regress of differentiated cells to a less differentiated state within their cell line with loss of stem cell niches in this tissue for implementation of the reparative processes (in particular, in the gastric mucosa) remains relevant [13].

EXTRACELLULAR MATRIX AND EPITHELIAL-MESENCHYMAL TRANSITION

The most striking example of the influence of the physicochemical properties of ECM on the phenotype and behavior of cells is the epithelial-mesenchymal transition (EMT), or the trans-differentiation phenomenon, when epithelial cells acquire a mobile fibroblastoid/ mesenchymal phenotype. The EMT program, along with the endothelial-mesenchymal transition (EndMT), revealed commonality of mechanisms working both in embryogenesis and wound healing, and in carcinogenesis, in particular during the formation of cancer stem cells and at the stage of invasive tumor growth [8, 17–19].

Activation and expression of transcription factors causing EMT occur through various signaling pathways, such as the Wnt-pathway, Sonic Hedgehog (Shh), Notch, and others, which can be triggered by different GFs (transforming growth factor beta (TGFβ), bone morphogenetic protein (BMP), epidermal growth factor (EGF), fibroblast growth factor (FGF), insulin-like growth factor 1 (IGF1), hepatocyte growth factor (HGF), platelet growth factor (PDGF)), signals from the ECM, and effects of hypoxia. Cells can integrate certain signals differently or respond to extracellular molecules with different sensitivity, depending on their state and microenvironment [18].

EMT is associated with loss of the apical-basal polarity in epithelial cells, tight intercellular contacts involving adhesive molecules (claudins, occludin, E-cadherin), which ensure the formation of an epithelial layer that is located on the basement membrane normally represented by type IV collagen and laminin, as well as by loss of expression of epithelial markers – cytokeratins. Epithelial cells acquire a fibroblastoid or mesenchymal phenotype due to the loss of intercellular contacts and a change in cell polarity. The ECM composition changes in parallel; fibronectin, N-cadherin, type I and III collagens begin to prevail, and the cells that have already changed their phenotype begin to express mesenchymal markers, such as vimentin, fibroblast-specific protein-1 (FSP-1), and α-smooth muscle actin (α-SMA). The acquired mobile mesenchymal phenotype allows the cells to invade through the basal layer with subsequent migration along the secreted fibronectin matrix [17, 18].

It is possible that EMT and reverse mesenchymal-epithelial transition (MET) exist as binary states of the cell. The flexible nature of the epithelial/mesenchymal state makes this process difficult to observe [18].

During EMT, the amount of type I and III collagen drastically increases in the ECM. Placing epithelial cells on matrices containing these types of collagen can induce EMT through various signaling pathways. The pathways of signal transmission also induce the expression of genes encoding MMP-2 and MMP-9 which cleave type IV collagen in the basal plate, facilitating tumor invasion [8, 18, 19].

As the composition of the ECM changes, the number of integrins on the cell surface increases, which contributes to the progression of EMT. Binding of latent TGFβ to integrins aVb6 and aVb8 induces proteolytic release of latent associated peptide (LAP) and activation of TGFβ. In response to TGFβ signaling, synthesis of type I collagen and fibronectin increases, which makes an additional contribution to EMT. Therefore, local accumulation of TGFβ is associated with the risk of initiating tumor growth through the development of EMT, while a decrease in the expression of TGFβ weakens EMT, invasion and tumor transformation itself.

Type I collagen, in turn, causes phosphorylation of IkB (inhibitor of kB) via integrin-linked kinase (ILK), leading to an increase in the amount of NF-κB localized in the nuclear region (kappa B nuclear transcription factor), which stimulates expression of Snail1 and lymphoid enhancer-binding factor-1 (LEF1) and induces EMT. An increase in the amount of type I collagen also activates the JNK pathway, the pharmacological inhibition of which cancels collagen-mediated migration and metastasis of breast cancer cells. The interaction of integrin b1 subunits with type I collagen in ECM correlates with direct suppression of E-cadherin and induction of N-cadherin [18, 19]. ECM remodeling not only changes the types of matrix proteins that interact with the cell membrane, but also affects the environment of soluble cytokines that promote EMT [18].

EMT precedes the emergence of stem cell properties in tumor cells [17, 20], which represent a small part of tumor cells capable of self-renewing, generating heterogeneity of the tumor cell population, metastasizing [21–23], and generating secondary tumors [24].

THE IMPORTANCE OF DYSREGULATION OF EXTRACELLULAR MATRIX MOLECULES IN THE DEVELOPMENT AND PROGRESSION OF CANCER

Modern ideas about carcinogenesis are shifting towards the crucial role of the ECM in this process, forming the cellular microenvironment and actively

regulating cell proliferation, adhesion, migration, and apoptosis [4, 18, 25–27]. The effect of ECM on cell differentiation has been proven, in particular, by return of the breast tumor cells to a normal phenotype during their culture on a basement membrane created on the basis of 3D substrates coated with antibodies blocking β1-integrin [4].

The main components of ECM interacting with tumor cells include fibronectin, laminin, collagen, proteoglycans, and glycosaminoglycans, in particular hyaluronic acid (HA). HA plays a crucial role in determining the compression properties of most tissues, participates in constant remodeling of ECM during embryogenesis and repair through interaction with cells of the immune system, is involved in tumor angiogenesis, and is an important modulator of the behavior of various cells in the tumor microenvironment [27]. HA is both a signal inducer for EMT and a substrate for cell migration; therefore, a change in the concentration of HA in some tissues (breast, prostate gland) is considered as a predictor of malignancy [4, 8, 27].

The formation of the HA-CD44 complex causes activation of the RhoGTPase signaling, leading to structural changes in actin assembly, cytoskeleton reorganization, transcription activation, growth of tumor cells, their migration and invasion, and disruption of the endothelial barrier. Many exact mechanisms of the effect of HA on immune cells are not known yet, but this interaction can both stimulate tumor angiogenesis and inhibit tumor growth through the induction of active immunity. One of the effects of the HA-CD44 signaling is involvement of β-catenin, the main protein of the Wnt-signaling pathway that controls cell polarity, proliferation, and a number of angiogenesis factors, such as VEGF-A97 and Il-898. The development of anti-angiogenic tumor therapy is based on the study of these mechanisms; moreover, such therapy is more effective in combination with α-interferon and chemical inhibitors of HA synthesis [27].

The most important role in tumor-stroma interaction is attributed to cancer-associated fibroblasts (CAFs), which are a heterogeneous cell population formed from various cells, including resident stromal fibroblasts, endothelial and smooth muscle cells, adipocytes, and vascular pericytes [28–30]. It is possible that the source of CAFs can also be epithelial cells that underwent EMT [30]. An important role in the formation of CAFs is assigned to bone marrow stromal cells recruited into the tumor microenvironment under the effect of chemokines secreted by tumor cells (CCL12, CCL16, etc.) and giving rise to MSCs [28, 29, 31].

Cross-talks between tumor epithelial cells and CAFs are formed by means of exosomes, extracellular vesicles from 30 to 100 nm in diameter, which are released by cells into the intercellular space and transmit information due to diverse biomolecules contained in them, such as proteins, DNA fragments, lipids, various GFs, miRNAs, and proteolytic enzymes [8, 17, 30, 32]. Exosome exchange determines the change in the spectrum of genes expressed by fibroblasts, the VCAM-1 integrin α4 signaling pathway is activated, the level of fibronectin in the ECM is increased, and the expression of VCAM-1 receptors in endotheliocytes is enhanced [17]. CAFs begin to secrete various CKs (TGFβ, CCL-10, CCL-5, etc.) that model the behavior of both immune cells (macrophages, lymphocytes) and tumors [17, 30, 33]. For example, CD9 positive fibroblast exosomes in scirrhous gastric cancer stimulate the migration and invasion of tumor cells associated with increased expression of MMP-2 [32].

Thus, CAFs begin to play an active role in tumor progression and metastasis, causing loss of E-cadherin expression and development of EMT [34]. During angiogenesis, formation of the immune status of the tumor microenvironment, and development of drug resistance, they become the main cells in the tumor stroma and can be important therapeutic targets [29–31, 33].

Moreover, in recent years it has been shown that changes in the stroma and the emergence of a CAFs-like fibroblast phenotype can precede the formation of a tumor, or the appearance of malignant epithelial cells. CAFs-secreted factors increase proliferative activity and mutagenesis in epithelial cells, activate angiogenesis, disrupt intercellular adhesion contacts, and suppress apoptosis, initiating a malignant phenotype in morphologically and genotypically normal epithelial cells [30].

It was found that CAFs-like fibroblasts are characterized by a decrease in the expression of CD36 (glycoprotein expressed on the surface of most cells) associated with high production of collagen and fibronectin [30]. Such CAFs-like fibroblasts were obtained, in particular, from healthy women with increased mammographic density; compared with fibroblasts obtained from women with low breast density, they were characterized by a pronounced ability to form desmoplasia [35]. With precancerous changes in the stroma, a decrease in the expression of CD36 and impairment of their functional state are observed in different stromal cells (adipocytes, fibroblasts, en-

dotheliocytes, immune cells). Thus, suppression of CD36 in endotheliocytes is accompanied by an increase in the angiogenesis; in preadipocytes, suppression of CD36 is associated with impairment of their differentiation into adipocytes; and in immune cells, it is accompanied by an increase in the population of M2 macrophages [30].

Repression of CD36 is associated with epigenetic changes, such as DNA methylation, modification of histones and nucleosome structure, or changes in miRNA expression, leading to a change in gene expression typical of CAFs [30, 36]. The phenotype of CAFs is associated with dysregulation of various signaling pathways, such as TGFβ, BMP, Wnt, Sonic hedgehog (Shh), PDGF, and some others [30].

Immune modulation and the development of inflammation caused by CAFs are considered as one of the mechanisms contributing to the growth and metastasis of the tumor. The immunosuppressive effect of CAFs in the tumor microenvironment is mediated by the activation of glycoprotein Chitinase 3Like1 (Chi3l1) in them, which determines the ability of fibroblasts to control the behavior of the tumor and its pro-inflammatory and immune environment and promotes tumor growth and a shift in the balance of the immune system to type 2 immunity [33].

CAFs can be the main cellular component of the tumor stroma and the main source of connective tissue components in ECM and various classes of proteolytic enzymes. Thus, in breast and pancreatic cancer, CAFs can make up to 80% of the tumor mass, causing pronounced desmoplasia [8, 30].

With an increase in the mass of tumor cells, their tissue microenvironment begins to experience the so-called solid stress, which causes compression of the blood and lymph vessels, deformation of healthy tissues and an increase in its resistance, which, in turn, causes solid stress in the tumor cells, leading to a change in gene expression and an increase in the rate of tumor cell proliferation and migration. The microvascular compression in the tumor area also results in a decrease in the effectiveness of chemotherapy and immunotherapy [4, 8].

Severe desmoplasia in pancreatic cancer is associated with the activation of stellate myofibroblast-like cells accompanied by an increase in the mechanical density of the microenvironment, that reflects the formation of positive feedback. Lysyl oxidase (LOX) secreted by tumor cells is responsible for cross-linking of collagen and elastin and an increase in the ECM rigidity, which leads to activation of integrins and a rise in Rho-generated tension in the cell and its facilitated movement along thickened and straightened collagen.

Inactivation of the ability of the stellate cells to remodel the ECM prevents mechanical release of TGFβ from its latent form. Persistent tumor rigidity induces high expression of TGFβ and EMT. Solid stress enhances hypoxia in the tumor cells, their proliferative activity, and resistance to chemotherapy. Inactivation of mechanosensory and remodeling ability of the stellate cells may be one of the areas in the treatment strategy. As such, all-trans retinoic acid suppresses the mechanosensitivity of stellate cells by decreasing the contractility of actomyosin (MLC-2), which disables the positive feedback between the increased ECM rigidity and stellate cell activation, resulting in reduced fibrosis and invasiveness of tumor cells [4].

The modulating effect on the tumor microenvironment is exerted by various ECM components and stromal cells (macrophages, dendritic cells, various populations of lymphocytes). So, an increase in the number of cancer-associated macrophages in the tumor microenvironment leads to an increase of the synthesis of type I, VI, and XIV collagen by fibroblasts. By modeling the activity of MMPs, it is accompanied by deposition, cross-linking, and straightening of collagen fibers, which facilitates the invasion of tumor cells [37]. Mast cells also affect remodeling of ECM, invasion and metastasis of tumor cells, and angiogenesis via neutral proteases (chymases, tryptases) secreted by them, which change the activity of MMPs, secretion of histamine, heparin, various growth factors (VEGF, FGF, TGFβ), tumor necrosis factor (TNF-α), and individual interleukins (IL-1, IL-6, IL-8) [38].

Therefore, tumor cells change the microenvironment in which they grow, interacting with cells of CT and ECM, and vice versa, which can cause both favorable conditions for tumor growth, invasion, and metastasis, and unfavorable conditions, in particular through activation of the immunity. Findings of recent studies drastically contrast with historically established ideas about the initiation of tumor growth in epithelial cells due to their mutations. In some types of cancer, the stroma goes beyond the role of a mediator in the tumor process. The changes in the signal and transcriptional program of stromal cells can precede (or act independently of) changes in epithelial cells and actually act as a driver of the tumor process [25, 27, 30, 35], that dramatically shifts the focus of the treatment strategy towards returning the original phenotype to the stromal elements. Such therapy can be aimed at removing CAFs by interfering with their

survival or normalizing their phenotype through pro-tumorigenic signal management [20, 30].

EXTRACELLULAR MATRIX AND FIELD CANCERIZATION

The concept of field cancerization formulated by R. Willis back in 1953 and actively developed at the present time is closely related with the system of CT, its cellular composition, the nature of the ECM, the spectrum of signaling molecules, and the activity of MMPs [39–43]. The main provisions of the concept are well confirmed in practice and include non-instantaneity of transformation; mosaic histological picture; tumor growth both due to transformation of cells entering the field zone and tumor proliferation; relapses caused not so much by non-radical treatment, but by maintaining this field or forming a new one with the emergence of a tumor according to the same laws [39, 44].

Zones of dysplasia and formation of blood vessels are considered as the first signs of field cancerization, while the size of the field can occupy both a part of the organ and extend to the entire organ. According to some authors, the field is associated with genetic and epigenetic lesions of the epithelium bordering the tumor growth zone [45–47], while others believe that the formation of the field is associated with the expression patterns of proteases and their inhibitors, inflammatory mediators, and immune signaling molecules. Big importance is attributed to the present macrophage line, accumulation of Treg lymphocytes [40–43], and the metabolic and hormonal status in the peritumoral zone [48].

The theory of field cancerization is constantly revised and updated and generally based on complex interaction between stromal and tumor cells by means of various signaling molecules changing the microenvironment of the tumor (GFs, CK, chemokines). Recently, great importance has been attributed to impairment of the regulatory role of miRNAs involved in posttranscriptional regulation of genes [34, 43]. So, in gastric cancer, an increase in the activity of some miRNAs (hsa-miR-10a, hsa-miR-483; hsa-miR-664a), which regulate cancer suppressor genes APC, RUNX1, PTEN, TP53, etc., is observed, which, in turn, is a consequence of chronic inflammation developing in the peritumoral zone [47].

A manifestation of field cancerization is evolution of somatic cells, as a result of which they acquire individual phenotypic characteristics (focal hyperplasia, metaplasia, dysplasia), which do not yet fully correspond to the tumor phenotype. The basis of this evolution is pro-oncogenic mutations which determine the formation of a mutant clone growing with formation of fields of cells predisposed to progression of changes to tumor cells; the cellular microenvironment plays a crucial role [43, 46]. In this context, precancerous diseases characterized by an increased risk of developing a tumor are an example of field cancerization [43, 46]. This is best illustrated by such precancerous diseases as Barrett's esophagus, prostatic intraepithelial neoplasia, and ductal carcinoma in situ in the breast, reflecting the growth of mutant cell lines evolving along the way to cancer [43].

An indirect indicator of field evolution or a high risk of tumor transformation is genetic or clonal diversity of cells within the field. The existence of field cancerization raises a number of practically important questions. Is medical modification of field cancerization possible, for example, the use of non-steroidal anti-inflammatory drugs that reduce the frequency of mutations in Barrett's esophagus or aspirin and 5-aminosalicylates in inflammatory bowel diseases, to prevent colorectal cancer? In addition, the effectiveness of treatment within the tumor field in precancerous diseases has been proven with respect to squamous cell carcinoma of the skin [46]. Is it necessary to remove the tumor field, which causes the risk of metachronous tumors, simultaneously with the tumor? Besides, the question of methods for visualizing the field (dysplastic lesions) during surgery also arises [43].

EXTRACELLULAR MATRIX IN THE FORMATION OF PREMETASTATIC NICHES

In recent years, ideas about the interaction between the tumor and the ECM during its progression and metastasis have significantly evolved. It has been shown that primary tumors have the ability to induce at a distance such microenvironment that will support the growth of tumor cells that have entered it. This new microenvironment formed away from the primary tumor site is called a premetastatic niche (PMN) [4, 49, 50]. Tumor cells entering the bloodstream from the primary focus die in large numbers, and only a part of them are able to survive and progress, being in the PMN [8, 49].

Tumor-derived secreted factors (TDSFs) and tumor exosomes, as well as stromal, immune cells and bone marrow-derived cells, through complex intercellular communication, determine the development of processes in niches, such as matrix remodeling, angiogenesis, immunosuppression, organotropism, and the

nature of biomarkers expressed by niche cells [4, 49].

It is assumed that remodeling of the ECM (accumulation of fibronectin, cross-linking of collagen using LOX) in the PMN occurs before tumor cells from the primary focus migrate into them, and then tumor cells that enter the vessels accumulate in the niches, that are characterized by higher tissue rigidity (this process is known as durotaxis) [4, 49]. An important role in ECM modification also belongs to prolyl 4-hydroxylase (P4HA), the expression of which increases under the effect of hypoxia and / or TGFβ and which causes deposition of high-stability collagen.

Fibronectin and hyaluronan in the ECM determine directional migration and increase the metabolic activity in the tumor cells. Fibronectin also promotes recruitment of bone marrow monocytes that turn into macrophages expressing VEGFR1. Neutrophils appearing in PMN due to leukotriene signaling (in particular, in lung PMN) also participate in the formation of an immunosuppressive environment by inhibiting CD8 + T-lymphocytes [49].

Many mechanisms of PMN formation are still not clear, in particular, the mechanism of metastatic tropism to certain organs, although recent studies have shown that tumor exosomes have specific integrin expression patterns that determine organotropism. Exosome proteomics revealed that oc6β4 and α6β1 exosomal integrins are closely associated with lung metastasis, and αvβ5 exosomal integrins are closely associated with liver metastasis. Targeted removal of these integrins reduces the absorption of exosomes by resident tissue cells and decreases metastasis to the lungs and liver [4].

It is assumed that cancer treatment can become more effective when it is targeted to various mechanisms of metastasis, in particular to the exosome-mediated mechanism. Exosomes can probably be used as a means of drug delivery to tumor cells, but many functions and mechanisms of exosome exchange have to be studied [4, 49, 50].

CONCLUSION

Thus, the works of recent years reflect a shift in the study of many pathological processes, in particular, tumor growth, to the area of the ECM state and CT cellular elements. The extracellular matrix and CT cells, primarily fibroblasts, are considered as active tissue components that determine cell proliferation, differentiation, migration, and apoptosis, as well as progression and metastasis of tumors, and initiation of tumor growth.

In recent years, the tissue (as well as its constituent elements) has been considered as a integrated structure, which is more than a simple sum of its constituents. The unique properties of the tissue arise from the collective behavior of its constituent components, and the architectural (structural), temporal, and dynamic aspects of tissue existence are integrated through feedback loops, which is clearly reflected in the formation of a cancerized field [30]. This understanding of the tissue, in particular cell-matrix interactions, defines a completely new treatment strategy in many diseases, including cancer.

REFERENCES

1. Shekhter A.B., Serov V.V. Inflammation, adaptive regeneration and dysregeneration (analysis of intercellular interactions). *Archives of Pathology.* 1991; 7: 7–14 (in Russ.).
2. Kaznacheev V.P., Subbotin M.Ya. Cases from the theory of general pathology. 2nd edition , 2006: 256 (in Russ.).
3. Naumova L.A. Pathological aspects of atrophic lesion in the gastric mucosa: features of clinical, structural, and functional manifestations in different morphogenetic types of atrophy (in Russ.). URL: https://surgumed.elpub.ru/jour/article/view/176?locale=ru_RU.
4. Walker C., Mojares E., Hernández A Del Río. Role of extracellular matrix in development and cancer progression. *Int. J. Mol. Sci*. 2018; 19 (10). DOI: 10.3390/ijms19103028.
5. Kaushik S., Pickup M.W., Weaver V.M. From transformation to metastasis: deconstructing the extracellular matrix in breast cancer. *Cancer Metastasis Rev*. 2016; 35 (4): 655–667. DOI: 10.1007/s10555-016-9650-0.
6. Sun Zhiqi, Guo Shengzhen S., Fässler R. Integrin-mediated mechanotransduction. *JBC*. 2016; 215 (4): 445–456. DOI: 10.1083/jcb.201609037.
7. Karsdal M.A., Nielsen M.J., Sand J.M., Henriksen K., Genovese F., Bay-Jensen A.C., Smith V., Adamkewicz J.I., Christiansen C., Leeming D.J. Extracellular matrix remodeling: the common denominator in connective tissue diseases. Possibilities for evaluation and current understanding of the matrix as more than a passive architecture, but a key player in tissue failure. *Assay Drug Dev. Technol.* 2013; 11 (2): 70–92. DOI: 10.1089/adt.2012.474.
8. Houg D.S., Bijlsma M.F. The hepatic pre-metastatic niche in pancreatic ductal adenocarcinoma. *Mol. Cancer*. 2018; 17 (1): 95. DOI: 10.1186/s12943-018-0842-9.
9. Humphries J.D., Chastney M.R., Askari J.A., Humphries M.J. Signal transduction via integrin adhesion complexes. *Cur*. *Opin. Cell Biol*. 2019; 56: 14–21. DOI: 10.1016/j.ceb.2018.08.004.
10. Sandbo N., Smolyaninova L.V., Orlov S.N., Dulin N.O. Regulation of differentiation and functioning of myofibroblasts by the cytoskeleton signaling system. *Advances in Biological Chemistry*. 2016; 56 (13): 259–282 (in Russ.).
11. Kechagia J.Z., Ivaska J., Roca-Cusachs P. Integrins as biomechanical sensors of the microenvironment. *Nat. Rev. Mol. Cell Biol*. 2019; 20 (8): 457–473. DOI: 10.1038/s41580-019-0134-2.

11. Habbig S., Bartram M.P., Müller R.U., Schwarz R., Andriopoulos N., Chen S., Sägmüller J.G., Hoehne M., Burst V., Liebau M.C., Reinhardt H.C., Benzing T., Schermer B. NPHP4, a cilia-associated protein, negatively regulates the Hippo pathway. *JBC*. 2011; 193 (4): 633–642. DOI: 10.1083/jcb.201009069.
12. Chacón-Martínez C.A., Koester J., Wickström S.A. Signaling in the stem cell niche: regulating cell fate, function and plasticity. *The Company of Biologists*. 2018; 145 (15). DOI: 10.1242/dev.165399.
13. Pennings S., Liu K.J., Qian H. The stem cell niche: interactions between stem cells and their environment. *Stem Cells Int*. 2018; 1–2: 1–2. DOI: 10.1155/2018/4879379.
14. Miller C., Crampin E., Osborne J. Maintaining the stem cell niche in multicellular models of epithelia. arXiv:1811.10781v1 [q-bio.TO] 27. 2018. https://arxiv.org/pdf/1811.10781.
15. Lucas B., Pérez L.M., Gálvez B.G. Importance and regulation of adult stem cell migration. *J. Cell Mol. Med*. 2018; 22 (2): 746–754. DOI: 10.1111/jcmm.13422.
16. Semba S., Kodama Y., Ohnuma K., Mizuuchi E., Masuda R., Yashiro M., Hirakavwa K., Yokozaki H. Direct cancer-stromal interaction increases fibroblast proliferation and enhances invasive properties of scirrhous-type gastric carcinoma cells. *Br. J. Cancer*. 2009; 101 (8): 1365–1373. DOI: 10.1038/sj.bjc.6605309.
17. Gonzalez D.M., Medici D. Signaling mechanisms of the epithelial-mesenchymal transition. *Science Signaling.* 2014; 7 (344): re8. DOI: 10.1126/scisignal.2005189.
18. Ye X., Weinberg R.A. Epithelial-mesenchymal plasticity: a central regulator of cancer progression. *Trends Cell Biol*. 2015; 25 (11): 675–686. DOI: 10.1016/j.tcb.2015.07.012.
19. Li H., Xu F., Li S., Zhong A., Meng X., Lai M. The tumor microenvironment: an irreplaceable element of tumor budding and epithelial-mesenchymal transition-mediated cancer metastasis. *Cell Adh. Migr*. 2016; 10 (4): 434–446. DOI: 10.1080/19336918.2015.1129481.
20. Chen C., Zimmermann M., Tinhofer I., Kaufmann A.M., Albers A.E. Epithelial-to-mesenchymal transition and cancer stem(-like) cells in head and neck squamous cell carcinoma. *Cancer Lett*. 2013; 338 (1): 47–56. DOI: 10.1016/j.canlet.2012.06.013.
21. Hao J., Zhang Y., Deng M., Ye R., Zhao S., Wang Y., Li J., Zhao Z. MicroRNA control of epithelial-mesenchymal transition in cancer stem cells. *Int. J. Cancer*. 2014; 135 (5): 1019–1027. DOI: 10.1002/ijc.28761.
22. Liu X., Fan D. The epithelial-mesenchymal transition and cancer stem cells: functional and mechanistic links. *Current Pharmaceutical Design*. 2015; 21 (10): 1279–1291. DOI: 10.2174/1381612821666141211115611.
23. Hollier B.G., Evans K., Mani S.A. The epithelial-to-mesenchymal transition and cancer stem cells: a coalition against cancer therapies. *J. Mammary Gland Biol. Neoplasia*. 2009; 14 (1): 29–43. DOI: 10.1007/s10911-009-9110-3.
24. Förster S., Gretschel S., Jöns T., Yashiro M., Kemmner W. THBS4, a novel stromal molecule of diffuse-type gastric adenocarcinomas, identified by transcriptome-wide expression profiling. *Mod. Pathol*. 2011; 24 (10): 1390–1403. DOI: 10.1038/modpathol.2011.99.
25. West J., Bianconi G., Severini S., Teschendorff A.E. Differential network entropy reveals cancer system hallmarks. *Scientific Reports*. 2012; 802. DOI: 10.1038/srep00802.
26. Spinelli F.M., Vitale D.L., Demarchi G., Cristina C., Alaniz L. The immunological effect of hyaluronan in tumor angiogenesis. *Clin. Transl. Immunology*. 2015; 4 (12): 1–9. DOI: 10.1038/cti.2015.35.
27. Augsten M. Cancer-associated fibroblasts as another polarized cell type of the tumor microenvironment. *Front Oncol*. 2014; 4: 62. DOI: 10.3389/fonc.2014.00062.
28. Kasashima H., Yashiro M., Nakamae H., Masuda G., Kinoshita H., Morisaki T., Fukuoka T., Hasegawa T., Sakurai K., Toyokawa T., Kubo N., Tanaka H., Muguruma K., Ohira M., Nakane T., Hino M., Hirakawa K. Bone marrow-derived stromal cells are associated with gastric cancer progression. *Br. J. Cancer*. 2015; 113 (3): 443–452. DOI: 10.1038/bjc.2015.236.
29. Gascard Ph., Tlsty Th.D. Carcinoma-associated fibroblasts: orchestrating the composition of malignancy. *Genes Dev*. 2016; 30 (9): 1002–1019. DOI: 10.1101/gad.279737.116.
30. Shi Y., Du L., Wang Y. Tumor-assiciated mesenchymal stem/stromal cell: emerging therapeutic targets. *Nat. Rev. Drug Discov*. 2017; 16: 35–52. DOI: 10.1038/nrd.2016.193.
31. Miki D., Zhu P., Zhang W., Mao Y., Feng Zh., Huang H., Zhang H., Li Y., Liu R., Zhang H., Qi Y., Zhu J.-K. Efficient generation of diRNAs requires components in the posttranscriptional gene-silencing pathway. *Scientific Reports*. 2017; 7: 301. DOI: 10.1038/s41598-017-00374-7.
32. Cohen N., Shani O., Raz Y., Sharon Y., Hoffman D., Abramovitz L., Erez N. Fibroblast drive an immunosuppressive and growth-promoting microenvironment in breast cancer via secretion of chitinase 3-like 1. *Oncogene*. 2017; 36 (31): 4457–4468. DOI: 10.1038/onc.2017.65.
33. Dhanota N., Arora S.K. Cancer stem cells: a cause or a consequence of field cancerization. *International Journal of Translational Research*. 2018; 1 (1): 14–16.
34. De Filippis R.A., Fordyce C., Patten K., Chang H., Zhao J., Fontenay G.V., Kerlikowske K., Parvin B., Tlsty Th. D. stress signaling from human mammary epithelial cells contributes to phenotypes of mammographic density. *Cancer Res*. 2014; 74 (18): 5032–5044. DOI: 10.1158/0008-5472.CAN-13-3390.
35. Kang N., Shah V.H., Urrutia R. Membrane-to-nucleus signals and epigenetic mechanisms for myofibroblastic activation and desmoplastic stroma: potential therapeutic targets for liver metastasis? *Mol. Cancer Res*. 2015; 13 (4): 604–612. DOI: 10.1158/1541-7786. MCR-14-0542.
36. Afik R., Zigmond E., Vugman M., Klepfish M., Shimshoni E., Pasmanik-Chor M., Shenoy A., Bassat E., Halpern Z., Geiger T., Sagi I., Varol C. Tumor macrophages are pivotal constructors of tumor collagenous matrix. *J. Exp. Med*. 2016; 213 (11): 2315–2331. DOI: 10.1084/jem.20151193.
37. Lazarev A.F., Bobrov I.P., Cherdantseva T.M., Klimachev V.V., Bryukhanov V.M., Avdalyan A.M., Lubennikov V.A., Gervald V.Ya. Mast cells and tumor growth. *Siberian Journal of Oncology*. 2011; 4 (46): 59–63 (in Russ.).
38. Rykov V.A. Field cancerization. *Archives of Pathology*. 1981; 10: 67–69 (in Russ.).
39. Stearman R., Dwyer-Nield L., Grady M.C., Malkinson A.M., Yeraci M.W. A macrophage gene expression signature defines

a field effect in the lung tumor microenvironment. *Cancer Res.* 2008; 68 (1): 34–43. DOI: 10.1158/0008-5472.CAN-07-0988.
40. Curtius K., Wright N.A., Graham T.A. An evolutionary perspective on field cancerization. *Nat. Rev. Cancer*. 2017; 18 (1): 19–32. DOI: 10.1038/nrc.2017.102.
41. Braakhuis B.J.M., Brakenhoff R.H., Leemans C.R. Second field tumor: a new opportunity for cancer preventing? *The Oncologist*. 2005; 10 (7): 493–500. DOI: 10.1634/theoncologist.10-7-493 theoncologist.alphamedpress.org/content/10/7/493.
42. Redente E.F., Orlicky D.J., Bouchard R.J. Tumour signaling to the bone marrow changes to the phenotype of monocytes and pulmonary macrophages during urethane-induced primary lung tumourogenesis in A/J mice. *Am. J. Pathol*. 2007; 170 (2): 693–708. DOI: 10.2353/ajpath.2007.060566.
43. Frank G.A. Cancer relapse: notion, essence, terminology. *Archives of Pathology*. 2006; 3: 23–26 (in Russ.).
44. Tabor M.P., Brakenhoff R.H., Ruijter-Schippers H.J., van der Wal J.E. et al. Multiple head and neck tumor frequently original from a single preneoplastic lesion. *Am. J. Pathol*. 2002; 161: 105–106. DOI: 10.1016/S0002-9440(10)64266-6.
45. Christensen S.R. Recent advances in field cancerization and management of multiple cutaneous squamous cell carcinomas. *Journal List*. *F1000Research.* 2018; 7: 690. DOI: 10.12688/f1000research.12837.1.
46. Pereira A.L., Magalhães L., Moreira F.C., Reis-das-Mercês L., Vidal A.F., Ribeiro-Dos-Santos A.M., Demachki S., Anaissi A.K.M., Burbano R.M.R., Albuquerque P., Dos Santos S.E.B., de Assumpção P.P., Ribeiro-Dos-Santos Â.K.C. Epigenetic field cancerization in gastric cancer: microRNAs as promising biomarkers. *Journal of Cancer*. 2019; 10 (6): 1560–1569. DOI: 10.7150/jca.27457.
47. Kit O.I., Frantsiyants E.M., Gevorkyan Yu.A., Komarova E.F., Salnikova M.M., Maleyko M.L. The state of tumor tissue sterois homeostasis in different morphological types of gastric cancer.. *Palliative Medicine and Rehabilitation.* 2011; 4: 35–38 (in Russ.).
48. Doglioni G., Parik S., Fendt S.M. Interactions in the (pre)metastatic niche support metastasis formation. *Frontiers in Oncology*. 2019; 9: 219. DOI: 10.3389/fonc.2019.00219.
49. Guo Ya., Ji X., Liu J., Fan D., Zhou Q., Chen Ch., Wang W., Wang G., Wang H., Yuan W., Ji Zh., Sun Zh. Effects of exosomes on pre-metastatic niche formation in tumors. *Mol. Cancer.* 2019; 18 (39): 39. DOI: 10.1186/s12943-019-0995-1.

Authors information

Naumova Lyudmila A., Dr. Sci. (Med.), Professor, Department of Pathological Physiology and General Pathology, Surgut State University, Khanty-Mansiysk Autonomous Area – Yugra, Russian Federation. ORCID 0000-0003-1145-3710.

Starodumova Valentina A., Post-Graduate Student, Department of Pathological Physiology and General Pathology, Surgut State University, Khanty-Mansiysk Autonomous Area – Yugra, Russian Federation. ORCID 0000-0001-8362-0608.

(✉) **Naumova Lyudmila A.,** e-mail: naumovala@yandex.ru.

Received 07.11.2019
Accepted 30.04.2020

УДК 616.329-018.7-06-006.66
https://doi.org/10.20538/1682-0363-2020-4-226-234

Barrett's esophagus and esophageal adenocarcinoma: biomarkers of proliferation, apoptosis, autophagy and angiogenesis

Petenyova E.S.[1], Salmina A.B.[2], Berdnikov S.I.[1], Salmin V.V.[2], Abramov V.G.[1], Medvedeva N.N.[2], Semichev E.V.[1]

[1] *Federal Siberian Research Clinical Center*
26, Kolomenskaya Str., Krasnoyarsk, 660037, Russian Federation

[2] *Krasnoyarsk State Medical University named after Prof. V.F. Voino-Yasenetsky*
1, Partizana Zheleznyaka Str., Krasnoyarsk, 660022, Russian Federation

ABSRACT

Aim. To analyze all known markers of proliferation, apoptosis, autophagy and angiogenesis in the pathogenesis of Barrett's esophagus and esophageal adenocarcinoma with the purpose of improvement of diagnostics and treatment quality.

Materials and methods. Analysis of the available scientific sources by Russian and foreign authors.

Results. Data on all the known markers has been structured and is supposed to be integrated into clinical practice in the diagnosis and treatment of Barrett's esophagus and esophageal adenocarcinoma at various stages of disease development

Key words: Barrett's esophagus, esophageal adenocarcinoma, proliferation, apoptosis, autophagy, angiogenesis, markers.

Conflict of interest. The authors declare no obvious or potential conflicts of interest related to the publication of this article.

Source of financing. The authors received no specific funding for this work.

For citation: Petenyova E.S., Salmina A.B., Berdnikov S.I., Salmin V.V., Abramov V.G., Medvedeva N.N., Semichev E.V. Barrett's esophagus and esophageal adenocarcinoma: biomarkers of proliferation, apoptosis, autophagy and angiogenesis. *Bulletin of Siberian Medicine.* 2020; 19 (4): 226–234. https://doi.org/10.20538/1682-0363-2020-4-226-234.

Пищевод Барретта и аденокарцинома пищевода: биомаркеры пролиферации, апоптоза, аутофагии и ангиогенеза (обзор литературы)

Петенёва Е.С.[1], Салмина А.Б.[2], Бердников С.И.[1], Салмин В.В.[2], Абрамов В.Г.[1], Медведева Н.Н.[2], Семичев Е.В.[1]

[1] *Федеральный Сибирский научно-клинический центр (ФСНКЦ)*
Россия, 660037, г. Красноярск, ул. Коломенская, 26

✉ *Petenyova E.S.,* e-mail: lenchik-dok@mail.ru.

[2] *Красноярский государственный медицинский университет (КрасГМУ) имени проф. В.Ф. Войно-Ясенецкого Россия, 660022, г. Красноярск, ул. Партизана Железняка, 1*

РЕЗЮМЕ

Цель: анализ известных маркеров пролиферации, апоптоза, аутофагии и ангиогенеза в патогенезе пищевода Барретта и аденокарциномы пищевода для улучшения качества диагностики и лечения.

Материалы и методы. Анализ доступной литературы российских и зарубежных авторов.

Заключение. Структурированы данные по известным маркерам, которые в дальнейшем планируется внедрить в клиническую практику при диагностике и лечении пищевода Барретта и аденокарциномы пищевода на разных стадиях развития заболеваний.

Ключевые слова: пищевод Барретта, аденокарцинома пищевода, пролиферация, апоптоз, аутофагия, ангиогенез, маркеры.

Конфликт интересов. Авторы декларируют отсутствие явных и потенциальных конфликтов интересов, связанных с публикацией настоящей статьи.

Источник финансирования. Авторы заявляют об отсутствии финансирования.

Для цитирования: Петенёва Е.С., Салмина А.Б., Бердников С.И., Салмин В.В., Абрамов В.Г., Медведева Н.Н., Семичев Е.В. Пищевод Барретта и аденокарцинома пищевода: биомаркеры пролиферации, апоптоза, аутофагии и ангиогенеза (обзор литературы). *Бюллетень сибирской медицины.* 2020; 19 (4): 226–234. https://doi.org/10.20538/1682-0363-2020-4-226-234.

INTRODUCTION

Barrett's esophagus is a pathological condition in which, under the influence of refluxate (stomach contents: hydrochloric acid, digestive enzymes, bile acids), the non-keratinizing squamous epithelium of the distal esophagus is replaced with specialized columnar epithelium with goblet cells, with the formation of areas with metaplasia and epithelial dysplasia. According to different authors, the frequency of Barrett's esophagus (BE) in the population is 2.4–4% and is a "precancerous disease", therefore, the problem of diagnosis, early detection of BE and monitoring of these patients is extremely important due to the high risk of malignization. In turn, esophageal cancer accounts for 3% and ranks 6th in the structure of all malignant diseases and is the third most common type of tumor of the gastrointestinal tract (after cancer of the stomach and rectum) [1]. The neoplastic progression of BE is expressed by the appearance of areas of metaplasia andan increase in the degree of epithelial dysplasia (low-grade dysplasia – high-grade dysplasia) [2–4]. With the continued effect of refluxate on the esophageal mucosa, in the absence of treatment, esophageal adenocarcinoma (EAC) develops. It is rarely detected in the initial stages of the disease due to the late onset of clinical symptoms which include pain syndrome (which, in clinical practice, is often perceived as a manifestation of other pathological conditions/diseases of the cardiovascular or bronchopulmonary systems), dysphagia, and respiratory issues in the form of a paroxysmal dry cough, and aggravation after eating and in the supine position. In this regard, the possibility of surgical treatment at the time of diagnosis usually does not exceed 50% [4]. The incidence of EAC against the background of BE is steadily increasing, amounting to up to 5% of patients with BE per year, while the five-year survival rate of patients with EAC is extremely low and, according to various sources, is no more than 15% [1, 2, 4]. Predicting malignization, a clear definition of markers will make it possible to track the course of BE, predict the transition to EAC, and, accordingly, facilitate early detection and timely treatment of this pathology.

The search for appropriate markers for the diagnosis of PB is inseparable from the pathogenesis of the disease. The pathogenesis of BE is not well understood. Metaplasia is considered a consequence of the long-term gastroesophageal reflux disease (GERD), in which there is constant contact of aggressive reflux factors with the stratified squamous epithelium of the esophagus.

The main risk factors are male gender, age over 50, clinical symptoms of GERD. Additional factors include Caucasian race, hiatal hernia, obesity (abdom-

inal type), smoking, family medical history and genetic predisposition.

Considering the above, it can be assumed that BE is a stage in the development of EAC. The reasons triggering the development of metaplasia and dysplasia, as well as the molecular mechanisms of the pathogenesis of these conditions, are still poorly understood. There are several theories of the BE development, and discussions continue regarding the mechanisms of the pathogenesis of this pathology.

It is known that in the presence of acid reflux, the flat non-keratinizing epithelium in the damaged mucous membrane of the esophagus is replaced by metaplastic columnar epithelium [2] (Fig. 1–4).

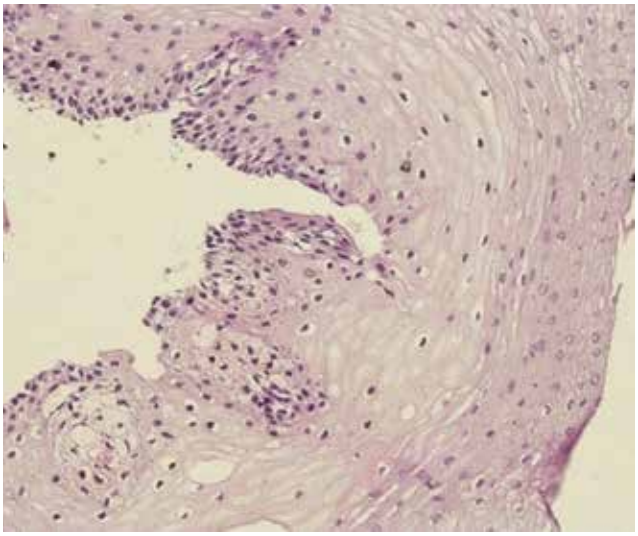

Fig. 1. The esophagus of a healthy person. Stained with hematoxylin and eosin, ×200

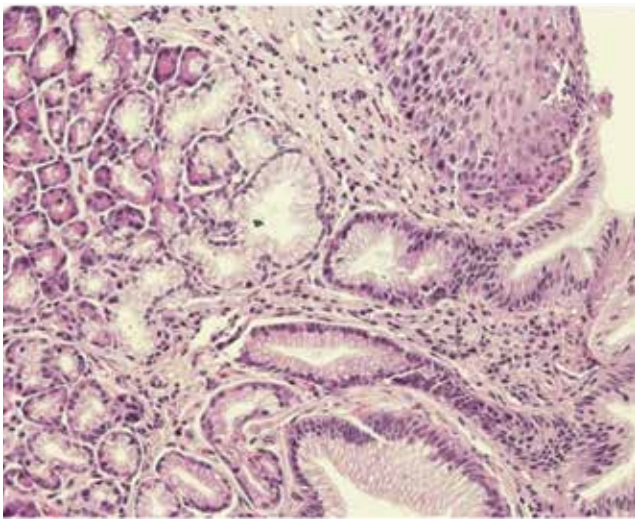

Fig. 2. The area of transition of the esophagus into the stomach in a healthy person. Stained with hematoxylin and eosin, ×200

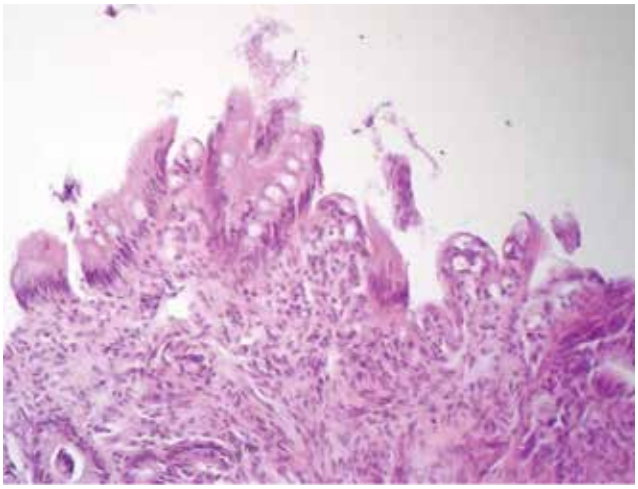

Fig. 3 The mucous membrane of the distal esophagus of a patient diagnosed with BE. Metaplastic type of mucous membrane. Stained with hematoxylin and eosin, ×200

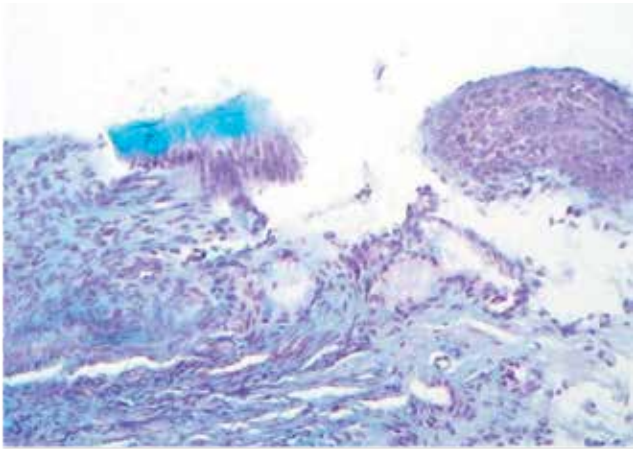

Fig. 4. The mucous membrane of the distal esophagus of a patient diagnosed with BE. Metaplastic type of mucous membrane. Kreiberg mucin staining, ×200

However, daily intraesophageal monitoring of pH and bilirubin revealed that mixed acid-biliary reflux predominates in up to 90% of patients with BE, which causes more severe damage to membranes and intercellular contacts due to the synergistic effect of hydrochloric acid, gastric acid enzymes and bile acid conjugates [4]. Conjugated lipophilic bile acids increase the permeability of apical cell membranes, thereby facilitating the diffusion of hydrogen protons into the tissue, which ultimately has the main damaging effect. Damage to the cells of the surface layer of the epithelium stimulates the regeneration and compensatory thickening of the epithelial layer under the influence of the epidermal growth factor, which leads to an increase in the length of the proliferation zone, the for-

mation and elongation of the papillae of the proper plate of the esophageal mucosa [6, 7]. At this time, the stem cells of the basal layer at the height of the papillae are exposed to acid, enzymes and bile acids. In this regard, the basal epithelial progenitor cell, being pluripotent, can differentiate not into a flat, but into a cylindrical epithelium that is more resistant to the influence of refluxate components (a "defense mechanism" against the action of aggressive reflux factors).

There are other theories of the mechanism of Barrett's metaplasia development. One of the first hypotheses for the development of BE, which consisted of the ascending migration of gastric epithelial cells from the esophageal-gastric junction as a reparative mechanism for replacing damaged acid and other components of esophageal mucosa refluxate, has by now yielded to the point of view that PB de novo develops from cells inherent in the esophagus and not migrating from the stomach [4].

According to modern concepts, factors in the formation of a malignant neoplasm include the ability of carcinogenic agents to cause damage to the cell genome. Malignant progression of any localization is characterized by an increase in proliferation and a decrease in apoptosis [8]. The esophagus is no exception in this regard. Neoplastic progression occurs in patients with acquired genetic instability, in which pathological clones of cells appear, in which aneuploidy is determined, which allows us to consider aneuploidy in PB as a marker of a high risk of malignant progression [9].

The progression of BE also affects the barrier function of the esophageal epithelium. Dysregulation of the complex of molecules of E-cadherin and β-catenin, which are responsible for cell adhesion, and a decrease in their expression on the cell membrane occurs at the late stages of dysplasia development. In Barrett's esophagus, a decrease in the expression of E-cadherin and β-catenin is observed with an increase in dysplasia [10]. Moreover, the more the expression of these proteins is reduced, the worse the prognosis in EAC is.

With an increase in the expression of cyclooxygenase-2, cell adhesion decreases, angiogenesis and proliferation increase, and apoptosis decreases [11].

Another potential point of studying the progression of BE in EAC is the expression of a marker such as maspin. Research in this area has shown that lesions of each pathological grade can be divided into subtypes that show different patterns of the subcellular distribution of maspin, including nuclear only (Nuc), combined nuclear and cytoplasmic (Nuc + Cyt), only cytoplasmic (Cyt) and in general negligible (Neg). Thus, the Cyt subtype of the maspin expression pattern can serve as a molecular marker of early EAC [12].

According to the literary sources, studies of differentially expressed genes (DEG) are being conducted as potential markers of the "transition" of Barrett's esophagus to esophageal adenocarcinoma. Considering the results of some studies, it can be assumed that a panel of differentially expressed genes can occur in cases of high sensitivity to the effects of "risk factors" in the development of EAC, as well as in the progression of this pathological condition [5].

There is data on the study of p504s and CD133 markers, which can act as markers of proliferation and in the future will be used for the differential diagnosis of benign metaplasia and EAC [2].

Phosphorylated histone H3 is a potential marker by which it will be possible to differentiate between low- and high-grade dysplasia and EAC. According to the literary sources, adenocarcinoma had higher rates of mitosis (in terms of phosphorylated histone H3) than high-grade dysplasia [13].

Autophagy is of some importance in the pathogenesis of BE. Autophagy is a highly conserved mechanism that is activated during cellular stress. Presumably, autophagy can be caused by acid reflux, which causes damage and inflammation and, therefore, contributes to the development of BE and EAC [49]. Currently, the role of autophagy in BE and EAC is poorly understood. According to various researchers, autophagy functions to improve cell survival after refluxate damage. Thus, autophagy may play a decisive role in the pathogenesis and progression of BE, which requires further study [14, 15, 40].

Another important and actively studied area is the mechanism of epigenetic drift is a gradual change in the DNA methylation profile with the age of the organism [16]. Presumably, this is a consequence of dysregulation of the molecular apparatus that maintains the normal methylation profile, which consists of the attachment of a methyl group to the cytosine in the CpG dinucleotide at position C5 of the cytosine ring [16–18]. Methylation in the promoter region of a gene usually leads to suppression of transcription of the corresponding gene. Methylated cytosine, in turn, can then be oxidized by special enzymes, which leads to its demethylation back into cytosine. Knowing that EAC is, as a rule, a consequence of BE, where normal squamous cell epithelium is replaced by intestinal

epithelium in response to chronic gastroesophageal acid-biliary reflux, and both of these conditions are characterized by loss of heterozygosity, aneuploidy, specific genetic mutations and clonal diversity, genome and epigenomic analyses can increase the accuracy of risk stratification [17]. Tests for detecting molecular changes associated with tumor progression can be used to improve the pathological assessment of BE/EAC and to select patients at high risk of developing these pathologies for more intensive follow-up [16].

One should also consider that the development of BE and, in the future, EAC is associated with certain demographic and behavioral factors, including gender, obesity/increased body mass index (BMI) and smoking [17–19].

Thus, the pathogenesis of BE is currently not fully understood; it is most likely to be multifactorial. Because of the strong relationship between EAC and BE and between BE and GERD, factors involved in the development of GERD have been the focus of attention in recent years in an attempt to explain the observed increase in the prevalence of EAC. The processes of increased proliferation and suppression of apoptosis, damage to the factors of the barrier function of the epithelium play an important role in the pathogenesis of BE and its progression into EAC.

According to the data we have analyzed, the following markers are most often used to diagnose and assess the prognosis in BE and EAC:

– Ki 67 protein expression,

– p53 gene mutation,

– BE aneuploidy,

– increased expression of COX-2 (low specificity, actively studied as a marker involved in the pathogenesis of PB),

– VEGFR (a marker of angiogenesis).

Table 1 summarizes the characteristics of some of the molecular markers.

Table 1

Markers of Barrett's Esophagus and Esophageal Adenocarcinoma	
Proliferation markers	***MUC-1*** "Intestinal" mucin. Its diagnostic sensitivity in BE is 95%. In 55% of cases, it is found in goblet cells. With severe dysplasia, i.e. progression of BE, its expression in cells increases [20].
	Ki-67 It is a classic marker of cell proliferation. Its expression makes it possible to isolate cells that are in the active phase of the cell cycle throughout its entire length (G1-, S-, G2- and M-phases). Ki-67 is absent only in the G0-period. If Ki-67 is less than 15%, the tumor is considered less aggressive; if it is more than 30%, the tumor is considered highly aggressive [21.22].
	CCK2R Cholecystokinin-2 (CCK2R) receptors are overexpressed in various malignant diseases and therefore attract some attention as potential markers for studying the progression of Barrett's esophagus into EAC [24].
	TFF1, TFF2 Trefoil factors are found in the secretions of goblet cells and Paneth cells and provide regulation of proliferation, differentiation and apoptosis [24].
	SATB1 SATB1 influences the expression of hundreds of genes, including some that are involved in the pathogenesis of human cancer. These data suggest that SATB1 may be involved in carcinogenesis and/or progression of human malignant tumors. SATB1 shows promise as a prognostic biomarker and a novel therapeutic target based on its expression level in solid tumors [25–27].
	Mcm2 Minichromosome maintenance protein is involved in all stages of cellular cycle. Representation in adenocarcinoma is 28.4% to 3.4% in non-progressive forms [28].
	P53 In the presence of mutations, accumulation occurs, including that in the nucleus of cells. The presence of the marker varies from 5% (no dysplasia); 10–20% for low-grade dysplasia, over 60% for high-grade dysplasia, and over 70% for adenocarcinoma [29, 30].
	PCNA (Proliferating cell nuclear antigen) is a nuclear non-histone protein required for DNA synthesis. It is an auxiliary protein for DNA polymerase alpha, which increases during the G1/S phase of the cell cycle. Expression of PCNA can be used as a marker of cell proliferation since cells proliferate for a longer time in the G1/S phase. In addition, this protein plays an important role in the metabolism of nucleic acids as a component of the mechanism of DNA replication and repair [10].
	P27 Inhibits the E/Cdk2 complex, which prevents the onset of the S stage of the cell cycle. The main types of damage are hypermethylation, decreased heterozygosity [28].

Table (continued)

Proliferation markers	***TGFα*** They stimulate VEGF secretion by acting on metaplastic PB cells [31].
	EGFR EGFR is an oncogene that encodes a transmembrane tyrosine kinase receptor. Its dysregulation has been linked to several types of human cancers [31].
	TGFβ It is central in the epithelial homeostasis, regulating both proliferation and differentiation. In normal cells, one of the functions of TGFβ is to induce cell-cycle block, and many epithelial tumors are resistant to this response. In contrast, TGFβ is involved in the epithelial-mesenchymal transition in tumor cells, especially at invasive margins, where this change in phenotype is believed to promote invasion and metastasis. Expression of TGFβ is increased in EAC compared to the normal esophagus and BE [31].
	erbB-2/Her2 receptor is amplified in approximately 10-50% of esophageal adenocarcinoma, with concomitant overexpression of mRNA or protein. Presumably, this lesion is a late stage in the carcinogenesis of Barrett's esophagus [31].
	Cyclooxygenase-2 (COX-2) is a key enzyme in the prostaglandin synthesis pathway. It is believed that chronic inflammation can stimulate tumor development, at least in part due to mediators such as prostaglandins, which suggests that COX-2 promotes carcinogenesis in BE. Increased expression of COX-2 is found during the progression from BE to EAC and is associated with proliferation and decreased survival [30, 31].
	MicroRNA **MicroRNA (miRNAs), a** class of endogenous and single-stranded RNA, is a subfamily of small non-coding regulatory RNA, 18–22 nt in size, involved in various physiological and pathological processes. miRNAs play an important role in oncogenesis by directly or indirectly regulating the expression of various oncogenes or tumor suppressors [32].
	CYFRA 21-1 One of the structural elements of epithelial cells, which forms their framework (cytoskeleton), and numerous cytokeratin proteins. There are about 25 types of proteins, and Cyfra 21-1 is used to diagnose some cancerous tumors [33].
	Fibronectin 1 Fibronectin 1 (FN1) is a member of the glycoprotein family located on the 2q35 chromosome. It has been reported that FN1 is activated in many tumors, and its expression is negatively associated with the prognosis and survival of cancer patients [34].
	Leptin It has been demonstrated that the expression of leptin and its receptor is present in cell cultures of some types of esophageal cancer, and the addition of recombinant leptin to these cell lines leads to a significant dose-dependent increase in cell proliferation and suppression of apoptosis [35].
	P21 The exact role of p21 in carcinogenesis has not yet been fully established. Studies show that in some types of tumors, loss of p21 is a sign of a poor chance of survival. However, situations are known when an increased concentration of this protein in cells positively correlates with the aggressiveness of the tumor and its ability to metastasize. This is particularly the case when p21 accumulates in the cytoplasm, and not in the cell nucleus [22, 31].
	CDX2 The cdx2 gene encodes a specific transcription factor; its protein is expressed in the early stages of small intestine development and may be important in the regulation of proliferation and differentiation of small intestinal epithelial cells. It is expressed in the nuclei of intestinal epithelial cells from the duodenum to the rectum. The protein is expressed in primary and metastatic tumors of the large intestine and is detected in intestinal metaplasia of the stomach and intestinal type of gastric cancer. It is not found in normal epithelial cells of the stomach [28, 36].
Markers of angiogenesis	***VEGF, VEGFR*** Provide neorevascularization of metaplastic tissues which is one of the early events supporting the tumor progression of BE [37].
	VEGFR -1,2 VEGFR-1 regulates angiogenesis through mechanisms that include ligand uptake, homo- and heterodimerization of receptors. Its function in angiogenesis may include its ligand-binding extracellular region, acting as a VEGF trap to modulate the function of VEGFR-2 (which in turn is a receptor for vascular endothelial growth). The study of these markers plays an important role in the creation of "compounds" aimed at suppressing vascular growth in tumors [37].
Markers of apoptosis	***P16*** The main types of damage are hypermethylation, decreased heterozygosity, mutations, and promotor methylation. A decrease in heterozyosity is observed in 75% of patients with adenocarcinoma [31].
	NF-kb (Nuclear Factor kappa B) is activated in various types of cancer. This mediator of carcinogenesis forces malignant tumor cells to avoid apoptosis from the checkpoint of the cell cycle. In recent years, many studies have been performed demonstrating that miRNAs and NF-κB play an important role in the development and progression of tumors [34].

Table (continued)

Markers of autophagy	**mTORC1 complex** regulates the signaling pathway leading to the activation of autophagy by phosphorylation and inhibition of the kinase activity of ULK1 (Unc-51-like kinase 1). After nutrient deprivation, mTORC1 repression is attenuated, and active ULK1 forms a complex with mAtg13, FIP200 (or RB1CC1), and Atg101, which leads to activation of autophagy [38].
	UV Radiation Resistance Associated Gene (UVRAG) is a tumor suppressor involved in autophagy. UVRAG, originally identified as a BECN1-binding macroautophagy/autophagy protein, UVRAG directs a variety of cellular processes to maintain homeostasis and genetic stability, including ER-Golgi transport, endosomal degradation, DNA repair, and centrosome integrity. Consequently, tumor cells may "seek to inactivate" UVRAG in some contexts to remove an important barrier to cancer development [15, 39, 45].
	ATG is a gene associated with autophagy. ATG8 protein is involved in autophagosome formation, load recognition, and recruitment to autophagosomes. At least seven homologues of ATG8 (mammalian ATG8, mATG8) are expressed in human cells. They are usually divided into two subfamilies of GABARAP (Gamma-aminobutyric acid receptor-associated protein A) proteins, including GABARAP / -L1 / -L2, as well as LC3, which includes LC3A (a, b) / B / C [14, 41−43].
	ULK1 is recruited into the Beclin-1-ATG14L-VPS34 complex through its interaction with ATG14L. Beclin-1 is activated by the phosphorylation of ULK1, and, therefore, the PI3 activity of the VPS34 kinase stimulates the production of PtdIns P, which is necessary for the formation and/or maturation of autophagosomes [37,38, 40].
	Lipid kinase VPS34 is an important mediator of many aspects of intracellular transport through the formation of phosphoinositide-3-phosphate (PI (3) P) on membranes [40, 44].

Based on the analysis of the literature available to us, it was revealed that studies in the field of etiology, the pathogenesis of BE and EAC, as well as verification of these pathological conditions, prognosis and choice of treatment methods, remain incomplete. There is a situation of untimely detection and, accordingly, late initiation of BE treatment, in connection with which the risk of EAC development increases. The literature analyzed shows a rather high risk of developing EAC against the background of BE which opens up new opportunities for us in the diagnosis and treatment of these pathological conditions. From our point of view, the most urgent are the issues of a detailed study of the markers of proliferation, apoptosis, autophagy and angiogenesis, the selection of the most significant of them for the early diagnosis of esophageal pathology and the use of markers as a possible immunobiological therapy for Barrett's esophagus and esophageal adenocarcinoma. Consequently, the study of this problem does not lose its relevance and requires further research.

REFERENCES

1. Vakhlyueva O.G. Clinical and diagnostic criteria for Barrett's esophagus and esophageal adenocarcinoma. *Bulletin of Medical Internet Conferences.* 2013; 3 (3): 517−519 (in Russ.).
2. Ahmad J., Arthur K., Maxwell P., Kennedy A., Johnston B.T., Murray L., McManus D.T. A cross sectional study of p504s, CD133, and Twist expression in the esophageal metaplasia dysplasia adenocarcinoma sequence. *Dis. Esophagus*. 2015; 28 (3): 276−282. DOI: 10.1111/dote.12181.
3. Pirogov S.S., Karseladze A.I. Molecular genetic studies in the diagnosis and evaluation of neoplastic progression of Barrett's esophagus. *Siberian Journal of Oncology*. 2008; 1: 85−94 (in Russ.).
4. Ter-Ovanesov M.D. Barrett's esophagus: etiology, pathogenesis, modern approaches to treatment (review). *Meditsinskiy Al'manakh*. 2011; 5: 41−48 (in Russ.).
5. Zali M.R., Zadeh-Esmaeel M.M., Rezaei-Tavirani M., Tabatabaei S.E., Ahmadi A.N. Barrett's esophagus transits to a cancer condition via potential biomarkers. *Gastroenterol Hepatol Bed Bench*. 2018; 11 (Suppl 1): S80−S84.
6. Kolomatskaya P.B. Barrett's esophagus. Epidemiology, ecology, pathogenesis, morphological characteristics, possibilities of endoscopic diagnostics. Literature review. *Vestnik of the Russian Scientific Center of Roentgenoradiology of the Ministry of Healthcare of the Russian Federation*. 2011; 4 (11): 11−14 (in Russ.).
7. Wu J., Ding J., Yang J., Guo X., Zheng Y. MicroRNA roles in the nuclear factor kappa B signaling pathway in cancer. *Front Immunol*. 2018; 9: 546. DOI: 10.3389/fimmu.2018.00546.
8. Reid B.J., Li X., Galipeau P.C., Vaughan T.L. Barrett's oesophagus and oesophageal adenocarcinoma: time for a new synthesis. *Nat. Rev. Cancer.* 2010; 10 (2): 87−101. DOI: 10.1038/nrc2773.
9. Götzel K., Chemnitzer O., Maurer L., Dietrich A., Eichfeld U., Lyros O., Moulla Y., Niebisch S., Mehdorn M., Jansen-Winkeln B., Vieth M., Hoffmeister A., Gockel I., Thieme R. In-depth characterization of the Wnt-signaling/β-catenin pathway in an in vitro model of Barrett's sequence. *BMC Gastroenterol*. 2019; 19 (1): 38. DOI: 10.1186/s12876-019-0957-5.
10. Hashimoto N. Expression of COX2 and p53 in rat esophageal cancer induced by reflux of duodenal contents. *ISRN Gastroenterol*. 2012; 2012: 914824. DOI: 10.5402/2012/914824.
11. Dzinic S.H., Mahdi Z., Bernardo M.M., Vranic S., Beydoun H., Nahra N., Alijagic A., Harajli D., Pang A., Saliganan D.M., Rahman A.M., Skenderi F., Hasanbegovic B., Dyson G., Beydoun R., Sheng S. Maspin differential expression patterns as a potential marker for targeted screening of esoph-

ageal adenocarcinoma/gastroesophageal junction adenocarcinoma. *PloS One.* 2019; 14 (4): e0215089. DOI: 10.1371/journal.pone.0215089.
12. Zhou Z., Lu H., Zhu S., Gomaa A., Chen Z., Yan J., Washington K., El-Rifai W., Dang C., Peng D. Activation of EGFR-DNA-PKcs pathway by IGFBP2 protects esophageal adenocarcinoma cells from acidic bile salts-induced DNA damage. *J. Exp. Clin. Cancer Res*. 2019; 38 (1): 13. DOI: 10.1186/s13046-018-1021-y.
13. Goodarzi M., Correa A.M., Ajani J.A., Swisher S.G., Hofstetter W.L., Guha S., Deavers M.T., Rashid A., Maru D.M. Anti-phosphorylated histone H3 expression in Barrett's esophagus, low-grade dysplasia, high-grade dysplasia, and adenocarcinoma. *Mod. Pathol*. 2009; 22 (12): 1612−1621. DOI: 10.1038/modpathol.2009.133.
14. Gan W., Zhang C., Siu K.Y., Satoh A., Tanner J.A., Yu S. ULK1 phosphorylates Sec23A and mediates autophagy-induced inhibition of ER-to-Golgi traffic. *BMC Cell Biol*. 2017; 18 (1): 22. DOI: 10.1186/s12860-017-0138-8.
15. Keown J.R., Black M.M., Ferron A., Yap M., Barnett M.J., Pearce F.G., Stoye J.P., Goldstone D.C. A helical LC3-interacting region mediates the interaction between the retroviral restriction factor Trim5α and mammalian autophagy-related ATG8 proteins. *J. Biol. Chem*. 2018; 293 (47): 18378−18386. DOI: 10.1074/jbc.RA118.004202.
16. Li S., Jang G.B., Quach C., Liang C. Darkening with UVRAG. *Autophagy*. 2019; 15 (2): 366−367. DOI: 10.1080/15548627.2018.1522911.
17. Agarwal A., Polineni R., Hussein Z., Vigoda I., Bhagat T.D., Bhattacharyya S., Maitra A., Verma A. Role of epigenetic alterations in the pathogenesis of Barrett's esophagus and esophageal adenocarcinoma. *Int. J. Clin. Exp. Pathol*. 2012; 5 (5): 382−396.
18. Kaz A.M., Grady W.M., Stachler M.D., Bass A.J. Genetic and epigenetic alterations in Barrett's esophagus and esophageal adenocarcinoma. *Gastroenterol. Clin. North Am*. 2015; 44 (2): 473−489. DOI: 10.1016/j.gtc.2015.02.015.
19. Luebeck E.G., Curtius K., Hazelton W.D., Maden S., Yu M., Thota P.N., Patil D.T., Chak A., Willis J.E., Grady W.M. Identification of a key role of widespread epigenetic drift in Barrett's esophagus and esophageal adenocarcinoma. *Clin. Epigenetics*. 2017; 9 (1): 113. DOI: 10.1186/s13148-017-0409-4.
20. Nieto T., Tomlinson C.L., Dretzke J., Bayliss S., Price M.J., Dilworth M., Beggs A.D., Tucker O. A systematic review of epigenetic biomarkers in progression from non-dysplastic Barrett's oesophagus to oesophageal adenocarcinoma. *BMJ Open*. 2018; 8 (6): e020427. DOI: 10.1136/bmjopen-2017-020427.
21. Butt M.A., Pye H., Haidry R.J., Oukrif D., Khan S.U., Puccio I., Gandy M., Reinert H.W., Bloom E., Rashid M., Yahioglu G., Deonarain M.P., Hamoudi R., Rodriguez-Justo M., Novelli M.R., Lovat L.B. Upregulation of mucin glycoprotein MUC1 in the progression to esophageal adenocarcinoma and therapeutic potential with a targeted photoactive antibody-drug conjugate. *Oncotarget*. 2017; 8 (15): 25080−25096. DOI: 10.18632/oncotarget.15340.
22. Sobecki M., Mrouj K., Camasses A., Parisis N., Nicolas E., Llères D., Gerbe F., Prieto S., Krasinska L., David A., Eguren M., Birling M.C., Urbach S., Hem S., Déjardin J., Malumbres M., Jay P., Dulic V., Lafontaine D.Lj., Feil R., Fisher D. The cell proliferation antigen Ki-67 organises heterochromatin. *Elife*. 2016; 5: e13722. DOI: 10.7554/eLife.13722.
23. Sun X., Bizhanova A., Matheson T.D., Yu J., Zhu L.J., Kaufman P.D. Ki-67 contributes to normal cell cycle progression and inactive X heterochromatin in p21 checkpoint-proficient human cells. *Mol. Cell. Biol*. 2017; 37 (17): e00569-16. DOI: 10.1128/MCB.00569-16.
24. Roy J., Putt K.S., Coppola D., Leon M.E., Khalil F.K., Centeno B.A., Clark N., Stark V.E., Morse D.L., Low P.S. Assessment of cholecystokinin 2 receptor (CCK2R) in neoplastic tissue. *Oncotarget*. 2016; 7 (12): 14605−14615. DOI: 10.18632/oncotarget.7522.
25. Jin E.H., Lee S.I., Kim J., Seo E.Y., Lee S.Y., Hur G.M., Shin S., Hong J.H. Association between promoter polymorphisms of TFF1, TFF2, and TFF3 and the risk of gastric and diffuse gastric cancers in a Korean population. *J. Korean Med. Sci*. 2015; 30 (8): 1035−1041. DOI: 10.3346/jkms.2015.30.8.1035.
26. Grzanka D., Kowalczyk A.E., Izdebska M., Klimaszewska-Wisniewska A., Gagat M. The interactions between SATB1 and F-actin are important for mechanisms of active cell death. *Folia Histochem. Cytobiol*. 2015; 53 (2): 152−161. DOI: 10.5603/fhc.a2015.0018.
27. Sunkara K.P., Gupta G., Hansbro P.M., Dua K., Bebawy M. Functional relevance of SATB1 in immune regulation and tumorigenesis. *Biomed. Pharmacother*. 2018; 104: 87−93. DOI: 10.1016/j.biopha.2018.05.045.
28. Wang S., Zeng J., Xiao R., Xu G., Liu G., Xiong D., Ye Y., Chen B., Wang H., Luo Q., Huang Z. Poor prognosis and SATB1 overexpression in solid tumors: a meta-analysis. *Cancer Manag. Res*. 2018; 10: 1471−1478. DOI: 10.2147/CMAR.S165497.
29. Grady W.M., Yu M. Molecular evolution of metaplasia to adenocarcinoma in the esophagus. *Dig. Dis. Sci*. 2018; 63 (8): 2059−2069. DOI: 10.1007/s10620-018-5090-8.
30. Duits L.C., Lao-Sirieix P., Wolf W.A., O'Donovan M., Galeano-Dalmau N., Meijer S.L., Offerhaus G.J.A., Redman J., Crawte J., Zeki S., Pouw R.E., Chak A., Shaheen N.J., Bergman J.J.G.H.M., Fitzgerald R.C. A biomarker panel predicts progression of Barrett's esophagus to esophageal adenocarcinoma. *Dis. Esophagus*. 2018; 32 (1): Doy: 102. DOI: 10.1093/dote/doy102.
31. Hashimoto N. Expression of COX2 and p53 in rat esophageal cancer induced by reflux of duodenal contents. *ISRN Gastroenterol*. 2012; 2012: 914824. DOI: 10.5402/2012/914824.
32. Clemons N.J., Phillips W.A., Lord R.V. Signaling pathways in the molecular pathogenesis of adenocarcinomas of the esophagus and gastroesophageal junction. *Cancer Biol. Ther*. 2013; 14 (9): 782−795. DOI: 10.4161/cbt.25362.
33. Wu J., Ding J., Yang J., Guo X., Zheng Y. MicroRNA roles in the nuclear factor kappa B signaling pathway in cancer. *Front. Immunol*. 2018; 9: 546. DOI: 10.3389/fimmu.2018.00546.
34. Gauthé M., Richard-Molard M., Rigault E., Buecher B., Mariani P., Bellet D., Cacheux W., Lièvre A. Prognostic value of serum CYFRA 21-1 1 in patients with anal canal squamous

cell carcinoma treated with radio (chemo) therapy. *BMC Cancer*. 2018; 18 (1): 417. DOI: 10.1186/s12885-018-4335-4.
35. Wang J., Deng L., Huang J., Cai R., Zhu X., Liu F., Wang Q., Zhang J., Zheng Y. High expression of Fibronectin 1 suppresses apoptosis through the NF-κB pathway and is associated with migration in nasopharyngeal carcinoma. *Am. J. Transl. Res*. 2017; 9 (10): 4502−4511.
36. Howard J.M., Pidgeon G.P., Reynolds J.V. Leptin and malignant tumors of the gastrointestinal tract. *Obesity and Metabolism*. 2011; 8 (2): 69−70 (in Russ.).
37. Johnson D.R., Abdelbaqui M., Tahmasbi M., Mayer Z., Lee H.W., Malafa M.P., Coppola D. CDX2 protein expression compared to alcian blue staining in the evaluation of esophageal intestinal metaplasia. *World J. Gastroenterol*. 2015; 21 (9): 2770−2776. DOI: 10.3748/wjg.v21.i9.2770.
38. Rahimi N. VEGFR-1 and VEGFR-2: two non-identical twins with a unique physiognomy. *Front. Biosci*. 2006; 11: 818−829. DOI: 10.2741/1839.
39. Nieto T., Tomlinson C.L., Dretzke J., Bayliss S., Price M.J., Dilworth M., Beggs A.D., Tucker O. A systematic review of epigenetic biomarkers in progression from non-dysplastic Barrett's oesophagus to oesophageal adenocarcinoma. *BMJ Open*. 2018; 8 (6): e020427. DOI: 10.1136/bmjopen-2017-020427.
40. Yang Y., He S., Wang Q., Li F., Kwak M.J., Chen S., O'Connell D., Zhang T., Pirooz S.D., Jeon Y.H., Chimge N.O., Frenkel B., Choi Y., Aldrovandi G.M., Oh B.H., Yuan Z., Liang C. Autophagic UVRAG promotes UV-induced photolesion repair by activation of the CRL4DDB2 E3 ligase. *Mol. Cell*. 2016; 62 (4): 507−519. DOI: 10.1016/j.molcel.2016.04.014.
41. Gan W., Zhang C., Siu K.Y., Satoh A., Tanner J.A., Yu S. ULK1 phosphorylates Sec23A and mediates autophagy-induced inhibition of ER-to-Golgi traffic. *BMC Cell Biol*. 2017; 18 (1): 22. DOI: 10.1186/s12860-017-0138-8.
42. Jeon P., Park J.H., Jun Y.W., Lee Y.K., Jang D.J., Lee J.A. Development of GABARAP family protein-sensitive LIR-based probes for neuronal autophagy. *Mol. Brain*. 2019; 12 (1): 33. DOI: 10.1186/s13041-019-0458-z.
43. Kauffman K.J., Yu S., Jin J., Mugo B., Nguyen N., O'Brien A., Nag S., Lystad A.H., Melia T.J. Delipidation of mammalian Atg8-family proteins by each of the four ATG4 proteases. *Autophagy.* 2018; 14 (6): 992−1010. DOI: 10.1080/15548627.2018.1437341.
44. Simons I.M., Mohrlüder J., Feederle R., Kremmer E., Zobel T., Dobner J., Bleffert N., Hoffmann S., Willbold D. The highly GABARAP specific rat monoclonal antibody 8H5 visualizes GABARAP in immunofluorescence imaging at endogenous levels. *Sci. Rep*. 2019; 9 (1): 526. DOI: 10.1038/s41598-018-36717-1
45. Pyo K.E., Kim C.R., Lee M., Kim J.S., Kim K.I., Baek S.H. ULK1 O-GlcNAcylation is crucial for activating VPS34 via ATG14L during autophagy initiation. *Cell Rep*. 2018; 25 (10): 2878-2890. e4. DOI: 10.1016/j.celrep.2018.11.042.
46. He S., Liang C. Frameshift mutation of UVRAG: Switching a tumor suppressor to an oncogene in colorectal cancer. *Autophagy.* 2015; 11 (10): 1939−1940. DOI: 10.1080/15548627.2015.1086523.
47. Kimos M.C., Wang S., Borkowski A., Yang G.Y., Yang C.S., Perry K., Olaru A., Deacu E., Sterian A., Cottrell J., Papadimitriou J., Sisodia L., Selaru F.M., Mori Y., Xu Y., Yin J., Abraham J.M., Meltzer S.J. Esophagin and proliferating cell nuclear antigen (PCNA) are biomarkers of human esophageal neoplastic progression. *Int. J. Cancer*. 2004; 111 (3): 415−417. DOI: 10.1002/ijc.20267.

Authors information

Petenyova Elena S., General Practitioner, Pulmonologist, Federal Siberian Research Clinical Center, Krasnoyarsk, Russian Federation. ORCID 0000-0003-1103-7848.

Salmina Alla B., Dr. Sci. (Med.), Professor, Head of the Department of Biological Chemistry with a Course of Medical, Pharmaceutical and Toxicological Chemistry, Krasnoyarsk State Medical University named after Prof. V.F. Voino-Yasenetsky, Krasnoyarsk, Russian Federation. ORCID 0000-0003-4012-6348.

Berdnikov Sergey I., Endoscopist, Federal Siberian Research Clinical Center, Krasnoyarsk, Russian Federation. ORCID 0000-0002-9196-589X.

Salmin Vladimir V., Dr. Sci.(Phys.-Math.), Head of the Department of Medical and Biological Physics, Krasnoyarsk State Medical University named after Prof. V.F. Voino-Yasenetsky, Krasnoyarsk, Russian Federation. ORCID 0000-0003-4441-9025.

Abramov Vladislav G., Head of the Department of Organization of Clinical Research, Development and Innovative Neurological Technology Implementation, Federal Siberian Research Clinical Center, Krasnoyarsk, Russian Federation. ORCID 0000-0003-4902-589X.

Medvedeva Nadeschda N., Dr. Sci. (Med.), Head of the Department of Anatomy and Human Histology, Krasnoyarsk State Medical University named after Prof. V.F. Voino-Yasenetsky, Krasnoyarsk, Russian Federation. ORCID 0000-0002-7757-6628.

Semichev Evgeny V., Dr. Sci. (Med.), Endoscopist, Head of the Research Department, Federal Siberian Research Clinical Center, Krasnoyarsk, Russian Federation. ORCID 0000-0003-2386-5798.

(✉) **Petenyova E.S.,** e-mail: lenchik-dok@mail.ru.

Received 25.10.2019
Accepted 30.04.2020

УДК 616.858-039:616.851-056.7]-055.2:575.113.2
https://doi.org/10.20538/1682-0363-2020-4-235-240

Atypical course of Parkinson's disease with clinical manifestations of Huntington's disease in a patient with an allele of 27 CAG repeats in the *HTT* gene

Nikitina M.A.[1], Bragina E.Yu.[2], Nazarenko M.S.[1, 2], Zhukova N.G.[1], Gomboeva D.E.[2], Nurzhanova K.F.[1], Tsentr N.V.[1], Alifirova V.M.[1]

[1] Siberian State Medical University
2, Moscow Trakt, 634050, Tomsk, Russian Federation

[2] Research Institute of Medical Genetics, Tomsk National Research Medical Center, Russian Academy of Sciences
10, Nab. Ushaiki Str., Tomsk, 634050, Russian Federation

ABSTRACT

Huntington's disease (HD) is an autosomal dominant progressive neurodegenerative disease. Its molecular cause is a cytosine-adenine-guanine (CAG) trinucleotide repeat dynamic expansion in the huntingtin (*HTT*) gene. Alleles with 36–39 CAG-repeats are incompletely penetrant, as individuals might develop symptoms but typically with a later age of onset. When repeats are equal or greater than 40, the symptoms of the disease occur. It is considered that CAG-repeats in the "intermediate" alleles (27–35 repeats) also cause the symptoms of the HD.

We present here the case of a patient who has clinical phenotype and family history of Parkinson's disease (PD), but 27 CAG-repeats. The feature of this patient is early development of non-motor manifestations such as cognitive impairment, psychotic disorders, early dystonia in a hand, camptocormia and poor response to levodopa. It is believed that the intermediate allele of *HTT* gene might modify the clinical phenotype of PD in this patient.

Key words: parkinsonism, Parkinson's disease, motor disorders, Huntington's disease, differential diagnosis, expansion of CAG-repeats, HTT, neurodegenerative diseases; genetics.

Conflict of interest. The authors declare no obvious or potential conflict of interest related to the publication of this article.

Source of financing. The study was performed with the support of Council for Grants of the President of the Russian Federation ("Clinical and epidemiological features of neurodegenerative diseases of the Tomsk Region", grant No. MK-813.2019.7).

For citation: Nikitina M.A., Bragina E.Yu., Nazarenko M.S., Zhukova N.G., Gomboeva D.E., Nurzhanova K.F., Tsentr N.V., Alifirova V.M. Atypical course of Parkinson's disease with clinical manifestations of Huntington's disease in a patient with an allele of 27 CAG repeats in the *HTT* gene. *Bulletin of Siberian Medicine.* 2020; 19 (4): 235–240. https://doi.org/10.20538/1682-0363-2020-4-235-240.

✉ *Nikitina Maria A.,* e-mail: nikitina_ma@mail.ru.

Атипичное течение болезни Паркинсона с клиническими проявлениями болезни Гентингтона у пациентки с аллелем 27 CAG-повторов в гене *HTT*

Никитина М.А.[1], Брагина Е.Ю.[2], Гомбоева Д.Е.[2], Назаренко М.С.[1, 2], Жукова Н.Г.[1], Нуржанова К.Ф.[1], Центр Н.В.[1], Алифирова В.М.[1]

[1] Сибирский государственный медицинский университет (СибГМУ)
Россия, 634050, г. Томск, Московский тракт, 2

[2] Научно-исследовательский институт (НИИ) медицинской генетики, Томский национальный исследовательский медицинский центр (НИМЦ) Российской академии наук
Россия, 634050, г. Томск, Набережная реки Ушайки, 10

РЕЗЮМЕ

Болезнь Гентингтона (БГ) – аутосомно-доминантное прогрессирующее нейродегенеративное заболевание, молекулярной причиной которого является динамическая мутация, связанная с экспансией тринуклеотидных CAG (цитозин-аденин-гуанин) повторов в гене гентингтина (*HTT*). Аллели с 36–39 CAG-повторами приводят к неполной пенетрантности и более позднему началу заболевания, тогда как клинические симптомы заболевания обязательно развиваются при количестве повторов 40 и более. В последнее время появляется все больше доказательств о связи CAG-повторов в диапазоне от 27 до 35 (промежуточные аллели) с отдельными клиническими проявлениями, характерными для БГ.

Нами описан клинический случай пациентки с фенотипом болезни Паркинсона (БП), отягощенный семейным анамнезом по данной патологии и промежуточным аллелем с 27 CAG-повторами. Особенностью было раннее развитие в дебюте болезни таких немоторных проявлений, как когнитивные и психотические расстройства; ранняя дистония в кисти и камптокормия, а также слабый ответ на леводопу. Предполагается, что промежуточный аллель гена HTT модифицирует клинический фенотип БП у этой пациентки.

Ключевые слова: паркинсонизм, болезнь Паркинсона, двигательные расстройства, болезнь Гентингтона, экспансия CAG-повторов, HTT, нейродегенеративные заболевания, генетика.

Конфликт интересов. Авторы декларируют отсутствие явных и потенциальных конфликтов интересов, связанных с публикацией настоящей статьи.

Источник финансирования. Исследование выполнено при поддержке Совета по грантам президента Российской Федерации (грант «Клинико-эпидемиологические особенности нейродегенеративных заболеваний Томской области» № МК-813.2019.7).

Для цитирования: Никитина М.А., Брагина Е.Ю., Гомбоева Д.Е., Назаренко М.С., Жукова Н.Г., Нуржанова К.Ф., Центр Н.В., Алифирова В.М. Атипичное течение болезни Паркинсона с клиническими проявлениями болезни Гентингтона у пациентки с аллелем 27 CAG-повторов в гене *HTT*. *Бюллетень сибирской медицины.* 2020; 19 (4): 235–240. https://doi.org/10.20538/1682-0363-2020-4-235-240.

INTRODUCTION

Huntington's disease (HD) is an autosomal dominant disease developing as a result of a mutation associated with a pathological increase in the number of CAG repeats in the first exon of the huntingtin gene (HTT) mapped at the 4p16.3 locus. On the basis of the mutant HTT gene, a large protein of the same name is synthesized, which has an elongated chain of glutamine residues in its composition, resulting in the formation of pathological connections between mutant huntingtin and other proteins that contribute to the cytotoxicity and selective death of striatum neurons which is characteristic of the disease [1, 2]. HD is the most common monogenic neurodegenerative disorder in populations of European origin [1].

The number of copies of CAG repeats in healthy individuals varies from 10 to 35, and the presence of at least one allele with 36 CAG repeats in the HTT gene leads to the development of HD. Carriers of

alleles within 36–39 CAG repeats are characterized by incomplete disease penetration, and the expansion of 40 or more CAG repeats leads to the development of a complete clinical picture of HD. The severity of symptoms and early onset of the disease correlate proportionally with an increase in the number of CAG repeats [3].

The carrier state of the so-called "intermediate" alleles (IAs) within the range of 27–35 CAG repeats is a characteristic of phenotypically healthy individuals. However, in recent years, some studies have appeared that note the correlation of "intermediate" alleles with a barely noticeable (subclinical), and sometimes explicit phenotypic manifestation of HD in some cases [3, 4]. A typical motor disorder in HD is characterized by both hyper- and hypokinesia, the latter is more pronounced in the early stages of the disease. However, hypokinesia prevails from the very beginning in the primary akinetic-rigid form of HD, a rare variant of Westphal, manifesting most often in the first two decades of life and characterized by a particularly unfavorable outcome [5].

Alleles with 36–39 CAG repeats that are associated with incomplete HD penetrance occur with a fairly high frequency among the general population. Thus, according to Kay C. and co-authors' study there is one carrier of the HD mutation for every 400 people among 7,315 individuals of European origin from the United States, Scotland, and Canada (this corresponds to a prevalence of 250 per 100,000 population) [6, 7]. Most often, individuals with the number of 36–37 CAG repeats were found in the studied cohorts (36 – 0.096%; 37 – 0.082%; 38 – 0.027%; 39 – 0.000%; ≥ 40 – 0.041%). The obtained data indicate an underestimation of the true prevalence of HD [8]. Unfortunately, similar estimates of CAG-repeat expansion prevalence in residents of different Russia regions are limited, which makes it necessary to conduct an all-Russian epidemiological study.

Regarding the "intermediate" alleles of the HTT gene, it was found that one IAs carrier with (27–35 CAG repeats) accounts for 16 examined individuals. It is especially important because IAs carriers are the source of the *de novo* HD mutation (sporadic cases of the disease) in subsequent generations, reaching 5–14% of the patients with HD total number [9]. According to an epidemiological study, the frequency of the intermediate alleles is 2.6% in Russian residents [10]. A fairly high frequency of "intermediate" alleles is also registered among patients with other neurological diseases: up to 3.5% among patients with HD, reaching the maximum frequency of 6.0% in patients with Alzheimer's disease [11, 12].

This article presents a clinical case of a patient with a phenotype that is largely compatible with the akinetic-rigid form of Parkinson's disease, but with features suggesting that an "intermediate" allele of the HTT gene (27 CAG repeats) modified the classic Parkinson's disease phenotype.

CLINICAL CASE

Patient K., female, 54 years old, noted general weakness, fatigue, and slowness of movements, which she associated with the stress, so she did not seek medical help. Over the next two years (up to the age of 56 years), poor left-hand control followed, interfering movements and performing any purposeful actions, with involuntary flexing of the fingers. Additionally, there was a tremor of the head and eyelids, increased hypokinesia in all types of activities, deterioration of handwriting, increased constipation, increased olfactory disfunction up to anosmia, and a constantly reduced mood background. Hypokinesia and hypomimia were present during the examination, as well as a slight inclination of the body forward (camptocormia) and slightly to the right (Pisa syndrome), small, shuffling step gait, disruption of balance control (rare falls up to once in 3–6 months) and clumsiness in fine motor skills. Symptoms of the disease prevailed on the left side of the body and in the left extremities.

The patient was examined. MRI of the brain: signs of microangiopathy with expansion of the basal cisterns, moderate atrophy of the frontal and parietal lobes cortex, rhinosinusitis. Electroencephalography: due to the high motor activity the EEG is overlaid by a myogram. Certain elements of epileptiform activity were registered for hyperventilation in the form of acute potentials, acute-slow wave complexes in the left central temporal area; irritation signs of subcortical and brainstem structures. Laboratory tests: antibodies to the thyroid-stimulating hormone receptor (TSH) in the blood: 2.3 mME/l; free thyroxine T4 in the blood: 12.7 nmol/l; anti-TPO in the blood: 3.3; hepatitis B virus antigen in the blood: negative; hepatitis C virus antigen in the blood: negative. General and biochemical blood tests: no pathology was detected. Ultrasound examination of the thyroid and parathyroid glands: diffuse changes in the thyroid gland were detected. Duplex scanning of brachiocephalic arteries with color Doppler mapping of blood flow: signs of carotid atherosclerosis without significant stenosis; tortuosity of the carotid arteries on both sides

with compression of the jugular veins; signs of extravasal dynamic impact on the vertebral arteries. Complex ultrasound examination of abdominal organs: moderate diffuse changes in the liver; signs of chronic cholecystitis. Radiography of the hands: deforming osteoporosis of the 1st degree. Ophthalmologist consultation: hypertensive arteriosclerosis; initial cataract in both eyes; destruction of the vitreous body of both eyes. Consultation of a general practitioner: hypertension of the 2nd stage; chronic heart failure of 0 stage, risk 2; hypertensive heart disease with a primary heart lesion without congestive heart failure. Surgeon consultation: constipation; scoliosis of the thoracic and lumbar spine levels.

The diagnosis of PD was established on the basis of physical and other examinations, since the signs and symptoms corresponded to the main diagnostic criteria of the disease: the presence of severe hypomimia, hypokinesia, rigidity and a sense of clumsiness with a symptom predominance in the left half of the body and limbs, as well as gait disorders of the "Parkinsonian" type, and the presence of postural instability. The patient has no children. According to the patient, her mother's brother also suffered from PD at the age of about 65. However, the patient's relative's medical history is not available. Dopamine receptor agonists and amantadine were prescribed (pramipexol 4.5 mg/day, amantadine 150 mg/day).

Six months later (at the age of 57), the woman noted a significant deterioration in the form of an increased severe body inclination to the right and forward. During the examination, there was a slight postural and kinetic tremor of the upper extremities without a rest tremor, slight tremor of the head and eyelids. Rigidity was observed with a predominance in the left extremities. Bradykinesia was moderate, but obvious, and the gait was shuffling. Postural reflexes were impaired (falls started to occur), but it was still possible to walk without assistance. According to validated clinical tools: the MDS-Unified Parkinson's Disease Rating Scale (MDS-UPDRS) III was 39 points, and the Unified Huntington's Disease Rating Scale (UHDRS) III was 24 points. Due to the deterioration of condition (increased stiffness and hypokinesia), the drug levodopa/carbidopa/entacapon (at a dose of 300 mg per day) was added to the antiparkinsonic therapy scheme, along with physical therapy. This pharmacological approach gave a slight improvement of the condition: slightly decreased rigidity, slightly decreased camptocormia, slightly improved gait. There was no clinically significant positive result after botulinum toxin injections for camptocormia correction.

Despite the presence of major symptoms, corresponding to PD (bradykinesia, rigidity and postural instability), the patient had several PD not corresponding non-motor manifestations after four years of the motor symptoms onset: pronounced cognitive impairment (13 points on the MoCA test and 18 points on the MMSE, which corresponds to moderately severe dementia), expressed anxiety and depressive disorders (according to HADS: subscale "anxiety" – 12 points, "depression" – 13), the presence of suicidal thoughts without suicidal behavior (according to the questionnaire C-CSSR) and no hallucinations. The young age of the onset is also notable (it is believed that the average age of PD onset is 65 years, the disease debuts earlier only in 10–15% of cases [13]). Such motor symptoms as camptocormia developed within three years from the onset of the disease, head tremor and the presence of involuntary flexor movements in the fingers of the left hand before the beginning of antiparkinsonic therapy were among motor disorders not filling the clinical picture of the disease.

In order to make a differential diagnosis of PD with other motor disorders manifesting as parkinsonism, a number of neurological tests were performed: there was a slight slowdown in initiation and hypometria of saccades, but eye movements were in full (in contrast to progressive supranuclear paralysis, in which postural instability is also observed). The patient could hold her tongue stuck out for 10 seconds without much effort (unlike Wilson – Konovalov's disease). Only mild vegetative symptoms were observed (diffuse hyperhidrosis, hypersalivation, moderately dry mouth, constipation in contrast to multi-system atrophy). For differential diagnosis between HD and PD, the Wartenberg glabellar reflex was tested, manifesting as a pronounced closing of the eyelids when a hammer strikes on the glabella (bridge of the nose) and considered an obligate sign of parkinsonism. The patient's glabellar reflex showed rapid habituation and the absence of pronounced closing of the eyelids when hitting the glabella.

Due to the lack of dramatic response to levodopa (although very high doses were not tested) and the presence of clinical manifestations not typical for patients with PD, but more characteristic for HD, molecular genetic analysis of the gene HTT was performed, in which the alleles associated with 27 and 20 CAG repeats were identified. The molecular genetic study of the number of HTT gene CAG-repeats was per-

formed using a polymerase chain reaction with fluorescently labeled primers according to the M. Bastepe, W. Xin, 2015 [14].

CONCLUSION

The phenotype of the patient K. basically corresponded to the PD. Taking into account the clinical diagnostic criteria of the International Parkinson and Movement Disorder Society for PD, she was found to have hypokinesia, asymmetric muscle rigidity, and postural instability - three of the main PD characteristics. However, one of the exclusion criteria ("red flag") was found: early-developing dementia with memory and speech disorders. In a clinical study, the symptoms of the disease were more fully evaluated using the UPDRS scale, in comparison with the UHDRS. The clinical picture also met the supporting criteria, and therefore the diagnosis of clinically established PD was verified.

Considering the fact that the "intermediate" alleles of the HTT gene have a noticeable effect on the deterioration of motor and cognitive functions [1], it seems likely that the presence of IAs in the patient's genotype modifies the classic phenotype. According to this fact, the results of the patient's glabellar reflex showed rapid habituation, as well as in patients with HD, whereas in PD no habituation was observed [2, 4]. Moreover, although the clinical phenotype of the patient mostly corresponded to PD, however, there was early dystonia, when the patient did not receive dopaminergic antiparkinsonian drugs.

Thus, taking into account early dystonia, poor response of motor symptoms to levodopa, and the results of neuropsychological testing indicating the presence of HD inherent signs, as well as clinical criteria, it can be concluded that the IAs carriage of the HTT gene modifies the PD phenotype in this patient. In world practice, several similar cases have been described, that is certainly of interest from the point of view of the need for medical and genetic counseling, both for differential diagnosis of the disease and risk assessment in the patient's family members, but at this stage it is important to accumulate data on the features of clinical manifestations of the huntingtin gene "intermediate" alleles carriers for a more complete characterization of subphenotypes.

REFERENCES

1. Cubo E., Ramos-Arroyo M.A., Martinez-Horta S., Martínez-Descalls A., Calvo S., Gil-Polo C. Clinical manifestations of intermediate allele carriers in Huntington disease. *Neurology*. 2016; 87 (6): 571–578. DOI: 10.1212/WNL.0000000000002944.
2. Illarioshkin S.N., Klushnikov S.A., Seliverstov Yu.A. Huntington's disease. Moscow: Atmosphere Publ. 2018: 472 (in Russ.). DOI: 10.12731/978-5-902123-69-9.
3. Apolinário T.A., Paiva C.L., Agostinho L.A. Intermediate alleles of Huntington's disease *HTT* gene in different populations worldwide: A Systematic Review. *Genet. Mol. Res.* 2017; 16 (2). DOI: 10.4238/gmr16029648.
4. Savitt D., Jankovic J. Clinical phenotype in carriers of intermediate alleles in the huntingtin gene. *J. Neurol. Sci*. 2019; 402: 57–61. DOI: 10.1016/j.jns.2019.05.010.
5. Reuter I., Hu M.T., Andrews T.C., Brooks D.J., Clough C., Chaudhuri K.R. Late onset levodopa responsive Huntington's disease with minimal chorea masquerading as Parkinson plus syndrome. *Journal of Neurology Neurosurgery & Psychiatry*. 2000; 68 (2): 238–241. DOI: 10.1136/jnnp.68.2.238.
6. Ha A.D., Jankovic J. Exploring the correlates of intermediate CAG repeats in Huntington disease. *Postgrad. Med.* 2011; 123 (5): 116–121. DOI: 10.3810/pgm.2011.09.2466.
7. Kay C., Collins J.A., Miedzybrodzka Z. et al. Huntington disease reduced penetrance alleles occur at high frequency in the general population. *Neurology*. 2016; 87 (3): 282–288. DOI: 10.1212/WNL.0000000000002858.
8. Kay C., Collins J.A., Wright G.E., Baine F., Miedzybrodzka Z., Aminkeng F., Semaka A.J., McDonald C., Davidson M., Madore S.J. The molecular epidemiology of Huntington disease is related to intermediate allele frequency and haplotype in the general population. *Am. J. Med. Genet. Part B. Neuropsychiatr. Genet.* 2018; 177 (3): 346–357. DOI: 10.1002/ajmg.b.32618.
9. Semaka A., Collins J.A., Hayden M.R. Unstable familial transmissions of Huntington disease alleles with 27-35 CAG repeats (intermediate alleles). *Am. J. Med. Genet. Part B. Neuropsychiatr. Genet.* 2010; 153B (1): 314–320. DOI: 10.1002/ajmg.b.30970.
10. Seliverstov Yu.A., Dranitsyna M.A., Kravchenko S.A., Klushnikov M.A., Illarioshkin S.N. Epidemiology of Huntington's disease in the Russian Federation. In: Parkinson's disease and movement disorders: guidelines for physicians based on materials of the IV National congress on Parkinson's disease and movement disorders; ed. S.N. Illarioshkin, O.S. Levin. Moscow: Luxury-Print Publ., 2017: 244–246 (in Russ.).
11. Menéndez-González M., Clarimón J., Allende I.R., Blázquez M., Martín E.S., Fernández C.G., Lleó A., Dols-Icardo O., Illán-Gala I., Morís G. et al. *HTT* gene intermediate alleles in neurodegeneration: Evidence for association with Alzheimer's disease. *Neurobiol. Aging*. 2019; 76: 215.e9–215.e14. DOI: 10.1016/j.neurobiolaging.2018.11.014.
12. Ha A.D., Jankovic J. Exploring the Correlates of Intermediate CAG Repeats in Huntington Disease. *Postgraduate Medicine*. 2011; 123 (5): 116–121. DOI: 10.3810/pgm.2011.09.2466.
13. Levin O.S., Fedorova N.V. Parkinson's disease; 5th ed. Moscow: MEDpress-inform Publ., 2016: 384 (in Russ.).
14. Bastepe M., Xin W. Huntington disease: molecular diagnostics approach. Current protocols in human genetics. 2015; 87: 9.26.1–9.26.23. DOI: 10.1002/0471142905.hg0926s87.

Authors information

Nikitina Maria A., Cand. Sci. (Med.), Associate Professor, Department of Neurology and Neurosurgery, Siberian State Medical University, Tomsk, Russian Federation. ORCID 0000-0002-2614-207X.

Bragina Elena Yu., Cand. Sci. (Biology), Senior Researcher, Population Genetics Laboratory, Research Institute of Medical Genetics, Tomsk NRMC, Tomsk, Russian Federation. ORCID 0000-0002-1103-3073.

Nazarenko Maria S., Dr. Sci. (Med.), Head of the Population Genetics Laboratory, Research Institute of Medical Genetics, Tomsk NRMC, Tomsk, Russian Federation. ORCID 0000-0002-0673- 4094.

Zhukova Natalya G., Dr. Sci. (Med.), Professor, Department of Neurology and Neurosurgery, Siberian State Medical University, Tomsk, Russian Federation. ORCID 0000-0001-6547-6622.

Gomboeva Densema E., Post-Graduate Student, Population Genetics Laboratory, Research Institute of Medical Genetics, Tomsk NRMC, Tomsk, Russian Federation. ORCID 0000-0002-7882-2093.

Nurzhanova Kseniya F., 5th-Year Student, Department of Pediatrics, Siberian State Medical University, Tomsk, Russian Federation. ORCID 0000-0002-4222-9765.

Tsentr Nikita V., 5th-Year Student, Department of General Medicine, Siberian State Medical University, Tomsk, Russian Federation. ORCID 0000-0002-7344-1726.

Alifirova Valentina M., Dr. Sci. (Med.), Professor, Head of the Department of Neurology and Neurosurgery, Siberian State Medical University, Tomsk, Russian Federation. ORCID 0000-0002-4140-3223.

(✉) **Nikitina Maria A.,** e-mail: nikitina_ma@mail.ru.

Received 14.03.2020
Accepted 29.09.2020

УДК 616.62-006.6-06-033.2:616.127
https://doi.org/10.20538/1682-0363-2020-4-241-246

A case of myocardial metastasis of bladder cancer

Shatov D.V., Grigoriev P.E., Shalanin V.V.

V.I. Vernadsky Crimean Federal University
4, Vernadsky Av., Simferopol, 295007, Russian Federation

ABSTRACT

The case of metastatic heart damage manifesting by a clinical picture of acute myocardial infarction in a patient with urothelial carcinoma of the urinary bladder is described. A 69-year old patient was admitted with the symptoms of acute myocardial infarction from the neurological department, where he was hospitalized due to a space-occupying lesion of the right hemisphere of the brain, which manifested in a convulsive episode with the development of left-sided spastic hemiparesis. After coronary angiography, percutaneous coronary intervention was performed for the lesions of the anterior interventricular branch of the left coronary artery. Despite the complex of the therapeutic measures, the patient died. A pathological study revealed urothelial carcinoma of the bladder with distant metastases to the brain and myocardium. This clinical case demonstrates the situation of intravital diagnosis of metastatic myocardial lesions, which requires a determination of the treatment approach in the described category of patients.

Key words: urothelial carcinoma of the bladder, metastases, metastatic heart damage, metastatic brain damage, myocardial infarction, heart lesion.

Conflict of interest. The authors declare the absence of obvious and potential conflicts of interest related to the publication of this article.

Source of financing. The authors state that there is no funding for the study.

For citation: Shatov D.V., Grigoriev P.E., Shalanin V.V. A case of myocardial metastasis of bladder cancer. *Bulletin of Siberian Medicine.* 2020; 19 (4): 241–246. https://doi.org/10.20538/1682-0363-2020-4-241-246.

Случай метастазирования рака мочевого пузыря в миокард

Шатов Д.В., Григорьев П.Е., Шаланин В.В.

Крымский федеральный университет имени В.И. Вернадского
Россия, 295007, Республика Крым, г. Симферополь, пр. Вернадского, 4

РЕЗЮМЕ

Представленный клинический случай метастатического поражения сердца у пациента проявился клиникой острого инфаркта миокарда при уротелиальной карциноме мочевого пузыря. Пациент 69 лет поступил с клиникой острого инфаркта миокарда из неврологического отделения, где находился по поводу объемного образования правого полушария головного мозга, манифестировавшего судорожным эпизодом с развитием левостороннего спастического гемипареза.

После проведения коронарографии было выполнено чрескожное коронарное вмешательство по поводу поражений передней межжелудочковой ветви левой коронарной артерии. Несмотря на проведенный комплекс лечебных мероприятий, пациент скончался. При патологоанатомическом исследовании обнаружена уротелиальная карцинома мочевого пузыря с отдаленными метастазами в головной мозг и

✉ *Shatov Dmitrii V.,* e-mail: dmitrii_shatov@mail.ru.

миокард. Клинический случай демонстрирует ситуацию прижизненной диагностики метастатических поражений миокарда, которая требует определения лечебного подхода у описанной категории пациентов.

Ключевые слова: уротелиальный рак мочевого пузыря, метастазы, метастазирование в сердце, метастазирование в головной мозг, инфаркт миокарда, поражение сердца.

Конфликт интересов. Авторы декларируют отсутствие явных и потенциальных конфликтов интересов, связанных с публикацией настоящей статьи.

Источник финансирования. Авторы заявляют об отсутствии финансирования.

Для цитирования: Шатов Д.В., Григорьев П.Е., Шаланин В.В. Случай метастазирования рака мочевого пузыря в миокард. *Бюллетень сибирской медицины.* 2020; 19 (4): 241–246. https://doi.org/10.20538/1682-0363-2020-4-241-246.

INTRODUCTION

Metastasis of urothelial bladder cancer (UBC) in the heart is a rare and dangerous case in clinical practice. To date, only 5 descriptions of UBC-metastasis in the heart have been discovered [1–5]; another 9 cases of metastases of the urogenital cancer (UC) in the heart with primary localization of the tumor in the urinary bladder (UB) were described in the article [6]. The clinical manifestations in such patients consist of impaired conduction, progression of heart failure due to obstruction of the exit tract of the right ventricle, effusion pericarditis with symptoms of pericardial tamponade and embolism of the pulmonary artery. In most of the cases described, patients lived (with rare exceptions) for no more than 1 month from the moment of verification and receiving medication, although in some cases pericardiocentesis, cytoreductive surgery and implantation of artificial pacemaker were performed. The cases described in the literature, as a rule, had other distant metastases; however, among them there were no patients with metastasis to the brain, which is why the case described in our article is relevant and significant.

The aim of the research was to describe the clinical case of metastasis of bladder cancer in the myocardium, taking into account the manifestation of the disease with neurological symptoms, which has not been previously described.

CLINICAL CASE

A 69-year old patient was admitted to the cardiology department with intensive care units of the N.A. Semashko Republican Clinical Hospital with complains of intense burning pains behind the sternum, which suddenly appeared 3 hours previous, dyspnea, general weakness, and sweating.

Prior to this, he was admitted to another medical institution with a diagnosis of the space-occupying lesion of the right hemisphere of the brain, a convulsive episode, and left-sided spastic hemiparesis. Computed tomography revealed the presence of extraaxial space-occupying formation adjacent to the parietal bone, measuring 4.5×3.0×7.0 cm, with density of 40–45 HU, accumulating contrast medium up to 80 HU, and mass effect with deformation of the right ventricle and surrounding structures. Decrease in the density of the brain substance to 18 HU was found perifocally (Fig. 1).

Over the past three days the patient was suffering from short-term episodes of sternal pain, which stopped on their own. On the day of admission, a prolonged pain attack occurred with the development of ST-segment elevation in I, II, III, aVL, V_2–V_6. Taking into account the contraindications for thrombolytic therapy, he was sent to the cardiology department for emergency coronary angiography and to determine the further treatment measures.

The general condition at admission was regarded as severe. Consciousness was clear. The skin was pale pink, dry, warm. The legs were pasty. The apical beat was in the 5th intercostal space. The boundaries of relative cardiac dullness were extended leftwards to the midclavicular line. The heart sounds were dull, regular. Blood pressure was 90/60 mm Hg, heart rate is 90 per minute. Respiratory rate was 18 per minute. Breathing during auscultation was rough, weakened in the lower parts on the right; at the same place crepitation was heard. The abdomen was painful in the lower sections. There were no signs of peritoneal irritation. The lower margin of the liver was located at the level of the costal arch and was painless. On electrocardiography the elevation of ST-segments in I, II, III, aVL, V_2–V_6 was found (Fig. 2).

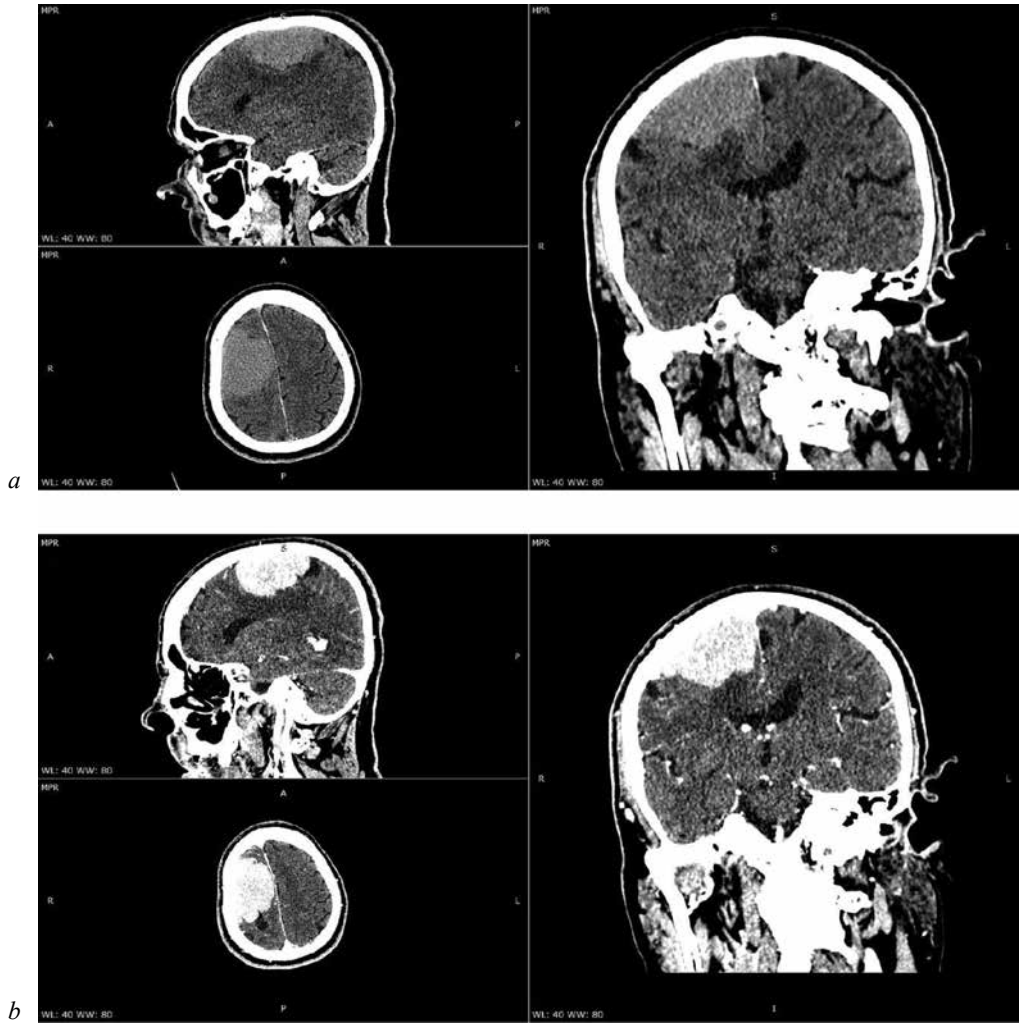

Fig. 1. Computed tomography of the patient's brain: *a* – without contrast enhancement; *b* – with contrast enhancement

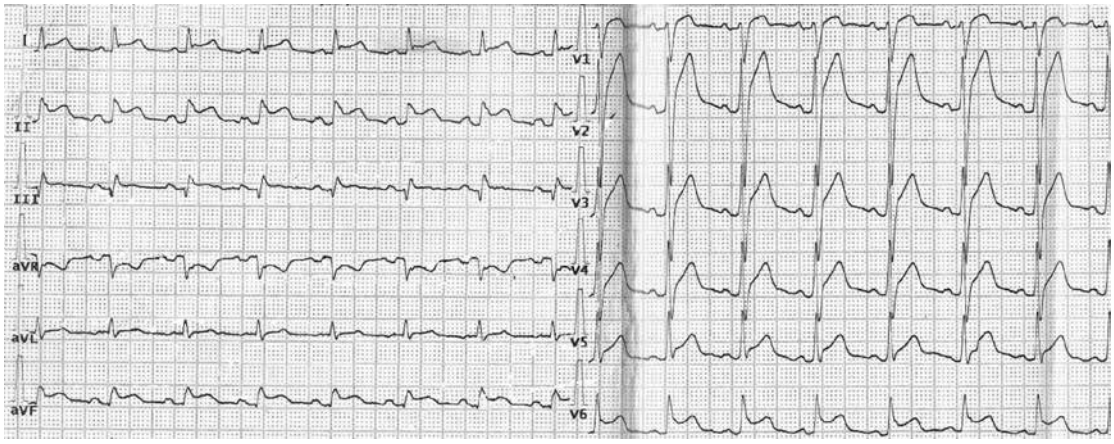

Fig. 2. Electrocardiogram of the patient during admission: speed 25 mm/s; voltage 10 mm

The following diagnose was made: CHD, circular myocardial infarction with ST-segment elevation, atherosclerosis of the coronary arteries, Killip II.

Complete blood count: hemoconcentration (hemoglobin 169 g/L, hematocrit 47%), leukocytosis up to $22.4*10^9$/L due to neutrophils (metamyelocytes 3%, stabs 42%, segmented 39%, toxigenic granularity of neutrophils – 50%). In the biochemical analysis of blood: urea – 17.7 μmol/L, creatinine – 126 μmol/L, total protein – 49 g/L, albumin – 28.9 g/L, potassium –

3.97 mmol/L, sodium – 124,7 mmol/L, cholesterol – 2.71 mmol/L, triglycerides – 2.27 mmol/L, HDL – 0.62 mmol/L, LDL – 1.42 mmol/L, LDH – 866 units/L, creatine kinase – 727 units/L. Coagulogram: PTI – 69.8%, INR – 1.44, fibrinogen A – 4.53 g/L, APTT - 31.7 sec., thrombin time – 20.1 sec.

30 minutes after admission, emergency coronarography was performed; it revealed atherosclerosis of the coronary arteries, the right type of coronary circulation. Stenosis of the orifice of the anterior interventricular branch (AIB) is about 50%, stenosis of the proximal third of the AIB is more than 70% with angiographic signs of instability, the intramural course of the distal third of the AIB in systole is more than 50%, stenosis of the proximal and middle thirds of the right coronary artery is about 40%. According to the results of coronarography, pre-dilatation, stenting and post-dilatation of stenosis of the proximal third of the AIB with good angiographic result were performed. The ECG after the intervention is shown in Fig. 3.

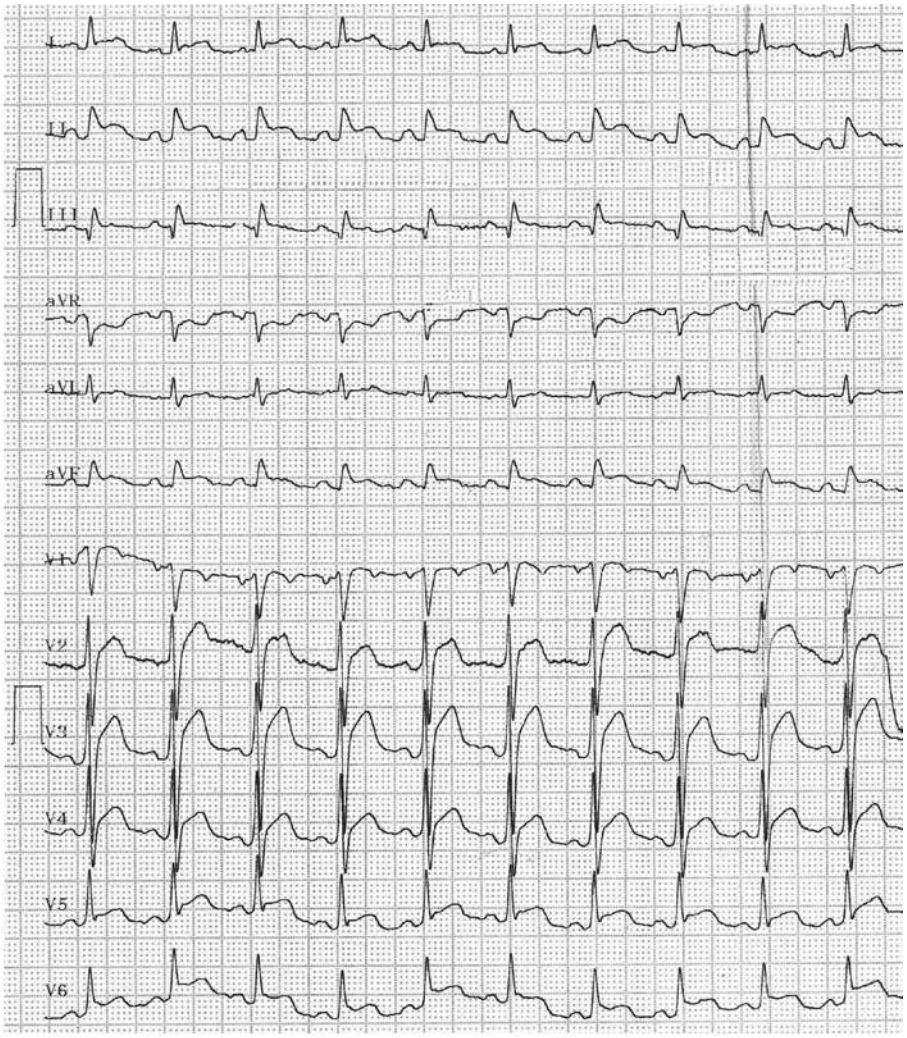

Fig. 3. Electrocardiogram of the patient after pre-dilatation, stenting and post-dilatation of stenosis of the proximal third of the AIB: speed; 25 mm/s.; voltage 10 mm

In the postoperative period, a chest X-ray and echocardiography were performed: aortic diameter in the ascending part is 4.6 cm, at the root – 3.5 cm, opening of the aortic valve cusps – 1.8 cm, the chambers are not enlarged, left ventricular wall hypertrophy is present (posterior wall – 1.3 cm, interventricular septum – 1.4 cm), ejection fraction – 54%, anteroposterior shortening – 22%, stroke volume – 29 ml, mitral and tricuspid insufficiency of the 1st degree are present. Disturbances of segmental contractility were not reliably detected due to tachycardia (heart rate – 140 per minute). Separation of pericardial layers along the contour of the left ventricle is 12 mm, along the contour of the right ventricle – 14 mm.

In the postoperative period, the symptoms of heart failure continued to progress, despite the ongoing therapy. 12 hours after the intervention, the patient died.

The autopsy revealed urothelial bladder cancer G2 ($T_3N_3M_1$) with metastases to the brain, heart, liver, kidneys, lungs, paraaortic lymph nodes, pelvic lymph nodes, pericardial carcinomatosis complicated with fibrinous-purulent pericarditis. In the brain, edema of the pia mater, severe dystrophy of glial cells, rarification fields, severe perivascular, pericellular edema, numerous metastases in the vessels of the pia mater and brain tissue, and plethora of the vessels were observed (Fig. 4). In the heart: the epicardium is thickened and edematous, with severe leukocyte infiltration and accumulations of fibrin, perivascular metastases; the muscular fibers are moderately hypertrophied and have a coiled course; dystrophy of myocardiocytes, focal fragmentation of muscle fibers; in the parenchyma – extensive areas of metastatic growth; around them – edema of the stroma of cardiomyocytes, signs of karyolysis and karyopyknosis; oxyphilia of the cytoplasm, focal swelling and clumpy decomposition of muscle fibers; loose leukocyte intermuscular infiltration, spasm of part of arterioles with reorientation of the endothelium, focal pronounced hyperemia, especially in the subendocardial vessels; signs of small focal perivascular intermuscular sclerosis; the walls of the vessels of the heart are unevenly thickened, dissociated, fibrous, sclerotic, the vessels are full-blooded (Fig. 5,6). In the urinary bladder: infiltrating growth of urothelial cancer G2 with the invasion of all layers of the wall.

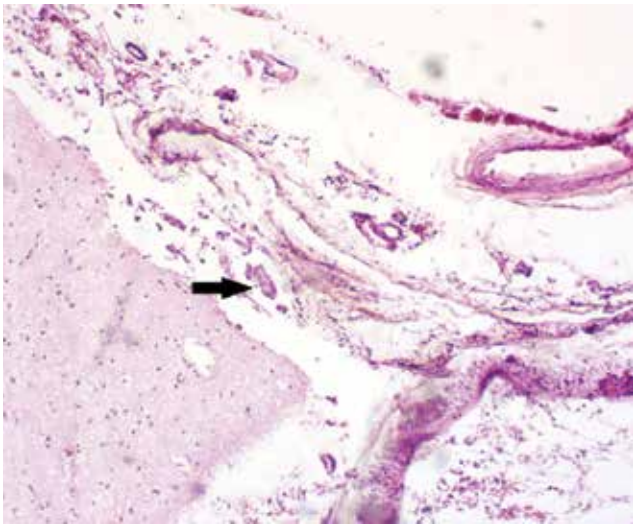

Fig. 4. Metastasis of urothelial bladder cancer in the brain (arrow); Hematoxylin and eosin stain ×100

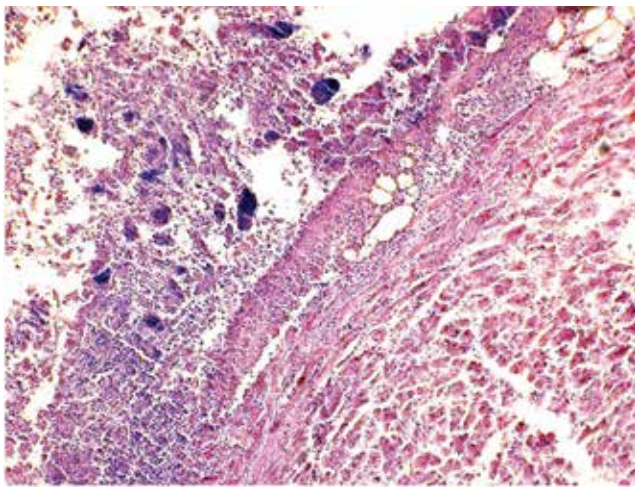

Fig. 5. A fragment of the patient's epicardium and pericardium. Hematoxylin and eosin stain; ×100

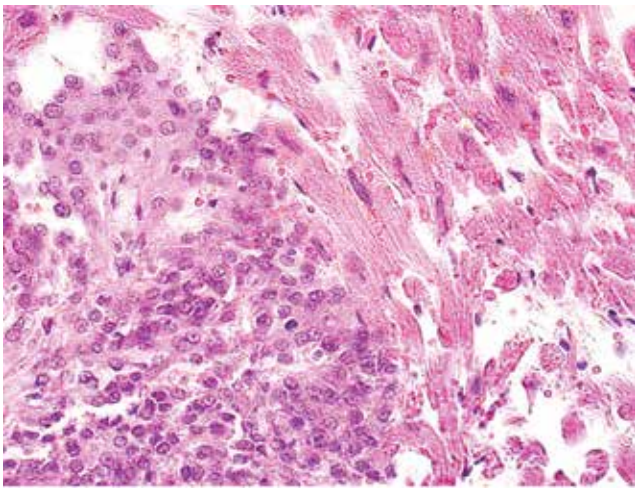

Fig. 6. Metastasis of urothelial bladder cancer (on the left) to the myocardium (on the right); hematoxylin and eosin stain ×100

DISCUSSION

The described clinical case is unique in the manifestation of UBC with a convulsive seizure and focal right hemisphere symptoms. Against the background of the progression of the disease in the form of the development of severe protein-energy insufficiency and the leukemoid reaction, the patient developed a clinical picture of acute circular myocardial infarction with ST-segment elevation, which required surgical intervention. Among the previously described cases, in one case under the metastasis being found in the myocardium, a two-chamber stimulator for resynchronization therapy was implanted, and 17 months after the manifestation of metastasis against the background of pains of ischemic genesis the patient died

during the consideration of palliative stenting of the branch involved in metastasis [1].

The given clinical case raises the question about the extents of invasive care for patients with distant heart metastases, which requires an individual approach to avoid the exposing of the patients to unnecessary suffering.

REFERENCES

1. Arscott W.T., Lal P., Mamtani R., O'Quinn R., Deo R., Jones J. Long-term survival after treating cardiac metastasis with radiation and immune therapy: a case report. *Cureus.* 2018; 10 (5): e2607. DOI: 10.7759/cureus.2607.
2. Schreiner M., Schneider B., Pauls S. Cardiac metastasis of a recurrent urothelial carcinoma of the bladder. *Rofo.* 2015; 187 (12): 1124–1126. (in German). DOI: 10.1055/s-0041-104181.
3. Yamac A.H., Insanic D., Bockmeyer C. Cardiac metastasis from a urothelial cell carcinoma: a commented case report. *Cardiovasc. Pathol.* 2014; 23 (3): 178–180. DOI: 10.1016/j.carpath.2014.01.005.
4. Blagova O.V., Aliyeva I.N., Bezrukov E.A., Ippolitov L.I., Polunin G.V., Kogan E.A., Sedov V.V., Mershina E.A., Sinitsyn V.E., Sarkisova N.D., Nedostup A.V., Fomin V.V. Acute decompensation of hypertensive heart disease in a patient with malignant urinary bladder paraganglioma: stages of diagnostics and treatment. *Rational Pharmacotherapy in Cardiology.* 2018; 14 (3): 370–378 (in Russ.). DOI: 10.20996/18196446-2018-14-3-370-378.
5. Kukharchik G.A., Dikarev K.V., Minkin S.R., Sorokin L.A., Koval I.N. A rare case of metastatic tumor of heart from bladder cancer. *Kardiologiia.* 2017; 57 (S1): 367–372 (in Russ.). DOI: 10.18087/cardio.2394.
6. Ueda N., Kawamura M., Nakazawa S., Hirai T., Kishikawa H., Nishimura K., Morimoto K. Complete atrioventricular block due to cardiac metastasis from bladder cancer: case report. *Hinyokika Kiyo.* 2014; 60 (10): 501–506.

Authors information

Shatov Dmitrii V., Cand. Sci. (Med.), Associate Professor, Department of Medicine of Emergency Conditions and Anesthesiology, Medical Academy n.a. S.I. Georgievsky, V.I. Vernadsky Crimean Federal University, Simferopol, Russian Federation. ORCID 0000-0003-2248-5400.

Grigoriev Pavel E., Dr. Sci. (Biology), Associate Professor, Professor, Department of Condensed Matter Physics, Physical Methods and Information Technology in Medicine, Physical and Technical Institute, V.I. Vernadsky Crimean Federal University, Simferopol, Russian Federation. ORCID 0000-0001-7390-9109.

Shalanin Valeriy V., Cand. Sci. (Med.), Associate Professor, Department of Pathological Anatomy with the Course of Dissection, Medical Academy n.a. S.I. Georgievsky, V.I. Vernadsky Crimean Federal University, Simferopol, Russian Federation. ORCID 0000-0001-5380-2048.

(✉) **Shatov Dmitrii V.,** e-mail: dmitrii_shatov@mail.ru.

Received 23.02.2020
Accepted 29.09.2020

E

F

G

H

I

K

L

M

N

O

P

R

S

T

U

V

Y

Z

ПРОФЕССОР СИБГМУ СОЗДАЛ УЧЕБНИК ПО ФАРМАКОЛОГИИ ДЛЯ РОССИЙСКИХ МЕДВУЗОВ

Учебник «Фармакология» под авторством заведующего кафедрой фармакологии, доктора медицинских наук, заслуженного работника высшей школы РФ, почетного профессора Сибирского государственного медицинского университета Александра Венгеровского опубликован в одном из крупнейших российских медицинских издательств «ГЭОТАР-Медиа» (Москва).

В учебнике освещаются современные проблемы общей и частной фармакологии, фармакологические свойства современных лекарственных средств, особенности их применения в медицинской практике и клинические подходы к фармакотерапии заболеваний. Действие лекарственных средств представлено в сравнительном плане, приведена информация о новых препаратах.

Издание рекомендовано для обучения студентов специальностей "Лечебное дело" и "Педиатрия", а также может быть использовано студентами медицинских вузов других специальностей. Учебному изданию Александра Исааковича присвоен гриф Министерства науки и высшего образования РФ.

«Фармакология – одна из основополагающих и важнейших дисциплин в профессиональной подготовке медицинских специалистов, которая бурно развивается и имеет широкие перспективы. У Томской школы фармакологов славная история. Выход в свет учебного издания знаменует преемственность ее лучших традиций и развитие их в стенах Сибирского государственного медицинского университета», - подчеркнул Александр Исаакович.

Издание в электронном варианте доступно на сайте издательства «ГЭОТАР-Медиа» и на образовательном ресурсе «Консультант студента». Печатная версия учебника «Фармакология» появится в Научно-медицинской библиотеке СибГМУ в ближайшее время.

Александр Венгеровский является автором 9 монографий, 11 учебников и учебных пособий, более 160 статей, опубликованных в ведущих российских и зарубежных журналах. В 2016 году Александру Исааковичу было присвоено звание «Почетный профессор СибГМУ» за выдающиеся достижения в научно-педагогической деятельности и значительный вклад в развитие науки и образования вуза.

Напомним, в 2012 году 4-е издание учебного пособия Александра Исааковича «Фармакология. Курс лекций» было опубликовано в издательстве «ГЭОТАР-Медиа», отмечено премией в сфере медицинского и фармацевтического образования России по итогам 2012 года как лучшее учебное издание для студентов, обучающихся по специальности «Лечебное дело», в 2016 году по результатам рейтинга Научно-медицинской библиотеки СибГМУ стало самым популярным электронным изданием среди читателей (количество просмотров страниц – 9225).

Кафедра фармакологии СибГМУ создана в 1891 году на медицинском факультете Императорского Томского университета впервые в Сибири. На базе кафедры сформировалась Томская научная школа фармакологии – одна из старейших в России. Основоположником сибирской школы фармакологов является ученик профессора П.В. Буржинского, академик АМН СССР, Заслуженный деятель науки РСФСР, лауреат Государственной (Сталинской) премии СССР Николай Вершинин. Николай Васильевич создал учебник «Фармакология как основа терапии», который выдержал 11 изданий и был обязательным руководством для студентов медицинских вузов СССР и Китайской Народной Республики.

bulletin.tomsk.ru

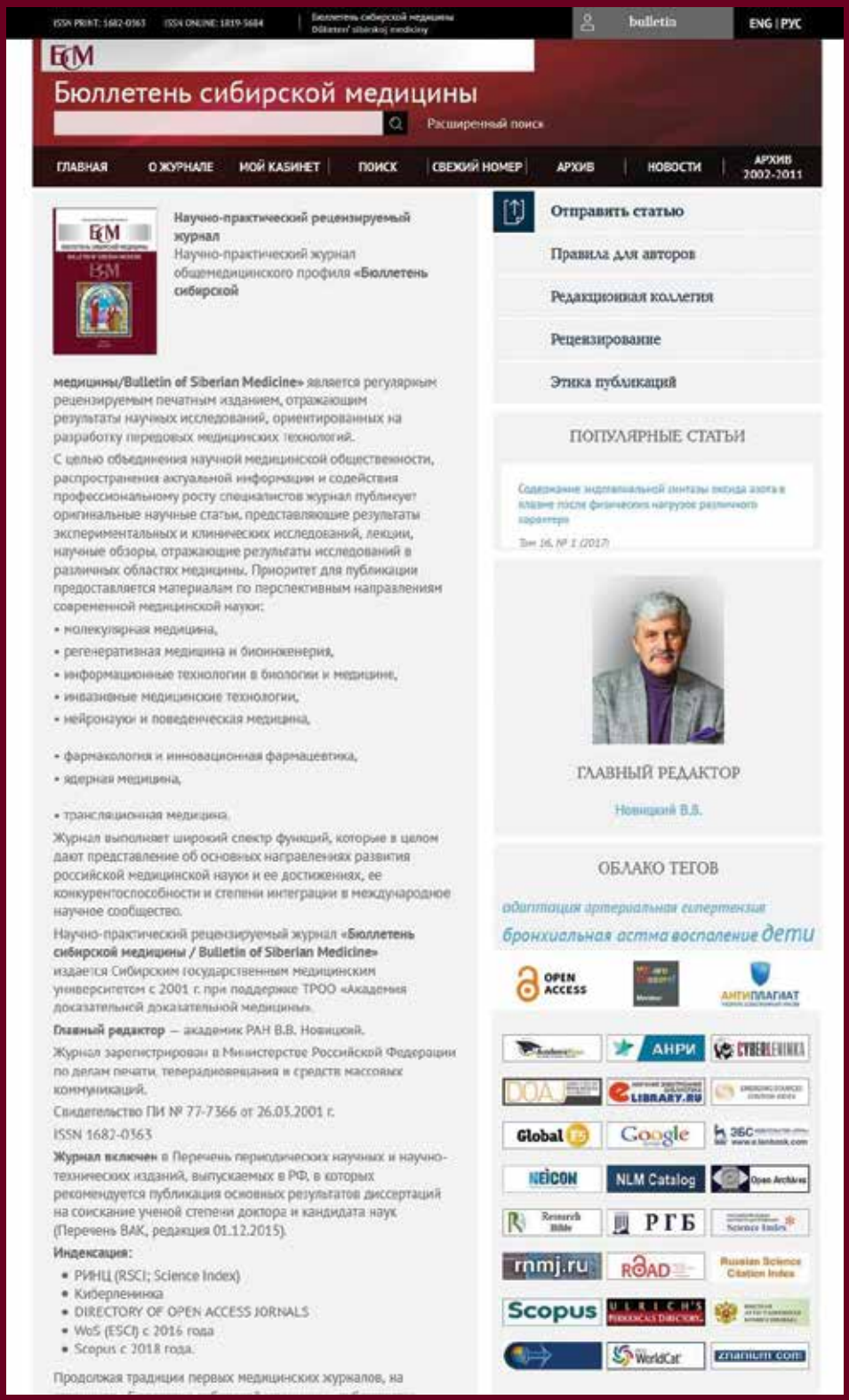

ISSN 1682-0363 (print)
ISSN 1819-3684 (on-line)
БЮЛЛЕТЕНЬ СИБИРСКОЙ МЕДИЦИНЫ
2020. Т. 19. № 4. 1–252
Подписной индекс 10650